

Vanessa Villalba Mouco

Late hunter-gatherers and early farmers in Iberia: an ancient DNA and isotope perspective

Director/es

Salazar García, Domingo Carlos
Haak, Wolfgang
Utrilla Miranda, Pilar

<http://zaguan.unizar.es/collection/Tesis>



© Universidad de Zaragoza
Servicio de Publicaciones

ISSN 2254-7606



Universidad
Zaragoza

Tesis Doctoral

LATE HUNTER-GATHERERS AND EARLY
FARMERS IN IBERIA: AN ANCIENT DNA AND
ISOTOPE PERSPECTIVE

Autor

Vanessa Villalba Mouco

Director/es

Salazar García, Domingo Carlos
Haak, Wolfgang
Utrilla Miranda, Pilar

UNIVERSIDAD DE ZARAGOZA
Escuela de Doctorado

2019

UNIVERSIDAD DE ZARAGOZA

Facultad de Filosofía y Letras

Departamento de Ciencias de la Antigüedad, Área de Prehistoria



Tesis doctoral

Vanessa Villalba Mouco

Directores

Pilar Utrilla Miranda

Domingo Carlos Salazar-García

Wolfgang Haak



Without data you're just another person with an opinion

William Edwards Deming

Esta tesis doctoral consiste en un compendio de artículos y cumple con la normativa establecida de por el Reglamento sobre Tesis Doctorales (Título IV, Capítulo III, arts. 19, 20 y 21). Todos los artículos que aquí se presentan componen una unidad temática, cronológica y metodológica. Esta tesis se compone de un total de cuatro artículos aceptados en revistas internacionales, todas ellas indexadas en el *Journal of Citation Reports* (JCR). Todos los artículos han sido elaborados y aceptados durante los años académicos de la realización de la tesis doctoral, entre los cursos 2015 y 2019. Además, esta tesis también incluye dos artículos que se encuentran en preparación.

Las referencias completas por orden cronológico de los trabajos científicos son las siguientes:

- **Villalba-Mouco, V.**, Sauqué, V., Sarasketa-Gartzia, I., Pastor, M. V., le Roux, P. J., Vicente, D., Utrilla, P., Salazar-García, D. C. (2018). Territorial mobility and subsistence strategies during the Ebro Basin Late Neolithic-Chalcolithic: A multi-isotope approach from San Juan cave (Loarre, Spain). *Quaternary International* 481, 28-41.
- **Villalba-Mouco, V.**, Sarasketa-Gartzia, I., Utrilla, P., Oms, F. X., Mazo, C., Mendiola, S., Cerbriá, A., Salazar-García, D. C. (2018). Stable isotope ratio analysis of bone collagen as indicator of different dietary habits and environmental conditions in Northeastern Iberia during the 4th and 3rd millennium cal BC. *Archaeological and Anthropological Sciences*. <https://doi.org/10.1007/s12520-018-0657-z>
- **Villalba-Mouco, V.**, Utrilla, P., Laborda, R., Lorenzo, J. I., Martínez-Labarga, C., Salazar-García, D. C. (2018). Reconstruction of human subsistence and husbandry strategies from the Iberian Early Neolithic: A stable isotope approach. *American journal of physical anthropology* 167 (2), 257-271.
- **Villalba-Mouco, V.**, Marieke S. van de Loosdrecht, M.S., Posth, C., Mora, R., Martínez-Moreno, J., Rojo-Guerra, M., Salazar-García, D.C., Royo-Guillén, J.I., Kunst, M., Rougier, H., Crevecoeur, I., Arcusa-Magallón, H., Tejedor-Rodríguez, C., García-Martínez de Lagran, I., Garrido-Pena, R., Alt, K.W., Utrilla, P., Krause, J., Haak, W. (2019). Survival of Late Pleistocene Hunter-gatherer ancestry in the Iberian Peninsula. *Current Biology* 29, 1-9. <https://doi.org/10.1016/j.cub.2019.02.006>

- **Villalba-Mouco, V.**, Montes, L., Bea, M., Salazar-García, D.C. (en preparación). Estudio de la movilidad de las comunidades de montaña durante el Calcolítico a través de isótopos de estroncio en esmalte humano: la cueva de los cristales (Sarsa de Surta, Huesca, España).
- **Villalba-Mouco, V.**, Utrilla, P., Sarasketa-Gartzia, Mazo., C., Salazar-García, D.C. (en preparación). Use and reuse of funerary spaces. Strontium isotopes and bayesian radiocarbon modelling to approach Late Neolithic/Chalcolithic funerary behaviour in Northern Iberia.

Además de las cuatro publicaciones (más dos en preparación) que se incluyen en esta tesis, también he contribuido en las siguientes publicaciones internacionales relacionadas con los análisis isotópicos y genómicos de otros restos humanos de la Península Ibérica:

- Sarasketa-Gartzia I., **Villalba-Mouco V.**, le Roux P., Arrizabalaga Á., Salazar-García D.C. (2018). Late Neolithic-Chalcolithic socio-economical dynamics in northern Iberia. A multi-isotope study on diet and provenance from Santimamiñe and Pico Ramos archaeological sites (Basque Country, Spain). *Quaternary International* 481, 14-27.
- Sarasketa-Gartzia, I., **Villalba-Mouco V.**, le Roux, P., Arrizabalaga, Á., Salazar-García, D.C. (2018). Anthropic resource exploitation and use of the territory at the onset of social complexity in the Neolithic-Chalcolithic Western Pyrenees: a multi-isotope approach. *Archaeological and Anthropological Sciences*. <https://doi.org/10.1007/s12520-018-0678-7>
- Olalde, I., Mallick, S., Patterson, N., Rohland, N., **Villalba-Mouco, V.**, Silva, M., Duliás, K., Edwards, C.J., Gandini, F., Pala, M., *et al.* (2019). The genomic history of the Iberian Peninsula over the past 8000 years. *Science*. *Science*, 363(6432), 1230 LP-1234.

ACKNOWLEDGEMENTS

Una tesis no son solo 4 años, sino una larga trayectoria que consigue que te apasione la investigación. Por ello, creo que es necesario empezar agradeciendo esta trayectoria a la educación pública y a mi profesora de secundaria de la asignatura de Biología Arantxa Hueto, quién me sacó de la cabeza ser peluquera y me aficionó al mundo de la biología molecular, así como a los profesores del Avempace. A “la Macu” y “el Goyo”, sin ellos quizás aún tendría la química y las mates pendientes. A mis compañeros y profesores de la Unitat de Antropologia Biològica de la Universitat de Barcelona, especialmente a Daniel Turbón quien hizo despertar mi interés por la evolución humana, a Carme Rissech, y a mi madrileña favorita Marta San Millán.

A mis compañeros del Departamento de Ciencias de la Antigüedad Marta Alcolea, Rafael Laborda, Paloma Lanau, Alejandro Sierra, Paloma Aranda y Luís Jiménez, con lo que he compartido oficina y campo, así como a todos los profesores del Departamento, especialmente Carlos Mazo, Lourdes Montes y Rafa Domingo, con los que he compartido veranos e inviernos de pincel, espátula y cervezas con tierra. Si a veranos de excavación inolvidables se refiere, no puedo pasar por alto a los miembros del CEPAP (Rafa Mora, Jorge Martínez, Susana Vega, Jeza Pizarro, Xavi Roda, Aitor Burguet y Laura Pinto y Anibal Nevado), los cuales me acogieron hace ya 10 años en su equipo. Con ellos aprendí y sigo aprendiendo arqueología. Por todos los buenos veranos que hemos pasado juntos en Sant Llorenç de Montgai, los QR, las PDAs, los karaokes, las fiestas en el zulo y con DJ Kelo, los baños en el pantano y por dejarme hacer el tejón con Jeza.

A todos los arqueólogos que han confiado en mí, y cuyos materiales he podido incluir en esta tesis. Sin su trabajo previo no habría sido posible. Por su comprensión y su paciencia cuando los resultados tardan en llegar.

A los miembros del CEA, mis chicos favoritos, y especialmente a Mario, por contagiarme su pasión por las cuevas, por su ayuda con las topos, las prospecciones, el muestreo de materiales, etc. A Daltón L., por facilitarnos siempre el trabajo de excavación con una escrupulosa metodología que solo el domina. A Moto, por intentar transmitirme una pequeña parte de todo lo que sabe. A los miembros del Boletín Aragón Subterráneo, unidos por la torpeza física y la agilidad verbal.

A mis compañeros de Geología y especialmente a las “Putas Amas de la Ciencia” Julia y Carmen, yo no he visto nunca doctoras tan pepinas y ecuanímes! A mis compañeros del Avempace Juan y Baza, y a las Kaxorras Andrea, María, Luzía, Lucy y Cartman, y a todos ellos que siempre están dispuestos a organizar vermouths cuando estoy en Zaragoza. A la Sede de UPyD, a la (Ru)Mancha y a Casa Germán por aguantarnos borrachos esos días.

A mi compañera y confidente de estancia sudafricana, Izaskun Sarasketa. Juntas creamos la simbiosis perfecta para sobrevivir a todos los contratiempos sudafricanos. Gracias por estar siempre ahí! Creo que sin ti no habría pisado la calle yo sola. Por nuestras nuestros días de laboratorio y nuestras noches de cerveza y Jagger en Kymberly Hotel.

Thanks to Johannes Krause for give the opportunity to stay in Jena during three months, the longest three months of my life. Also thanks to Stephan Schiffels and Choonwong Jeong to keep the office open to discuss new data. Thanks to all the technicians who always make easy to work in the lab, thanks for your patience. Thanks to all my colleagues of the SHH-MPI, my home the last two years and a half. Thanks for sharing with me a piece of your wisdom, for showing that Science is even stronger if is made in a team. Thanks for Flower Power nights, hiking and kayaking days, barbecues, Christmas markets and retreats. Gracias especialmente al padrísimo pinche coate de oficina y laboratorio, el chingón Rodrigo Barquera. Thanks to Ben Rohrlach for helping me with the popgen methods and the English. Thanks to my group of exotic Bavarian women (Maïté Rivollat, Kerttu Majander, Karen Giffin and Ayshin Ghalichi), the best Bollywood dancer Aditya Kumar, the best popgen teachers Marieke van de Loosdrecht and Cosimo Posth, the bioinformatic rescuers Thiseas Lamnidis and Stephen Clayton and my gym partner Ke Wang. Thanks to my sweet ‘Melkkühe vom Magdelstiege’ Rabia Yüksel, Jil Annabell Leonhardt, and Antonia Rausch, and my flatmate and colleague Erini Skourtanioti. Jena can be the warmest place with all of you despite the low temperatures. Gracias también a Iñigo Olalde por prestarme su ayuda desde el otro lado del océano. Gracias a Eva Fernández por su compañía en Jena.

Thanks to the external reviewers of my PhD thesis and the defense referees for taking their time in read the thesis.

Gracias a mis tres directores de tesis. Gracias mi directora Pilar Utrilla por confiar ciegamente en mi capacidad investigadora, y por darme todo su apoyo cuando creí que la investigación ya

no era para mí. Por buscar siempre lo mejor para mi carrera investigadora, sin importarle mi ausencia en el departamento por largas temporadas. Gracias por llegar tan alto manteniendo siempre una posición tan cercana a tus estudiantes.

Gracias a mi codirector Domingo Carlos Salazar-García por formar parte de esta dirección. Por su generosidad a la hora de dejarme incluir en esta tesis cualquier material que yo considerase importante. Por todos los buenos momentos en Sudáfrica, por salvarnos de nuestra primera noche de homeless en Capetown, por las cenas de chuletón en el Hussar Grill, las cervezas con margarita en el Mejicano (también en el de Jena) y en general, por toda su ayuda en Sudáfrica.

Thank to my codirector Wolfgang Haak. Thanks for supervising my official “three months research stay” and for giving me the opportunity to go back to Jena and being part of this wonderful scientific environment. Thanks for trusting in my capacity to learn and for being patient with my slow bioinformatic learning process and my English. Thanks for let me be part of your Iberian projects and extend my stay in Jena after this PhD. Thanks for let me know that if the scientific career fails, I still on time to turn into the weather forecast lady, just is needed to change the Magdalenian and Epigravettian technocomplex by sun, clouds and rain symbols!

Gracias a mi familia, a mis abuelos Pepo y Pilar, a mis tíos Merche y Fernando, a mi prima Sandra, a mi tato Fer, siempre dispuesto a insultarme incluso a miles de kilómetros de distancia. Especialmente gracias a mi madre, por comprender mi ausencia en muchos momentos en los que debería estar, por hacer todo lo posible para llegar hasta aquí. Gracias a Rafa, porque día tras día y chapa tras chapa consiguió convertirme en una friki de la Prehistoria y de la Arqueología. Gracias por ser un poco menos gañán y hacer el esfuerzo de conocer otros países. Gracias a Valentina, por no olvidarse de mí y mostrar su afecto con una carrera de más de cinco segundos cuando nos volvemos a ver después de una larga temporada. Para todos los que la conozcáis sabréis que esto implica mucho.

1 Table of Contents

2	ABSTRACT	15
3	INTRODUCTION	17
4	BACKGROUND	19
4.1	The Neolithic: Origins and Diffusion	19
4.1.1	Theories about the Neolithic diffusion	20
4.1.2	The origin of the Neolithic in the Iberian Peninsula and the Mesolithic substrate	21
4.1.3	Iberian Middle and Late Neolithic-Chalcolithic	28
4.2	DNA and the Neolithisation process	30
4.2.1	HG genetic substrate	30
4.2.2	The Genetic studies contribution to the knowledge of the Neolithic	31
4.2.3	Post-Neolithic genomic transformation	34
4.3	Isotopic studies to approach the Neolithic lifestyle	35
4.3.1	Stable isotopes and the study of the Neolithic subsistence patterns	35
4.3.2	Strontium isotopes and the study of the prehistoric mobility patterns	38
5	OBJECTIVES	41
6	ISOTOPES: PRINCIPLES	43
6.1	Isotopic fractionation	43
6.2	Mass spectrometers	44
6.3	Isotope analysis in archaeological remains: diet and mobility studies	45
6.3.1	Carbon and nitrogen isotopes: diet studies	45
6.3.2	Strontium isotopes: mobility studies	54
7	GENOMICS	61
7.1	History of genetics	61
7.2	Ancient DNA background	62
7.2.1	Characteristics of ancient DNA	64
7.2.2	Genomic advances	68
8	ISOTOPE METHODOLOGY	75
8.1	Carbon and Nitrogen isotopes procedures	75
8.1.1	Bone Preparation	76
8.1.2	Collagen extraction	76
8.1.3	Filtering and ultrafiltering	76
8.1.4	Freezing and lyophilisation	77
8.1.5	Collagen microweight and carbon and nitrogen isotope ratio measurements	77
8.1.6	Data analysis	78
8.2	Strontium isotope procedures	78
8.2.1	Enamel sample preparation for strontium isotope analysis	79
8.2.2	Digestion	80
8.2.3	Strontium separation chemistry by ion-exchange columns and preparation for analysis	80
8.2.4	Strontium isotope ratio measurements and quality controls	81
8.2.5	Data analysis	81
9	aDNA METHODOLOGY	83
9.1	Lab processing	83
9.1.1	Sampling and sample processing of ancient human remains	83
9.1.2	DNA extraction	84
9.1.3	Library preparation	85

9.1.4	Shotgun screening and in-solution enrichment of nuclear DNA (1240k capture) and mtDNA (mitocapture).....	89
9.2	Bioinformatic data processing.....	90
9.2.1	Read processing	90
9.2.2	Assessment of ancient DNA authenticity	90
9.2.3	Genotyping and merging with data set.....	93
9.3	Population genomic analysis.....	93
9.3.1	Clustering analysis.....	93
9.3.2	F-statistics.....	94
9.3.3	qpWave/qpAdm	99
9.3.4	Phenotypic traits	100
9.3.5	Mitochondrial and Y-chromosomal haplogroups.....	100
9.3.6	Kinship.....	101
10	RESULTS.....	105
10.1	Reconstruction of human subsistence and husbandry strategies from the Iberian Early Neolithic: A stable isotope approach	107
10.2	Territorial mobility and subsistence strategies during the Ebro Basin Late Neolithic-Chalcolithic: A multi-isotope approach from San Juan cave (Loarre, Spain).....	123
10.3	Stable isotope ratio analysis of bone collagen as indicator of different dietary habits and environmental conditions in Northeastern Iberia during the 4th and 3rd millennium cal BC....	138
10.4	Estudio de la movilidad de las comunidades de montaña durante el Calcolítico a través de isótopos de estroncio en esmalte humano: la cueva de los cristales (Sarsa de Surta, Huesca, España)156	
10.5	Use and reuse of funerary spaces. Strontium isotopes and bayesian radiocarbon modelling to approach Late Neolithic/Chalcolithic funerary behaviour in Northern Iberia.....	188
3. RESULTS	196
3.1 Radiocarbon analysis	196
<p>The two phases model (Pre-Fire and Post-Fire burial stages) showed a Model agreement index of 102% ($A_{\text{model}}=102.6\%$) (Figure 4 and Table S2). Individual agreement index was higher than 60% in all the samples and range between 111.7 to 74.8% (Table S2). In this case, boundaries estimated by the model are reflecting a burial use from 3810-3170 cal B.C. (Boundary Start, 95,4% of probability) to 2880-2570 (Boundary Fire, 95,4% of probability), which acts as a transition to the second phase which ends at 2562-2325 cal B.C. (Boundary End, 95,4% of probability). Table S2 show the unmodelled and modelled radiocarbon dates according to two phase bayesian modelling. Figure 4 shows the multiple plot for the two modelled phases and the summarized modelled radiocarbon dates of each phase using Kerner plot (Bronk Ramsey, 2017).....</p>		
3.2 Sr and provenance study	197
10.6	Survival of Late Pleistocene Hunter-gatherer ancestry in the Iberian Peninsula.....	225
11	DISCUSSION	255
11.1	Discussion of carbon and nitrogen isotopic results	255
11.1.1	Fish consumption abandonment during the Neolithic.....	255
11.1.2	Husbandry practices during Early Neolithic	258
11.1.3	Diet continuity or a methodological bias?	261
11.1.4	Environmental influence on isotopic values	262
11.2	Discussion of strontium results	267
11.2.1	Method accuracy to estimate the bioavailable Sr range.....	267
11.2.2	Archaeological discussion of strontium results.....	269
11.3	Archaeological discussion of aDNA results	274

11.3.1	El Mirón admixture.....	274
11.3.2	Aurignacian lineage survival in Magdalenian-associated individuals.....	275
11.3.3	Second arrival of Villabruna like-ancestry related to the Azilian technocomplex.....	275
11.3.4	Differences between Villabruna components in the Magdalenian, Azilian and Mesolithic individuals	278
11.3.5	The Last Iberian HGs Canes 1 and La Braña 1 and their Eastern HG ancestry.....	280
11.3.6	No African connections during Mesolithic times	281
11.3.7	The genetic legacy of hunter-gatherers in Iberian farmers.....	282
11.3.8	LBK and Cardial-related routes of the Neolithic expansion.....	284
12	CONCLUSIONS AND FUTURE PERSPECTIVES.....	287
13	BIBLIOGRAPHY	295
14	ANNEX	323

2 ABSTRACT

The transition from foraging to farming is one of the most drastic shifts visible in the archaeological record. In Europe, the so-called ‘Meso-Neolithic transition follows a chronological gradient from the origin in the Near East to Western Europe, following two main routes: the Danubian inland route and the Mediterranean route. In this sense, the Iberian Peninsula, located in the southwestern part of Europe is a key region to study the transition from foraging to farming in the most distant end of the expansion. Previous studies have pointed out that the previous local hunter-gatherers were genetically very distinct from the newly arriving farmers. Mitochondrial DNA analysis showed an almost complete replacement of the hunter-gatherer mitochondrial haplogroups at the beginning of the Neolithic. Analysis of autosomal genome-wide data confirms that most of the genetic ancestry of farmers is derived directly from Anatolian Neolithic groups with a limited admixture of hunter-gatherer ancestry along the routes of expansion.

In terms of subsistence, it is also possible to track a substantial change in the lifestyle of the first Neolithic communities in comparison with previous hunter-gatherer groups. The new food producing economy caused a decrease in dietary diversity. We observe a systematic abandonment/negligence/disregard of marine resources albeit a persistence of hunting, and usually combined with management of domestic livestock and crops. Farming also included a variety of husbandry strategies, such as feeding animals with special fodder or human waste products, the use of enclosures for animal keeping, transhumance and the use of natural fertilizers on crops. The analysis of stable isotope analysis (carbon and nitrogen) in bone collagen from faunal and human remains is the most common used technique to study the new farming strategies as well as human diet. In addition, strontium isotopes, which are able to provide insights about the provenance of individuals, can help to correlate dietary shifts in specific individuals, and are also useful to explore the demographic structure of a community.

The aim of this thesis is to study the impact of the Neolithic arrival to the Iberian Peninsula on autochthonous hunter-gatherers and their lifestyle and the evolution of the following Neolithic communities. Here, I applied the most advanced methods currently used in paleogenomic research, such as Next Generation Sequencing (NGS) and the capture of 1240K informative SNPs of the human genome. Thanks to these methods we have been able to recover genome-wide data from eleven individuals ranging from ~ 13000 cal BP to 5000 cal BP. Moreover, we have produced more than 200 carbon ($\delta^{13}\text{C}$) and nitrogen ($\delta^{15}\text{N}$) isotopic collagen values,

increasing considerably the dataset available for the Iberian Peninsula at this period, and even more so for the isotopic collagen data available on Early Neolithic fauna remains. In addition, we have generated the first big published data set of more than 80 strontium values ($^{87}\text{Sr}/^{86}\text{Sr}$) of human enamel and created a preliminary bioavailable strontium map of the Pre-Pyrenean landscape with more than 100 samples.

The genetic results showed a unique genetic structure in Iberian HG, resulting from admixture of individuals related to Goyet Q-2 (Magdalenians) and Villabruna (Western Hunter-Gatherers) genetic clusters. This suggests a survival of two lineages of Late Pleistocene ancestry in Holocene western Europe, in particular the Iberian Peninsula, whereas HG ancestry in most other regions was largely replaced by Villabruna-like ancestry. Traces of the dual hunter-gatherer lineages (Goyet Q-2 and Villabruna) were also found in Iberian Early Neolithic individuals, arguing for admixture with local Iberian hunter-gatherers. Early Neolithic individuals with higher amounts of Goyet Q-2 like ancestry were located in Southern Iberia, possibly reflecting the previous hunter-gatherer structure in that territory. During Middle Neolithic times this signal start to be more homogenized but the Iberian sites continued having a higher Goyet-2-like ancestry.

The results of the stable isotope analysis suggest a higher importance of animal husbandry than agriculture/crop farming/plant cultivation, although the domestic species studied did not show a special feeding signal compared to the wild ones. Besides, the large data set available now for humans from the Late Neolithic and the Chalcolithic period allows to test the presence of two different eco-geographic regions with statistics significance in isotopic values. The use of strontium isotopes with the radiocarbon dates has allowed us to distinguish different burial phases despite a common terrestrial diet.

3 INTRODUCTION

The main issue that this thesis aims to address is the impact that the Neolithic arrival to the Iberian Peninsula had on the autochthonous hunter-gatherer groups and their lifestyle. Previous theses defended in the ‘Departamento de Ciencias de la Antigüedad, Área de Prehistoria’ have focused on the same transitional time period albeit from different perspectives, such as environmental transformations ([Alcolea, 2017](#)) and the analysis of timing vs. cultural traits ([Laborda, 2018](#)). Following this line, the broader question has here specifically been addressed from a biomolecular point of view and focused on the analysis of human remains. The main biomolecular techniques performed in this thesis have been isotopic (carbon, nitrogen and strontium) and ancient DNA (aDNA) genomic analysis.

Carbon and Nitrogen stable isotopes have been performed with the aim to answer the impact that plant and animal husbandry had on the diet of the first farmer societies compared to the hunter-gatherer ones, and their potential transformation through time. Traditionally, the reconstruction of subsistence patterns was addressed by indirect evidences like the study of faunal and plant remains (e.g. [Castaños 2004](#); [Zapata et al. 2004](#)), and lithic assemblages and pottery styles recovered from the archaeological context (e.g. [Mazzucco and Gibaja 2018](#)). On the other hand, strontium isotope analysis has been performed to study the mobility of these societies, considered mostly sedentary during the Neolithic times. Along the archaeological record it is also possible to identify the presence of exotic objects which provides indirect evidences of individual mobility and cultural shifts (e.g. [García Sanjuán et al. 2013](#)). In this sense, aDNA is the main technical approach used to identify large population movements in the past (migration patterns) commonly associated with major cultural changes (e.g. [Haak et al. 2015](#); [Olalde et al. 2018](#)). This set of biomolecular techniques applied directly on human remains allows a direct and quantifiable analysis from which we are able to individualize the results in an individual, spatial and/or temporal scale, providing more accurate and reliable past reconstructions.

The Neolithic is the time period on which this thesis is focusing most. Nevertheless, to understand the transition and the evolution of the Neolithic it is necessary to explore backwards and forwards in time. This necessitated essentially the addition of other chronological periods, basically the Mesolithic and Chalcolithic, to the research plan of this Doctoral Thesis. A specific geographical delimitation of this thesis has not been possible because of the variety of techniques. Some of them, like aDNA analysis, require bigger sampling areas and time periods to cover the real genetic heterogeneity of the period studied and its changes over time. Unlike the isotopes, which do not allow the direct comparison among different territories or chronological periods. The individuals analyzed in this thesis were recovered from sites distributed along the Iberian Peninsula, although most of them coming from the North-eastern Iberia (where the isotope studies were focused on). Along the discussion chapter as well as in the published papers included in this thesis, the discussion of the data has been addressed from a Peninsular perspective. As mentioned before, in the case of the discussion of the isotopic results, sometimes it was mandatory to reduce the scale to smaller regions due to the environmental effect (see Chapter 9.1.4). On the contrary, in the discussion of the aDNA results, the discussion has a broader scale including also nearby countries.

This thesis was done in a compendium article modality and consist on four accepted articles with a thematic unity. Moreover, data from another article which is in the review processing form has been included in this manuscript. The thesis has been structured in four main blocks. The first one is the “Background” where is explained the archaeological background in the knowledge of the Neolithic and briefly their pre- and post- Neolithic societies focusing mainly on Iberia Peninsula, as well as an overview of isotope and aDNA techniques to approach the archaeological questions about this time period in the region. Secondly, I developed a chapter about “Isotope principles” in which I describe the technique: chemical description of isotopes, biogeochemical cycle of each one, methodological aspects and limitations. The third chapter is a homologous of the second one but describing “DNA principles”: the discovery of aDNA preservation in old biological samples, the characteristics of ancient DNA, and new advances in the field. The fourth is the “Article compendium”. Fifth is the “Discussion” of the articles in two main subchapters, one for isotopic analysis and the other for aDNA analysis and, finally, there is a “Conclusion and future perspectives” chapter.

4 BACKGROUND

4.1 The Neolithic: Origins and Diffusion

The so-called Neolithic revolution has been considered one of the most important outcomes in humankind. A vast number of studies from different disciplines suggest the Fertile Crescent as the place for the origin of the European Neolithic lifestyle. The transition to a more sedentary live-style seems to have its main explanation on the warmer weather condition at the end of the Pleistocene, during the Bølling/Allerød period (Shennan, 2018; Wright et al., 2003). The climatic amelioration made the habitat richer in resources, which resulted on a more sedentary lifestyle already present during the Natufian period, where first food storage and production has been attested around 12,000-13,000 cal BP (Arranz-Otaegui, et al., 2018; Bar-Yosef, 1983; Boyd, 2006; Valla, 1981).

The first clear evidences of Neolithisation (food producer societies) appear during the Early Holocene Levant PPNA (*Pre-Pottery Neolithic A*) in the Fertile Crescent, with plant domestication represented by wheat, barley, rye lentils and peas (Flannery 1973; Willcox et al., 2009) followed shortly after by animal domestication represented by goat and sheep firstly and cattle and pig later (Larson et al., 2007; Zeder, 2008). This change in the economy and lifestyle boosted the population size (Shennan, 2018) in that area and spread fast from the Levant to Western Anatolia and Cyprus, where the Neolithic arrives as a 'package' (Peltenburg et al., 2000). After that, the so-called Neolithic package, normally defined by an increase of material culture including first pottery and polished stone together with domestic plants and animals spreads towards the Balkans where it developed the Starčevo culture (Biagi and Spataro, 2005). It was there where the Neolithic started to accumulated cultural changes along the main two geographical routes. One of these groups followed the Danube river and resulted in the LBK ware culture (*Linearbandkeramik*), which eventually spread throughout Central Europe between 5500 and 4900 cal BC (Manning et al., 2014). The other group spread faster through Western Europe by the Mediterranean coast and led to the *Impressa* (between 5800 and 5400

cal BC) and Cardial ware cultures (between 5500 and 4900 cal BC) (Binder and S  n  part, 2010).

4.1.1 Theories about the Neolithic diffusion

Probably the main debate about the transition from foraging and gathering to farming and herding is the way in which it happened. Conceptually, there are two extreme models to explain the spread of early farming:

- *Cultural Diffusion* where farming, animal husbandry and the technological changes that conform the Neolithic package were transmitted within Europe from one group to the next one without people displacement. The model assumed that the Hunter Gatherers (HG) in Europe adopted the new technology and husbandry strategies from Early Farmers from the Near East, without none or negligible admixture between both groups (Tilley, 1994; Whittle, 1996).
- *Demic Diffusion* where the human displacement was the major source of Neolithic spread. This migration hypothesis was firstly proposed by Gordon Childe and his Theory of the Oasis (Childe 2013) where he noticed a space-temporal spread of pottery from Levant into Europe. Later, Childe also proposed that this population movement was driven by demographic pressure (Childe 1964). Finally, Ammerman and Cavalli-Sforza (Ammerman, 1973; Ammerman and Cavalli-Sforza, 1971) introduced the *Wave of advance* model. They also noticed that both models *Cultural* and *Demic diffusion* are not mutually exclusive and some of them could play different roles in different territories (Ammerman and Cavalli-Sforza, 2014).

Nowadays, we know that Neolithic expansion was a more complicated process which involved not only the mobility of people, but also domestic species and ideas. Researchers from different disciplines give more support to the *Demic model* (e.g Brandt et al. 2015; Isern et al. 2017; Lemmen et al. 2011; Zeder 2008). On the other hand, the migration process did not have to affect equally different parts of Europe, and HG could play a role in the acculturation process of some territories. Moreover, the differences in time of Neolithic arrival could also influence the potential relation with the local Hunter-Gatherers. This intermediate model is known as

Dual Model and suggest that population substitution and acculturation process were part of the Europe Neolithisation (e.g [Juan-Cabanilles and Martí Oliver 2017](#); [Sampietro et al. 2007](#)).

4.1.2 The origin of the Neolithic in the Iberian Peninsula and the Mesolithic substrate

The Mediterranean expansion route represented by *Impressa* and Cardial ware spread faster than the central Europe route represented by the LBK and seems to reach the Iberian Peninsula first ([Zilhão, 2001](#)) (**Figure 1**). This differences in Neolithic times arrival could have an influence in the potential relation with the local Hunter-Gatherers. In Iberia, we can distinguish three main chrono-cultural contexts during the Early Neolithic: Pre-Cardial phase which is only restricted to the Mediterranean façade ([Bernabeu et al., 2009; 2011](#)); the Cardial ware commonly spread in Mediterranean and South-Atlantic coastal areas ([Martins et al., 2015](#)); and the so-called Epicardial ware, the latest but the most extended Early Neolithic assemblage ([Rojo-Guerra et al. 2006](#)). Additionally, in Andalucia there is a specific Early Neolithic group represented by the characteristic style of the Almagra ware ([García Borja et al. 2014](#); [Pellicer Catalán and Acosta Martínez 1997](#)).

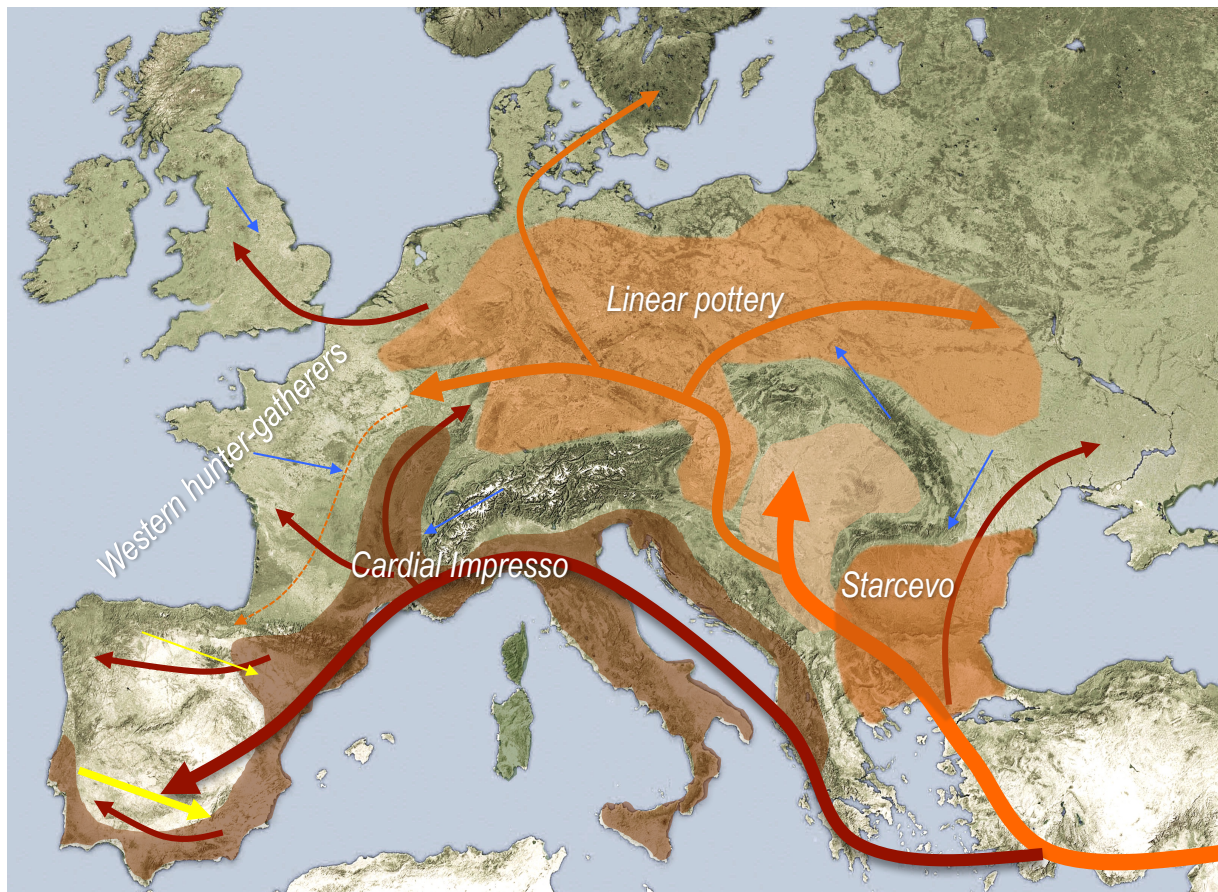


Figure 1: European map with the Early Neolithic expansion from Western Anatolia into Europe, following two main routes: the LBK ware-related group and the Impresso-Cardial ware-related group. Map adapted from [Haak et al. 2015](#)

In this chapter, we will describe the main characteristics of all these Early Neolithic groups and the archaeological context about the previous Hunter Gatherers groups located in the same areas.

4.1.2.1 Pre-Cardial phase: Impressa horizon (5800 to 5500 cal BC)

The *Impressa* ware spreads from the West of the Balkan and Italian Peninsulas to France (Provence and Languedoc) around 5900 cal BC. It is in Italy and Southwestern France where most of the sites associated with *Impressa* ware are concentrated ([Binder and Sénépart 2010](#); [Guilaine and Manen 2007](#)). This pre-cardial phase probably arrives up to the Iberian Peninsula from France at 5600 cal BC ([Bernabeu et al., 2009, 2011](#); [Binder and Sénépart, 2010](#)). The *Impressa* ware is very diverse but nevertheless, the most common characteristic decoration is composed by the so-called *sillon d'impression* and vertical cardial impressions ([Manen, 2007](#)). Only some vestiges of pottery recovered from Iberian sites like Mas d'Is, El Barranquet and Cova d'en Pardo (all located in Alicante), are potentially attributed to the *Impressa* ware. For

all those site, the radiocarbon dates were older than 5500 BC (Bernabeu et al., 2009, 2011) (Figure 2). It is possible that other sites with old radiocarbon dates as Guixeres de Vilobí or El Cavet with radiocarbon dates around 5,600 cal BC (Martins et al., 2015) had some *Impressa*-like influences but not as clearly detectable due to the heterogeneity of the *Impressa* group (Manen, 2007) (Figure 2).

The register of the Pre-Cardial phase is very scarce for the moment and their potential relation with local HG is still unknown. Based on the oldest radiocarbon dates for Iberian Pre-Cardial groups, it is still not possible to confirm the direct contact with the local Geometric Mesolithic groups. But, in Southern France (Languedoc) where the *Impressa* groups and their chronology is very-well-known, the temporal hiatus is shorter, with the last Castelnovian Mesolithic ranging between 6300-5600 cal BC (Perrin and Defranould, 2016) and first *Impressa* around 5500 cal BC (Perrin and Binder, 2011; Perrin et al., 2018).



Figure 2: Pottery fragments with potential Impressa decoration technique from Barranquet and Mas d'Is sites, Alicante (Spain). Picture taken from Bernabeu et al., 2011.

4.1.2.2 The Cardial world (5500 to 4900 cal BC)

Cardial was defined by the sequence found in Arene Candide in Savona (Liguria, Italy) (Brea, 1949). This phenomenon spreads homogeneously in Iberia (Martins et al., 2015), Southwestern France (Perrin et al., 2018) and Northern Africa (Manen, 2007) from 5600 to 4900 cal BC. Cardial phenomenon appear more or less at the same time in all these territories, which would

be compatible with a maritime pioneering colonization via leap-frop sailing (Isern et al., 2017; Zilhão, 2001) (Figure 1). Nevertheless, most of the oldest radiocarbon dates associated to Cardial vestiges appear in Iberia (including Portugal) (Davis and Simões, 2016; Martins et al., 2015). This has been interpreted the Cardial as the evolution of the *Impressa* ware with reflux into France (Guilaine, 2018).

Cardial vestiges are located in open-air-settlements, rock shelters and cave sites but always link to coastal, estuarine or big basin river areas, with a lesser impact on inland ones. Inside Iberia, most of the Early Neolithic sites with Cardial pottery are distributed along the Mediterranean coastline (Oms, 2017) and the half-south of the Atlantic coastline (Carvalho, 2011) (Figure 3). The Ebro Valley is the best well-known natural corridor where the Cardial ware was spread from coastal to inland Peninsula (Laborda, 2018). There is a gradient along the corridor, with older and high-density number of Cardial sites in the Middle Ebro Valley (Baldellou 2011; Laborda 2018; Villalba-Mouco et al. 2018) than in the Upper Ebro Valley, where the Cardial ware is very scarce (Fernández Eraso et al. 1997; Rojo-Guerra et al. 2018) (Figure 1).

The potential relation of first Cardial groups with the local HG seems to be not well supported based on the radiocarbon dates in the Mediterranean areas. This chronological gap is even higher in the area of Catalonia, where there is a chrono-cultural hiatus between the Notch and Denticulate Mesolithic groups (7000-6500 cal BC) and the first Cardial ware groups (5500 cal BC), with the absence of Geometric Mesolithic. This chronological gap matches with the 8.2 K climatic event (8200 cal BP) and is also observed in the lower-southern Ebro Basin (González-Sampériz et al., 2009). Meanwhile, in more southern Mediterranean areas and the rest of the Ebro Valley this gap does not exist and the presence of Geometric Mesolithic has been attested between 6200 and 5900 cal BC (García-Puchol et al. 2018; García-Puchol et al. 2017). Despite the chronological information still showing a gap between the Geometric Mesolithic (6200-5900 cal BC) and the oldest pottery evidences (5600 cal BC) (Bernabeu et al., 2009), the enduring of Geometric traditions in the first Early Neolithic groups point out possible contact in an unknown area.

Exceptionally, the Late Mesolithic Muge and Sado shell midden sites located in the Tagus estuary (Portugal) were occupied for a longer period: from 6100 to 5600 cal BC in Moita do Sebastião and from 6200 to 5500 cal BC in Cabeço da Arruda (Zilhao, 1993). These Late Mesolithic sites have been interpreted as complex HG groups due to the evidences of some

cultural characteristics that suggest permanence at the site, like the presence of post holes associated with hut building and big burial spaces (Jackes and Alvim, 1999). These features have been interpreted as a systematic occupation of the estuarine areas, which is also reflected in the shell midden conformations. Their latest radiocarbon dates are similar to the first Cardial sites in the area (Davis and Simões, 2016), pointing out this region as a possible contact area.



Figure 3: Cardial ware from the Early Neolithic sites Cova de l'Or and Cova de les Cendres (Alicante). Picture taken from [García Borja 2017](#).

4.1.2.3 Epi-Cardial assemblage (5460 to 4800 cal BC)

The so-called Epicardial assemblage corresponds with an aggregate of decorative techniques dated between 5460-4800 cal BC despite the highest density of sites dating between 5300 and 4800 cal BC (Laborda, 2018; Oms, 2017) (Figure 4). Stratigraphically it was defined as a new Early Neolithic phase after the Cardial horizon but nowadays, is also defined in sites where the Cardial phase is absent (Rojo-Guerra et al. 2006). Inside these extensive sets of decorative

techniques which involved the epicardial assemblage, some are already present in the Cardial ware and others as the *Boquique* are exclusive but not always present (Laborda, 2018).

Despite their presence in Catalonia, Portugal, Cantabria and Andalucía (closer to coastal areas), the two big clusters of Epicardial sites are located in the Central Plateau (e.g. Rodilla, Fuente Celada, Pancorbo, La Lámpara, etc.) and the Prepyrenean area (e.g. Trocs, Olvena, Torrollón, Colomera, etc.) (Rojo-Guerra et al. 2013, 2018; Laborda 2018; Oms et al. 2013). In this last area where the 'Epicardial' coexist with a Late Cardial phase around 5200 cal BC. Moreover, Cueva de Chaves located in the Middle Ebro Valley, represents the only example where Cardial and *Boquique* have been found together (level Ia), pointing out a possible coexistence of both or the presence of intrusive elements inside the archaeological level (Utrilla and Laborda 2018). The areas where the Neolithic arrived with certain delay, like North or Northwest of Iberia (5000 cal BC), only the incised-impressed group has been attested (Arias, 2007) (Figure 4).

The densest Mesolithic area where the Epicardial assemblage is settled down later is the Cantabrian region. By the fifth millennium cal BC, in this region it is possible to distinguish between fully Neolithic sites with evidences of farming and others without disruption in the economic patterns since the Mesolithic (Arias, 2007). These two kind of sites can be related to the presence of Neolithic and HG populations at the same time in the same area, but also with the different function of each site (Barandiarán and Cava 2000). Moreover, despite the Early Neolithic starting later in the Cantabrian region than in the Upper Ebro Valley, the Cantabrian Mesolithic groups could have some connections with the Mediterranean Early Neolithic groups, possibly via the Ebro Valley (Arias, 2007).

During the end of the sixth millennium cal BC, Geometric Mesolithic from the Upper Ebro Valley present diverse characteristics that have been suggested as a sign of acculturation process: 1) the presence of *Columbella rustica* from the Mediterranean sea in sites (Álvarez-Fernández, 2011), 2) the presence of Late Mesolithic and Early Neolithic levels recorded in the same site (Cava 1994) or; 3) the endure of the geometric lithic technology traditions since the Mesolithic in the Upper Ebro Valley and Neolithic groups located close to the Mediterranean coastline (Montes et al. 2016).

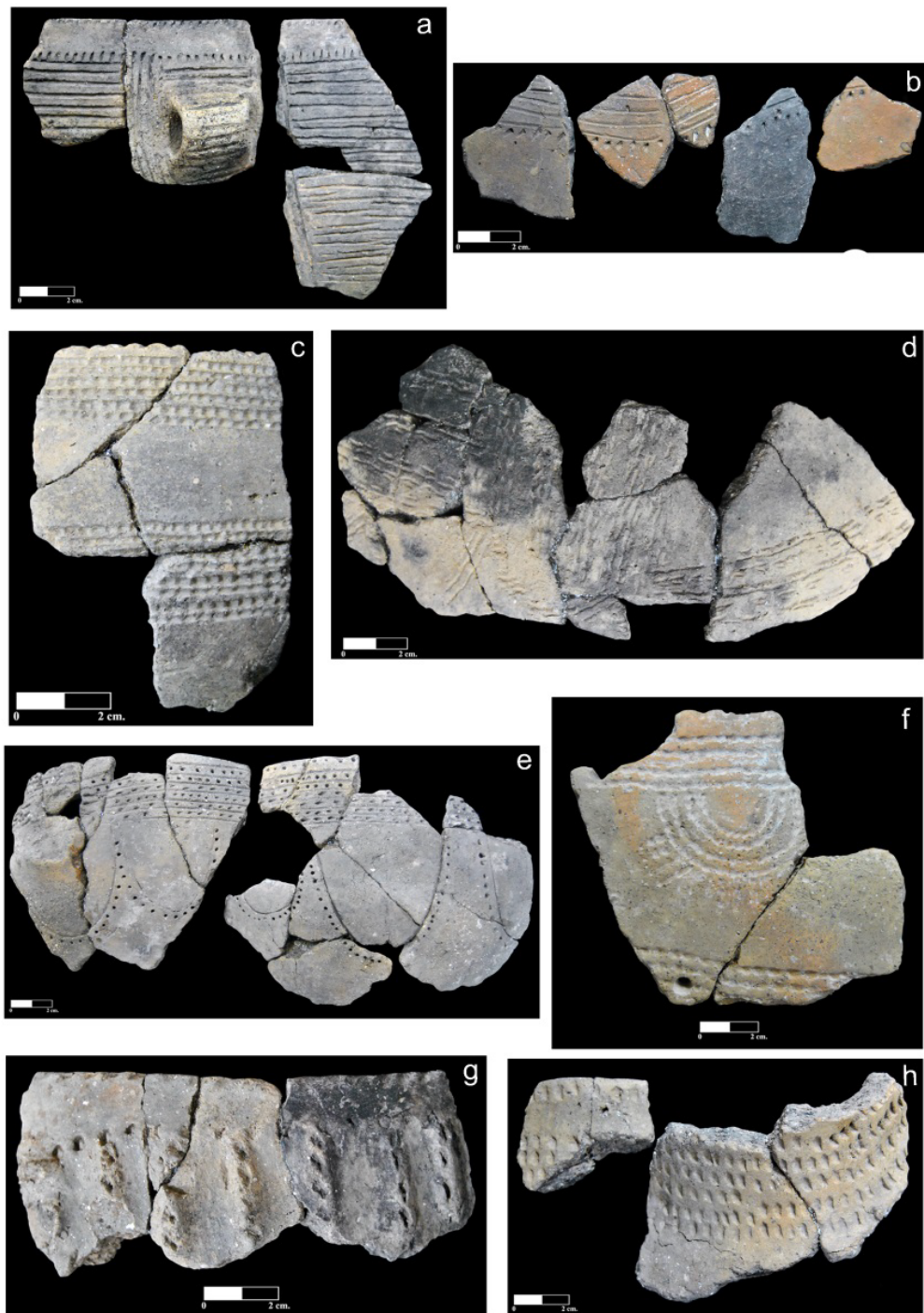


Figure 4: Epi-Cardial ware with incised and impressed techniques from Cova de Els Trocs (Rojo-Guerra et al., 2013).

In the North Central Plateau, the information about the previous Mesolithic groups is very scarce, and the Neolithic arrival has been interpreted as the colonization of an empty territory (Delibes and Manzano 2000). This situation contrasts with what was proposed for the French territory, where the presence of the Epicardial has been interpreted as the acculturation process of the local HG (Van Willigen, 2004). Other authors infer some parallels between ‘Epicardial’ assemblage and the LBK-like ware in Southern France (Guilaine and Manen, 1995; van

Willigen, 2018). In Galicia and Northern Portugal preservation problems due to the acidity of the soils and coastal transgression invalidates the possibility of having a well-documented radiocarbon data set for Mesolithic and Neolithic periods (Arias, 2007).

4.1.2.4 Almagra ware in Andalucía (5420 to 4750 cal BC)

The Almagra or “Cultura de Cuevas” ware group is located in Southern Iberia and is represented by a specific pottery with ovoid shape, conical bottom and red ochre over the surface or just filling the impressed decoration patterns (García-Borja et al. 2014; Martín-Socas et al. 2018). Most of the sites where the Almagra ware was recovered are cave sites with some exceptions in the Guadalquivir basin (Gavilán and Escacena 2009). This group is recorded from 5420 to 4750 cal BC, with a higher density between 5300 and 4800 cal BP, and shows different decorations patterns and manufacture techniques (García-Borja et al. 2014) (Figure 5). The presence of a characteristic residual cardial decoration make some researchers to propose an *Impressa*-like origin. The penetration route could have been the same as the other *Impressa* sites located in Alicante (Bernabeu et al., 2009), but with a high number of stylistic mutations due to a fast spread or it was introduced via Africa by *Impressa* groups from Southern Italy (García-Borja et al. 2014) (Figure 5).

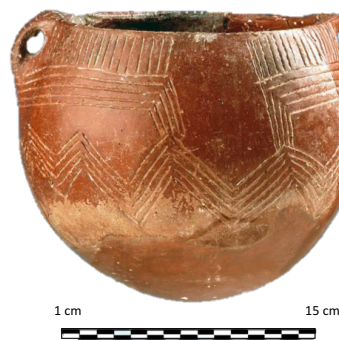


Figure 5: Almagra ware recovered from Cueva de los Murciélagos de Zuheros (Córdoba). Picture taken from [Valdiosera et al., 2018](#).

4.1.3 Iberian Middle and Late Neolithic-Chalcolithic

The Middle Neolithic archaeological remains are very scarce in Iberia, and they present a clear bias depending on the geographical area. One of the exceptions is the *Sepulcros de Fosa* culture, very well studied and restricted to the Northeast of Iberia, covering Catalonia (Muñoz 1965) and Lower Ebro Valley in Aragón (Royo, 1987). It is also possible to find Middle Neolithic

first collective burials (Salazar-García et al., 2016), megalithic burials in the Central Plateau (Rojo-Guerra et al. 2015) or cave sites in the Atlantic or Mediterranean regions (Silva 2003; Zilhão and Real 1984) which use is prolonged in time up to the Chalcolithic.

The Chalcolithic period is traditionally defined by the emergence of copper elements and the develop of big settlements, sometimes associated with defensive-style architecture (Esquivel & Navas, 2007). This last characteristic only seems to appear clearly in the southern of the Iberian Peninsula, with the denominated Millares Culture (e.g. Sanjuán 2013; Valera et al. 2014). In the rest of the Iberian Peninsula, the Late Neolithic-Chalcolithic transition is scarcely defined. In fact, it is possible that this transition does not even strictly exist and rather results from the evolution of villages present in the most advanced phases of the Neolithic (e.g. Blasco et al. 2007). This continuity is also perceptible in most of the sepulchral caves and megalithic structures over time, where radiocarbon dates show a continued use from the 4th to the 3rd millennium cal B.C. (e.g Fernández-Crespo 2016; Utrilla et al 2015). Moreover, it is possible to find some copper materials normally associated with burial contexts as prestigious grave goods (Blasco and Ríos, 2010), but not as evidence of a massive replacement of commonly used tools such as flint blades, bone industry, polished stones or pottery without singular characteristics from a unique period (Pérez-Romero et al., 2017). In this context, except for the copper elements which are not always present, the Late Neolithic-Chalcolithic transition cannot be clearly delimited. Moreover, the archaeological evidence of Late Neolithic- Chalcolithic settlements from the upper half part of the Iberian Peninsula is very scarce. In this upper-half there are only examples of Chalcolithic villages in the north central plateau (e.g. Delibes et al. 1995 and Díaz-Andreu et al. 1992). The causes for this absence are probably erosive episodes and modern agrarian works that affected the conservation of the sites (Montes and Domingo 2014). As a result, the knowledge about this Late Neolithic-Chalcolithic period on great parts of Iberia is basically based on burial structures (e.g. Andrés 1998), anthropological studies and molecular studies on human remains (e.g. Alt et al. 2016; Guixé 2011; Salazar García 2011; Szécsényi-Nagy et al. 2017).

Only Bell-Beaker ware, always associated to burials and some domestic contexts, could be consistently identified as a new component, although it seems to appear when the villages defined as Chalcolithic had already been settled (Blasco et al., 2007). The origin of this European phenomenon is still debated.

4.2 DNA and the Neolithisation process

4.2.1 HG genetic substrate

The Last Glacial Maximum (LGM) played an important role in the dispersal of Pleistocene HG and it has been proposed as the main cause of a genetic bottleneck represented by the loss of mtDNA M haplogroup in Europe (Posth et al., 2016). Probably, the southern latitudes were less affected by this climatic shift and they became into *refugia* (Stewart and Stringer, 2012). By this way, Iberian Peninsula formed a European periglacial *refugium* for HG and thus served as a potential source for the re-peopling of Northern latitudes shortly after (Fu et al., 2016). The post-LGM genetic signature in Western and Central Europe was dominated by ancestry similar to individuals from the ‘Villabruna’ cluster, commonly described as Western Hunter Gatherer (WHG) ancestry (Fu et al., 2016) and largely represented by Epi-Paleolithic and Mesolithic cultures. Villabruna Cluster conformed a cline from Western HG (WHG) to Eastern HG (EHG), which replaced earlier genetic clusters, such as those characterized by *El Mirón*- and *Věstonice*-like ancestry, which are associated with the Magdalenian and Gravettian cultures in central and western Europe, respectively (Fu et al., 2016) (Figure 6). However, given the wide geographic spread of individuals attributed to the *Villabruna* cluster, it remains unclear where this cluster had originated.

The Holocene Iberian HG were attributed to Villabruna cluster: La Braña 1 in Castilla y León (Mathieson et al., 2015; Olalde et al., 2014) and Canes 1 in Asturias (González-Forbes et al., 2017). The other Holocene HG reported was Chan in Galicia (González-Forbes et al., 2017), noting that the individual differed from the predominant WHG ancestry profile without exploring this observation further (Figure 6).

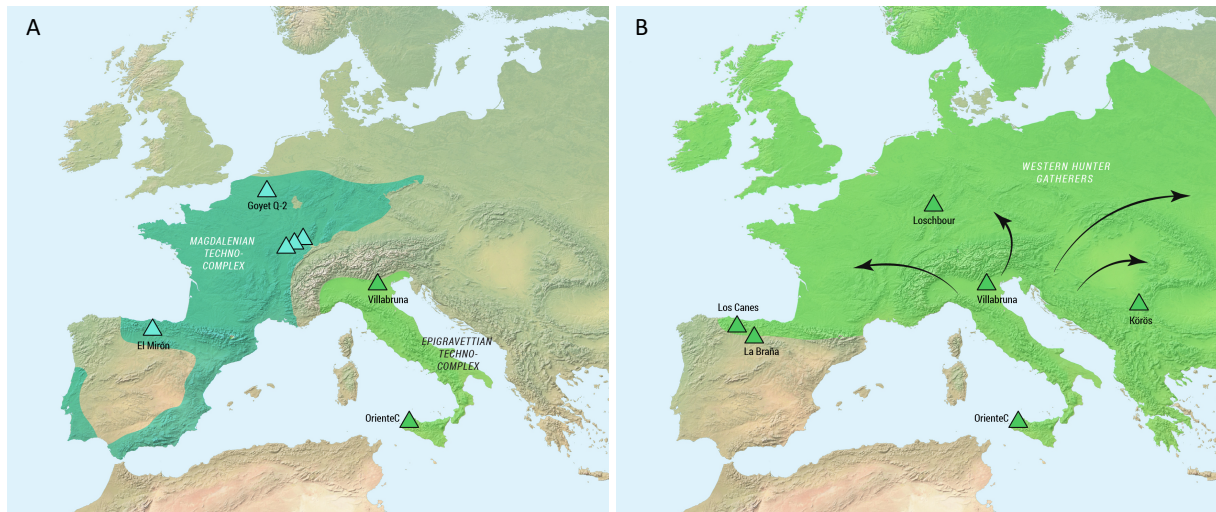


Figure 6: A) Genetic landscape in Europe after LGM; B) Genetic landscape in Europe between 14,000 and 7,000 cal BP.

In this thesis, we include new Iberian HG to understand better the HG genetic ancestry of Southwestern Europe study on how was the replacement of Magdalenian-related ancestry (represented in Iberia by El Mirón individual) by the broadly spread WHGs.

4.2.2 The Genetic studies contribution to the knowledge of the Neolithic

Genetics shows the strongest evidence to distinguish between migration or acculturation processes. This discipline fully supports the hypothesis of a main demic diffusion of Near Eastern early farmers with certain degree of admixture among different local groups of HG along the expansion routes (Haak et al., 2015; Lazaridis et al., 2016; Lipson et al., 2017).

Uniparental markers (mtDNA and Y chromosome), transmitted by maternal or parental line generation by generation, have been used to track population discontinuities. mtDNA showed the introduction of new mitochondrial haplogroups which were absent before the Neolithic arrival in Europe: K, J, W, X, H, HV, V, T2 and N1a (Brandt et al. 2015; Haak et al. 2005; Gamba et al. 2011). We also see the introduction of G2a, J2, E3b and F* Y-haplogroups at the same time (Brandt et al., 2015), suggesting that the expansion of the Neolithic was driven by both sexes (Figure 7).

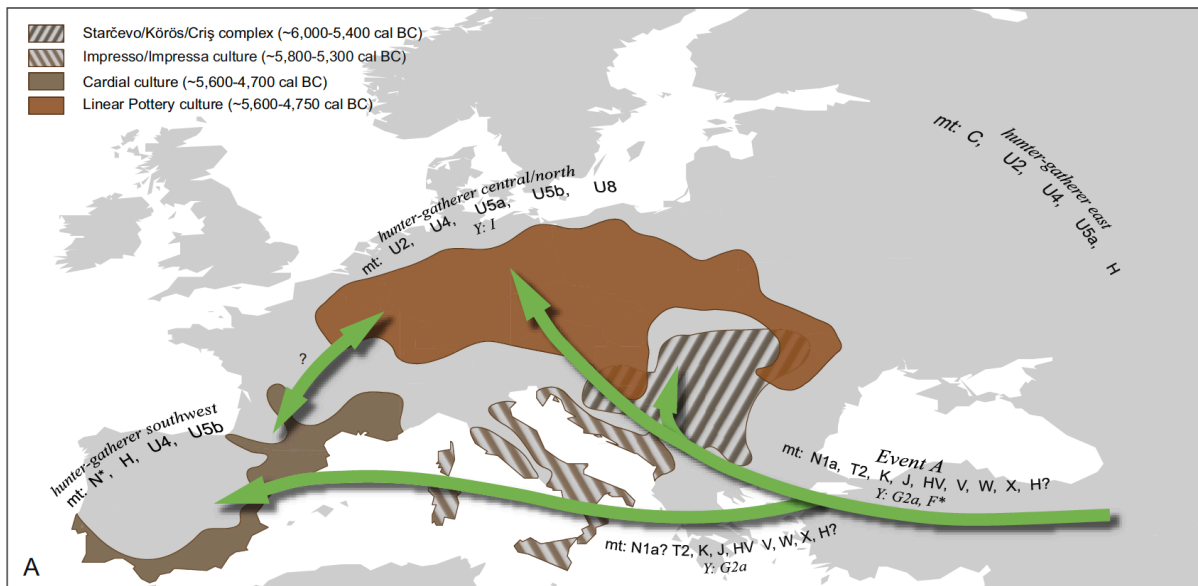


Figure 7: Distributions of mitochondrial and Y-Chromosome haplogroups during the Neolithic, following (Brandt et al., 2015).

Nowadays, this evidence is much stronger with the genome-wide aDNA analysis, where we apply the capture of more than one million of autosomal markers inherited by each progenitor (see chapter 5). The genomic data also shows this incoming signal from Anatolian Neolithic groups into Europe, almost replacing the previous Hunter-Gatherer genetic component (Haak et al., 2015; Mathieson et al., 2015). That has been interpreted as a big population replacement with only a small introgression of the Hunter-Gatherer ancestry in the new incoming farmer genomes related to Anatolia Neolithic. This trait can be observed using principal component analysis (PCA). This method, which allows assessing the genetic affinities qualitatively, shows Neolithic individuals spread along a cline from Anatolian Neolithic to WHG (Haak et al., 2015). Concretely, we can observe that Early Neolithic and Central Europe populations like LBK are closer to Anatolia Neolithic than Early Neolithic from Western Europe like Cardial or Middle Neolithic populations that are closer to WHG, but never overlapping with them because they have different genetic ancestries. Formal statistics also show that all the Neolithic individuals from Europe conform a clade with Anatolia Neolithic using the test $f_4(HG, \text{Anatolia } N; \text{test population}; Mbuti)$, highlighting that all the Neolithic individuals shared more genetic ancestry with Anatolia Neolithic (the majority component) than with any HG. But, using *ADMIXTURE* or *qpAdm* models (see chapter 7), we prove that the individuals are distributed along the cline observed on PCA based on their HG ancestry proportion (Haak et al., 2015) which increase along the time (higher HG ancestry in Middle Neolithic than Early Neolithic) and distance from

Anatolia (higher HG ancestry in Cardial than LBK), suggesting an increase of admixture along the Neolithic expansion (**Figure 8**).

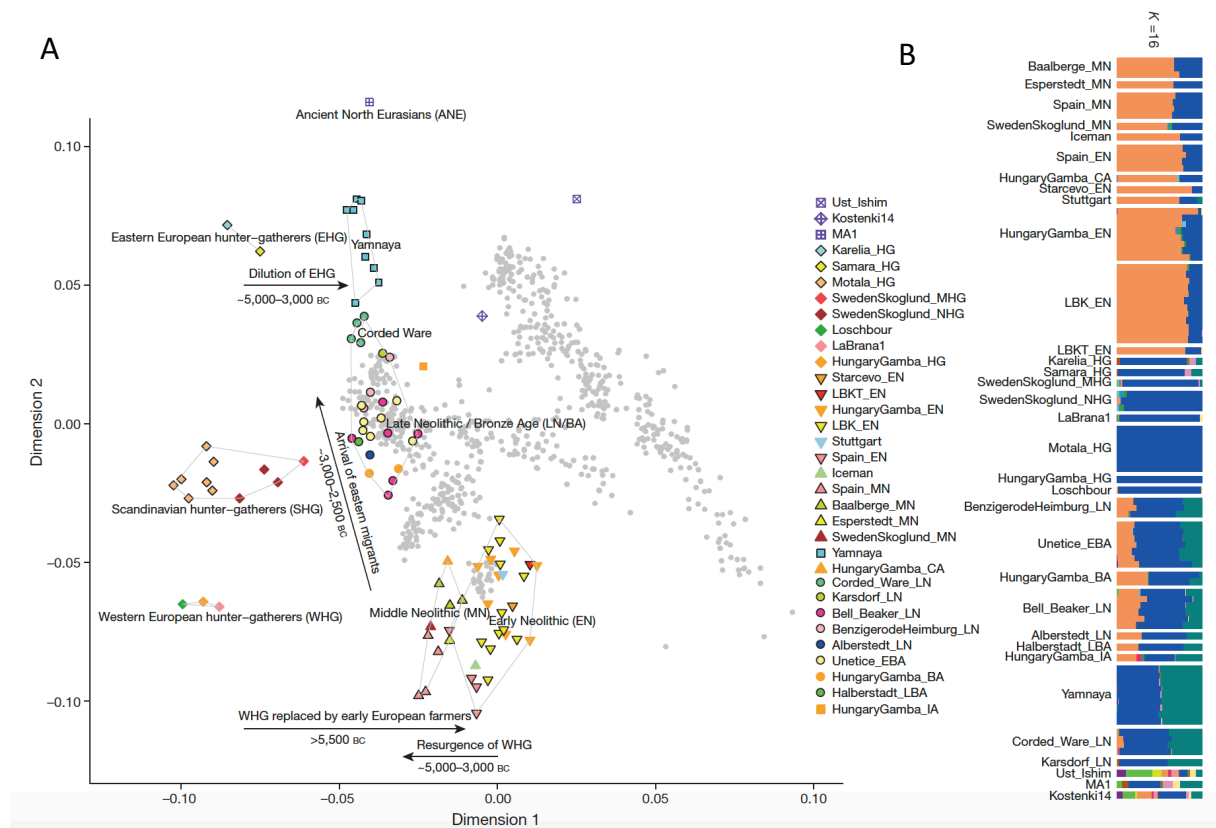


Figure 8: HG resurgence in Middle Neolithic populations showed from PCA (A) and ADMIXTURE (B) analysis from [Haak et al. 2015](#).

There are also some exceptions where a full genetic HG were found in Early Neolithic context like in Kőros (Hungary) ([Gamba et al., 2014](#)), or mixed individuals with 50% of HG and Anatolia ancestries, like in Lepenski Vir Early Neolithic site, which suggest a first generation admixture among hunter-gatherers and incoming farmers ([Hofmanová et al., 2016](#)). There are also examples of full HG ancestry survival in an unadmixed way in Germany during the Middle Neolithic in the Blätterhole site, or with percentages un to around 70% of HG ancestry in the same site ([Lipson et al., 2017](#)).

The relatively fast expansion of Early Neolithic individuals associated with farming practises from Western Anatolia into Europe resulted in a relatively low genetic variability in the reported Neolithic genomes. This lack of genetic differentiation makes it difficult to distinguish between the Mediterranean and Danubian expansion routes of Neolithic lifeways postulated by the archaeological record ([Binder and Sénépart, 2010](#); [Manning et al., 2014](#)). In Iberia, the

percentage of HG ancestry has been estimated around 10% (Haak et al., 2015; Mathieson et al., 2015; Olalde et al., 2015). The first Early Neolithic (EN) genome from Cova Bonica suggested that individual CB13 received either all or the majority of their HG ancestry *en route* from Western Anatolia to Iberia (Olalde et al., 2015). But, increasing the number of HG and EN individuals analysed across Europe, a strong correlation between HG ancestries in the Farmer genomes and geography has been observed, pointing out the presence of different admixture events along the expansion routes (Lipson et al., 2017). This means that, the HG ancestry from the Early Farmers from Western Europe is more similar to the WHG from Western Europe too. Moreover, the HG ancestry of Iberian Neolithic groups have been used to trace the movement of Middle Neolithic groups from Southwestern Europe to Britain along the Atlantic Coast (Olalde et al., 2018). This movement corresponds well with the Megalithic burial practices of these regions observed in the archaeological record (Masset, 1993; Sherratt, 1995).

4.2.3 Post-Neolithic genomic transformation

During the Middle Neolithic and Copper Age we find a resurgence of HG ancestry in the whole of Europe (Haak et al., 2015; Lipson et al., 2017) and specially in the Iberian Peninsula; the resurgence of HG ancestry could be driven by the incorporation of male HGs to the Neolithic groups (Mathieson et al., 2018) (**Figure 8**). Moreover, it is during the Copper Age when we start to see some sporadic African gene flow in both sides of the Mediterranean, Iberia and North Africa (Fregel et al., 2018; Olalde et al., 2019) not already attested before. At the same time in the Russian steppe, the Yamnaya herders had a completely different genomic makeup as the result of the admixture of Caucasus/Iran Neolithic and Eastern HGs, known as steppe ancestry (Haak et al., 2015). This ancestry almost replaces the Anatolian-like-ancestry present in LBK individuals during the Late Neolithic Corded Ware (Haak et al., 2015). This phenomenon is spread fast from Central Europe to Britain (Olalde et al., 2018) and shortly after to Iberia (Martiniano et al., 2017; Valdiosera et al., 2018) with a clear male biased represented by R1b Y-haplogroup and associated to the Bell Beaker phenomenon (Allentoft et al., 2015; Haak et al., 2015; Olalde et al., 2018). The directionality of the phenomenon or the source/s of expansion is still unclear. In Iberia, the first traced steppe ancestry appeared in some Bell Beakers burials from the Central Plateau, but is broadly spread to the whole Peninsula during the Bronze Age (Olalde et al., 2019) (**Figure 9**).

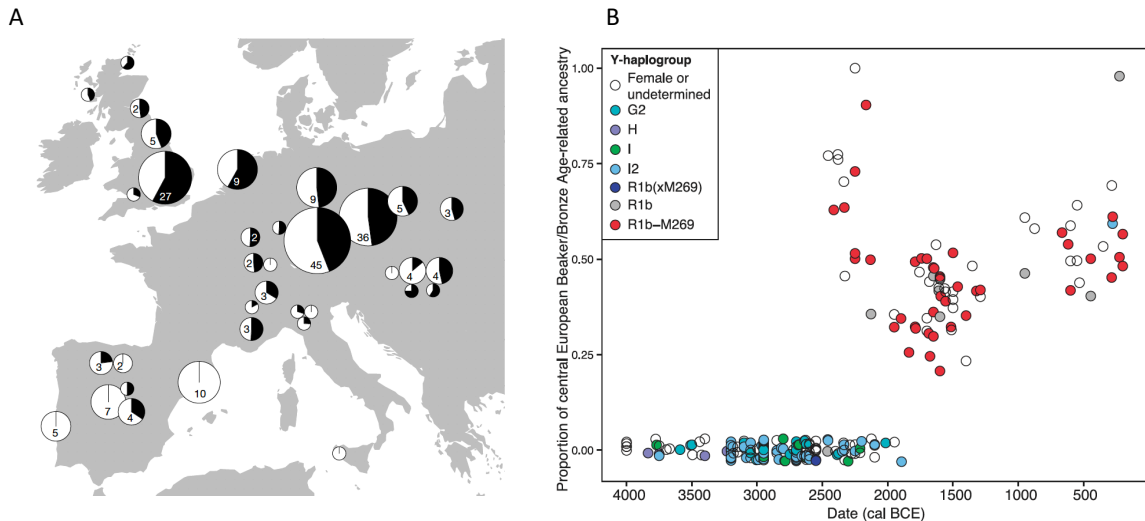


Figure 9: **A)** proportion of Steppe ancestry (in black) in the Bell Beaker-associated groups estimated with qpAdm with the model Steppe + Anatolia N + WHG (Olalde et al. 2018). **B)** proportion of Steppe ancestry from Beaker/Bronze Age from Central Europe in Iberian populations estimated with qpAdm (Olalde et al. 2019).

4.3 Isotopic studies to approach the Neolithic lifestyle

4.3.1 Stable isotopes and the study of the Neolithic subsistence patterns

One of the major topics of the Neolithic research is the impact of farming in subsistence patterns, as well as the study of dietary changes between Hunter Gatherers and Farmers (Schulting 2015). There are different biomolecular techniques to approach this question but maybe the most common extended way is the application of stable isotope analysis. The use of carbon ($\delta^{13}\text{C}$) and nitrogen ($\delta^{15}\text{N}$) stable isotope ratios from bone collagen gives a quantitative assessment of protein consumption (Lee-Thorp, 2008; Makarewicz and Sealy, 2015). This quantitative dietary approach has been useful in establishing subsistence patterns of first farmers, the socio-economic impact of farming, and animal and plant management practises at the time (e.g., Balasse et al. 2014, 2016; Cabal 2005; Lillie and Richards 2000; Lubell et al. 1994; Navarrete et al. 2017; Schulting 1998).

The $\delta^{13}\text{C}$ measurement is suitable to distinguish between protein from marine and terrestrial resources (Schoeninger and DeNiro, 1984). A full marine diet has been estimated in a $\delta^{13}\text{C}$ value of $\sim 12\text{‰}$ in contrast to a full terrestrial diet which usually shows $\sim 20\text{‰}$ very broadly (Richards and Hedges, 2003) (Figure 10). This information is very important in the coastal areas where we see a shift in the consumption from marine to terrestrial resources during the

Mesolithic-Neolithic so-called transition (Tauber, 1981; 1986). In Europe in general we appreciate a higher consumption of marine resources by hunter gatherers in the Atlantic (Schulting 2015) than in the Mediterranean (Mannino et al., 2011, 2012). In Iberia, the Mediterranean Mesolithic (García-Guixé et al. 2006; Salazar-García et al. 2014) show less marine or estuarine resources than the Atlantic Mesolithic (Arias 2005; Lubell et al. 1994) (Figure 11). But, during the Neolithic period there is a common abandonment of the marine resources in both areas, with few or no contribution (Watterman, 2012; Salazar-García et al. 2018). However, the resolution of this technique does not allow the detection of sporadic consumption of marine resources. Estuarine aquatic resources, commonly consumed in the Western Mediterranean, might have lower $\delta^{13}\text{C}$ values than expected (e.g., Salazar-García et al. 2014), so special care should be taken interpreting their consumption in the region (Figure 10).

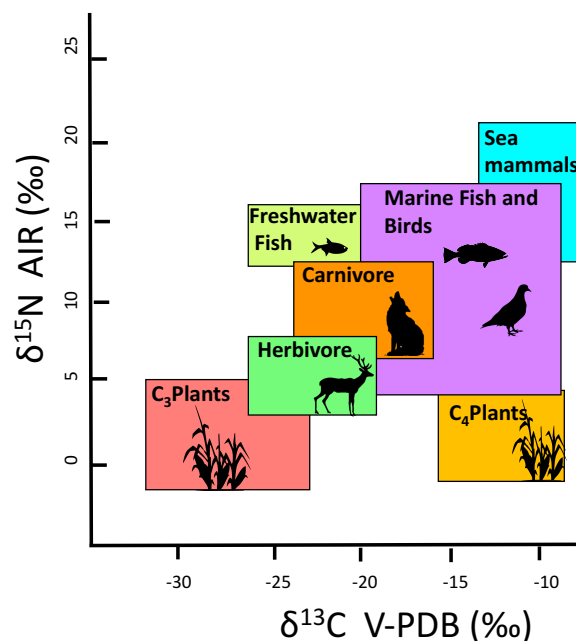


Figure 10: $\delta^{13}\text{C}$ and $\delta^{15}\text{N}$ range values in different plants and animal groups.

The ^{13}C measurement is also useful to detect the consumption of plants with different photosynthetic pathways (C_3 and C_4) (van der Merwe, 1982). C_3 plants has a mean $\delta^{13}\text{C}$ value of -26‰ and C_4 plants has a value of -12.5‰ (O’Leary, 1981; 1988) (Figure 10). This scenario makes more difficult the distinction among different diets with C_4 or marine resources but fortunately, there is no archaeobotanical evidence of C_4 resources commonly consumed in Iberian Peninsula during Mesolithic and Neolithic times. The first evidences date back to the

Middle Bronze Age and increase the importance during the Late Bronze Age in the Iberian Peninsula (Buxó and Piqué 2008: 161).

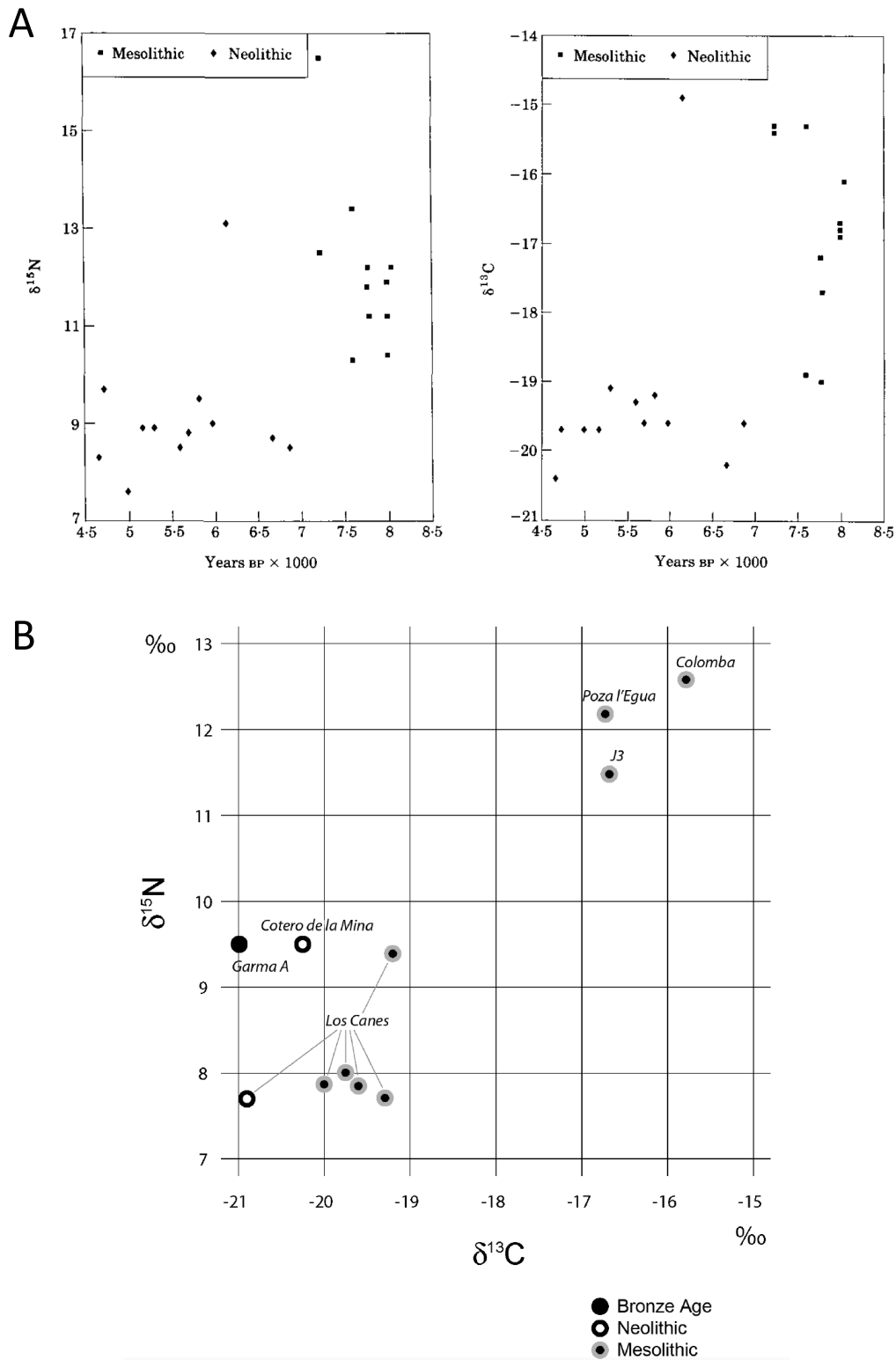


Figure 11: Marine vs terrestrial diet during Mesolithic and Neolithic. A) Mesolithic-Neolithic transition in Muge region (Portugal) from Lubell and Jackes, 1994. B) Mesolithic-Neolithic

transition in Northern Iberian from [Arias 2007](#) (Colomba, Poza l'Egua J3 and Canes are Mesolithic individuals; Cotero de la Mina and Garma A are Neolithic individuals).

$\delta^{15}\text{N}$ values can be used to establish the trophic level a specific organism holds in the food chain of its environment, with an overall agreed estimated increase of 3-5‰ per trophic step ([Bocherens and Drucker, 2003](#)). Aquatic ecosystems always present longer and more complicated food webs, so the diets based on these resources show higher $\delta^{15}\text{N}$ than diets based on terrestrial resources ([Minagawa and Wada, 1984](#)). Using the same principles, it is also possible to detect the nursing effect in subadult individuals or a preferable consumption of subadult species ([Fuller et al., 2006](#)). Contrary to the marine resources, the consumption of freshwater fish increase $\delta^{15}\text{N}$ independently on the increase of $\delta^{13}\text{C}$ values ([Lillie et al. 2011](#)) (**Figure 10**).

Apart from the diet, $\delta^{13}\text{C}$ and $\delta^{15}\text{N}$ values can also give an overview about the management of the resources and the husbandry strategies during the Neolithic and following periods. $\delta^{13}\text{C}$ values help to distinguish between open or close-forested environments, with the plants that grow in closed environments showing lower $\delta^{13}\text{C}$ values ([O'Leary, 1981](#); [Tieszen, 1991](#)); the $\delta^{15}\text{N}$ values increase due to arid conditions or vary depending on soil type ([Ambrose, 1993](#); [Handley et al., 1999](#)). Moreover, $\delta^{15}\text{N}$ values have proved to be useful to infer manuring strategies and also possible to detect domestic species-specific feeding with manured resources ([Bogaard et al., 2007](#)). Based on that and comparing the values, it is possible to infer if wild and domestic herbivores have a common plant resource consumption, or if domestics were fed differently. The variety of values can be translated into different husbandry strategies. All these features make always recommendable sampling enough set of faunal remains (plant remains if available too) from the same archaeological context. Analysing the values of fauna and humans together can offer more information about aspects of the ecology of the first anthropic ecosystems during the onset of the Neolithic.

A technical overview as well as a further description about isotopes is given in chapter 6 and 8.

4.3.2 Strontium isotopes and the study of the prehistoric mobility patterns

Strontium isotope ratios ($^{87}\text{Sr}/^{86}\text{Sr}$) of tooth enamel can provide insight on the use of the territory by tracking individual mobility ([Bentley, 2013](#)), understanding mobility as temporal or permanent territorial movements of individuals for an unknown reason. In this sense,

$^{87}\text{Sr}/^{86}\text{Sr}$ have proved to be useful in many archaeological issues which involve human or animal displacements: livestock mobility patterns and transhumance activities (e.g. [Bogaard et al., 2014](#); [Valenzuela-Lamas et al., 2016](#)), seasonal mobility of wild species (e.g. [Britton et al. 2009, 2011](#); [Copeland et al. 2016](#)) and female exogamy in hominins and prehistoric cultures (e.g. [Copeland et al. 2011](#); [Knipper et al. 2017](#)).

Contrary to what happens with carbon and nitrogen stable isotope analysis, the strontium isotope analysis performed in human remains with the aim to infer the mobility are underrepresented in Iberia, even more during the Early Neolithic. Most of the analysis have been performed in latter chronologies mostly Late Neolithic-Chalcolithic and Bell Beaker sites, when the human remains record increase (e.g. [Alt et al. 2016](#); [Diaz-Zorita-Bonilla 2013](#); [Sarasketa-Gartzia et al. 2018](#)). Outside Iberia, strontium isotope analyses are better represented in all the chronologies and they have been useful to track first generation movements of people during the Neolithic arrival ([Borić and Price, 2013](#)), infer different mobility patterns according with the sex determination ([Haak et al., 2008](#)) or the interaction among the contemporaneous groups ([Price, et al., 2001](#)).

A technical overview as well as a further description about strontium isotopes is given in the chapter 6 and 8. Other methods like DNA (explained in chapter 7 and 9) can open the overview and complement the strontium isotope analysis to understand better the population movements.

5 OBJECTIVES

The main objective of this doctoral thesis is to study the impact of the Neolithic phenomenon inside the Iberian Peninsula by using several biomolecular techniques.

This issue has been addressed using different methods, specifically aDNA and isotopes (see chapter 4 and 5 for a method introduction). Nuclear aDNA and strontium isotopes have been applied to understand the movement of people at a macro- (DNA) and microscale (strontium isotopes). Changes in subsistence strategies and lifestyle were addressed applying carbon and nitrogen isotopes on humans and wild and domestic fauna bone collagen (see chapter 4 and 6 for a method introduction).

Despite this thesis does not include data from all areas of the Iberian Peninsula, the results have been integrated with a Peninsular overview and discussion.

In summary, these are the main goals of this work:

1. Understand the genomic structure in Iberia amongst last hunter-gatherer populations
2. Evaluate the genomic impact of the Neolithic arrival into Iberia.
3. Characterize the HG ancestry in the Neolithic groups and study in detail the potential different HG ancestries among the Neolithic groups from different territories.
4. Test potential local admixture events between HG and Early Farmers, especially in regions that initially were more influenced by expanding farmers.
5. Clarify if there are different genomic make-ups in the cultural Neolithic Cardial and Epicardial groups.
6. Test the presence of potential different arrival routes of the Early Neolithic groups.

7. Study the change of the subsistence strategies between published HGs, Neolithic and Post-Neolithic peoples in the Iberia Peninsula.
8. Evaluate the possible change of diet during Post-Neolithic times.
9. Evaluate the mobility of the Neolithic populations generally considered fully sedentary.
10. Study the environmental influence among different sites and chronologies that might have an influence in the isotopic value backgrounds and interpretation.

6 ISOTOPES: PRINCIPLES

Atoms are composed by protons, electrons and neutrons. Protons and neutrons are located in the nucleus of the atom and the electrons are circulating around the nucleus. The atomic mass is calculated by the number of protons and neutrons while the atomic number, which defines the element, is characterized only by the number of protons. Based on that, we can find heavy or light atoms of the same element, depending of the number of neutrons. These are the isotopes, atoms of the same chemical element that have different atomic weight because they have different number of neutrons (Sharp, 2017: 6).

The ‘stable’ isotopes do not decay by time, unlike the "radioactive" isotopes that have a limited lifetime which depends on the chemical element where they come from. Others, like strontium isotopes are named “radiogenic” because they are created from the decomposition of a *radioactive* ones. Stable isotopes were discovered by Thomson et al. (1921), the inventor of the mass spectrometer, instrument with which the different isotopic species are quantified.

6.1 Isotopic fractionation

Different stable isotopes from the same atoms are present in nature. To understand why some substances are more enriched by the light or the heavy one we need to explain the concept of *isotopic fractionation* (Briscoe and Robinson, 1925). The isotopic fractionation factor between two substances A and B in the reaction $A_1X + B_2X \longrightarrow A_2X + B_1X$ is defined in the following equation, where 1 and 2 refer to the light and the heavy isotope of the element A and B:

$$\text{Isotopic fractionation} = \frac{(A_2/A_1)X_A}{(B_2/B_1)X_B}$$

This means that some metabolic processes are conditioned by the weight of the substances involved in the chemical reactions. Atoms with different atomic mass have different behavior against the same chemical reaction, which creates differences among the substrate and the material analyzed.

6.2 Mass spectrometers

The Mass spectrometer is the device for measuring the different isotopic composition of each substance (**Figure 12**). All mass spectrometers are based on the principle of deflecting ionized atoms in a magnetic and/or electrostatic field. The acceleration of the different ionized atoms with different masses can be used to calculate the isotope ratios. This quantification can be measured thanks to 3 basic components of every spectrometer: 1) the source where the sample is ionized; 2) the analyser which deflects the ionized atoms as a function of mass; and 3) the collector, where the relative intensities from different ionized atoms are measured and recorded (**Figure 12**).

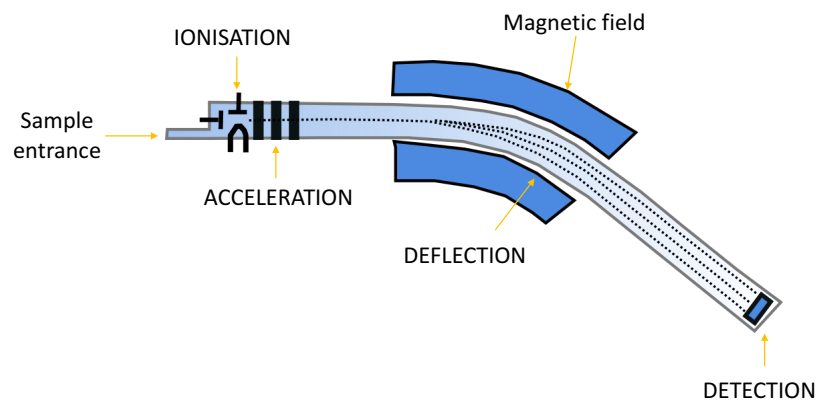


Figure 12: Diagram of spectrometer with the 3 basic components: 1) atomic ionisation and acceleration; 2) deflection of ionized atoms; and 3) intensity detection.

The mass spectrometer measures the proportion of isotopes in one sample regarding the isotopic proportion of a reference material. All the measurements are referenced to a standard material with a known isotopic composition in order to allow very precise comparisons among different laboratories. Standards from the National Institute for Standards and Technology (NIST) or International Atomic Energy Agency (IAEA) are needed to calibrate the Mass spectrometer (Coplen, 1996; Coplen and Clayton, 1973; Coplen et al. 1983; Hut, 1987). The calculated value (δ) is done in parts per thousand (‰) following the next equation, where R is the elemental ratio in the sample and in the standard.

$$\delta = \left[\left(\frac{R_{sample}}{R_{standard}} \right) - 1 \right] \times 1000 (\text{‰})$$

Applying this equation, we can obtain positive or negative values, depending on the standard reference value. Carbon isotope ratios are reported relative to the Upper Cretaceous Peedee

formation of South Carolina (PeeDee Belemnite, PDB) and by definition, the $\delta^{13}\text{C}$ value of PDB is zero (Cai and Qiu, 1984) and all the carbon values measured in biologic materials are going thus to be negative. In the case of the nitrogen, the referenced standard is the atmospheric nitrogen (N_2), called AIR. By definition, $\delta^{15}\text{N}$ value of AIR is 0‰ (Mariotti, 1983). In this case, all the nitrogen values measured in biologic materials are going to be positive. Strontium isotope ($^{87}\text{Sr}/^{86}\text{Sr}$) values are usually reported relative to SRM987, with reference value of 0.710255 from NIST and the measured range of values in bio-mineral materials are always very close to this value.

6.3 Isotope analysis in archaeological remains: diet and mobility studies

To understand how the isotope ratio changes among different substrates (organic or inorganic) and tissues from the individual analysed (human or animal) it is necessary to understand the biogeochemical cycles of the different elements and their isotopic fractionation at every step. In this chapter, I will describe the most common isotopes and target tissues used in archaeology as well as the biogeochemical cycles of the elements. Finally, I will describe the quality controls and limitations of each method.

6.3.1 Carbon and nitrogen isotopes: diet studies

The isotopic elements and the kind of material analysed to carry out dietary studies in archaeological remains are very diverse but, the best well-known ones and the most commonly used are the carbon ($\delta^{13}\text{C}$) and nitrogen ($\delta^{15}\text{N}$) isotope analysis performed on the bone collagen. This method is based on the premise that “we are what we eat”, which means that the isotopic composition of the individual’s diet determines the isotopic composition of their tissues. Basically, the collagen values of $\delta^{13}\text{C}$ and $\delta^{15}\text{N}$ allow us to distinguish between the consumption of some kind of plants, as well as the terrestrial, marine or potentially lacustrine/fluvial origin of different food resources (Lee-Thorp, 2008; Makarewicz and Sealy, 2015) (Figure 10). To understand better why this technic allows dietary discrimination, we have to understand the key aspects in the biogeochemical cycles of every element analysed.

6.3.1.1 Biogeochemical cycle of Carbon

There are two stable isotopes of carbon in nature, ^{13}C and ^{12}C . Their natural abundances are 1.1% and 98.9%, respectively (Hoefs, 1987; Schoeninger, 1990). The major source of non-biological carbon is contained in the oceans. When the dissolved carbon (CO_2) is transferred from oceans to atmosphere, CO_2 molecules are depleted in ^{13}C (Schoeninger and Moore, 1992). Both, atmospheric CO_2 and oceanic CO_2 go inside the biological cycle via photosynthesis, which fixes the atoms of inorganic CO_2 into organic molecules.

The terrestrial plants have two main photosynthetic pathways: C_3 and C_4 , referring to the number of carbon atoms from CO_2 that are fixed in the first molecule of the photosynthesis cycle (O'Leary, 1981; Smith and Epstein, 1971) (Figure 13). In the C_3 photosynthesis, the discrimination of the ^{13}C (the heavier isotope) by the enzyme ribulose biphosphate carboxylase/oxidase (RUBISCO), which fix the CO_2 to the first component of the photosynthesis cycle, is higher than in C_4 photosynthetic pathways. In C_4 plants, the CO_2 is concentrated in bundle-sheath cells prior to release to RUBISCO. This previous step makes C_4 plants less discriminative in the capture of ^{13}C than the C_3 plants. The C_4 photosynthesis pathway has been interpreted as an adaptation for lower pressure of CO_2 and high solar radiation, more typical from tropical climates, or very dry areas (Ehleringer et al., 1997). There is an extra photosynthetic pathway present in crassulacean plants (CAM), as a result of another adaptation to arid conditions. CAM plants show a similar photosynthetic pathway as C_4 , but it only happens during the night (O'Leary, 1988) (Figure 13).

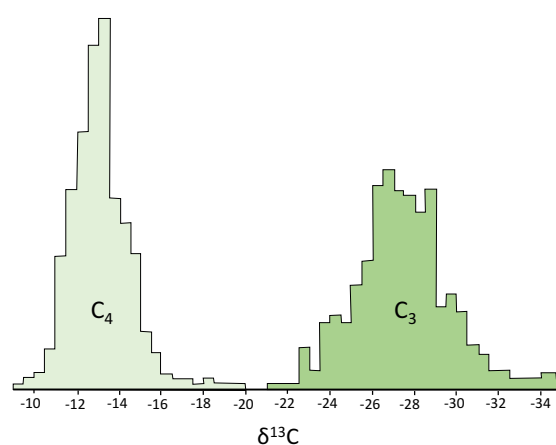


Figure 13: C_3 and C_4 $\delta^{13}\text{C}$ ranges, adapted from (O'Leary, 1988).

C₃ plants include most of the bushes, trees and grass from temperate ecosystems. The most interesting C₃ plants for diet are cereals (e.g. barley, wheat and rice), nuts, and most of fruits and vegetables. Among the C₄ plants consumed we have e.g. corn, millet, sugarcane or sorghum, all of them absent during Early Prehistory. CAM plants include succulent and crassulaceous plants, without almost no representant in human diet.

The step of CO₂ fixation from atmosphere by the primary producers generates the isotopic fractionation useful to estimate the consumption of plants with different photosynthetic pathways. Atmospheric carbon has a δ¹³C value of -7‰ although an estimated value of -5 or -6‰ previous to the massive fossil fuel carbon burn must be acknowledged (Bada et al., 1990; Keeling, 1961; Marino and McElroy, 1991). C₃ plants which take in this carbon present a δ¹³C mean value of -26.5 ‰ in C₃ (ranging from -22 to -34 ‰ δ¹³C), and C₄ plants show a mean value of -12.5 ‰ (ranging from -7 to -20 ‰ δ¹³C) with less variation. CAM plants show an average value of -11 ‰ δ¹³C (O'Leary, 1988; Tieszen, 1991) (Figure 13, Figure 14).

Primary producers in the oceans (e.g. phytoplankton and algae) take CO₂ from different sources (Hoefs, 1987). Among them, we have the terrestrial detritus washed by the rivers into oceans with similar values to terrestrial plants, dissolved CO₂ from the atmosphere (δ¹³C -7‰), or dissolved carbonic acid (HCO₃⁻) coming from the dissolution of bicarbonates (H₂CO₃) of marine shells that make up the limestones (δ¹³C 0‰) (Schoeninger and Moore, 1992) (Figure 14). All these elements are present in the ocean in an equilibrium reaction: CO₂ + H₂O → H₂CO₃ → HCO₃⁻ + H⁺. This mix of values makes the ocean primary producers to be more enriched in ¹³C isotope than the terrestrial ones, which have a mean value of δ¹³C -20 ‰, an intermediate value between the terrestrial C₃ and C₄ plants (Smith and Epstein, 1971). Freshwater first producers use a mix of dissolved CO₂ and carbon from terrestrial detritus which makes δ¹³C values much more unpredictable (Rau, 1978; Schell, 1983) (Figure 14).

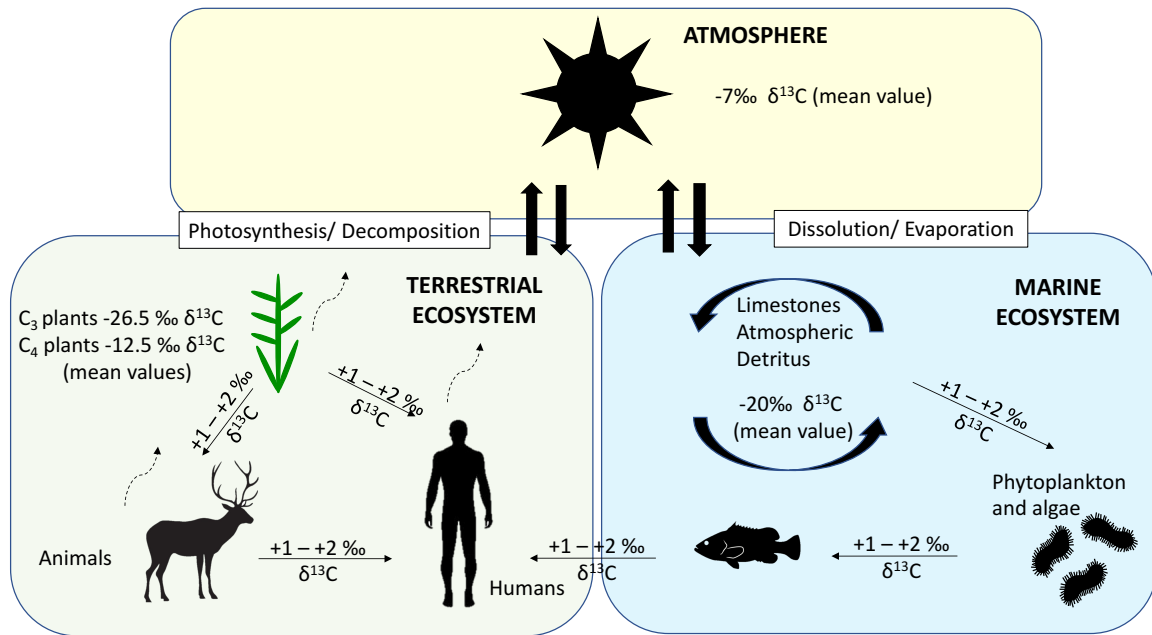


Figure 14: Biogeochemical cycle of Carbon element with the most important steps for dietary interpretation of carbon isotope analysis.

Plant $\delta^{13}\text{C}$ values are reflected in their consumer tissues. DeNiro and Epstein (1978) showed in a controlled feeding experiment that the $\delta^{13}\text{C}$ values of the animal consumer were almost the same as the $\delta^{13}\text{C}$ values of their diet. Looking into the collagen values specifically, another controlled experiment showed that the collagen only reflects the consumption of proteins, because the aminoacids consumed are mostly used to build new collagen (Ambrose and Norr, 1993; Tieszen and Fagre, 1993). Finally, only a small trophic effect is observed among the food chain, calculated in an increase of $+1$ to $+2\text{‰ } \delta^{13}\text{C}$ in every step (Lee-Thorp, 2008). Based on these principles, $\delta^{13}\text{C}$ values are useful to discriminate among marine or terrestrial diets in animals and humans too, although alone could lead to misinterpretation due to overlap with C₃-C₄ ecosystems (Figure 14).

6.3.1.2 Biogeochemical cycle of Nitrogen

Nitrogen also present two stable isotopes, ^{15}N , which represents the 0.36%, and ^{14}N , which represents 99.64% of natural abundance (Hoefs, 1987). N_2 is the gas with the highest representation in the atmosphere (78.1%), with a uniform isotopic composition and a $\delta^{15}\text{N}$ value of 0‰, by definition (Mariotti, 1983) (Figure 15). However, most of biological organisms cannot take the inorganic atmospheric N_2 directly. Only terrestrial plants with symbiotic

relations with cyanobacteria or green/blue algae from marine or freshwater ecosystems can fix N_2 in organic components directly (Delwiche and Steyn, 1970). This process incorporates nitrogen into the biological cycle with $\delta^{15}N$ values close to 0‰ (same as the atmospheric value) (Schoeninger and Moore, 1992) (Figure 15).

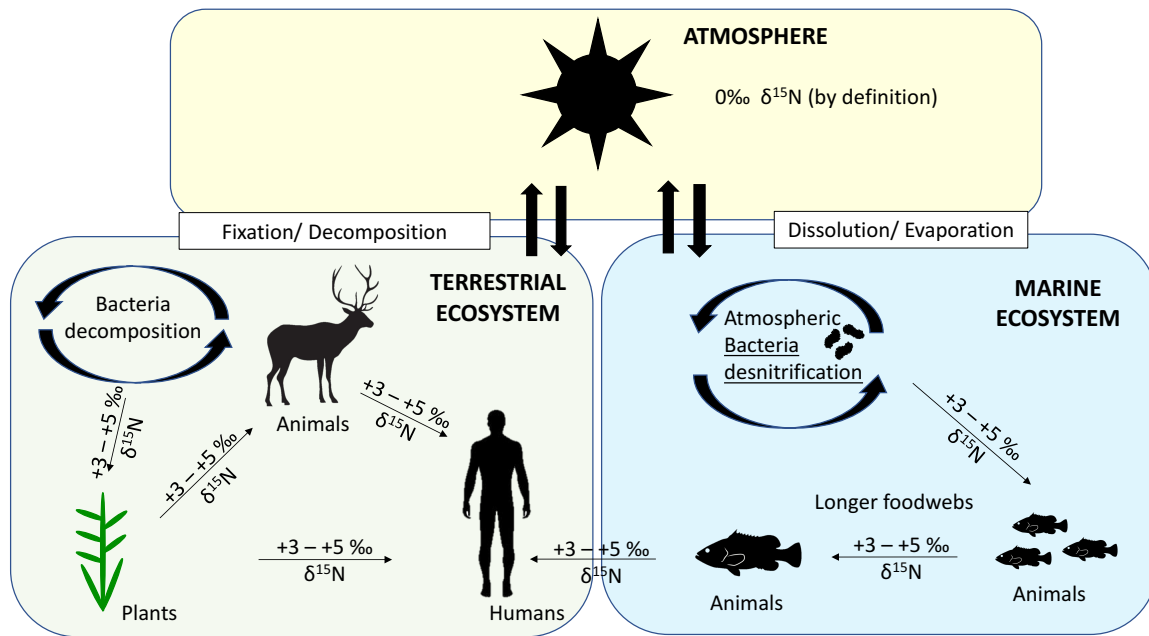


Figure 15: Biogeochemical cycle of Nitrogen element with the most important steps for dietary interpretation of nitrogen isotope analysis.

Another process that produces the reincorporation of nitrogen into the biological cycle comes from the bacterial decomposition of dead organisms into organic molecules with nitrogen content like nitrates (NO_3^-). These organic components are enricher in ^{15}N than the N_2 from the atmosphere. This is the reason why fixing- N_2 plant could show a lower $\delta^{15}N$ than plants which only use nitrates from the bacterial decomposition (Delwiche and Steyn, 1970). A range of values from +1 to +4 ‰ $\delta^{15}N$ are observed in the terrestrial plants because the bacterial action and nitrates catchment are conditioned by many environmental factors like aridity, leaching, anoxia and salinity (Ambrose, 1991; Handley and Raven, 1992; Heaton, 1987; Shearer et al., 1978). In the oceans, the vast majority of available nitrogen is produced by bacterial denitrification instead of from the dissolved atmospheric N_2 , creating higher $\delta^{15}N$ values in all marine organisms (Wada, 1980) (Figure 15).

The $\delta^{15}N$ values experiment also what is known as a *trophic-level effect*. This effect consists on an enrichment of ^{15}N compared to ^{14}N with every step of the food chain. This effect has been

observed in all the ecosystems and trophic relationships, like in invertebrates (Wada, 1980), marine vertebrates (Minagawa and Wada, 1984; Schoeninger and DeNiro, 1984; Wada, 1980), and terrestrial vertebrates (Schoeninger, 1985, 1988; Schoeninger and DeNiro, 1984). The trophic-level-effect has been estimated in an enrichment of +3 to +5 ‰ $\delta^{15}\text{N}$ (Bocherens and Drucker, 2003; Vogel et al., 1990) although some researchers suggest this range could be wider among species and different physiological conditions (Hedges and Reynard, 2007), and have been estimated in ca. 6‰ combining short-scale studies from red blood cells with measured offsets in other studies (O'Connell et al., 2012). One well-known example of this increase in the $\delta^{15}\text{N}$ values is the breastfeeding, which is reflected in an increase of +2 to +3 ‰ $\delta^{15}\text{N}$ values more than the adult individuals (Fuller et al., 2006). The metabolic explanation of the ^{15}N increasing is that the bonds among ^{14}N atoms are broken easily during the metabolic reactions and consequently more ^{14}N is excreted in the urea, remaining more ^{15}N for synthesis of new proteins (Ambrose, 1991; Schoeninger and Moore, 1992) (**Figure 15**).

In long marine food chains, due to the higher number of steps along the foodweb, the ^{15}N enrichment is higher, resulting in distinct high $\delta^{15}\text{N}$ values in most marine foods and consumers (Minagawa and Wada, 1984) compared to the terrestrial ones (Schoeninger and DeNiro, 1984). In the freshwater ecosystems, the food web are also longer than the terrestrial ones, and so that the same $\delta^{15}\text{N}$ values as the marine foods can be observed. Contrary, the $\delta^{13}\text{C}$ values do not increase as much as in the marine organism (e.g. (Lillie et al., 2011).

For all these reasons, a combined carbon and nitrogen stable isotope analysis is highly recommended, even more if we want to address questions about the potential marine/freshwater/ C_4 plants consumption. Important as well is always to have a very good knowledge of the time period and the environmental conditions of our samples come from (**Figure 15**).

6.3.1.3 Target tissue: bone collagen

The bone is composed by organic and inorganic parts. Approximately, two thirds of the bone tissue correspond to the organic part (Brothwell, 1987). The main organic component is represented by collagen, a large protein that represents around the 90% of the bone organic content. Bone acquires a hard consistency because elastic collagen is surrounded by an inorganic hard matrix which represents one third of the bone tissue. The main component from

this inorganic part is hydroxyapatite, a kind of calcium phosphate (White and Folken, 2005) (Figure 16).

Bones can suffer diagenesis, which produces a modification of the original isotopic ratio (Hedges, 2002; Price et al., 1992). This is the reason why the analyses tend to be performed on the organic portion of the bone (the collagen), where different quality controls are defined to check collagen preservation and the diagenetic incorporation of some materials during the depositional phase (Ambrose, 1990; DeNiro, 1985) (explained below). To perform the isotopic analysis in bone collagen it will be necessary to remove the inorganic part of the bones (Figure 16). A full explanation of this process is described in the methods section.

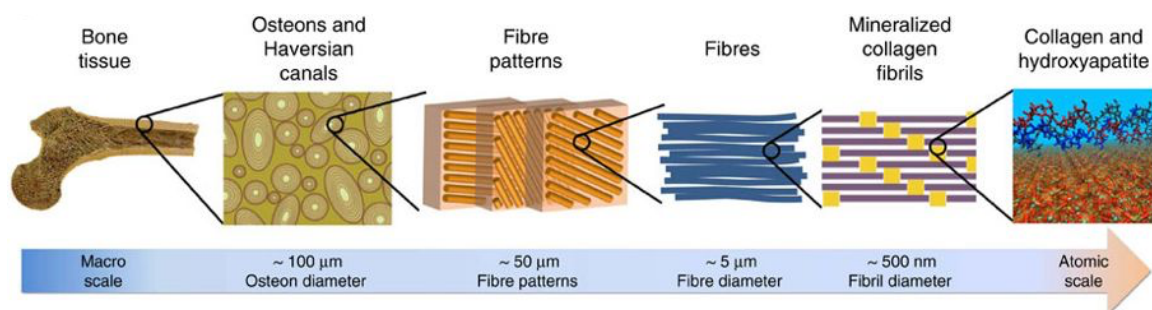


Figure 16: Structure of bone collagen from Nair, et al, (2013).

Another factor which can alter isotopic values of bone collagen is the portion of the bone analysed (Hedges et al., 2007). In this case, the variation is due to collagen remodelling rate of different parts of the bone and age of the individual analysed. Remodelling involves the removal of bone tissue and the substitution by a new one. The function of this mechanism is thought to be reparative of the of microscopic damage (Scheuer and Black, 2000: 24) (Figure 16). The remodelling rate varies depending on the part of bone. It is estimated that around 5% of the adult compact bone is remodelled every year, while around 25% of the spongy bone is renewed during the same period of time (Martin et al., 1998). Despite the different rates of renewing, the physiological remodelling is a coordinated process between bone formation and resorption without affecting the size nor shape of the bone (Enlow, 1963; Garn, 1970).

The bone remodelling process creates an average of the diet information included in the bone collagen and should be taken into account during the interpretation of results. In order to reflect a comparable average of years it is highly recommended to use the same kind of bone when possible. There are also some studies which combine the analysis of collagen from bones with

high amount of cortical portion and other with cancellous, with the aim of finding out the latest changes produced on the individual diet (Cox and Sealy, 1997).

6.3.1.4 Quality controls

There are many established quality controls for the isotopic analysis performed in collagen samples. These quality checks help to identify if the collagen is very degraded or contaminated, which would render useless data for interpretation. The use of ultrafilters to keep only the long molecules (>30 KDa) is one of the quality steps carried out along the process. This allows us to keep the best quality collagen molecules, which is especially important in the case of old samples. There are also quality indicators that should be taken into account.

The easiest quality indicator to measure the collagen degradation is the measure of the collagen yield following the formula:

$$\text{Collagen yield (\%)} = \frac{(\text{Collagen mass})}{(\text{Bone mass})} \times 100$$

Where *Collagen mass* is the weight of the total amount of collagen extracted after lyophilisation and *Bone mass* is the weight of the bone sample used to extract the collagen. The minimum acceptable percentage range is between 1 and 0.5% (van Klinken, 1999) although it is necessary to use another quality indicator when the collagen yield is below 2% (Ambrose, 1990). If we use ultrafilters the collagen yield is always lower, because we discarded all the collagen smaller than 30KDa. This is the reason why collagen yield is not considered when collagen is ultrafiltered if all other parameters are within acceptable ranges (see below).

We can also measure the collagen integration and preservation with other parameters reported by the spectrometer. To explore the collagen integrity we measure the molecular weight (in percentage) of C % and N %. In fresh collagen, they have been estimated in 35 and 11-16% respectively (Ambrose, 1990). In archaeological samples is still valid a value >13% for C and >5% for N if the rest of the quality parameters of those samples are correct (Michael P Richards et al., 2000). The last indicator used is the elemental C:N ratio, corrected for the mass differences between carbon (12) and nitrogen (14). In absence of contaminants, the ratio ranges between 2.9 and 3.6 (DeNiro, 1985). We also use international and in-house standards with well-known isotopic composition to calibrate the measurements in order to assure the accuracy. We also test the precision on the measurements with the repeated measurements of standards

and sample replicates. An extended explanation of this process can be found in the method section.

In this thesis, we have applied all of the possible quality controls. However, because of the use of ultrafilters, the collagen yield cannot count as a determinant one.

6.3.1.5 Limitations of diet estimation using carbon and nitrogen isotopes from bone collagen.

Stable isotope analysis has some limitations to estimate the diet. Nitrogen of the diet mainly come from the consumption of aminoacids, of which the proteins are composed. Therefore, the $\delta^{15}\text{N}$ values only reflect the protein intake and not the whole diet. Carbon comes from different sources of macronutrients (proteins, lipids and carbohydrates) but it has been proved that the bone collagen $\delta^{13}\text{C}$ value mainly comes from the proteins too (Ambrose and Norr, 1993). We should take this into account when we estimate the diet because high protein products (e.g. meat, fish, dairy products) that are reflected in the isotopic signature of the collagen could mask the low protein products (e.g. vegetables, fruits, cereals). That means, the plant consumption can be masked by the animal product intake, because the amount of proteins is always higher in the animal than in plant products with a same weight/mass (Van Klinken et al., 2002).

Another aspect to take into consideration is collagen turnover, which is low during adulthood and therefore reflects an average diet of the last years before the individual died (Robert E M Hedges et al., 2007; Hill, 1998). Moreover, subadult individuals could still show a breastfeeding or weaning isotopic signal (Herrscher et al., 2017), as well as having isotopic values that reflect a narrower window of time before death because of their faster collagen turnover (Valentin, 2002).

The environmental conditions can modify the expected values for carbon and nitrogen. The $\delta^{13}\text{C}$ values could reflect many features about plant physiology (Seibt et al., 2008). The range of $\delta^{13}\text{C}$ values in plants is mainly related to the CO_2 catchment efficiency from the atmosphere, which depends on many environmental factors such as luminosity, water availability and temperature (O'Leary, 1981; Tieszen, 1991). As It has been said before, plants take organic nitrogen from the soil, resulting in their $\delta^{15}\text{N}$ values showing variations depending on natural or anthropic factors which affect the soil-plant system (Szpak, 2014). Among the natural factors, the presence of organic material in the soil, temperature and water availability could be

the most significant ones (Ambrose, 1991; Handley et al., 1999). Otherwise, human ecosystem modifications like the use of fertilisers may also modify the expected $\delta^{15}\text{N}$ along the food web (Bogaard et al., 2007). All these factors have an impact in the primary producers, which produces a bias in the next steps along the foodchain. The environmental conditions can show variability along the timescale and among different geographical areas. That is what makes so difficult the direct comparison of diet along different time periods and regions. (Drucker et al., 2003; Goude and Fontugne, 2016; Tornero et al., 2018).

6.3.2 Strontium isotopes: mobility studies

The geochemical signature of the strontium isotopes is widely used to link archaeological individuals to some geological areas, and infer by this way the potential mobility during their life. The strontium is taken from geological materials and pass from the soil through the food chain up to skeleton and teeth, where strontium substitutes calcium. The pioneer use of strontium isotope analysis to study geographical movements of different animal species was performed by ecologists (e.g. Gosz et al., 1983; Ericson, 1985). This method is based on matching the isotope signature of the individual to the biologically available signature at a suspected location of origin (Bentley, 2006).

6.3.2.1 Geographical distribution of strontium isotope values

In nature we can find four strontium isotopes. Three of them are non-radiogenic (^{84}Sr with an abundance of $\sim 0.56\%$; ^{86}Sr with an abundance of 9.87% and ^{88}Sr with an abundance of 82.53%). The radiogenic one is ^{87}Sr , which is formed over time by the decay of ^{87}Rb , with a half-life of 4.88×10^{10} years (49 billion years) (Bentley, 2006). The geographical distribution of strontium isotope values along the geosphere will depend on two main factors: 1) the age of the rocks, and 2) the original Rb/Sr ratio of the rocks.

The Rb/Sr decay is used in geochronology, and $^{87}\text{Sr}/^{86}\text{Sr}$ ratio is a function of the relative abundances of Rb and Sr in rocks. Due to that, the decrease of Rb follows the following decay equation, where ^{87}Rb is the current amount of ^{87}Rb , $^{87}\text{Rb}_0$ is the initial amount of ^{87}Rb , λ is the decay constant and t is the time.

$$^{87}\text{Rb} = ^{87}\text{Rb}_0 e^{-\lambda t}$$

Due to the decay of ^{87}Rb directly producing ^{87}Sr , the loss of the first one correlates with the increase of the second one in a 1:1 relation through time. Therefore, the Rb/Sr decay system creates a set of values where the age of the rocks will be a source of variation: older rocks have a long decay of Rb and thus, higher amount of ^{87}Sr . As an example, modern rocks as the basalts usually present a range of values of 0.703-0.704, and old granites can arrive up to 0.710 (Bentley, 2006).

There are several geochemical differences between Rb and Sr which have an effect on solubility and exchange capacity. Sr is an alkaline earth element with +2 valence, which is easily substitute by Ca^{2+} in many minerals and bioapatite because of their same valence and similar ionic radius. On the other hand, Rb is an alkaline metal, which is substituted in many minerals by K^+ because they share similar ionic radius values. These different chemical characteristics of Rb and Sr, make the Rb/Sr ratio variable among different types of rocks, and also among different minerals inside the rock. The original Rb/Sr ratio would therefore be another factor that creates variation of the $^{87}\text{Sr}/^{86}\text{Sr}$ values among the rocks (Bentley, 2006).

6.3.2.2 Geochemical cycle of strontium isotopes

The Sr will pass to plants and animals and arrive to rivers and oceans by the sediment transport. The time scale of this process is not comparable with the decay of ^{87}Rb , with a half-life of 49 billion years, meaning that the Sr values does not change significantly during prehistorical and historical periods, and we can assume that they are constant. Moreover, contrary to what happens with carbon and nitrogen stable isotopes, also the isotopic fractionation can be negligible in the case of $^{87}\text{Sr}/^{86}\text{Sr}$ due to the large atomic mass of both isotopes (Graustein and Armstrong, 1983) (Figure 17).

The strontium from the geosphere is released from the rocks to the soil due to the weathering mainly, but also by ground and stream water, atmospheric deposition (wind, rain and sea spray) (Bentley, 2006). Due to rock weathering is usually the major component, we are able to correlate the local bedrock with the $^{86}\text{Sr}/^{87}\text{Sr}$ ratio in the soils (Capo et al., 1998; Hodell et al., 2004). Nevertheless, it has been proved that plants always reflect a more consistent average of the local bioavailable values than the soil (e.g. Benson et al., 2003; Poszwa et al., 2002) (Figure 17).

This averaging effect (lower ranges of variability) increase up the food chain because animals eat a mix of plant materials from a local area and the diet is also average among the time of the tissue formation (Burton et al., 1999) (Figure 17).

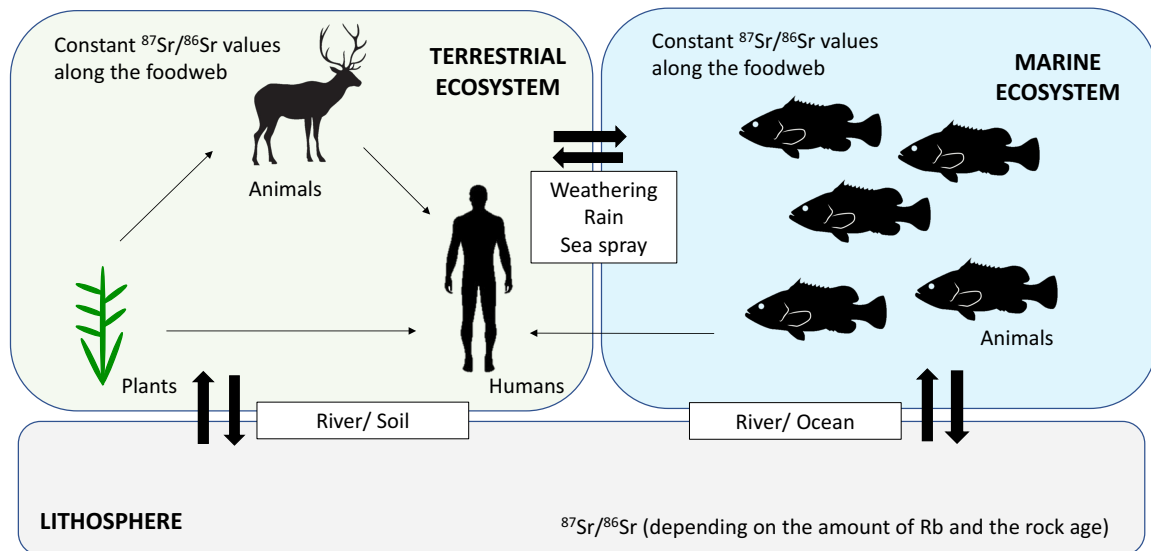


Figure 17: Geochemical cycle of Strontium element with the most important steps for mobility interpretation of strontium isotope analysis.

The soil values can be modified by external factors. Probably the most common one is the *Sea spray effect*. Contrary to what happens with the $^{87}\text{Sr}/^{86}\text{Sr}$ ratio of the rivers, the seawater ratio has been estimated to possess a unique value of 0.7092, which represents an average ratio of the continental crust around the world (Bentley, 2006). Nevertheless, this value changed along the different geological periods between 0.707-0.709, and nowadays is remained in the marine limestones from different geological periods (McArthur et al., 2001). In coastal areas, bedrock substrates can be modified by the sea spray effect by incorporating certain amount of marine strontium with the same $^{87}\text{Sr}/^{86}\text{Sr}$ ratio as marine water (0.7092). This effect could increase or decrease the $^{87}\text{Sr}/^{86}\text{Sr}$ ratio of the shoreline and surrounding areas depending on the bedrock baseline value. In modern ecosystems the atmospheric pollution and the use of agricultural fertilizers may also modify the $^{86}\text{Sr}/^{87}\text{Sr}$ ratio from soil and ground water (Åberg et al., 1998) (Figure 17).

6.3.2.3 Calculation of local bioavailable $^{87}\text{Sr}/^{86}\text{Sr}$ range

If we want to characterize the displacement of different species, we need to know the 'local' strontium isotope baseline. For archaeological studies, we usually named 'local' the area where the individual was recovered, even if acknowledging that most of individuals come from burial places. To calculate the isotopic signature of the 'local' values archaeological rodent teeth, as well as modern plants (Hoppe et al., 1999) and snails (Price et al., 2002), were sampled and measured from different geological areas around the archaeological sites from which material was studied.

We must keep in mind, however, that the $^{87}\text{Sr}/^{86}\text{Sr}$ ratio in modern materials can be bias by the anthropogenic strontium coming from environmental pollution or the use of agricultural fertilizers (Otero et al., 2005). This is why, for each geological area studied, the most pristine areas were selected for sampling, always avoiding direct contact with fields and constructions. Furthermore, different types of plants, with different root depth, were also chosen for sampling in each area to minimize the potential bias. An alternative to this would be to sample archaeological teeth of different local species (Bentley, 2004; Price et al., 2002), but sometimes this is not possible for specific geological areas, plus adds the uncertainty of animal provenance amongst non-microfaunal remains.

6.3.2.4 Diagenetic strontium

As already mentioned, strontium is very similar to calcium, which can be substituted by it in phosphates and apatites from the skeleton (Ezzo, 1994). The first mobility studies used the values from the teeth (Sr is only incorporated during the mineralization process) with the values from the bones (where the Sr is incorporated along the life), to track the potential movements of the species during their life (Ericson, 1985). Nowadays we know that the contact with water and soil can incorporate Sr in bones, what is known as diagenetic effect (Hedges, 2002; Tuross et al., 1989). Different treatments have been suggested (e.g Nielsen-Marsh and Hedges, 2000; Sillen, 1986) but it is still not clear if they are useful and there is no way to quantify the potential amount of contaminant Sr. Therefore, the use of bones has been put aside as a reliable value to estimate the last residence place. Now, it is commonly accepted to use instead tooth enamel, which is less porous and the potential diagenetic Sr can be easily removed performing an acid treatment plus the mechanical abrasion of the surface.

6.3.2.5 The target tissue: tooth enamel

The enamel is formed by the ameloblasts in a process named amelogenesis. Basically, this process only happens once and the enamel is not remodelled although enamel is lost and modified by mechanical abrasion (tooth wear) (White and Folkens, 2005: 107) (Figure 18).

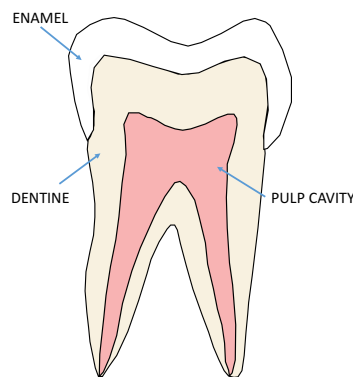


Figure 18: basic structure of tooth. Enamel, located in the outer surface is the target tissue for Sr analysis.

The mineralization of the enamel teeth present different phases. The first one consists on the synthesis and secretion of the amelogenins by the ameloblasts. It is only during the last phase of maturation when the hidroxyapatite crystals incorporate mineral ions (including Strontium in place of Calcium) and the mature enamel is created (Fincham et al., 1999). This process takes months-years and the mineralization takes place in different directions (Montgomery and Evans, 2006). This is the reason why in human studies, researchers tend to measure the bulk enamel instead of serial analysis as in herbivore studies, where the direction of the growth and mineralization is well known (Britton et al., 2011) However, the mineralization process occurs at different times in each type of dental piece, and there are some studies which combine the measurement of different teeth to estimate the mobility in a short-time scale (e.g. Müller et al., 2003)

6.3.2.6 Quality Controls

In the case of strontium isotope analysis, we need to address a higher number of quality controls than in carbon and nitrogen isotope analysis, especially during the Sr isolation in the laboratory. Firstly, it is mandatory to work in the so-called clean laboratories. Clean laboratories are equipped with a system to create a positive pressure to avoid the contamination of environmental strontium coming from outside air. To make sure that there is no Sr contaminant

we add one blank per every batch that is treated as the rest of the samples and measured with the spectrometer as well. The same as happens with the other isotopes, there are international standards that serve for the calibration of the spectrometer and to normalise the results. The international standard is called SMR987 and is processed in the same way as the samples and the blanks (Copeland et al., 2008). To estimate the potential diagenetic contaminations, we also measure the concentration of Sr in the archaeological samples and we check the coherence along the archaeological materials.

During the spectrometer measuring, we need make sure that the intensity signal for ^{88}Sr is between 20 and 25 V. We also need to nullify the interference signals from Krypton (Kr), Rubidium (Rb) using the normalization curve of $^{88}\text{Sr}/^{86}\text{Sr}$ with a value of 8.375209 and $^{84}\text{Sr}/^{86}\text{Sr}$ must be between the values 0.055 and 0.057 (Copeland et al., 2008).

6.3.2.7 Limitations

The main limitation of this technique is that there is no way to measure contamination with specific parameter as it happens in carbon and nitrogen isotope analysis, apart from the concentration estimation. The results interpretation are also limited. This is because there are many different areas with the same $^{87}\text{Sr}/^{86}\text{Sr}$ values across the world, because as we have seen, this value depends mainly on the geological age of the bedrock. This makes very difficult to point out a specific area for the individual origin. There is also a problem with the underestimation of the 'non local' individuals because the 'local values' not always means no human movements. The displacements could have happened before or after the enamel mineralization and/or involve areas with the same bioavailable $^{87}\text{Sr}/^{86}\text{Sr}$ values. Moreover, many deposits show overlapping $^{87}\text{Sr}/^{86}\text{Sr}$ values and that makes very difficult to stablish a clear range for every geologic substrate. Finally, another not solved question is the number of bioavailable samples needed to determinate with confidence the local range for each geological sampling area.

7 GENOMICS

7.1 History of genetics

Nothing was known about genetics when Robert Hooke described the cell for the first time in the 17th century, nor Virchow when he formulated the Cellular theory “*omnis cellula e cellula*” in the 19th century (Mazzarello, 1999; Wilson, 1947). With this theory, he proposed that the continuity of life depends on cell division and that every cell is the basic unit for reproduction without the mention of any aspect related to heritability.

In parallel, Charles Darwin presented the ‘Theory of Evolution and the concept of Natural Selection’ in the book *The origin of the species* in 1859 (Darwin, 1859). In his time, the concept of Natural Selection lacked a genetic explanation. In 1865, Gregor Mendel presented the result of his experiments carried out with peas (*Pisum sativum*) and formulated the famous Mendel’s laws. All these concepts together were eventually integrated into the new Neo-Darwinian theory (Dobzhansky, 1937) in the 20th century, when genetics was recognized as a scientific discipline.

On the other hand, many studies performed on *Drosophila melanogaster* allowed to formulate the concept of genes as a structural and functional unit ordered along the chromosomes. By that time, the discipline of Population Genetics emerged. Influential scholars such as Hardy and Weinberg (1908) or Fisher (1918) reformulated the Theory of Evolution linking selection, mutation, genetic drift and migration with the field of population genetics.

Many advances in molecular genetics were made after World War II. The general dogma of molecular biology was formulated (DNA→ RNA→ Proteins), and in 1953 Watson and Crick proposed/discovered the double-helix structure of DNA molecules based on Rosalind Franklin observations from x-ray diffraction (Watson and Crick, 1953). The knowledge about the DNA structure gave the main clues to understand the replication process and how to duplicate DNA. In 1977, Sanger and colleagues developed the first DNA sequencing technique (Sanger et al., 1977), and in 1986 Kary Mullis described the Polymerase Chain Reaction (PCR), which made him win the Nobel Prize of Chemistry in 1993 (Mullis and Faloona, 1987). In the 1990s, the Human Genome project was started, which was carried out simultaneously by two research groups, one headed by Craig J. Venter, which published the results in *Science* and one by

Francis Collins which published at the same time in *Nature* in 2001 (Consortium et al., 2001; Venter et al., 2001). This is generally considered as the starting point of the Genomic Era.

7.2 Ancient DNA background

Ancient DNA (aDNA) studies are a relatively novel discipline, which allows us to shed light on the genetic variability of the past, and how it has been shaped to form the current state we observe today. This study of aDNA can be applied to many different organisms and as a result the first 20 years of this young field have dealt with the genetic characterization of extinct species (**Figure 19**). Lately, and after overcoming major issues concerning DNA contamination, aDNA has increasingly focused on human history, offering a direct insight of migration and population turnover in the past, and pathogen evolution, approaching past pandemics and pathogen-host interactions (Krause and Pääbo, 2016).



Figure 19: Extinct organisms from which DNA sequences has been recovered. From bottom left to top right: quagga, marsupial wolf, sabre-toothed cat, moa, mammoth, cave bear, blue antelope, giant ground sloth, Aurochs, mastodon, New Zealand coot, South Island piopio, Steller's sea cow, Neanderthal, Aptornis defossor, Shasta ground sloth, pig-footed bandicoot, moa-nalo and Myotragus balearicus (from Hofreiter et al. 2001).

First aDNA studies were carried out by Higuchi et al. (1984) and Pääbo (1985). Both studies showed that is possible to retrieve DNA molecules from ancient specimens. The first one recovered and cloned mitochondrial DNA (mtDNA) fragments from the extinct equid Quagga (*Quagga quagga*) in a bacterial vector (Higuchi et al., 1984). The second one claimed for first time that the genetic material of Egyptian mummy tissues was still located in the cellular

nucleus, although it was probably contamination (Pääbo, 1985).

The first real advances in the field of aDNA were only possible after the invention of the Polymerase Chain Reaction (PCR) by Kary Mullis in 1986 (Mullis and Faloona, 1987). The automatization of amplification cycles with PCR and the use of thermally-stable Taq-Polymerases increased vastly the efficiency of the reactions. Together with the discovering of the DNA preservation in calcified biological materials like bone and teeth (Hagelberg et al., 1989) rather than tissue increased the number of studies based on aDNA (Pääbo, 1989).

First aDNA studies were able to retrieve fragments of multicopy DNA sequences such as mitochondrial DNA (mtDNA). Apart from the high copy number, mtDNA has an elevated mutation rate, specially, in the non-coding hypervariable regions (HVR I and II) which made the mtDNA the best molecular marker to study the genetic diversity of human populations at that moment (Wilson et al., 1985). The mtDNA variability observed is classified in groups, called haplogroups, which are defined by a specific set of stable mutations (haplotypes). First studies showed the phylogeographic distribution of the haplogroups and the coalescence estimation time pointed out the African continent as the origin of the mitochondrial variability (Cann et al., 1987), around 170,000 years ago (Ingman et al. 2000) whereas Neanderthal and modern humans diverged ~500,000 years ago (Kriings et al. 1999). PCR aDNA studies also revealed by first time the genetic discontinuity between Hunter-Gatherers (Bramanti et al. 2009) and first Farmers who both contributed to the genetic pool of the modern Europeans (Haak et al. 2005) (**Figure 20**).

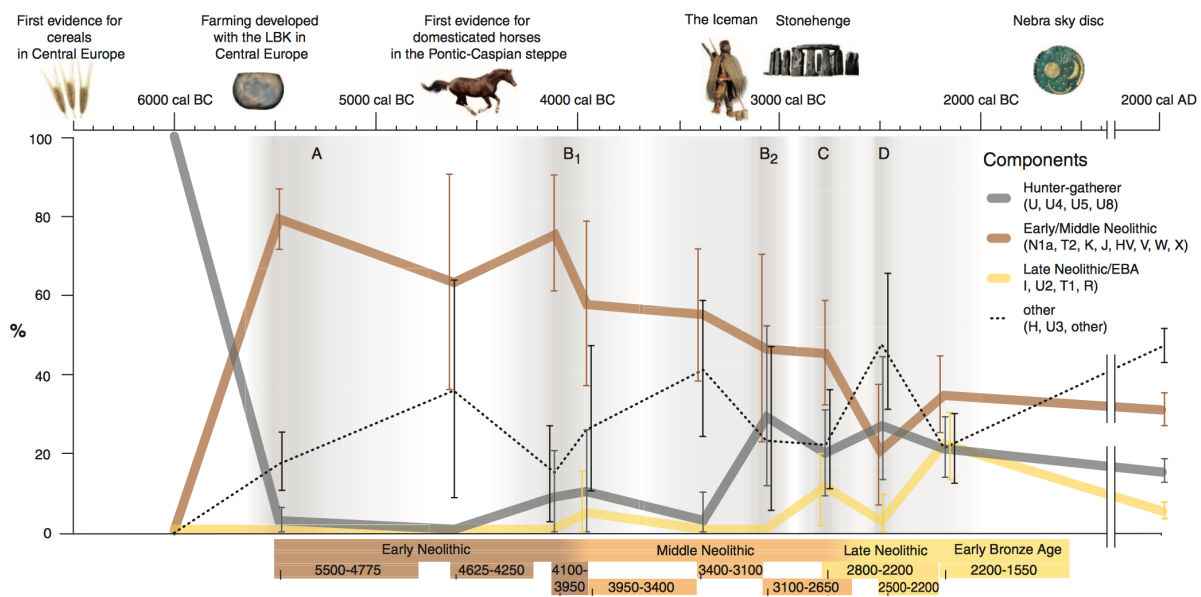


Figure 20: Mitochondrial haplogroups in central Europe from the Mesolithic to nowadays (Brandt et al., 2013)

The situation changed with the arrival of high-throughput DNA sequencing at the beginning of this millennium. PCR is no longer applied to target directly specific regions of the genome anymore. Instead, DNA extracts are turned into genomic libraries which can be sequenced directly or further reamplified for selected regions along the entire genome by means of targeted hybridization capture protocols (see chapter 7.2.2).

These new advances have allowed to recover thousands of ancient genomes all around the world and correlate the most important past phenomenon suggested by archaeology with population movements (e.g Fu et al., 2016; Haak et al., 2015). Human DNA will not be the only target. DNA extracted from bones and teeth also contains information beyond the individual. DNA from bacterial communities (commensal or pathogens) and even DNA viruses, can also survived in ancient tissues and provide information about the host-pathogen interaction, selection and coevolution (Key et al. 2017).

7.2.1 Characteristics of ancient DNA

7.2.1.1 Highly degraded DNA

Genetic material recovered from ancient samples is a highly degraded and has a limited survival time which makes very difficult to recover the genetic sequences from past organisms. Both

factors, age and environmental conditions are the factors which influence most in survival time, although the environmental conditions of preservation is the most important one (Willerslev and Cooper, 2005). Thus, the oldest surviving aDNA evidence coming from the arctic regions (around 200,000 years old) (Willerslev et al., 2003, 2007), or permafrost areas (560,000-780,000 years old) (Orlando et al., 2013). The oldest aDNA recovered from temperate areas come from the 430,000 years old Pleistocene site Sima de los Huesos (Atapuerca) (Meyer et al., 2016).

Postmortem DNA decay is mainly caused by cellular enzymes released from the cytoplasm. Then, nutrients from the cytoplasm engage environmental microorganisms which also contribute to the degradation (Hebsgaard et al. 2005). Chemically, these processes are mainly hydrolysis and oxidation. Hydrolysis produces DNA fragmentation, depurination and deamination (Hansen et al. 2001; Hofreiter et al. 2001) (Figure 21). Oxidation creates base transformations and crosslinks which correlate negatively with the amplification success (Höss et al. 1996).

Depurination is the major cause of DNA fragmentation (Lindahl, 1993). The N-glycosyl bond between the sugar and adenine or guanine residue is cleaved resulting in an abasic site, where the DNA backbone is prone to break and become fragmented (Briggs et al., 2007; Sawyer et al., 2012) (Figure 21).

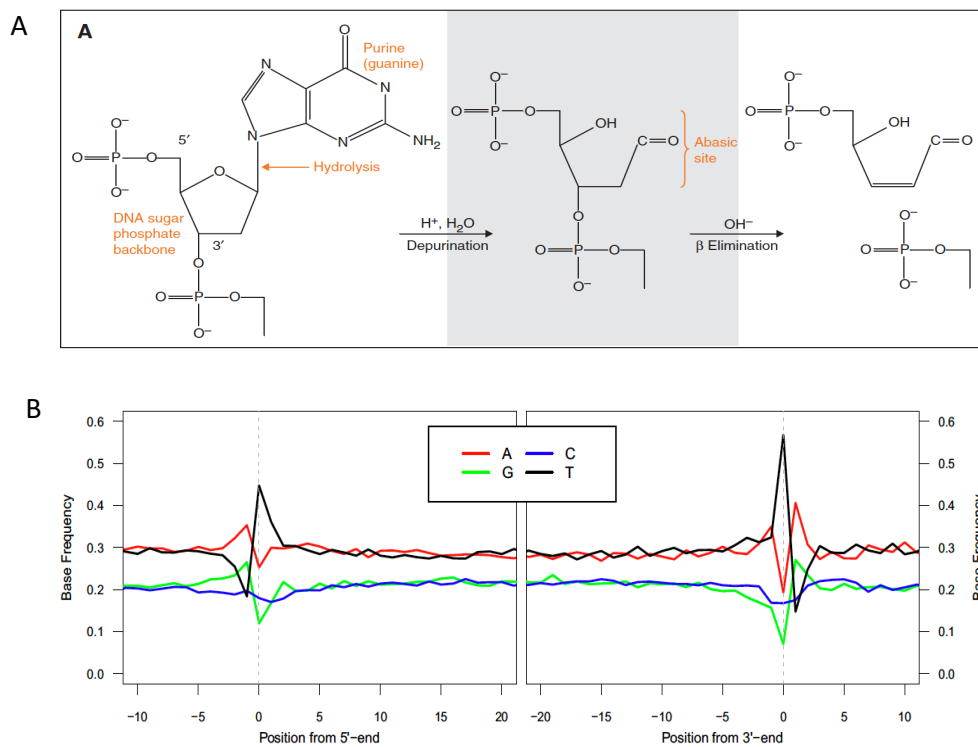


Figure 21: DNA damage: Depurination. A) Process of depurination, N-glycosyl bond between the sugar and the base is cleaved (from [Dabney et al., 2013a](#)); B) DNA fragmentation pattern with a decrease of adenine and guanine at the start point because of the depurination (from [Dabney et al., 2013b](#)).

The deamination of cytosine to uracil creates miscoding lesions in aDNA ([Hansen et al. 2001](#); [Hofreiter et al. 2001](#)). During DNA amplification, the polymerases incorporate adenine (A) instead of guanine (G) across the uracil (U) on the complementary strand, which in the next phase of copying will introduce a thymine (T) across the A on the complementary strand, leading to characteristic C to T and G to A substitutions at deaminated cytosine sites. The process is more likely to occur in terminal single stranded overhangs ([Lindahl, 1993](#)) and shows an exponential decrease of substitutions in the internal part of the sequence ([Briggs et al., 2007](#); [Brotherton et al., 2007](#)). Consequently, aDNA molecules are expected to show increased damage at the terminal ends of the molecule, i.e. C to T at the 5' end as well as the reverse complement G to A substitution at the 3' end. The enzyme Uracil DNA Glycosylase (UDG) can be used to minimise the number of miscoding lesions (C > T, G > A) in aDNA sequences by excising the uracil residues prior to amplification (see methods section) (**Figure 22**).

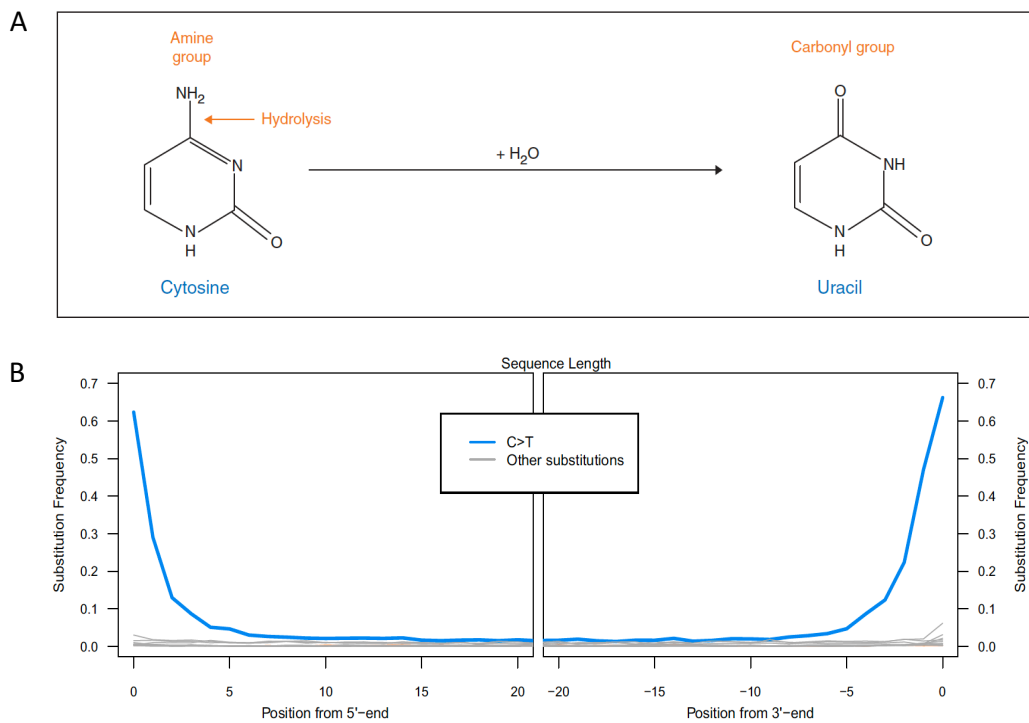


Figure 22: DNA damage: Deamination. A) Deamination of cytosine to Uracil (from [Dabney et al., 2013a](#)). B) C to T substitutions at the 5' and 3' ends (from [Dabney et al., 2013b](#)).

A vast proportion of ancient DNA molecules are usually degraded to less than 50 pb length on average ([Green et al., 2010](#)). PCR based methods have therefore had only very limited power to amplify sequences from such short and damaged DNA fragments, as only a few fragments are long enough (impossible in molecules with less than 40 bp) to allow the hybridization of two PCR primers ([Krause and Pääbo, 2016](#)). Moreover, the presence of miscoding lesions at the end of the aDNA fragments can prevent the correct priming and thus render such damaged fragments inaccessible for PCR. Lastly, the very limited length of the amplified sequence after priming can compromise the sequence identification in downstream analysis.

7.2.1.2 Contamination problems

Due to DNA degradation aDNA studies have to deal with very low amount of endogenous DNA (DNA of the target organism) which rarely exceeds 5% ([Green et al., 2010](#)). This makes it difficult to sequence DNA efficiently from the target individuals unless capture protocols are applied (See Genomic advances). The presence of other kinds of DNA (ancient or modern) not only decreases the sequencing efficiency but can also introduce contamination. PCR-based studies specially increase contamination problems due to the high power of amplification

without specificity (Willerslev and Cooper, 2005). The sources of contamination can come from the environment where the archaeological samples were deposited (environmental ancient contamination) or from the moment when the samples were excavated and manipulated (modern contamination, usually from humans).

Here, so-called DNA-capture protocols can help to increase the amount of endogenous DNA (see chapter 9.1.4) while various bioinformatic filtering tools allow to distinguish between modern and ancient human DNA sequences (see chapter 9.2.2). Here, the characteristics DNA damage patterns described above are used to distinguish aDNA molecules from contaminant sequences.

7.2.2 Genomic advances

The advent of next generation sequencing technologies paired with advanced bioinformatics processing pipeline have revolutionized the aDNA research. It is now possible to generate entire genomes from prehistoric individuals at comparable resolution to modern-day genomic data.

7.2.2.1 Method optimization

7.2.2.1.1 Change in sampling strategy: Petrous bone

Improved sampling methods and a more systematic search for best quality DNA samples have made it possible to retrieve DNA from samples from warmer and wetter climates, which was not possible before (See characteristics of aDNA). Archaeological samples have typically low amounts of endogenous DNA and this content is even lower in temperate ecosystems, where DNA is more degraded (Llorente et al., 2015). Until 2014, teeth were the preferred skeletal element to retrieve aDNA from. Here, the pulp chamber and the root cementum were the main target (Adler et al., 2011; Higgins et al., 2013), but *compacta* from long bones was also often used. In a seminal study by Gamba and colleagues it was shown that petrous bone yielded consistently higher amount of endogenous DNA than teeth, with 4 to 16-fold more endogenous DNA on the whole (Gamba et al., 2014) (Figure 23).

The petrous portion of the temporal bone (*Pars petrosa ossis temporalis*), also called petrous bone, is located in the internal base of the skull. The petrous portion houses the organs located in the inner ear, which constitute the sense of hearing (cochlea) and equilibrium (vestibular

system and semicircular channels). All the organs are included within the otic capsule, which has been shown to be the part with the high endogenous DNA content (Pinhasi et al., 2015) (Figure 23).

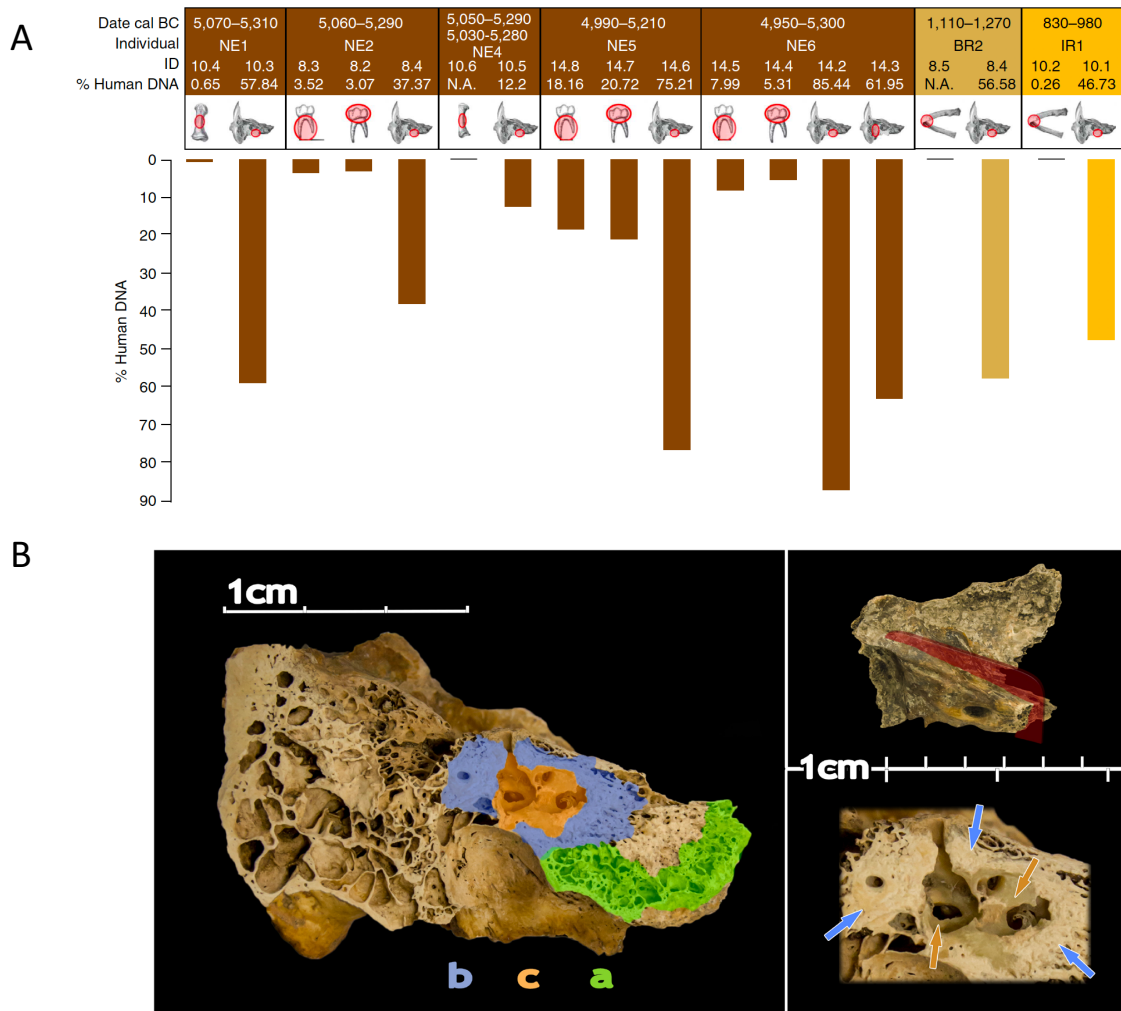


Figure 23: A) Differences in aDNA retrieval (endogenous DNA content) in various bones and teeth tested (Gamba et al., 2014); B) Longitudinal cut through a human petrous portion detailing the target area (c) with best DNA preservation (Pinhasi et al., 2015).

7.2.2.1.2 Improvements of DNA extraction and library protocols

New lab procedures using an improved silica-based extraction protocol has allowed the retrieval of shorter DNA molecules (Dabney et al. 2013). Additionally, DNA library protocols which have the advantage of immortalizing DNA extracts by making them amplifiable, also have empowered the retrieval and sequencing of very short fragments as the generic adaptors that are ligated to each end of the molecules serve as an external PCR priming sites (Kircher et

al., 2012; Meyer and Kircher, 2010) (Figure 24). Single-stranded library protocol further improves the targets, single-stranded (SS) DNA in addition to denatured double-stranded (DS) molecules (Figure 24). In addition, it has been shown that the SS-library protocols showed more efficiency in fishing short molecules in part owing to the reduction of purification steps to remove the excess of adaptors (Meyer et al., 2012). Both library protocols have the advantage of retaining DNA damage patterns characteristic for aDNA molecules, which are widely used to evaluate DNA authenticity (see methods section).

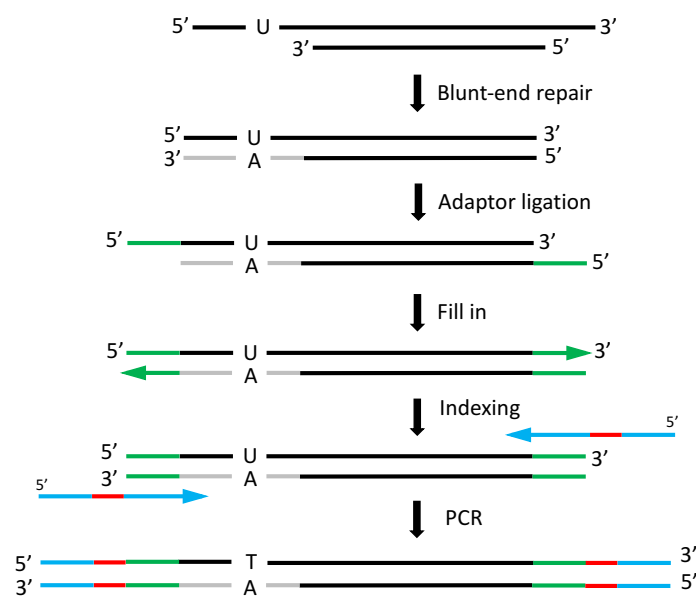


Figure 24: Schematic representation of the main steps involved in double-stranded DNA library preparation.

7.2.2.2 DNA-capture protocols

Ancient human DNA extracts usually contain many different sources of DNA, which can be endogenous, i.e. from the targeted human sample, or exogenous such as soil-derived from environmental DNA (plant, fungi, microbial, etc.) or human contamination. This often makes sequencing human DNA less efficient and costly. Consequently, targeted DNA hybridization capture protocols are used to enriching for molecules that represent the genetic variability of interest, i.e. human DNA in this case.

The first capture protocol on aDNA samples was described by Briggs et al., (2009). This method, called primer extension capture (PEC), used a 5'-biotinylated oligonucleotide primers

which anneal to a specific target region. These target regions together with adaptors and barcodes are amplified using DNA polymerases, resulting in a double stranded association between primer and target, including the 5' adaptors. Biotinylated primers plus targets are captured by streptavidin-coated magnetic beads, and then eluted from them. Finally, targets are further amplified with adaptor priming sites.

7.2.2.2.1 In-solution DNA capture

While various DNA capture methods exist, such as solid-array techniques (Burbano et al., 2010) or capture protocols use probes with streptavidin-coated magnetic beads that bind target DNA (Maricic et al., 2010), the most widely used are in-solution capture protocols because they require no special equipment and allow fast processing and guarantee a high specificity (Figure 25).

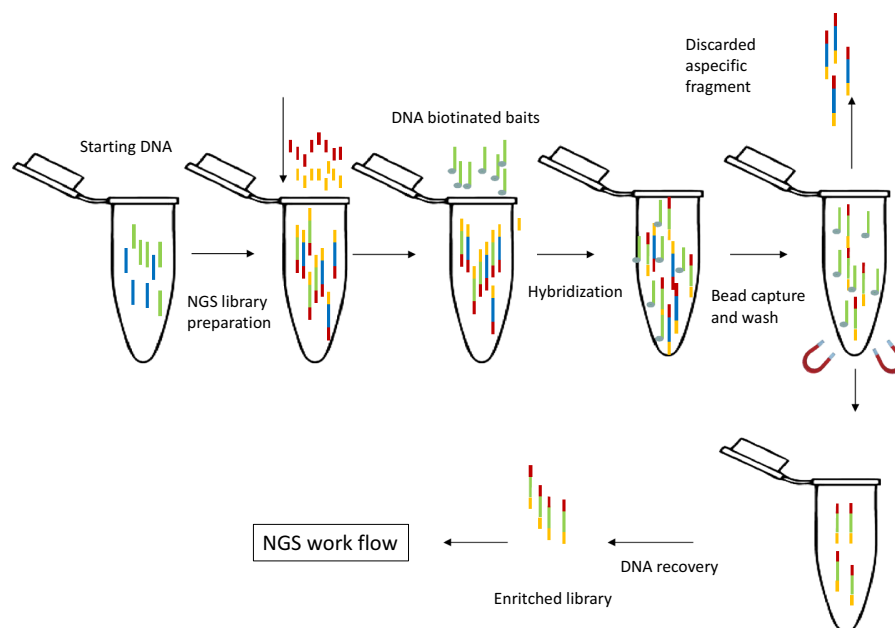


Figure 25: In-solution capture workflow adapted from (Rizzi et al., 2012).

7.2.2.2.2 Probes

Probes in use are designed by Agilent technologies exclusively for MPIs in Jena and Leipzig and Harvard Medical School (Boston) using proprietary protocols. The 50-mer probes either side of the targeted variant cover a 105 bp flanking region in addition to two probes each of

which carries one of the two alleles. In sum, a total of four probes are used to target each SNP in the panels used (Fu et al., 2013). The probes are single-stranded and carry a 5'biotinylated primer site. During hybridization, the probes pair with complementary denatured ssDNA fragments of the ancient DNA libraries and these molecules are then concentrated with magnetic streptavidin beads using a magnet. After purification steps the targeted DNA molecules are eluted from the beads and further amplified (Fu et al., 2013; Gnrke et al., 2009) (Figure 26).

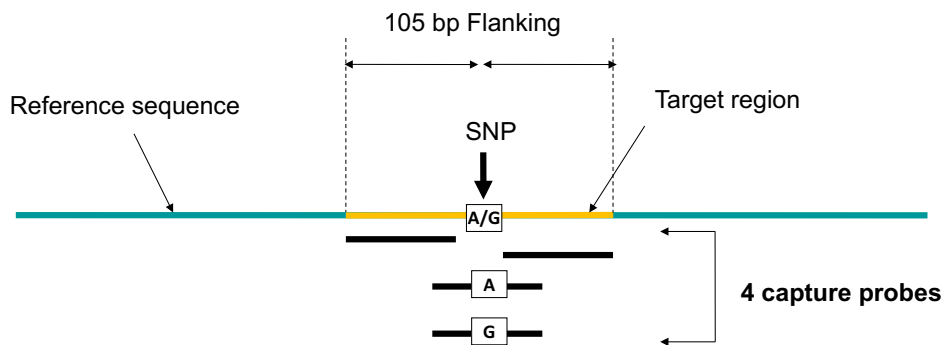


Figure 26: Scheme of the probe design for a targeted SNP.

7.2.2.2.3 Probe panels

- The in-house **1240K panel** contains 1.2 million variants in the human genome, of which 560K SNPs overlap with the commercially available Human Origins (HO) Affymetrix array and >600,000 additional SNPs that were ascertained in Yoruba and San and are informative for non-African populations. The 1240K array was first described in Mathieson et al., (2015).
- The in-house **Mitochondrial genome capture** contains probes which cover the entire mitogenome (RSRS). Mitogenome is covered by 52 bp capture probes with 3 bp tiling.
- **Big Yoruba panel:** this panel was developed to obtain an outgroup-ascertained set of SNPs for African populations (Skoglund et al., 2017). It contains 814,242 transversions that are polymorphic between the archaic Denisovan (Meyer et al., 2012) and Neanderthal (Prüfer et al., 2014) genomes and two Yoruba individuals.
- **Archaic panel:** This panel includes all SNPs where Yoruba carry one allele in high frequency while the archaic genomes (Neanderthals and Denisovans) carry

the alternative. Archaic capture is applied to ancient individuals to look for archaic admixture (Fu et al., 2016).

- **Pathogen captures:** There are also specific set of probes which cover the entire genome of some pathogens, e.g. *Yersinia pestis* (plague) (Spyrou et al., 2018), *Salmonella enterica* (Vågene et al., 2018), etc.

7.2.2.3 Next Generation Sequencing (NGS)

Before Second and more broadly Next Generation Sequencing, the most widely used sequencing technique was following the method first described by Sanger (Sanger et al., 1977). The ‘Sanger method’ is based on synthesis chain termination. The complementary chain of a single stranded DNA is synthesized in four different slots. Every slot contains normal dNTP (dATP, dGTP, dCTP y dTTP) and one single kind of ddNTP (ddATP, ddGTP, ddCTP y ddTTP) which stops the DNA synthesis. That creates fragments with different sizes that can be sorted by size in an electrophoresis gel. The automatization of Sanger method consists on the incorporation of ddNTPs labelled with different fluorochroms and light signals are recorded and automatically sorted by fragment size (Figure 27).

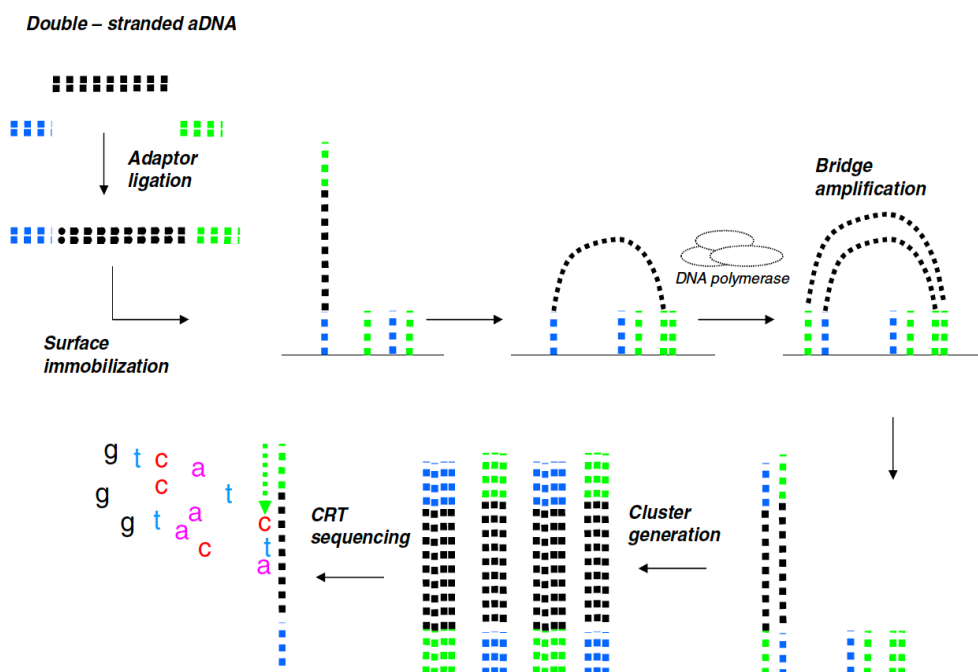


Figure 27: Illumina NGS workflow adapted from (Rizzi et al., 2012).

In contrast to long read length Sanger sequencing techniques, only partly suited to aDNA, the short length reads of second and next generation sequencing techniques offered great

opportunities for ancient DNA research as the DNA fragments could be sequenced without shearing of DNA molecules. DNA library preparation protocols were equally suited to short fragmented read length and only required end repair steps to utilize the vast majority of short molecules that could be recovered from aDNA extracts (see chapter 7.2.2 and 9.1).

DNA polymerase adds fluorescent nucleotides one by one in a DNA template strand. Libraries are used as a template to incorporate labelled nucleotides going through the its universal adaptors. Each incorporated nucleotide is identified by its fluorescent tag. Additionally, the introduction of individuals barcoding inside the adaptors makes also possible to track and identify the sample after sequencing (Kircher et al., 2012; Meyer and Kircher, 2010) (**Figure 27**). The main point of NGS, also known as massive parallel sequencing, is that millions of fragments (DNA libraries) are simultaneously synthesized at the same time (Consortium et al., 2001; Venter et al., 2001). Thus, Illumina NGS instruments can generate multiple terabases (Tb) of data per run, which would require a bioinformatic processing. The automatization of the high throughput sequencing process makes possible to sequence many human genomes at the same time.

8 ISOTOPE METHODOLOGY

Once time the bones and teeth were identified and selected in their respective museums, I proceeded with the sampling strategy. This varied depending on the isotope analysis. Bones were used for carbon and nitrogen analysis in order to approach the subsistence strategies, and teeth were only used for strontium isotope analysis to approach the mobility patterns. An overview description of the different approaches is described in the chapter 4. In this chapter, I will describe the laboratory procedure of each isotope technique.

The sampling selection was different and adapted to different techniques and archaeological characteristics of each site. To see an accurate description of the sampling selection performed on each study, please consult the “Materials” section of the publications.

8.1 Carbon and Nitrogen isotopes procedures

We used carbon and nitrogen stable isotopes to approach the subsistence strategies during the Iberian Early Neolithic and Late Neolithic-Chalcolithic periods. The carbon and nitrogen isotope sample preparation and analysis of all the bone samples was carried out at the Department of Archaeology of the University of Cape Town (South Africa) (**Figure 28**).

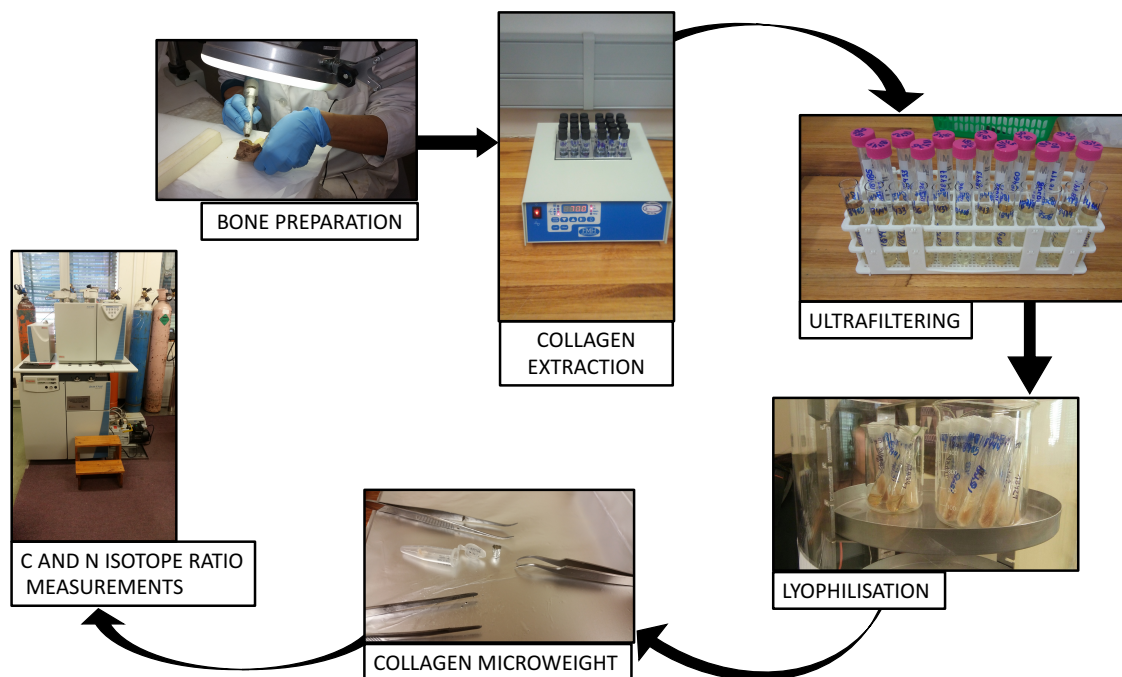


Figure 28: Standard procedure for C and N isotopic analysis.

8.1.1 Bone Preparation

The bone samples were cleaned by removing the bone outer layer to avoid the introduction of some contaminants by mechanical abrasion using a 220 Dremel 3500 drill. Approximately 300 mg of cleaned bone sample is use for the next steps (**Figure 28**).

8.1.2 Collagen extraction

Next step consists on retaining the organic part of the bone and removing the inorganic one. In our method, we are specifically interested on extracting and isolating the majority structural protein present in bones, collagen. The protocol includes some steps to remove the potential contaminants but, a minimal amount of another kind of bone of bone protein can be retained (e.g phosphoproteins or fibronectins) (**Figure 28**).

Collagen extraction was done following the Longin (1971) method with the addition of an ultrafiltration step (Brown et al., 1988). Approximately 300 mg of cleaned bone samples from each individual were introduced in 0.5M HCl solution at 5°C in order to keep low the speed of bone demineralization and therefore damage less the sample. This process can take one or two weeks and you need to check the consistency of the bone and change the acid solution every 4-5 days until demineralized. When the bone acquires a flexible consistency with no trace of hard surface it is considered fully demineralized. Demineralized samples were rinsed three times with deionized water to remove the acid traces until pH became neutral. If the consistency of collagen was too soft that it became prone to dismantling, a pipette was used to remove the acid and to add the water. Finally, tubes must be filled with bidistilled water and 1-3 drops of HCl 0.5M were added to get a final pH of 3 to start the process of gelatinization. Collagen was then gelatinized at 70°C for 48 hours using a heater block (FMH instruments, South Africa). This acidic and high temperature environmental conditions allow to brake the collagen triplex helix make it soluble (**Figure 28**).

8.1.3 Filtering and ultrafiltering

The resulting solution containing the gelatinized collagen is filtered with a 9 ml EZEE-filter (Elkay, United Kingdom) to remove small (<8 µm) insoluble particles. The filtration process is mandatory in this protocol. The ultrafiltration process is not fully standardized but is highly recommended in order to remove small organic substances like humic acids, as well as for

retaining for analysis only the less degraded collagen proteins. With the ultrafilters we collect the largest collagen protein chains, the best quality ones (>30,000 kDa or >10,000 kDa, depending on the ultrafilter selected) (Liden et al., 1995). Moreover, the gelatinization process could create a preferential loss of some aminoacids which can originate a bias in the C:N ratio that we use as quality control (see chapter 4.3.1.4). Ultrafiltration process solves this issue because it discards the low weight collagen chains (Grupe, 2001) (**Figure 28**).

We have used 30 kDa ultrafilters (Amicon, Germany) for all our samples. The ultrafilters were cleaned with a run of centrifugation of 0.5M NaOH at 2500 rpm followed by three more runs of centrifugation with bidistilled water using a centrifuge at 2500 rpm (Thermo Fisher Scientific Megafuge 16, USA). The gelatinized collagen is transferred with the help of a pipette into the ultrafilters and they are centrifuged during variable times depending on the filtering speed of each sample. The time of centrifugation must be controlled carefully in order to not lose the entire collagen solution. Finally, we get a solution of ~500 μ L enriched in > 30kDa collagen chains. We rinsed the filter with another 500 μ L to collect the potential collagen trapped arriving up to 1 mL of total volumen. We keep the <30 kDa fraction in case there is not enough > 30kDa collagen (**Figure 28**).

8.1.4 Freezing and lyophilisation

The final solution (~1 mL) was frozen at -20 to -35 °C in tubes covered by parafilm for at least 24h. Then, only once they are totally frozen, we carry the samples from the freezer to the freeze-dryer as soon as possible to avoid the collagen melting. The parafilm cover is pierced with a needle to prevent the brake of the tube during the process and allowing the evaporated water to leave the test tube. The lyophilisation process takes 48 hours and consists on the removal of the water by sublimation (from solid to gas). Finally, we transfer the collagen from the tubes to eppendorfs and we weight it to calculate the collagen yield (**Figure 28**).

8.1.5 Collagen microweight and carbon and nitrogen isotope ratio measurements

Duplicates of ca. 0.5 mg (0.45-0.55mg) of collagen per sample were weighed into tin capsules, and loaded into the mass spectrometer. The microbalance was cleaned with ethanol among samples in order to avoid cross-contamination. The carbon and nitrogen isotope ratio measurements were performed using a Finnigan Delta plus XP continuous-flow isotope ratio

mass spectrometer (Thermo Fisher Scientific, USA) after being combusted in an elemental analyser Flash EA 1112 interfaced with it (Thermo Fisher Scientific, USA) directly at the Isotope Facilities of the University of Cape Town. Stable Carbon isotope ratios were expressed relative to the VPDB scale (Vienna Pee Dee Belemnite), and stable Nitrogen isotope ratios were measured relative to the AIR scale (atmospheric N₂), using the delta notation (δ) in parts per thousand (‰).

The accuracy of measurements was monitored using international and in-house standards with well-known isotopic composition (MG: $\delta^{13}\text{C}$ 21.3 ± 0.3 , $\delta^{15}\text{N}$ $7.3 \pm 0.1\text{‰}$; seal: $\delta^{13}\text{C}$ $12.7 \pm 0.1\text{‰}$; $\delta^{15}\text{N}$ $15.6 \pm 0.1\text{‰}$; valine: $\delta^{13}\text{C}$ $27.7 \pm 0.1\text{‰}$; $\delta^{15}\text{N}$ $15.6 \pm 0.1\text{‰}$). Precision was determined with the repeated measurements of standards and sample replicates, determined an average analytical error lower than 0.1‰ (1 σ) for $\delta^{13}\text{C}$ and $\delta^{15}\text{N}$ in standards and in sample replicates. All the samples were measured in duplicate. Samples which showed bad quality of collagen according to Ambrose (1993), DeNiro (1985) and Van Klinken (1999) parameters were not considered for interpretation of the results (more information in chapter 4.3.1.4) (**Figure 28**).

8.1.6 Data analysis

Once the samples with low quality were discarded, we calculated the average and the standard deviation of the duplicated measurements. We determined an acceptable analytical error something below 0.1‰ (1 σ) between sample replicates.

We use non-parametric statistical analysis, Mann-Whitney test for one variable and Kruskal-Wallis test for more than one variable, when we want to test for significant differences among groups of isotopic values (e.g. males and females or adults and subadults groups). We also performed Multi Dimensional Scale analysis (MDS) in the Isotope discussion chapter as clustering method to infer eco-geographical regions based on collagen isotopic values.

8.2 Strontium isotope procedures

We used strontium isotopes from tooth enamel to approach the provenance and mobility patterns of humans from different phases of the Neolithic in Northern Iberian sites that we got the access. The strontium isotope analysis of all the teeth samples was carried out at the

Department of Geology of the University of Cape Town (South Africa). Strontium isotope procedures, contrary to what happens with carbon and nitrogen ones, need *clean* laboratories to avoid the presence of environmental strontium in the laboratory where samples are prepared. Moreover, the process also changes depending of the material analysed: archaeological teeth, modern plants or modern snails (**Figure 29**).

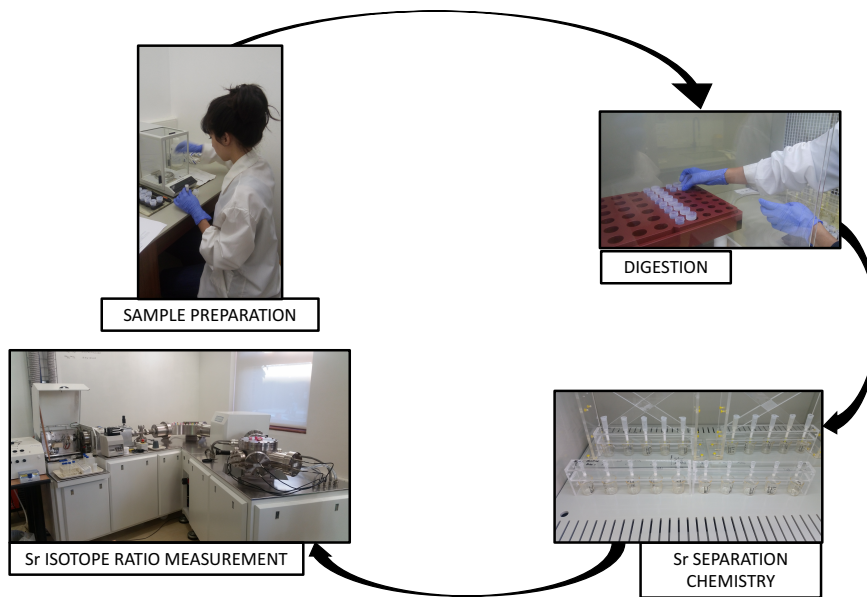


Figure 29: Standard procedure for Sr isotopic analysis.

8.2.1 Enamel sample preparation for strontium isotope analysis

This step of the process can be performed outside the cleanlab but always using sterilized material and gloves. A transversal portion of enamel (ca. 20 mg, from the top of the crown to the end) was cleaned by abrasion and possible dentine remains were removed using a Dremel 3500 drill bit, rinsed and ultrasonicated for 20 minutes in MilliQ water. We kept the enamel samples over the hood until the water dried out. Diamond drill bits were cleaned with ethanol and ultrasonicated in MilliQ water between samples to avoid cross-contamination (Budd et al., 2000).

Modern snail shells and microfauna teeth were cleaned following the same procedure as that for enamel. In this case, we took ca. 40 mg of shell and microfauna teeth. For modern plants, the procedure need a previous step of calcination of the green parts during 8h at 500°C (**Figure 29**).

8.2.2 Digestion

The objective of this step is to make the samples soluble in order to proceed with the strontium separation chemistry. The cleaned enamel sample was digested with 2mL bi-distilled 65% HNO₃ in a closed Teflon beaker placed on a hotplate at 140 °C for an hour. Digested samples were then dried and redissolved in 1.5 mL of bi-distilled 2M HNO₃. These redissolved samples were centrifuged at 4000 rpm for 20 minutes, and the supernatant was collected for strontium separation chemistry. In the case of the archaeological samples only, a separate fraction for each sample in this step was used to calculate the concentration with ⁸⁸Sr intensity (V) regression equation built with SRM987 standard from NIST (National Institute of Standards and Technology, Gaithersburg, MD, USA).

The same procedure is performed with the snail shells. For plants, the digestion is done with 48% HF and bi-distilled 65% HNO₃ (4:1 respectively) as it is described in Copeland et al. (2016). No strontium concentrations were measured in modern samples because diagenetic effects were not expected (Figure 29).

8.2.3 Strontium separation chemistry by ion-exchange columns and preparation for analysis

Strontium was isolated with 200µl of Eichrom Sr.Spec resin loaded in Bio-Spin Disposable Chromatography Bio-Rad Columns following the method of Pin et al. (1994). The pre-conditioning of the columns was done with 2 x 1mL 2M HNO₃. The samples were loaded on the column in two times (2x 0.75 µL), and then washed six times with 2M HNO₃. Finally, we collected the strontium in 1.5 mL of bi-distilled water inside a Teflon beaker. The separated strontium fraction for each sample was dried down at 120°C during 6-8 h, dissolved in 2 ml 0.2% bi-distilled HNO₃, and diluted to 200 ppb Sr concentrations for isotope analysis. The columns were cleaned after the process using 6.2 M HCl, MilliQ H₂O, 7M HNO₃ and MilliQ H₂O again (Figure 29).

The concentrations were measured extrapolating the measured Sr values with MC-ICP ThermoFisher XSeries 2 into a calibration curve built with different known standards concentrations.

8.2.4 Strontium isotope ratio measurements and quality controls

$^{87}\text{Sr}/^{86}\text{Sr}$ ratios were measured using a NuPlasma HR multicollector inductively-coupled-plasma mass spectrometer (MC-ICP-MS). Sample analyses were referenced to bracketing analyses of SRM987, using a $^{87}\text{Sr}/^{86}\text{Sr}$ reference value of 0.710255 from NIST. All strontium isotope data are corrected for isobaric rubidium interference at 87 amu using the measured signal for ^{85}Rb and the natural $^{85}\text{Rb}/^{87}\text{Rb}$ ratio. Instrumental mass fractionation was corrected using the measured $^{86}\text{Sr}/^{88}\text{Sr}$ ratio and the exponential law, and a true $^{86}\text{Sr}/^{88}\text{Sr}$ value of 0.1194. Results for repeat analyses of an in-house carbonate standard processed and measured with the batches of samples in this study ($^{87}\text{Sr}/^{86}\text{Sr} = 0.708936$; 2 sigma 0.000041; n=33) are in agreement with long-term results for this in-house standard ($^{87}\text{Sr}/^{86}\text{Sr}$; 0.708915; 2 sigma 0.000047; n=125). For every two batches one blank was added to assess the cleanliness of the process; there was no peak and, thus, no contamination from external Sr in any of the batches (**Figure 29**).

8.2.5 Data analysis

The range of values of the bioavailable samples was represented and compared with the human values in order to see if the human ones fall inside or outside the range. We always include the outliers in the range representation (highest, lowest and intermediate values). To compare different if bioavailable areas were significantly different, different non-parametrical Kruskal-Wallis statistical tests were performed.

9 aDNA METHODOLOGY

9.1 Lab processing

9.1.1 Sampling and sample processing of ancient human remains

The dense parts of the petrous bone have been identified as the best bone from which to retrieve nuclear DNA (Gamba et al., 2014; Pinhasi et al., 2015). Traditionally, teeth have long been used as another skeletal element with relatively high endogenous DNA because they are protected in the alveoli, which encapsulate the pulp cavity (Adler et al., 2011; Higgins et al., 2013), which has been shown to allow the recovery of blood-borne pathogens (Andrades Valtueña et al., 2017; Bos et al., 2011; Spyrou et al., 2018). Teeth and petrous bones are not always available in our case, and so other bones have been also included.

In this work, different bones and teeth (molars) have been sampled in the clean room facilities of the Max Planck Institute for the Science of Human History (MPI-SHH) in Jena, Germany. Prior to sampling, samples were irradiated with UV-light for 30 min at all sides. Different sampling methods were used for different bone types, including sandblasting, grinding with a mortar and pestle, and cutting and drilling into the denser regions at low speed using a Kavo dental drill hand-piece. Prior to sampling, teeth surfaces were cleaned with a low concentration bleach solution (10%) and wiped off with water later. For some of the teeth, the crown was separated from the root by cutting along the cementum/enamel junction with a hand saw, followed by drilling into the pulp chamber at low speed (Posth et al., 2018) to collect tooth powder. For others, the complete tooth was ground into powder using a Retsch mixer mill (Szécsényi-Nagy et al., 2017) (Figure 30).

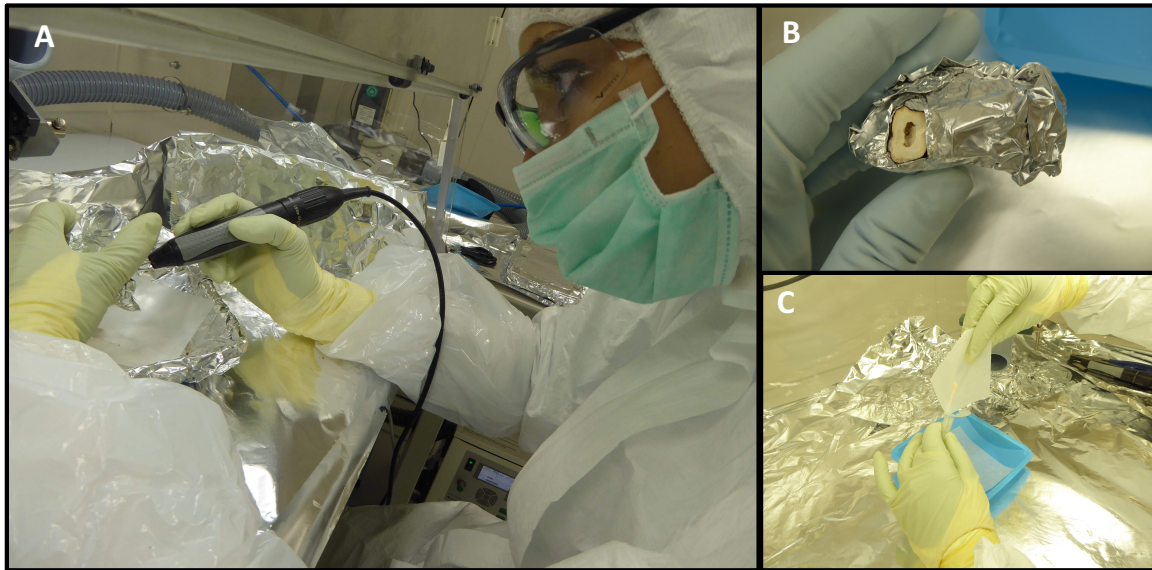


Figure 30: Sample processing in the aDNA clean lab. A) Drilling; B) Drilled pulp chamber; C) Aliquoting tooth powder for DNA extraction.

9.1.2 DNA extraction

The DNA extraction describes the bio-chemical isolation of DNA molecules from bone and tooth powder. This also entails the digestion and lysis of other biomolecules present in the bone tissue, such as proteins, humic acids and tannins that could inhibit the downstream analysis.

DNA extraction was carried out following a modified version of the silica-based extraction protocol by Dabney et al. (2013). We started with an initial amount of 50-100 mg of bone or tooth powder. Samples were digested to release the DNA from the powder with the 1 ml of extraction buffer per sample (900 μ l of 0.5M EDTA, 75 μ l of UV H₂O and 25 μ l of 10 mg/mL Proteinase K) in a rotator at 37 °C for 16-24h. EDTA chelates hydroxyapatite and Proteinase K has the function of digesting proteins by cleaving peptide bonds. The suspension was centrifuged (2 minutes at 14,000 rpm) and the supernatant transferred to a new 50 ml Falcon tube containing 10 ml binding buffer per sample (4.77 ml of 5M Guanidine hydrochloride, 4 ml Isopropanol at 40% and filled up to 10 ml with UV H₂O) and 400 μ l of Sodium Acetate, mixed and then onto silica columns (High Pure Viral Nucleic Acid Kit; Roche). The silica columns with the conjugated DNA were first washed with 450 μ l wash buffer (High Pure Viral Nucleic Acid Kit; Roche) and then the DNA was eluted in 100 μ L TET (TE-buffer with 0.05% Tween). This method has been shown to yield a higher amount of short-DNA molecules when compared to other methods (Rohland and Hofreiter, 2007). The differences between the Dabney

et al. 2013 protocol and the Rohland and Hofreiter (2007) protocol are: the composition of the binding buffer (previously sodium acetate, sodium chloride, and guanidine thiocyanate), the increase of the volume of binding buffer relative to that of the extraction buffer, and the replacement of silica suspension to silica spin columns adapted to falcon tubes to enable load large volumes (Dabney, Knapp, et al., 2013) (**Figure 31**).

Two extraction blanks were included in each extraction batch to check for cross-contamination between samples and background contamination from the lab environment and the chemicals that were used.

9.1.3 Library preparation

Double-stranded (ds) DNA libraries with unique index pairs (Kircher et al., 2012) following a protocol by Meyer and Kircher (2010) and partial Uracil DNA Glycosylase treatment (UDG-half) (explained below) was used (Rohland et al., 2015). Uracil DNA Glycosylase (UDG) is an enzyme which prevents the mutagenesis in *E. coli* by excising uracil residues, leaving abasic sites and initiating the Base Excision Repair (BER) (Briggs et al., 2010; Krokan and Bjørås, 2013). The enzyme has a positively charged channel which binds to ssDNA or dsDNA and scans the sequence for Uracil residues, which are then subsequently cleaved. As a result, the UDG enzymatic reaction reduces C to T and G to A misincorporations in the final sequence reads (**Figure 31, Figure 24**).

Concretely, 25 μ L DNA extract were used for incomplete Uracil DNA Glycosylase treatment ('UDG-half') in order to retain a partial damage pattern characteristic for ancient DNA. This treatment removes deaminated cytosines (Uracils) except for the final nucleotides at the 5' and 3' read ends (Briggs et al., 2010). We used USER enzyme, which combines UDG and endonuclease VIII. UDG catalyzes the excision of uracil leaving abasic sites, and the endonuclease VIII cleaves the molecule the abasic sites leaving 5' and 3' phosphate groups on both sides. The USER enzyme (0.072 U) was included in a mastermix solution which also contained Buffer Tango (1.2 x), ATP (1.2 mM), BSA (0.2 mg/ml), dNTP (0.1 mM) and UV H₂O in a final volume of 50 μ l per sample. After 30 min at 37°, a UDI inhibitor (0.1343 U) is added, which stops the reaction. This results in the excision/cleavage of all damaged sites, except for those at a dephosphorylated 5'U terminus, which retain a damage pattern with around 10% of C to T transitions at the first sites to authenticate the DNA reads as ancient, whilst guaranteeing maximum sequence fidelity on the remainder of the read.

We repaired the overhanging 5' and 3' terminal ends of the DNA fragments synthesizing DNA in the direction 5' to 3' with the presence of a complementary DNA template and removing overhanging nucleotides with exonuclease activity in 3' to 5' direction, using T4 DNA Polymerase (NBE) (1.65 μ l, 0.085 U). We then used T4 Polynucleotide Kinase (PNK) (3 μ l, 0.515 U) to transfer phosphate groups from ATP and attach them to the 5' hydroxy-ends, and at the same time remove the 3' phosphate. Both reactions happen incubating libraries at 25 °C for 20 min, and then at 12°C for 10 min in the thermocycler. Then, we purified the library products with MinElute kit as is described below. We start mixing library products independently with PB buffer and load onto MinElute Columns and incubating there during 1 to 2 minutes. Supernatant is discarded spinning the columns during 30 seconds at 13,000 rpm. Following, columns were washed with 700 μ l of PE buffer and the supernatant is discarded spinning the columns during 30 seconds at 13,000 rpm. After two dry spin of 1 minute at 13,000 rpm, columns are located in a new 1.5 ml LoBind tubes and libraries where 20 μ l of pre-heated EB containing 0.05% of Tween were added during 1 minute and eluted spinning the columns during 1 minute at 13,000 rpm (**Figure 31, Figure 24**).

After a purification step, Illumina adaptors were ligated using the Quick Ligation Kit (NBE) which contains ligation buffer and ATP (20 ml at 1x), and the adaptors separately (1 μ l at 0.25 μ M) in a total volume of 40 μ l. The T4 DNA ligase was added (0,125 U) later and ligates the ends of the DNA duplex with 5' phosphate group with the Illumina P5 and P7 adapters. The adapters lack 5' phosphates to avoid potential adapter dimers. The ligation reaction was carried out at room temperature (20 minutes at 22°C in the thermocycler). The process of adapter ligation is not directional, which creates DNA molecules with the same kind of adapters at both ends (5' and 3'). Such molecules will conform hairpin structures and will not interfere during the downstream steps. After the adaptor ligation there is another purification step with MinElute column kit (described before).

The remaining 20 μ l nicks between adaptors and DNA sequences are removed/filled in with the Bst 2.0 DNA polymerase which contains DNA polymerase activity and displaces the adapter strand and new elongation of the strand in 5' to 3' direction thereby closing the nick between adapter and molecule. The 'adapter fill in' mastermix contains Isothermal Buffer (4 μ l at 1x), dNTPs (0.20 μ l at 0.125 mM), Bst Polymerase (2 μ l at 0.4 U) and UV-Water up to a

volume of 40 μl . This reaction happens in the thermocycler, during 30 minutes at 37 °C, followed by 10 minutes at 80 °C.

After this step, we quantify the DNA copy number of molecules in our libraries, and calculate the number of splits to perform the following index PCR reaction. The qPCR reaction was set up in the clean lab environment using the 10 μl of the DyNAmo SYBP Green qPCR Kit (0.5 x) (Thermo Fisher Scientific), an aliquot of each library (1 μl of 1:10 dilution), 1 μl of IS7/IS8 primers (0.5 μM) (Meyer and Kircher, 2010), while the amplification was carried on a LightCycler 480 (Roche) in the ‘modern lab’. qPCR reactions have an initial denaturation at 95°C for 10 min and 40 cycles of 95°C for 30 seconds, 60°C for 60 seconds, and 72°C for 30 seconds, followed by a melting curve with continuous recording of emission from 60-95°C. The success of the library preparation for each sample is validated by comparing it to the amount of DNA molecules in a known positive control (cave bear) as well as to the library blanks (Figure 31, Figure 24).

After quantification, a unique pair of index combinations were assigned to each library (Kircher et al., 2012). All reactions are adapted to contain less than 1.5×10^0 molecules. Indexing PCR mastermix contains 10 μl of Pfu Turbo Buffer at 1 x, 1.5 μl of BSA at 0.3 mg/ml, 1 μl of dNTPs at 0.25 mM, 1 μl of Pfu Turbo Polymerase at 0.025 U and 2 μl of each P5 and P7 at 0.2 μM . DNA and UV-water were adapted to reach the required concentration. Indexes and the full-length adapters were added by PCR amplification using PfuTurbo DNA Polymerase (Agilent) and 5'-tailed IS5/IS6 primers outside of the cleanroom. PCR reaction was set up at 95°C for 2 min and 10 cycles of 95°C for 30 seconds, 58°C for 30 seconds, and 72°C for 1 minute, followed by a final elongation at 72°C for 10 min. After amplification, the indexed libraries were purified with MinElute columns (Qiagen) (process already described) and eluted in 50 μl EBT (EB containing 0.05% of Tween) and quantified with using the DyNAmo SYBP Green qPCR Kit and IS5/IS6 primers (Thermo Fisher Scientific) on the LightCycler 480 (Roche), as it was described in the previous qPCR reaction (Meyer and Kircher, 2010). Herculase II Fusion DNA Polymerase (Agilent) and the same IS5/IS6 primers were used for the subsequent amplification of the indexed products up to a copy number of 10×10^{-13} molecules/ μL . After purification, the indexed libraries were quantified precisely using a TapeStation (TapeStation Nucleic Acid System, Agilent 4200) in order to dilute and combine the library aliquots to a 10nM equimolar pool (Figure 31, Figure 24).

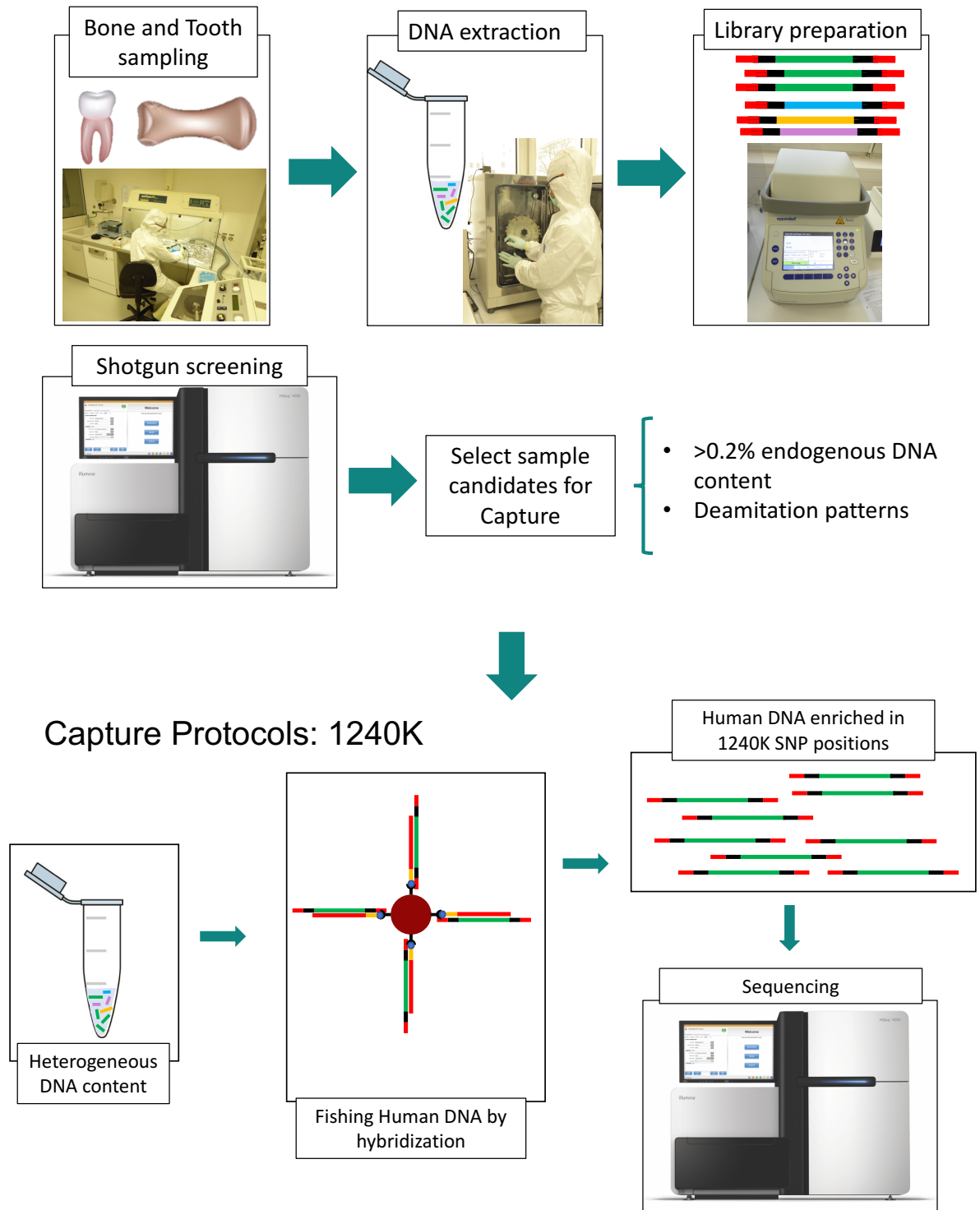


Figure 31: Schematic process of laboratory methods (to see a more detailed Schematic representation of the main steps involved in double-stranded DNA library preparation, see Figure 24).

9.1.4 Shotgun screening and in-solution enrichment of nuclear DNA (1240k capture) and mtDNA (mitocapture)

The pooled double indexed libraries were sequenced on an Illumina HiSeq2500 platform for a depth of ~5 million read cycles, using either a single (1x75bp reads) or double end (2x50bp reads) configuration. Reads were demultiplexed by their respective index combinations and then further processed with EAGER 1.92.32 (Peltzer et al., 2016) to assess the quality and quantity of endogenous human DNA in each library. Libraries that showed a damage pattern characteristic for ancient DNA and >0.2% of the reads mapping to the human reference sequence were selected for targeted in-solution capture. Prior to capture, the selected libraries were amplified using the IS5/IS6 primer set to reach a concentration of ~200-400 ng/mL. Following this, the libraries were hybridized in-solution to different oligonucleotide probe sets synthesized by Agilent Technologies to enrich for the complete mitogenome (mtDNA capture, (Maricic et al., 2010)) and for 1,196,358 informative nuclear SNP markers (1240k capture, (Fu et al., 2015; Mathieson et al., 2015)) (Figure 31).

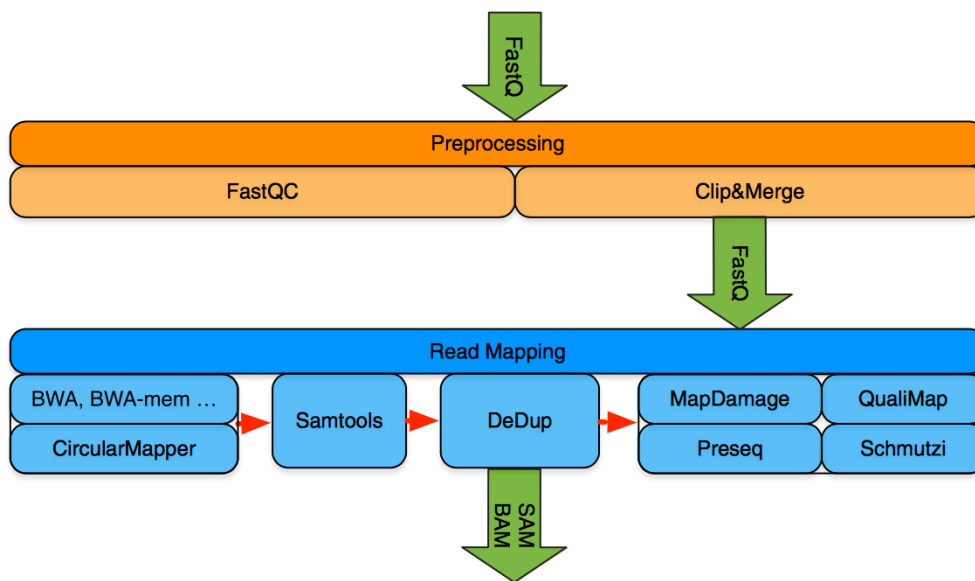


Figure 32: Part of the workflow of the EAGER pipeline used in read processing (Figure from Peltzer et al., 2016).

9.2 Bioinformatic data processing

9.2.1 Read processing

Sequenced libraries were demultiplexed according to individual library indexes, allowing for at most one mismatch. Library adapters were clipped using AdapterRemoval v2.2.0 (Schubert et al., 2016) before mapping to the reference genome to maximise mapping efficiency. For paired-end reads, we restricted to merge fragments with an overlap of at least 30 bp. Finally, single-end reads shorter than 30 bp were discarded. Mapped DNA fragments were assembled to the Human Reference Genome Hs37d5 using the Burrows-Wheeler Aligner (BWA, v0.7.12-r1039) *aln* and *samse* commands (-l 16500, -n0.01, -q30) (Li and Durbin, 2009). Reads with mapped quality Phred scored below 30 were not retained.

After mapping, PCR duplicates were removed using DeDup v0.12.1 from samtools (Li et al., 2009), which eliminates the clonality from PCR amplifications, which are needed to reach the required concentrations for shotgun (SG) sequencing and capture (mt and 1240K). This step is important to estimate the true X-fold coverage of a site, in particular for downstream analyses that require the true ratio of heterozygote allele calls, e.g. phenotypic traits, or when estimating background contamination (Korneliussen et al. 2014).

9.2.2 Assessment of ancient DNA authenticity

The assessment of ancient DNA authenticity is a crucial step since modern DNA molecules are ubiquitous and thus the most common source of contamination. The first step to minimise contamination with modern DNA is to restrict work to dedicated clean labs (see above). However, there are also bioinformatics tools that can help to identify and estimate contamination *post hoc*. We are able to distinguish aDNA molecules from modern DNA molecules as the former is usually present in low abundance and highly degraded (see characteristics of aDNA). Three main bioinformatics methods were used to estimate contamination:

9.2.2.1 DNA damage and fragment length

DNA damage is caused by the deamination of cytosines at the end of DNA molecules, which creates the characteristic misincorporation pattern of aDNA. This pattern is used to assess the

authenticity of the DNA reads (Briggs et al., 2009; Hofreiter et al., 2001). Extra-corporal or post mortem degradation processes occur very rapidly, which suggests that reads without a characteristic damage pattern highly likely derive from modern DNA contamination. We used MapDamage v.2.0.6 (Jónsson et al., 2013) embedded in EAGER 1.92.32 (Peltzer et al., 2016) to determine and plot the deamination rate pattern of the sequenced libraries. Despite it was not used in this work, we can complement the analysis using PMD tools when we have enough data (Skoglund et al., 2014). This tool filters for damage reads and thus allows the comparison between damaged and total number of reads, whereby a difference between the two observations indicates the presence of modern contamination. Following the DNA damage assessment, we trimmed the mapped reads for downstream analysis, which reduced the damage signal to less than 2%. The number of bp trimmed depended on the library architecture (2 bp for UDG-half libraries, and up to 10 bp for non-UDG libraries).

Fragment length can also be used to assess the quality of DNA libraries. As we expect aDNA to be highly degraded, the presence of long DNA fragments as estimated by the fragment length distribution indicate contamination from modern DNA.

DNA damage and fragment lengths are qualitative assessments that should always be considered alongside the following contamination estimation methods (points 9.2.2.2, 9.2.2.3 and 9.2.2.4).

9.2.2.2 Sex determination

The genetic sex is determined by use of the X-ratio (X-Chromosome mapped reads/ autosomal mapped reads) and Y-ratio (Y-Chromosome mapped reads/ autosomal mapped reads). For uncontaminated libraries we expect an X-ratio of approximately one, and a Y-ratio of approximately zero for females. Conversely, an X-ratio and Y-ratio of one half is expected in males (Fu et al., 2016) (**Figure 33**). Individuals that fall in an intermediate position may indicate the presence of DNA contamination.

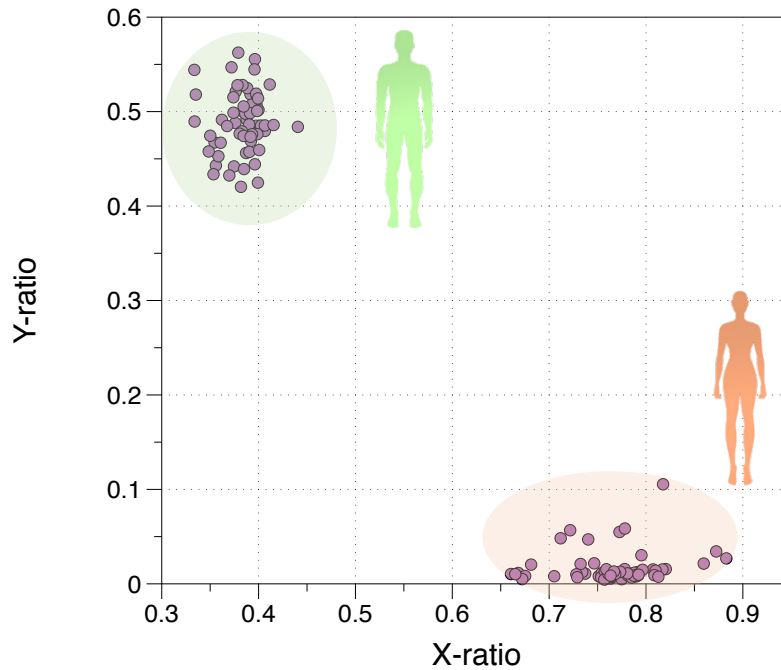


Figure 33: Genetic sex determination calculating X and Y-ratios.

9.2.2.3 Mitochondrial contamination

Mitochondrial DNA (mtDNA) constitutes a circular haploid genome with a high copy number per cell, which renders it a good estimator for contamination. This high copy number makes it possible to retrieve sufficiently high amounts of mtDNA reads from ancient samples. The haploid nature implies contamination if more than one haplotype is observed.

To test mtDNA reads for the presence of contaminated lineages, we used Geneious R8.1.974 (Kearse et al., 2012) to call consensus sequences from the read assemblies of all individuals. Then, the program ContamMix 1.0.10 was used to estimate the mitochondrial contamination levels in the consensus sequences from the mito-captured libraries taking a worldwide mitochondrial dataset that encompass all plausible contaminating sequences to compare as a potential contamination source (Fu, Mittnik, et al., 2013). Moreover, the read assembly was checked visually with Geneious R8.1.974 for potential heterozygous calls to compare with the contamination estimates from ContamMix.

9.2.2.4 X-Chromosome contamination in males

Males are haploid for the X chromosome and so, as with mtDNA sequences, only homozygotic calls are expected for male individuals. Testing the heterozygosity for the polymorphic positions in the X chromosome for males is the only way to test for nuclear DNA contamination.

Method 2 from the ANGSD package was applied to libraries from male individuals to test for the heterozygosity of polymorphic sites on the X chromosome that were covered at least twice (Korneliussen et al., 2014). To facilitate contamination estimation we merged low coverage libraries from the same individual, *i.e.* libraries with less than 200 SNPs on the X-chromosome, into a single BAM file using samtools v0.1.19 (Li et al., 2009). Finally, merged libraries with less than 3% contamination were selected for downstream population genetic analyses.

9.2.3 Genotyping and merging with data set.

For the non-UDG libraries, SNP genotyping was applied to clipped and unclipped BAM files, calling only the transversions for the unclipped BAM files to avoid the ancient DNA damage, and merged to include the extra SNPs in the combined genotype file. For UDG-half libraries, genotypes were called directly from the 2 bp trimmed BAM files using pileupCaller (<https://github.com/stschiff/sequenceTools/tree/master/srcpileupCaller>). PileupCaller will randomly call one base per position with probabilities equal to the observed read frequencies, effectively treating the human genome as a pseudo-haploid genome. Genotyped data were merged with the Human Origins panel (~600K SNPs) (Patterson et al., 2012) and 1240K SNP panel (Mallick et al., 2016).

9.3 Population genomic analysis

9.3.1 Clustering analysis

All of the analyses performed here are exploratory and clustering methods without explicit associated statistical significance tests. However, these methods are potentially very useful for identifying possible population and demographic structure. For example, it would be useful to know if one is studying homogeneous populations, or if a population contains subpopulations that are genetically distinct (Patterson et al., 2006). These methods are also useful for detecting

signals of admixture, though this is not formally tested. In this thesis, the two following clustering methods have been employed:

9.3.1.1 Principal Components Analysis (PCA)

PCA was first introduced to the study of genetic data by Luca Cavalli-Sforza's team (Menozzi et al., 1978). Here, we leverage information from multiple variables, i.e. 600,000 SNPs from the Human Origins panel, and use PCA to reduce the dimensionality of the multivariate data, which is expressed in a hierarchical order of orthogonal principal components that explain the data best (usually PC1 and PC2). PCA was applied to modern-day West Eurasian populations from the Human Origins panel (Lazaridis et al., 2016) using *smartpca* v10210 (EIGENSOFT) with the option *SHRINKMODE* (Patterson et al., 2006) enabled to calculate principal components upon which aDNA samples were projected.

9.3.1.2 Multi Dimensional Scaling

Multi-Dimensional-Scaling (MDS) translates information about pairwise distances among individuals/populations from a distance matrix to an N -dimensional scale. Two dimensions are often used to visualize the data in a simple scatter plot. MDS can be computed directly from a matrix of F_{st} values (genetic distances calculated with the variation of allele frequencies among populations). It is also possible to transform F_3 -outgroup statistics, which are essentially a measure of similarity, into distances, i.e. a measure of dissimilarity, by calculating the value: $1-F_3$. In doing so, the private genetic drift of the population/individuals is ignored, and only distances in the path of shared genetic drift are measured (Fu et al., 2016).

We performed Multi-Dimensional Scaling (MDS) using the R package *cmdscale* to plot the genetic dissimilarity among hunter-gatherers (HG), using the transformed $[1-F_3(X; Y, Mbuti)]$ pairwise values from all pairwise combinations (Fu et al., 2016).

9.3.2 F-statistics

F-statistics measure levels of shared genetic drift between populations, where drift is defined to be the change in the allele frequencies in a population over the time. Drift is inferred from allele frequencies (including only SNPs that are understood to be neutral, i.e. not under selection) between different populations.

There are many kinds of F-statistics, however every form of order greater than two can be expressed as a linear combination of F_2 -statistics. F_2 -statistics can be interpreted as the variance of the difference in allele frequencies between two populations (**Figure 34**).

For example, for populations A and X, and where a'_i is the frequency of the i th allele in population A, x'_i is the frequency of the i th allele in population X, and N is the total number of SNPs of interest, we calculate the observed value of the associated F_2 -statistics as

$$F_2(A, X) = \frac{1}{N} \sum_i^N [(a'_i - x'_i)]^2.$$

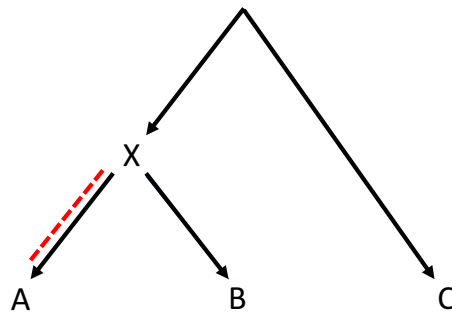


Figure 34: a schematic diagram of $F_2(A, X)$, which measures the genetic drift between the two populations (A and X) and it is used as branch length between populations A and X.

The F-statistics reported in this thesis were calculated using qpDstat from ADMIXTOOLS (<https://github.com/DReichLab>). We used the 1240K SNP panel to increase the potential number of SNPs shared by the ancient individuals, which could improve the power of resolution in the associated significance tests. Standard errors were calculated with the default block jackknife option. We report and plot three standard errors for all F-statistics.

9.3.2.1 Three population test

In a tree formed by three populations, denoted X, A and B, the F_3 -statistic can be decomposed into the following linear combination of F_2 -statistics:

$$F_3(C; A, B) = \frac{1}{2} [F_2(C, A) + F_2(C, B) - F_2(A, B)].$$

It can be seen that this statistic measures the shared genetic drift between population C, and the most recent common ancestor of populations A and B. Assuming a tree-like evolutionary history, this statistic must always be positive, because the genetic drift between population C and population A, and population C and population B are always larger than the genetic drift between population A and population B (**Figure 35**).

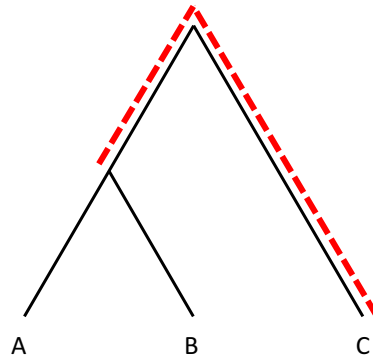


Figure 35: schematic diagram of a F_3 -statistics formulated in the way $F_3(C;A,B)$, which measures allele frequency difference between the focal population (C) and the most recent common ancestor of populations A and B.

9.3.2.1.1 F_3 -admixture $F_3(C; A, B)$

Negative F_3 -statistics are only observable if population C has admixed with population A, population B (or both but in unequal proportions). Only in this case can the distances between populations X and A, and populations C and B be shorter than the distance between populations A and B. To perform this test, diploid data is required, and so in the case of pseudo-haploid genomes it is necessary to work at the population level (**Figure 36**).

9.3.2.1.2 F_3 -outgroup $F_3(O; A, B)$

This test is used to calculate the shared genetic drift between populations A and B since the divergence from the outgroup (O) (Reich et al., 2009). The genetically closest population to your test population (A or B as the test population yields a symmetric result) will get the highest positive value (**Figure 36**).

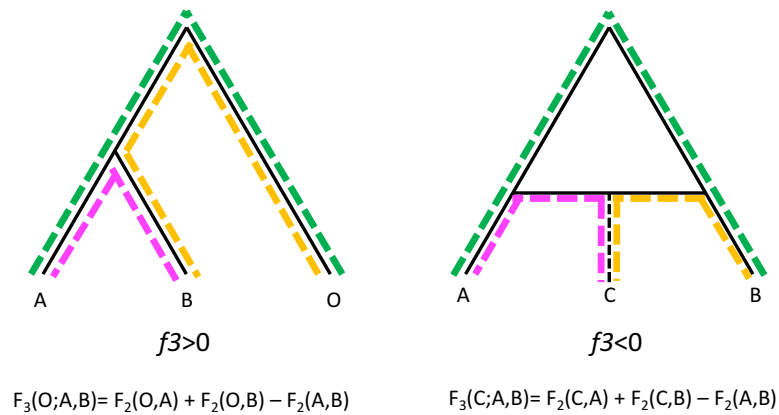


Figure 36: The F_3 -statistic tree topologies. The left tree shows an F_3 -outgroup which always is positive, and right tree shows admixture scenario for that the F_3 -admixture will be negative.

9.3.2.2 Four population test

The F_4 -statistic was introduced by Reich et al. (2009) and is the unstandardized form of the so-called D-statistic from the BABA/ABBA test described in Green et al., (2010) to evaluate Neanderthal ancestry in non-Africans, and the formal way to test for admixture and population structure. This test estimates the allele frequency balance among populations and outgroups. The null hypothesis (AABB) for the statistic $F_4(A,B;C,D)$ assumes a symmetrical tree and is thus consistent with $F_4(A,B;C,D) = 0$. If the F_4 -values are significantly different from 0, this means that the tree topology is incorrect, i.e. tree asymmetry, either because of admixture between populations either side of the main branches A,B and C,D, or because the assumed bifurcating topology is incorrect. Positive values are expected if there was gene flow between populations C and A or between populations D and B (the BABA tree). Conversely, negative values are expected if there was gene flow between populations C and B or populations D and A (the ABBA tree) (Figure 37).

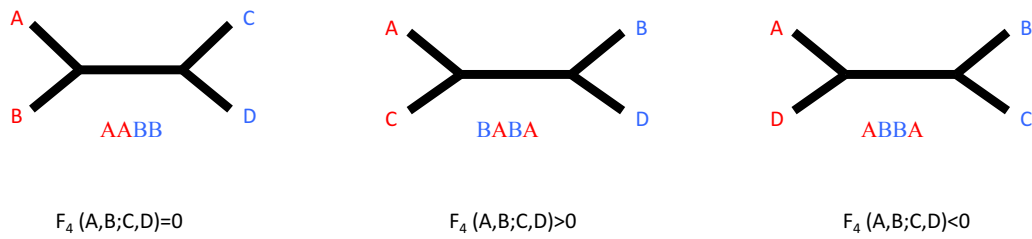


Figure 37: Three different unrooted trees from the ABBA/BABA test and the corresponding F_4 -values.

If population D is substituted by an Outgroup (O), positive values are only expected if there is gene flow between C and A and negative if the gene flow is between C and B.

There are different ways to apply the F_4 -test and it can be used to test for cladality with respect to the outgroups, or for admixture.

9.3.2.2.1 Cladality or Admixture test $F_4(A, B; C, D)$

An F_4 -value consistent with zero is expected if populations A and B are cladal with respect to population C, and the population D (tree symmetry). If population C violates the cladality of populations A and B by being differentially related to one of the two, the resulting F_4 -statistic is expected to be positive if populations C and A are genetically more similar than populations C and B, or negative if populations C and B are genetically more similar than C and A (**Figure 38**).

The differential relation to one of the two populations could imply admixture between population C and populations A or B (**Figure 38**).

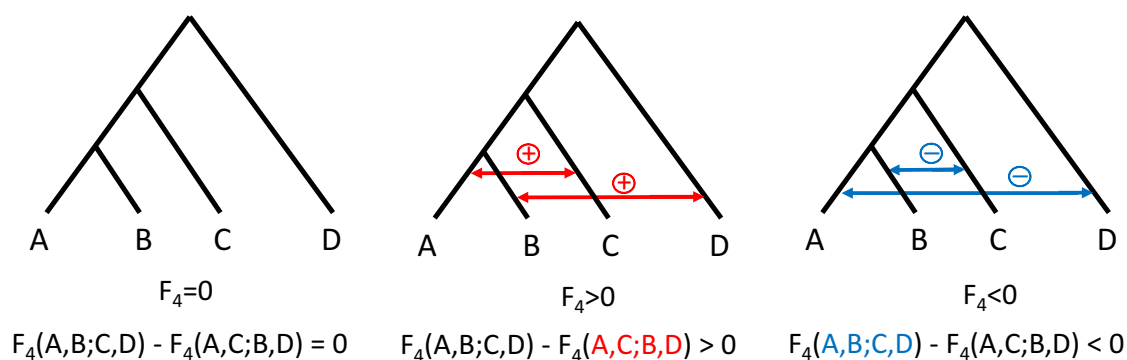


Figure 38: A schematic diagram of the 3 different scenarios considered for the 4-population tree and its expected F_4 -value.

9.3.3 qpWave/qpAdm

qpWave/qpAdm are an extension of the F-statistic framework first implemented in Haak et al. (2015) and an updated version is available in the ADMIXTOOLS package (<https://github.com/DReichLab>). The combined methods allow researchers to test for the number of contributing ancestral sources to a target population, and to quantify the proportion of genetic ancestry contributed by each source. The ancestry proportions in the target population are inferred based on how the target population is differentially related to a set of outgroups via the reference populations.

This method creates a matrix with the elements made up of all the possible combinations of the form $F_4(R_1, R_j; O_1, O_j)$. Using this matrix, qpWave can estimate the minimum number of independent sources of gene flow needed to adequately explain a set of target populations. To estimate the admixture proportions, qpAdm calculates the proportions of the References in the Target population.

An advantage of this method is that the F_4 -statistics are only affected by the drift shared among references and outgroup populations, but not by any specific drift in the reference or target populations. This means that it is not necessary to use as a reference population the population which directly contributed to the ancestry on the target population. The reference population need only be cladal to the test population.

9.3.4 Phenotypic traits

Ancient DNA also allows the study of genetic variants that are considered to be under selection. The temporal dimension of aDNA is of particular interest as it allows the observation of allele frequency shifts through time, i.e. before and after potential events or in the light of long-standing selective constraints. Some phenotypic analysis on ancient individuals were based on the study of a specific allele commonly associated with lactase persistence in Europeans (Burger et al. 2007). The first large-scale phenotypic analysis on ancient individuals was possible through the application of the 1240K SNP capture to a sufficiently large number of ancient individuals from different time periods (Mathieson et al., 2015). The 1240K SNP panel includes a set of 30,000 SNPs that are phenotypically informative or under selection.

In this work, we used a select set of 36 SNPs covered in the 1240K SNP panel to infer phenotypic traits including diet, pigmentation or immunity from ancient individuals. The genotype likelihood was calculated based on the number of reads (using a quality filter q30) for each specific position to determine the presence of either the ancestral or derived allele (van de Loosdrecht et al., 2018).

9.3.5 Mitochondrial and Y-chromosomal haplogroups

An in-house mtDNA capture assay was used to recover complete mitochondrial genomes from ancient individuals. We used samtools v1.3.1 to extract reads from the mitocapture read data (Maricic et al., 2010) and mapped these to the revised Cambridge Reference Sequence (rCRS; Andrews et al., 1999) and called consensus sequences from read assemblies using Geneious R8.1.974 (Kearse et al., 2012). Consensus sequences were exported in *fasta* format and analysed in Haplogrep 2 (Weissensteiner et al., 2016) to determinate mitochondrial haplotypes.

For Y-chromosomal haplogroup determination, Y-chromosomal SNPs (Y-SNPs) of the 1240K SNP panel were called from all male individuals using pileupCaller with MajorityCalling mode, (<https://github.com/stschiff/sequenceTools>), and mapped with quality greater than 30. Y-chromosomal haplogroups were called from the overlap with the list of Y-SNPs that accompanied the *yhaplo* script (Poznik, 2016).

9.3.6 Kinship

Traditionally, mt- and Y-haplogroups, together with short tandem repeat genotypes (STR), have been used to estimate maternal and paternal relatedness among individuals from the same site (Haak et al., 2008; Knipper et al., 2017). Now, genome-wide autosomal data can also be used to assess the degree of relatedness. To date, there are several methods that are used for estimating the degree of relatedness between ancient individuals.

9.3.6.1 PWMR

Calculating the pairwise mismatch rate (PWMR) requires the least amount of data, as it directly counts the number of shared SNPs between two individuals. The PWMR was calculated from the 1240K genotype files directly, and can be filtered for pairs of individuals that shared at least 1,000 SNPs (van de Loosdrecht et al., 2018). A median PWMR value, denoted b , is used for unrelated pairs of individuals (b , is theoretically expected to be 0.25). In turn, the PWMR between two identical individuals, or monozygotic twins, is expected to be zero. However, due to the pseudo-haploid mode of calling genotypes that was applied, is never exactly zero. The value a , is calculated by dividing the median by two ($a=b/2$, and thus should theoretically be equal to 0.125). From this value, we calculate the degree of relatedness for each pairwise sample. For example, for first degree relatives we would expect a value equal to $b*3/4$, and $b*7/8$ for second degree, or $b*13/16$ for individuals related in the third degree (Monroy Kuhn et al. 2018) (Figure 39).

The PWMR, denoted y , can trivially be transformed into a coefficient of relatedness (x) using the following formula $x=(b-y)/a$. Here, the coefficient of relatedness is expected to equal 1 in case of two identical individuals or monozygotic twins, 0.5 for first degree relatives (parent-offspring, full siblings) or 0.25 for second degree (grandparents-grandchildren or uncle/aunt-nephew/niece). Higher degrees of relatedness are difficult to distinguish because that the values we are estimating are shrinking on a logarithmic scale, but the standard errors do not (Monroy Kuhn et al. 2018). However, for unrelated individuals the coefficient of relatedness is expected to be very close to zero. Based on this threshold we can apply a normalization with respect to the median value, and relate the PWMR to the coefficient of relatedness (Figure 39).

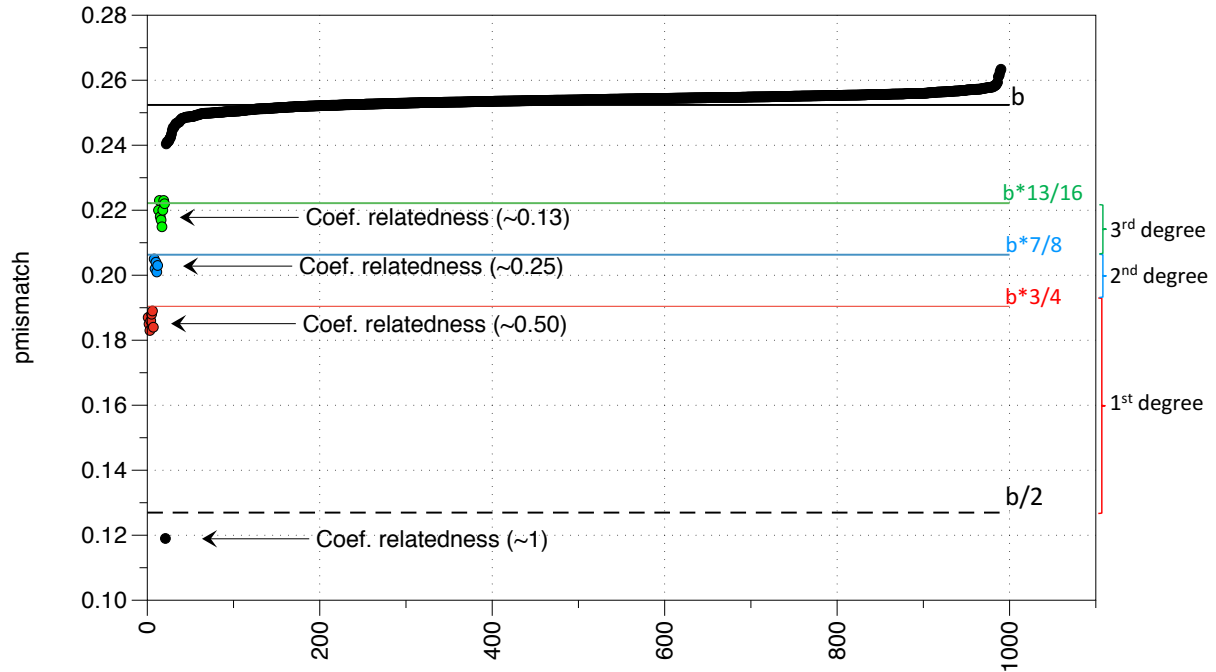


Figure 39: Pairwise mismatch rate along different kinship degree and their correspondence with the coefficient of relatedness, considering the median value (b) as the Pairwise mismatch rate for unrelated individuals.

9.3.6.2 READ

Relationship Estimation from Ancient DNA (READ) is another method that aims to estimate the degree of genetic kinship among individuals (Monroy Kuhn et al., 2018). This method can reliably identify identical twins or same individuals and first and second-degree relatedness among individuals based on the proportion of non-matching alleles (P_0). The results have to be corrected to take into account background genetic relatedness within each subpopulation. After the correction, p_0 is expected to be between 0 and 0.625 for identical twins, between 0.625 and 0.8125 for first degree related individuals, between 0.8125 and 0.90625 for second degree related individuals, and greater than 0.90625, for all other degrees of relatedness (which are reported as “unrelated”) (Figure 40).

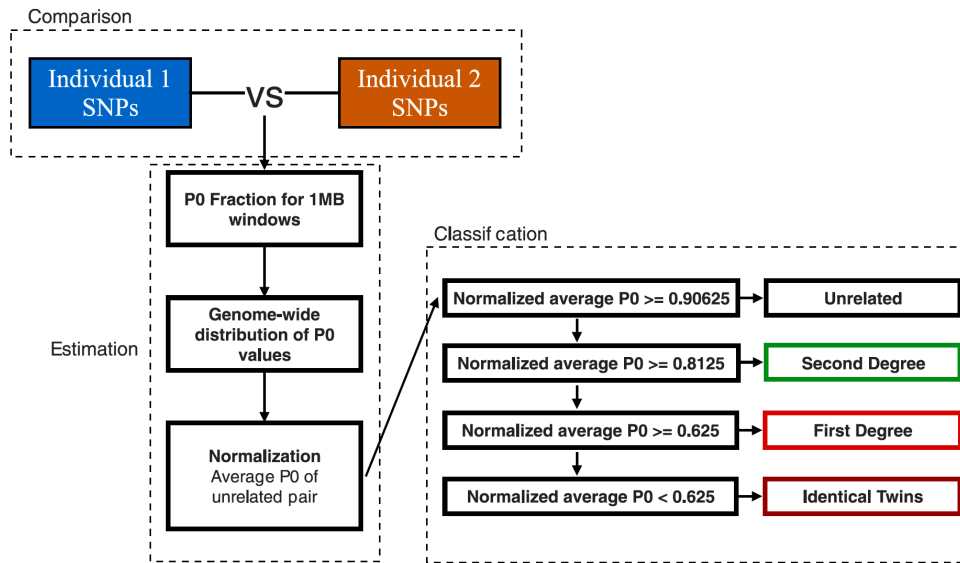


Figure 40: READ workflow to estimate 1st and 2nd degree of kinship between two individuals (Figure from Monroy Kuhn et al., 2018).

10 RESULTS

This chapter is composed of four published articles plus another two in preparation. First, it is shown the published articles related to the isotopic analysis (three already published and two in preparation) and secondly the published article related to genomics.

In order to be able to follow the Discussion chapter a subchapter numeration has been done to every article and its reference will appear along the discussion following this order:

9.1 Reconstruction of human subsistence and husbandry strategies from the Iberian Early Neolithic: A stable isotope approach.

Villalba-Mouco, V., Utrilla, P., Laborda, R., Lorenzo, J. I., Martínez-Labarga, C., Salazar-García, D. C. (2018). Reconstruction of human subsistence and husbandry strategies from the Iberian Early Neolithic: A stable isotope approach. *American journal of physical anthropology* 167 (2), 257-271.

9.2 Territorial mobility and subsistence strategies during the Ebro Basin Late Neolithic-Chalcolithic: A multi-isotope approach from San Juan cave (Loarre, Spain).

Villalba-Mouco, V., Sauqué, V., Sarasketa-Gartzia, I., Pastor, M. V., le Roux, P. J., Vicente, D., Utrilla, P., Salazar-García, D. C. (2018). Territorial mobility and subsistence strategies during the Ebro Basin Late Neolithic-Chalcolithic: A multi-isotope approach from San Juan cave (Loarre, Spain). *Quaternary International* 481, 28-41.

9.3 Stable isotope ratio analysis of bone collagen as indicator of different dietary habits and environmental conditions in Northeastern Iberia during the 4th and 3rd millennium cal BC.

Villalba-Mouco, V., Sarasketa-Gartzia, I., Utrilla, P., Oms, F. X., Mazo, C., Mendiola, S., Cerbría, A., Salazar-García, D. C. (2018). Stable isotope ratio analysis of bone collagen as indicator of different dietary habits and environmental conditions in Northeastern Iberia during

the 4th and 3rd millennium cal BC. *Archaeological and Anthropological Sciences*.
<https://doi.org/10.1007/s12520-018-0657-z>

9.4 Estudio de la movilidad de las comunidades de montaña durante el Calcolítico a través de isótopos de estroncio en esmalte humano: la cueva de los cristales (Sarsa de Surta, Huesca, España)

Villalba-Mouco, V., Montes, L., Bea, M., Salazar-García, D.C. (*In prep.*). Estudio de la movilidad de las comunidades de montaña durante el Calcolítico a través de isótopos de estroncio en esmalte humano: la cueva de los cristales (Sarsa de Surta, Huesca, España).

9.5 Use and reuse of funerary spaces. Strontium isotopes and bayesian radiocarbon modelling to approach Late Neolithic/Chalcolithic funerary behaviour in Northern Iberia.

Villalba-Mouco, V., Utrilla, P., Sarasketa-Gartzia, Mazo., C., Salazar-García, D.C. (*In prep.*). Use and reuse of funerary spaces. Strontium isotopes and bayesian radiocarbon modelling to approach Late Neolithic/Chalcolithic funerary behaviour in Northern Iberia.

9.6 Survival of Late Pleistocene Hunter-gatherer ancestry in the Iberian Peninsula.

Villalba-Mouco, V., Marieke S. van de Loosdrecht, M.S., Posth, C., Mora, R., Martínez-Moreno, J., Rojo-Guerra, M., Salazar-García, D.C., Royo-Guillén, J.I., Kunst, M., Rougier, H., Crevecoeur, I., Arcusa-Magallón, H., Tejedor-Rodríguez, C., García-Martínez de Lagran, I., Garrido-Pena, R., Alt, K.W., Utrilla, P., Krause, J., Haak, W. (2019). Survival of Late Pleistocene Hunter-gatherer ancestry in the Iberian Peninsula. *Current Biology* 29, 1-9.
<https://doi.org/10.1016/j.cub.2019.02.006>

10.1 Reconstruction of human subsistence and husbandry strategies from the Iberian Early Neolithic: A stable isotope approach



Received: 25 August 2017 | Revised: 11 May 2018 | Accepted: 12 May 2018

DOI: 10.1002/ajpa.23622

RESEARCH ARTICLE

WILEY 

Reconstruction of human subsistence and husbandry strategies from the Iberian Early Neolithic: A stable isotope approach

Vanessa Villalba-Mouco¹  | Pilar Utrilla¹ | Rafael Laborda¹ | José Ignacio Lorenzo¹ |
Cristina Martínez-Labarga²  | Domingo C. Salazar-García^{3,4}

¹Departamento de Ciencias de la Antigüedad, Grupo Primeros Pobladores del Valle del Ebro (PPVE), Instituto de Investigación en Ciencias Ambientales (IUCA), Universidad de Zaragoza, Pedro Cerbuna 12, Zaragoza 50009, Spain

²Centro di Antropologia molecolare per lo studio del DNA antico Dipartimento di Biologia, Università degli Studi di Roma "Tor Vergata" Via della Ricerca Scientifica 1, Roma 00173, Italia

³Departamento de Geografía, Prehistoria y Arqueología, Grupo de Investigación en Prehistoria IT-622-13 (UPV-EHU)/ IKERBASQUE-Basque Foundation for Science, Vitoria, Spain

⁴Department of Geological Sciences, University of Cape Town, Cape Town, South Africa

Correspondence

Vanessa Villalba-Mouco, Departamento de Ciencias de la Antigüedad, Universidad de Zaragoza, Pedro Cerbuna 12, 50009, Zaragoza, Spain.

Email: vmouco@unizar.es

and

Domingo C. Salazar-García, Departamento de Geografía, Prehistoria y Arqueología, Universidad del País Vasco-Euskal Herriko Unibertsitatea, C/ Francisco Tomás y Valiente s/n. 01006, Vitoria-Gasteiz, Spain.
Email: domingocarlos.salazar@ehu.es

Funding information

Fundación Ibercaja-CAI (2016); Research Stay Scholarship; Gobierno de Aragón and the Fondo Social Europeo; Predoctoral Scholarship, Grant/Award Number: BOA20150701025; Transiciones Climáticas y Adaptaciones Sociales en la Prehistoria de la Cuenca del Ebro, Grant/Award Number: HAR2014-59042-P; PPVE research group (H-07: Primeros Pobladores del Valle del Ebro); BBVA Foundation; I Ayudas a Investigadores, Innovadores y Creadores Culturales

Abstract

Objectives: The Early Neolithic involved an important social and economic shift that can be tested not only with the material culture, but also through biomolecular approaches. The Iberian Peninsula presents few Early Neolithic sites where fauna and humans can be analyzed together from an isotopic perspective. Here we present an isotopic study on the site of Cueva de Chaves as an example for understanding the dietary and economical changes that took place during Early Neolithic in Iberia.

Material and methods: Here we apply carbon and nitrogen stable isotope analysis to bone collagen from 4 humans and 64 faunal samples from 14 different species. The large dataset belongs to the same unique chrono-cultural context secured by 20 radiocarbon dates. Three direct new radiocarbon dates were carried out on the human remains analyzed.



Results: Faunal isotope values show no significant differences between wild and domestic herbivores, although the latter have more homogeneous values. Domestic pigs, potentially considered omnivorous, also show signatures of a herbivore diet. Human isotopic results show a diet mainly based on terrestrial C₃ resources and possibly high meat consumption. The only individual found buried with a special funerary treatment presents a slightly different protein intake, when taking into account the long contemporaneous baseline analyzed.

Discussion: Similar values between wild and domestic species could be the result of common feeding resources and/or grazing on the same parts of the landscape. The herbivore diet seen amongst domestic pigs rules out feeding on household leftovers. High meat consumption by humans would support the hypothesis of the existence of a specialized animal husbandry management community in which agriculture was not intensively developed. Our results suggest that the development of agricultural practices and animal husbandry were not necessarily associated together in the early stages of the Western Mediterranean Neolithic.

KEYWORDS

animal management, cardial, carbon and nitrogen stable isotopes, funerary practices, domestication, radiocarbon dating

Reconstruction of human subsistence and husbandry strategies from the Iberian Early Neolithic: A stable isotope approach

Vanessa Villalba-Mouco¹  | Pilar Utrilla¹ | Rafael Laborda¹ | José Ignacio Lorenzo¹ |
Cristina Martínez-Labarga²  | Domingo C. Salazar-García^{3,4}

¹Departamento de Ciencias de la Antigüedad, Grupo Primeros Pobladores del Valle del Ebro (PPVE), Instituto de Investigación en Ciencias Ambientales (IUCA), Universidad de Zaragoza, Pedro Cerbuna 12, Zaragoza 50009, Spain

²Centro di Antropologia molecolare per lo studio del DNA antico Dipartimento di Biologia, Università degli Studi di Roma "Tor Vergata" Via della Ricerca Scientifica 1, Roma 00173, Italia

³Departamento de Geografía, Prehistoria y Arqueología, Grupo de Investigación en Prehistoria IT-622-13 (UPV-EHU)/ IKERBASQUE-Basque Foundation for Science, Vitoria, Spain

⁴Department of Geological Sciences, University of Cape Town, Cape Town, South Africa

Correspondence

Vanessa Villalba-Mouco, Departamento de Ciencias de la Antigüedad, Universidad de Zaragoza, Pedro Cerbuna 12, 50009, Zaragoza, Spain.

Email: vvmouco@unizar.es

and

Domingo C. Salazar-García, Departamento de Geografía, Prehistoria y Arqueología, Universidad del País Vasco-Euskal Herriko Unibertsitatea, C/Francisco Tomás y Valiente s/n. 01006, Vitoria-Gasteiz, Spain.

Email: domingocarlos.salazar@ehu.es

Funding information

Fundación Ibercaja-CAI (2016); Research Stay Scholarship; Gobierno de Aragón and the Fondo Social Europeo; Predoctoral Scholarship, Grant/Award Number: BOA20150701025; Transiciones Climáticas y Adaptaciones Sociales en la Prehistoria de la Cuenca del Ebro, Grant/Award Number: HAR2014-59042-P; PPVE research group (H-07: Primeros Pobladores del Valle del Ebro); BBVA Foundation; I Ayudas a Investigadores, Innovadores y Creadores Culturales

Abstract

Objectives: The Early Neolithic involved an important social and economic shift that can be tested not only with the material culture, but also through biomolecular approaches. The Iberian Peninsula presents few Early Neolithic sites where fauna and humans can be analyzed together from an isotopic perspective. Here we present an isotopic study on the site of Cueva de Chaves as an example for understanding the dietary and economical changes that took place during Early Neolithic in Iberia.

Material and methods: Here we apply carbon and nitrogen stable isotope analysis to bone collagen from 4 humans and 64 faunal samples from 14 different species. The large dataset belongs to the same unique chrono-cultural context secured by 20 radiocarbon dates. Three direct new radiocarbon dates were carried out on the human remains analyzed.

Results: Faunal isotope values show no significant differences between wild and domestic herbivores, although the latter have more homogeneous values. Domestic pigs, potentially considered omnivorous, also show signatures of a herbivore diet. Human isotopic results show a diet mainly based on terrestrial C₃ resources and possibly high meat consumption. The only individual found buried with a special funerary treatment presents a slightly different protein intake, when taking into account the long contemporaneous baseline analyzed.

Discussion: Similar values between wild and domestic species could be the result of common feeding resources and/or grazing on the same parts of the landscape. The herbivore diet seen amongst domestic pigs rules out feeding on household leftovers. High meat consumption by humans would support the hypothesis of the existence of a specialized animal husbandry management community in which agriculture was not intensively developed. Our results suggest that the development of agricultural practices and animal husbandry were not necessarily associated together in the early stages of the Western Mediterranean Neolithic.

KEYWORDS

animal management, animal husbandry, carbon and nitrogen stable isotopes, funerary practices, domestication, radiocarbon dating

1 | INTRODUCTION

The rise of the Neolithic involved important cultural, economic, genetic and environmental changes in many places, including the Western

Mediterranean (Salazar-García and García-Puchol, 2017a). These changes are relatively easy to prove throughout the archaeological record. The so-called Neolithic package normally includes an increase of material culture including first pottery and polished stone, and then

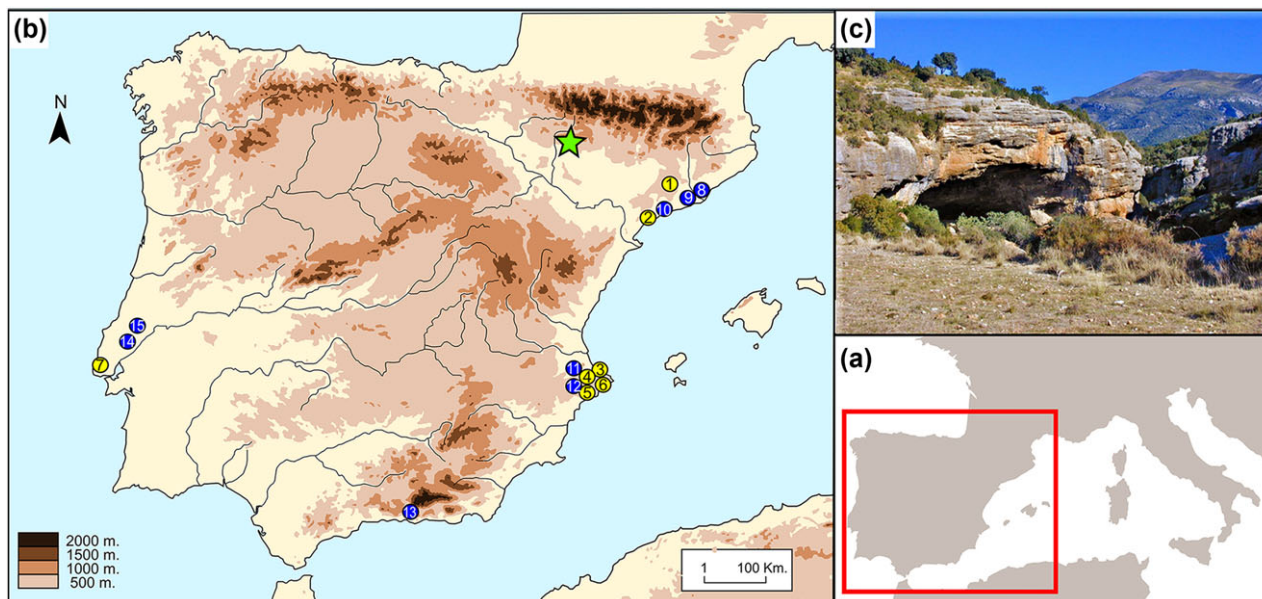


FIGURE 1 Location map. (a) Location of the Iberian Peninsula inside Western Europe; (b) Map of the Iberian Peninsula with the Earliest Cardial Neolithic sites but without human remains from this chronology (yellow dots: 1: Guixeres de Vilobí; 2: Cavet; 3: Barranquet; 4: Cova d'en Pardo; 5: Mas d'Is; 6: Cova de les Cendres; 7: Lápia das Lameiras) and sites with Cardial human remains directly dated (blue dots: 8: Plaça de la Vila de Madrid; 9: Cova Bonica; 10: Cova Foradada; 11: Cova de l'Or; 12: Cova de la Sarsa; 13: Cueva de Nerja; 14: Galeria da Cisterna and 15: Gruta do Caldeirão.) The star shows the location of Cueva de Chaves (c) Cueva de Chaves [Color figure can be viewed at wileyonlinelibrary.com]

domestication of animals and cereals (Edwards et al., 2007; Guilaine and Manen, 2007; Zapata, Peña-Chocarro, Pérez-Jordá, & Stika, 2004; Zilhão, 2001).

Different types of studies have shown the Fertile Crescent as the origin of the Neolithic cultures that spread throughout Europe and northern Africa (Lemmen, Gronenborn, & Wirtz, 2011; Zeder, 2008). The demographic expansion spread towards the Balkan Peninsula, where the Neolithic is then genetically and culturally differentiated into two population groups (Fernández et al., 2014; Olalde et al., 2015). One of these groups followed the Danube river and resulted in the LBK ware culture (*Linearbandkeramik*), which eventually spread throughout Central Europe between 5500 and 4900 cal BC (Manning et al., 2014). The other group spread faster through Western Europe by the Mediterranean coast and led to the *Impressa* ware culture (between 5800 and 5400 cal BC), and the Cardial ware culture (between 5500 and 4900 cal BC) (Binder and Sénépart, 2010). The Cardial expansion seemed to reach the Iberian Peninsula first (Gamba et al., 2012), although the presence of some vestiges of *Impressa* ware has been suggested at some coastal sites (Bernabeu, Molina, Esquembre, Ortega, Boronat, 2009). In any case, it is clear that the arrival of farming practices to Iberia arrived mainly through maritime colonization (Isern, Zilhão, Fort, & Ammerman, 2017; Zilhão, 2001). This maritime pioneering is in agreement with the fact that the first Neolithic sites are situated in the coastal region and have Cardial pottery (Bernabeu, García-Puchol, & Orozco-Köhler, 2018), whereas inland Early Neolithic sites occur later and show no Cardial pottery (Rojo-Guerra, Kunst, Garrido-Pena, & García-Martínez de Lagrán, 2006).

1.1 | Cueva de Chaves and its importance in the neolithization of Iberia

Cueva de Chaves is a cave located in the northeast of Iberia, at 663 m. a.s.l. (metres above sea level) in the Prepyrenean mountain range of Sierra de Guara (Bastarás, Huesca, Aragón; UTM: 735325.00 X; 4678636.00 Y; ETRS 89, Datum 30) (Figure 1). The site was excavated between 1984 and 2007 under the direction of Pilar Utrilla (Paleolithic levels) and Vicente Baldellou (Neolithic levels). The cave has about 225 m of extension, of which 110 m were potentially inhabitable (Baldellou, 2012). Cueva de Chaves was occupied during the Paleolithic (Solutrean and Magdalenian), Neolithic and, sporadically, the Bronze Age and Late Roman periods. Neolithic deposits from levels Ia and Ib date to the Early Neolithic period (Ia 5600-5300 cal BC; Ib 5300-5000 cal BC). These two chronologically consecutive levels have in them domestic fauna (Castaños, 2004), Cardial pottery (Baldellou, 2012; Utrilla and Laborda, 2018) and schematic rock art painted on pebbles (Utrilla and Baldellou, 2002, 2007) (Figure 2, Table 1).

Cueva de Chaves represents an interesting case study, as it is located inland but its radiocarbon dates show the use of the cave mostly as a settlement during the early stages of the Neolithic colonization of Iberia, overlapping with short-life radiocarbon dates from other nearby Cardial coastal Early Neolithic sites such as Guixeres de Vilobí, El Cavet (Martins et al., 2015), Cova de les Cendres, Cova d'En Pardo, Barranquet, Mas D'Is (Bernabeu et al., 2009), Cueva de Nerja (García-Borja, Aura Tortosa, Jordá Pardo, & Salazar García, 2014), Caldeirão (Zilhão, 1992), Galeria da Cisterna-Almolda (Martins et al., 2015; Zilhão, 2001) and Lapias das Lameiras (Davis and Simões, 2016). Moreover, only few sites in Iberia have human remains recovered from Cardial levels that have been directly dated: Caldeirão

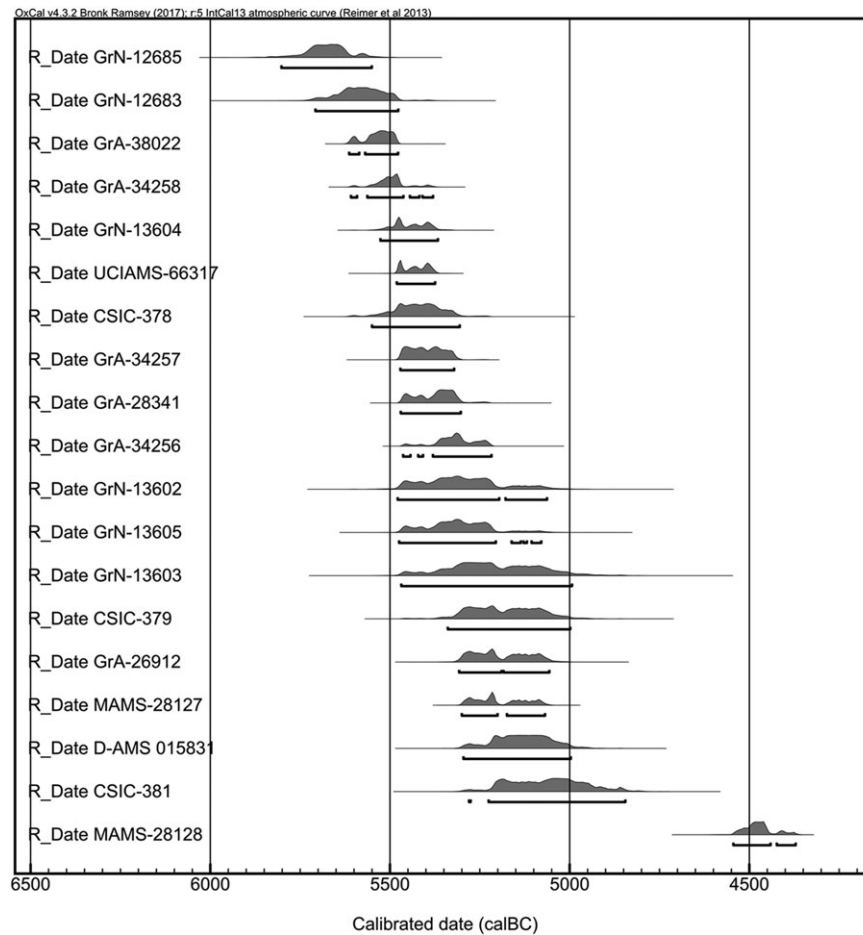


FIGURE 2 AMS radiocarbon dates from Cueva de Chaves. All dates have been calibrated with OxCal v4.2.3 and using the IntCal13 calibration curve (Bronk Ramsey, 2009; Reimer et al., 2013)

TABLE 1 AMS radiocarbon dates from the Early Neolithic levels of Cueva de Chaves, calibrated with OxCal v4.2.3 using the IntCal13 calibration curve (Bronk Ramsey, 2009; Reimer et al., 2013)

Lab code	Sample	^{14}C age	1 σ Cal BC	2 σ Cal BC	Reference
GrN-12685	charcoal	6770 \pm 70	5723-5627	5799-5550	Baldellou, 2012
GrN-12683	charcoal	6650 \pm 80	5634-5515	5707-5478	Baldellou, 2012
GrA-38022	<i>Ovis aries</i>	6580 \pm 35	5550-5486	5614-5479	Baldellou, 2012
GrA-34258	charcoal	6530 \pm 40	5528-5473	5609-5380	Baldellou, 2012
GrN-13604	charcoal	6490 \pm 40	5487-5379	5527-5368	Baldellou, 2012
UCIAMS-66317	<i>Ovis aries</i>	6470 \pm 25	5479-5382	5481-5374	Baldellou, 2012
CSIC-378	charcoal	6460 \pm 70	5483-5363	5549-5306	Baldellou, 2012
GrA-34257	charcoal	6410 \pm 40	5468-5357	5471-5322	Baldellou, 2012
GrA-28341	acorn	6380 \pm 40	5464-5315	5471-5303	Baldellou, 2012
GrA-34256	charcoal	6335 \pm 40	5367-5295	5464-5218	Baldellou, 2012
GrN-13602	charcoal	6330 \pm 90	5465-5216	5478-5063	Baldellou, 2012
GrN-13605	charcoal	6330 \pm 70	5374-5219	5474-5079	Baldellou, 2012
GrN-13603	charcoal	6260 \pm 100	5325-5062	5469-4991	Baldellou, 2012
CSIC-379	charcoal	6230 \pm 70	5299-5076	5340-4999	Baldellou, 2012
GrA-26912	human	6230 \pm 45	5298-5079	5308-5057	Baldellou, 2012
MAMS 29127	human	6227 \pm 28	5292-5081	5299-5070	This article
D-AMS 015831	human	6180 \pm 54	5213-5057	5296-4998	This article
CSIC-381	charcoal	6120 \pm 70	5207-4963	5281-4845	Baldellou, 2012
MAMS 28128	human	5645 \pm 31	4518-4452	4544-4373	This article

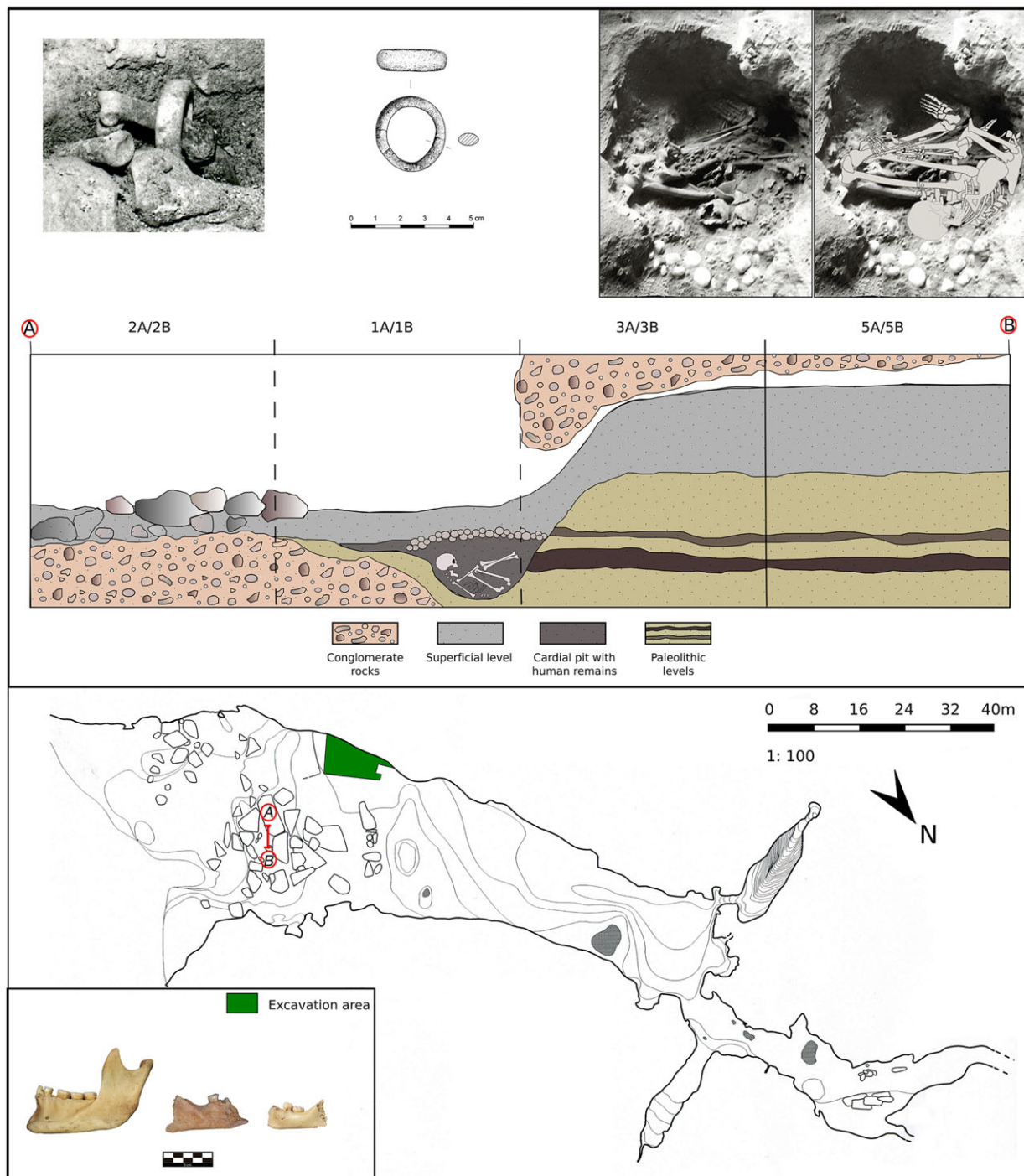


FIGURE 3 Early Neolithic human remains from Cueva de Chaves and their position in the topography. (a) Early Neolithic human remains sampled and recovered from the excavation area reflected in the topography; (b) Stratigraphic profile in the area where the Cardial burial was found; and (c) Detailed picture of the ring recovered from the Cardial burial and the archaeological drawing detailing the position of the skeleton [Color figure can be viewed at wileyonlinelibrary.com]

(Zilhão, 1992), Galería da Cisterna-Almonda (Martins et al., 2015), Cova de la Sarsa (García-Borja, Salazar-García, Pérez, Pardo, & Casanova, 2011), Cova de l'Or (Olalde et al., 2015), Cova Foradada (Oms, Cebrià, Morales, & Pedro, 2015), Vila de Madrid (Pou, Martí, Jordana, Malgosa, & Gibaja, 2010), Cova Bonica (Oms et al., 2017), Cueva de Nerja (Salazar-García, Pérez-Ripoll, García-Borja, & Jordá Pardo, 2017b) and now Cueva de Chaves. Of all of these sites, only Cueva de Chaves has an individual in complete anatomical articulation. This individual was buried in a pit with a flexed position, had an associated

ring, and was covered by red pigment and pebbles. All these features could be representative of the less well known Cardial funerary rituals (Utrilla, Lorenzo, Baldellou, Sopena, & Ayuso, 2008) (Figure 3).

Cueva de Chaves was mostly a habitat settlement, although it also had some areas dedicated to funerary practices. Besides the funerary area (Utrilla et al., 2008), evidence of different daily activities typical of a Neolithic community have been discovered inside the cave, shedding light on the broad Neolithic lifestyle: evidence of hunting (Castaños, 2004; Domingo, 2009), butchery and harvest activities

(Domingo, 2014; López García, 1992; López García and López-Sáez, 2000; Mazzucco, Clemente-Conte, Gassiot, & Gibaja, 2015), schematic art representations in pebbles, (Utrilla and Baldellou, 2002, 2007), fireplaces and storage structures (Alcolea, Utrilla, Piqué, Laborda, & Mazo, 2017; Sánchez, 2013). Many of these tasks can be recorded separately, and evidence of most of them together usually happen only in open-air settlements such as La Draga (Bosch, Chinchilla, & Tarrús, 2011) and Guixeres de Vilobí (Oms, Esteve, Mestres, Martín, & Martins, 2014a). In this sense, it is considered that Cueva de Chaves is mainly an example of a settlement located inside a cave (Alcolea et al., 2017). Moreover, the environmental conditions of the cave resulted in conservation of its archaeological material, making Cueva de Chaves an essential site to understand the neolithization process of Iberia. Unfortunately, the Neolithic levels were intentionally destroyed in 2007 to build an illegal enclosure for animals of a private hunting ground situated around the cave, so almost nothing is left at the archaeological site (Sentence num. 00255/2016 11/11/16).

1.2 | Isotopic analysis for dietary and environmental reconstructions

The use of carbon ($\delta^{13}\text{C}$) and nitrogen ($\delta^{15}\text{N}$) stable isotope ratios from bone collagen gives a quantitative assessment of protein consumption (e.g., Lee-Thorp, 2008). Stable isotope analysis of Early Neolithic remains has proved useful to establish the socio-economic impact of farming (e.g., Arias, 2007; Lillie and Richards, 2000; Lubell, Jackes, Schwarcz, Knyf, & Meiklejohn, 1994; Schulting, 1998). This quantitative dietary approach has been useful in establishing subsistence patterns of the first farmers, as well as shedding light on animal and plant management practises at the time (e.g., Balasse et al., 2014, 2016; Navarrete et al., 2017).

The $\delta^{13}\text{C}$ measurement is suitable to distinguish between protein from marine and terrestrial resources (Schoeninger and De Niro, 1984), as well as proteins from plants with different photosynthetic pathways (C_3 and C_4) (Van der Merwe, 1982) and different environments (Goude and Fontugne, 2016). Estuarine aquatic resources, commonly consumed in the Western Mediterranean might have lower $\delta^{13}\text{C}$ values than expected (e.g., Salazar-García et al., 2014), so special care should be taken interpreting their consumption in the region. In addition, $\delta^{15}\text{N}$ values can be used to establish the trophic level a specific organism holds in the food chain of its environment, with an overall agreed estimated increase of 3-5‰ per trophic step (Bocherens and Drucker, 2003). Using the same principles, it is also possible to detect domestic species-specific feeding (Navarrete et al., 2017) and manuring practises due to high $\delta^{15}\text{N}$ values (Bogaard, Heaton, Poulton, & Merbach, 2007; Bogaard et al., 2013). Analyzing the values of fauna and humans together can offer more information about aspects of the ecology of the first anthropic ecosystems during the onset of the Neolithic. Here we have reconstructed dietary habits and trophic structure of the Early Neolithic ecosystem from Cueva de Chaves.

The main limitation of stable isotope analysis in bone collagen is that it mainly reflects protein consumption, resulting in a considerable amount of animal proteins masking plant food consumption (Hedges and Reynard, 2007). Another aspect to take into consideration is

collagen turnover, which is low during adulthood and therefore reflects an average diet of the last years before the individual died (Hedges, Clement, Thomas, & O'Connell, 2007; Hill, 1998). Subadult individuals could still show a breastfeeding or weaning isotopic signal (Herrscher, Goude, & Metz, 2017), as well as having isotopic values that reflect a narrower window of time before death because of their faster collagen turnover (Valentin, 2002).

2 | MATERIAL AND METHODS

This study focuses on the Early Neolithic levels Ia (5600-5300 cal BC) and Ib (5300-5000 cal BC). Both levels are consecutive to each other and show no radiocarbon discontinuity when considering short-life dates (Table 1, Figure 2). New and previous direct human radiocarbon dates overall confirm this. Therefore, materials from both levels have been considered as one common Early Neolithic assemblage, and samples were taken indifferently from both.

2.1 | Human and faunal remains

Initially, the MNI (minimum number of individuals) recovered from Cueva de Chaves was 8, based on the number of mandibles. One of the individuals was found in correct anatomical position and buried in a pit. The other seven were found disarticulated and commingled with other archaeological material, some of them in superficial levels (Figure 3). Because of this unclear attribution of the human remains, all skeletal material that defined the MNI (seven mandibles and one rib from the isolated individual) was directly radiocarbon dated. A total of 4 of the individuals were dated to the Early Neolithic period: three adults and one subadult. Three of them (two adults and the subadult) date from the beginning of the Early Neolithic, and one adult individual dates to the end of the Early Neolithic (Table 1, Figure 2). This last individual was included in the isotopic analysis, but the results are to be considered with caution because the date is more recent than those of the remaining individuals. The subadult individual (S-UCT 21023) was estimated to be around 4 years old, according to its dental eruption pattern (Ubelaker, 1989); no other subadult remains were found to help infer more aspects about individual health and lifestyle. Mandible S-UCT 21025 belongs to an adult individual; presenting a robust appearance (pronounced gonion and chin) associated with male traits, a molar wear pattern corresponds with 25-35 years of age (following Brothwell, 1981), and shows neither *antemortem* dental loss nor caries, although dental calculus is present. Mandible S-UCT 19600 shows a more gracile aspect, although only one fragment of the mandibular body is present and thus makes it impossible to determinate sex. However, the molar wear pattern corresponds to an individual of 25-35 years of age (Brothwell, 1981), as seen in the only tooth present (M1), and *antemortem* loss is observed by alveolar reabsorption of P2, M2 and M3 on the right side of the mandible. The individual found in correct anatomical position (S-UCT 21024) was identified as an adult male based on morphology of the innominate (Utrilla et al., 2008), and his pubic symphyseal surface corresponds to Todd's (1920) Phase IX, which corresponds to 44-50 years of age. His mandible also shows a heavy wear, in this case corresponding to 33-45 years of age

TABLE 2 NR (number of remains) and MNI (minimum number of individuals) faunal remains by taxa categories from Cueva de Chaves (information extracted from Castaños, 2004)

	Cueva de Chaves (Ia) NR	Cueva de Chaves (Ia) MNI	Cueva de Chaves (Ib) NR	Cueva de Chaves (Ib) MNI	Total NR	Total MNI
<i>Bos taurus</i>	235	12	200	14	435	26
<i>Ovis/Capra</i>	1967	68	4196	120	6163	188
<i>Sus domesticus</i>	504	37	713	41	1217	78
<i>Canis familiaris</i>	15	1	21	1	40	2
<i>Equus ferus</i>	5	1	7	2	12	3
<i>Bos primigenius</i>	5	2	7	1	12	9
<i>Capra pyrenaica</i>	55	5	123	11	178	16
<i>Cervus elaphus</i>	393	14	664	13	1057	27
<i>Capreolus capreolus</i>	20	3	58	6	78	9
<i>Sus ferus</i>	46	7	108	13	154	20
<i>Canis lupus</i>	5	1	2	2	7	3
<i>Vulpes vulpes</i>	57	11	55	9	112	20
<i>Ursis arctos</i>	15	1	13	2	28	3
<i>Felis silvestris</i>	7	2	19	2	26	4
<i>Lynx pardina</i>	4	1	6	1	10	2
<i>Meles meles</i>	47	4	77	7	124	11
<i>Martes sp.</i>	7	3	8	1	15	4
<i>Oryctolagus cuniculus</i>	1156	58	1796	96	2952	154
<i>Lepus granatensis</i>	89	15	45	5	134	20
TOTAL	4632	246	8122	347	12754	593

according to Brothwell (1981), and also shows *antemortem* loss of both third molars as well as caries in one of the second molars and dental calculus on one incisor.

The Neolithic levels from Cueva de Chaves have the highest amount of faunal remains when compared to other Early Neolithic sites from Iberia (Castaños, 2004). Both domestic and wild species recovered from the Early Neolithic levels show an equal percentage of representation: 49.6% of the total remains are domestic, and 51.4% are wild (Castaños, 2004) (Table 2). For this study a total of 64 faunal remains of 14 different taxa were selected following the classification of Castaños (2004). The taxa analyzed consists of: *Ovis/Capra*, *Sus domesticus*, *Bos taurus*, *Capra pyrenaica*, *Capreolus capreolus*, *Equus caballus*, *Cervus elaphus*, *Meles meles*, *Vulpes vulpes*, *Canis sp.*, *Buteo buteo*, *Felis silvestris*, *Oryctolagus cuniculus* and *Lepus granatensis*. Only adult faunal specimens have been sampled in order to avoid altered values due to suckling or weaning effects (Fogel, Tuross, & Owsley, 1989; Fuller, Fuller, Harris, & Hedges, 2006). *Canis sp.* and *Felis silvestris* are considered as carnivores because of the lack of evidence to define them as either domestic or wild. We have followed Castaños (2004) for determination of domestic or wild *Sus* specimens, but ruled out subadult specimens, which are impossible to distinguish between domestic and wild, as well as large-sized pig remains following Navarrete and Saña (2017).

2.2 | Isotopic analysis

Isotope analysis of the Cueva de Chaves samples was carried out at the Stable Isotope Laboratories of the University of Cape Town (South Africa). A total of 68 samples were cleaned by removing the

bone outer layer by mechanical abrasion using a 220 Dremel 3500 drill. Collagen extraction for carbon ($\delta^{13}\text{C}$) and nitrogen ($\delta^{15}\text{N}$) isotope analysis was done following the Longin (1971) method with the addition of an ultrafiltration step (Brown, Nelson, Vogel, & Southon, 1988). Approximately 300 mg of cleaned bone samples from each specimen were demineralized in 0.5M HCl solution at 5 °C until fully demineralization. Demineralized samples were rinsed three times with deionized water until pH became neutral. The samples were gelatinized at 70 °C for 48 hr using a heater block (FMH instruments, South Africa). This solution was filtered with a 9 ml EZEE-filter (Elkay, United Kingdom) to remove small (<8 μm) particles and ultrafiltered with 30 kDa ultrafilters (Amicon, Germany) using a centrifuge (Thermo Fisher Scientific Megafuge 16, USA) at 2500 rpm during variable times depending on the filtering speed of each sample. The final solution was then frozen and lyophilized for 48 hr. Finally, duplicate about 0.5 mg of collagen per sample was weighed into tin capsules, and loaded into the mass spectrometer.

The carbon and nitrogen isotope ratio measurements were performed using a Finnigan Delta plus XP continuous-flow isotope ratio mass spectrometer (Thermo Fisher Scientific, USA) after being combusted in an elemental analyser Flash EA 1112 interfaced with it (Thermo Fisher Scientific, USA). Stable Carbon isotope ratios were expressed relative to the VPDB scale (Vienna Pee Dee Belemnite), and stable Nitrogen isotope ratios were measured relative to the AIR scale (atmospheric N_2), using the delta notation (δ) in parts per thousand (‰). Repeated analysis of internal and international standards determined an analytical precision of 0.1‰ (1 σ) or less for $\delta^{13}\text{C}$ and $\delta^{15}\text{N}$. All analyses were carried out in duplicate.

TABLE 3 Cueva de Chaves S-UCT code, species, sampled bone, archaeological level, biological age group, $\delta^{13}\text{C}$ and $\delta^{15}\text{N}$ average values, collagen control indicators (%C, %N, C:N elemental) and radiocarbon dates

S-UCT code	Species	Sampled bone	Archaeological level	Age group	Average $\delta^{13}\text{C}$ ‰	Average $\delta^{15}\text{N}$ ‰	C (%)	N (%)	C: N Elemental	Radiocarbon date (uncalibrated)
18534	<i>Ovis aries/ Capra hircus</i>	tibia	lb	adult	-19.9	3.9	40.4	13.8	3.4	-
18538	<i>Ovis aries/ Capra hircus</i>	radius	lb	adult	-19.6	4.7	41.2	14.9	3.2	-
18537	<i>Ovis aries/ Capra hircus</i>	innominate	lb	adult	-19.5	4.6	43.0	15.5	3.2	-
18536	<i>Ovis aries/ Capra hircus</i>	phalanx	lb	adult	-19.7	4.8	38.6	13.4	3.4	-
18535	<i>Ovis aries/ Capra hircus</i>	calcaneus	lb	adult	-19.8	3.4	42.7	15.3	3.3	-
18533	<i>Ovis aries/ Capra hircus</i>	tibia	lb	adult	-19.6	3.7	40.1	14.4	3.2	-
18540	<i>Ovis aries</i>	talus	lb	adult	-19.5	4.7	41.0	14.7	3.2	-
18539	<i>Ovis aries</i>	talus	lb	adult	-20.1	3.5	41.5	14.5	3.3	-
18541	<i>Ovis aries</i>	talus	lb	adult	-19.9	5.3	39.8	13.7	3.4	-
18580	<i>Bos taurus</i>	mandible	la	adult	-19.6	6.2	40.6	14.2	3.3	-
18581	<i>Bos taurus</i>	innominate	la	adult	-19.6	3.7	41.3	14.5	3.3	-
18582	<i>Bos taurus</i>	tarsus	la	adult	-19.1	5.4	42.5	15.5	3.2	-
18583	<i>Bos taurus</i>	calcaneus	lb	adult	-19.8	4.4	43.0	15.6	3.2	-
18584	<i>Bos taurus</i>	humerus	lb	adult	-19.6	5.1	34.4	11.6	3.5	-
18585	<i>Bos taurus</i>	cranial fragment	lb	adult	-20.1	3.4	32.8	11.3	3.4	-
18569	<i>Cervus elaphus</i>	radius	lb	adult	-20.1	3.9	41.0	14.5	3.3	-
18571	<i>Cervus elaphus</i>	femur	lb	adult	-20.2	3.7	41.7	14.8	3.3	-
18570	<i>Cervus elaphus</i>	humerus	lb	adult	-20.1	4.4	40.0	13.9	3.4	-
18572	<i>Cervus elaphus</i>	humerus	la	adult	-20.0	3.4	39.5	13.9	3.3	-
18573	<i>Cervus elaphus</i>	humerus	la	adult	-19.9	3.1	42.7	15.4	3.2	-
18574	<i>Cervus elaphus</i>	mandible	la	adult	-18.8	4.6	41.2	15.0	3.3	-
18544	<i>Capreolus capreolus</i>	scapula	lb	adult	-20.9	4.8	38.9	13.3	3.4	-
18545	<i>Capreolus capreolus</i>	talus	lb	adult	-19.1	4.7	40.8	14.0	3.4	-
18543	<i>Capreolus capreolus</i>	scapula	lb	adult	-19.9	3.9	41.9	14.4	3.4	-
18542	<i>Capreolus capreolus</i>	metapodia	la	adult	-20.1	3.7	43.2	15.5	3.2	-
18575	<i>Capra pyrenaica</i>	cranial fragment	la	adult	-19.7	3.5	41.6	14.7	3.3	-
18578	<i>Capra pyrenaica</i>	metapodia	lb	adult	-19.5	3.9	42.8	14.9	3.3	-
18579	<i>Capra pyrenaica</i>	humerus	lb	adult	-19.5	2.7	39.4	13.9	3.3	-
18576	<i>Capra pyrenaica</i>	innominate	la	adult	-19.6	2.7	39.4	13.9	3.3	-
18577	<i>Capra pyrenaica</i>	scapula	lb	adult	-19.5	3.3	41.0	14.2	3.4	-
18549	<i>Equus caballus</i>	talus	lb	adult	-21.1	5.1	41.3	14.6	3.3	-
18550	<i>Equus caballus</i>	phalanx	lb	adult	-20.1	3.4	36.3	12.7	3.3	-
18547	<i>Equus caballus</i>	radius	la	adult	-21.2	5.1	41.1	14.4	3.3	-
18546	<i>Equus caballus</i>	metapodia	la	adult	-20.4	3.7	28.1	9.8	3.3	-
18548	<i>Equus caballus</i>	calcaneus	lb	adult	-21.0	5.1	41.8	14.6	3.3	-
18568	<i>Oryctolagus cuniculus</i>	femur	la	adult	-20.2	0.9	38.2	13.6	3.3	-
18564	<i>Oryctolagus cuniculus</i>	femur	la	adult	-21.9	1.4	42.4	14.6	3.4	-
18565	<i>Oryctolagus cuniculus</i>	femur	la	adult	-21.1	5.4	40.7	14.6	3.3	-
18566	<i>Oryctolagus cuniculus</i>	femur	la	adult	-22.0	5.5	35.9	12.3	3.4	-
18567	<i>Oryctolagus cuniculus</i>	femur	la	adult	-21.5	4.7	41.9	14.5	3.4	-
18559	<i>Lepus granatensis</i>	metapodia	la	adult	-21.6	2.5	42.4	15.2	3.3	-
18560	<i>Lepus granatensis</i>	tibia	la	adult	-22.0	2.8	42.0	15.1	3.2	-
18561	<i>Lepus granatensis</i>	innominate	la	adult	-20.8	5.5	43.3	15.7	3.2	-
18563	<i>Lepus granatensis</i>	tibia	la	adult	-21.9	2.7	69.3	15.3	5.3	-
18554	<i>Sus domesticus</i>	calcaneus	la	adult	-20.5	3.6	35.8	12.4	3.4	-
18551	<i>Sus domesticus</i>	humerus	la	adult	-20.6	4.5	42.0	15.1	3.2	-
18552	<i>Sus domesticus</i>	maxilla	la	adult	-20.2	5.8	38.4	13.1	3.4	-
18553	<i>Sus domesticus</i>	radius	la	adult	-19.5	5.3	39.5	13.6	3.4	-
18555	<i>Sus domesticus</i>	calcaneus	la	adult	-19.9	4.1	42.4	15.2	3.2	-

(Continues)

TABLE 3 (Continued)

S-UCT code	Species	Sampled bone	Archaeological level	Age group	Average $\delta^{13}\text{C}$ ‰	Average $\delta^{15}\text{N}$ ‰	C (%)	N (%)	C: N Elemental	Radiocarbon date (uncalibrated)
18586	<i>Meles meles</i>	radius	lb	adult	-18.3	8.0	43.4	15.6	3.2	-
18587	<i>Meles meles</i>	calcaneus	lb	adult	-18.3	7.9	42.0	15.1	3.2	-
18588	<i>Meles meles</i>	vertebra	lb	adult	-18.1	7.5	42.1	15.2	3.2	-
18594	<i>Meles meles</i>	mandible	la	adult	-18.3	7.6	43.9	15.5	3.3	-
18597	<i>Meles meles</i>	femur	la	adult	-17.7	9.7	42.7	15.1	3.3	-
18590	<i>Canis sp.</i>	metatarsus	la	adult	-19.4	5.8	41.8	14.8	3.3	-
18591	<i>Canis sp.</i>	metatarsus	la	adult	-19.5	6.0	40.6	14.2	3.3	-
18592	<i>Canis sp.</i>	scapula	la	adult	-18.2	7.6	42.6	15.4	3.2	-
18593	<i>Canis sp.</i>	tibia	la	adult	-19.3	9.9	43.4	15.3	3.3	-
18525	<i>Felis silvestris</i>	ulna	lb	adult	-19.1	6.8	42.0	15.0	3.3	-
18526	<i>Felis silvestris</i>	tibia	lb	adult	-18.6	4.7	42.5	15.1	3.3	-
18527	<i>Felis silvestris</i>	humerus	lb	adult	-19.5	6.5	42.7	15.1	3.3	-
18596	<i>Felis silvestris</i>	long bone diaphysis	la	adult	-18.9	6.2	41.7	15.2	3.2	-
18595	<i>Vulpes vulpes</i>	cranial fragment	la	adult	-18.2	7.9	42.0	15.2	3.2	-
18589	<i>Buteo buteo</i>	radius	la	adult	-20.0	8.8	42.7	15.2	3.3	-
19600	<i>Homo sapiens</i>	mandible	la	adult	-19.1	9.0	37.7	13.2	3.3	5645 ± 31
21023	<i>Homo sapiens</i>	mandible	la	infant	-19.1	8.8	40.2	13.8	3.4	6180 ± 54
21024	<i>Homo sapiens</i> (84C)	phalanx	la	adult	-18.5	10.6	44.0	15.6	3.3	6230 ± 45
21025	<i>Homo sapiens</i>	mandible	la	adult	-19.4	9.5	44.3	16.0	3.3	6227 ± 28

3 | RESULTS

Bone samples from 4 humans and 64 animals were analyzed from the Early Neolithic levels of Cueva de Chaves. The $\delta^{13}\text{C}$ and $\delta^{15}\text{N}$ results are presented in Table 3 and plotted in Figure 4. All the samples from Cueva de Chaves yielded enough collagen from the >30 kDa fraction for analysis in duplicate, and %C (around ≥ 30), %N (around ≥ 10) and C:N ratio (2.9–3.6) values indicate a good collagen quality, according to Ambrose (1993), De Niro (1985), and Van Klinken (1999). The $\delta^{13}\text{C}$ and $\delta^{15}\text{N}$ values were obtained from the >30 kDa fraction of the lyophilized collagen.

Herbivore $\delta^{13}\text{C}$ values range between -22.0‰ and -18.8‰ with a mean value of -20.2 ± 0.8 [1σ] ‰. The taxa with the smallest $\delta^{13}\text{C}$ values are rabbits and hares, which usually present ^{13}C -depleted values in the region (Salazar-García et al., 2014; Villalba-Mouco et al., 2018), and show a high deviation. Herbivore $\delta^{15}\text{N}$ values range between 0.9‰ and 6.2‰, with a mean value of 4.0 ± 1.1 [1σ] ‰, defining the trophic baseline of the ecosystem foodweb. In this case, rabbit and hares also present the lowest values and the highest deviation of $\delta^{15}\text{N}$ values (see Table 1, Figure 3). These herbivore $\delta^{13}\text{C}$ and $\delta^{15}\text{N}$ values are consistent with typical values for a terrestrial C_3 European ecosystem (De Niro and

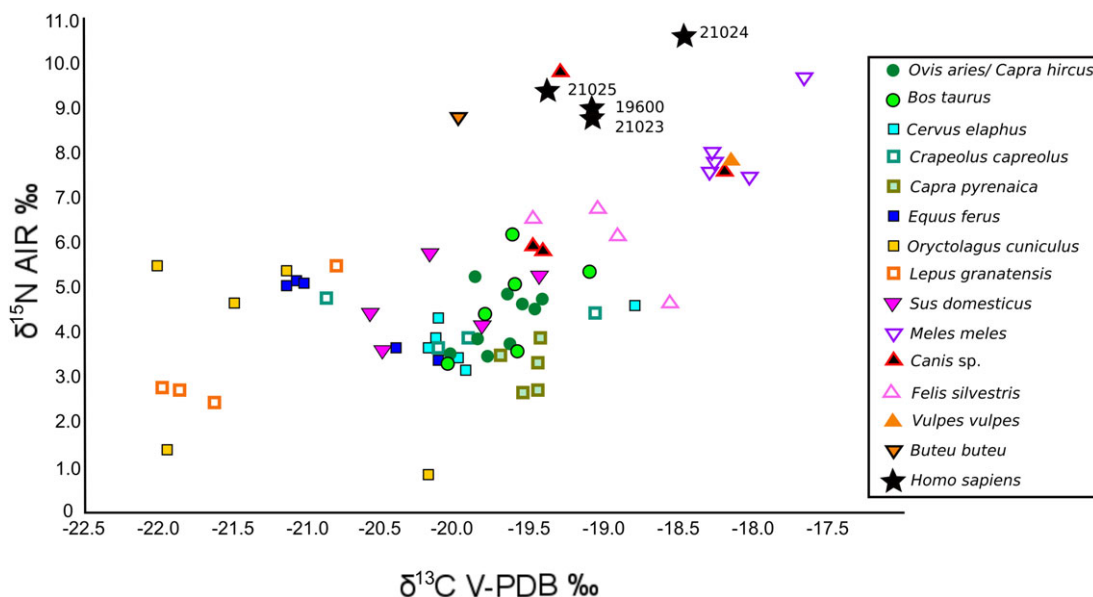


FIGURE 4 Scatter plot of human and fauna bone collagen $\delta^{13}\text{C}$ and $\delta^{15}\text{N}$ values from Cueva de Chaves. The X and Y axes are plotted at different scales in order to make all the samples more visible [Color figure can be viewed at wileyonlinelibrary.com]

Epstein, 1978; Schwarcz and Schoeninger, 1991). If we divide the sample between domestic (*Ovis/Capra* and *Bos taurus*; $\delta^{13}\text{C}$ mean: -19.7 ± 0.2 [1 σ] ‰; $\delta^{15}\text{N}$ mean: 4.4 ± 0.8 [1 σ] ‰) and non-lagomorph wild herbivores (*Cervus elaphus*, *Capreolus capreolus*, *Capra pyrenaica* and *Equus caballus*; $\delta^{13}\text{C}$ mean: -20.0 ± 0.6 [1 σ] ‰; $\delta^{15}\text{N}$ mean: 3.9 ± 0.8 [1 σ] ‰), they show no differences in $\delta^{13}\text{C}$ ($p = 0.074$) nor $\delta^{15}\text{N}$ ($p = 0.086$) values.

Domestic pig livestock (*Sus domesticus*) were classically considered as potential omnivores. Their $\delta^{13}\text{C}$ values range between -20.6‰ and -19.5‰ , with a mean value of -20.1 ± 0.5 [1 σ] ‰ and place them in the same range as all other medium- and large-sized herbivores. Their $\delta^{15}\text{N}$ values range between 3.6‰ and 5.8‰ , with a mean value of 4.7 ± 0.9 [1 σ] ‰, which does not show the increase expected for a change of trophic level (Bocherens and Drucker, 2003; Minagawa and Wada, 1986). A nonparametric Mann Whitney test indicates no significance differences between the means for herbivores (not including ^{13}C -depleted lagomorphs) and pigs in $\delta^{13}\text{C}$ ($p: 0.260$) or in $\delta^{15}\text{N}$ ($p: 0.236$).

Carnivore $\delta^{13}\text{C}$ values range between -20.0‰ and -17.7‰ , with a mean value of -18.8 ± 0.7 [1 σ] ‰, and their $\delta^{15}\text{N}$ values range between 4.7‰ and 9.9‰ , with a mean value of 7.4 ± 1.4 [1 σ] ‰. These values position them in a higher trophic level than both herbivores and potential omnivores. Overall, the non-parametric Mann Whitney test shows significant differences between pigs and carnivores in $\delta^{13}\text{C}$ ($p: 0.004$) and $\delta^{15}\text{N}$ ($p: 0.003$) values. However, the non-parametric Kruskal Wallis test reveals significant differences in $\delta^{13}\text{C}$ values between *Canis sp.*, *Felis silvestris*, and *Meles meles* ($p: 0.043$). Dunn's Post Hoc test also shows further significant differences between *Meles meles* and *Felis silvestris* ($p: 0.033$) and between *Meles meles* and *Canis sp.* ($p: 0.033$). These significant differences can define the specific diet of each species. Only *Felis silvestris* and *Canis sp.* appear to have an isotopically similar diet (Dunn's Post Hoc test $p: 1.000$). The non-parametric Kruskal Wallis test reveals no significant differences in $\delta^{15}\text{N}$ values between *Canis sp.*, *Felis silvestris*, and *Meles meles* ($p: 0.089$). *Vulpes vulpes* and *Buteo buteu* are not included in the statistical analysis because of their low sample number.

The four human $\delta^{13}\text{C}$ values (including the subadult individual) range between -19.4‰ and -18.5‰ , with a mean value of -19.0 ± 0.4 [1 σ] ‰, and the $\delta^{15}\text{N}$ values are between 8.8‰ and 10.6‰ , with a mean value of 9.5 ± 0.8 [1 σ] ‰. These average values portray a terrestrial diet based mainly on C_3 terrestrial resources, and defines the highest values of the local trophic ecosystem foodweb. Of interest is that the only individual recovered from an actual Cardial burial shows higher $\delta^{13}\text{C}$ (by 0.7‰) and $\delta^{15}\text{N}$ (by 1.5‰) values than the average from the other three individuals. In any case, because of the low number of samples, these results need to be interpreted with caution (Figure 4).

4 | DISCUSSION

4.1 | Wild and domestic herbivores

No significant differences were found between wild and domestic herbivores. These similar values could point towards a possible common plant resource consumption for both wild and domestic herbivores. Different environmental factors may have an effect on stable isotope values (Drücker et al., 2003; Goude and Fontugne, 2016). The

$\delta^{13}\text{C}$ values help to distinguish between open or close-forested environments, with the plants that grow in closed environments showing lower $\delta^{13}\text{C}$ values (O'Leary, 1981; Tieszen, 1991); the $\delta^{15}\text{N}$ values increase due to arid conditions or vary depending on soil type (Ambrose, 1993; Handley et al., 1999). Therefore, another possible explanation for these similar values between wild and domestic species could be linked to a shared environment and/or the use of the same parts of the landscape for grazing. These data could suggest foddering domestic animals with wild plants. The use of wild plants such as *Juniperus* for foddering was previously suggested by an anthracological study in the most recent Early Neolithic level (Alcolea et al., 2017). The use of *Juniperus* as fodder has been documented in the Central Pyrenees (Villar and Fernández, 2000) and in ovicaprine coprolites from the prehistoric La Fangade archaeological site in France (Bouby, 2014; Chabal et al., 2009).

In either scenario, the use of wild plant species as fodder for domestic animals reflect that the population relied more on animal husbandry than agricultural practices. This hypothesis is in agreement with palynological studies that suggest a low impact of crop management at the site except during the last stages of the Early Neolithic (López García and López Sáez, 2000). Some authors suggest that this could be the result of not having potential agricultural fields close to Cueva de Chaves (Mazzucco et al., 2015). In this sense, the absence of grains makes it isotopically difficult to test if manuring practices played an important role in the early stages of Iberian Neolithic agriculture. However, the fact that both wild and domestic animals have a similar $\delta^{15}\text{N}$ values suggests that no manure signal is present (Bogaard, Heaton, Poulton, & Merbach, 2007; Bogaard et al., 2013).

The Cueva de Chaves domestic herbivore data also present little dispersion. Specifically, domestic ovicaprids show the smallest dispersion in both $\delta^{13}\text{C}$ and $\delta^{15}\text{N}$ values and suggest a common environment and feeding that could be associated with stabling practices to protect the livestock from the wild carnivores as described for other Iberian Early Neolithic sites (Oms et al., 2014b; Saña et al., 2015). This common feeding/environment would imply the absence of sheep flocks or transhumance activities amongst the Early Neolithic community living in the cave (Martín et al., 2015). However, since bulk bone collagen reflects an average of the last years of life, it is difficult to find differences in isotopic values resulting from the seasonal movements between environments; sequential $\delta^{13}\text{C}$ and $\delta^{18}\text{O}$ isotopic analysis of teeth would be necessary to prove the absence of these types of husbandry practices (Tornero et al., 2016, 2018). Even so, non-transhumance activities would be in agreement with the characteristics of a big settlement such as Cueva de Chaves, and would confirm that it was not a site for short residence periods as is typical for mountain sites linked to sheep-herding activities (Rojo-Guerra et al., 2013).

Isotopic tests between wild and domestic herbivores have been carried out in order to test differences in husbandry management practices in other contemporary Iberian sites such as La Draga or Cova de Frare (Navarrete et al., 2017). At the first site, the domestic fauna showed higher $\delta^{13}\text{C}$ and $\delta^{15}\text{N}$ values (Navarrete et al., 2017). These slight isotopic differences could suggest different feeding strategies, such as using agricultural crops as one of the potential fodders for domestic species. The reason for these higher $\delta^{13}\text{C}$ and $\delta^{15}\text{N}$ values could be the use of natural fertilizers. Although the presence of

crops in La Draga is clear (Antolín, 2016; Antolín and Buxó, 2011;), the increase in $\delta^{15}\text{N}$ values is quite low to propose an intensive manuring effect (Bogaard et al., 2013). However, the other Early Neolithic site, Cova de Frare, presents no isotopic differences between wild and domestic herbivores (Navarrete et al., 2017), likewise as observed at Cueva de Chaves.

4.2 | Omnivores: Pig livestock

Suids are omnivores with a flexible ecological niche because of their opportunistic feeding (Macdonald and Barrett, 1993; Schley and Roper, 2003). Humans have taken advantage of this to feed domestic pigs (*Sus domesticus*) with whatever suited them. As a result, the diet of pigs has proved to reflect many aspects of human community structure in both prehistoric (Madgwick, Mulville, & Stevens, 2012) and historic periods (Halley and Rosvold, 2014). In this sense, two main management models for pig husbandry have been proposed. The first one is based on a free-range management where pigs feed on their own and most of the diet comes from plants (Madgwick et al., 2012), resulting in an herbivorous isotopic signal. The other one is the household management one, where pigs feed on leftovers and human debris and therefore commonly show a mixed isotopic signature resulting from combining the different types of foods consumed by humans in each case (Balasse et al. 2016; Madgwick et al., 2012; Müldner and Richards, 2005; Privat, O'Connell, & Richards, 2002; Richards, Fuller, & Molleson, 2006). Some authors consider that both suid husbandry management models can occur simultaneously in what is called a "household model" with mixed diets only depending on the size of livestock (Navarrete et al., 2017). Other authors argue that pig management practices change according to the chrono-cultural period, showing more household feeding of pigs in historic rather than prehistoric times (Madgwick et al., 2012).

Domestic pigs from Cueva de Chaves show a significant difference in their $\delta^{13}\text{C}$ ($p: 0.007$) and $\delta^{15}\text{N}$ ($p: 0.007$) values with carnivores, but no significant difference with herbivores from the same ecosystem ($\delta^{13}\text{C} = p: 0.237$; $\delta^{15}\text{N} = p: 0.203$). Having the same $\delta^{15}\text{N}$ range as herbivores shows they are in a same trophic level, ruling out a significant input of animal protein in their diet (Bocherens and Drucker 2003). The $\delta^{15}\text{N}$ values are also the same for ruminant and non-ruminant herbivores, suggesting that isotopic digestive fractionation could cause an incorrect herbivore profile in pigs (Halley and Rosvold, 2014; Hedges, 2003). This herbivore trophic attribution would be compatible with a free-range pig husbandry management similar to what is proposed for the Early Neolithic Iberian sites of Cova del Frare and Serra de Mas Bonet (Navarrete et al., 2017). However, and contrary to what is observed at these sites, Cueva de Chaves has a large-sized pig livestock, more similar to the one from La Draga where an herbivore pig diet has also been suggested (Navarrete et al., 2017). Furthermore, Cueva de Chaves is one of the biggest pig husbandry communities in the Iberian Early Neolithic according to the number of pig remains recovered ($n = 1217$) (Castaños, 2004), followed by La Draga ($n = 1048$) (Saña, 2011), and shows mostly an infant and juvenile specimen slaughtering pattern as at La Draga (Saña, 2011). This kind of husbandry management is more usual in a household model (Halstead and Isaakidou, 2011), where number of

pigs is limited by pig size, which is bigger as a result of feeding them with animal fat and protein in order to slaughter them earlier (Balasse et al., 2016).

All these aforementioned traits lead us to propose, a controlled and limited dispersion range for suid husbandry, or their keeping in an enclosure where they would be fed only plant foods (Hadjikoumis, 2012; Halstead and Isaakidou, 2011). In this sense, anthracological evidence shows the importance of acorns in Cueva de Chaves during the older Early Neolithic level (Alcolea et al., 2017; Zapata, Baldellou, & Utrilla, 2008) when the presence of a woodland environment is suggested (Alcolea et al., 2017). The consumption of acorns could have decreased over time (Hamilton et al., 2009), parallel to the woodland clearing at the recent Early Neolithic level (Alcolea et al., 2017).

It is also necessary to consider that, as ethnography shows (Halstead and Isaakidou, 2011), a fattening diet based on animal products could take place at the end of the pig's life and would therefore not be shown in the collagen bulk signature. However, it seems that the overall introduction of leftover feeding of pigs happened over time, linked to the complexity of the settlements (Madgwick et al., 2012). An even bigger dataset would be required to get more in-depth information on pig management in the Neolithic levels from Cueva de Chaves.

4.3 | Wild and domestic carnivores

The canine data show the highest dispersion inside the carnivore group. This could be translated into a heterogeneous feeding pattern that could be linked to their wild or domestic status. Two of them (S-UCT 18592 and S-UCT 18593) are closer to the human isotopic values and could be associated to domestic adscription, because in that case most of their diet depends on human provided or leftover foods (Reitsema, Kozłowski, & Makowiecki, 2013). This would be in agreement with the dog surrogacy hypothesis, which considers dogs to be a good proxy to recover information on prehistoric human diet whenever human remains are not available (e.g., Guiry and Grimes, 2013). The other two canine values (S-UCT 18590 and S-UCT 18591) show lower values than expected for a full carnivore diet but could be in agreement with a high consumption of depleted ^{13}C and ^{15}N rabbits and hares and their wild adscription. It is also important to highlight that wolves are a highly mobile species and they can reflect the isotopic values from different environments (Blanco, 2017).

In the case of wild cats (*Felis silvestris*) their $\delta^{13}\text{C}$ and $\delta^{15}\text{N}$ values do not show clear evidence of household feeding, suggesting a combination of human leftover and small prey hunting in their diet. Regarding other wild carnivores, only the data for one *Vulpes vulpes* is positioned inside the range of *Meles meles*. While *Vulpes vulpes* mainly feed on rabbits (López-Martín, 2017), *Meles meles* eat mainly earthworms but have a huge range of food resources including rabbits (Virgós, 2005), which are abundant in the Early Neolithic levels of Cueva de Chaves (Castaños, 2004). Because the *Meles meles* $\delta^{13}\text{C}$ and $\delta^{15}\text{N}$ values are very close to those of *Vulpes vulpes*, it could be argued that the specimens analyzed consumed abundant rabbit. The problem when looking at the Chaves baseline is that rabbits have lower $\delta^{13}\text{C}$ and $\delta^{15}\text{N}$ values than what would fit the pattern if *Vulpes vulpes* and *Meles meles* were mainly consuming them, so it is possible that both

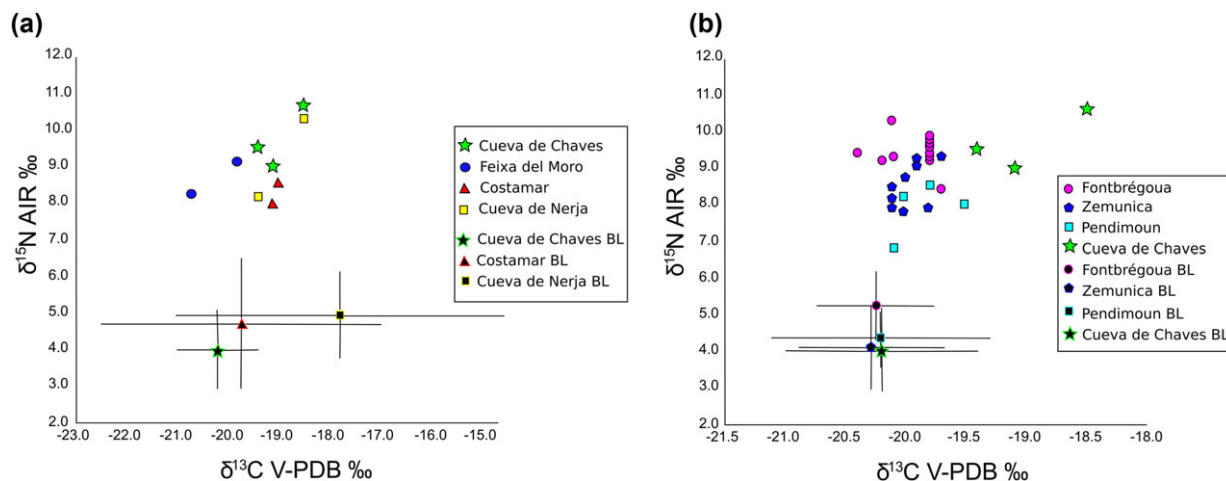


FIGURE 5 (a) Plot of bone collagen $\delta^{13}\text{C}$ and $\delta^{15}\text{N}$ values of different Early Neolithic adult humans from Iberia [Costamar (Salazar-García, 2009); Cueva de Nerja (Salazar-García et al., 2017b); Feixa del Moro (Remolins et al., 2016) and Cueva de Chaves (this study)]; (b) Plot of bone collagen $\delta^{13}\text{C}$ and $\delta^{15}\text{N}$ values of different Early Neolithic from the Western Mediterranean region [Fontbrégoua (France) (Le Bras-Goude et al., 2009), Pendimoun (Le Bras-Goude et al., 2006), 3: Zemunica (Croatia) (Guiry et al., 2017) and Cueva de Chaves (this study)]. The X and Y axes are plotted at different scales in order to make all the samples more visible. The $\delta^{13}\text{C}$ and $\delta^{15}\text{N}$ baselines were calculated with contemporaneous herbivore data of each site when was available excluding domestic pigs. Subadult individuals were excluded; BL: Baseline [Color figure can be viewed at wileyonlinelibrary.com]

badgers and foxes also scavenged human refuse (López-Martín, 2017; Virgós, 2005). The addition of freshwater resources like amphibians or reptiles in the diet could be also compatible with the *Meles meles* isotopic values. The intermittent water flux of the ravines close to Cueva de Chaves (Ortega Becerril, 2010), however, makes the consumption of riverine fish less plausible.

4.4 | Human dietary reconstruction

Humans from Cueva de Chaves present isotopic values that show a protein diet based mainly on C_3 terrestrial resources. The $\delta^{15}\text{N}$ human values are 5.5‰ higher than herbivore values (wild and domestic) and 4.8‰ higher than the suid values. Because there are no significant isotopic differences between wild and domestic herbivores, it is difficult to know which of these resources humans relied on more. Perhaps little of the protein intake came from lagomorphs and horses, which show lower $\delta^{13}\text{C}$ values than what would be expected from the main protein source of the human diet. This would be compatible with the higher importance of domestic animal resources put forward by the zooarchaeological study (Castaños, 2004) (Table 2).

Regarding plant consumption, and keeping in mind the isotopic masking effect of animal protein on plant foods, the high $\delta^{15}\text{N}$ values could suggest that plant foods were not the central element of their protein diet, which would be based on animal resources (Bocherens and Drucker, 2003). Previous studies suggested a high consumption of plant resources at Cueva de Chaves based on the presence of a pit structure full of charred acorns dated back to the Early Neolithic (Zapata et al., 2008). However, isotopically it seems more probable that domestic animals (mainly suids) were fed acorns, which would have been consumed by humans only sporadically. Furthermore, there is no isotopic evidence whatsoever for the consumption of C_4 resources.

Looking at the human sample in more detail, there is a quite homogeneous group of three individuals, including the subadult individual who does not show a breastfeeding or weaning signal (Fuller et al., 2006). Amongst this first group the $\delta^{15}\text{N}$ values are high and can be explained by abundant meat consumption (higher by 5.1‰ in $\delta^{15}\text{N}$ values and by 1‰ in $\delta^{13}\text{C}$ values than herbivores). The single individual who does not cluster with the others is individual S-UCT 21024, whose body was recovered from a special burial. This individual shows higher $\delta^{15}\text{N}$ and $\delta^{13}\text{C}$ values (by 6.6‰ and 1.7‰ higher than herbivores, respectively; 1.5‰ and 0.7‰ higher than the other humans, respectively) (Figure 4). For this individual, a small input of another type of protein resource could be suggested, perhaps marine or estuarine protein consumption in low quantities but enough as to be recorded in the isotopic collagen composition. Cueva de Chaves is located close to the Solencio ravine, which presents a torrential water flux, something likely not compatible with the extensive presence of freshwater fish. Moreover, the higher $\delta^{15}\text{N}$ and $\delta^{13}\text{C}$ values at the same time is more common for marine than freshwater resource consumption (Lillie, Budd, & Potekhina, 2011). If this was the case and the individual had eaten marine or estuarine fish, as they are not available locally, this would be another point to support the existence of coastal-inland routes for this time period. This has been proposed previously by schematic rock art studies (Hernández Pérez, 2016; Utrilla and Baldellou, 2002) as well as by the huge set of Cardial pottery and marine shells used for Cardial decoration recovered at the site (Utrilla and Laborda, 2018).

When plotting together all the adult Early Neolithic humans from Iberia (3 sites, 9 adult humans including Cueva de Chaves), individual S-UCT 21024 from Cueva de Chaves shows the highest $\delta^{13}\text{C}$ and $\delta^{15}\text{N}$ values only followed by one individual from Cueva de Nerja where a small C_4 input has been suggested (Salazar-García et al., 2017b) (Figure 5a). In contrast to Cueva de Nerja, no faunal remains have shown typical values from C_4 ecosystems at Cueva de Chaves,

so the hypothesis of marine protein intake is more plausible for this individual, as well as due to the presence of a higher $\delta^{15}\text{N}$ increase at Cueva de Chaves than at Cueva de Nerja in comparison to their respective faunal baselines. This would imply that the Cueva de Chaves first farmers arrived to the Iberian coast and penetrated fast into Iberia, and not through the Pyrenees as it was proposed in some works (Utrilla et al., 1998). Strontium isotope analysis in dental enamel could help to know more about the mobility of this Cardial individual with a special burial treatment during his life as long as the migration happened after the enamel mineralization and if the geology of the two areas (where the enamel mineralization took place and Cueva de Chaves) were different (Bentley 2013; Price, Burton, & Bentley, 2002).

At a broader scale encompassing the Western Mediterranean (Salazar-García, Fontanals-Coll, Goude, & Subirà, 2018), when plotting bone collagen $\delta^{13}\text{C}$ and $\delta^{15}\text{N}$ values from different Early Neolithic adult humans, we see how Chaves fits into the expected Early Neolithic mainly terrestrial protein diet intake. Even so, humans from different sites present variability and they cluster depending on their location and suggesting that human diets are not similar between all communities, although the baselines for each site show an overlap. In this sense, we observe again that individuals from Cueva de Chaves exhibit a trend that corresponds to the consumption of a significant quantity of food items with high $\delta^{13}\text{C}$ and $\delta^{15}\text{N}$ values and individual S-UCT 21024 from Cueva de Chaves is also positioned in the highest top-right part of the graph, perhaps due to some marine or estuarine protein intake (Figure 5b). In any case, comparing only humans from different ecosystems should be done with caution, as variations in the ecosystem baselines of each site might result in incomparable data.

5 | CONCLUSIONS

This study represents one of the few Early Neolithic isotope analysis studies carried out on the Iberian Peninsula where humans and a large set of fauna coming from the same chrono-cultural context have been analyzed together. While the number of domestic animal remains reflects the importance of animal husbandry at inland early farming communities, animal dietary strategies show a basic husbandry management. Domestic and wild species showed similar values, suggesting the use of common resources or areas for grazing. Even the domestic pig showed an herbivorous diet, ruling out a human leftover feeding. The human isotopic dietary study shows a high animal protein intake by all individuals. This high meat consumption would be related to the existence of a specialized animal husbandry management community in which agriculture was not intensively developed. The values from one individual might reflect a slight isotopic signature of marine or estuarine protein intake at some point of the individual's life. There was no isotopic evidence for the consumption of C_4 resources either by humans or fauna.

ACKNOWLEDGMENTS

VVM, DCSG, PU, and CML designed this work, VVM carried out sampling and labwork, VVM and DCSG made the analysis and the data

interpretation and VVM, DCSG, RL, PU, and JIL have contributed with the archaeological context. This study is part of VVM's Doctoral Thesis. VVM has a predoctoral scholarship funded by the Gobierno de Aragón and the Fondo Social Europeo (BOA20150701025), and carried out a research stay at the University of Cape Town funded by the Fundación Ibercaja-CAI (2016) and DCSG's UCT Research Developing Grant. DCSG acknowledges funding for this research from the BBVA Foundation (I Ayudas a Investigadores, Innovadores y Creadores Culturales). VVM, PU and RL are members of the Spanish project HAR2014-59042-P (Transiciones climáticas y adaptaciones sociales en la prehistoria de la Cuenca del Ebro), and VVM, PU, RL and JIL are members of the regional government of Aragón PPVE research group (H-07: Primeros Pobladores del Valle del Ebro). All authors thank the Museo de Huesca for allowing the use of their installations. They thank Ian Newton for technical assistance, Maricruz Sopena for archaeological drawings, Marta Alcolea for her useful comments, Rafael Larma for the topography of the cave and James Fellows Yates for the proofreading in English.

ORCID

Vanessa Villalba-Mouco  <http://orcid.org/0000-0002-9357-5238>

Cristina Martínez-Labarga  <http://orcid.org/0000-0003-0439-0379>

REFERENCES

- Alcolea, M., Utrilla, P., Piqué, R., Laborda, R., & Mazo, C. (2017). Fuel and acorns: Early Neolithic plant use from Cueva de Chaves (NE Spain). *Quaternary International*, 457, 228–239.
- Ambrose, S. H. (1993). Isotopic analysis of paleodiets: Methodological and interpretative considerations. In: M. K. Stanford (Ed.), *Investigations of ancient human tissue: Chemical analyses in anthropology* (pp. 59–130). Langhorne: Gordon and Breach Science Publishers.
- Antolín, F. (2016). Local, intensive and diverse? Early farmers and plant economy in the North-East of the Iberian Peninsula (5500–2300 Cal BC). *Advances in archaeobotany*, 2, Groningen.
- Antolín, F., & Buxo, R. (2011). L'explotació de les plantes al jaciment de la Draga: Contribució a la història de l'agricultura i de l'alimentació vegetal del neolític a Catalunya. In A. Bosch, J. Chinchilla, & J. Tarrús (Eds.), *El poblament lacustre del neolític antic de la draga: Excavacions de 2000–2005* (pp. 147–174). Girona: MAC-CASC.
- Arias, P. (2007). Neighbours but diverse: Social change in northwest Iberia during the transition from the Mesolithic to the Neolithic (5500–4000 cal BC). In A. Whittle, & V. Cummings (Eds.), *Going over: The mesolithic-neolithic transition in North-West Europe*, (pp. 53–71), Oxford: Oxford University Press.
- Balasse, M., Evin, A., Tornero, C., Radu, V., Fiorillo, D., Popovici, D., ... Bălăşescu, A. (2016). Wild, domestic and feral? Investigating the status of suids in the Romanian Gumelnița (5th mil. cal BC) with biogeochemistry and geometric morphometrics. *Journal of Anthropological Archaeology*, 42, 27–36.
- Balasse, M., Tornero, C., Bréhard, S., Ughetto-Monfrin, J., Voinea, V., & Bălăşescu, A. (2014). Cattle and sheep herding at Cheia, Romania, at the turn of the fifth millennium cal BC: A view from stable isotope analysis. *Proceedings of the British Academy*, 198 115–142.
- Baldellou, V. (2012). La Cueva de Chaves (Bastarás-Casbas, Huesca). *SAGNVTVM Extra*, 12, 141–144.
- Bentley, R. A. (2013). Mobility and the diversity of early Neolithic lives: Isotopic evidence from skeletons. *Journal of Anthropological Archaeology*, 32, 303–312.
- Bernabeu, J., García-Puchol, O., & Orozco-Köhler, T. (2018). New insights relating to the beginning of the Neolithic in the eastern Spain: Evaluating empirical data and modelled predictions. *Quaternary International*, 470, 439–450.

- Bernabeu, J., Molina, L., Esquembre, M. A., Ortega, J. R., Boronat, J. (2009). La cerámica impresa mediterránea en el origen del Neolítico de la Península Ibérica. *De Méditerranéen Et D'ailleurs... Mèlanges Offerts à Jean Guilaine*, (pp 83–95). Toulouse.
- Binder, D., & Sénépart, I. (2010). La séquence de l'Impresso-Cardial de l'abri Pendimoun et l'évolution des assemblages céramiques en Provence. In C. Manen, F. Convertini, D. Binder, & I. Sénépart (Eds.), *Premières sociétés paysannes de méditerranée occidentale. Structures des productions céramiques* (pp. 149–167). Toulouse: Société Préhistorique Fañçaise, Mémoire, 51.
- Blanco, J. C. (2017). *Lobo—Canis lupus*. En: *Enciclopedia virtual de los vertebrados españoles*. In A. Salvador & I. Barja (Eds.), Madrid: Museo Nacional de Ciencias Naturales. Available at: <http://www.vertebradosibericos.org/>
- Bocherens, H., & Drucker, D. (2003). Trophic level isotopic enrichment of carbon and nitrogen in bone collagen: Case studies from recent and ancient terrestrial ecosystems. *International Journal of Osteoarchaeology*, 13, 46–53.
- Bogaard, A., Fraser, R., Heaton, T. H., Wallace, M., Vaiglova, P., Charles, M., ... Stephan, E. (2013). Crop manuring and intensive land management by Europe's first farmers. *Proceedings of the National Academy of Sciences of the United States of America*, 110, 12589–12594.
- Bogaard, A., Heaton, T. H. E., Poulton, P., & Merbach, I. (2007). The impact of manuring on nitrogen isotope ratios in cereals: Archaeological implications for reconstruction of diet and crop management practices. *Journal of Archaeological Science*, 34, 335–343.
- Bosch, A., Chinchilla, J., & Tarrús, J. (2011). El poblado lacustre del neolítico antic de La Draga. Excavacions 2000–2005 (Vol. 9). Monografies del Centre d'Arqueologia Subaquatica de Catalunya.
- Bouby, L. (2014). *Agriculture dans le bassin du Rhône du bronze final à l'antiquité. Agrobiodiversité, économie, cultures*. Toulouse: Archives d'Écologie Préhistorique.
- Bronk Ramsey, C. (2009). Bayesian analysis of radiocarbon dates. *Radiocarbon*, 51, 337–360.
- Brown, T. A., Nelson, D. E., Vogel, J. S., & Southon, J. R. (1988). Improved collagen extraction by modified Longin method. *Radiocarbon*, 30, 171–177.
- Castaños, P. M. (2004). Estudio arqueozoológico de los macromamíferos del Neolítico de la Cueva de Chaves (Huesca). *Saldvie*, 4, 125–172.
- Chabal, L., Bouby, L., Figueiral, I., Catanzano, J., Leroy, F., Guibal, F., & Greck, S. (2009). Vivre sur un littoral lagunaire au Bronze final: Milieu et activités humaines d'après les macrorestes végétaux du site palafitique de La Fangade, étang de Thau (Sète, Hérault). *Des Hommes Et Des Plantes: Exploitation Du Milieu Et Gestion Des Ressources Végétales De La Préhistoire à Nos Jours, XXXe Rencontres Internat. d'Archéo. et D'Hist. d'Antibes*, 22–24.
- Davis, S. J., & Simões, T. (2016). The velocity of ovis in prehistoric times: The sheep bones from early Neolithic Lameiras, Sintra, Portugal. In M. Diniz, C. Neves, & A. Martins (Eds.), *O neolítico em Portugal antes do horizonte 2020: Perspectivas em debate*. Lisboa: Associação de arqueólogos portugueses (pp. 51–66). Monografias da AAP, Lisboa, Portugal.
- De Niro, M. J. (1985). Postmortem preservation and alteration of in vivo bone collagen isotope ratios in relation to paleodietary reconstruction. *Nature*, 317, 806–809.
- De Niro, M. J., & Epstein, S. (1978). Influence of diet on the distribution of carbon isotopes in animals. *Geochimica Et Cosmochimica Acta*, 42, 495–506.
- Domingo, R. (2009). Caracterización funcional de los microlitos geométricos: el caso del Valle del Ebro. *El mesolítico geométrico en la Península Ibérica* (pp. 375–389). Departamento de Ciencias de la Antigüedad, Universidad de Zaragoza, Zaragoza.
- Domingo, R. (2014). Beyond Chaves: Functional analysis of neolithic blades from the Ebro Valley. In J. Marreiros, N. Bicho, & J. F. Gibaja (Eds.), *International conference on use-wear analysis 2012* (pp. 672–681) Faro.
- Drucker, D., Bocherens, H., Bridault, A., & Billiou, D. (2003). Carbon and nitrogen isotopic composition of red deer (*Cervus elaphus*) collagen as a tool for tracking palaeoenvironmental change during the Late-Glacial and Early Holocene in the northern Jura (France). *Palaeogeogr Palaeoclimatol Palaeoecol*, 195(3), 375–388.
- Edwards, C. J., Bollongino, R., Scheu, A., Chamberlain, A., Tresset, A., Vigne, J. D., ... Burger, J. (2007). Mitochondrial DNA analysis shows a Near Eastern Neolithic origin for domestic cattle and no indication of domestication of European aurochs. *Proceedings of the Royal Society*, 274, 1377–1385.
- Fernández, E., Pérez-Pérez, A., Gamba, C., Prats, E., Cuesta, P., Anfruns, J., ... Turbón, D. (2014). Ancient DNA analysis of 8000 B.C. Near Eastern farmers supports an early Neolithic pioneer maritime colonization of mainland Europe through Cyprus and Aegean Islands. *PLOS Genetics*, 10, e1004401–e1004416.
- Fogel, M. L., Tuross, N., & Owsley, D. W. (1989). Nitrogen isotope tracers of human lactation in modern and archaeological populations. *Annual Report of the Director, Geophysical Laboratory 1988–89* (pp. 111–117). Carnegie Institute of Washington.
- Fuller, B. T., Fuller, J. L., Harris, D. A., & Hedges, R. E. M. (2006). Detection of breastfeeding and weaning in modern human infants with carbon and nitrogen stable isotope ratios. *American Journal of Physical Anthropology*, 129, 279–293.
- Gamba, C., Fernández, E., Tirado, M., Deguilloux, M. F., Pemonge, M. H., Utrilla, P., ... Arroyo-Pardo, E. (2012). Ancient DNA from an Early Neolithic Iberian population supports a pioneer colonization by first farmers. *Molecular Ecology*, 21, 45–56.
- García, B. P., Aura, T. E., Jordá Pardo, J. F., & Salazar-García, D. C. (2014). La cerámica neolítica de la Cueva de Nerja (Málaga, España): salas del Vestíbulo y la Mina. *Archivo de Prehistoria Levantina*, 30, 81–131.
- García-Borja, P., Salazar-García, D. C., Pérez, A., Pardo, S., & Casanova, V. (2011). El Neolítico Antiguo Cardial y la Cova de la Sarsa (Bocairent, Valencia). *Nuevas Perspectivas A Partir de su Registro Funerario. Munibe*, 62, 175–195.
- Goude, G., & Fontugne, M. (2016). Carbon and nitrogen isotopic variability in bone collagen during the Neolithic period: Influence of environmental factors and diet. *Journal of Archaeological Science*, 70, 117–131.
- Guilaine, J., & Manen, C. (2007). From Mesolithic to early Neolithic in the western Mediterranean. In A. Whittle & V. Cummings (Eds.), *Going over: The mesolithic-neolithic transition in North-west Europe* (Vol. 144, pp. 21–51). London: Proceedings of the British Academy.
- Guiry, E. J., & Grimes, V. (2013). Domestic dog (*Canis familiaris*) diets among coastal Late Archaic groups of northeastern North America: A case study for the canine surrogacy approach. *Journal of Anthropological Archaeology*, 32, 732–745.
- Guiry, E. J., Karavanić, I., Klindžić, R. Š., Talamo, S., Radović, S., & Richards, M. P. (2017). Stable isotope palaeodietary and radiocarbon evidence from the Early Neolithic Site of Zemunica, Dalmatia, Croatia. *European Journal of Archaeology*, 20, 235–256.
- Hadjikoumis, A. (2012). Traditional pig herding practices in southwest Iberia: Questions of scale and zooarchaeological implications. *Journal of Anthropological Archaeology*, 31, 353–364.
- Halley, D. J., & Rosvold, J. (2014). Stable isotope analysis and variation in medieval domestic pig husbandry practices in northwest Europe: Absence of evidence for a purely herbivorous diet. *Journal of Archaeological Science*, 49, 1–5.
- Handley, L. L., Austin, A. T., Stewart, G. R., Robinson, D., Scrimgeour, C. M., Raven, J. A., ... Schmidt, S. (1999). The $\delta^{15}\text{N}$ natural abundances of ecosystem samples reflects measures of water availability. *Aust J Plant Physiol*, 26, 185–199.
- Hamilton, J., Hedges, R. E., & Robinson, M. (2009). Rooting for pigfruit: pig feeding in Neolithic and Iron Age Britain compared. *Antiquity*, 83(322), 998–1011.
- Hedges, R. E., & Reynard, L. M. (2007). Nitrogen isotopes and the trophic level of humans in archaeology. *Journal of Archaeological Science*, 34, 1240–1251.
- Halstead, P., & Isaakidou, V. (2011). A Pig Fed by Hand is Worth Two in the Bush: Ethnoarchaeology of Pig Husbandry in Greece and its Archaeological Implications. In U. Albarella & A. Trentacoste (Eds.), *Ethnozooarchaeology: The Present and Past of Human-Animal Relationships* (pp. 160–174). Oxford: Oxbow.
- Herrscher, E., Goude, G., & Metz, L. (2017). Longitudinal study of stable isotope compositions of maternal milk and implications for the palaeo-diet of infants. *Bulletins et Mémoires de la Société d'Anthropologie de Paris*, 29 (3-4), 131–139.

- Hedges, R. E. (2003). On bone collagen—Apatite-carbonate isotopic relationships. *International Journal of Osteoarchaeology*, 13, 66–79.
- Hedges, R. E., Clement, J. G., Thomas, C. D. L., & O'Connell, T. C. (2007). Collagen turnover in the adult femoral mid-shaft: Modeled from anthropogenic radiocarbon tracer measurements. *American Journal of Physical Anthropology*, 133, 808–816.
- Hernández Pérez, M. S. (2016). Arte Macroesquemático vs. Arte Esquemático. Reflexiones en torno a una relación intuitiva. In J. J. Cabanilles, (Ed.), *Del neolítico a l'edat del bronze en el mediterrani occidental. Estudis en homenatge a Bernat Martí Oliver* (pp. 481–490). Servei d'Investigació Prehistòrica, Museu de Prehistòria de València, València.
- Hill, P. A. (1998). Bone remodelling. *British Journal of Orthodontics*, 25, 101–107.
- Isern, N., Zilhão, J., Fort, J., & Ammerman, A. J. (2017). Modeling the role of voyaging in the coastal spread of the Early Neolithic in the West Mediterranean. *Proceedings of the National Academy of Sciences of the United States of America*, 114, 897–902.
- Le Bras-Goude, G., Binder, D., Formicola, V., Duday, H., Couture-Veschambre, C., Hublin, J. J., & Richards, M. (2006). Stratégies de subsistance et analyse culturelle de populations néolithiques de Ligurie: Approche par l'étude isotopique ($\delta^{13}\text{C}$ et $\delta^{15}\text{N}$) des restes osseux. *Bulletins Et Mémoires De La Société D'Anthropologie De Paris*, 18, 43–53.
- Le Bras-Goude, G., Binder, D., Zémour, A., & Richards, M. P. (2009). New radiocarbon dates and isotope analysis of Neolithic human and animal bone from the Fontbrégoua Cave (Salernes, Var, France). *Journal of Anthropological Sciences*, 88, 167–178.
- Lee-Thorp, J. A. (2008). On isotopes and old bones. *Archaeometry*, 50, 925–950.
- Lemmen, C., Gronenborn, D., & Wirtz, K. W. (2011). A simulation of the Neolithic transition in Western Eurasia. *Journal of Archaeological Science*, 38, 3459–3470.
- Lillie, M., Budd, C., & Potekhina, I. (2011). Stable isotope analysis of prehistoric populations from the cemeteries of the Middle and Lower Dnieper Basin, Ukraine. *Journal of Archaeological Science*, 38, 57–68.
- Lillie, M. C., & Richards, M. (2000). Stable isotope analysis and dental evidence of diet at the Mesolithic–Neolithic transition in Ukraine. *Journal of Archaeological Science*, 27, 965–972.
- Longin, R. (1971). New method of collagen extraction for radiocarbon dating. *Nature*, 230, 241–242.
- López García, P. (1992). Análisis polínicos de cuatro yacimientos arqueológicos situados en el Bajo Aragón. In P. Utrilla (Ed.), *Aragón/Litoral mediterráneo. Intercambios culturales durante la prehistoria* (pp. 235–242). Zaragoza: Institución Fernando el Católico.
- López García, P., & López Sáez, J. A. (2000). Le paysage et la phase épipaléolithique-mésolithique dans les Pre-Pyrénées aragonaises et le bassin moyen de l'Ebre à partir de l'analyse palynologique, en Les derniers chasseurs cueilleurs d'Europe occidentale (13.000-5.5000 av J.C.). *Annales Littéraires*, 699, 59–69.
- López-Martín, J. M. (2017). Zorro—*Vulpes vulpes*. In: A. Salvador & I. Barja (Eds.), *Enciclopedia virtual de los vertebrados españoles*. Madrid: Museo Nacional de Ciencias Naturales. <http://www.vertebradosibericos.org/>
- Lubell, D., Jackes, M., Schwarcz, H., Knyf, M., & Meiklejohn, C. (1994). The Mesolithic-Neolithic transition in Portugal: Isotopic and dental evidence of diet. *Journal of Archaeological Science*, 21, 201–216.
- Madgwick, R., Mulville, J., & Stevens, R. E. (2012). Diversity in foddering strategy and herd management in late Bronze Age Britain: An isotopic investigation of pigs and other fauna from two midden sites. *Environmental Archaeology*, 17, 126–140.
- Manning, K., Timpson, A., Colledge, S., Crema, E., Edinborough, K., Kerig, T., & Shennan, S. (2014). The chronology of culture: A comparative assessment of European Neolithic dating approaches. *Antiquity*, 88, 1065–1080.
- Martins, H., Oms, F. X., Pereira, L., Pike, A., Rowsell, K., & Zilhão, J. (2015). Radiocarbon dating the beginning of the Neolithic in Iberia: New results, new problems. *Journal of Mediterranean Archaeology*, 28, 105–131.
- Mazzucco, N., Clemente-Conte, I., Gassiot, E., & Gibaja, J. F. (2015). Insights into the economic organization of the first agro-pastoral communities of the NE of the Iberian Peninsula: A traceological analysis of the Cueva de Chaves flaked stone assemblage. *Journal of Archaeological Science: Reports*, 2, 353–366.
- Macdonald, D., & Barrett, P. (1993). *Collins field guide: Mammals of Britain and Europe* (pp. 197). London: Harper Collins Publishers.
- Minagawa, M., & Wada, E. (1986). Nitrogen isotope ratios of red tide organisms in the East China Sea: A characterization of biological nitrogen fixation. *Marine Chemistry*, 19, 245–259.
- Müldner, G., & Richards, M. P. (2005). Fast or feast: Reconstructing diet in later medieval England by stable isotope analysis. *Journal of Archaeological Science*, 32, 39–48.
- Navarrete, V., Colonese, A. C., Tornero, C., Antolín, F., Von Tersch, M., Subirà, M. E., ... Saña, M. (2017). Feeding management strategies among the early Neolithic pigs in the NE of the Iberian Peninsula. *International Journal of Osteoarchaeology*, 27(5), 839–852.
- Navarrete, V., & Saña, M. (2017). Size changes in wild and domestic pig populations between 10,000-800 cal BC in the Iberian Peninsula: Evaluation of natural versus social impacts in animal populations during the first domestication stages. *The Holocene*. <http://dx.doi.org/10.1177/2F0959683617693902>
- O'Leary, M. H. (1981). Carbon isotope fractionation in plants. *Phytochemistry*, 20(4), 553–567.
- Olalde, I., Schroeder, H., Sandoval-Velasco, M., Vinner, L., Lobón, I., Ramirez, O., ... Lalueza-Fox, C. (2015). A common genetic origin for early farmers from Mediterranean Cardial and Central European LBK cultures. *Molecular Biology and Evolution*, 32, 3132–3142.
- Oms, F. X., Cebrià, A., Morales, J. I., & Pedro, M. (2015). Una inhumació cardial a la cova Foradada (Calafell, Baix Penedès)? In X. Esteve, C. Miró, M. Molist, & G. Sabaté (Eds.), *Jornades d'Arqueologia del penedès* (pp. 59–64). Vilafranca del Penedès: Institut d'Estudis Penedesencs.
- Oms, F. X., Daura, J., Sanz, M., Mendiola, S., Pedro, M., & Martínez, P. (2017). First evidence of collective human inhumation from the cardial neolithic (Cova Bonica, Barcelona, NE Iberian Peninsula). *Journal of Field Archaeology*, 42, 43–53.
- Oms, F. X., Esteve, X., Mestres, J., Martín, P., & Martins, H. (2014a). La neolitización del nordeste de la Península Ibérica: Datos radiocarbónicos y culturales de los asentamientos al aire libre del Penedés. *Trabajos De Prehistoria*, 71, 42–55.
- Oms, F. X., López-García, J. M., Mangado, X., Martín, P., Mendiola, S., Morales, J. I., ... Yubero, M. (2014b). Hàbitat en cova i espai pels ramats ca. 6200-6000 BP: Dades preliminars de la Cova Colomera (Prepirineu de Lleida) durant el neolític antic. *Sagvntvm. Papeles Del Laboratorio De Arqueologia De Valencia*, 45, 25–38.
- Ortega Becerril, J. A. (2010). El estudio de la morfología de los ríos en roca. Implicaciones hidrológicas y evolutivas en dos barrancos españoles. *Boletín Geológico y Minero*, 118, 803–811.
- Pou, R., Martí, M., Jordana, X., Malgosa, A., & Gibaja, J. F. (2010). L'enterrament del Neolític antic de la Plaça Vila de Madrid (Barcelona): Una estructura funerària del VIè mil·lenni aC. *Quarhis*, 6, 94–107.
- Price, T. D., Burton, J. H., & Bentley, R. A. (2002). The characterization of biologically available strontium isotope ratios for the study of prehistoric migration. *Archaeometry*, 44, 117–135.
- Privat, K. L., O'Connell, T. C., & Richards, M. P. (2002). Stable isotope analysis of human and faunal remains from the Anglo-Saxon cemetery at Berinsfield, Oxfordshire: Dietary and social implications. *Journal of Archaeological Science*, 29, 779–790.
- Reimer, P. J., Bard, E., Bayliss, A., Beck, J. W., Blackwell, P. G., Bronk Ramsey, C., ... Van der Plicht, J. (2013). IntCal13 and Marine13 radiocarbon age calibration curves 0-50,000 Years cal BP. *Radiocarbon*, 55, 1869–1887.
- Reitsema, L. J., Kozłowski, T., & Makowiecki, D. (2013). Human-environment interactions in medieval Poland: A perspective from the analysis of faunal stable isotope ratios. *Journal of Archaeological Science*, 40, 3636–3646.
- Remolins, G., Gibaja, J. F., Allié, F., Fontanals, M., Martín, P., Masclans, A., ... Llovera, X. (2016). The Neolithic necropolis of La Feixa del Moro (Juberri, Andorra): New data on the first farming communities in the Pyrenees. *Comptes Rendus Palevol*, 15, 537–554.
- Richards, M. P., Fuller, B. T., & Molleson, T. I. (2006). Stable isotope palaeodietary study of humans and fauna from the multi-period (Iron Age,

- Viking and Late Medieval) site of Newark Bay, Orkney. *Journal of Archaeological Science*, 33, 122–131.
- Rojo-Guerra, M. A., Kunst, M., Garrido-Pena, R., & García-Martínez de Lagrán, I. (2006). La neolitización de la meseta norte a la luz del c-14: Análisis de 47 dataciones absolutas inéditas de dos yacimientos domésticos del valle de Ambrona, Soria, España. *Archivo De Prehistoria Levantina*, 26, 39–100.
- Rojo-Guerra, M., Peña-Chocarro, L., Royo, J. I., Tejedor, C., García-Martínez de Lagrán, I., Arcusa, H., ... Alt, K. W. (2013). Pastores trashumantes del Neolítico antiguo en un entorno de alta montaña: secuencia crono-cultural de la Cova de Els Trocs (San Feliú de Verí, Huesca). *BSAA Arqueología*, 79, 9–55.
- Salazar-García, D. C. (2009). Estudio de la dieta en la población neolítica de Costamar. Resultados preliminares de análisis de isótopos estables de Carbono y Nitrógeno. In E. Flors (Ed.), *Torre la Sal (ribera de cabanes, castellón). la evolución del paisaje antrópico desde la prehistoria hasta el medioevo* (pp. 411–418). Monografies de Prehistòria i Arqueologia Castellonenques 8. archaeology, Springer.
- Salazar-García, D. C., Aura, J. E., Olària, C. R., Talamo, S., Morales, J. V., & Richards, M. P. (2014). Isotope evidence for the use of marine resources in the Eastern Iberian Mesolithic. *Journal of Archaeological Science*, 42, 231–240.
- Salazar-García, D. C., & García-Puchol, O. (2017a). Current thoughts on the Neolithisation process of the Western Mediterranean. In O. García-Puchol & D. C. Salazar-García (Eds.), *Times of neolithic transition along the Western mediterranean* (pp. 1–11), Springer, Cham.
- Salazar-García, D. C., Fontanals-Coll, M., Goude, G., & Subirà, E. (2018). To “seafood” or not to ‘seafood’? An isotopic perspective on dietary preferences at the Mesolithic-Neolithic transition in the Western Mediterranean. *Quaternary International*, 470, 497–510.
- Salazar-García, D. C., Pérez-Ripoll, M., García-Borja, P., & Jordá Pardo, J. F. (2017b). A terrestrial diet close to the coast: A case study from the Neolithic levels of Nerja Cave (Málaga, Spain). In O. García-Puchol & C. Salazar-García (Eds.), *Times of neolithic transition along the Western Mediterranean* (pp. 281–307). Springer: Fundamental Issues in Archaeology.
- Sánchez, P. (2013). La organización microespacial del Neolítico de la cueva de Chaves. *Bolskan*, 24, 11–25.
- Saña, M. (2011). La gestió dels recursos animals. In A. Bosch, J. Chinchilla, & J. Tarrús (Eds.), *El poblat lacustre del neolític antic de la draga. Excavacions 2000–2005* (pp. 177–212). Girona: Museu d'Arqueologia de Catalunya (Monografies del CASC, 9).
- Saña, M., Antolín, F., Zapata, M., Castells, L., Craig, O. E., Benaiges, M. E., & Spiteru, C. (2015). Prácticas agropecuarias durante el Neolítico antiguo y medio en la cueva de Can Sadurní (Begues, Barcelona). In V. Gonçalves, M. Diniz, & A. C. Sousa (Eds.), *V congresso do neolítico peninsular* (pp. 57–66). Lisboa: Centro do Arqueologia da Universidade de Lisboa.
- Schley, L., & Roper, T. J. (2003). Diet of wild boar *Sus scrofa* in Western Europe, with particular reference to consumption of agricultural crops. *Mammal Review*, 33, 43–56.
- Schoeninger, M. J., & DeNiro, M. J. (1984). Nitrogen and carbon isotopic composition of bone collagen from marine and terrestrial animals. *Geochimica Et Cosmochimica Acta*, 48, 625–639.
- Schulting, R. J. (1998). Slighting the sea: Stable isotope evidence for the transition to farming in northwestern Europe. *Documenta Praehistorica*, 25, 18.
- Schwarcz, H. P., & Schoeninger, M. J. (1991). Stable isotope analysis in human nutritional ecology. *American Journal of Physical Anthropology*, 34, 283–321.
- Tieszen, L. L. (1991). Natural variations in the carbon isotope values of plants: implications for archeology, ecology and paleoecology. *Journal of Archaeological Science*, 18, 227–248.
- Tornero, C., Aguilera, M., Ferrio, J. P., Arcusa, H., Moreno-García, M., García-Reig, S., & Rojo-Guerra, M. (2018). Vertical sheep mobility along the altitudinal gradient through stable isotope analyses in tooth molar bioapatite, meteoric water and pastures: A reference from the Ebro valley to the Central Pyrenees. *Quaternary International*, 484, 94–106.
- Tornero, C., Balasse, M., Bălăşescu, A., Chataigner, C., Gasparyan, B., & Montoya, C. (2016). The altitudinal mobility of wild sheep at the Epi-Gravettian site of Kalavan 1 (Lesser Caucasus, Armenia): Evidence from a sequential isotopic analysis in tooth enamel. *Journal of Human Evolution*, 97, 27–36.
- Ubelaker, D. H. (1989). Human skeletal remains: excavation, analysis, interpretation. In *Manual on Archaeology 2 Taraxacum* (first ed.). Washington.
- Utrilla, P., Cava, A., Alday, A., Baldellou, V., Barandiaran, I., Mazo, C., & Montes, L. (1998). Le passage du mésolithique au néolithique ancien dans le Bassin de l'Ebre (Espagne) d'après les datations C14. *Préhistoire européenne*, 12, 171–194.
- Utrilla, P., & Baldellou, V. (2002). Cantos pintados neolíticos de la Cueva de Chaves (Bastarás, Huesca). *Saldue*, 2, 45–126.
- Utrilla, P., & Baldellou, V. (2007). *Les galets peints de la grotte de Chaves* (pp. 73–88). Toulouse: Préhistoire, Arts et Sociétés LXII.
- Utrilla, P., & Laborda, R. (2018). La Cueva de Chaves (Bastarás, Huesca), el gran lugar de habitat del prepirineo: 15000 años de ocupación. *Trabajos De Prehistoria*, 75, 1–22.
- Utrilla, P., Lorenzo, J. I., Baldellou, V., Sopena, M. C., & Ayuso, P. (2008). Enterramiento masculino en fosa, cubierto de cantos rodados, en el neolítico antiguo de la cueva de Chaves. In M. S. Hernández, J. A. Soler, & J. A. López (Eds.), *IV congreso del neolítico peninsular. Museo arqueológico de alicante (MARQ)* (Vol. 2, pp. 131–140), Alicante.
- Valentin, J. (2002). Basic anatomical and physiological data for use in radiological protection: Reference values. *Annals of the ICRP*, 32, 1–185.
- Van der Merwe, N. J. (1982). Carbon isotopes, photosynthesis, and archaeology: Different pathways of photosynthesis cause characteristic changes in carbon isotope ratios that make possible the study of prehistoric human diets. *American Scientist*, 70, 596–606.
- Van Klinken, G. J. (1999). Bone collagen quality indicators for palaeodietary and radiocarbon measurements. *Journal of Archaeological Science*, 26, 687–695.
- Villalba-Mouco, V., Sauqué, V., Sarasketa-Gartzia, I., Pastor, M. V., J., Le Roux, P., Vicente, D., Utrilla, P., ... Alazar-García, D. C. (2018). Territorial mobility and subsistence strategies during the Ebro Basin Late Neolithic-Chalcolithic: A multi-isotope approach from San Juan cave (Loarre, Spain). *Quaternary International*, 481, 28–41.
- Villar, L., & Fernández, J. V. (2000). Usos etnobotánicos de la “Sabina albar” y arbustos que le acompañan en Aragón. *ONF Les Dossiers Forestiers*, 6, 130–139.
- Virgós, E. (2005). Tejón—Meles meles. In: L. M. Carrascal & A. Salvador (Eds.), *Enciclopedia virtual de los vertebrados españoles*. Madrid: Museo Nacional de Ciencias Naturales. <http://www.vertebradosibericos.org/>
- Zapata, L., Baldellou, V., & Utrilla, P. (2008). Bellotas de cronología neolítica para consumo humano en la cueva de Chaves (Bastarás, Huesca). In M. S. Hernández, J. A. Soler, & J. A. López (Eds.), *IV Congreso del neolítico peninsular. Museo arqueológico de alicante (MARQ)* (pp. 402–410), Alicante.
- Zapata, L., Peña-Chocarro, L., Pérez-Jordá, G., & Stika, H. P. (2004). Early Neolithic agriculture in the Iberian Peninsula. *Journal of World Prehistory*, 18, 283–325.
- Zeder, M. A. (2008). Domestication and early agriculture in the Mediterranean Basin: Origins, diffusion, and impact. *Proceedings of the National Academy of Sciences of the United States of America*, 105, 11597–11604.
- Zilhão, J. (1992). *Gruta do caldeirão O neolítico antigo*. Lisbon: Instituto Português do Património Arquitectónico e Arqueológico.
- Zilhão, J. (2001). Radiocarbon evidence for maritime pioneer colonization at the origins of farming in west Mediterranean Europe. *Proceedings of the National Academy of Sciences of the United States of America*, 98, 14180–14185.

How to cite this article: Villalba-Mouco V, Utrilla P, Laborda R, Lorenzo JI, Martínez-Labarga C, Salazar-García DC. Reconstruction of human subsistence and husbandry strategies from the Iberian Early Neolithic: A stable isotope approach. *Am J Phys Anthropol*. 2018;167:257–271. <https://doi.org/10.1002/ajpa.23622>

10.2 Territorial mobility and subsistence strategies during the Ebro Basin Late Neolithic-Chalcolithic: A multi-isotope approach from San Juan cave (Loarre, Spain).

Quaternary International 481 (2018) 28–41



Contents lists available at ScienceDirect

Quaternary International

journal homepage: www.elsevier.com/locate/quaint



Territorial mobility and subsistence strategies during the Ebro Basin Late Neolithic-Chalcolithic: A multi-isotope approach from San Juan cave (Loarre, Spain)



Vanessa Villalba-Mouco ^{a, b, *}, Víctor Sauqué ^{c, d}, Izaskun Sarasketa-Gartzia ^e,
M. Victoria Pastor ^f, Petrus J. le Roux ^g, Diana Vicente ^f, Pilar Utrilla ^{a, b},
Domingo C. Salazar-García ^{h, i, **}

^a Departamento de Ciencias de la Antigüedad, Grupo de investigación Primeros Pobladores del Valle del Ebro (PPVE), Universidad de Zaragoza, Pedro Cerbuna 12, 50009, Zaragoza, Spain

^b Instituto Universitario de Investigación en Ciencias Ambientales de Aragón (IUCA), Universidad de Zaragoza, Pedro Cerbuna 12, 50009, Zaragoza, Spain

^c Grupo Aragosaurus-IUCA, Departamento de Ciencias de la Tierra, Facultad de Ciencias, Universidad de Zaragoza, Spain

^d Laboratorio de Zooarqueología y Tafonomía de Zonas Áridas (LaZTA), IDACOR CONICET-UNC, H. Yrigoyen 174, 5000, Córdoba, Argentina

^e Departamento de Geografía, Prehistoria y Arqueología, Euskal Herriko Unibertsitatea, Francisco Tomás y Valiente s/n., 01006, Vitoria-Gasteiz, Spain

^f Facultad de Filosofía y Letras, Universidad de Zaragoza, Pedro Cerbuna 12, 50009, Zaragoza, Spain

^g Department of Geological Sciences, University of Cape Town, South Africa

^h Department of Archaeology, University of Cape Town, Upper Campus, Beattie Building, University Avenue 5, 7701, Cape Town, South Africa

ⁱ Grupo de Investigación en Prehistoria IT-622-13 (UPV-EHU)/IKERBASQUE-Basque Foundation for Science, Vitoria, Spain

ARTICLE INFO

Article history:

Received 14 December 2016

Received in revised form

11 May 2017

Accepted 26 May 2017

Available online 17 June 2017

Keywords:

Carbon and nitrogen isotopes

Strontium isotopes

Iberian prehistory

Social structure

Mobility patterns

ABSTRACT

The use of isotopic analysis in human and animal remains from the Holocene has proved to be a very useful tool to explore the exploitation and adaptation of past populations to different environments. In this study we present isotopic analysis results of carbon, nitrogen and strontium from the Late Neolithic-Chalcolithic site of San Juan cave (Loarre, Spain). We analysed 33 humans, divided in adult and subadult groups, and 16 animals recovered from the same archaeological context. Stable isotope analysis of carbon and nitrogen has allowed to distinguish an homogeneous subsistence pattern during the Late Neolithic-Chalcolithic transition. The use of strontium isotopes ($^{87}\text{Sr}/^{86}\text{Sr}$) in human dental enamel suggests 19% (4 out of 21) are non-local individuals, based on comparison with the local bioavailable $^{87}\text{Sr}/^{86}\text{Sr}$ range calculated using microfauna teeth from the archaeological context, modern plants and snails. This new study gives information about Late Neolithic communities located in the north-east of the Iberian Peninsula, and it allows inference of the socio-economic structure, territorial mobility and individual provenance of humans.

© 2017 Elsevier Ltd and INQUA. All rights reserved.



Contents lists available at ScienceDirect

Quaternary International

journal homepage: www.elsevier.com/locate/quaint

Territorial mobility and subsistence strategies during the Ebro Basin Late Neolithic-Chalcolithic: A multi-isotope approach from San Juan cave (Loarre, Spain)



Vanessa Villalba-Mouco ^{a, b, *}, Víctor Sauqué ^{c, d}, Izaskun Sarasketa-Gartzia ^e,
M. Victoria Pastor ^f, Petrus J. le Roux ^g, Diana Vicente ^f, Pilar Utrilla ^{a, b},
Domingo C. Salazar-García ^{h, i, **}

^a Departamento de Ciencias de la Antigüedad, Grupo de investigación Primeros Pobladores del Valle del Ebro (PPVE), Universidad de Zaragoza, Pedro Cerbuna 12, 50009, Zaragoza, Spain

^b Instituto Universitario de Investigación en Ciencias Ambientales de Aragón (IUCA), Universidad de Zaragoza, Pedro Cerbuna 12, 50009, Zaragoza, Spain

^c Grupo Aragosaurus-IUCA, Departamento de Ciencias de la Tierra, Facultad de Ciencias, Universidad de Zaragoza, Spain

^d Laboratorio de Zooloquología y Tafonomía de Zonas Áridas (LaZTA), IDACOR CONICET-UNC, H. Yrigoyen 174, 5000, Córdoba, Argentina

^e Departamento de Geografía, Prehistoria y Arqueología, Euskal Herriko Unibertsitatea, Francisco Tomás y Valiente s/n., 01006, Vitoria-Gasteiz, Spain

^f Facultad de Filosofía y Letras, Universidad de Zaragoza, Pedro Cerbuna 12, 50009, Zaragoza, Spain

^g Department of Geological Sciences, University of Cape Town, South Africa

^h Department of Archaeology, University of Cape Town, Upper Campus, Beattie Building, University Avenue 5, 7701, Cape Town, South Africa

ⁱ Grupo de Investigación en Prehistoria IT-622-13 (UPV-EHU)/IKERBASQUE-Basque Foundation for Science, Vitoria, Spain

ARTICLE INFO

Article history:

Received 14 December 2016

Received in revised form

11 May 2017

Accepted 26 May 2017

Available online 17 June 2017

Keywords:

Carbon and nitrogen isotopes

Strontium isotopes

Iberian prehistory

Social structure

Mobility patterns

ABSTRACT

The use of isotopic analysis in human and animal remains from the Holocene has proved to be a very useful tool to explore the exploitation and adaptation of past populations to different environments. In this study we present isotopic analysis results of carbon, nitrogen and strontium from the Late Neolithic-Chalcolithic site of San Juan cave (Loarre, Spain). We analysed 33 humans, divided in adult and subadult groups, and 16 animals recovered from the same archaeological context. Stable isotope analysis of carbon and nitrogen has allowed to distinguish an homogeneous subsistence pattern during the Late Neolithic-Chalcolithic transition. The use of strontium isotopes ($^{87}\text{Sr}/^{86}\text{Sr}$) in human dental enamel suggests 19% (4 out of 21) are non-local individuals, based on comparison with the local bioavailable $^{87}\text{Sr}/^{86}\text{Sr}$ range calculated using microfauna teeth from the archaeological context, modern plants and snails. This new study gives information about Late Neolithic communities located in the north-east of the Iberian Peninsula, and it allows inference of the socio-economic structure, territorial mobility and individual provenance of humans.

© 2017 Elsevier Ltd and INQUA. All rights reserved.

1. Introduction

Stable isotope measurements in human and animal remains has proved to be a very useful tool to explore the exploitation and environment adaptation of past populations (e.g. Makarewicz and

Sealy, 2015). Specifically, stable isotope ratio analysis of carbon ($\delta^{13}\text{C}$) and nitrogen ($\delta^{15}\text{N}$) of bone collagen is a common method used to quantitatively approach protein dietary input from both prehistoric and historical populations (e.g. Salazar-García et al., 2016a). $\delta^{13}\text{C}$ values are suitable to discriminate between the consumption of terrestrial and aquatic resources (e.g. Carvalho and Petchey, 2013; Lillie et al., 2011; Schoeninger and DeNiro, 1984), as well as of plants with different photosynthetic pathways (i.e. C_3 and C_4) (e.g. Lee-Thorp, 2008; Van der Merwe, 1982). $\delta^{13}\text{C}$ values are lower in estuarine and brackish fish, giving rise to what has been defined as the “fish paradox” when interpreting human fish consumption in the past (Salazar-García et al., 2014a). $\delta^{15}\text{N}$ values

* Corresponding author. Departamento de Ciencias de la Antigüedad, Universidad de Zaragoza, Pedro Cerbuna 12, 50009, Zaragoza, Spain.

** Corresponding author. Department of Archaeology, University of Cape Town, Upper Campus, Beattie Building, University Avenue 5, 7701, Cape Town, South Africa.

E-mail addresses: vvmouco@unizar.es (V. Villalba-Mouco), domingocarlos.salazar@uv.es (D.C. Salazar-García).

are able to provide information about the trophic level a specific organism holds in the food chain of its environment (Bocherens and Drucker, 2003; Minagawa and Wada, 1986). $\delta^{15}\text{N}$ values are considered to increase generally between 3‰ and 5‰ with each trophic level up the foodweb (Bocherens and Drucker, 2003; Schwarcz and Schoeninger, 1991). Some researchers suggest this range could be wider (Hedges and Reynard, 2007), being estimated in ca. 6‰ combining short-scale studies from red blood cells with measured offsets in other studies (O'Connell et al., 2012). It is necessary to highlight that diet studies based on stable isotope analysis of bone collagen present two important traits to take into account: 1) collagen turnover is low during adulthood and therefore reflect an average diet of the last 10–20 years before the individual died (Hedges et al., 2007); and 2) collagen stable isotope ratios mainly reflect protein sources and this is the reason why plant food consumption could be masked by diets high in protein content (Ambrose and Norr, 1993). To complement isotopic dietary information from bone collagen, the study of trapped plant micro-remains (starches and phytoliths) inside dental calculus can be very useful to detect plant consumption (e.g. Power et al., 2014; Salazar-García et al., 2013a).

Strontium isotope ($^{87}\text{Sr}/^{86}\text{Sr}$) analyses of tooth enamel have the potential to provide insight on the use of a geological area by tracking territorial mobility of the individuals studied (Bentley, 2013; Copeland et al., 2011). $^{87}\text{Sr}/^{86}\text{Sr}$ ratios vary depending on the geology and bedrock age, and, because there is no isotopic fractionation due to their very small relative mass differences, they are incorporated directly into the foodweb (plants, animals, and eventually humans). Strontium is fixed during enamel mineralization and reflects the bioavailable strontium values from the region where an individual lived when enamel mineralization took place (Bentley, 2006; Ericson, 1985; Price et al., 2002). Enamel from second (M2) and third (M3) molars from the same human individuals are preferentially selected for this kind of analysis as they allow comparison of a childhood signature not influenced by breastfeeding and weaning (M2) with a signature from early adulthood (M3) (Hillson, 1996).

Although prehistoric dietary studies based on stable isotope ratio analysis have been increasing during the last decade in Spain (e.g. Arias, 2005; Fontanals-Coll et al., 2015; García-Guixé et al., 2006; Salazar-García et al., 2013b), territorial mobility studies based on strontium isotope analysis are still scarce in Iberia (Díaz-Zorita, 2014; Salazar-García, 2012a; Waterman et al., 2014). Most of the previous studies have focused on the “transition to agriculture”, leaving some gaps on other “transitions” between the Late Neolithic and the so-called Metal Ages in the Iberian Peninsula (López-Costas et al., 2015; McClure et al., 2011; Salazar-García, 2012b).

The aim of this paper is to bridge this gap by assessing, through a multi-isotope study of the Late Neolithic-Chalcolithic collective burial of San Juan cave in the Ebro Basin (Huesca, Spain), the socio-economical dynamics at the onset of metallurgy in northeast Iberia.

2. San Juan cave site and its archaeological context

Late Neolithic-Chalcolithic and early Bronze Age periods in Iberia are characterized by the presence of a high number of burials where people were usually buried together in shared spaces (Andrés, 1998). The use of both caves and rock shelters as burial sites is contemporary to the use of megalithic tombs during the Late Neolithic in northeastern Iberia (Fernández-Crespo, 2010). Overall, some authors suggest that the use of different types of burials was linked to different groups of people, or to people with different socio-economic status (Chapman, 1981; Hodder, 1984; Renfrew, 1976; Sherratt, 1990). In northeastern Iberia, there is still no solid

explanation for the differential use of the diverse types of burials (Andrés, 1998, 2005). However, some studies from the middle-high Ebro Valley reveal an overrepresentation of adult male individuals in Megalithic tombs, while subadults and female individuals are more abundant in cave burials (Fernández-Crespo and de-la-Rúa, 2015). Since at the site here studied there has been no sex or age selection when burying the remains, they are more representative of the whole past population of the region. San Juan cave is one of very few sites in the Ebro Basin for which the entire human burial population is available. Additionally, there are very few anthropological studies on the total sample of human remains recovered from the burial caves in the Ebro Basin, and to date there are no multi-isotopic studies carried out on these samples. Furthermore, the end of the Neolithic is still poorly understood in northeastern Iberia, where there are no clear limits between the Neolithic and Chalcolithic periods unlike what happens in the south when the Millares culture appears. In this context, the site of San Juan cave is of interest to fill in this gap.

San Juan cave is a burial site located between the Ebro Valley and the pre-Pyrenean mountain range, close to the town of Loarre, Huesca, Spain (X.697155; Y. 4688532, UTM30N, WGS84). It is a $2.5 \times 1.5 \times 1.5$ m. limestone cave situated in the western slope of Los Vallazos gorge, at 983.37 m.a.s.l. (metres above sea level) (Fig. 1). This site was excavated by M. Victoria Pastor and Diana Vicente in 2007 (Pastor and Vicente, 2009) in the framework of a rescue excavation of the Gobierno de Aragón. Material culture recovered as grave goods include stone and bone beads, *Cardium* and *Dentalia* seashells, two bone and wild board tusk pendants, flint tools, and some ceramic pot fragments. Also comingled with the human remains were several faunal remains (Pastor and Vicente, 2009). Since the collective burial has no clear archaeological stratigraphy, direct radiocarbon dates from several of the human remains show that the burial site was used mainly during the Late Neolithic-Chalcolithic, with only a single date pointing to the Bronze Age (Table 1, Fig. 2). The individuals were deposited individually and accumulatively over the surface of the cave. Most of the human remains were found commingled and disarticulated, with no anatomical connexions, suggesting that buried corpses were displaced to accommodate new ones (Pastor and Vicente, 2009).

3. Materials and methods

3.1. Study of faunal and human remains

Faunal taxonomic identification has been based on the works of Fernandez (2001), Pales and Lambert (1971), Rowley-Conwy et al. (2012), and Sanchís (2010), as well as on the zooarchaeological reference collection of the University of Zaragoza (UZ) and the Natural Science Museum of Zaragoza. In order to assess the skeletal representation of the assemblage from San Juan cave, we used the Number of Remains (NR), the Number of Identified Specimens (NISP) and the Minimum Number of Individuals (MNI), all of which have been calculated in accordance with Brain (1981) and Lyman (1994). Hillson (1992) and Morris (1978) were followed in order to determine age at death, dental replacement and degree of dental eruption. The degree of long bone epiphyses fusion was measured following Morris (1972). Different types of carnivore tooth marks have been differentiated (pits, punctures, grooves, furrowing, crenulated edges and impact points) according to the definitions of Binford (1981), Haynes (1980, 1983), and Sala (2012).

The total amount of human remains present at the site is 2148 bones and bone fragments according to a previous study (Gimeno, 2009). In that study, the Minimum Number of Individuals (MNI) was calculated to 47. No postcranial element is complete, so the MNI, sex and age diagnoses were based on cranial and mandibular

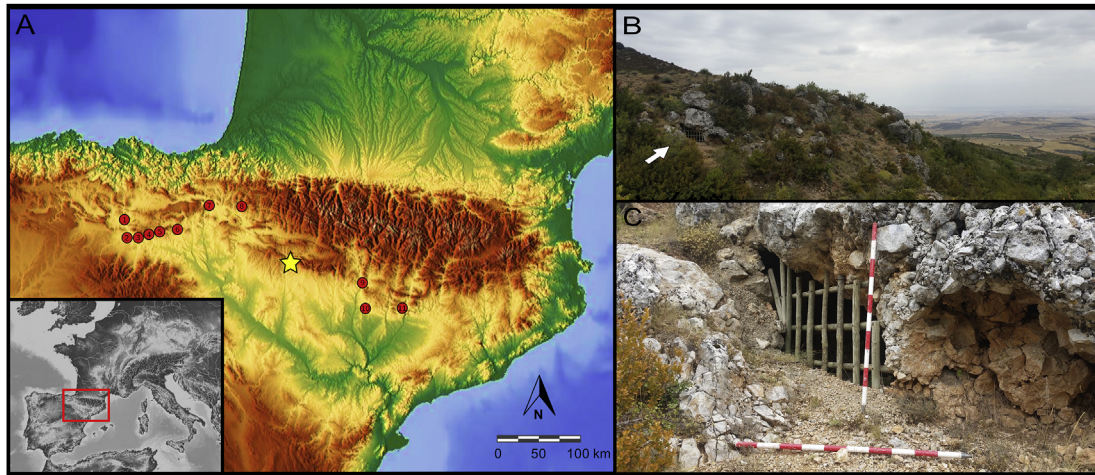


Fig. 1. Location map. A) Map of Sepulchral Late Neolithic-Chalcolithic caves in the Ebro Basin with anthropological studies and direct radiocarbon dates [1: Fuente Hoz (Basabe and Bennassar, 1983); 2: Las Yurdinas, 3: Peña Larga, 4 and 5: Los Husos I and II, 6: Peña Marañón (Fernández-Crespo, 2016); 7: Hombres Verdes (Fuste, 1982); 8: Zatoya (Lorenzo, 1989); 9: Peña de las Forcas (Lorenzo, 2014); 10: Los de los Moros de Alins del Monte (Rodanés et al., 2016); and 11: Forat de Conqueta (García-Guixé, 2011)]. The star shows the location of San Juan cave; B) Picture of San Juan cave and its surrounding landscape with the two different ecosystems: Pre-Pyrenean mountain range (left side of the picture), and Ebro Valley (right side of the picture) (The arrow indicates the entrance of San Juan cave); C) Detailed picture of San Juan cave.

Table 1
AMS radiocarbon dates of 6 individuals from San Juan cave calibrated with OxCal v4.2.3 and using the IntCal13 calibration curve (Bronk Ramsey, 2009; Reimer et al., 2013).

Lab code	Sample	^{14}C age	1 σ Cal BC	2 σ Cal BC	Cultural Period	Reference
GrA-38270	Vertebra	4620 \pm 30	3496–3359	3512–3348	Late Neolithic	Pastor and Vicente, 2009
GrA-38268	Crania	4120 \pm 30	2856–2624	2866–2579	Late Neolithic-Chalcolithic	Pastor and Vicente, 2009
GrA-3795	Rib	4110 \pm 30	2851–2586	2865–2575	Late Neolithic-Chalcolithic	Pastor and Vicente, 2009
D-AMS 09112	Mandible	4087 \pm 28	2835–2576	2858–2499	Late Neolithic-Chalcolithic	This paper
D-AMS 019113	Mandible	4053 \pm 35	2830–2492	2847–2474	Late Neolithic-Chalcolithic	This paper
GrA-38396	Humerus	3285 \pm 30	1611–1529	1629–1500	Bronze Age	Pastor and Vicente, 2009

elements, only using post-cranial elements to obtain information about pathologies and lifestyles (Gimeno, 2009).

In the present study only mandibles are considered and analysed, with the aim of avoiding stable isotope value duplicates from a same individual. Furthermore, in the context of a collective burial whose remains are all in secondary position, sampling mandibles allows to associate isotopic data obtained from bone and teeth of each individual. Although not as diagnostic as other elements,

mandibles might in some cases be able to provide information about sex and age. However, they should be checked with other skeletal elements that give higher accuracy in the sex and age determination (Brothwell, 1989; Buikstra and Ubelaker, 1994). The impossibility of associating mandibles with other skeletal elements of a same individual that are more useful for sex-determination at this site, has lead us to be cautious and avoid using sex-categories to discuss the isotopic data. Regarding age estimation, mandibles have

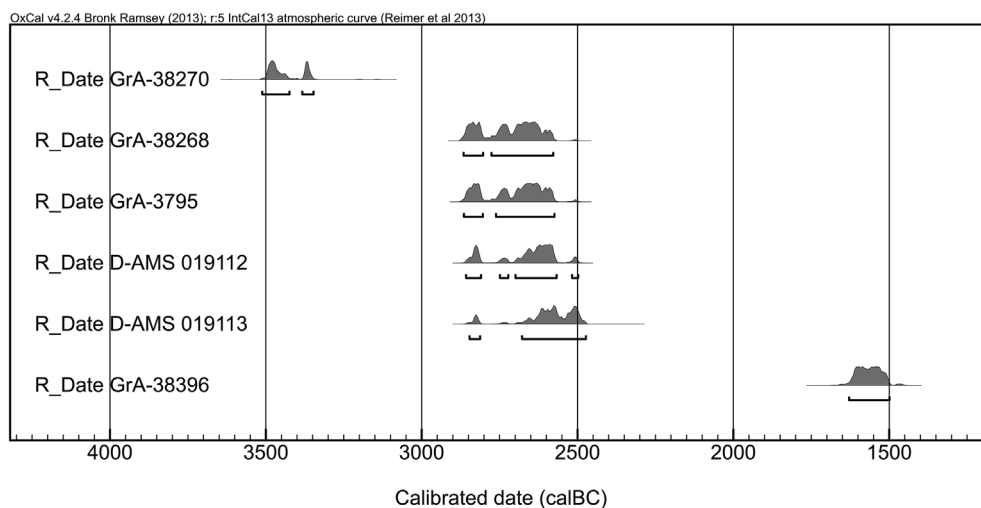


Fig. 2. AMS radiocarbon dates from San Juan cave. All dates have been calibrated with OxCal v4.2.3 and using the IntCal13 calibration curve (Bronk Ramsey, 2009; Reimer et al., 2013).

been divided into four age categories following [Buikstra and Ubelaker \(1994\)](#): infant (0–3 years), child (3–6 years), adolescent (12–20 years) and adult (>20 years). Subadult individual age was calculated using the eruption dental pattern ([Ubelaker, 1989](#)), and mandibles with totally developed permanent dentition have been classified as adults. Adult individual age was not considered, but molar wear patterns were nevertheless studied. Since molar wear patterns can be influenced by multiple factors and therefore not be reliable for estimating specific adult age ([El Aidi et al., 2011](#)), this study only correlates the degree of wear patterns itself to $\delta^{13}\text{C}$ and $\delta^{15}\text{N}$ isotopic values (not inferred age from them). Following this, mandibles with preserved molars were divided according to wear scores from [Brothwell \(1989\)](#): low wear (from 2 to 3 wear scores), medium wear (from +3+ to +4), high wear (from 5 to +5) and very high wear (more than +5 in all molars).

3.2. Collagen extraction and CN analysis

Samples from 33 humans and 16 animals of 6 different species were taken from the archaeological burial for analysis ([Table 2](#)). Sample preparation and analysis were carried out in dedicated facilities of the Department of Archaeology at University of Cape Town (South Africa), as described below.

Prior to analysis, external contaminants were removed by manual abrasion using a Dremel 3500 drill with a diamond grinder bit attached. Collagen extraction for carbon ($\delta^{13}\text{C}$) and nitrogen ($\delta^{15}\text{N}$) isotope analysis was done following the [Longin \(1971\)](#) method with the addition of an ultrafiltration step ([Brown et al., 1988](#)) as described in the procedure in [Salazar-García et al. \(2014a\)](#). Approximately 300 mg of bone samples from each specimen were demineralized in 0.5 M HCl solution at 5 °C until fully demineralized (over the course of a week in all cases). When demineralization finished, samples were rinsed three times with deionized water until pH became neutral, before starting gelatinization at 70 °C for 48 h using a heater block (FMH instruments, South Africa). This was followed by filtering with a 9 ml EZEE-filter (Elkay, United Kingdom) to remove small (<8 μm) particles and ultrafiltering with 30 kDa ultrafilters (Amicon, Germany) using a centrifuge (Thermo Fisher Scientific Megafuge 16, USA) at 2500 rpm during variable times depending on the filtering speed of each sample. The solution was then frozen and lyophilized. Finally, ca. 0.5 mg of collagen was weighed into tin capsules in duplicate per sample, and loaded into the mass spectrometer.

The carbon and nitrogen isotope ratio measurements were performed using a Finnigan Delta plus XP continuous-flow isotope ratio mass spectrometer (Thermo Fisher Scientific, USA) after being combusted in an elemental analyser Flash EA 1112 interfaced with it (Thermo Fisher Scientific, USA). Stable carbon isotope ratios were expressed relative to the VPDB scale (Vienna PeeDee Belemnite), and stable nitrogen isotope ratios were measured relative to the AIR scale (atmospheric N_2), using the delta notation (δ) in parts per thousand (‰). Repeated analysis of internal and international standards (Valine, MG and Seal) determined an analytical error better than 0.1‰ (1 σ) for $\delta^{13}\text{C}$ and $\delta^{15}\text{N}$. All analysis were carried out in duplicate.

3.3. Sample preparation for strontium isotope analysis

Thirty-two tooth samples from 21 humans were selected for strontium isotope analysis. Second and third molars were preferentially selected and sampled for each individual when possible. When not available, premolars or canines were chosen instead of second molars ([Table 2](#)). This sampling strategy ensured having two different windows to the individual's life: childhood (M2, P, C) and early adulthood (M3) ([Hillson, 1996](#)). Sample preparation and

analysis were done in dedicated facilities of the Departments of Archaeology and Geology of the University of Cape Town (South Africa), as described below.

Prior to analysis, enamel surfaces were cleaned by abrasion, rinsed and ultrasonicated for 20 min in MilliQ water. Diamond drill bits were cleaned with ethanol and ultrasonicated in MilliQ water between samples to avoid cross-contamination ([Budd et al., 2000](#)). After this, ca. 20 mg of cleaned enamel sample was digested with 2 mL of distilled 65% HNO_3 in a closed Teflon beaker placed on a hotplate at 140 °C for an hour. Digested samples were then dried and redissolved in 1.5 ml of 2 M distilled HNO_3 . These redissolved samples were centrifuged at 4000 rpm for 20 min, and the resulting supernatant was collected for strontium separation chemistry. A separate fraction for each sample was used to calculate the Sr concentration; ^{88}Sr intensity (V) regression equation was built with the SRM987 standard from the NIST (National Institute of Standards and Technology, Gaithersburg, MD, USA).

Strontium was isolated with 200 μl of Eichrom Sr.Spec resin loaded in 2 ml Bio-Spin Disposable Chromatography *Bio-Rad* Columns following the method of [Pin et al. \(1994\)](#). The separated strontium fraction for each sample was dried down, dissolved in 2 ml 0.2% distilled HNO_3 and diluted to 200 ppb Sr concentrations for isotope analysis. $^{87}\text{Sr}/^{86}\text{Sr}$ ratios were measured using a NuPlasma HR multicollector inductively-coupled-plasma mass spectrometer (MC-ICP-MS). Sample analyses were referenced to bracketing analyses of SRM987, using a $^{87}\text{Sr}/^{86}\text{Sr}$ reference value of 0.710255 from the NIST. All strontium isotope data are corrected for isobaric rubidium interference at 87 amu using the measured signal for ^{85}Rb and the natural $^{85}\text{Rb}/^{87}\text{Rb}$ ratio. Instrumental mass fractionation was corrected using the measured $^{86}\text{Sr}/^{88}\text{Sr}$ ratio and the exponential law, and a true $^{86}\text{Sr}/^{88}\text{Sr}$ value of 0.1194. Results for repeat analyses of an in-house carbonate standard processed and measured with the batches of samples in this study ($^{87}\text{Sr}/^{86}\text{Sr} = 0.708936$; 2 sigma 0.000041; $n = 33$) are in agreement with long-term results for this in-house standard ($^{87}\text{Sr}/^{86}\text{Sr}$; 0.708915; 2 sigma 0.000047; $n = 125$).

To discern possible non-local individuals, the $^{87}\text{Sr}/^{86}\text{Sr}$ bioavailable range from the site and region were estimated by preparing and analysing microfauna teeth, modern snails and plants from two sampling areas, following [Bentley et al. \(2004\)](#) and [Price et al. \(2001\)](#). Except for the site, for which 5 microfauna teeth were also analysed, from every sampling area only 5 plants and 5 snail shells were sampled and analysed. The same Sr extraction and purification procedure previously described was used on the microfauna teeth and modern snail shells ([Price et al., 2002](#)). The sample preparation used for modern plants was similar to that described in [Copeland et al. \(2016\)](#). No strontium concentrations were measured in modern samples.

4. Results

4.1. Anthropological study on mandibles

The minimum number of individuals (MNI) was calculated to 33 based on the number of mandibles and mandible fragments, as in the previous carried out anthropological study ([Gimeno, 2009](#)). A number of 24 belonged to adults (73%), 2 belonged to adolescents (6%), and 7 belonged to children (21%). In 19 adult mandibles it was possible to measure the wear pattern based on criteria from [Brothwell \(1989\)](#). Most of the mandibles from inside this group, 58%, belonged to individuals that showed a medium molar wear pattern (from +3 to +4). They are followed by 26% that showed a low wear pattern (from 2 to 3), and by 16% that showed a high molar wear pattern (from 5 to +5). None of the mandibles showed a molar wear pattern higher than +5 score. In 5 adult mandibles it

Table 2
San Juan cave S-UCT code, $\delta^{13}\text{C}$ and $\delta^{15}\text{N}$ values, species, biological age group, collagen control indicators (yield, %C, %N, C:N elemental), $^{87}\text{Sr}/^{86}\text{Sr}$ ratios, Sr concentration (ppm) and sampled bone and tooth, [l.w: low wear (from 2 to 3 score); m.w: medium wear (from +3 to +4 score); h.w: high wear (from 5 to +5 score); scores according with Brothwell (1989); C: canine; P1: premolar 1; P2: premolar 2; M2: second molar; and M3: third molar].

S-UCT code	Species	$\delta^{13}\text{C}$ ‰	$\delta^{15}\text{N}$ ‰	Age	Molar wear pattern	Collagen yield (%)	C (%)	N (%)	C: N (Elemental)	Sampled bone (sample code)	Sampled tooth	$^{87}\text{Sr}/^{86}\text{Sr}$	Sr conc. (ppm)
18472	Human	-18.9	10.9	Child	–	7.2	42.1	15.2	3.2	Mandible (M1)	–	–	–
18480	Human	-19.4	10.3	Child	–	4.6	42.8	15.3	3.3	Mandible (M9)	–	–	–
18492	Human	-19.5	10.6	Child	–	2.2	39.9	13.8	3.4	Mandible (M28a)	–	–	–
18493	Human	-19.4	10.1	Child	–	2.1	42.1	14.5	3.4	Mandible (M28b)	P2	0.708520	110.3
18499	Human	-18.4	9.1	Child	–	4.4	43.4	15.7	3.2	Mandible (M40)	–	–	–
18500	Human	-19.5	11.6	Child	–	6.7	44.1	15.9	3.2	Mandible (M41)	–	–	–
18477	Human	-19.2	10.4	Child	–	5.8	42.9	15.4	3.2	Mandible (M6)	M2	0.708569	127.6
18474	Human	-19.3	10.8	Adolescent	–	2.3	41.5	14.4	3.4	Mandible (M3)	M2	0.708383	119.2
18488	Human	-19.4	10.8	Adolescent	–	2.4	40.9	14.1	3.4	Mandible (M19)	M2	0.708495	121.3
18475	Human	-19.3	10.4	Adult	l.w.	2.2	35.9	12.3	3.4	Mandible (M4)	M2	0.708375	222.4
18484	Human	-19.3	10.1	Adult	l.w.	7.8	43.6	15.7	3.2	Mandible (M13)	M2	0.707750	338.0
											M3	0.707838	285.9
18485	Human	-19.1	10.4	Adult	l.w.	4.9	40.8	14.2	3.4	Mandible (M14)	M2	0.708076	222.2
											M3	0.708424	226.3
18495	Human	-19.4	10.4	Adult	l.w.	5.1	43.6	15.8	3.2	Mandible (M32)	–	–	–
18502	Human	-19.2	9.9	Adult	l.w.	6.5	43.2	15.6	3.2	Mandible (C1)	M2	0.708351	133.0
											M3	0.708361	128.1
18473	Human	-19.7	9.7	Adult	m.w.	2.2	39.9	13.6	3.4	Mandible (M2)	P2	0.708095	168.4
18478	Human	-19.2	10.6	Adult	m.w.	4.8	43.5	15.4	3.3	Mandible (M7)	M2	0.708095	323.2
											M3	0.708278	316.2
18479	Human	-19.5	9.9	Adult	m.w.	1.6	39.9	14.1	3.3	Mandible (M8)	M2	0.708331	77.87
18483	Human	-19.3	11.0	Adult	m.w.	1.4	43.3	14.8	3.4	Mandible (M12)	M2	0.708412	85.99
											M3	0.708313	75.41
18487	Human	-19.1	10.0	Adult	m.w.	2.8	41.0	14.6	3.3	Mandible (M17)	M2	0.708424	141.2
											M3	0.708345	147.5
18494	Human	-19.6	10.4	Adult	m.w.	2.7	42.3	14.9	3.3	Mandible (M30)	M2	0.710787	80.16
18496	Human	-19.3	9.8	Adult	m.w.	5.7	43.1	15.5	3.3	Mandible (M33)	–	–	–
18501	Human	-19.6	10.5	Adult	m.w.	3.2	42.3	15.0	3.3	Mandible (M42)	P1	0.710415	79.99
18503	Human	-19.4	9.2	Adult	m.w.	2.7	39.3	14.1	3.2	Mandible (C3)	M2	0.708484	211.2
											M3	0.708430	225.5
18504	Human	-19.2	10.2	Adult	m.w.	4.1	39.4	13.8	3.3	Mandible (C7)	M2	0.711710	76.44
											M3	0.711142	75.36
18505	Human	-18.7	11.2	Adult	m.w.	2.2	39.5	13.7	3.4	Mandible (C13)	M2	0.708392	175.9
											M3	0.708384	150.6
18476	Human	-19.0	10.9	Adult	h.w.	3.5	39.4	10.9	3.3	Mandible (M5)	M2	0.708316	103.7
											M3	0.708756	143.5
18482	Human	-19.2	11.0	Adult	h.w.	2.4	42.2	11.0	3.3	Mandible (M11)	P1	0.708465	150.1
18491	Human	-19.7	9.6	Adult	h.w.	2.5	41.4	9.6	3.4	Mandible (M24)	M2	0.708196	170.5
											M3	0.708145	201.9
18486	Human	-19.4	10.6	Adult	–	5.3	43.6	10.6	3.3	Mandible (M15)	–	–	–
18489	Human	-19.2	10.9	Adult	–	1.1	38.7	10.9	3.4	Mandible (M20)	–	–	–
18490	Human	-19.9	9.4	Adult	–	2.8	43.1	9.4	3.3	Mandible (M23)	–	–	–
18481	Human	-19.4	10.2	Adult	–	4.6	42.6	10.2	3.3	Mandible (M10)	–	–	–
18498	Human	-19.5	10.2	Adult	–	3.7	42.3	10.2	3.3	Mandible (M39)	–	–	–
18506	<i>Ovis aries</i>	-20.0	4.9	Adult	–	7.0	43.9	15.7	3.3	Metapodial	–	–	–
18509	<i>Ovis aries</i>	-18.5	8.7	Adult	–	6.0	44.0	15.8	3.2	Tibia	–	–	–
18510	<i>Ovis aries</i>	-19.1	6.2	Adult	–	2.1	41.3	14.7	3.3	Metapodial	–	–	–
18507	<i>Ovis aries</i>	-20.2	6.6	Subadult	–	3.3	40.4	14.3	3.3	Metapodial	–	–	–
18508	<i>Ovis aries</i>	-20.0	6.8	Subadult	–	7.6	41.0	14.8	3.2	Metapodial	–	–	–
18520	<i>Ovis aries</i>	-19.5	6.9	Subadult	–	5.9	43.2	15.6	3.2	Radius	–	–	–
18511	<i>Oryctolagus cuniculus</i>	-21.4	3.7	Adult	–	3.4	42.2	14.9	3.3	Humerus	–	–	–
18512	<i>Oryctolagus cuniculus</i>	-21.7	5.1	Adult	–	4.7	41.6	14.9	3.3	Femur	–	–	–
18513	<i>Oryctolagus cuniculus</i>	-21.5	3.6	Adult	–	6.2	44.3	16.0	3.2	Femur	–	–	–
18514	<i>Oryctolagus cuniculus</i>	-21.3	5.0	Adult	–	5.7	43.8	15.9	3.2	Ulna	–	–	–
18515	<i>Oryctolagus cuniculus</i>	-22.1	4.6	Subadult	–	4.1	41.9	14.6	3.3	Femur	–	–	–
18516	<i>Oryctolagus cuniculus</i>	-20.3	7.6	Subadult	–	4.6	42.1	15.0	3.3	Femur	–	–	–
18517	<i>Sus domesticus</i>	-19.8	10.5	Subadult	–	5.4	43.5	15.7	3.2	Mandible	–	–	–
18521	<i>Meles meles</i>	-16.8	5.3	Adult	–	4.4	42.4	15.1	3.3	Femur	–	–	–
18522	<i>Vulpes vulpes</i>	-18.9	7.9	Adult	–	5.4	42.8	15.3	3.3	Skull	–	–	–
18523	<i>Felis silvestris</i>	-19.1	6.7	Adult	–	8.8	42.7	15.5	3.2	Skull	–	–	–
18524	<i>Meles meles</i>	-18.7	11.4	Adult	–	3.7	42.9	15.4	3.2	Skull	–	–	–

was not possible to assess the molar wear pattern due to post-mortem or ante-mortem molar loss. In 2 cases, the ante-mortem molar loss was associated to degenerative traits, suggesting an older age inside the adult group. No sexual identification has been attempted, as no human remains were found in primary position to test if the mandibular dimorphic traits are in agreement with sexual dimorphism of the innominate bone or other more diagnostic skeletal elements (Buikstra and Ubelaker, 1994). Distribution of biological age and wear pattern of the sample analysed is included in Table 2 and Fig. 3.

4.2. Zooarchaeological and environmental reconstructions

More than a hundred faunal remains are present at the San Juan cave burial. Of these, 79 have been taxonomically identified, and 36 have been classified as indeterminate (Table 3). Overall, the MNE (Minimum Number of Skeletal Elements) is 74. The most frequently represented elements are metapodials (12), ribs (10), vertebrae (10), pelvis (8), and teeth (7). The long bones show an analogous representation, comprising in order of decreasing frequency tibiae (9), femora (8), humeri (6), and radiuses (4). Complete or fragmented crania are less represented (5), as well as mandibles (1). Most of the taxonomically assigned remains belong to *Oryctolagus cuniculus* (European rabbit, $n = 59$), followed by *Ovis aries* (sheep, $n = 10$), *Felis silvestris* (wildcat, $n = 5$), *Vulpes vulpes* (red fox, $n = 4$), *Meles meles* (European badger, $n = 3$), *Sus domesticus* (pig, $n = 3$) and *Lepus granatensis* (Iberian hare, $n = 2$) (Table 3, Fig. 4). As far as the elements classified by size are concerned, all these elements belong to the small-sized category (20–100 kg). Furthermore, microfaunal remains from *Bufo bufo*, *Arvicola sapidus*, *Talpa europaea* and *Serpentes* indet. have also been recovered. Regarding the number of individuals, *Oryctolagus cuniculus* (MNI = 4) is the predominant taxon in the assemblage, representing 36% of the total. The species *Ovis aries* is the next most abundant taxa (MNI = 2, one juvenile and one adult), representing 18% of all. The remaining taxa are represented by only one individual (Fig. 4).

Carnivore marks are abundant in the assemblage. They appear in 29 remains, representing 33.7% of the sample. All the herbivores except *Sus domesticus* show alterations produced by carnivores. The Iberian hare is the mammal with the highest percentage of modified remains (100%), although only two elements have been recovered from this taxon. The herbivore with the next highest percentage of modified remains by carnivores is *Oryctolagus cuniculus*, with 40% from a sample of 59 remains. The sheep present 37.5% of its remains with carnivore marks from a total of 8. The main types of carnivore tooth marks found are pits, scores, punctures, crenulated edges and scooping outs. Considering all the taxa as a whole, the most modified elements are the tibiae (88%),

followed by the pelvis (62%) and the humeri (50%). The other elements show less modification, with a percentage equal to or less than 25%. Pits and scores are the most abundant tooth marks, present in a total of 15 and 12 skeletal remains respectively. Furrowing has been confirmed in six remains. Furthermore, the breakage caused by carnivores is recorded by the presence of crenulated edges (Number of Remains = 6) and scooping outs (Number of Remains = 2), and eight remains have been found showing evidence of digestion. However, no remains show evidence of anthropic cut marks. Despite the cave being a burial, there seems to be no anthropogenic influence in the origin of the faunal assemblage, suggesting the cave was possibly used at some point as a carnivore den in which red fox or wild cat accumulated herbivore remains.

This assemblage, although scarce, is useful to make environmental inferences from the past, as the herbivores present at San Juan cave are associated with various types of landscapes. The leporids (*Oryctolagus cuniculus* and *Lepus granatensis*) indicate open environments (Gálvez-Bravo, 2011; Purroy, 2011). On the other hand, *Sus domesticus* and *Ovis aries* prefer a broad range of habitats (Rowley-Conwy et al., 2012). The carnivores of San Juan cave (*Meles meles*, *Felis silvestris* and *Vulpes vulpes*) are opportunistic carnivores that populate wooded habitats ranging from Mediterranean to high mountainous areas (Palomo, 2007). Taking all this into account, the purported landscape at the time of the burials would be similar to what we currently find in the area around the cave, the mouth of which opens at a ravine with rocky walls, but close to the open environment suitable for leporids of the Hoya de Huesca.

4.3. Carbon and nitrogen stable isotope ratios

Bone samples from 33 humans and 16 animals were analysed from San Juan cave. The $\delta^{13}\text{C}$ and $\delta^{15}\text{N}$ results are presented in Table 2 and plotted in Fig. 5. All the samples from San Juan cave yielded enough collagen at the >30 kDa fraction for analysis in duplicate. Their %C, %N and C:N elemental ratio values indicate a good collagen quality (Ambrose, 1993; Van Klinken, 1999).

Herbivore $\delta^{13}\text{C}$ values range between -22.1‰ and -18.5‰ with a mean value of -20.5 ± 1.1 [1 σ] ‰. These $\delta^{13}\text{C}$ values are consistent with typical values for a terrestrial C_3 European ecosystem (De Niro and Epstein, 1978; Schwarcz and Schoenniger, 1991). The high deviation is caused by ^{13}C -depleted rabbit $\delta^{13}\text{C}$ values. Herbivore $\delta^{15}\text{N}$ values are between 3.6‰ and 8.7‰, with a mean value of 5.8 ± 1.6 [1 σ] ‰, defining the trophic baseline of the ecosystem foodweb. The highest values belong to adult ovicaprids, which also show the biggest dispersion of $\delta^{15}\text{N}$ values, followed by subadult rabbit values, showing their possible nursing effect (Fogel et al., 1989). Carnivore $\delta^{13}\text{C}$ values range between -19.1‰ and -16.8‰ , with a

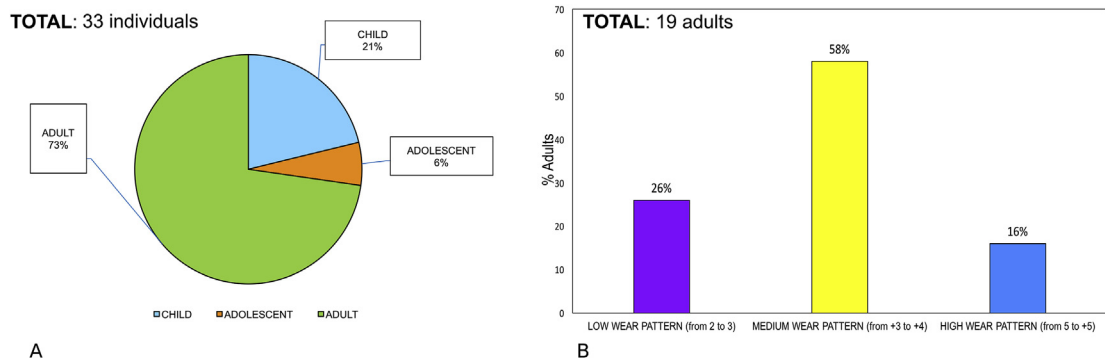


Fig. 3. A) Distribution of biological age; and B) molar wear pattern groups of the samples analysed (see text for details).

Table 3
NR (Number of Remains), NISP (Number of Identified Specimens), MNE (Minimum Number of Elements) by taxa and size categories from San Juan cave faunal assemblage [dP4: third milk molar; m2: second lower molar; P4: fourth upper premolar; P3: third upper premolar; M1: first upper molar].

Sample code	Element	Taxa	NR	NISP	NME	NMI
NIG 11678	Vertebrae	<i>Oryctolagus cuniculus</i>	7	7	7	2
NIG 11678	Metacarpals/Metatarsals	<i>Oryctolagus cuniculus</i>	9	9	9	1
NIG 11678	Scapula	<i>Oryctolagus cuniculus</i>	2	2	2	2
NIG 11678	Pelvis	<i>Oryctolagus cuniculus</i>	8	8	7	4
NIG 11678	Tibia	<i>Oryctolagus cuniculus</i>	8	8	7	4
NIG 11678	Humerus	<i>Oryctolagus cuniculus</i>	6	6	6	3
NIG 11678	Femur	<i>Oryctolagus cuniculus</i>	7	7	7	4
NIG 11678	Radius	<i>Oryctolagus cuniculus</i>	3	3	3	2
NIG 11678	Ribs	<i>Oryctolagus cuniculus</i>	9	9	9	1
NIG 11678	Tibia	<i>Lepus granatensis</i>	1	1	1	1
NIG 11678	Femur	<i>Lepus granatensis</i>	1	1	1	1
NIG 11678	Long bone	<i>Ovis aries</i>	1	1	1	1
NIG 11678	Radius	<i>Ovis aries</i>	1	1	1	1
NIG 11678	Metatarsus	<i>Ovis aries</i>	2	2	2	1
NIG 11678	Metacarpus	<i>Ovis aries</i>	1	1	1	1
NIG 11678	Scaphocuboide	<i>Ovis aries</i>	1	1	1	1
NIG 11678	Lumbar vertebra	<i>Ovis aries</i>	1	1	1	1
NIG 11678	Ribs	<i>Ovis aries</i>	1	1	1	1
NIG 11678	dP4	<i>Ovis aries</i>	2	2	1	1
NIG 11678	m2	<i>Ovis aries</i>	1	1	1	1
NIG 11678	Tibia	<i>Ovis aries</i>	1	1	1	1
NIG 11678	Mandible	<i>Sus domesticus</i>	1	1	1	1
NIG 11678	M1	<i>Sus domesticus</i>	2	2	1	1
NIG 11678	Skull fragment	<i>Felis silvestris</i>	1	1	1	1
NIG 11678	Maxilar P4 and P3	<i>Felis silvestris</i>	1	1	1	1
NIG 11678	Incisive	<i>Felis silvestris</i>	1	1	1	1
NIG 11678	Skull fragment	<i>Felis silvestris</i>	1	1	1	1
NIG 11678	Pelvis	<i>Felis silvestris</i> ?	1	1	1	1
NIG 11678	Atlas	<i>Meles meles</i>	1	1	1	1
NIG 11678	Skull	<i>Meles meles</i>	1	1	1	1
NIG 11678	M1	<i>Meles meles</i>	1	1	1	1
NIG 11678	Cervical vertebra	<i>Vulpes vulpes</i>	1	1	1	1
NIG 11678	Maxilar P4 and M1	<i>Vulpes vulpes</i>	1	1	1	1
NIG 11678	Skull fragment	<i>Vulpes vulpes</i> ?	2	2	1	1
NIG 11678	Skull fragment	Indet.	1			
NIG 11678	Indeterminate	Mammals	12			
Total			101	88	83	10

mean value of -18.4 ± 1.1 [1σ] ‰. Three of four $\delta^{13}\text{C}$ values (-19.1‰ , -18.9‰ and -18.7‰) are consistent with typical values for a terrestrial C_3 european ecosystem (De Niro and Epstein, 1978; Schwarcz and Schoenniger, 1991), while a *Meles meles*, shows an unusual higher value (-16.8‰). This could be explained if it comes from a foreign ecosystem or if it consumes small mammals, reptiles or carrion from big mammals (Martín et al., 1995). Carnivore $\delta^{15}\text{N}$ values are between 5.3‰ and 11.5‰ , with a mean value of 7.9 ± 2.7 [1σ] ‰, positioning this group in a higher trophic level than the

herbivores. The highest $\delta^{15}\text{N}$ data belongs also to *Meles meles*. There is only one $\delta^{13}\text{C}$ and $\delta^{15}\text{N}$ value from a subadult omnivore, *Sus domesticus* ($\delta^{13}\text{C} = -19.8\text{‰}$; $\delta^{15}\text{N} = 10.5\text{‰}$), which is placed above carnivores, possibly caused by a nursing effect (Fogel et al., 1989; Fuller et al., 2006) and/or by feeding on anthropic wastes (Müldner and Richards, 2005).

The human $\delta^{13}\text{C}$ values range between -19.9‰ and -18.4‰ , with a mean value of -19.3 ± 0.3 [1σ] ‰. Human $\delta^{15}\text{N}$ values go between 9.1‰ and 11.6‰ , with a mean value of 10.3 ± 0.6 [1σ] ‰.

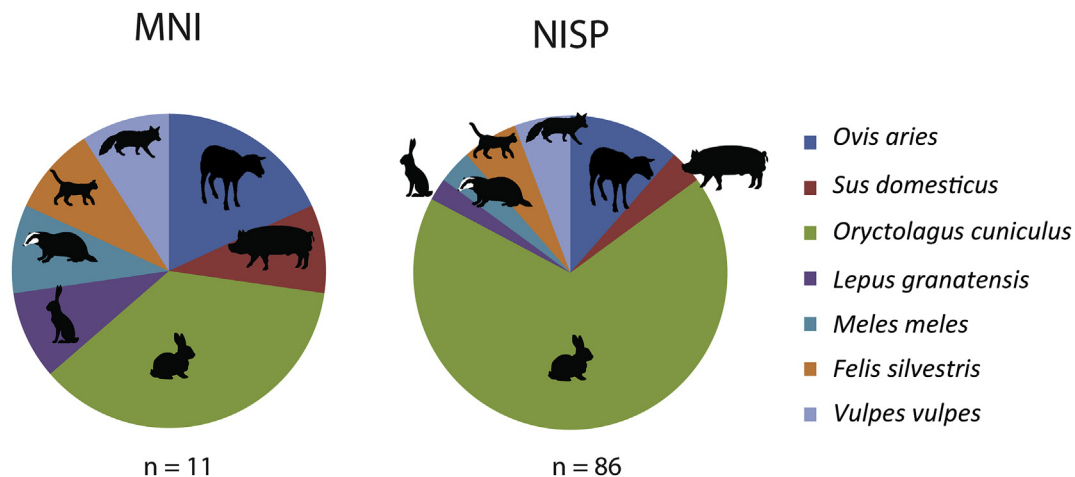


Fig. 4. % MNI (Minimum Number of Individuals) and % NISP (Number of Identified Specimens) of the faunal assemblage from San Juan cave.

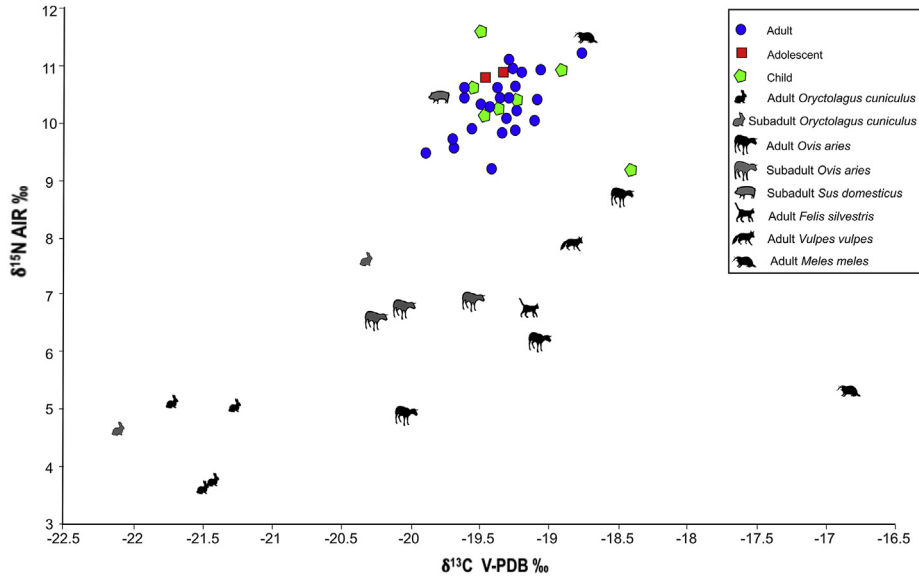


Fig. 5. Scatter plot of human and animal bone collagen $\delta^{13}\text{C}$ and $\delta^{15}\text{N}$ values from San Juan cave.

These values show that human dietary protein was mainly coming from C_3 terrestrial resources, with no evidence of regular aquatic resource consumption, and that humans are at a higher trophic level than contemporary adult herbivores ($\delta^{15}\text{N}$ 5.3‰ higher than the mean) and even carnivores ($\delta^{15}\text{N}$ 2.4‰ higher than the mean).

A non-parametric statistical test (Mann-Whitney) reveals that isotopic values do not differ between age groups (adult and sub-adult, $\delta^{13}\text{C}$: $p = 0.744$; $\delta^{15}\text{N}$: $p = 0.292$), and children (3–12 years), not showing breastfeeding or weaning influence amongst the latter (Fuller et al., 2006). A non-parametric statistical test (Kruskal-Wallis) was applied to test if there were different $\delta^{13}\text{C}$ and $\delta^{15}\text{N}$ values among the different groups of molar wear patterns observed. No significant differences can be seen nor in $\delta^{13}\text{C}$ ($p = 0.777$) or in $\delta^{15}\text{N}$ ($p = 0.832$) values among the different molar wear pattern groups (Fig. 6).

4.4. $^{87}\text{Sr}/^{86}\text{Sr}$ results

4.4.1. Bioavailable strontium from modern samples

The results of plants and snails analysed to determine bioavailable $^{87}\text{Sr}/^{86}\text{Sr}$ are presented in Table 4. Different geological

zones sampled around San Juan cave are shown in Fig. 7. Strontium isotope ratios in the proximity of San Juan cave, (Cretaceous-Miocene) show a range between 0.709984–0.708291 for plants and 0.708943–0.708243 for snails. Paleogene deposits show a similar bioavailable $^{87}\text{Sr}/^{86}\text{Sr}$ values with a range between 0.708306–0.708249 for plants and 0.708188–0.707986 for snails (Fig. 8). The range of bioavailable $^{87}\text{Sr}/^{86}\text{Sr}$ values from the geological area where San Juan cave is located was higher than that for the bioavailable range from the Paleogene deposits. This is probably due to San Juan cave being situated in a transition Cretaceous-Miocene geological area.

The range of bioavailable $^{87}\text{Sr}/^{86}\text{Sr}$ values for plants was larger than for snails. The range in this group is likely caused by the different kinds of plants sampled, herbaceous, bushes and trees, which take water from different depths within the ground. The small range for $^{87}\text{Sr}/^{86}\text{Sr}$ values from snails reflects the extremely limited movement over the landscape.

4.4.2. Strontium in archaeological material

$^{87}\text{Sr}/^{86}\text{Sr}$ enamel ratios from small vertebrates, small-medium sized mammals and humans were analysed. They include 32

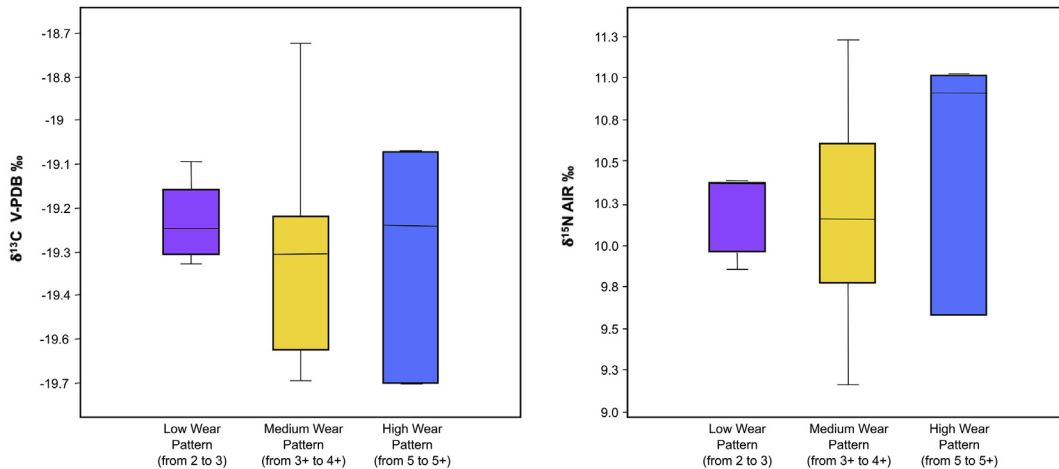


Fig. 6. Box plot of bone collagen $\delta^{13}\text{C}$ and $\delta^{15}\text{N}$ values of different wear pattern measured in adults from San Juan cave according to Brothwell (1989). Boxes represent the median value and 1st and 3rd quartiles, whiskers are 1.5 times the interquartile range.

Table 4
 $^{87}\text{Sr}/^{86}\text{Sr}$ and Sr concentration (ppm) of bioavailable samples: sample type or genus/specie, S-UCT code and corresponding geologic area.

Sample type/Genus/Specie	Origin	S-UCT Code	Geological zone	$^{87}\text{Sr}/^{86}\text{Sr}$	Sr conc. [ppm]
Snail (<i>Helix</i> sp.)	modern	18277	Cretaceous-Miocene	0.708943	–
Snail (<i>Helix</i> sp.)	modern	18278	Cretaceous-Miocene	0.708275	–
Snail (<i>Helix</i> sp.)	modern	18279	Cretaceous-Miocene	0.708729	–
Snail (<i>Helix</i> sp.)	modern	18280	Cretaceous-Miocene	0.708266	–
Snail (<i>Helix</i> sp.)	modern	18281	Cretaceous-Miocene	0.708243	–
Herbaceous	modern	18113	Cretaceous-Miocene	0.709984	–
Bush (<i>Buxus sempervirens</i>)	modern	18114	Cretaceous-Miocene	0.708322	–
Tree (<i>Quercus ilex</i>)	modern	18115	Cretaceous-Miocene	0.708915	–
Bush (<i>Juniperus</i> sp.)	modern	18116	Cretaceous-Miocene	0.708291	–
Bush (<i>Rubus ulmifolius</i>)	modern	18117	Cretaceous-Miocene	0.708378	–
Tooth (<i>Oryctolagus</i> sp.)	archaeological	18419	Cretaceous-Miocene	0.708490	167.1
Tooth (<i>Oryctolagus</i> sp.)	archaeological	18420	Cretaceous-Miocene	0.709047	140.0
Tooth (<i>Oryctolagus</i> sp.)	archaeological	18423	Cretaceous-Miocene	0.708710	177.0
Tooth (<i>Bufo</i> sp.)	archaeological	18421	Cretaceous-Miocene	0.708885	129.7
Tooth (<i>Talpa</i> sp.)	archaeological	18422	Cretaceous-Miocene	0.708506	167.1
Snail (<i>Helix</i> sp.)	modern	18307	Continental Paleogene	0.707986	–
Snail (<i>Helix</i> sp.)	modern	18308	Continental Paleogene	0.708031	–
Snail (<i>Helix</i> sp.)	modern	18309	Continental Paleogene	0.708096	–
Snail (<i>Helix</i> sp.)	modern	18310	Continental Paleogene	0.708004	–
Snail (<i>Helix</i> sp.)	modern	18311	Continental Paleogene	0.708189	–
Herbaceous	modern	18143	Continental Paleogene	0.708306	–
Bush (<i>Pistacia lentiscus</i>)	modern	18144	Continental Paleogene	0.708249	–
Tree (<i>Pinus</i> sp.)	modern	18145	Continental Paleogene	0.708283	–
Bush (<i>Juniperus</i> sp.)	modern	18146	Continental Paleogene	0.708270	–
Bush (<i>Buxus sempervirens</i>)	modern	18147	Continental Paleogene	0.708060	–

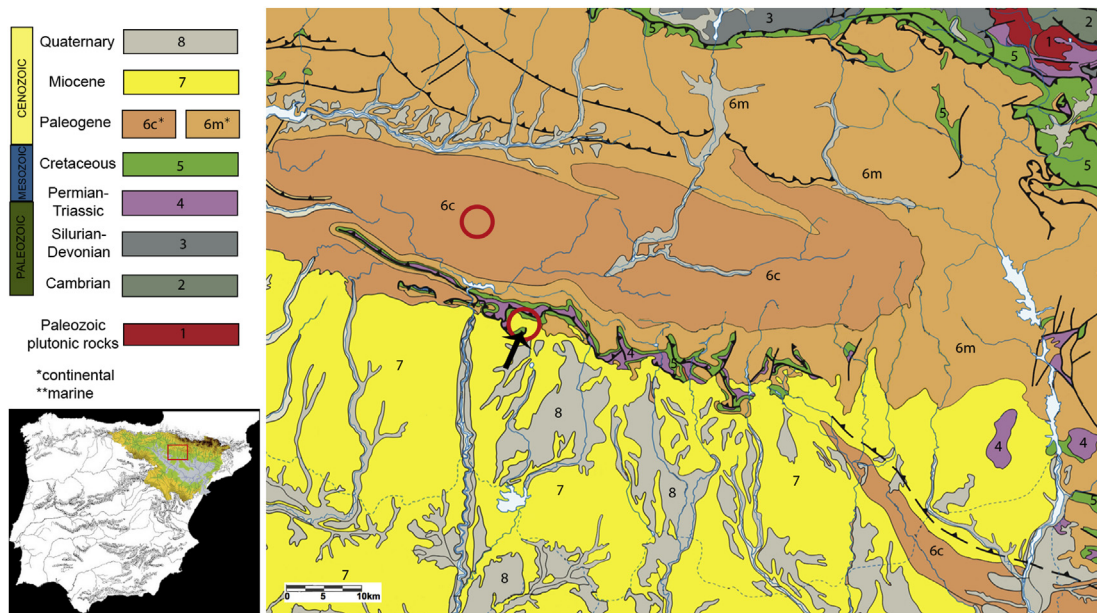


Fig. 7. Simplified geological map of the area of the Ebro Basin discussed in the text. The tip of the arrow indicates the location of San Juan cave and the circles show the sampling areas for bioavailable $^{87}\text{Sr}/^{86}\text{Sr}$ range.

samples from 21 human individuals, 3 samples from rabbit (*Oryctolagus cuniculus*), and 2 samples from mole (*Talpa europaea*) and toad (*Bufo Bufo*). $^{87}\text{Sr}/^{86}\text{Sr}$ and Sr concentration (ppm) results from San Juan cave human enamel are presented in Table 2, and small vertebrate enamel results are presented in Table 4. A plot with enamel and bioavailable $^{87}\text{Sr}/^{86}\text{Sr}$ values from San Juan cave is shown in Fig. 8.

There are only four individuals (M42: 0.710415 -second molar-; M30: 0.710787-second molar-; C7: 0.711710 -second molar- and 0.711142 -third molar-; M13: 0.707750 -second molar- and 0.707838 -third molar-) whose $^{87}\text{Sr}/^{86}\text{Sr}$ values are outside of the local bioavailable $^{87}\text{Sr}/^{86}\text{Sr}$ range, and not within the Paleogene

bioavailable $^{87}\text{Sr}/^{86}\text{Sr}$ range showed in the present study. The M13 individual shows a $^{87}\text{Sr}/^{86}\text{Sr}$ value lower than the bioavailable $^{87}\text{Sr}/^{86}\text{Sr}$ range of the two zones (surroundings of the caves with Cretaceous-Miocene transition and Paleogene deposits), and M42, M30 and C7 individuals have a higher value than the bioavailable $^{87}\text{Sr}/^{86}\text{Sr}$ range from both. The high $^{87}\text{Sr}/^{86}\text{Sr}$ values from both the second and third molars of individuals C7 and M13 suggest that these individuals spent their childhood and early adulthood in the same place, where both molars mineralized (Hillson, 1996). There was no great difference between inter-tooth analysis from same individuals, being the highest variation of 0.0006 (C7 individual; M2-M3) and 0.0001 the lowest (C1 individual; M2-M3).

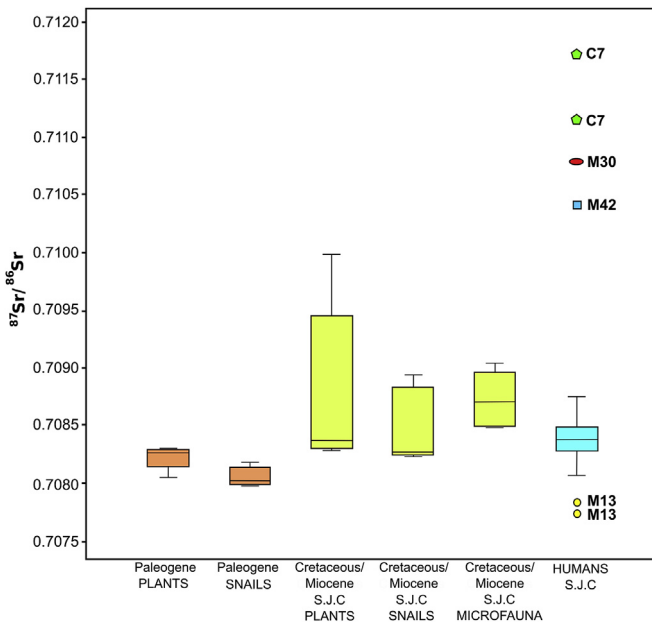


Fig. 8. Box plot of $^{87}\text{Sr}/^{86}\text{Sr}$ range for bioavailable samples from different geologic areas, modern plant and modern snails, microfauna teeth taken from the archaeological burial context and human teeth. Boxes represent the median value and 1st and 3rd quartiles, whiskers are 1.5 times the interquartile range. The outlier values are shown [S.J.C: San Juan cave].

Differences between individuals are higher than inter-tooth analyses done in same individuals (Fig. 9). Two bone samples of these four non-local individuals were sent to DirectAMS laboratories in Seattle (Washington) to be dated by Radiocarbon with AMS. These new radiocarbon dates refer to M30 (4087 ± 28 BP) and M42 (4053 ± 35 BP) (Table 1, Fig. 2).

5. Discussion

San Juan cave is a typical collective burial site from the Late Neolithic-Chalcolithic period situated on the Ebro Basin (Rodanés

et al., 2016). The radiocarbon record for San Juan cave shows the use of the cavity during all the Late Neolithic-Chalcolithic period and, sporadically, also during the Bronze Age (Table 1, Fig. 2). The high number of radiocarbon dates from the Late Neolithic-Chalcolithic period suggests a greater sepulchral use during this phase. This recurrent use of the cavity is also proved by the kind of grave goods found inside the cave, which show high concentrations of material attributed to the Late Neolithic-Chalcolithic period (Pastor and Vicente, 2009). These grave goods have parallels with other sepulchral sites located in the high Ebro Valley, for example those from the sites of San Juan Ante Portam Latinam (Etxeberria et al., 1999) and Cueva de Abautz (Utrilla et al., 2015).

It is possible that when the cave began to have a less intensive use, carnivores visited the cave more regularly and accumulated their preys in it. This could explain the high percentage of faunal remains with carnivore marks. A few herbivore remains do not have carnivore modifications, so it is not possible to rule out the intentional accumulation by humans. Faunal and human remains are commingled with each other because of human bone reacommodations, making this impossible to distinguish between casual or intentional accumulation by humans. Apart from that, all faunal remains seem to be in the same archaeological context.

The domestic faunal remains recovered from San Juan cave show overall high $\delta^{15}\text{N}$ values, which could be associated to it being a warm ecosystem where organic nitrogen is taken by plants more efficiently (Amundson et al., 2003; Handley et al., 1999). This idea would be supported by environmental studies done in Estanya Lake, in the Pre-Pyrenean range, which portray a warmer climatic phase in the Recent Holocene (4200–2000 cal. BP) for the region (González-Sampérez et al., 2017). However, in this case the high $\delta^{15}\text{N}$ values can't be explained by warmer conditions alone, because most of wild faunal remains (rabbits and carnivores) do not show increased $\delta^{15}\text{N}$ values similar to the ones observed amongst contemporary domestic animals. Only one subadult rabbit shows a higher value ($\delta^{15}\text{N} = 7.6\text{‰}$) that could be due to a nursing effect (Fogel et al., 1989). Carnivores present in the sample (*Felis silvestris*, *Vulpes vulpes* and *Meles meles*) do not show elevated $\delta^{15}\text{N}$ values compared with domestic herbivores (only 1.1‰ higher). Only one *Meles meles* presents an elevated $\delta^{15}\text{N}$ value that might be caused by carrion feeding (Martín et al., 1995). In the case of the carnivores,

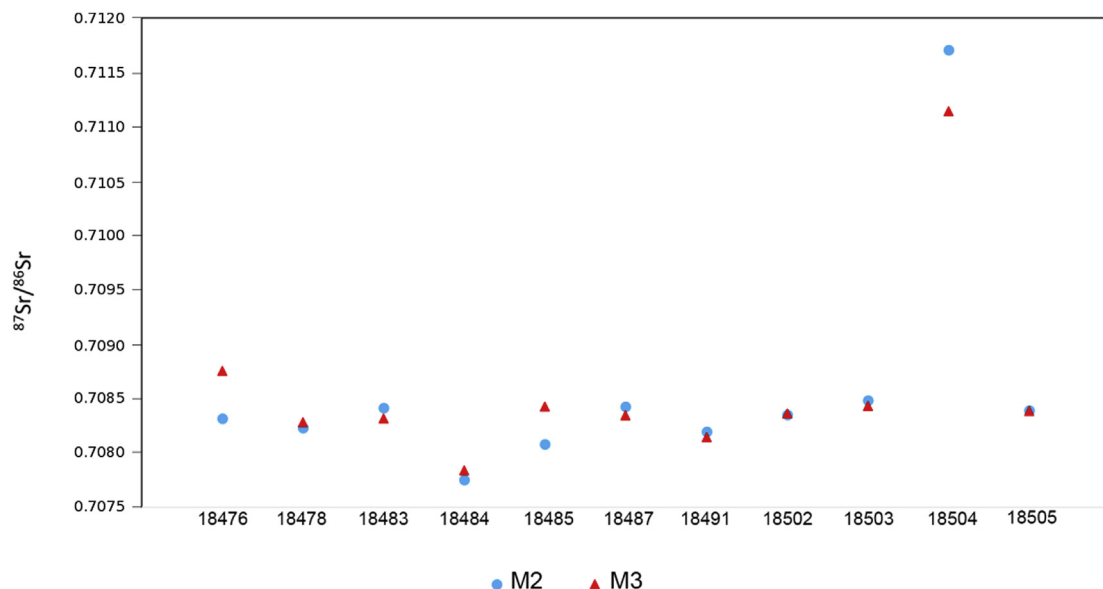


Fig. 9. Plot of $^{87}\text{Sr}/^{86}\text{Sr}$ ratios of human enamel inter-tooth samples from same individuals. The legend shows the molar piece: second molar (M2: completed mineralization during childhood) and third molar (M3: completed mineralization during early adulthood). Horizontal axis refers to the S-UCT code.

the low $\delta^{15}\text{N}$ values could be explained by a sporadic domestic herbivore intake and a more usual wild herbivore intake that would have lower $\delta^{15}\text{N}$ values (e.g. rabbits). On the other hand, higher $\delta^{15}\text{N}$ values from domesticated herbivores could be explained by the use of composted fodder (Bogaard et al., 2007), as suggested by some authors for these chronologies in near-by regions (Salazar-García, 2012b). We should anyway consider the possibility that all human and faunal remains might not be strictly contemporaneous, as not all of them have been directly radiocarbon dated (Fig. 5).

The huge variability observed in $\delta^{15}\text{N}$ and $\delta^{13}\text{C}$ values from domestic adult ovicaprids could be explained by the presence of different sheep flocks (Martín et al., 2015) and also transhumance livestock activities, which are suggested by other isotopic studies in the recent Holocene of the Iberian Peninsula (Valenzuela-Lamas et al., 2016). Sequential $\delta^{13}\text{C}$ and $\delta^{18}\text{O}$ isotopic analysis done in ovicaprid teeth (Tornero et al., 2016) are necessary to discriminate if the differences in $\delta^{15}\text{N}$ and $\delta^{13}\text{C}$ ovicaprid values are due to transhumance activities or not. It is also possible that these range of values are due to livestock coming from different origins, perhaps through trading, or that all remains are after all not strictly contemporaneous.

The human isotope values from San Juan cave indicate a quite homogeneous protein diet based on C_3 terrestrial resources, and consistent with domestic herbivores being consumed preferentially. Differences between herbivore and human $\delta^{15}\text{N}$ values ($\delta^{15}\text{N}$ enrichment of 2.4‰) suggest a moderate animal protein intake assuming 3–5‰ as typical $\delta^{15}\text{N}$ collagen enrichment (Bocherens and Drucker, 2003). A mixed diet with a moderate animal intake combined with a plant food intake could be in agreement with the $\delta^{15}\text{N}$ values. Nevertheless, there are some limitations that are necessary to take into account. The most important limitation is the exclusive use of San Juan cave as a burial site. If the burial was shared by different communities, there is a risk that the $\delta^{15}\text{N}$ values from the few available faunal remains do not represent all available faunal resources at the time. Indeed, as this is something very difficult to prove at a burial site, it is necessary to calculate a common $\delta^{15}\text{N}$ baseline for all human individuals. Besides, the animal sample is very small and the $\delta^{15}\text{N}$ values for wild medium- and large-sized herbivores are unknown, being difficult to prove their consumption (much less to try to quantify it). There is, however, no isotopic evidence of the consumption of C_4 resources. Additionally, a regular feeding of marine or freshwater resources has not been observed, something supported by the lack of ictiofaunal remains recovered at the cave and surrounding sites (Fig. 5). Furthermore, all marine malacofaunal materials recovered at the site are perforated and suggested to be used as decorative beads and pendants (Pastor and Vicente, 2009). This is all consistent with the presence of exchange networks but not with the consumption of these resources.

The limited anthropological capacity of the human sample has not allowed making sex diagnoses, so possible differences between sexes cannot be tested as in other isotopic studies from the Neolithic period in the Western Mediterranean (Le Bras-Goude et al., 2009; Fontanals-Coll et al., 2015). However, no differences between adults and subadults have been observed. Only one of the five infants has high $\delta^{15}\text{N}$ values (1.3‰ higher than the mean adult value), probably as a result of the last moments of breastfeeding, at the transition to weaning (Fogel et al., 1989; Fuller et al., 2006). The remaining infants have similar values to adults, with one of them presenting the lowest $\delta^{15}\text{N}$ value of the whole population. This could be growth-related physiological processes, a signal of change in the diet, or both of them (Beaumont et al., 2013; Reynard and Tuross, 2015). Furthermore, and alternatively to specific ages amongst the adult individuals, dental wear from adult specimens analysed was checked against the isotopic values. No differences in

$\delta^{13}\text{C}$ and $\delta^{15}\text{N}$ values were observed among individuals with different molar wear pattern (Fig. 6). It is possible that macro-wear tooth and protein consumption are here not correlated, making it necessary to use dental microwear to test this relationship as done in previous studies (Salazar-García et al., 2016a). Macrowear pattern could be associated with age in this case (Brothwell, 1989), but it is not possible to associate it to a discriminatory agent regarding protein consumption.

This homogeneous C_3 terrestrial based dietary subsistence pattern is representative of the Late Neolithic-Chalcolithic and the beginning of the Bronze Age. While no other previous isotopic studies have been carried out before for the Late Neolithic-Chalcolithic or Bronze Age in the Ebro Basin, there is data available from other surrounding Iberian regions for this chronology: La Pijotilla and Valencina-Castilleja in the south (Díaz-Zorita, 2014); Cova Moura, Paimogo I and Feteiras II in the west (Waterman et al., 2015); Cova do Santo in the north-west (López-Costas et al., 2015); and Cova de la Pastora, Avenc dels dos Forats (McClure et al., 2011), La Vital (Salazar-García, 2012b), Cova dels Diablets (Salazar-García, 2014b) and Coveta del Frare (García-Borja et al., 2013) in the east of the Iberian Peninsula. When plotting all human carbon and nitrogen isotope values available for the surrounding regions, we can see that there is not a large difference among the five areas and San Juan cave in the Ebro Basin (north-east) (Fig. 10). San Juan cave only presents slight differences in their $\delta^{13}\text{C}$ values regarding north and north-west plotted sites. It also shows some differences in both $\delta^{13}\text{C}$ and $\delta^{15}\text{N}$ values with two southern sites. In both cases, standard deviations calculated for these groups are not overlapping, although the slight differences with the southern sites could be due to the low number of individuals analysed in that area ($n = 8$). Therefore, an homogeneous C_3 terrestrial diet with no clear marine input was the common feeding pattern during the Late Neolithic-Chalcolithic Period among the different regions of Iberia.

$^{87}\text{Sr}/^{86}\text{Sr}$ data show that only 4 of 21 individuals (19% of the total studied population) come from further afield than the surroundings of San Juan cave: M13, M42, M30 and C7 (Fig. 8). Non-local individuals found in a sepulchral cave could have different meanings. They could be actual migrants that travelled at some point during their life to settle at a community living close to San Juan

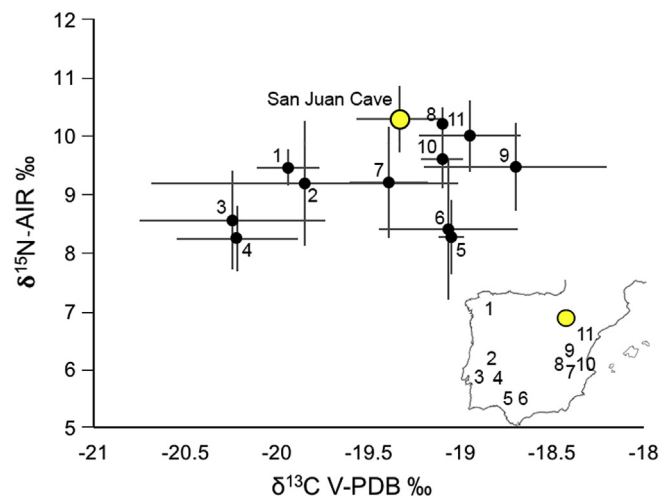


Fig. 10. Plot of bone collagen $\delta^{13}\text{C}$ and $\delta^{15}\text{N}$ values of different Late Neolithic-Chalcolithic and Bronze sites from Iberian Peninsula [1: Cova do Santo (López-Costas et al., 2015); 2,3,4: Cova Moura, Paimogo I and Feteiras II (Waterman et al., 2015); 5, 6: Valencina-Castilleja and La Orden-Seminario (Díaz-Zorita, 2014); 7, 8, 9, 10, 11: La Vital (Salazar-García, 2012b), Coveta del Frare (García-Borja et al., 2013), Cova de la Pastora, Avenc dels dos Forats (McClure et al., 2011), Cova dels Diablets (Salazar-García, 2014b)]. The position of the numbers is approximate.

cave, where they were eventually buried. Or, alternatively, could mean that the site was used as a shared funerary space by communities living in a wider area encompassing different major geological regions other than the one from the immediate burial surrounding. In order to better assess these two possibilities, distances should be considered. If a non-local individual shows values compatible with those from nearby geological areas, we can't rule out the possibility that the individual is no real migrant but instead was transported to the cave from its "local" community once dead. However, if the non-local values correspond to geological domains situated further away, it is less plausible that the corpse was brought into the cave from far away distances, and we are possibly talking in this case of a real migrant.

Individual M13 shows $^{87}\text{Sr}/^{86}\text{Sr}$ values lower than those from San Juan cave surroundings (Cretaceous-Miocene) and nearby Paleogene deposits. If it is considered that lower $^{87}\text{Sr}/^{86}\text{Sr}$ values come from more recent geologic deposits (Bentley, 2006), it is possible to speculate that individual M13 came from the flattest area of the Ebro Valley, which is dominated exclusively by Miocene-Quaternary deposits. Furthermore, since both second and third molar values are similar and lower than the local range, it is quite possible that this individual arrived only after the mineralization of the third molar occurred during early adulthood (Hillson, 1996). As Miocene-Quaternary deposits exist close to the cave in a southern direction, individual M13 could well be either a migrant or an example of corpse transportation from a local community. Furthermore, as this study has confirmed that Paleogene deposits show similar $^{87}\text{Sr}/^{86}\text{Sr}$ values to those from San Juan cave immediate surroundings (Cretaceous-Miocene), and knowing that a huge part of the Ebro Valley is dominated by this type of deposits, it is difficult to know if migrants coming from this latter type of geology could be also masked among the sample population (i.e. even if non-locals, they would have same values as local people).

Individuals C7, M30 and M42 show higher $^{87}\text{Sr}/^{86}\text{Sr}$ values than the bioavailable Sr range from San Juan cave surroundings (Cretaceous-Miocene) and nearby Paleogene deposits. C7 also shows similar values for second and third molars, suggesting as well a movement after his early adulthood (Hillson, 1996). Noteworthy is that $^{87}\text{Sr}/^{86}\text{Sr}$ values from these non-local individuals (M42, M30 and C7) are consistent with published bioavailable $^{87}\text{Sr}/^{86}\text{Sr}$ data from the southwest of the Iberian Peninsula (Waterman et al., 2014), as well as from Lower Triassic deposits of northern Iberia (Villalba-Mouco et al., 2017). Because of proximity, it is likely that these individuals arrived from other regions with abundant Lower Triassic formations: the Iberian System in the south of San Juan cave or the Navarre Pyrenees in the north (visible on the geological map from Instituto Geológico y Minero, Ministerio de Ciencia e Innovación, Gobierno de España; (<http://www.imgc.es/>)). In this two cases the Lower Triassic deposits with considerable surface area are more than 100 km away from San Juan cave, and it is therefore likely that these three individuals (M30, M42 and C7) are actual migrants coming from afar. As a result, and further supported by the fact that all this far away region is full of cavities potentially available for burying the dead, the corpse-transportation hypothesis is in the case of individuals M30, M42 and C7 case less plausible than in the case of individual M13.

Only two of the non-local individuals have been directly radiocarbon dated: M30 (4087 ± 28 BP) and M42 (4053 ± 35 BP). That both of these dates correspond to the later stages of the Late Neolithic-Chalcolithic suggest that the purported higher mobility pattern would have started only at the end of the Late Neolithic-Chalcolithic period (Fig. 2). This proposed higher mobility scenario could be also common amongst other communities of the Ebro Basin with same cultural attribution. It could also be that San Juan cave started to be used overall more during this stage, and therefore

have more probability of detecting the non-locals by randomly sampling for dating. As a result of this uncertainty, it is necessary to perform more intensive radiocarbon studies in collective burials of the region as done elsewhere in Iberia (e.g. Salazar-García et al., 2016b). A more detailed study encompassing a wider variety of geological sampling areas for better portraying the bioavailable strontium map of Iberia would also help in profiling better provenance and territorial mobility of these past farming communities.

6. Conclusions

This study represents the first multi-isotope analysis of dietary and mobility strategies from the Ebro Basin Late Neolithic-Chalcolithic period. The isotopic dietary study shows a mixed diet based on C_3 terrestrial resources, with domestic herbivores as probably the main protein source. The individuals buried in San Juan cave did not consume marine or freshwater resources, at least enough as to have it reflected on the bone collagen signature. No differences in $\delta^{13}\text{C}$ and $\delta^{15}\text{N}$ values are observed between adults and subadults, nor between different molar wear patterns. Only four individuals are potentially detectable non-locals, as their $^{87}\text{Sr}/^{86}\text{Sr}$ values are different from those of the immediate geological surrounding of the cave and the region. This mobility pattern seems to have happened at the end of the cave's use as burial site, during the end of the Late Neolithic-Chalcolithic period, as shown by the radiocarbon dates of these individuals. The $^{87}\text{Sr}/^{86}\text{Sr}$ bioavailable values that exist today for the Iberian Peninsula suggest different origins for these non-local individuals: one from Miocene-Quaternary deposits, and three from Lower Triassic geologic regions. The flattest part of the Ebro Valley is dominated by a Miocene-Quaternary geology, but the closest Lower Triassic geologies to San Juan cave are in the Navarre Pyrenees to the north or at the Iberian System to the south. Both of them are located more than 100 km away from the place of burial, suggesting a migration movement of at least these three individuals.

Acknowledgements

VVM has a predoctoral scholarship funded by the Gobierno de Aragón and the Fondo Social Europeo (BOA20150701025), and did a research stay at the University of Cape Town funded by the Fundación Ibercaja-CAI (2016). DCSG acknowledges funding for this research from the BBVA Foundation (I Ayudas a Investigadores, Innovadores y Creadores Culturales). VVM and PU are members of the Spanish project HAR2014-59042-P (Transiciones climáticas y adaptaciones sociales en la prehistoria de la Cuenca del Ebro), and of the regional government of Aragón PPVE research group (H-07: Primeros Pobladores del Valle del Ebro). ISG has a predoctoral scholarship funded by Basque Government and is a member of the Spanish project HAR2014-53536-P and IT-662-13. VS is supported by the Ministerio de Ciencia, Tecnología e Innovación Productiva, Consejo Nacional de Investigaciones Científicas y Técnicas (CONICET) of Argentina (Postdoctoral Fellowship)(Resolución N°4256). All authors would like to thank the Museo de Huesca for allowing the use of their installations, as well as to the Centro de Espeleología de Aragón (CEA) for the help with sampling modern materials. We would also like to thank Feyrooza Rawoot, Kerryn Gray and Ian Newton for technical assistance, and Chrystel Tinguely for help obtaining the Sr concentration values. We would also like to thank the two anonymous reviewers for their useful comments, who helped improve the manuscript.

References

Ambrose, S.H., 1993. Isotopic analysis of paleodiets: methodological and

- interpretative considerations. In: Stanford, M.K. (Ed.), *Investigations of Ancient Human Tissue: Chemical Analyses in Anthropology*. Gordon and Breach Science Publishers, Langhorne, pp. 59–130.
- Ambrose, S.H., Norr, L., 1993. Experimental evidence for the relationship of the carbon isotope ratios of whole diet and dietary protein to those of bone collagen and carbonate. In: Lambert, J.B., Gruppe, G. (Eds.), *Prehistoric Human Bone: Archaeology at the Molecular Level*. Springer Verlag, Berlin, pp. 1–37.
- Amundson, R., Austin, A.T., Schuur, E.A.G., Yoo, K., Matzek, V., Kendall, C., Uebersax, A., Brenner, D., Baisden, W.T., 2003. Global patterns of the isotopic composition of soil and plant nitrogen. *Glob. Biogeochem. Cycles* 17 (1), 1031.
- Andrés, M.T., 1998. *Colectivismo funerario neo-eneolítico. Aproximación metodológica sobre datos de la Cuenca Alta y Media del Ebro*. Institución Fernando el Católico. Diputación de Zaragoza, Zaragoza.
- Andrés, M.T., 2005. Concepto y análisis del cambio cultural: su percepción en la materia funeraria del Neolítico y Eneolítico. In: *Monografías Arqueológicas*, vol. 42. Departamento de Ciencias de la Antigüedad, Universidad de Zaragoza, Zaragoza.
- Arias, P., 2005. Determinaciones de isótopos estables en restos humanos de la región Cantábrica. Aportación al estudio de la dieta de las poblaciones del Mesolítico y Neolítico. *Munibe (Antropología-Arkeología)* 57, 359–374. Home-naje a Jesús Altuna.
- Basabe, J.M., Bennassar, I., 1983. Estudio antropológico del yacimiento de Fuente Hoz (Anúncia, Álava). *Estud. Arqueol. Alavesa* 11, 77–119.
- Beaumont, J., Gledhill, A., Lee-Thorp, J., Montgomery, J., 2013. Childhood diet: a closer examination of the evidence from dental tissues using stable isotope analysis of incremental human dentine. *Archaeometry* 55 (2), 277–295.
- Bentley, R.A., 2006. Strontium isotopes from the earth to the archaeological skeleton: a review. *J. Archaeol. Method Theory* 13 (3), 135–187.
- Bentley, R.A., 2013. Mobility and the diversity of early Neolithic lives: isotopic evidence from skeletons. *J. Anthropol. Archaeol.* 32 (3), 303–312.
- Bentley, R.A., Price, T.D., Stephan, E., 2004. Determining the 'local' Sr-87/Sr-86 range for archaeological skeletons: a case study from Neolithic Europe. *J. Archaeol. Sci.* 31 (4), 365–375.
- Binford, L.R., 1981. *Bones: Ancient Men and Modern Myths*. Academic Press, New York, p. 320.
- Bocherens, H., Drucker, D., 2003. Trophic level isotopic enrichment of carbon and nitrogen in bone collagen: case studies from recent and ancient terrestrial ecosystems. *Int. J. Osteoarchaeol.* 13 (1–2), 46–53.
- Bogaard, A., Heaton, T.H., Poulton, P., Merbach, I., 2007. The impact of manuring on nitrogen isotope ratios in cereals: archaeological implications for reconstruction of diet and crop management practices. *J. Archaeol. Sci.* 34 (3), 335–343.
- Brain, C.K., 1981. *The Hunters or the Hunted? An Introduction to African Cave Taphonomy*. University of Chicago Press, Chicago.
- Bronk Ramsey, C., 2009. Bayesian analysis of radiocarbon dates. *Radiocarbon* 51 (1), 337–360.
- Brothwell, D.R., 1989. The relationship of tooth wear to aging. In: Iscan, M.Y. (Ed.), *Age Markers in the Human Skeleton*. Thomas, Springfield, pp. 303–316.
- Brown, T.A., Nelson, D.E., Vogel, J.S., Southon, J.R., 1988. Improved collagen extraction by modified Longin method. *Radiocarbon* 30, 171–177.
- Budd, P., Montgomery, J., Barriero, B., Thomas, R.G., 2000. Differential diagenesis of strontium in archaeological human dental tissues. *Appl. Geochem.* 15, 687–694.
- Buikstra, J.E., Ubelaker, D.H., 1994. Standards for Data Collection from Human Skeletal Remains. In: *Arkansas Archaeological Survey Research Series (Fayetteville)*.
- Carvalho, A.F., Petchey, F., 2013. Stable isotope evidence of Neolithic palaeodiets in the coastal regions of Southern Portugal. *J. Isl. Coast. Archaeol.* 8 (3), 361–383.
- Chapman, R., 1981. The emergence of formal disposal areas and the 'problem' of Megalithic tombs in prehistoric Europe. In: Chapman, R., Kinnes, I., Randsborg, K. (Eds.), *The Archaeology of Death*. Cambridge University Press, Cambridge, pp. 71–82.
- Copeland, S.R., Cawthra, H.C., Fisher, E.C., Lee-Thorp, J.A., Richard, M.C., le Roux, P.J., Hodgkins, J., Marean, C.W., 2016. Strontium isotope investigation of ungulate movement patterns on the pleistocene paleo-agulhas plain of the greater Cape floristic region, South Africa. *Quat. Sci. Rev.* 141, 65–84.
- Copeland, S.R., Sponheimer, M., de Ruiter, D.J., Lee-Thorp, J.A., Codron, D., le Roux, P.J., Grimes, V., Richards, M.P., 2011. Strontium isotope evidence for landscape use by early hominins. *Nature* 474 (7349), 76–78.
- De Niro, M.J., Epstein, S., 1978. Influence of diet on the distribution of carbon isotopes in animals. *Geochim. Cosmochim. Acta* 42, 495–506.
- Díaz-Zorita, M., 2014. *The copper age. In: South-west Spain: a Bioarchaeological Approach to Prehistoric Social Organisation*. Durham University, Durham (Doctoral thesis).
- El Aidi, H., Bronkhorst, E.M., Huysmans, M.C.D.N.J.M., Truin, G.J., 2011. Multifactorial analysis of factors associated with the incidence and progression of erosive tooth wear. *Caries Res.* 45 (3), 303–312.
- Ericson, J.E., 1985. Strontium isotope characterization in the study of prehistoric human ecology. *J. Hum. Evol.* 14, 503–514.
- Etxeberria, F., Fernández, S., Zumalabe, F.J., Vegas, J.I., Herrasti, L., Armendáriz, A., 1999. La sepultura colectiva de San Juan ante Portam Latinam (Laguardia, Álava). *Saguntum Extra* 2, 439–445.
- Fernández-Crespo, T., 2010. Caracterización antropológica y tratamiento funerario de las poblaciones del Neolítico a la Edad del Bronce en la comarca de La Rioja: estado de la cuestión. *Munibe. Suplemento* 32, 414–424.
- Fernández-Crespo, T., de-la-Rúa, C., 2015. Demographic evidence of selectiveburial in megalithic graves of northern Spain. *J. Archaeol. Sci.* 53, 604–617.
- Fernández-Crespo, T., 2016. El papel del fuego en los enterramientos neolíticos finales/calcolíticos iniciales de los abrigos de la Sierra de Cantabria y sus estribaciones (valle medio-alto del Ebro). *Trab. Prehis.* 73 (1), 128–146.
- Fernandez, H., 2001. *Ostéologie comparée des petites ruminants eurasiatiques sauvages et domestiques (genres Rupicapra, Ovis, Capra et Capreolus): diagnose différentielle du squelette appendiculaire*. Université de Geneva, Geneva (Doctoral thesis).
- Fogel, M.L., Tuross, N., Owsley, D.W., 1989. Nitrogen isotope tracers of human lactation in modern and archaeological populations, Annual Report of the Director, Geophysical Laboratory 1988–89. Carnegie Inst. Wash. 111–117.
- Fontanals-Coll, M., Subirà, M.E., Bonilla, M.D.Z., Dubosq, S., Gibaja, J.F., 2015. Investigating palaeodietary and social differences between two differentiated sectors of a Neolithic community, La Bòbila Madurell-Can Gambús (north-east Iberian Peninsula). *J. Archaeol. Sci. Rep.* 3, 160–170.
- Fuller, B.T., Fuller, J.L., Harris, D.A., Hedges, R.E.M., 2006. Detection of breastfeeding and weaning in modern human infants with carbon and nitrogen stable isotope ratios. *Am. J. Phys. Anthropol.* 129, 279–293.
- Fuste, M., 1982. Restos humanos de la Cueva de los Hombres Verdes en Urbiola (Navarra). *Trab. Arqueol. Navar.* 3, 41.
- Gálvez-Bravo, L., 2011. *Conejo – Oryctolagus cuniculus*. In: Salvador, A., Cassinello, J. (Eds.), *Enciclopedia Virtual de los Vertebrados Españoles*. Museo Nacional de Ciencias Naturales, Madrid. <http://www.vertebradosibericos.org/>.
- García-Borja, P., Pérez Fernández, A., Biosca Cirujeda, V., Ribera i Gomes, A., Salazar-García, D.C., 2013. Los restos humanos de la Coveta del Frare (Font de la Figuera, València). In: García-Borja, P., Revért, E., Ribera, A., Biosca, V. (Eds.), *El Naiximent d' un Poble. Historia i Arqueologia de la Font de la Figuera*, pp. 47–60. Ajuntament de la Font de la Figuera.
- García-Guixé, E., 2011. *Estudi paleoantropològic i paleopatològic del sepulcre col·lectiu de Forat de Conqueta (Santa Linya, Lleida)*. Treballs d'arqueologia 17, 37–98.
- García-Guixé, E., Subirà, M.E., Richards, M.P., 2006. Paleodiets of humans and fauna from the Spanish mesolithic site of el collado. *Curr. Anthropol.* 47 (3), 549–556.
- Gimeno, B., 2009. Estudio antropológico de la cueva sepulcral de Lohar. *Saldvie Estud. Prehist. Arqueol.* 9, 369–392.
- González-Sampériz, P., Aranbarri, J., Pérez-Sanz, A., Gil-Romera, G., Moreno, A., Leunda, M., Sevilla-Callejo, M., Corella, J.P., Morellón, M., Oliva, B., Valero-Garcés, B., 2017. Environmental and climate change in the southern Central Pyrenees since the Last Glacial Maximum: a view from the lake records. *Catena* 149, 668–688.
- Handley, L.L., Austin, A.T., Robinson, D., Scrimgeour, C.M., Raven, J.A., Heaton, T.H.E., Schmidt, S., Stewart, G.R., 1999. The N15 natural abundance ($\delta^{15}N$) of ecosystem samples reflects measures of water availability. *Aust. J. Plant Physiol.* 26, 185–199.
- Haynes, G., 1980. Evidence of carnivore gnawing on Pleistocene and Recent mammalian bones. *Paleobiology* 6 (3), 341–351.
- Haynes, G., 1983. A guide for differentiating mammalian carnivore taxa responsible for gnaw damage to herbivore limb bones. *Paleobiology* 9 (2), 164–172.
- Hedges, R.E.M., Clement, J.G., Thomas, C.D.L., O'Connell, T.C., 2007. Collagen turnover in the adult femoral mid-shaft: modeled from anthropogenic radiocarbon tracer measurements. *Am. J. Phys. Anthropol.* 133, 808–816.
- Hedges, R.E.M., Reynard, L.M., 2007. Nitrogen isotopes and the trophic level of humans in archaeology. *J. Archaeol. Sci.* 34, 1240–1251.
- Hillson, S., 1992. *Mammal Bones and Teeth: an Introductory Guide to Methods of Identification*. Institute of Archaeology, University College London, London.
- Hillson, S., 1996. *Dental Anthropology*. Cambridge University Press, Cambridge.
- Hodder, I., 1984. Burials, houses, women and men in the European Neolithic. In: Miller, D., Tilley, C. (Eds.), *Ideology, Po and Prehistory*. Cambridge University Press, Cambridge, pp. 51–68.
- Le Bras-Goude, G., Schmittb, A., Loison, G., 2009. Comportements alimentaires, aspects biologiques et sociaux au Néolithique: le cas du Crès (Hérault, France). *Comptes Rendus Palevol* 8 (1), 79–91.
- Lee-Thorp, J.A., 2008. On isotopes and old bones. *Archaeometry* 50 (6), 925–950.
- Lillie, M., Budd, C., Potekhina, I., 2011. Stable isotope analysis of prehistoric populations from the cemeteries of the Middle and Lower Dnieper Basin, Ukraine. *J. Archaeol. Sci.* 38 (1), 57–68.
- Longin, R., 1971. New method of collagen extraction for radiocarbon dating. *Nature* 230, 241–242.
- López-Costas, O., Müldner, G., Cortizas, A.M., 2015. Diet and lifestyle in Bronze age northwest Spain: the collective burial of Cova do Santo. *J. Archaeol. Sci.* 55, 209–218.
- Lorenzo, J.I., 1989. Restos óseos humanos. In: Barandiaran, I., Cava, A. (Eds.), *El yacimiento prehistórico de Zatoya (Navarra)*. Evolución ambiental cultural a fines del Tardiglacial y en la primera mitad del Holoceno. *Trabajos de Arqueología Navarra* 8. Institución Príncipe de Viana del Departamento de Educación y Cultura del Gobierno de Navarra, pp. 209–219.
- Lorenzo, J.I., 2014. Estudio antropológico de los restos de Forcas II. In: Utrilla y, P., Mazo, C. (Eds.), *La Peña de las Forcas (Graus, Huesca)*. Un asentamiento estratégico en la con uencia del Esera y el Isabena. *Monografías Arqueológicas/ Prehistoria* 46, Zaragoza, pp. 337–341.
- Lyman, R.L., 1994. *Vertebrate Taphonomy*. Cambridge University Press, Cambridge.
- Makarewicz, C.A., Sealy, J., 2015. Dietary reconstruction, mobility, and the analysis of ancient skeletal tissues: expanding the prospects of stable isotope research in archaeology. *J. Archaeol. Sci.* 56, 146–158.
- Martín, P., García-González, R., Nadal, J., Vergés, J.M., 2015. Perinatal ovicaprine remains and evidence of shepherding activities in early Holocene enclosure

- caves: el mirador (sierra de atapuerca, Spain). *Quat. Int.* 414, 316–329.
- Martín, R., Rodríguez, A., Delibes, M., 1995. Local feeding specialization by badgers (*Meles meles*) in a Mediterranean environment. *Oecologia* 101 (1), 45–50.
- McClure, S.B., García, O., de Togores, C.R., Culleton, B.J., Kennett, D.J., 2011. Osteological and paleodietary investigation of burials from Cova de la Pastora, Alicante, Spain. *J. Archaeol. Sci.* 38 (2), 420–428.
- Minagawa, M., Wada, E., 1986. Nitrogen isotope ratios of red tide organisms in the East China Sea: a characterization of biological nitrogen fixation. *Mar. Chem.* 19 (3), 245–259.
- Morris, P., 1972. A review of mammalian age determination methods. *Mammal. Rev.* 2, 69–104.
- Morris, P., 1978. The use of teeth for estimating the age of wild mammals. In: Butler, P.M., Joysey, K.A. (Eds.), *Development, Function and Evolution of Teeth*. Academic Press, London, pp. 483–494.
- Müldner, G., Richards, M.P., 2005. Fast or feast: reconstructing diet in later medieval England by stable isotope analysis. *J. Archaeol. Sci.* 32 (1), 39–48.
- O'Connell, T.C., Kneale, C.J., Tasevska, N., Kuhnle, G.G., 2012. The diet-body offset in human nitrogen isotopic values: a controlled dietary study. *Am. J. Phys. Anthropol.* 149 (3), 426–434.
- Pales, L., Lambert, C., 1971. Atlas ostéologique pour servir à la identification des mammifères du quaternaire. CNRS, Bordeaux.
- Palomo, L.J., 2007. In: Gisbert, J., Blanco, J.C. (Eds.), *Atlas y libro rojo de los mamíferos terrestres de España*. Organismo Autónomo de Parques Nacionales.
- Pastor, M.V., Vicente, D., 2009. La cueva sepulcral neolítica/calcolítica de San Juan en Loarre (Huesca). *Saldvie Estud. Prehist. Arqueol.* 9, 335–368.
- Pin, C., Briot, D., Bassin, C., Poitrasson, F., 1994. Concomitant separation of strontium and samarium-neodymium for isotopic analysis in silicate samples, based on specific extraction chromatography. *Anal. Chim. Acta* 298 (2), 209–217.
- Power, R.C., Salazar-García, D.C., Wittig, R.M., Henry, A.G., 2014. Assessing use and suitability of scanning electron microscopy in the analysis of micro remains in dental calculus. *J. Archaeol. Sci.* 49, 160–169.
- Price, T.D., Bentley, R.A., Gronenborn, D., Lüning, J., Wahl, J., 2001. Human migration in the linearbandkeramik of central Europe. *Antiquity* 75, 593–603.
- Price, T.D., Burton, J.H., Bentley, R.A., 2002. The characterization of biologically available strontium isotope ratios for the study of prehistoric migration. *Archaeometry* 44 (1), 117–135.
- Purroy, F.J., 2011. *Liebre ibérica – Lepus granatensis*. In: Salvador, A., Cassinello, J. (Eds.), *Enciclopedia Virtual de los Vertebrados Españoles*. Museo Nacional de Ciencias Naturales, Madrid. <http://www.vertebradosibericos.org/>.
- Reimer, P.J., Bard, E., Bayliss, A., Beck, J.W., Blackwell, P.G., Bronk Ramsey, C., Grootes, P.M., Guilderson, T.P., Hafflidason, H., Hajdas, I., Hatté, C., Heaton, T.J., Hoffmann, D.L., Hogg, A.G., Hughen, K.A., Kaiser, K.F., Kromer, B., Manning, S.W., Niu, M., Reimer, R.W., Richards, D.A., Scott, E.M., Southon, J.R., Staff, R.A., Turney, C.S.M., Van der Plicht, J., 2013. *IntCal13 and Marine13 radiocarbon age calibration curves 0–50,000 Years cal BP*. *Radiocarbon* 55 (4), 1869–1887.
- Renfrew, A.C., 1976. Megaliths, territories, and populations. In: De Laet, S.J. (Ed.), *Acculturation and Continuity in Atlantic Europe*, pp. 198–220. Tempel, Brugge, Belgium.
- Reynard, L.M., Tuross, N., 2015. The known, the unknown and the unknowable: weaning times from archaeological bones using nitrogen isotope ratios. *J. Archaeol. Sci.* 53, 618–625.
- Rodanés, J.M., Lorenzo, J.I., Aranda, P., 2016. Enterramientos en cuevas y abrigos en el Alto Aragón durante el Neolítico y la Edad del Bronce. In: Bonet, H. (Ed.), *Del neolítico a l'edat del bronze en el Mediterrani occidental*. Estudis en homenatge a Bernat Martí Oliver. TV SIP 119, pp. 411–426. Valencia.
- Rowley-Conwy, P., Albarella, U., Dobney, K., 2012. Distinguishing wild boar from domestic pigs in prehistory: a review of approaches and recent results. *J. World Prehistory* 25 (1), 1–44.
- Sala, N., 2012. *Tafonomía de yacimientos kársticos de carnívoros en el Pleistoceno*. Departamento de Paleontología. Universidad Complutense de Madrid, Madrid (Doctoral thesis).
- Salazar-García, D.C., 2012a. *Isótopos, dieta y movilidad en el País Valenciano*. Aplicación a restos humanos del Paleolítico medio al Neolítico final. Universitat de València, Valencia (Doctoral thesis).
- Salazar-García, D.C., 2012b. *Aproximación a la dieta de la población calcolítica de La Vital a través del análisis de isótopos estables del carbono y del nitrógeno sobre restos óseos*. In: Pérez, G., Bernabeu, J., Carrión, Y., García-Puchol, O., Molina, L.L., Gómez, M. (Eds.), *La Vital (Gandia, Valencia)*. Vida y muerte en la desembocadura del Serpis durante el III y el I milenio a.C. Museu de Prehistòria de València-Diputació de València (TV. 113), pp. 139–143. València.
- Salazar-García, D.C., Aura, J.E., Olària, C.R., Talamo, S., Morales, J.V., Richards, M.P., 2014a. Isotope evidence for the use of marine resources in the Eastern Iberian Mesolithic. *J. Archaeol. Sci.* 42, 231–240.
- Salazar-García, D.C., 2014b. *Estudi de la dieta en la població de Cova dels Diablets mitjançant anàlisi d'isòtops estables del carboni i del nitrogen en collagen ossi*. Resultats preliminars. In: Aguilera Arzo, G.A., Monroig, D., García-Borja, P. (Eds.), *La Cova dels Diablets (Alcalà de Xivert, Castelló)*. Prehistòria a la Serra d'Irta. Diputació de la Castelló, Castellón, pp. 67–78.
- Salazar-García, D.C., Romero, A., García-Borja, P., Subirà, M.E., Richards, M.P., 2016a. A combined dietary approach using isotope and dental buccal-microwear analysis of human remains from the Neolithic, Roman and Medieval periods from the archaeological site of Tossal de les Basses (Alicante, Spain). *J. Archaeol. Sci. Rep.* 6, 610–619.
- Salazar-García, D.C., García-Puchol, O., de Miguel-Ibañez, M.P., Talamo, S., 2016b. Earliest evidence of neolithic collective burials from Eastern Iberia: radiocarbon dating at the archaeological site of Les Llometes (Alicante, Spain). *Radiocarbon* 58 (3), 679–692.
- Salazar-García, D.C., de Lugo Enrich, L.B., Álvarez García, H.J., Benito Sánchez, M., 2013b. Estudio diacrónico de la dieta de los pobladores antiguos de Terrinches (Ciudad Real) a partir del análisis de isótopos estables sobre restos óseos humanos. *Rev. Española Antropol. Física* 34, 6–14.
- Salazar-García, D.C., Power, R.C., Serrà, A.S., Villaverde, V., Walker, M.J., Henry, A.G., 2013a. Neanderthal diets in central and southeastern Mediterranean Iberia. *Quat. Int.* 318, 3–18.
- Sanchis, A., 2010. *Los lagomorfos del Paleolítico medio de la región central y sudoriental del Mediterráneo ibérico*. Caracterización tafonómica y taxonómica. Universitat de València, Valencia (Doctoral Thesis).
- Sherratt, A., 1990. The genesis of megaliths: monumentality, ethnicity and social complexity in Neolithic north-west Europe. *World Archaeol.* 22 (2), 147–167.
- Schoeninger, M.J., DeNiro, M.J., 1984. Nitrogen and carbon isotopic composition of bone collagen from marine and terrestrial animals. *Geochim. Cosmochim. Acta* 48, 625–639.
- Schwarcz, H.P., Schoeninger, M.J., 1991. Stable isotope analysis in human nutritional ecology. *Yearb. Phys. Anthropol.* 34, 283–321.
- Tornero, C., Balasse, M., Bălăşescu, A., Chataigner, C., Gasparyan, B., Montoya, C., 2016. The altitudinal mobility of wild sheep at the Epigravettian site of Kalavan 1 (Lesser Caucasus, Armenia): evidence from a sequential isotopic analysis in tooth enamel. *J. Hum. Evol.* 97, 27–36.
- Ubelaker, D.H., 1989. *Human skeletal remains: excavation, analysis, interpretation*. In: *Manual on Archaeology 2 Taraxacum*, first ed. Washington.
- Utrilla, P., Mazo, C., Domingo, R., 2015. Fifty thousand years of prehistory at the cave of Abautz (arraitz, Navarre): a nexus point between the Ebro valley, aquitaine and the cantabrian corridor. *Quat. Int.* 364, 294–305.
- Valenzuela-Lamas, S., Jiménez-Manchón, S., Evans, J., López, D., Jornet, R., Albarella, U., 2016. Analysis of seasonal mobility of sheep in Iron Age Catalonia (north-eastern Spain) based on strontium and oxygen isotope analysis from tooth enamel: first results. *J. Archaeol. Sci. Rep.* 6, 828–836.
- Van der Merwe, N.J., 1982. Carbon isotopes, photosynthesis, and archaeology: different pathways of photosynthesis cause characteristic changes in carbon isotope ratios that make possible the study of prehistoric human diets. *Am. Sci.* 70 (6), 596–606.
- Van Klinken, G.J., 1999. Bone collagen quality indicators for palaeodietary and radiocarbon measurements. *J. Archaeol. Sci.* 26, 687–695.
- Villalba-Mouco, V., Sarasketa-Gartzia, I., Utrilla, P., Montes, L., Mazo, C., Salazar-García, D.C., 2017. *Burial Caves, Shared Spaces*. Subsistence and Territorial Mobility during the Neolithic in the North-East Iberian Peninsula: a Multi-isotopic Approach. Archaeological Science, UK.
- Waterman, A.J., Peate, D.W., Silva, A.M., Thomas, J.T., 2014. In search of homelands: using strontium isotopes to identify biological markers of mobility in late prehistoric Portugal. *J. Archaeol. Sci.* 42, 119–127.
- Waterman, A.J., Tykot, R.H., Silva, A.M., 2015. Stable isotope analysis of diet-based social differentiation at late prehistoric collective burials in south-western Portugal. *Archaeometry*. <http://dx.doi.org/10.1111/arcm.12159>.


10.3 Stable isotope ratio analysis of bone collagen as indicator of different dietary habits and environmental conditions in Northeastern Iberia during the 4th and 3rd millennium cal BC.

Archaeological and Anthropological Sciences
<https://doi.org/10.1007/s12520-018-0657-z>

ORIGINAL PAPER



Stable isotope ratio analysis of bone collagen as indicator of different dietary habits and environmental conditions in northeastern Iberia during the 4th and 3rd millennium cal B.C.

Vanessa Villalba-Mouco¹  · Izaskun Sarasketa-Gartzia² · Pilar Utrilla¹ · F. Xavier Oms³ · Carlos Mazo¹ · Susana Mendiola⁴ · Artur Cebrià³ · Domingo C. Salazar-García^{5,6}

Received: 12 October 2017 / Accepted: 20 May 2018
© Springer-Verlag GmbH Germany, part of Springer Nature 2018

Abstract

The Late Neolithic and Chalcolithic periods are poorly understood in northeastern Iberia. Most of the information comes from the sepulchral structures rather than habitat settlements. The high number of individuals usually recovered from this types of collective burial spaces, together with the low number of direct radiocarbon dates available on them, forces us to be cautious and consider all the studied assemblages as belonging to the so-called Late Neolithic-Chalcolithic time period. To evaluate human dietary patterns of the Late Neolithic-Chalcolithic populations from the northeast of Iberia, stable carbon and nitrogen isotope analysis was carried out on 78 humans and 32 faunal bones from Cova de la Guineu (Font-rubí, Barcelona) and Cueva de Abauntz (Arraitz, Navarra), both of them sepulchral sites. Results show a common dietary pattern in both sites, indicating an homogeneous protein diet based on C₃ terrestrial resources and no isotopic evidence of the consumption of C₄ plants. Only one individual from Cueva de Abauntz, who directly dates to the first moments of the use of the cave as a burial place, suggests a different protein intake. The inter-population analysis shows a significant difference between both human and faunal $\delta^{13}\text{C}$ values, suggesting an environmental influence on the isotope values depending on the geographic location. This effect should not be discarded and always assessed with baseline isotopic values in future studies at each area of Iberia and for different chronological moments.

Keywords Sepulchral caves · Late Neolithic-Chalcolithic · Carbon and nitrogen isotopes · Cova de la Guineu · Cueva de Abauntz



Stable isotope ratio analysis of bone collagen as indicator of different dietary habits and environmental conditions in northeastern Iberia during the 4th and 3rd millennium cal B.C.

Vanessa Villalba-Mouco¹ · Izaskun Sarasketa-Gartzia² · Pilar Utrilla¹ · F. Xavier Oms³ · Carlos Mazo¹ · Susana Mendiola⁴ · Artur Cebrià³ · Domingo C. Salazar-García^{5,6}

Received: 12 October 2017 / Accepted: 20 May 2018
© Springer-Verlag GmbH Germany, part of Springer Nature 2018

Abstract

The Late Neolithic and Chalcolithic periods are poorly understood in northeastern Iberia. Most of the information comes from the sepulchral structures rather than habitat settlements. The high number of individuals usually recovered from this types of collective burial spaces, together with the low number of direct radiocarbon dates available on them, forces us to be cautious and consider all the studied assemblages as belonging to the so-called Late Neolithic-Chalcolithic time period. To evaluate human dietary patterns of the Late Neolithic-Chalcolithic populations from the northeast of Iberia, stable carbon and nitrogen isotope analysis was carried out on 78 humans and 32 faunal bones from Cova de la Guineu (Font-rubí, Barcelona) and Cueva de Abauntz (Arraitz, Navarra), both of them sepulchral sites. Results show a common dietary pattern in both sites, indicating an homogeneous protein diet based on C₃ terrestrial resources and no isotopic evidence of the consumption of C₄ plants. Only one individual from Cueva de Abauntz, who directly dates to the first moments of the use of the cave as a burial place, suggests a different protein intake. The inter-population analysis shows a significant difference between both human and faunal $\delta^{13}\text{C}$ values, suggesting an environmental influence on the isotope values depending on the geographic location. This effect should not be discarded and always assessed with baseline isotopic values in future studies at each area of Iberia and for different chronological moments.

Keywords Sepulchral caves · Late Neolithic-Chalcolithic · Carbon and nitrogen isotopes · Cova de la Guineu · Cueva de Abauntz

✉ Vanessa Villalba-Mouco
vvmouco@unizar.es

✉ Domingo C. Salazar-García
domingocarlos@gmail.com

¹ Departamento de Ciencias de la Antigüedad, Grupo Primeros Pobladores del Valle del Ebro (PPVE), Instituto de Investigación en Ciencias Ambientales (IUCA), Universidad de Zaragoza, Pedro Cerbuna 12, 50009 Zaragoza, Spain

² Departamento de Geografía, Prehistoria y Arqueología, Universidad del País Vasco-Euskal Herriko Unibertsitatea, C/Francisco Tomás y Valiente s/n., 01006 Vitoria-Gasteiz, Spain

³ Seminari d'Estudis i Recerques Prehistòriques (SERP), Secció de Prehistòria i Arqueologia, Universitat de Barcelona, C/Montalegre 6-8, 08001 Barcelona, Spain

⁴ Departamento de Prehistoria, Arqueología, Historia Antigua, Historia Medieval y Ciencias y Técnicas Historiográficas, Universidad de Murcia, C/Santo Cristo 1, 30001 Murcia, Spain

⁵ Grupo de Investigación en Prehistoria IT-622-13 (UPV-EHU)/ IKERBASQUE-Basque Foundation for Science, Vitoria, Spain

⁶ Department of Geology, University of Cape Town, Cape Town, South Africa

Introduction

The Chalcolithic period is traditionally defined by the emergence of copper elements and associated to the beginning of defensive-style architecture (Esquivel and Navas 2007). This last characteristic only seems to appear clearly in the southeast of the Iberian Peninsula, with the denominated Millares Culture (e.g. García Sanjuán 2013; Valera et al. 2014). In the rest of the Iberian Peninsula, the Neolithic-Chalcolithic transition is scarcely defined. In fact, it is possible that this transition does not even strictly exist and rather results from the evolution of villages present in the most advanced phases of the Neolithic (e.g. Blasco et al. 2007). This continuity is also perceptible in most of the sepulchral caves over time, where radiocarbon dates show a continued use from the 4th to the 3rd millennium cal B.C. (Fernández-Crespo 2016; Utrilla et al. 2015; Villalba-Mouco et al. 2017). Moreover, it is possible to find some copper materials normally associated with burial contexts as prestigious grave goods (Blasco and Ríos 2010), but not as evidence of a massive replacement of commonly

used tools such as flint blades, bone industry, polished stones or pottery without singular characteristics from a unique period (Pérez-Romero et al. 2017). In this context, except for the copper elements which are not always present, the Late Neolithic-Chalcolithic transition cannot be clearly delimited. Only Bell-Beaker ware, always associated to burial contexts, could be consistently identified as a new component, although it seems to appear when the villages defined as Chalcolithic had already been settled (Blasco et al. 2007). In this sense, genomic studies pointed out that Bell-Beaker-related individuals showed different genetic ancestries along Europe, suggesting a cultural diffusion rather than long-distance movement of people (Olalde et al. 2018).

Finally, the archaeological evidence of Late Neolithic-Chalcolithic settlements from the upper half part of the Iberian Peninsula is very scarce. There are only examples of Chalcolithic villages in the north central plateau (e.g. Delibes et al. 1995; Díaz-Andreu et al. 1992). The causes for this absence are probably erosive episodes and modern agrarian works that affected the conservation of the sites (Montes and Domingo 2014). As a result, the knowledge about this Late Neolithic-Chalcolithic period on great parts of Iberia is basically based on burial structures (e.g. Andrés 1998), anthropological studies (e.g. García-Guixé 2011; Gimeno 2009), radiocarbon dates (e.g. Salazar-García et al. 2016a), isotope studies (Fernández-Crespo et al. 2016; García-Borja et al. 2013; McClure et al. 2011; Salazar-García 2011, 2014; Sarasketa-Gartzia et al. 2017; Villalba-Mouco et al. 2017) and DNA analysis (Alt et al. 2016; Olalde et al. 2018; Szécsényi-Nagy et al. 2017).

In this context, the aim of this work is to use an isotopic approach to study the subsistence patterns and the environmental influence from two different Late Neolithic-Chalcolithic communities from the northeast of the Iberian Peninsula which are located in different geographical areas. These new isotopic data are provided to contribute increasing the scarce knowledge existing from the Late Neolithic-Chalcolithic period in most of Iberia. Moreover, we aim to discuss if it is possible to directly compare contemporary human isotopic data from different locations in Iberia due to environmental influences on the isotopic values of both fauna and humans.

$\delta^{13}\text{C}$ and $\delta^{15}\text{N}$ stable isotope from collagen bone: diet and environment

Stable isotope ratio analysis of carbon and nitrogen has many uses in ecology (e.g. Ambrose and DeNiro 1986; Vogel 1978), plant physiology (e.g. Smith and Epstein 1971; Tieszen 1991) and geochemistry (Craig 1953). All this knowledge has been used in archaeology to know more about past human subsistence strategies (e.g. Lee-Thorp 2008) and environmental conditions (e.g. Drucker et al. 2003; Goude and Fontugne 2016).

$\delta^{13}\text{C}$ and $\delta^{15}\text{N}$ values of bone collagen allow a direct and quantitative assessment of protein dietary input in animals (e.g. Guiry and Grimes 2013) and humans (e.g. Salazar-García et al. 2016b). $\delta^{13}\text{C}$ values can discriminate between the consumption of terrestrial and aquatic resources (e.g. Lubell et al. 1994; Schoeninger and DeNiro 1984) and also help to detect freshwater and estuarine fish consumption (e.g. Lillie et al. 2011; Richards et al. 2015; Salazar-García et al. 2014). Moreover, $\delta^{13}\text{C}$ can discriminate the intake of plants with different photosynthetic pathways and the animals that consumed them (i.e. C_3 and C_4) (e.g. Laffranchi et al. 2016; Schwarcz and Schoeninger 1991; Van der Merwe 1982). Otherwise, $\delta^{15}\text{N}$ values are able to provide information about the trophic level that an specific organism holds in the food chain (Bocherens and Drucker 2003; Minagawa and Wada 1986). They are considered to increase generally between 3 and 5‰ with each trophic level up inside the food web (Bocherens and Drucker 2003; Schwarcz and Schoeninger 1991), although some researchers suggest this range could be wider (Hedges and Reynard 2007; Szpak 2014).

Diet studies based on stable isotope analysis of bone collagen reflect an average diet of the last 10–15 years before the individual died, depending on the collagen turnover rate of the studied bones (Hedges et al. 2007). In addition, stable isotope ratios mainly reflect protein sources, resulting in having plant intake masked by animal protein consumption due to the higher density of proteins in animal lean meat than in plant foods (Ambrose and Norr 1993). In that case, the study of plant microremains trapped inside dental calculus by microscopy (e.g. Power et al. 2014; Salazar-García et al. 2013a), or metagenomics analysis (e.g. Weyrich et al. 2017) can be very useful to detect plant consumption and complement isotopic dietary information in this regard.

From an environmental point of view, $\delta^{13}\text{C}$ could reflect many features about plant physiology (Seibt et al. 2008). The range of $\delta^{13}\text{C}$ values in plants is mainly related to the CO_2 catchment efficiency from the atmosphere, which depends on many environmental factors such as luminosity, water availability and temperature (O'Leary 1981; Tieszen 1991). This $\delta^{13}\text{C}$ variability is not only recorded in plants, as it is introduced also in higher trophic levels through their consumption, and plays an important role in the study of shepherding and livestock management (Tornero et al. 2016a). Plants also take organic nitrogen from the soil, resulting in their $\delta^{15}\text{N}$ values showing variations depending on natural or anthropic factors which affect the soil-plant system (Szpak 2014). Among the natural factors, the presence of organic material in the soil, temperature and water availability could be the most significant ones (Ambrose 1991; Handley et al. 1999). Otherwise, human ecosystem modifications like the use of fertilisers may also modify the expected $\delta^{15}\text{N}$ along the food web (Bogaard et al. 2007). All these features can be tested in bone collagen values (Drucker et al. 2003; Goude and Fontugne 2016;

Heaton et al. 1986) and help us know more about past environmental conditions.

Archaeological context from the studied sites

Cova de la Guineu

Cova de la Guineu is a sepulchral cave located in the village of Font-rubí (Alt Penedès, Barcelona) (X. 377972; Y. 4664374, UTM31N, WGS84) at 738 m above sea level (m.a.s.l.) (Fig. 1). The site was discovered by the Associació d'Estudis Científics i Culturals de Mediona (AECCM) in the seventies, but the first archaeological intervention was conducted by Josep Mestres in 1983. Nowadays, the cave continues being excavated by Xavier Oms and Artur Cebrià (Oms et al. 2016a; Oms et al. 2016b). The excavation process verified the use of the cavity since the Epipalaeolithic and up to the Bronze Age (11–4 ka BP). The burial use of the cave took place during the 4th and second half of the 3rd millennium cal B.C. (Fig. 2, Table 1), working as a paradolmenic structure (Oms et al. 2016a).

The archaeological materials and grave goods recovered from the sepulchral levels help to prove a continuous funerary use during time: (1) the oldest phase dates from the Late Neolithic, represented by discoidal bone and seashell beads, and V-perforated buttons typical from the end of the 4th millennium cal. BC (Alday 1995); (2) a second phase is represented with the presence of a specific and regional Bell-Beaker pottery called Salomó (Harrison 1974) and a large set of lithic industry based on long flint blades and arrows, corresponding with the Chalcolithic period at the first half of the 3rd millennium; and (3) a third phase with some fragments of carinated pottery, typical from the beginning of the Bronze Age (Oms et al. 2016a). Only one metallic tool was found outside the cave (Oms et al. 2016a). Most of the human remains were found commingled and disarticulated as a result of accumulative primary and secondary burials and clandestine

activities. The first anthropological study gave an MNI (Minimal Number of Individuals) of 30 (Mercadal and Campillo 1995), but human remains recovered from the cave continue being studied by S. Mendiola. The faunal remains are largely present in the sepulchral level and many of these are burned and show cut marks. They were interpreted as food-offerings (Oms et al. 2016a).

Cueva de Abauntz

Cueva de Abauntz is another sepulchral cave located in the village of Arraitz (Navarra) (X. 610735; Y. 4763270, UTM30N, WGS84) at 610 m.a.s.l. (Fig. 3). The cave was excavated by Pilar Utrilla and Carlos Mazo over ten campaigns (Utrilla et al. 2015). In this case, the use of the cave dates back to the Middle Palaeolithic, with the presence of Mousterian tools and a large amount of macrofauna remains (Altuna et al. 2002), and arrives up to the Late Roman Period when the cavity was used as a hiding place for coins and metallic tools (Utrilla et al. 2014a). During the Late Neolithic-Chalcolithic, the cavity was used as a burial space where the human corpses were accumulated inside individually. The MNI of the three later campaigns was of 108, calculated with dental elements (Utrilla et al. 2014b). The preference type of burial was the simple inhumation, but there were also pit and cist burials inside the cave (Utrilla et al. 2007). Some of the human remains were burned, the same as happens in other nearby burial cave sites (Fernández-Crespo 2016) probably as corpse treatment (Utrilla et al. 2015). The high number of radiocarbon dates performed shows the use of the cavity as a burial enclosure during one millennia, from the 4th to the 3rd millennium cal B.C. (Fig. 2, Table 1). All the archaeological materials recovered at the site from this period are basically grave goods, with a predominance of bone industry composed by awls and spatulas (more present in pit burials), and pedunculated and leaf-shaped points, necklace beads and pendants made from the teeth of wild boar.

Fig. 1 Location map. **a** Location of the Iberian Peninsula inside Western Europe. **b** Map of the northeast of the Iberian Peninsula, the star shows the location of Cova de la Guineu. **c** Topography of Cova de la Guineu with plan and profile views

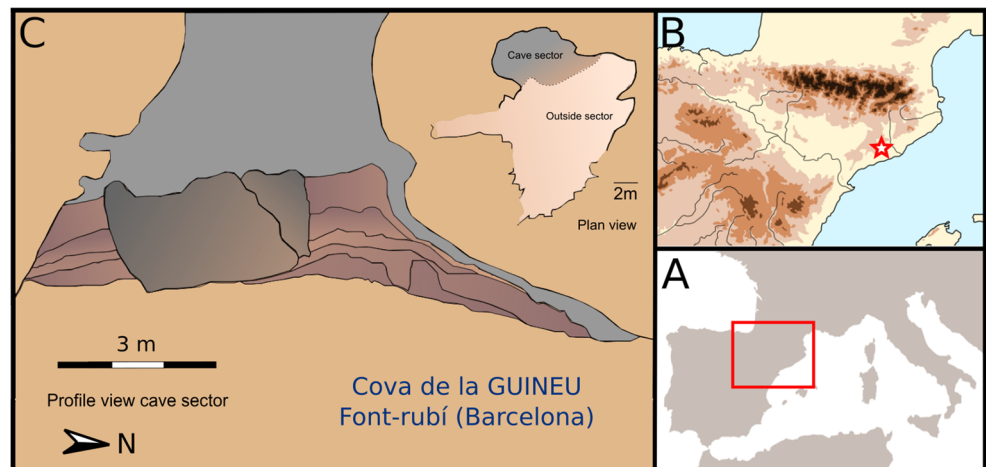
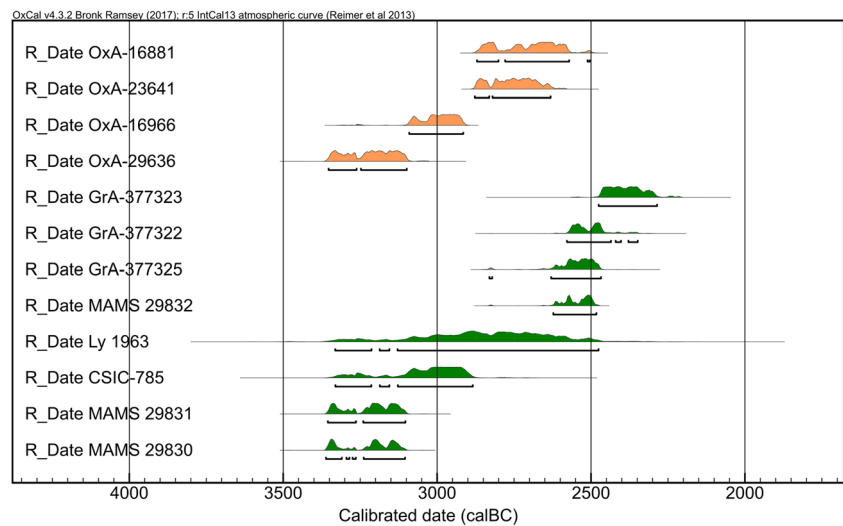


Fig. 2 AMS radiocarbon dates from Cova de la Guineu (in orange) and Cueva de Abauntz (in green) sepulchral levels. All dates have been calibrated with OxCal v4.2.3 and using the IntCal13 calibration curve (Bronk Ramsey 2009; Reimer et al. 2013)



Metallic tools are not very common, but they were present (Utrilla et al. 2007).

Materials and methods

Human and faunal remains

The sampling strategy was different for each archaeological site. It was adapted to the characteristics of the site and the availability of sampling material, with the aim to obtain the maximum information from the remains. The possibility of carrying out one diachronic study in both sites was impossible due to all the human remains appeared commingled and disarticulated, not having enough economic resources to

radiocarbon date all the individuals. However, the dates obtained give an approximated timeframe for the burials.

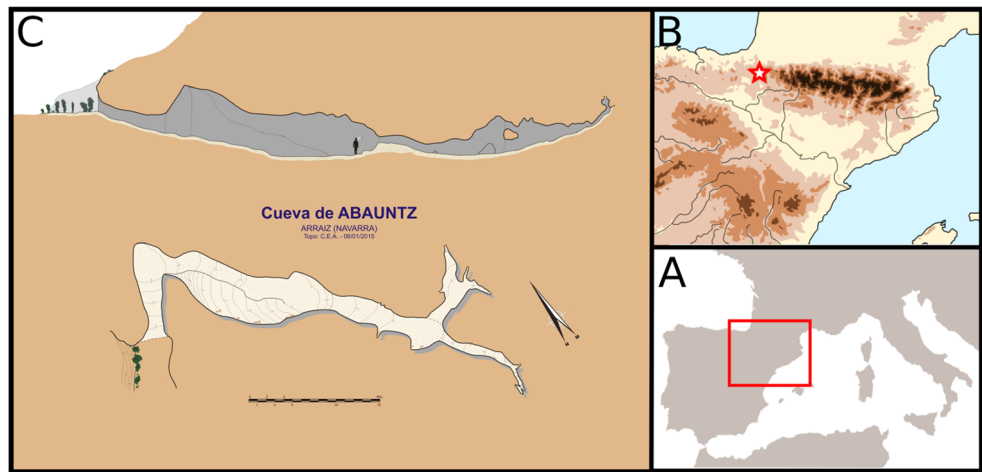
Cova de la Guineu

The anthropological report of Cova de la Guineu indicated that the talus was the most abundant bone among the human remains. However, this element was not chosen for the study because of its large spongy portion that could reflect a short-time diet closer to life's end (Cox and Sealy 1997). The next skeletal element with a higher frequency among the available remains was the humerus, which has an overall good preservation and helps to distinguish age groups. Therefore this skeletal element was chosen one for sampling. Specifically, the part of the humerus that showed more repetitions was the left olecranean fossa, with a completed or fragmented distal

Table 1 AMS radiocarbon dates from the Sepulchral Late Neolithic-Chalcolithic levels of Cova de la Guineu and Cueva de Abauntz, calibrated with OxCal v4.2.3 using the IntCal13 calibration curve (Bronk Ramsey 2009; Reimer et al. 2013)

Lab code	Sample	^{14}C age	2σ Cal BC	Site	Reference
OxA-29636	Human bone (phalanx)	4513 ± 30	3353–3099	Cova de la Guineu	This study
OxA-16966	Human bone (ulna)	4385 ± 32	3091–2916	Cova de la Guineu	Oms et al. 2016a
OxA-23641	Charcoal (<i>Quercus</i> sp.)	4156 ± 28	2878–2632	Cova de la Guineu	Oms et al. 2016a
OxA-16881	Human bone (patella)	4110 ± 38	2871–2505	Cova de la Guineu	Oms et al. 2016a
MAMS 29830	Human bone (mandible)	4534 ± 24	3362–3105	Cueva de Abauntz	This study
MAMS 29831	Human bone (mandible)	4523 ± 24	3356–3104	Cueva de Abauntz	This study
CSIC-785	Human bone (no specification)	4370 ± 70	3331–2885	Cueva de Abauntz	Utrilla et al. 2007
Ly-1963	Charcoal	4240 ± 140	3332–2476	Cueva de Abauntz	Utrilla et al. 2007
MAMS 29832	Human bone (mandible)	4040 ± 23	2622–2484	Cueva de Abauntz	This study
GrA-377325	Human bone (no specification)	4025 ± 35	2831–2468	Cueva de Abauntz	Utrilla et al. 2007
GrA-377322	Human bone (no specification)	3975 ± 35	2579–2349	Cueva de Abauntz	Utrilla et al. 2007
GrA-377323	Human bone (no specification)	3900 ± 35	2476–2286	Cueva de Abauntz	Utrilla et al. 2007

Fig. 3 Location map. **a** Location of the Iberian Peninsula inside Western Europe. **b** Map of the northeast of the Iberian Peninsula, the star shows the location of Cueva de Abauntz. **c** Topography of Cueva de Abauntz with plan and profile views



epiphysis. Thirty-nine human left olecranean fossas were sampled: 18 classified as *adult* (when the epiphysis is fused), nine as *possible adult* (when only the fossa is present but the dimensions are the same as samples defined as adult), nine as *subadult* (when the epiphysis is unfused) and three as *possible subadult* (when the dimensions are equivalent to subadult samples but the epiphysis is absent). One phalanx was sampled in only one individual found in primary position to avoid the destruction of other skeletal elements (Table 2). The impossibility of associating humerus with other skeletal elements of a same individual makes impossible the sex-determination nor accurate age estimation of the individuals.

Cova de la Guineu faunal samples were taken from all species present: five rabbits (*Oryctolagus cuniculus*), two deer (*Cervus elaphus*), six domestic ovicaprids (*Ovis aries/Capra hircus*), two suids (*Sus domesticus*), one horse (*Equus ferus*) and one mustelid (genus unknown). Animal samples came from the funerary archaeological level but were not able to be selected based on a minimum number of individuals (MNI). Even so, we tried to select the same skeletal elements with a farther location to each other inside the cave whenever was possible. All the animal samples were adults, except for one pig sample (S-UCT 19023) (Table 2).

Cueva de Abauntz

Cueva de Abauntz presents many human remains burned. The bones with clear signs of thermic alteration were discarded for sampling. Besides this limitation, we must also acknowledge that long bones were highly fragmented and made it difficult to get an accurate MNI with them. Of the remaining available skeletal material, mandibles were the most appropriate element to be assured that no the same individual was sampled twice; and they also presented a good preservation. The number of mandibles was large enough to have a representative sample of the individuals buried at the site. Moreover, they are a suitable skeletal element for retrieving information about

age, which is very important in isotopic studies where $\delta^{13}\text{C}$ and $\delta^{15}\text{N}$ are physiologically and age related (Beaumont et al. 2013). In this case, adults and subadults were distinguished more accurately according to bone dimensions and the presence of deciduous dentition (Ubelaker 1989). Finally, human samples consist of 40 mandibles divided in three biological age groups according to Buikstra and Ubelaker (1994): eight *child* (second permanent molar erupted; \approx up to 12 years), four *adolescent* (third permanent molar in the process of eruption; \approx up to 18 years) and 28 *adult* (full permanent dentition; $>$ 18 years) (Table 3). The impossibility of associating mandibles with other skeletal elements more useful for sex determination (Buikstra and Ubelaker 1994) has lead us to be cautious and avoid using sex-categories to discuss the isotopic data.

Cueva de Abauntz faunal samples consist of two cattle (*Bos taurus*), six ovicaprids (*Ovis aries/Capra hircus*), four suids (*Sus domesticus*), two felids (*Felis* sp.) and one horse (*Equus ferus*). Animal samples were not selected based on MNI because of the scarcity of remains. Even so, we tried to select animal samples that were located far away from each other inside the cave. These faunal remains appeared commingled with the human remains, assuming a common stratigraphical level. Some faunal remains showed thermic alterations, which suggest they are from the same time period as the human remains. All the faunal samples were adults, except for one pig (S-UCT 19090), one ovicaprid (S-UCT 19083) and the horse (S-UCT 19094) (Table 3).

Collagen extraction and $\delta^{13}\text{C}$ and $\delta^{15}\text{N}$ analysis

Sample preparation and analysis were carried out at the isotope dedicated facilities of the University of Cape Town (South Africa), as described below.

Before the analysis, visible contaminants were removed by abrasion using a Dremmel 3500 drill with a diamond grinder bit attached. Collagen extraction for carbon ($\delta^{13}\text{C}$) and nitrogen ($\delta^{15}\text{N}$) isotope analysis was extracted following the

Table 2 Cova de la Guineu stable isotope ratio results, including S-UCT code, species, sampled bone, biological age group [P. adult: possible adult; P. subadult: possible subadult], %Collagen (> 30 kDa fraction), $\delta^{13}\text{C}$, $\delta^{15}\text{N}$ and collagen quality indicator (%C, %N, C:N elemental) average values

S-UCT code	Archaeological ID	Species	Sampled bone	Age Group	Collagen (%) (> 30 kDa fraction)	$\delta^{13}\text{C}$ (‰)	$\delta^{15}\text{N}$ (‰)	% C	% N	C:N (elemental)
18979	Gn.RX.293	Human	Humerus	Subadult	4.73	-19.0	7.8	41.5	15.4	3.1
18981	Gn.M.323	Human	Humerus	Subadult	8.70	-19.4	6.4	43.1	15.5	3.2
19027	Gn'1331.VII.Ia(b) C11.366F	Human	Phalanx	Subadult	8.43	-18.6	9.5	40.7	14.8	3.2
18977	Gn.M.327	Human	Humerus	Subadult	5.27	-18.9	8.8	41.5	15.5	3.1
18980	Gn.M.321	Human	Humerus	Subadult	4.48	-18.9	7.4	41.6	15.3	3.2
18990	Gn.Rx.396	Human	Humerus	Subadult	0.92	-19.5	8.1	41.5	14.5	3.3
18999	Gn.Rx.12157	Human	Humerus	Subadult	1.64	-19.4	8.3	41.7	15.1	3.2
19000	Gn.Rx.13291	Human	Humerus	Subadult	2.82	-19.3	8.6	33.2	11.9	3.2
19005	Gn. Rx. 17370	Human	Humerus	Subadult	1.68	-19.1	8.3	28.3	10.0	3.3
18988	Gn.M.335	Human	Humerus	P. subadult	3.05	-19.2	9.0	37.7	13.5	3.3
19003	Gn.Rx. 13311	Human	Humerus	P. subadult	0.83	-19.9	8.4	41.2	14.5	3.3
19006	Gn.Rx.17371	Human	Humerus	P. subadult	1.50	-19.5	7.4	36.2	12.4	3.4
18972	E5.11	Human	Humerus	P. adult	4.01	-19.6	8.7	42.5	15.4	3.2
18974	Gn.Rx.99	Human	Humerus	P. adult	0.67	-19.8	9.4	33.2	10.8	3.6
18975	Gn.M.324	Human	Humerus	P. adult	3.99	-19.4	8.5	41.7	14.7	3.3
18986	Gn.M.333	Human	Humerus	P. adult	1.40	-19.2	9.4	41.9	14.4	3.4
18989	Gn.M.338	Human	Humerus	P. adult	6.38	-19.5	8.6	38.9	14.0	3.2
18991	Gn.Rx.401	Human	Humerus	P. adult	1.44	-19.7	8.8	30.9	10.8	3.4
18993	Gn.Rx.7838	Human	Humerus	P. adult	1.47	-19.2	9.5	35.8	12.7	3.3
18995	Gn.RX.7847	Human	Humerus	P. adult	2.44	-19.3	10.1	38.4	13.7	3.3
18996	Gn.RX.7849	Human	Humerus	P. adult	4.83	-19.1	8.2	42.0	15.6	3.1
18973	Gn.Rx.10	Human	Humerus	Adult	0.86	-19.8	9.5	38.3	12.8	3.5
18976	Gn.M.326	Human	Humerus	Adult	2.12	-19.3	9.0	36.9	13.0	3.3
18978	Gn.M.328	Human	Humerus	Adult	1.24	-19.2	9.2	43.4	15.3	3.3
18982	Gn.M.329	Human	Humerus	Adult	4.66	-19.4	9.2	42.9	15.4	3.2
18983	Gn.Rx.330	Human	Humerus	Adult	2.03	-19.4	8.4	36.2	12.7	3.3
18984	Gn.M.331	Human	Humerus	Adult	5.76	-18.8	9.0	40.2	14.3	3.3
18985	Gn.M.332	Human	Humerus	Adult	2.67	-19.3	8.7	39.5	13.8	3.3
18987	Gn.M.334	Human	Humerus	Adult	0.39	-19.5	9.1	28.0	9.4	3.5
18992	Gn.Rx.1286	Human	Humerus	Adult	1.20	-19.4	8.5	37.3	13.0	3.4
18994	Gn.RX.7841	Human	Humerus	Adult	1.98	-19.1	9.3	39.1	14.1	3.2
18997	Gn.RX.7853	Human	Humerus	Adult	1.70	-19.3	8.2	39.3	14.2	3.2
18998	Gn.RX.12156	Human	Humerus	Adult	0.70	-19.3	8.8	25.7	9.2	3.3
19001	Gn.Rx. 13294	Human	Humerus	Adult	3.27	-19.3	8.7	39.9	14.4	3.2
19002	Gn.RX.13309	Human	Humerus	Adult	3.01	-19.4	9.9	39.9	14.3	3.3
19004	Gn.RX.17368	Human	Humerus	Adult	1.21	-19.4	8.7	39.4	13.3	3.4
19007	Gn.Rx.17836	Human	Humerus	Adult	2.84	-19.3	8.6	41.9	14.8	3.3
19008	Gn.RX.7844	Human	Humerus	Adult	5.01	-19.5	9.9	41.7	14.9	3.3
19009	17842	Human	Humerus	Adult	0.79	-19.2	9.0	37.7	13.0	3.4
19010	Gn/E3/1047	<i>Oryctolagus cuniculus</i>	Diaphysis	Adult	2.79	-21.1	2.3	41.8	15.0	3.3
19011	Gn/E3/1046	<i>Oryctolagus cuniculus</i>	Vertebra	Adult	2.50	-20.5	3.7	41.1	14.9	3.2
19012	Gn/E3/589	<i>Oryctolagus cuniculus</i>	Maxilla	Adult	1.73	-20.9	4.9	40.3	13.5	3.5
19013	Gn/E3/1039	<i>Oryctolagus cuniculus</i>	Maxilla	Adult	2.66	-20.3	2.6	42.5	14.8	3.3
19014	Gn/E3/795	<i>Oryctolagus cuniculus</i>	Mandible	Adult	0.83	-20.8	2.6	33.1	11.8	3.3
19015	Gn/D3/47	<i>Ovis aries/Capra hircus</i>	Tibia	Adult	1.02	-20.4	4.4	38.6	13.7	3.3
19016	GN/E2/175B	<i>Ovis aries/Capra hircus</i>	Scapula	Adult	0.12	-19.4	4.3	39.7	14.0	3.3

Table 2 (continued)

S-UCT code	Archaeological ID	Species	Sampled bone	Age Group	Collagen (%) (> 30 kDa fraction)	$\delta^{13}\text{C}$ (‰)	$\delta^{15}\text{N}$ (‰)	% C	% N	C:N (elemental)
19017	Gn/D1/272	<i>Ovis aries/Capra hircus</i>	Humerus	Adult	3.74	-20.1	4.2	41.5	14.7	3.3
19018	Gn/D1/862	<i>Ovis aries/Capra hircus</i>	Cranial fragment	Adult	8.93	-19.7	4.1	42.1	15.3	3.2
19019	Gn/D1/461a	<i>Ovis aries/Capra hircus</i>	Vertebra	Adult	4.46	-19.7	6.4	42.6	15.4	3.2
19020	Gn/D1/906	<i>Ovis aries/Capra hircus</i>	Phalanx	Adult	5.89	-20.4	4.3	43.3	15.6	3.2
19021	Gn/D1/532	<i>Cervus elaphus</i>	Metapodia	Adult	2.30	-19.7	3.7	41.7	15.1	3.2
19022	Gn/D1/842	<i>Cervus elaphus</i>	Maxilla	Adult	2.27	-19.9	3.8	41.3	14.9	3.2
19023	Gn/D3/832	<i>Sus domesticus</i>	Mandible	Subadult	1.64	-19.5	5.8	37.4	13.0	3.4
19024	Gn/D1/859	<i>Sus domesticus</i>	Mandible	Adult	3.98	-19.3	5.5	43.2	15.5	3.2
19025	Gn/D3/845	<i>Equus ferus</i>	Phalanx	Adult	1.20	-20.8	2.6	33.6	11.8	3.3
19026	Gn/D1/568	<i>Mustelidae</i>	Mandible	Adult	3.96	-18.5	8.2	42.3	14.8	3.3

Longin (1971) method with the addition of an ultrafiltration step (Brown et al. 1988). Approximately 300 mg of chunk bone samples from each specimen were demineralised in 0.5 M HCl solution at 5 °C until fully demineralisation (over the course of a week in most cases). When demineralisation finished, samples were rinsed three times with deionised water until pH became neutral and then started the gelatinisation at 70 °C during 48 h using a heater block (FMH instruments, South Africa). The solutions were filtered with a 5-mm EZEE-filter (Elkay, United Kingdom) and ultrafiltered with 30 kDa ultrafilters previously cleaned with 0.5 M NaOH (Amicon, Germany) using a centrifuge (Thermo Fisher Scientific Megafuge 16, USA) at 2500 rpm during variable times depending on the filtering speed of each sample. After that, solutions were frozen and lyophilised. Finally, duplicate ca. 0.5 mg of collagen per sample was microweighed into tin capsules and loaded into the mass spectrometers.

The carbon and nitrogen isotope ratio measurements were performed using a Finnigan Delta plus XP continuous-flow isotope ratio mass spectrometer (Thermo Fisher Scientific, USA) after being combusted in an elemental analyser Flash EA 1112 interfaced with it (Thermo Fisher Scientific, USA). Stable carbon isotope values were calibrated and expressed relative to the reference V-PDB scale (Vienna PeeDee Belemnite), and stable nitrogen isotope values were calibrated and expressed relative to the reference AIR scale (atmospheric N_2), using the delta notation (δ) in parts per thousand (‰). The accuracy of measurements was monitored using international and in-house standards with well-known isotopic composition (MG: $\delta^{13}\text{C}$ 21.3 ± 0.3 , $\delta^{15}\text{N}$ 7.3 ± 0.1 ‰; seal: $\delta^{13}\text{C}$ 12.7 ± 0.1 ‰; $\delta^{15}\text{N}$ 15.6 ± 0.1 ‰; valine: $\delta^{13}\text{C}$ 27.7 ± 0.1 ‰; $\delta^{15}\text{N}$ 15.6 ± 0.1 ‰). Precision was determined with the repeated measurements of standards and sample replicates, determined an average analytical error below than 0.1‰ (1 σ) for $\delta^{13}\text{C}$ and $\delta^{15}\text{N}$ in standards and in sample replicates. All the samples were measured in duplicate. Samples which showed

bad quality of collagen according to Ambrose (1993), DeNiro (1985) and Van Klinken (1999) parameters were not considered for interpretation of the results.

Results

The results from both sepulchral caves are presented in Figs. 4 and 5, as well as in Tables 2 and 3. The results of the different sites are shown in different sections but are compared together at the end.

Cova de la Guineu $\delta^{13}\text{C}$ and $\delta^{15}\text{N}$ results

Bone samples from 39 humans and 17 fauna were analysed from Cova de la Guineu. The $\delta^{13}\text{C}$ and $\delta^{15}\text{N}$ results are presented in Table 2 and plotted in Fig. 4. Only one sample from Cova de la Guineu (S-UCT 19016, ovicaprid) did not yield enough collagen at the > 30 kDa fraction to run the analysis in duplicate. However, for all samples (including the latter mentioned) the %C, %N and C:N elemental ratio values indicate a good collagen quality according to Ambrose (1993), DeNiro (1985) and Van Klinken (1999). As we use ultrafiltration, we have not considered the 1% of collagen as a quality control when all other indicators were acceptable.

Herbivore $\delta^{13}\text{C}$ values range between -21.1‰ and -19.4‰, with a mean value of -20.3 ± 0.5 [1 σ]‰ ($n = 14$). These $\delta^{13}\text{C}$ values are consistent with typical values for a terrestrial C_3 European ecosystem (DeNiro and Epstein 1978; Schwarcz and Schoeniger 1991). Leporids, together with the horse value, show ^{13}C -depleted values the same as happen in other studies (Villalba-Mouco et al. 2017), and wild herbivores (*Cervus elaphus*) ($\delta^{13}\text{C} = 19.8 \pm 0.2$ ‰) are enclosed inside the $\delta^{13}\text{C}$ domestic herbivore range (*Ovis aries/Capra hircus*) ($\delta^{13}\text{C} = 19.9 \pm 0.4$ ‰), showing no difference between them. Herbivore $\delta^{15}\text{N}$ values range between

Table 3 Cueva de Abautz stable isotope ratio results, including S-UCT code, species, sampled bone, biological age group, %Collagen (> 30 kDa fraction), $\delta^{13}\text{C}$ and $\delta^{15}\text{N}$ average values, collagen control indicators (%C, %N, C:N elemental) and radiocarbon dates

S-UCT code	Archaeological ID	Species	Sampled bone	Age group	Collagen (%) (> 30 kDa fraction)	$\delta^{13}\text{C}$ (‰)	$\delta^{15}\text{N}$ (‰)	%C	%N	C: N (elemental)
19064	Ab.4F.139.1	Human	Mandible	Child	3.45	-20.2	8.9	39.8	14.4	3.2
19063	Ab.27D.342.155	Human	Mandible	Child	5.71	-20.5	9.0	44.1	15.6	3.3
19058	Ab.2F.95.2	Human	Mandible	Child	7.22	-20.5	9.0	44.1	15.6	3.3
19056	Ab.3D.142.2.68	Human	Mandible	Child	2.76	-20.0	8.3	43.7	15.3	3.3
19067	Ab.5C.b1b2.159	Human	Mandible	Child	3.72	-20.3	9.1	43.0	15.6	3.2
19059	Ab.1D.146.11	Human	Mandible	Child	2.05	-19.3	9.8	40.4	14.7	3.2
19060	Ab.3D.142.2.67	Human	Mandible	Child	4.81	-20.0	9.7	41.6	15.1	3.2
19062	Ab.27-33.100?	Human	Mandible	Child	4.46	-20.0	8.5	42.9	15.7	3.2
19057	Ab.35E.401.6	Human	Mandible	Adolescent	2.57	-20.7	7.9	39.5	14.2	3.3
19061	Ab.9C.230.860	Human	Mandible	Adolescent	4.78	-20.6	9.3	43.4	15.0	3.4
19065	Ab.3C.161.19.134	Human	Mandible	Adolescent	2.40	-20.8	8.9	41.3	14.7	3.4
19066	Ab.7A.146.295	Human	Mandible	Adolescent	2.80	-20.4	8.3	40.8	14.5	3.2
19033	Ab.29F.rev.2	Human	Mandible	Adult	3.17	-20.3	8.8	39.8	14.6	3.2
19038	Ab.25D.371.746	Human	Mandible	Adult	1.74	-20.5	9.5	37.6	13.5	3.2
19039	Ab.23D.421.221	Human	Mandible	Adult	4.26	-19.8	9.0	40.8	15.3	3.1
19041	Ab. 23D/F.rev.	Human	Mandible	Adult	5.68	-20.2	8.2	42.8	15.7	3.2
19042	Ab.2C.64.42	Human	Mandible	Adult	2.79	-20.1	9.1	39.9	14.6	3.2
19045	Ab.rev(35)439	Human	Mandible	Adult	2.83	-20.2	8.8	40.8	14.7	3.2
19047	Ab.4B.100.638	Human	Mandible	Adult	2.96	-20.5	9.1	41.1	14.7	3.3
19049	Ab.29F.b1.2	Human	Mandible	Adult	5.28	-20.1	8.8	42.9	15.6	3.2
19051	Ab.25D.nivel I. X:375	Human	Mandible	Adult	4.40	-20.3	9.5	43.5	15.8	3.2
19055	Ab.25D.nivel I.430-431	Human	Mandible	Adult	4.96	-20.1	8.4	43.1	15.5	3.2
19028	Ab.25D.371.768	Human	Mandible	Adult	2.37	-20.1	9.0	38.1	13.7	3.2
19029	Ab.21D.360.7	Human	Mandible	Adult	4.75	-19.3	11.3	41.7	15.1	3.2
19034	Ab.rev(35).146	Human	Mandible	Adult	2.30	-19.6	9.2	41.0	15.3	3.1
19035	Ab.rev(35).672	Human	Mandible	Adult	2.89	-20.1	9.1	39.7	14.7	3.1
19036	Ab.rev(35).619	Human	Mandible	Adult	5.55	-20.1	9.0	42.2	15.7	3.1
19037	Ab.27-33.109	Human	Mandible	Adult	3.08	-20.2	8.2	41.7	15.5	3.1
19053	Ab.19E.364.2	Human	Mandible	Adult	2.38	-19.9	8.8	38.6	13.7	3.3
19030	Ab.1A.169.169	Human	Mandible	Adult	6.32	-20.8	9.3	42.5	15.2	3.3
19040	Ab.27-33.108	Human	Mandible	Adult	4.52	-19.9	9.0	41.2	15.3	3.1
19044	Ab.25C.nivel I.x: 375 (17)	Human	Mandible	Adult	2.80	-20.2	8.6	41.0	14.8	3.2
19048	Ab.21D.360.8	Human	Mandible	Adult	4.09	-20.4	9.7	41.2	14.8	3.3
19046	Ab.rev(35).126	Human	Mandible	Adult	2.36	-20.3	9.0	38.8	14.0	3.2
19031	Ab.27C.r.50	Human	Mandible	Adult	5.06	-20.3	8.8	41.2	14.8	3.3
19043	Ab.25D.r.845	Human	Mandible	Adult	3.05	-20.4	9.5	38.0	14.0	3.2
19054	Ab.23D/E.rev.181	Human	Mandible	Adult	2.96	-19.9	9.4	40.5	14.5	3.3
19032	Ab.23r.421.219	Human	Mandible	Adult	5.72	-20.3	9.2	42.8	15.6	3.2
19050	Ab.35E.430.138	Human	Mandible	Adult	2.61	-20.0	9.2	41.2	14.8	3.2
19052	Ab.25E.rev.51	Human	Mandible	Adult	3.69	-19.7	9.6	41.4	19.7	3.3
19074	Ab.27-33E/F.389	<i>Bos taurus</i>	Tibia	Subadult	4.86	-22.1	4.6	40.4	14.7	3.2
19075	Ab.35E.430.173	<i>Bos taurus</i>	Talus	Adult	6.29	-21.6	4.3	42.5	15.7	3.2
19084	Ab.27-33EF.203-215	<i>Ovis aries/Capra hircus</i>	Phalanx	Adult	1.30	-22.5	3.8	37.8	13.2	3.3
19079	Ab.11D.rev.144	<i>Ovis aries/Capra hircus</i>	Talus	Adult	3.56	-20.9	3.3	42.2	15.6	3.2
19080	Ab.3C.rev.43	<i>Ovis aries/Capra hircus</i>	Talus	Adult	1.69	-21.2	4.6	41.6	15.2	3.2
19082	Ab.7B.rev.11	<i>Ovis aries/Capra hircus</i>	Mandible	Adult	2.09	-20.6	3.6	40.4	14.7	3.2

Table 3 (continued)

S-UCT code	Archaeological ID	Species	Sampled bone	Age group	Collagen (%) (> 30 kDa fraction)	$\delta^{13}\text{C}$ (‰)	$\delta^{15}\text{N}$ (‰)	%C	%N	C: N (elemental)
19083	Ab.3C.rev.31	<i>Ovis aries/Capra hircus</i>	Tibia	Subadult	4.32	-21.0	5.1	41.8	15.6	3.1
19092	Ab.25C.rev.127	<i>Ovis aries/Capra hircus</i>	Femur	Adult	1.75	-21.4	4.4	35.8	12.7	3.3
19086	Ab.4F.139.7	<i>Sus domesticus</i>	Ulna	Adult	1.21	-20.7	4.1	42.0	14.4	3.4
19087	Ab.7BCD.rev.68	<i>Sus domesticus</i>	Maxilla	Adult	3.23	-21.1	5.8	39.7	13.8	3.3
19089	Ab.5D.196.13a78	<i>Sus domesticus</i>	Phalanx	Adult	4.57	-20.1	9.4	42.3	15.5	3.2
19090	Ab.5D.196.13a78	<i>Sus domesticus</i>	Maxilla	Subadult	7.72	-20.6	6.3	40.7	14.5	3.3
19094	Ab.5C.300.38	<i>Equus ferus</i>	Metapodia	Subadult	7.82	-21.5	4.9	42.3	15.3	3.2
19076	Ab.3C5C.rev.34	<i>Felis</i> sp.	Radius	Adult	4.63	-19.0	7.8	42.2	15.4	3.2
19091	Ab.3C.rev.32	<i>Felis</i> sp.	Vertebra	Adult	5.77	-18.8	6.6	42.3	15.4	3.2

2.3‰ and 6.4‰, with a mean value of $3.9 \pm 1.1 [1\sigma]\%$, defining the trophic baseline of the ecosystem food web for the region at the time. The lowest $\delta^{15}\text{N}$ value belongs to a horse and the highest to an ovicaprid. Most of the $\delta^{15}\text{N}$ domestic herbivore values (*Ovis aries/Capra hircus*) show similar $\delta^{15}\text{N}$ values to the wild ones (*Cervus elaphus*) except for one sample whose $\delta^{15}\text{N}$ value is higher (S-UCT 19019, $\delta^{15}\text{N} = 6.4$).

There are only two omnivores, whose $\delta^{13}\text{C}$ values are -19.5‰ and -19.3‰, with a mean value of $-19.4 \pm 0.2 [1\sigma]\%$ ($n = 2$). Their $\delta^{15}\text{N}$ values are 5.8‰ and 5.5‰ with a mean value of $5.7 \pm 0.2 [1\sigma]\%$. The difference between $\delta^{15}\text{N}$ herbivores and $\delta^{15}\text{N}$ omnivores values is not as high as a complete trophic level change (1.8‰) (Bocherens and Drucker 2003). The singular carnivore datum from a mustellidae shows a $\delta^{13}\text{C}$ value of -18.5‰ and a $\delta^{15}\text{N}$ value

of 8.2‰, showing also a C_3 terrestrial environment and placing it in a higher trophic level (4.3‰ higher than herbivores and 3.2‰ higher than omnivores).

The human $\delta^{13}\text{C}$ values range between -19.9‰ and -18.6‰, with a mean value of $-19.3 \pm 0.3 [1\sigma]\%$ ($n = 39$). Human $\delta^{15}\text{N}$ values range between 7.4‰ and 9.9‰, with a mean value of $8.8 \pm 0.7 [1\sigma]\%$. Humans are in a higher trophic level than herbivores ($\delta^{15}\text{N}$ 4.9‰ higher) and even omnivores ($\delta^{15}\text{N}$ 3.1‰ higher). The single carnivore value is in the same trophic level as humans (Fig. 4). A non-parametric statistical test (Mann-Whitney) reveals that isotopic $\delta^{13}\text{C}$ values do not differ between age groups (adult and subadult, $\delta^{13}\text{C}$ $p = 0.142$). However, the same test shows a difference in $\delta^{15}\text{N}$ between these two groups that is statistically significant ($\delta^{15}\text{N}$ $p = 0.007$), showing lower $\delta^{15}\text{N}$ values in the subadult

Fig. 4 Scatter plot of human and fauna bone collagen $\delta^{13}\text{C}$ and $\delta^{15}\text{N}$ values from Cova de la Guineu

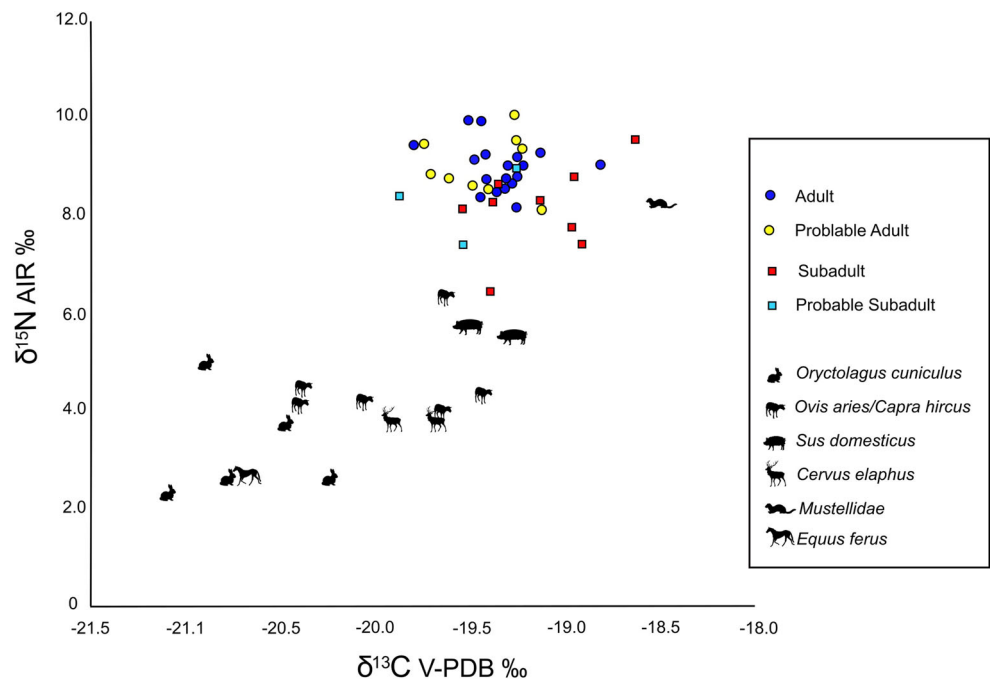
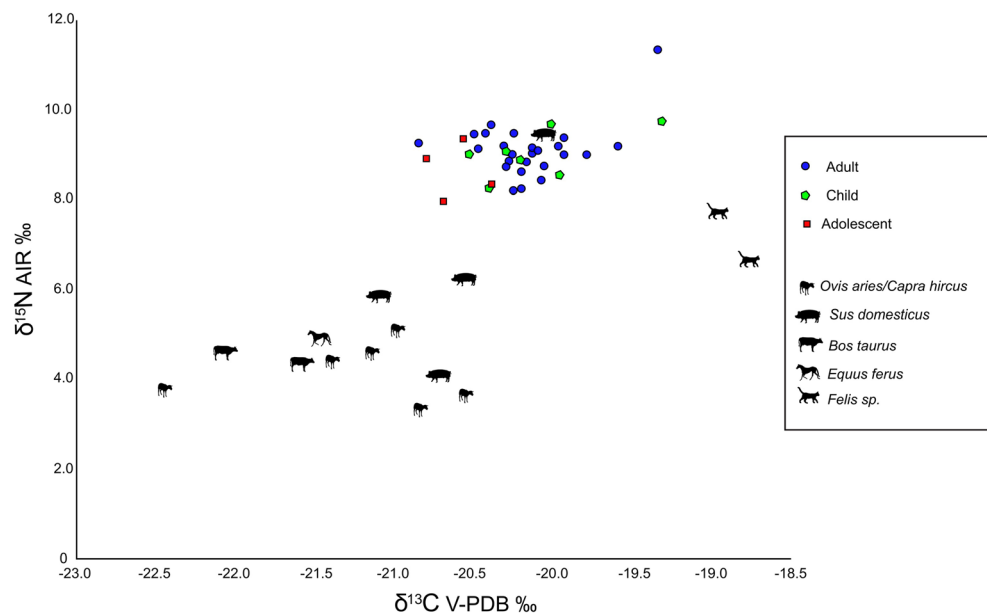


Fig. 5 Scatter plot of human and fauna bone collagen $\delta^{13}\text{C}$ and $\delta^{15}\text{N}$ values from Cova de Abauntz



group. Possible adult and possible subadult categories were ruled out of this statistical test.

Cueva de Abauntz $\delta^{13}\text{C}$ and $\delta^{15}\text{N}$ results

Bone samples from 40 humans and 15 animals were analysed from Cueva de Abauntz. The $\delta^{13}\text{C}$ and $\delta^{15}\text{N}$ results are presented in Table 3 and plotted in Fig. 5. All the samples yielded enough collagen at the $>30\text{-kDa}$ fraction for analysis in duplicate, but three duplicates were ruled out because they did not show a good collagen C:N elemental ratio (DeNiro 1985). All the other runs show good collagen quality parameters (%C, %N and C:N elemental ratio) according to Ambrose (1993), DeNiro (1985) and Van Klinken (1999). Herbivore $\delta^{13}\text{C}$ values range between -22.5 and -20.6‰ with a mean value of $-21.4 \pm 0.6 [1\sigma]\text{‰}$ ($n=9$). These $\delta^{13}\text{C}$ values are consistent with typical values for a terrestrial C_3 European ecosystem (DeNiro and Epstein 1978; Schwarcz and Schoeniger 1991). Herbivore $\delta^{15}\text{N}$ values range between 3.3 and 5.1‰ with a mean value of $4.3 \pm 0.6 [1\sigma]\text{‰}$, defining the trophic baseline of the ecosystem food web. The higher and lower values belong to different ovicaprids. In this case, no wild herbivore was analysed, as none was found in the available faunal assemblage of the site.

There are four omnivores, whose $\delta^{13}\text{C}$ values range between -21.1‰ and -20.1‰ , with a mean value of $-20.6 \pm 0.4 [1\sigma]\text{‰}$. Their $\delta^{15}\text{N}$ values range between 4.1‰ and 9.4‰ , with a mean value of $6.4 \pm 2.2 [1\sigma]\text{‰}$, although the variability is high enough for not grouping of all of them in a single category. Carnivores are only represented by two felids with a $\delta^{13}\text{C}$ mean value of $-$

$18.9 \pm 0.1 [1\sigma]\text{‰}$ and a $\delta^{15}\text{N}$ mean value of $7.2 \pm 0.8 [1\sigma]\text{‰}$. Their $\delta^{15}\text{N}$ places carnivores in a higher trophic level than herbivores (2.9‰) and slightly more over omnivores (0.8‰).

The human $\delta^{13}\text{C}$ values range between -19.3‰ and -20.5‰ , with a mean value of $-20.2 \pm 0.3 [1\sigma]\text{‰}$ ($n=40$). Their $\delta^{15}\text{N}$ values range between 8.2‰ and 11.3‰ , with a mean value of $9.0 \pm 0.6 [1\sigma]\text{‰}$. Humans are clearly in a higher trophic level than herbivores ($\delta^{15}\text{N}$ 4.7‰ higher) and also in a higher step than omnivores ($\delta^{15}\text{N}$ 2.6‰ higher) and carnivores ($\delta^{15}\text{N}$ 1.8‰ higher). There is an adult human (S-UCT 19029) whose $\delta^{15}\text{N}$ values are enriched in 2.3‰ compared to the human mean. The direct radiocarbon date for this human is 4534 ± 24 BP (MAMS-29830), contemporary to sample S-UCT 19048 (MAMS-29831: 4523 ± 24 BP) whose $\delta^{15}\text{N}$ values are enclosed in the human mean (Table 1, Fig. 5). A non-parametric statistical test (Mann-Whitney) reveals no significant differences between age groups (adult and subadult), $\delta^{13}\text{C}$ data ($p=0.063$) and $\delta^{15}\text{N}$ values ($p=0.373$).

Inter-population $\delta^{13}\text{C}$ and $\delta^{15}\text{N}$ analysis

A non-parametric statistical test (Mann-Whitney) reveals that isotopic results from each site differ significantly in their $\delta^{13}\text{C}$ values ($p=1.05 \times 10^{-12}$) but not in their $\delta^{15}\text{N}$ values ($p=0.062$). Inter-population analysis has been also applied to the herbivores from both sites to assess if the difference could be associated to different environments rather than dietary patterns via the same statistical test. It reveals also significant differences only in their $\delta^{13}\text{C}$ values ($p=0.0004$), not in their $\delta^{15}\text{N}$ values ($p=0.1644$) (Fig. 6).

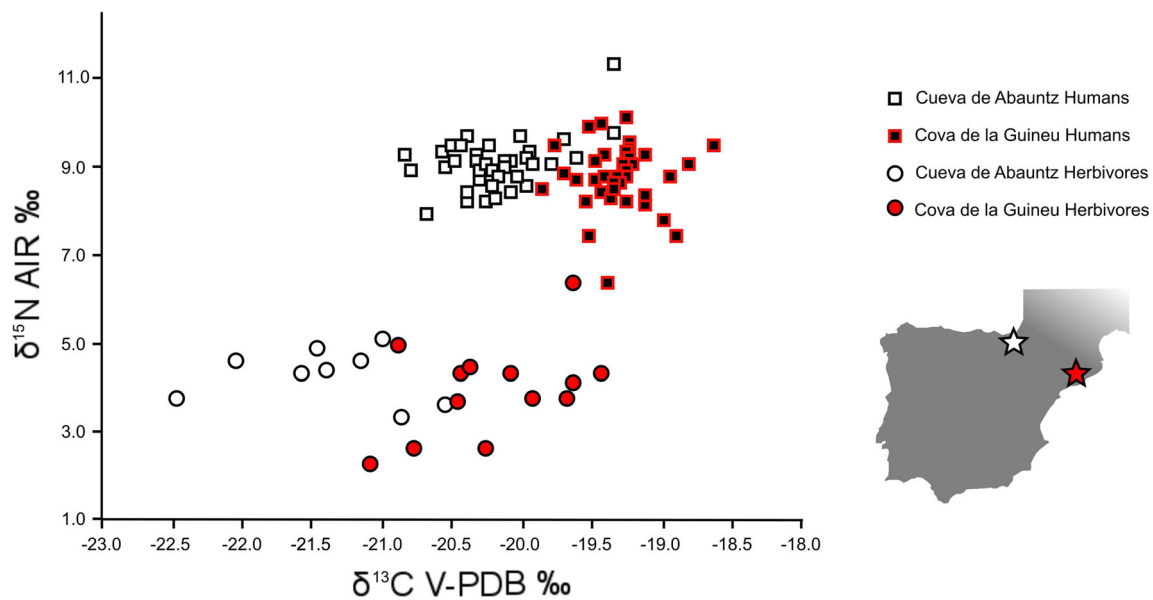


Fig. 6 Scatter plot of human and fauna bone collagen $\delta^{13}\text{C}$ and $\delta^{15}\text{N}$ values from Cova de la Guineu and Cueva de Abauntz according to their location inside Iberia

Discussion

Collective burials and, specially, sepulchral caves, usually present an heterogeneous archaeological record that limits an in-depth discussion. The first limitation can be found in the chronological heterogeneity of the human remains, which ideally should be all directly radiocarbon dated to ensure the attribution of each individual to one or another chronological period (e.g. Salazar-García et al. 2016a). However, this is not always possible due to budgetary constrictions, and only a few specimens can be dated (e.g. Villalba-Mouco et al. 2017). Secondly, it is difficult to know if the humans buried together belonged to the same community/settlement or if they came from different ones (potentially from environments with different availability of resources). In this case, the isotopic baselines from the different populations buried in a same burial enclosure might be different. These two limitations are applied to both human and faunal remains. Furthermore, faunal remains are normally poorly represented in the burial spaces and very possibly do not represent all species consumed. All these limitations are considered in the following discussion for both sepulchral sites.

Cova de la Guineu

All fauna $\delta^{13}\text{C}$ and $\delta^{15}\text{N}$ values from Cova de la Guineu group together by species and suggest a similar environment, as well as discarding a big shift in isotope values due to potential chronological differences. Domestic (*Ovis aries/Capra hircus*) and wild ungulates (*Cervus elaphus*) are in the same range for $\delta^{13}\text{C}$ and $\delta^{15}\text{N}$ values, probably related to the use of shared areas for grazing (Villalba-Mouco et al. 2018).

Different isotopic values between wild and domestic fauna can be also due to feeding from different ecosystems (e.g. aquatic resources in terrestrial ecosystem) (Schulting et al. 2017; Müldner et al. 2014) or to the introduction of manuring practices that would imply an enrichment in $\delta^{15}\text{N}$ of domestic plants potentially consumed by domestic animals (Bogaard et al. 2007). But in this case, only one sheep/goat falls into the pig range (higher $\delta^{13}\text{C}$ and $\delta^{15}\text{N}$ values) suggesting a distinctive diet and/or provenance for this specimen, or even a different chronological period attribution (Fig. 4).

The average $\delta^{15}\text{N}$ difference between herbivores and domestic omnivores (*Sus domesticus*) is of 1.8‰. This slight increment suggests the omnivore attribution of the pigs, pointing out at a small input of animal protein in their diet (Fig. 4).

The only carnivore data available was a mustelid. It shows $\delta^{13}\text{C}$ and $\delta^{15}\text{N}$ values slightly higher than human mean but in the same trophic level according to Bocherens and Drucker (2003). This little increase could be in agreement with mustelid generalist and opportunistic diet, which can include carrion feeding and another species normally non-consumed by humans as micromammals, reptiles and different kind of invertebrates (Barja 2017; Mangas 2017) (Fig. 4).

Human samples show homogeneous isotopic values, especially the adult group where values are probably not influenced by physiological factors related to growth and/or development (Beaumont et al. 2013). The $\delta^{13}\text{C}$ human values indicate a quite homogeneous animal protein diet based on C_3 terrestrial resources, with no evidence of regular aquatic nor C_4 resource consumption. Otherwise, the $\delta^{15}\text{N}$ human values suggest a high importance of animal proteins in human diet, showing a $\delta^{15}\text{N}$ value increase of 4.9‰ higher than herbivores

and 2.4‰ higher than omnivores. If we analyse the possible species consumed one by one, we can also suggest that $\delta^{15}\text{N}$ values from rabbits and horse do not fit with ca. 3–5‰ the theoretical enrichment (Bocherens and Drucker 2003). In this sense, we could suggest animal protein consumed by humans could come mainly from ovicaprids. This is despite the fact that red deer consumption could also fit isotopically, because the archaeozoological data for this period in the region points out to a decrease in hunting followed by the rise of husbandry practices (Saña 2013). The consumption of other domestic animals like pig could be less regular, as well as those from rabbit and horse, according to $\delta^{15}\text{N}$ enrichment (Bocherens and Drucker 2003) (Fig. 4). Due to the limitation of stable isotope analysis on bone collagen, we cannot discuss the amount of plant foods consumed (Hedges and Reynard 2007). However, if a high proportion of proteins were coming from plant resources, we would not expect the observed increase in $\delta^{15}\text{N}$ human values (Fahy et al. 2013). A non-parametric statistical test (Mann-Whitney) reveals differences between adult and subadult groups, showing subadults lower $\delta^{15}\text{N}$ values, possibly due to the physiological process associated to the increase of collagen turnover during the growth and/or a changes in the diet (Hedges et al. 2007; Beaumont et al. 2013).

Cueva de Abauntz

The domestic herbivores recovered from Cueva de Abauntz group together in their $\delta^{13}\text{C}$ and $\delta^{15}\text{N}$ values, which could be associated to a common environment and chronological period. The average of $\delta^{15}\text{N}$ isotopic enrichment between herbivores and domestic omnivores (*Sus domesticus*) in this case is 2.1‰, similar as at Cova de la Guineu. Assuming that all the pig remains were contemporary, the household model could be proposed since the $\delta^{15}\text{N}$ values are very different among pigs (Madgwick et al. 2012), showing a variety of types of diet: values compatible with an herbivore diet (e.g. S-UCT 19086), a carnivore diet (e.g. S-UCT 18989), even so a mixed omnivore diet (e.g. S-UCT 19087). This heterogeneous feeding pattern seem to be more frequent in a household management model, where the number of pigs is small and they are fed with human leftovers (Halley and Rosvold 2014) (Fig. 5).

Carnivore values were represented by felids (*Felis* sp.). Their elevated $\delta^{13}\text{C}$ values in comparison with humans suggest they were feeding on different resources, perhaps a diet based on micromammals, reptiles and birds (Lozano 2017), which are not commonly consumed by humans.

Most of the human samples from Cueva de Abauntz show homogeneous isotopic values except for one individual outlier that will be discussed separately. The $\delta^{13}\text{C}$ human values show that human dietary protein was mainly coming from C_3 terrestrial resources, with no evidence of regular aquatic or C_4 resource consumption. The $\delta^{15}\text{N}$ human values suggest

a high importance of animal proteins in human diet, showing a $\delta^{15}\text{N}$ enrichment of 4.7‰ compared to herbivore average, and 2.6‰ compared to omnivore average (Fig. 5). Looking into the possible species consumed, we cannot rule out any herbivore intake based on the faunal and human isotopic values (Bocherens and Drucker 2003). On the other hand, a 2.6‰ $\delta^{15}\text{N}$ enrichment between humans and omnivores is too small to conclude that pig was the preferential intake. Our results would be consistent with a mixed diet that could include ovicaprids and bovids preferably and pig and plant protein potentially in lower amount.

As mentioned before, there is only one outlier adult human (S-UCT 19029) shifted to a higher position of the plot. This human shows an enrichment of 2.3‰ in $\delta^{15}\text{N}$ values and 0.9‰ in $\delta^{13}\text{C}$ values regarding to human mean values. The consumption of enough freshwater resources as to be reflected in the isotopic signature could be one possibility. This type of dietary outlier has already been reported in other Iberian sites for other chronologies, and they are usually linked to fish consumption (Guiry et al. 2015). The detection of intake of freshwater resources is not straightforward, but it seems that high $\delta^{15}\text{N}$ values are a common characteristic when freshwater resource exploitation is present (Lillie et al. 2011). The Ultzama River goes a few metres away from Cueva de Abauntz, making it plausible that riverine fish could have been consumed even if not knowing where was the location of the settlement/s where the individuals buried in Cueva de Abauntz lived. Otherwise, the consumption of marine resources is unlikely because the increase with respect to the other individuals is mainly in $\delta^{15}\text{N}$ values but not in $\delta^{13}\text{C}$, which would be less negative if the individual showed a marine diet (Richards and Hedges 1999). The consumption of estuarine resources, which have lower $\delta^{13}\text{C}$ and $\delta^{15}\text{N}$ values than marine ones (Salazar-García et al. 2014), could be another explanation given that Cueva de Abauntz is only ca. 80 km away from Atlantic sea lochs and marine marshes. Finally, a preference consumption of pig livestock could also be suggested for this individual (4.9‰ enrichment in $\delta^{15}\text{N}$ between this human sample and the pig mean) (Fig. 5).

The direct radiocarbon date of this human sample is contemporary to another human sample analysed (S-UCT 19048) whose isotopic values fit well within the human mean (Fig. 2). This probably discards the isotopic difference due to a different chronological attribution of the remains and could be reflecting that some humans have different access to some types of resources due to several reasons. Carbon and nitrogen have been explored in respect to hierarchy in medieval societies, finding high protein diet in higher status burials (Trautmann et al. 2017). During Prehistory, and especially in the case of collective burial caves, assessing different social positions is difficult to test. The association of specific individuals to grave goods could shed light on this (Blasco and Ríos 2010), but unfortunately in the case of Cueva de Abauntz

having all skeletal remains and grave goods comingled makes this impossible (Utrilla et al. 2015). Another way to approach the study of hierarchy in prehistoric burial sites could be the study of funerary structures (Fernández-Crespo and de-la-Rúa 2015). Cueva de Abauntz presents some particular burials in pits and cists inside the cave (Utrilla et al. 2007), but none include these two earlier individuals (S-UCT 19029 and S-UCT 19048). Both of these directly dated individuals came from a small rock niche, without any specific burial structure nor grave goods.

Other non-dietary explanations could be argued to justify these differences too. A non-local origin of this individual could be one option that should be further studied through strontium isotope analysis of the population (Waterman et al. 2014). In this sense, the combination of carbon and nitrogen together with strontium isotope ratio analysis could give us more information about this unequal protein intake, as it is already done for the same chronology in nearby territories (Sarasketa-Gartzia et al. 2017; Villalba-Mouco et al. 2017).

Inter-population analysis

The human isotope values from both sites portray a quite homogeneous overall diet among humans. This homogeneous pattern of diet based on C_3 terrestrial resources seems to be general along the entire Iberian Peninsula during the Late Neolithic and Chalcolithic (e.g. Alt et al. 2016; Díaz-Zorita 2014; Fernández-Crespo et al. 2016; Fontanals-Coll et al. 2015; García-Borja et al. 2013; López-Costas et al. 2015; McClure et al. 2011; Sarasketa-Gartzia et al. 2017; Villalba-Mouco et al. 2017; Salazar-García 2011; Salazar-García et al. 2013b; Salazar-García 2014; Waterman et al. 2016). The reason of this homogeneity could be the consolidated economy based on agriculture and livestock, together with a higher mobility among the different communities and the increase of trade networks, not only in prestigious objects (Schuhmacher and Banerjee 2012) but also in food products. Isotopic analyses in fauna remains could give us more clues about animal trade, as happens in other chronologies (Salazar-García et al. 2017).

In any case, and even if the dietary interpretation does not vary, it is noteworthy to mention that there are significant differences between $\delta^{13}C$ human values from Cova de la Guineu and $\delta^{13}C$ human values from Cueva de Abauntz (Mann-Whitney test, $p = 1.05 \times 10^{-12}$) (Fig. 6). This observed $\delta^{13}C$ differences among humans is also present among herbivores (Mann-Whitney test, $p = 0.0004$), which define the baseline of each ecosystem. This suggests that the observed human difference between sites should not be attributed to diet, but most possibly to the existence of enough environmental differences to be recorded in the collagen $\delta^{13}C$ values along the food web. Plants are very sensitive to different environmental factors (altitude, temperature, luminosity or water

availability) and their physiological adaptation to its factors can generate a variation in their isotopic values as happens with C_3 and C_4 adaptations (O'Leary 1981; Ambrose 1991). This spectrum of values has been used to assess several aspects about past environmental conditions when studying the $\delta^{13}C$ and $\delta^{15}N$ isotopic values of a species with a fixed diet over time (e.g. Stevens et al. 2008; González-Guarda et al. 2017). Moreover, this gradual $\delta^{13}C$ and $\delta^{15}N$ variation among different environments is very helpful to discriminate altitudinal movements in herbivores with a high precision method based on serial dentine analysis (Tornero et al. 2016b). In our case, results reflect the influence of environment from at least two areas in Iberia (the Western Prepyrenees and the Northeastern coast of Iberia). These differences demand caution when interpreting human diets from different sites that are not contemporary and/or not in a same area, as it is possible that the environmental influence is responsible for changes otherwise attributed to different subsistence patterns and social structures (Fernández-Crespo and Schulting 2017), as has been demonstrated in neighbouring territories (Herrscher and Bras-Goude 2010; Goude and Fontugne 2016).

Conclusions

This study represents a comparative isotopic analysis between two burial caves dated back to the Late Neolithic-Chalcolithic Period from the Western Prepyrenees and the Northeastern coast of Iberia. The isotopic dietary approach shows a diet based on C_3 terrestrial resources, common for the whole Iberian Peninsula during this period. A preferential herbivore intake as main protein source, probably domestic, has been proposed for both sites. Moreover, isotopic human values also suggest that the consumption of domestic pig was not very frequent, at least not enough to leave a clear sign in human bulk collagen values. The present study also reveals a significantly different carbon isotope signature in humans and herbivore baselines from both sites, suggesting an environmental effect between these two Iberian areas, and suggests caution when interpreting diet in isotopic studies comparing human values from different regions and/or chronologies.

Acknowledgments VVM has a predoctoral scholarship funded by the Gobierno de Aragón and the Fondo Social Europeo (BOA20150701025) and did a research stay at the University of Cape Town funded by the Fundación Ibercaja-CAI (2016) and DCSG's UCT and BBVA research grants. VVM, CMP and PU are members of the Spanish project HAR2014-59042-P (Transiciones climáticas y adaptaciones sociales en la prehistoria de la Cuenca del Ebro), and VVM, CMP and PU are members of the regional government of Aragón PPVE research group (H-07: Primeros Pobladores del Valle del Ebro). ISG has a predoctoral scholarship funded by Basque Government and is a member of the Spanish project HAR2014-53536-P and IT-662-13. All authors would like to thank the Museo de Navarra, specially to Jesús García Gazólaz for allowing the study of Cueva de Abauntz in the

Universidad de Zaragoza facilities, as well as to the Centro de Espeleología de Aragón (CEA), specially Mario Gisbert for the topography of Cueva de Abauntz. We also thank Víctor Sauqué for the help with fauna identification and Jesús Laborda and J. Ignacio Lorenzo for their help in the transport of the archaeological material, as well as Ian Newton for the technical assistance.

References

- Alday A (1995) Los elementos de adorno personal de la cueva del Moro de Olvena y sus derivaciones cronológico-culturales. *Bolskan* 12, 193–214
- Alt KW, Zesch S, Garrido-Pena R, Knipper C, Szécsényi-Nagy A, Roth C, Tejedor-Rodríguez C, Held P, García-Martínez-de-Lagrán I, Navitainuck D, Arcusa H, Rojo-Guerra MA (2016) A community in life and death: the Late Neolithic megalithic tomb at Alto de Reinoso (Burgos, Spain). *PLoS One* 11(1):e0146176
- Altuna J, Mariezcurrera K, Elorza M (2002) Arqueozoología de los niveles Paleolíticos de la Cueva de Abauntz (Arraiz, Navarra). *Saldvie* 2, 1–26
- Ambrose SH (1991) Effects of diet, climate and physiology on nitrogen isotope abundances in terrestrial foodwebs. *J Archaeol Sci* 18(3): 293–317
- Ambrose SH (1993) Isotopic analysis of paleodiets: methodological and interpretative considerations. In: Stanford MK (ed) *Investigations of ancient human tissue: chemical analyses in anthropology*. Gordon and Breach Science Publishers, Langhorne, pp 59–130
- Ambrose SH, DeNiro MJ (1986) The isotopic ecology of East African mammals. *Oecologia* 69(3):395–406
- Ambrose SH, Norr L (1993) Experimental evidence for the relationship of the carbon isotope ratios of whole diet and dietary protein to those of bone collagen and carbonate. In: Lambert JB, Gruppe G (eds) *Prehistoric human bone: archaeology at the molecular level*. Springer Verlag, Berlin, pp 1–37
- Andrés MT (1998) Colectivismo funerario neo-eneolítico. Aproximación metodológica sobre datos de la Cuenca Alta y Media del Ebro. Institución Fernando el Católico. Diputación de Zaragoza, Zaragoza
- Barja I (2017) Marta – *Martes martes*. In: Salvador, A., Barja, I. (Eds.), *Enciclopedia Virtual de los Vertebrados Españoles*. Museo Nacional de Ciencias Naturales, Madrid. <http://www.vertebradosibericos.org/>
- Beaumont J, Gledhill A, Lee-Thorp J, Montgomery J (2013) Childhood diet: a closer examination of the evidence from dental tissues using stable isotope analysis of incremental human dentine. *Archaeometry* 55(2):277–295
- Blasco C, Ríos P (2010) La función del metal entre los grupos campaniformes. Oro versus cobre. El ejemplo de la Región de Madrid. *Trab Prehist* 67(2):359–372
- Blasco C, Delibes G, Baena J, Liesau C, Ríos P (2007) El poblado calcolítico de Camino de las Yeseras (San Fernando de Henares, Madrid): un escenario favorable para el estudio de la incidencia campaniforme en el interior peninsular. *Trab Prehist* 64(1):151–163
- Bocherens H, Drucker D (2003) Trophic level isotopic enrichment of carbon and nitrogen in bone collagen: case studies from recent and ancient terrestrial ecosystems. *Int J Osteoarchaeol* 13(1–2):46–53
- Bogaard A, Heaton THE, Poulton P, Merbach I (2007) The impact of manuring on nitrogen isotope ratios in cereals: archaeological implications for reconstruction of diet and crop management practices. *J Archaeol Sci* 34:335–343
- Bronk Ramsey C (2009) Bayesian analysis of radiocarbon dates. *Radiocarbon* 51(1):337–360
- Brown TA, Nelson DE, Vogel JS, Southon JR (1988) Improved collagen extraction by modified Longin method. *Radiocarbon* 30:171–177
- Buikstra JE, Ubelaker DH (1994) Standards for data collection from human skeletal remains. In: *Arkansas Archaeological Survey Research Series* (Fayetteville)
- Cox G, Sealy J (1997) Investigating identity and life histories: isotopic analysis and historical documentation of slave skeletons found on the Cape Town foreshore, South Africa. *Int J Hist Archaeol* 1(3): 207–224
- Craig H (1953) The geochemistry of the stable carbon isotopes. *Geochim Cosmochim Acta* 3(2–3):53–92
- Delibes G, Herrán JI, Santiago J, de Val J (1995) Evidence for social complexity in the Copper Age of the Northern Meseta. In: Lillios KT (ed) *The origins of complex societies in late prehistoric Iberia*. International Monographs in Prehistory 8, pp. 44–63
- DeNiro MJ (1985) Post-mortem preservation and alteration of in vivo bone collagen isotope ratios in relation to palaeodietary reconstruction. *Nature* 317:806–809
- DeNiro MJ, Epstein S (1978) Influence of diet on the distribution of carbon isotopes in animals. *Geochim Cosmochim Acta* 42:495–506
- Díaz-Andreu M, Liesau C, Castaño A (1992) El poblado calcolítico de La Loma de Chiclana (Vallecas, Madrid). *Excavaciones de urgencia realizadas en 1987*. *Arqueología, Paleontología y Etnografía* 3:31–116
- Díaz-Zorita M (2014) *The Copper Age*. In: *South-west Spain: a bioarchaeological approach to prehistoric social organisation*. Durham University, Durham (Doctoral thesis)
- Drucker D, Bocherens H, Bridault A, Billiou D (2003) Carbon and nitrogen isotopic composition of red deer (*Cervus elaphus*) collagen as a tool for tracking palaeoenvironmental change during the Late-Glacial and Early Holocene in the northern Jura (France). *Palaeogeogr Palaeoclimatol Palaeoecol* 195(3):375–388
- Esquivel JA, Navas E (2007) Geometric architectural pattern and constructive energy analysis at Los Millares Copper Age Settlement (Santa Fé de Mondújar, Almería, Andalusia). *J Archaeol Sci* 34(6):894–904
- Fahy GE, Richards M, Riedel J, Hublin JJ, Boesch C (2013) Stable isotope evidence of meat eating and hunting specialization in adult male chimpanzees. *Proc Natl Acad Sci* 110(15):5829–5833
- Fernández-Crespo T (2016) El papel del fuego en los enterramientos neolíticos finales/calcolíticos iniciales de los abrigos de la Sierra de Cantabria y sus estribaciones (valle medio-alto del Ebro). *Trab Prehist* 73(1):128–146
- Fernández-Crespo T, de-la-Rúa C (2015) Demographic evidence of selectiveburial in megalithic graves of northern Spain. *J Archaeol Sci* 53:604–617
- Fernández-Crespo T, Schulting RJ (2017) Living different lives: early social differentiation identified through linking mortuary and isotopic variability in Late Neolithic/Early Chalcolithic north-central Spain. *PLoS One* 12(9):e0177881
- Fernández-Crespo T, Mujika JA, Ordoño J (2016) Aproximación al patrón alimentario de los inhumados en la cista de la Edad del Bronce de Ondarre (Aralar, Guipúzcoa) a través del análisis de isótopos estables de carbono y nitrógeno sobre colágeno óseo. *Trab Prehist* 73(2):325–334
- Fontanals-Coll M, Díaz-Zorita Bonilla M, Subirà ME (2015) A palaeodietary study of stable isotope analysis from a high-status burial in the copper age: the Montelirio megalithic structure at Valencina de la Concepción–Castilleja de Guzmán, Spain. *Int J Osteoarchaeol* 26(3):447–459
- García Sanjuán L (2013) El asentamiento de la Edad del Cobre en Valencina de la Concepción: Estado actual de la investigación, debates y perspectivas. In: Sanjuán LG, Vargas JM, Hurtado V, Ruiz T, Cruz R (eds) *El asentamiento prehistórico de Valencina de la Concepción (Sevilla): Investigación y tutela en el 150 aniversario del descubrimiento de La Pastora*. Universidad de Sevilla, Sevilla, pp 21–60

- García-Borja P, Pérez Fernández A, Biosca Cirujeda V, Ribera i Gomes A, Salazar-García DC (2013) Los restos humanos de la Coveta del Frare (Font de la Figuera, València). In: García-Borja P, Revert E, Ribera A, Biosca V (eds) *El Naiximent d'un Poble. Historia i Arqueologia de la Font de la Figuera*. Ajuntament de la Font de la Figuera, pp. 47–60
- García-Guixé E (2011) Estudi paleoantropològic i paleopatològic del sepulcre col·lectiu de Forat de Conqueta (Santa Linya, Lleida). *Treballs d'Arqueologia* 17:37–98
- Jimeno B (2009) Estudio antropológico de la cueva sepulcral de Loarre. *Saldvie* 9:369–392
- González-Guarda E, Domingo L, Tomero C, Pino M, Hernández MH, Sevilla P, Villalvicencio N, Agustí J (2017) Late Pleistocene ecological, environmental and climatic reconstruction based on megafauna stable isotopes from northwestern Chilean Patagonia. *Quat Sci Rev* 170:188–202
- Goude G, Fontugne M (2016) Carbon and nitrogen isotopic variability in bone collagen during the Neolithic period: influence of environmental factors and diet. *J Archaeol Sci* 70:117–131
- Guiry EJ, Grimes V (2013) Domestic dog (*Canis familiaris*) diets among coastal Late Archaic groups of northeastern North America: a case study for the canine surrogacy approach. *J Anthropol Archaeol* 32(4):732–745
- Guiry EJ, Hillier M, Richards MP (2015) Mesolithic dietary heterogeneity on the European Atlantic coastline: stable isotope insights into hunter-gatherer diet and subsistence in the Sado Valley, Portugal. *Curr Anthropol* 56:460–470
- Halley DJ, Rosvold J (2014) Stable isotope analysis and variation in medieval domestic pig husbandry practices in Northwest Europe: absence of evidence for a purely herbivorous diet. *J Archaeol Sci* 49:1–5
- Handley LL, Austin AT, Stewart GR, Robinson D, Scrimgeour CM, Raven JA, Heaton THE, Schmidt S (1999) The $\delta^{15}\text{N}$ natural abundances ($\delta^{15}\text{N}$) of ecosystem samples reflects measures of water availability. *Aust J Plant Physiol* 26:185–199
- Harrison RJ (1974) Ireland and Spain in the Early Bronze Age. *J R Soc Antiqu Irel* 104:52–73
- Heaton THE, Vogel H, Von la Chevallerie G, Gollet G (1986) Climatic influence on the isotopic composition of bone nitrogen. *Nature* 322:822–823
- Hedges REM, Reynard LM (2007) Nitrogen isotopes and the trophic level of humans in archaeology. *J Archaeol Sci* 34:1240–1251
- Hedges RE, Clement JG, Thomas CDL, O'Connell TC (2007) Collagen turnover in the adult femoral mid-shaft: modeled from anthropogenic radiocarbon tracer measurements. *Am J Phys Anthropol* 133:808–816
- Herrscher E, Bras-Goude L (2010) Southern French Neolithic populations: isotopic evidence for regional specificities in environment and diet. *Am J Phys Anthropol* 141(2):259–272
- Laffranchi Z, Huertas AD, Brobeil SAJ, Torres AG, Cantal JAR (2016) Stable C & N isotopes in 2100 year-BP human bone collagen indicate rare dietary dominance of C4 plants in NE-Italy. *Sci Rep* 6:1–8
- Lee-Thorp JA (2008) On isotopes and old bones. *Archaeometry* 50(6):925–950
- Lillie M, Budd C, Potekhina I (2011) Stable isotope analysis of prehistoric populations from the cemeteries of the Middle and Lower Dnieper Basin, Ukraine. *J Archaeol Sci* 38(1):57–68
- Longin R (1971) New method of collagen extraction for radiocarbon dating. *Nature* 230:241–242
- López-Costas O, Müldner G, Cortizas AM (2015) Diet and lifestyle in Bronze Age northwest Spain: the collective burial of Cova do Santo. *J Archaeol Sci* 55:209–218
- Lozano J (2017) Gato montés – *Felis silvestris*. In: Salvador A, Barja I (eds) *Enciclopedia Virtual de los Vertebrados Españoles*. Museo Nacional de Ciencias Naturales, Madrid <http://www.vertebradosibericos.org/>
- Lubell D, Jackes M, Schwarz H, Knyf M, Meiklejohn C (1994) The Mesolithic-Neolithic transition in Portugal: isotopic and dental evidence of diet. *J Archaeol Sci* 21(2):201–216
- Madgwick R, Mulville J, Stevens RE (2012) Diversity in foddering strategy and herd management in late Bronze Age Britain: an isotopic investigation of pigs and other fauna from two midden sites. *Environ Archaeol* 17:126–140
- Mangas JG (2017) Garduña – *Martes foina*. In: Salvador A, Barja I (eds) *Enciclopedia Virtual de los Vertebrados Españoles*. Museo Nacional de Ciencias Naturales, Madrid <http://www.vertebradosibericos.org/>
- McClure SB, García O, de Togores CR, Culleton BJ, Kennett DJ (2011) Osteological and paleodietary investigation of burials from Cova de la Pastora, Alicante, Spain. *J Archaeol Sci* 38(2):420–428
- Mercadal O, Campillo D (1995) Patologia de la població prehistòrica de la cova de la Guineu (Fontrubí, Alt Penedès, Barcelona). Proceedings of the IX European meeting of the Paleopathology Association - I Congreso Nacional de Paleopatología (Barcelona, 1992). *Museu d'Arqueologia de Catalunya*. Barcelona, pp. 229–232
- Minagawa M, Wada E (1986) Nitrogen isotope ratios of red tide organisms in the East China Sea: a characterization of biological nitrogen fixation. *Mar Chem* 19(3):245–259
- Montes L, Domingo R (2014) La ocupación de las Sierras Exteriores durante el Calcolítico. In: Utrilla P, Mazo C (eds) *La Peña de las Forcas* (Graus, Huesca). Un asentamiento estratégico en la confluencia del Ésera y el Isábena. *Monografías Arqueológicas/Prehistoria* 46, Universidad de Zaragoza, Zaragoza, pp 409–426
- Müldner G, Britton K, Ervynck A (2014) Inferring animal husbandry strategies in coastal zones through stable isotope analysis: new evidence from the Flemish coastal plain (Belgium, 1st–15th century AD). *J Archaeol Sci* 41:322–332
- O'Leary MH (1981) Carbon isotope fractionation in plants. *Phytochemistry* 20(4):553–567
- Olalde I, Brace S, Allentoft ME, Armit I, Kristiansen K, Booth T, Rohland N, Mallick S, Szécsényi-Nagy A, Mittnik A, Altena E, Lipson M, Lazaridis I, Harper TK, Patterson NJ, Broomandkoshbacht N, Diekmann Y, Faltyskova Z, Fernandes DM, Ferry M, Harney E, de Knijff P, Michel M, Oppenheimer J, Stewardson K, Barclay A, Alt KW, Liseau C, Ríos P, Blasco C, Vega Miguel J, Menduina García R, Avilés Fernández A, Bánffy E, Bernabò-Brea M, Billoin D, Bonsall C, Bonsall L, Allen T, Büster L, Carver S, Castells Navarro L, Craig OE, Cook GT, Cunliffe B, Denaire A, Dinwiddie KE, Dodwell N, Ermée M, Evans C, Kuchařík M, Farré JF, Fowler C, Gazonbeck M, Garrido Pena R, Haber-Uriarte M, Haduch E, Hey G, Jewett N, Knowles T, Massy K, Pfrengle S, Lefranc P, Lemercier O, Lefebvre A, Heras C, Galera V, Bastida A, Lomba J, Majó T, McKinley JJ, McSweeney K, Gusztáv MB, Modi A, Kulcsár G, Kiss V, Czene A, Patay Z, Endródi A, Köhler K, Hajdu T, Szczeny T, Dani J, Bernert Z, Hoole M, Cheronet O, Velemínský P, Dobeš M, Candilio F, Brown F, Flores R, Herrero-Corral AM, Tusa S, Carnieri E, Lentini L, Valenti A, Zazini A, Waddington C, Delibes G, Guerra-Doce E, Neil B, Brittain M, Luke M, Mortimer R, Desideri J, Besse M, Brüken G, Furmanek M, Haluszko A, Mackiewicz M, Rapiński A, Leach S, Soriano I, Lillios KT, Cardoso JL, Pearson MP, Włodarczak P, Price TD, Prieto P, Rey PJ, Risch R, Rojo Guerra MA, Schmitt A, Serralongue J, Silva AM, Smrčka V, Vergnaud L, Zilhão J, Caramelli D, Higham T, Thomas MG, Kennett DJ, Fokkens H, Heyd V, Sheridan JA, Sjögren KG, Stockhammer PW, Krause J, Pinhasi R, Haak W, Barnes I, Lalueza-Fox C, Reich D (2018) The Beaker phenomenon and the genomic transformation of Northwest Europe. *Nature* 555:190–196
- Oms FX, Cebrià A, Mestres J, Morales JJ, Pedro M, Vergès JM (2016a) Campaniforme i metal·lúrgia en un espai sepulcral del III mil·lenni cal. BC: la Cova de la Guineu (Font-rubí, Alt Penedès). In: Esteve X, Miró C, Molist N, Sabaté G (eds) *Jornades d'Arqueologia del*

- Penedès, Institut d'Estudis Penedesencs, Vilafranca del Penedès: pp. 109–116
- Oms FX, Mestres J, Cebrià A, Morales JI, Nadal J, Pedro M, Mendiola S, Martín P, Fullola JM (2016b) La Cova de la Guineu (Font-Rubí, Barcelona) i les relacions plana-muntanya al Penedès durant el neolític inicial. In: Cabanilles JJ (ed) *Del neolític a l'edat del bronze en el Mediterrani occidental. Estudis en homenatge a Bernat Martí Oliver.*, Servei d'Investigació Prehistòrica. *Trabajos Varios* n° 119, pp. 97–107
- Pérez-Romero A, Iriarte E, Galindo-Pellicena MA, García-González R, Rodríguez L, Castilla M, Francés-Negro M, Santos E, Valdiosera C, Arsuaga JL, Alday A, Carretero JM (2017) An unusual Pre-Bell Beaker copper age cave burial context from El Portalón de Cueva Mayor site (Sierra de Atapuerca, Burgos). *Quat Int* 433:142–155
- Power RC, Salazar-García DC, Wittig RM, Henry AG (2014) Assessing use and suitability of scanning electron microscopy in the analysis of micro remains in dental calculus. *J Archaeol Sci* 49:160–169
- Reimer PJ, Bard E, Bayliss A, Beck JW, Blackwell PG, Bronk Ramsey C, Grootes PM, Guilderson TP, Hafliðason H, Hajdas I, Hatt e C, Heaton TJ, Hoffmann DL, Hogg AG, Hughen KA, Kaiser KF, Kromer B, Manning SW, Niu M, Reimer RW, Richards DA, Scott EM, Southon JR, Staff, R.A., Turney CSM, Van der Plicht J (2013) *IntCal13 and Marine13 radiocarbon age calibration curves 0-50,000 years cal BP.* *Radiocarbon* 55(4):1869–1887
- Richards MP, Hedges REM (1999) Stable isotope evidence for similarities in the types of marine foods used by Late Mesolithic humans at sites along the Atlantic coast of Europe. *J Archaeol Sci* 26:717–722
- Richards MP, Karavanić I, Pettitt P, Miracle P (2015) Isotope and faunal evidence for high levels of freshwater fish consumption by late glacial humans at the late upper palaeolithic site of Šandalja II, Istria, Croatia. *J Archaeol Sci* 61:204–212
- Salazar-García DC (2011) Aproximación a la dieta de la población calcolítica de La Vital a través del análisis de isótopos estables del carbono y del nitrógeno sobre restos óseos. In: Pérez G, Bernabeu J, Carrión Y, García-Puchol O, Molina LL, Gómez M (eds) *La Vital (Gandia, Valencia). Vida y muerte en la desembocadura del Serpis durante el III y el I milenio a.C.* Museu de Prehistòria de València-Diputació de València (T.V. 113), València, pp. 139–143
- Salazar-García DC (2014) Estudi de la dieta en la població de Cova dels Diablets mitjançant anàlisi d'isòtops estables del carboni i del nitrogen en col·lagen ossi. Resultats preliminars. In: Aguilera Arzo GA, Monroig D, García-Borja P (eds) *La Cova dels Diablets (Alcalà de Xivert, Castelló). Prehistòria a la Serra d'Irta.* Diputació de la Castelló, Castellón, pp. 67–78
- Salazar-García DC, Power RC, Serra AS, Villaverde V, Walker MJ, Henry AG (2013a) Neanderthal diets in central and southeastern Mediterranean Iberia. *Quat Int* 318:3–18
- Salazar-García DC, de Lugo Enrich LB, Alvarez García HJ, Benito Sánchez M (2013b) Estudio diacrónico de la dieta de los pobladores antiguos de Terrinches (Ciudad Real) a partir del análisis de isótopos estables sobre restos óseos humanos. *REAF* 34:6–14
- Salazar-García DC, Aura JE, Olària CR, Talamo S, Morales JV, Richards MP (2014) Isotope evidence for the use of marine resources in the eastern Iberian Mesolithic. *J Archaeol Sci* 42:231–240
- Salazar-García DC, García-Puchol O, de Miguel-Ibañez MP, Talamo S (2016a) Earliest evidence of neolithic collective burials from eastern Iberia: radiocarbon dating at the archaeological site of Les Llometes (Alicante, Spain). *Radiocarbon* 58(3):679–692
- Salazar-García DC, Romero A, García-Borja P, Subirà ME, Richards MP (2016b) A combined dietary approach using isotope and dental buccal microwear analysis of human remains from the Neolithic, Roman and Medieval periods from the archaeological site of Tossal de les Basses (Alicante, Spain). *J Archaeol Sci Rep* 6:610–619
- Salazar-García DC, Pérez-Ripoll M, García-Borja P, Jordá Pardo JF (2017) A terrestrial diet close to the coast: a case study from the Neolithic levels of Nerja Cave (Málaga, Spain). In: García-Puchol O, Salazar-García C (eds) *Times of Neolithic transition along the western Mediterranean. Fundamental issues in archaeology*, Springer, pp. 281–307
- Saña M (2013) Domestication of animals in the Iberian peninsula. Origins and spread of domestic animals in Southwest Asia and Europe, Left Coast Press, pp. 195–22
- Sarasketa-Gartzia I, Villalba-Mouco V, le Roux P, Arrizabalaga Á, Salazar-García DC (2017) Late Neolithic-Chalcolithic socio-economical dynamics in northern Iberia. A multi-isotope study on diet and provenance from Santimamiñe and Pico Ramos archaeological sites (Basque Country, Spain). *Quat Int*
- Schoeninger MJ, DeNiro MJ (1984) Nitrogen and carbon isotopic composition of bone collagen from marine and terrestrial animals. *Geochim Cosmochim Acta* 48:625–639
- Schuhmacher TX, Banerjee A (2012) Procedencia e intercambio de marfil en el Calcolítico de la Península Ibérica. *Rubricatum: revista del Museu de Gavà* 5:289–298
- Schulting RJ, Vaiglova P, Crozier R, Reimer PJ (2017) Further isotopic evidence for seaweed-eating sheep from Neolithic Orkney. *J Archaeol Sci Rep* 11:463–470
- Szwarcz HP, Schoeninger MJ (1991) Stable isotope analysis in human nutritional ecology. *Yearb Phys Anthropol* 34:283–321
- Seibt U, Rajabi A, Griffiths H, Berry JA (2008) Carbon isotopes and water use efficiency: sense and sensitivity. *Oecologia* 155:411–454
- Smith BN, Epstein S (1971) Two categories of $^{13}C/^{12}C$ ratios for higher plants. *Plant Physiol* 47(3):380–384
- Stevens RE, Jacobi R, Street M, Germonpré M, Conard NJ, Münzel SC, Hedges RE (2008) Nitrogen isotope analyses of reindeer (*Rangifer tarandus*), 45,000 BP to 9,000 BP: Palaeoenvironmental reconstructions. *Palaeogeogr Palaeoclimatol Palaeoecol* 262(1):32–45
- Szécényi-Nagy A, Roth C, Brandt G, Rihuete-Herrada C, Tejedor-Rodríguez C, Held P, García-Martínez-de-Lagrán I, Arcusa Magallón H, Zesch S, Knipper C, Bánffy E, Friederich S, Meller H, Bueno P, Barroso R, Balbín R, Herrero-Corral AM, Flores R, Alonso C, Jiménez J, Rindlisbacher L, Oliart C, Freireiro MI, Soriano I, Vicente O, Micó R, Lull V, Soler J, López JA, Roca de Togores C, Hernández MS, Jover FJ, Lomba J, Avilés A, Lillios KT, Silva AM, Magalhães M, Oosterbeek LM, Cunha C, Waterman AJ, Roig J, Martínez A, Ponce J, Hunt M, Mejías-García JC, Carlos Pecero JC, Cruz-Auñón R, Tomé T, Carmona E, Cardoso JL, Araújo AC, Liesau von Lettow-Vorbeck C, Blasco C, Ríos P, Pujante A, Royo-Guillén JI, Esquembre MA, Dos Santos VM, Parreira R, Morán E, Méndez E, Vega y Miguel J, Mendiña R, Martínez V, López O, Krause J, Pichlerf SL, Garrido-Pena R, Kunst M, Risch R, Rojo-Guerra MA, Haak W, Alt KW (2017) The maternal genetic make-up of the Iberian Peninsula between the Neolithic and the Early Bronze Age. *Sci Rep* 7:15644
- Szpak P (2014) Complexities of nitrogen isotope biogeochemistry in plant-soil systems: implications for the study of ancient agricultural and animal management practices. *Front Plant Sci* 5:288
- Tieszen LL (1991) Natural variations in the carbon isotope values of plants: implications for archeology, ecology and paleoecology. *J Archaeol Sci* 18:227–248
- Tomero C, Aguilera M, Ferrio JP, Arcusa H, Moreno-García M, García-Reig S, Rojo-Guerra M (2016a) Vertical sheep mobility along the altitudinal gradient through stable isotope analyses in tooth molar bioapatite, meteoric water and pastures: a reference from the Ebro valley to the central Pyrenees. *Quat Int*
- Tomero C, Balasse M, Bălăşescu A, Chataigner C, Gasparyan B, Montoya C (2016b) The altitudinal mobility of wild sheep at the Epigravettian site of Kalavan 1 (Lesser Caucasus, Armenia): evidence from a sequential isotopic analysis in tooth enamel. *J Hum Evol* 97:27–36
- Trautmann B, Wißing C, Díaz-Zorita M, Bis-Worch C, Bocherens H (2017) Reconstruction of socioeconomic status in the Medieval

- (14th-15th century) population of Grevenmacher (Luxembourg) based on growth, development and diet. *Int J Osteoarchaeol* 27: 947–957
- Ubelaker DH (1989) Human skeletal remains: excavation, analysis, interpretation. In: *Manual on archaeology 2 Taraxacum*, first ed. Washington
- Utrilla P, Mazo C, Lorenzo JI (2007) Enterramientos humanos en el Calcolítico de Abauntz. In: *La tierra te sea leve. Arqueología de la Muerte en Navarra*, pp. 66–72. Museo de Navarra
- Utrilla P, Laborda R, Sebastián M, (2014a) La reocupación de cuevas prehistóricas del Prepirineo oscense en época romana. Modelización mediante tig's. In: Duplá A, Escribano MV, Sancho L, Villacampa MA (eds) *Miscelánea de estudios en homenaje a Guillermo Fatás Cabeza*, Institución Fernando el Católico, pp. 673–682
- Utrilla P, Mazo C, Lorenzo JI (2014b) Rituales funerarios en el calcolítico de Abauntz. Un ejemplo de lesión con supervivencia. *Salduie* 13-14, pp. 297–314
- Utrilla P, Mazo C, Domingo R (2015) Fifty thousand years of prehistory at the cave of Abauntz (Arraitz, Navarre): a nexus point between the Ebro valley, aquitaine and the cantabrian corridor. *Quat Int* 364:294–305
- Valera AC, Silva AM, Romero JE (2014) The temporality of Perdigoões enclosures: absolute chronology of the structures and social practices. *SPAL* 23:11–26
- Van der Merwe NJ (1982) Carbon isotopes, photosynthesis, and archaeology: different pathways of photosynthesis cause characteristic changes in carbon isotope ratios that make possible the study of prehistoric human diets. *Am Sci* 70(6):596–606
- Van Klinken GJ (1999) Bone collagen quality indicators for palaeodietary and radiocarbon measurements. *J Archaeol Sci* 26:687–695
- Villalba-Mouco V, Sauqué V, Sarasketa-Gartzia I, Pastor MV, le Roux PJ, Vicente D, Utrilla P, Salazar-García DC (2017) Territorial mobility and subsistence strategies during the Ebro Basin Late Neolithic-Chalcolithic: a multi-isotope approach from San Juan cave (Loarre, Spain). *Quat Int*
- Villalba-Mouco V, Utrilla P, Laborda R, Lorenzo JI, Martínez-Labarga C, Salazar-García DC (2018) Reconstruction of human subsistence and husbandry strategies from the Iberian Early Neolithic: a stable isotope approach. *Am J Phys Anthropol*
- Vogel JC (1978) Recycling of carbon in a forest environment. *Oecol Plant* 13(1):89–94
- Waterman AJ, Peate DW, Silva AM, Thomas JT (2014) In search of homelands: using strontium isotopes to identify biological markers of mobility in late prehistoric Portugal. *J Archaeol Sci* 42:119–127
- Waterman AJ, Tykot RH, Silva AM (2016) Stable isotope analysis of diet-based social differentiation at late prehistoric collective burials in south-western Portugal. *Archaeometry* 58(1):131–151
- Weyrich LS, Duchene S, Soubrier J, Arriola L, Llamas B, Breen J, Morris AG, Alt KW, Caramelli D, Dresely V, Farrell M, Farrer AG, Francken M, Gully N, Haak W, Hardy K, Harvati K, Held P, Holmes EC, Kaidonis J, Lalueza-Fox C, de la Rasilla M, Rosas A, Semal P, Soltysiak A, Townsend G, Usai D, Wahl J, Huson DH, Dobney K, Cooper A (2017) Neanderthal behaviour, diet, and disease inferred from ancient DNA in dental calculus. *Nature* 544(7650):357–361

10.4 Estudio de la movilidad de las comunidades de montaña durante el Calcolítico a través de isótopos de estroncio en esmalte humano: la cueva de los cristales (Sarsa de Surta, Huesca, España)

Estudio de la movilidad territorial de las comunidades de montaña durante el Calcolítico a través de isótopos de estroncio en esmalte humano: la Cueva de los Cristales (Sarsa de Surta, Huesca, España)

Vanessa Villalba-Mouco¹, Lourdes Montes¹, Manuel Bea¹, Domingo C. Salazar-García^{2,3}.

¹ Departamento de Ciencias de la Antigüedad, Grupo Primeros Pobladores del Valle del Ebro (PPVE), Instituto de Investigación en Ciencias Ambientales (IUCA), Universidad de Zaragoza, Pedro Cerbuna 12, 50009 Zaragoza, España.

² Grupo de Investigación en Prehistoria IT-622-13 (UPV-EHU)/ IKERBASQUE Basque Foundation for Science, Vitoria, España.

³ Department of Geological Sciences, University of Cape Town, Cape Town, South Africa.

Correspondencia: Vanessa Villalba Mouco (vvmouco@unizar.es)

Resumen

Durante el Neolítico Final y los inicios del Calcolítico se produce un aumento del registro arqueológico, sobre todo de origen funerario. Las zonas más altas del Prepirineo comienzan a ser pobladas de manera más frecuente pero, debido a sus condiciones ambientales menos favorables y a la ausencia de poblados específicos, se han interpretado como visitas esporádicas. Este argumento genera discusión cuando además de yacimientos de ocupación, encontramos enterramientos en lugares poco accesibles. Con el objetivo de profundizar en el conocimiento de estas comunidades de montaña, hemos realizado el estudio de los isótopos de estroncio en esmalte dental de los individuos localizados en la Cueva de los Cristales (Sarsa de Surta, Huesca, España), localizada a unos 1.300 metros sobre el nivel del mar (m.s.n.m.), y

que solo presenta un nivel de tipo funerario. Los resultados obtenidos muestran unos valores de estroncio compatibles con un origen prepirenaico. A su vez, se han encontrado diferentes valores entre los individuos, cuyos valores también estarían presentes en otras zonas del Prepireneo.

Abstract

During the Late Neolithic and the beginning of the Chalcolithic periods there is an increase of the abundance of the archaeological record in Iberia, mostly regarding burials. In this sense, the higher Prepyrenean areas started to be settled more frequently, but the worse weather conditions here make researchers to suggest mostly sporadic visits. This argument generates a big debate when, added to the increase of the archaeological record also do the number of burial sites in less accessible places increase. With the aim of shed more light into the knowledge of these Chalcolithic mountain groups, we have carried out strontium isotope analysis of human enamel of individuals from the funerary cave Cueva de los Cristales (Sarsa de Surta, Huesca, España), located at 1.300 meters above the sea level. Our results point to a Prepyrenean origin of the Chalcolithic groups despite to differences found among the individual values, which can also be related to a different location in the Prepyrenean area.

Palabras clave: Neolítico Final-Calcolítico, cueva sepulcral, Prepireneo, movilidad, arqueología.

Keywords: Late Neolithic-Chalcolithic, sepulchral cave, Prepyrenees, mobility, archaeology.

Entidad financiadora del proyecto:

Beca predoctoral del Gobierno de Aragón y el Fondo Social Europeo (BOA20150701025).

Estancias de investigación de Ibercaja-CAI (2017).

1. INTRODUCCIÓN

Durante el final del Neolítico y a lo largo del Calcolítico se observa de manera indudable en toda la Península Ibérica un aumento en el registro arqueológico de tipo funerario: cuevas o abrigos sepulcrales en los lugares en las que la orografía lo permite (e.g. [Utrilla et al., 2015](#); [Fernández-Crespo, 2016](#); [Salazar-García et al., 2016](#)), construcción de sepulcros megalíticos (e.g. [Atl et al., 2015](#); [Aranda Jiménez et al., 2018](#)), e incluso la reutilización de dólmenes que ya habían sido usados como lugares de enterramiento durante el Neolítico ([Fernández-Eraso y Mujika-Alustiza, 2013](#)). Todo ello sugiere la posibilidad de un aumento demográfico, más allá de cambios en el ritual que aumentaron la visibilidad actual de estos enterramientos. Las causas de este incremento de la población podrían residir en la existencia de movimientos migratorios, hipótesis avalada por la importación de objetos exógenos ([Schuhmacher y Banerjee, 2012](#)), o bien, por el crecimiento intrínseco de la población Neolítica presente en la Península, tal y como apuntan los estudios de ADN mitocondrial en Iberia, ya que no se observan grandes cambios entre Neolítico y Calcolítico ([Szécsényi-Nagy et al., 2017](#)).

Sea como fuere, tanto el crecimiento demográfico como la existencia de redes de comercio e intercambio suelen ir asociados a un incremento de la movilidad entre comunidades que cada vez están más especializadas en la gestión ciertos tipos de recursos. El resultado de esta consolidación económica genera una homogenización del consumo de estos recursos, algo que se hace evidente en los estudios de dieta basados en el análisis de isótopos estables del colágeno óseo de humanos en cronologías del Neolítico Final y el Calcolítico (e.g. [McClure et al., 2011](#); [Salazar-García 2011, 2014](#); [García-Borja et al., 2013](#); [Fontanals-Coll et al., 2015](#); [López-Costas et al., 2015](#); [Fernández-Crespo et al., 2016](#); [Waterman et al., 2016](#); [Sarasketa-Gartzia et al., 2018](#); [Villalba-Mouco et al., 2018a](#)).

Durante el Calcolítico encontramos signos de esta movilidad poblacional reflejados en la ocupación de territorios que hasta este momento no estaban presentes. De esta manera, aumenta la presencia de yacimientos arqueológicos o, al menos, la densidad de materiales que nos permiten reconocerlos, en las zonas más elevadas de la Península Ibérica ([Gassiot et al., 2014](#)). Entre estos puntos destaca el Pirineo, con yacimientos datados en ~2500 cal BC ([Laborda et al., 2017](#)). Estos lugares elevados y con unas condiciones climáticas menos

favorables plantean un uso puntual, tal vez periódico y recurrente, muchas veces relacionado con la ganadería (Rojo *et al.*, 2013, Montes *et al.*, 2016a).

El concepto de movilidad territorial no guarda relación con el concepto de migración. Consideramos movilidad a la distribución espacial de los individuos o comunidades a lo largo de su vida, sin estar estrictamente ligado a cambios culturales, algo que estaría más relacionado con movimientos migratorios. Dentro de las técnicas moleculares aplicadas a restos humanos y faunísticos, encontraríamos el estudio de ADN antiguo como pilar fundamental para identificar grandes movimientos poblacionales del pasado (Haak *et al.*, 2015, Olalde *et al.*, 2018). Por otra parte, el análisis de isótopos de estroncio nos ayuda a dilucidar los movimientos a nivel individual o grupal dentro de grupos poblacionales que pueden ser perfectamente homogéneos desde un punto de vista genético (Haak *et al.*, 2008; Knipper *et al.*, 2017).

1.1 El Neolítico Final y el Calcolítico en las Sierras exteriores del Pirineo

Las sierras exteriores del Pirineo son un territorio habitado durante toda la prehistoria debido a la numerosa presencia de cuevas y abrigos (Montes y Domingo, 2014), a su ambiente mixto entre valle y montaña (que favorece la diversidad de recursos disponibles), y a la existencia de unas condiciones climáticas más suaves que las presentes en alta montaña (González-Sampériz *et al.*, 2017). A lo largo de todo el Prepirineo encontramos ejemplos de ocupación en todas las cronologías: Paleolítico Medio (e.g. Utrilla *et al.*, 2010, Mora *et al.*, 2008), Paleolítico Superior (e.g. Utrilla y Laborda, 2018, Martínez-Moreno *et al.*, 2010), Mesolítico (e.g. Domingo *et al.*, 2018) y Neolítico (e.g. Utrilla y Laborda, 2018, Mazzucó *et al.*, 2013). Durante el Neolítico Medio la presencia de asentamientos decrece drásticamente, encontrando hasta la fecha restos humanos solo en Cova de Els Trocs (Rojo-Guerra *et al.*, 2013) y Cueva de Chaves (Villalba-Mouco *et al.*, 2018b). Durante el Calcolítico, en las sierras exteriores aumenta el número de yacimientos de tipo funerario, véase dólmenes (e.g. Calvo, 1991a; 1991b) como cuevas sepulcrales (e.g. Lorenzo, 2014) (Figura 1). Las fechas radiocarbónicas que tenemos para ambos tipos de enterramientos colectivos parecen solaparse en el tiempo, lo que todavía supone una incógnita es la selección de un tipo de

recinto u otro como lugar de enterramiento, y que algunos investigadores están tratando de estudiar mediante diversos enfoques ([Fernández-Crespo et al., 2015; 2017](#)).

La evidencia de existencia de poblados del Neolítico Final y Calcolítico continúa siendo nula en esta zona. Se han llevado a cabo trabajos de prospección arqueológica pero los materiales recuperados en superficie no son atribuibles de manera exclusiva al periodo Calcolítico. Tanto el sílex como las cerámicas, muchas de ellas lisas o con cordones aplicados, también están presentes en otros periodos cronológicos ([Pérez-Romero et al., 2017](#)), por lo que los hallazgos aislados no nos ayudan a establecer una cronología relativa cuando aparecen fuera de contexto estratigráfico o crono-cultural.

Pese a la ausencia de poblados específicos y de abundantes cantidades de material, se han encontrado estructuras y objetos de almacenaje, algo que indica, al menos, la existencia de ocupaciones relativamente cortas que generalmente se han relacionado con la explotación ganadera ([Baldellou, 1987; Montes y Martínez Bea, 2006](#)). Los estudios faunísticos llevados a cabo por P. Castaños muestran la importancia de los ovicaprinos para las comunidades que habitaron la región prepirenaica, y esta zona concreta conocida como Tierra Bucho ([Montes et al., 2016a; 2016b](#)). Otros taxones también presentes en el territorio podrían indicar que estas poblaciones no estarían sujetas a importantes patrones de movilidad. En esta línea se documenta el cerdo, que no cabe relacionar con actividades trashumantes ([Montes et al., 2016a; 2016b](#)).

1.2 El yacimiento de la Cueva de los Cristales

El yacimiento de la Cueva de los Cristales se sitúa a unos 1.300 m.s.n.m., en el Cordal del Sevil, en la ladera Este del barranco formado por el río Isuala, en el antiguo municipio de Sarsa de Surta, hoy término municipal de Aínsa-Sobrarbe (Huesca, España). La cavidad, tapizada de cristales de calcita en sus paredes, se compone de un vestíbulo y una cámara interior de unos 7 m de desarrollo, unidos a través de un paso estrecho (**Figura 1b y 2**). Es en la sala interior donde aparecieron los primeros restos humanos, aparentemente depositados en superficie sin ningún otro tipo de tratamiento ([Montes y Domingo, 2001-2002](#)). El resto de huesos humanos fueron obtenidos en la campaña de excavación de 2007 ([Montes y Martínez Bea,](#)

2006). Todos ellos aparecieron desarticulados y entremezclados, tal vez como resultado de la simple deposición sobre la superficie de la cámara interior. Este tratamiento del cadáver es típico de los enterramientos colectivos en cuevas funerarias de cronología calcolítica (e.g. Guixé *et al.*, 2009, Gimeno, 2009). A su vez, esta cronología fue corroborada mediante dataciones de radiocarbono realizadas directamente sobre los restos humanos de la Cueva de los Cristales, así como en otros yacimientos cercanos a la zona (**Tabla 1**). En la excavación de la Cueva de los Cristales apenas se recuperaron algunos fragmentos de cerámica lisa, de indudable factura prehistórica, que se suponen asociados a los enterramientos, y escasos restos de fauna, todos ellos de ovicáprido. Al no haber sido datados directamente no permiten afirmar su relación con los enterramientos, y por su aspecto, algunos pudieran ser incluso actuales.

1.3 Isótopos de estroncio y estudio de la movilidad territorial

Los estudios de movilidad basados en el análisis de isótopos de estroncio han demostrado ser de gran utilidad en arqueología, tanto en animales (e.g. Britton *et al.*, 2009; Copeland *et al.*, 2016) como en humanos (e.g. Copeland *et al.*, 2011; Haak *et al.*, 2008), aunque su análisis continúa siendo escaso a escala peninsular (Salazar-García, 2012; Diaz-Zorita, 2014; Sarasketa *et al.*, 2018., Villalba-Mouco *et al.*, 2018c).

El análisis de la ratio de los isótopos de estroncio ($^{87}\text{Sr}/^{86}\text{Sr}$) en el esmalte de las piezas dentales puede proporcionar evidencias, a escala individual, acerca del uso del territorio y su movilidad a través de él (Bentley, 2013). Al contrario de lo que ocurre con los isótopos de carbono y nitrógeno, los isótopos de estroncio ($^{87}\text{Sr}/^{86}\text{Sr}$) no presentan fraccionamiento isotópico, por lo que se incorporan directamente a la cadena alimentaria a través del agua, circulando por plantas y animales, hasta alcanzar los tejidos humanos. El esmalte humano, a diferencia de lo que ocurre con los huesos, se forma durante la infancia (en el caso de la dentición permanente) y no sufre remodelaciones durante la vida del individuo.

En este sentido, la ratio $^{87}\text{Sr}/^{86}\text{Sr}$ depende directamente de la geología de la zona, mostrando diferencias de acuerdo con la edad de las rocas del sustrato y la cantidad de ^{87}Rb que éstas posean. Esta ratio de $^{87}\text{Sr}/^{86}\text{Sr}$, común a una litología, queda fijada en el esmalte dental

durante su mineralización y refleja los valores de estroncio biodisponible de la región dónde el individuo vivió y dónde tuvo lugar la mineralización de su esmalte (Bentley, 2006; Ericson, 1985; Price et al., 2002). Los segundos y terceros molares son las piezas que suelen ser seleccionadas en estos tipos de estudios puesto que permiten realizar comparaciones entre los valores de la infancia (tiempo de mineralización del segundo molar) y el inicio de la etapa adulta (tiempo de mineralización del tercer molar) (Hillson, 1996). Las piezas dentales deciduas, cuyo esmalte mineraliza durante el periodo de embarazo, o las piezas dentales cuyo esmalte mineraliza durante la posible etapa de lactancia, son descartados del análisis ya que diferentes procesos fisiológicos pueden afectar a los valores de $^{87}\text{Sr}/^{86}\text{Sr}$.

Diferentes condiciones ambientales, como el efecto de los aerosoles marinos (Bentley, 2006), así como el arrastre de diferentes materiales geológicos por fenómenos atmosféricos como la lluvia, el arrastre de materiales por los ríos y su deposición, pueden alterar los valores esperados de estroncio para una litología determinada (Sjögren et al., 2016). Por ello, es necesario calcular el valor biodisponible de un territorio mediante el muestreo de plantas y caracoles actuales (Price et al., 2002), y compararlos con los valores obtenidos en el esmalte humano.

2. MATERIAL Y MÉTODOS

2.1 Los restos humanos de la Cueva de los Cristales

El número total de restos humanos recuperados de la Cueva de los Cristales es de 17 (Alconchel, 2013). Aunque *a priori* son escasos, el estado de conservación de los mismos y los elementos anatómicos presentes han permitido inferir datos importantes a nivel antropológico, como son el establecimiento del Número Mínimo de Individuos (MNI), la estimación de la edad biológica de los mismos, así como la determinación del sexo (Alconchel, 2013). En base a estos parámetros, en Cueva de los Cristales se cuantificó un MNI de 6 individuos, entre los cuales se encontraron dos individuos de categoría infantil II (6 a 12 años) y de sexo indeterminable, 3 adultos, dos de ellos masculinos y otro de sexo indeterminado, y un individuo juvenil determinado como femenino (Alconchel, 2013). Los métodos empleados en el diagnóstico sexual se basaron en la morfología craneana y mandibular (Brothwell, 1993;

Campillo y Subirà, 2004). Dado que ninguno de los métodos está basado en la morfología del coxal (e.g. Bruzek, 2002), y ya que los restos aparecieron desarticulados, hemos decidido excluir la información relacionada con el sexo de los individuos de nuestro estudio. Entre los huesos recuperados no se observó ninguna patología aparente a nivel macroscópico. La mayoría de las piezas dentales que aparecieron aisladas no están repetidas y no se pueden atribuir a individuos específicos. Entre las piezas dentales recuperadas, tan solo una parece estar afectada por la presencia de caries y dos de ellas por hipoplasia del esmalte. Estas patologías están presentes en dentición permanente completamente desarrollada (Alconchel, 2013). Finalmente, 5 piezas dentales correspondientes a 4 individuos diferentes fueron las seleccionadas para llevar a cabo el análisis de los isótopos de estroncio (Tabla 3). Todas las piezas dentales escogidas estaban asociadas a mandíbulas o al maxilar, con lo que descartamos la posibilidad de estar muestreando un individuo dos veces. Además, de esta forma se obtiene más información acerca de los aspectos biológicos del individuo: edad aproximada mediante los patrones de erupción dental (Ubelaker, 1978) y la existencia de posibles patologías (Ortner, 2003). Cuando ha sido posible, se han seleccionado segundos (M2) y terceros molares (M3) procedentes de un mismo individuo, con el objetivo de inferir posibles movimientos en diferentes etapas de la vida, durante la infancia, cuando mineraliza el segundo molar, y al inicio de la etapa adulta, cuando mineraliza el tercer molar (Hillson, 1996) (Tabla 3). Los dientes deciduos o piezas dentales cuya mineralización se produce durante época de lactancia (incisivos y primeros molares), fueron descartados para evitar una posible inferencia maternal en los valores isotópicos. Esta estrategia de muestreo ya ha sido puesta a punto en estudios anteriores de cronologías similares realizados en territorios adyacentes (Sarasketa-Gartzia et al., 2018a; 2018b).

2.2 Cálculo de los valores de $^{87}\text{Sr}/^{86}\text{Sr}$ biodisponibles de entorno

Para saber qué valores de Sr presentan los seres vivos en los diferentes sustratos geológicos, es necesario no solo analizar las muestras arqueológicas, sino también muestras actuales que muestran los valores de Sr biodisponible que presenta cada zona. Para ello, escogemos muestras biológicas inmóviles, como pueden ser las plantas, o de movilidad muy reducida, como pueden ser los caracoles. Para este estudio se han muestreado cinco plantas y cinco caracoles para cada ambiente y área geológica diferente en el entorno. En total hemos

analizado muestras de cuatro zonas geográficas diferentes situadas a lo largo de Prepirineo. (**Tabla 2**). Las principales son dos: los alrededores de la Cueva de los Cristales y la Cueva Dróllica, cuya etapa geológica de formación se correspondería con el Paleoceno-Eoceno inferior (denominada “Zona Cuevas”), y el entorno a los Dólmenes cercanos a ambas cuevas (Capilleta, Pueyoril y Caseta de las Balanzas), denominada “Zona Dólmenes” y que se corresponde con una geología del Eoceno Medio-Superior (**Figura 3**). A su vez, hemos incluido dos nuevas áreas geográficas más alejadas: el entorno de la localidad de Arén, cuya geología también se corresponde con el Paleoceno-Eoceno inferior, y el entorno de la localidad de Gabasa, cuya geología se corresponde una zona de transición Paleoceno-Cretácico Superior (**Figura 3**).

Se han seleccionado diversas áreas geológicas similares con el objetivo de aumentar la precisión de nuestro estudio, ya que el arrastre de materiales desde el Pirineo (de una edad geológica más antigua) podría haber tenido una mayor influencia en alguna de las zonas, creando un mosaico de valores en el Prepirineo. En este trabajo también se añaden los datos obtenidos de la zona prepirenaica en estudios anteriores ([Villalba-Mouco et al., 2018](#)).

2.3 Preparación y análisis de Sr en muestras arqueológicas

2.3.1 Muestras de esmalte dental

La preparación de las muestras arqueológicas se llevó a cabo en el *Department of Archeology* y *Department of Geology* de la Universidad de Cape Town (Sudáfrica). De cada pieza dental se tomó una porción longitudinal de esmalte de unos 20 mg. Cada uno de los fragmentos fue limpiado mediante abrasión con una Dremel 3500 con broca de cabeza de diamante, tanto en su parte externa, para eliminar posibles restos del sustrato arqueológico, como su porción interna, para eliminar la posible dentina asociada. Tras la limpieza por abrasión, las porciones de esmalte fueron lavadas con agua MilliQ (ultra destilada y filtrada) y sometidas a ultrasonidos durante 20 minutos. Para cada muestra se empleó una broca de cabeza de diamante diferente, todas ellas previamente estaban lavadas con etanol y sometidas a ultrasonidos en agua MilliQ para evitar la contaminación cruzada ([Budd et al., 2000](#)). El siguiente paso fue la digestión del esmalte en 2 ml de HNO₃ al 65% previamente destilado dos

veces dentro de recipientes de teflón en una placa térmica a 140 °C durante una hora. Una vez digerido el esmalte, se procede al secado y redisolución de las muestras en 1,5 ml de HNO₃ bidestilado de concentración 2M. Estas muestras redisueltas son las que se centrifugan a 4000 rpm durante 20 min y de las cuales, se recolecta el sobrenadante. En este paso, una porción de volumen específico se utilizó para conocer la concentración de Sr en las muestras mediante el uso de una curva de calibración obtenida a partir del estándar SRM987 y su señal de intensidad de ⁸⁸Sr (V) emitida a diferentes concentraciones. El resto del volumen se utilizó para llevar a cabo la separación química del estroncio mediante columnas cromatográficas de resina de 200µl, modelo Eichrom Sr.Spec de Bio-Spin Disposable Chromatography Bio-Rad Columns, siguiendo el métodos descrito en Pin et al. (1994). La fracción de estroncio que se eluye en el paso final de su separación es secada y disuelta de nuevo en 2 ml de HNO₃ bidestilados al 0.2% de concentración y finalmente es diluido hasta 200 ppb de concentración de Sr para llevar a cabo su medición mediante el espectrómetro de masas. La medición de la ratio ⁸⁷Sr/⁸⁶Sr se llevó a cabo en un espectrómetro *NuPlasma HR multicollector inductively-coupled-plasma* (MC-ICP-MS). Todas las muestras fueron referenciadas respecto al estándar SRM987 que presenta un valor de referencia de ⁸⁷Sr/⁸⁶Sr de 0,710255 (valores obtenidos del National Institute of Standards and Technology, NIST). También se procedió a la corrección de la señal de interferencia isobárica causada por rubidio mediante la medición de ⁸⁵Rb y el ratio ⁸⁵Rb/⁸⁷Rb. La corrección del fraccionamiento isotópico se realizó mediante la medición de la ratio ⁸⁶Sr/⁸⁸Sr y tomando como señal de ⁸⁶Sr/⁸⁸Sr el valor de 0,1194.

Como controles del proceso, se procedió a la medida de los estándares procesados a la vez que las muestras de este estudio (⁸⁷Sr/⁸⁶Sr = 0,708936; 2 sigma 0,000041; n=33) y se vio que los valores eran coherentes con los datos que se tenían hasta el momento en el laboratorio (⁸⁷Sr/⁸⁶Sr; 0,708915; 2 sigma 0,000047; n=125). También se procesaron blancos en cada set de extracción de estroncio para descartar la contaminación cruzada en algún punto del proceso (Tabla 3, Figura 4b).

2.4 Muestras biológicas actuales para el cálculo de Sr biodisponible

Los rangos de los valores de ⁸⁷Sr/⁸⁶Sr biodisponibles de dos áreas geológicas diferentes fueron calculados con plantas y caracoles siguiendo las indicaciones de Bentley (2004) y Price (2001).

La extracción y purificación de estroncio fue la misma que la descrita anteriormente en el caso de las conchas de caracol. En el caso de las plantas, fue necesario la previa calcinación de las partes verdes y la digestión de las cenizas, que en este caso se llevó a cabo mediante HF al 48% y HNO₃ bidestilado al 65% en proporciones 4:1, respectivamente tal y como queda descrito en Copeland et al. (2016). En el caso de las muestras actuales no se procedió a la medida de las concentraciones de Sr ya que se asume que las muestras actuales no quedarían afectadas por la posible incorporación diagenética (Tabla 2, Figura 4a).

3. RESULTADOS

3.1. Estroncio biodisponible de las muestras biológicas actuales.

Los resultados de los valores de ⁸⁷Sr/⁸⁶Sr biodisponible de plantas y caracoles de las diferentes zonas de estudio muestreadas se presentan en la Tabla 2 y la Figura 4a. Lo primero que hicimos fue aplicar el test estadístico Mann-Whitney a las zonas “Zona Cuevas” y “Arén” para comprobar si se pueden considerar zonas diferentes a pesar de compartir la geología, o bien se pueden unificar sus valores. El resultado de este test indica que no existen diferencias significativas entre estas tres zonas (p=0,734), por lo que agrupamos los valores de Sr biodisponible de todas ellas para ganar potencial estadístico a la hora de determinar la procedencia de los individuos. El resto de áreas de muestreo las mantenemos por separado ya que pertenecen a geologías diferentes. Nos parece interesante destacar que la mayoría de los *outliers* (4/5) (Figura 4a) quedan representados por especies arbóreas o arbustivas, cuyas raíces se agarran de manera más profunda al estrato y nunca por caracoles.

Finalmente, nuestro rango de valores para el Paleoceno-Eoceno Inferior (Zona Cuevas y Arén) es de 0,707885-0,709424, el de la Zona Dólmenes (Eoceno Medio-Superior) es de 0,707869-0,708110, y para Gabasa (Paleoceno-Cretácico Superior) es de 0,708375-0,709246. El rango de valores publicados para Loarre (Cretácico-Mioceno) es de 0,708243-0,709984, y para Bailo (Oligoceno Superior-Mioceno Inferior) es de 0,707986-0,708306, ambas zonas localizadas también en el Prepirineo (Villalba-Mouco et al., 2018).

3.2. Valores de estroncio de las muestras arqueológicas

Hemos realizado el análisis de isótopos de Sr en cinco piezas dentales de cuatro individuos calcolíticos recuperados en la Cueva de los Cristales. La ratio $^{87}\text{Sr}/^{86}\text{Sr}$ y las concentraciones de Sr en partes por millón (ppm) de las muestras de esmalte humano aparecen en la **Tabla 3**. Los datos de $^{87}\text{Sr}/^{86}\text{Sr}$ de esmalte dental humano aparecen en la **Figura 4b**. Todos los individuos poseen unos valores de $^{87}\text{Sr}/^{86}\text{Sr}$ en el esmalte dental de compatible con los valores de $^{87}\text{Sr}/^{86}\text{Sr}$ biodisponible de diversas zonas del Prepirineo (Figura 4a). Si nos centramos en su entorno más cercano, los valores de $^{87}\text{Sr}/^{86}\text{Sr}$ humanos quedan englobados dentro del rango del entorno de la Cueva de los Cristales (Zona Cuevas, así como todas las zonas cuyo sustrato geológico es el Paleoceno), y dos de ellos, lo que supone un 50% de la muestra, (0739.sup.26 y segundo molar de 0739.sup.20) quedarían incluidos a su vez dentro del rango de la zona de los Dólmenes (Sustrato geológico Eoceno), que queda englobado dentro de los valores de la Zona cuevas, pero presentando siempre unos valores de $^{87}\text{Sr}/^{86}\text{Sr}$ menores (**Figura 4b**). El individuo 0739.sup.20 es el único que presenta valores $^{87}\text{Sr}/^{86}\text{Sr}$ sobre diferentes piezas dentales (M2 y M3) mostrando valores de $^{87}\text{Sr}/^{86}\text{Sr}$ más bajos en su segundo molar (M2) (común a los valores biodisponibles del Paleoceno más bajos y los valores Eoceno) y valores de Sr más altos en su tercer molar (M3) (**Figura 4b, Tabla 3**).

4. DISCUSIÓN

Para llevar a cabo el estudio isotópico de movilidad territorial de los individuos de la Cueva de los Cristales hemos realizado un intenso mapeo de los valores de estroncio biodisponible en el Prepirineo, a los que, a su vez, hemos añadido los recopilados en la bibliografía procedentes de áreas geográfica cercanas ([Villalba-Mouco et al., 2018](#)). La primera observación que extraemos de los datos es que existe un gran solapamiento entre los valores de las zonas, algo que estaría relacionado con la cronología de los estratos, ya que la mayoría se atribuyen a diversas etapas incluidas entre el Paleoceno y el Eoceno. Aun así, a excepción de los lugares de contacto geológico, como ocurre en la Cueva de San Juan de Loarre ([Villalba-Mouco et al., 2018](#)), vemos que existe una correlación entre valores de Sr más altos en zonas del Prepirineo con estratos geológicos más antiguos que, a su vez, coinciden, en general, con las zonas más elevadas. Gracias a ello vemos, por ejemplo, en la región denominada “Zona Cuevas” (ca. 1.300 m s.n.m.) unos valores más elevados que en la zona Dólmenes (ca. 800 m s.n.m.) aunque sus valores más bajos se solapen con ésta última (**Figura 4a, Tabla 3**).

Los individuos de la Cueva de los Cristales muestran valores que superan a los comunes encontrados en zonas más bajas (Zona Dólmenes) pero también otros exclusivos de las zonas más altas (Zona Cuevas), sugiriendo la existencia de comunidades que las habitarían de manera permanente o semipermanente. Estos valores, compatibles con las regiones más altas del Prepirineo, también están presentes en los segundos molares, lo que significa que los individuos se podrían encontrar en esta zona desde su infancia, aunque no podamos determinar los posibles movimientos del individuo a partir de esta etapa y la edad de la muerte ya que no poseemos los terceros molares de tres de los cuatro humanos analizados. A su vez, dos de los individuos, podrían atribuirse a ambas zonas (Cuevas y Dólmenes): individuo 0739.sup.26 (medición realizada en el M2, S-UCT 18415) y el individuo 0739.sup.20 (medición realizada en el M2, S-UCT 18416). En el caso de este último, también tenemos los valores de su tercer molar (M3, S-UCT 18417), que se solapan exclusivamente con la “Zona Cuevas”. Este cambio en los valores de Sr de su esmalte podría estar indicando un movimiento desde las zonas más bajas de Tierra Bucho (en nuestro caso la Zona de los Dólmenes, ca. 870 m s.n.m.) a las zonas de montaña más altas, donde se encuentra la Cueva de los Cristales (1.320 m s.n.m.) (**Figura 1 y 2**).

Entre las cavidades cercanas a la Cueva de los Cristales, se ubica la Cueva Drólica (ca. 1.200 m s.n.m.), localizadas a unos centenares de metros la una de la otra. A diferencia de Cueva de los Cristales, cuya función es exclusivamente funeraria, Cueva Drólica presenta niveles de habitación que son contemporáneos al uso funerario de Cueva de los Cristales (**Tabla 1**). También aparecieron en ella algunos restos humanos, pero hasta el momento todos ellos datan de una cronología más avanzada. Cabe destacar que en Cueva Drólica apareció un gran vaso campaniforme cuyas dimensiones apuntan a su uso como recipiente de almacenaje ([Montes y Martínez Bea, 2006](#)). Por el contrario, en Cueva de los Cristales solo se encontraron escasos fragmentos de cerámica lisos, sin decoración campaniforme, muchas veces asociada a contextos funerarios ([Blasco, 2007](#)).

El hecho de encontrar una cueva con niveles de habitación y no exclusivamente funerarios apoyaría la hipótesis sobre la existencia de estancias más o menos largas en la zona. La montaña cuenta con los recursos suficientes, aunque quizás las condiciones climáticas no parezcan las idóneas. Aunque las ocupaciones no fueran permanentes, el hecho de que los

esmaltes marquen la señal de Sr de estas zonas y no de las más bajas del Prepireneo nos indica que la conexión con las zonas más altas sería muy frecuente. Por el contrario, ninguno de los individuos analizados presenta valores de Sr que sobrepasen a los valores de Sr biodisponible en las Sierra prepirenaicas, lo que nos hace descartar, con cierta seguridad, un poblamiento de larga estancia en las zonas más altas del Pirineo (superando los 1.500 m s.n.m.), dominada por la presencia de estratos geológicos más antiguos y, por tanto, con valores de Sr potencialmente más elevados (Bentley, 2006) (Figura 3).

Como ya hemos visto, varias zonas del Prepireneo comparten unos valores de Sr comunes, por lo que no podemos descartar una procedencia diferente de los individuos. Por ello, es necesario siempre complementar los estudios isotópicos con los datos arqueológicos disponibles. Basándose en los datos arqueológicos proporcionados por los yacimientos, en Tierra Bucho se ha propuesto la presencia de movimientos anuales en altitud para aprovechar los pastos de los puertos inmediatos (Asba, Sevil) correspondientes con la denominada “Zona Dólmenes” (Montes *et al.*, 2016a y b). A su vez, se propone que podrían existir largas estancias centradas en Cueva Dróllica (“Zona Cuevas”), que serían aprovechadas por la cabaña ganadera del grupo, en un régimen de trasterminancia o trashumancia altitudinal, aprovechando no sólo las herbáceas como pasto, sino también la elevada producción de bellotas del quercetal de la época (Montes *et al.*, 2016a y b). El análisis en serie de esmalte de ovicápridos domésticos podría ayudarnos a resolver esta cuestión (Valenzuela-Lamas *et al.*, 2016), aunque *a priori*, la presencia de diferentes valores de Sr en el esmalte humano, así como valores intermedios entre ambas zonas, podría apoyar esta hipótesis.

En estudios futuros sería interesante comparar los datos de los individuos de los dólmenes cercanos de Capilleta, Caseta de las Balanzas y Pueyoril para ver si encontramos valores isotópicos compatibles con ambas zonas.

5. CONCLUSIONES

Se ha llevado a cabo un estudio de los valores biodisponibles de estroncio a lo largo del Prepireneo junto al análisis de estroncio del esmalte dental de los individuos calcolíticos recuperados en el yacimiento de la Cueva de los Cristales. Hemos comprobado que las zonas

más montañosas del Prepirineo muestran todas ellas unos valores similares. Por ello, no se ha podido determinar con precisión la zona de origen de los individuos. Aun así, dos individuos muestran valores inferiores que podrían corresponderse con zonas geológicas más recientes, como las que se encuentran más próximas al Valle del Ebro, donde dominan los depósitos cuaternarios, o las zonas más bajas del Prepirineo, donde dominan los depósitos del Eoceno, que muestran valores inferiores y conforman un relieve menos abrupto que el de las sierras Prepirenaicas.

Nuestros resultados sugieren que durante el Calcolítico habría comunidades habitando estos dos tipos de paisaje, ya que encontramos valores de Sr que son exclusivos de las zonas más montañosas y que no encontramos en las áreas más bajas del Prepirineo, aunque existirían movimientos entre unas y otras en distintas etapas de la vida. Ninguno de nuestros individuos presenta valores fuera del rango de la zonas dominada por depósitos Paleocenos, lo que nos hace descartar un poblamiento permanente de las zonas más altas del Pirineo, donde aparecen estratos geológicos más antiguos con valores de estroncio potencialmente más elevados.

AGRADECIMIENTOS

Queríamos transmitir las gracias a Izaskun Sarasketa y Fayrooza Ragoot por la ayuda y asistencia en el trabajo de laboratorio, a Rafael Laborda y Mario Gisbert por la ayuda en la localización de la cavidad, la recogida de muestras para el cálculo del Sr biodisponible de la zona de “Las Cuevas” y la realización de la topografía de la Cueva de los Cristales. Gracias también a Pilar Mouco por la ayuda en la recogida de muestras para Sr biodisponible en la zona de “Los Dólmenes” y a Rafael Domingo por la cesión de las fotografías. Este trabajo forma parte de la tesis doctoral de V. V-M. financiada con una beca predoctoral del Gobierno de Aragón y el Fondo Social Europeo (BOA20150701025) y ha realizado una estancia Predoctoral en la Universidad de Cape Town con la ayuda Económica de las Estancias de investigación de Ibercaja-CAI (2016), cuya supervisión y gastos asociados han corrido a cargo de D. C. S-G. L. M., M. B. y V. V-M forman parte del grupo de investigación (H-14: Primeros Pobladores del Valle del Ebro) y del proyecto (Gaps and Sites: Vacíos y ocupaciones en la Prehistoria de la Cuenca del Ebro) (ref.: HAR2017-85023-P).

BIBLIOGRAFÍA

- Alconchel, L. (2013) Paleoantropología del alto Vero en el Calcolítico: las cuevas Drólica y de los Cristales y el dolmen de la Caseta de las Balanzas. *Bolskan* 24, 27–38
- Alt, K. W., Zesch, S., Garrido-Pena, R., Knipper, C., Szécsényi-Nagy, A., Roth, C., Tejedor-Rodríguez, C., Held, P., García-Martínez-de-Lagrán, I., Navitainuck, D., Arcusa, H., Rojo-Guerra, M. A. (2016). A Community in Life and Death: The Late Neolithic Megalithic Tomb at Alto de Reinoso (Burgos, Spain). *PLOS ONE*, 11(1), e0146176.
- Aranda Jiménez, G., Lozano Medina, Á., Sánchez Romero, M., Díaz-Zorita Bonilla, M., & Bocherens, H. (2018). Chronology of Megalithic Funerary Practices in Southeastern Iberia: The Necropolis of Panoria (Granada, Spain). *Radiocarbon*, 60(1), 1–19. <https://doi.org/DOI: 10.1017/RDC.2017.96>
- Baldellou, V. (1987) Avance al estudio de la Espluga de la Puyascada. *Bolskan*, (4), 3–42.
- Britton, K., Grimes, V., Dau, J., & Richards, M. P. (2009). Reconstructing faunal migrations using intra-tooth sampling and strontium and oxygen isotope analyses: a case study of modern caribou (*Rangifer tarandus granti*). *Journal of Archaeological Science* 36(5), 1163-1172.
- Brothwell, D. R. (1993). Desenterrando huesos: la excavación, tratamiento y estudio de restos del esqueleto humano. FCE. Madrid.
- Bruzek, J. (2002). A method for visual determination of sex, using the human hip bone. *American Journal of Physical Anthropology* 117(2), 157–168.
- Budd, P., Montgomery, J., Barrierro, B., Thomas, R.G. (2000). Differential diagenesis of strontium in archaeological human dental tissues. *Applied Geochemistry* 15, 687–694.
- Copeland, S.R., Cawthra, H.C., Fisher, E.C., Lee-Thorp, J.A., Richard, M.C., le Roux, P.J., Hodgkins, J., Marean, C.W. (2016). Strontium isotope investigation of ungulate movement patterns on the pleistocene paleo-agulhas plain of the greater Cape floristic region, South Africa. *Quaternary Science Reviews* 141, 65–84.
- Copeland, S.R., Sponheimer, M., de Ruiter, D.J., Lee-Thorp, J.A., Codron, D., le Roux, P.J., Grimes, V., Richards, M.P., 2011. Strontium isotope evidence for landscape use by early hominins. *Nature* 474 (7349), 76–78.
- Gassiot Balbé, E., Julià Brugués, R., Rodríguez Antón, D., Bal-Serín, M.-C. Pèlach Mañosa, A., Mazzucco, N., Pérez Obiol, R. (2014). La alta montaña durante la Prehistoria: 10 años

- de investigación en el Pirineo catalán occidental. *Trabajos de Prehistoria*, 71(2), 261–281
- Bentley, R.A. (2006). Strontium isotopes from the earth to the archaeological skeleton: a review. *Journal of Archaeological Method and Theory* 13 (3), 135–187.
- Bentley, R.A. (2013). Mobility and the diversity of early Neolithic lives: isotopic evidence from skeletons. *Journal of Anthropological Archaeology* 32 (3), 303–312.
- Bentley, R.A., Price, T.D., Stephan, E. (2004). Determining the 'local' Sr-87/Sr-86 range for archaeological skeletons: a case study from Neolithic Europe. *Journal of Archaeological Science* 31 (4), 365–375.
- Blasco, C., Delibes, G., Baena, J., Liesau, C., Ríos, P. (2007). El poblado calcolítico de Camino de las Yeseras (San Fernando de Henares, Madrid): un escenario favorable para el estudio de la incidencia campaniforme en el interior peninsular. *Trabajos de Prehistoria*, 64(1), 151–163.
- Calvo, M. J., 1991a: Excavaciones en el dolmen de la Capilleta (Paules de Sarsa-Ainsa, Huesca). *Arqueología Aragonesa* 1986-1987, 89–90.
- Calvo, M. J., 1991b: Excavaciones en el dolmen de la Caseta de las Balanzas en Selva Grande (Almazorre-Bárcabo, Huesca), *Arqueología Aragonesa* 1986-1987, 87–88.
- Campillo, D., Subirà, M. E. (2004). Antropología física para arqueólogos. Ariel Prehistoria. Barcelona.
- Díaz-Zorita, M., 2014. The copper age. In: South-west Spain: a Bioarchaeological Approach to Prehistoric Social Organisation. Durham University, Durham (Doctoral thesis).
- Domingo, R., Alcolea, M., Bea, M., Mazo, C., Montes, L., Picazo, J., Rodanés, J.M., Utrilla, P. (2018). Call it home: Mesolithic dwellings in the Ebro Basin (NE Spain). *Journal of Archaeological Science: Reports*, 18, 1036–1052. <https://doi.org/https://doi.org/10.1016/j.jasrep.2017.12.034>
- Ericson, J.E. (1985). Strontium isotope characterization in the study of prehistoric human ecology. *Journal of Human Evolution* 14, 503–514.
- Fernández-Crespo, T. (2016). El papel del fuego en los enterramientos neolíticos finales/calcolíticos iniciales de los abrigos de la Sierra de Cantabria y sus estribaciones (valle medio-alto del Ebro). *Trabajos de Prehistoria*, 73(1), 128–146.
- Fernández-Crespo, T., de-la-Rúa, C. (2015). Demographic evidence of selective burial in megalithic graves of northern Spain. *Journal of Archaeological Science*, 53, 604–617.
- Fernández-Crespo, T., Mujika, J. A., Ordoño, J. (2017). Aproximación al patrón alimentario de

- los inhumados en la cista de la Edad del Bronce de Ondarre (Aralar, Guipúzcoa) a través del análisis de isótopos estables de carbono y nitrógeno sobre colágeno óseo. *Trabajos de Prehistoria*, 73(2), 325–334.
- Fernández-Crespo, T., Schulting, R. J. (2017). Living different lives: Early social differentiation identified through linking mortuary and isotopic variability in Late Neolithic/ Early Chalcolithic north-central Spain. *PLOS ONE*, 12(9), e0177881.
- Fernández-Eraso, J., Mujika-Alustiza, J. A. (2013). La estación megalítica de la Rioja Alavesa: Cronología, orígenes y ciclos de utilización/The megalithic station of the Rioja Alavesa: chronology, origins and utilisation cycles. *Zephyrus*, 71, 89-106.
- Fontanals-Coll, M., Díaz-Zorita Bonilla, M., Subirà, M. E. (2015). A Palaeodietary Study of Stable Isotope Analysis from a High-status Burial in the Copper Age: The Montelirio Megalithic Structure at Valencina de la Concepción–Castilleja de Guzmán, Spain. *International Journal of Osteoarchaeology*, 26(3), 447–459.
- García-Borja, P., Perez Fernandez, A., Biosca Cirujeda, V., Ribera i Gomes, A., Salazar-García, D.C., (2013). Los restos humanos de la Coveta del Frare (Font de la Figuera, Valencia). In: García-Borja, P., Revert, E., Ribera, A., Biosca, V. (Eds.), *El Naiximent d' un Poble. Historia i Arqueologia de la Font de la Figuera*, pp. 47–60. Ajuntament de la Font de la Figuera.
- González-Sampériz, P., Aranbarri, J., Pérez-Sanz, A., Gil-Romera, G., Moreno, A., Leunda, M., Sevilla-Callejo, M., Corella, J.P., Morellón, M., Oliva, B., Valero-Garcés, B. (2017). Environmental and climate change in the southern Central Pyrenees since the Last Glacial Maximum: A view from the lake records. *CATENA*, 149, 668–688.
- Rojo-Guerra, M., Peña-Chocarro, L., Royo, J. I., Tejedor, C., García-Martínez de Lagrán, I., Arcusa, H., Garrido-Pena, R., Moreno, M., Mazzucco, N., Gibaja, J.F., Ortega, D.; Kromer, B., Alt, K.W. (2013). Pastores trashumantes del Neolítico antiguo en un entorno de alta montaña: secuencia crono-cultural de la Cova de Els Trocs (San Feliú de Veri, Huesca). *BSAA Arqueología*, 79, 9–55.
- Guixé, E. G. (2009). Estudi paleoantropològic i paleopatològic del sepulcre col·lectiu de Forat de Conqueta (Santa Linya, Lleida). *Treballs d'arqueologia*, 17, 37–98.
- Haak, W., Brandt, G., de Jong, H. N., Meyer, C., Ganslmeier, R., Heyd, V., Hawkesworth, C., Pike, A. W. G., Meller, H., Alt, K. W. (2008). Ancient DNA, Strontium isotopes, and

- osteological analyses shed light on social and kinship organization of the Later Stone Age. *Proceedings of the National Academy of Sciences*, pnas-0807592105.
- Haak, W., Lazaridis, I., Patterson, N., Rohland, N., Mallick, S., Llamas, B., Brandt, G., Nordenfelt, S., Harney, E., Stewardson, K., Fu, Q., Mittnik, A., Bánffy, E., Economou, C., Francken, M., Friederich, S., Garrido Pena, R., Hallgren, F., Khartanovich, V., Khokhlov, A., Kunst, M., Kuznetsov, P., Meller, H., Mochalov, O., Moiseyev, V., Nicklisch, N., Pichler, S.L., Risch, R., Rojo Guerra, M.A., Roth, C., Szécsényi-Nagy, A., Wahl, J., Meyer, M., Krause, J., Brown, D., Anthony, D., Cooper, A., Alt, K.W., Reich, D. (2015). Massive migration from the steppe was a source for Indo-European languages in Europe. *Nature*, 522, 207.
- Hillson, S. (1996). *Dental Anthropology*. Cambridge University Press, Cambridge.
- Knipper, C., Mittnik, A., Massy, K., Kociumaka, C., Kucukkalipci, I., Maus, M., Wiitenborn, F., Metz, S. E., Staskiewicz, A., Krause, J., Stockhammer, P. W. (2017). Female exogamy and gene pool diversification at the transition from the Final Neolithic to the Early Bronze Age in central Europe. *Proceedings of the National Academy of Sciences*, 201706355.
- Laborda, R., Villalba-Mouco, V., Lanau, P., Gisbert, M., Sebastián, M., Domingo, R., Montes, L. (2017). El Puerto Bajo de Góriz (Parque Nacional de Ordesa y Monte Perdido). Ocupación y explotación de un paisaje de alta montaña desde la prehistoria hasta el siglo XX. *Bolskan*, (26), 9–30.
- López-Costas, O., Müldner, G., Martínez Cortizas, A. (2015). Diet and lifestyle in Bronze Age Northwest Spain: the collective burial of Cova do Santo. *Journal of Archaeological Science*, 55, 209–218.
- Lorenzo, J. I. (2014). Estudio antropológico de los restos de Forcas II. In: Utrilla P., Mazo, C. (Eds.), *La Peña de las Forcas (Graus, Huesca). Un asentamiento estratégico en la confluencia del Ésera y el Isábena. Monografías Arqueológicas/ Prehistoria 46, Universidad de Zaragoza, Zaragoza*, pp. 337–341.
- Martínez-Moreno, J., Mora, R., de la Torre, I. (2010). The Middle-to-upper Palaeolithic transition in Cova Gran (Catalunya, Spain) and the extinction of Neanderthals in the Iberian peninsula. *Journal of Human Evolution*, 58(3), 211–226.
- Gimeno, B. (2009). Estudio antropológico de la cueva sepulcral de Loarre. *Saldvie: Estudios de Prehistoria y Arqueología*, (9), 369–392.

- Mazzucco, N., Clemente-Conte, I., Baldellou, V., Gassiot Ballbè, E. (2013). The management of lithic resources during the V millennium cal BC at Espluga de la Puyascada (La Fueva, Huesca). *Preistoria Alpina* (47/1), 17–30.
- McClure, S. B., García, O., Roca de Togores, C., Culleton, B. J., Kennett, D. J. (2011). Osteological and paleodietary investigation of burials from Cova de la Pastora, Alicante, Spain. *Journal of Archaeological Science*, 38(2), 420–428.
- Montes, L., Martínez, Bea. (2006). El yacimiento campaniforme de Cueva Drólica (Sarsa de Surta, Huesca). *Saldvie* 6, 297–316.
- Montes, L., Domingo, R. (2001-2002). Epipaleolítico y Neolítico en las sierras exteriores de Aragón. Prospecciones, Sondeos y excavaciones 2001. *Saldvie* II, 323–336.
- Montes, L., Domingo, R. (2014). La ocupación de las Sierras Exteriores durante el Calcolítico. In: Utrilla P., Mazo, C. (Eds.), *La Peña de las Forcas (Graus, Huesca). Un asentamiento estratégico en la confluencia del Ésera y el Isábena. Monografías Arqueológicas/Prehistoria 46, Universidad de Zaragoza, Zaragoza* pp. 409–426.
- Montes, L., Bea, M., Domingo, R., Sánchez, P., Alcolea, M., Sebastián, M. (2016b). La gestión prehistórica de un territorio en la montaña Prepirenaica: Tierra Bucho (Huesca, España). *Munibe Antropologia-Arkeologia* 67, 349–362.
- Montes, L., Domingo, R., Sebastián, M., & Lanau, P. (2016a). ¿Construyendo un paisaje? Megalitos, arte esquemático y cabañeras en el Pirineo central. *ARPI, 04 Extra* (Homenaje a R. de Balbín Behrmann), 248–263.
- Mora, R., Martínez-Moreno, J., Casanova, J. (2008). Abordando la noción de “variabilidad musterense” en Roca dels Bous (Prepireneo suroriental, Lleida). *Trabajos de Prehistoria*, 65(2), 13–28.
- Olalde, I., Brace, S., Allentoft, M. E., Armit, I., Kristiansen, K., Booth, T., Rohland, N., Mallick, S., Szécsényi-Nagy, A., Mittnik, A., Altena, E., Lipson, M., Lazaridis, I., Harper, T.K., Patterson, N.J., Broomandkoshbacht, N., Diekmann, Y., Faltyskova, Z., Fernandes, D.M., Ferry, M., Harney, E., de Knijff, P., Michel, M., Oppenheimer, J., Stewardson, K., Barclay, A., Alt, K.W., Liseau, C., Ríos, P., Blasco, C., Vega Miguel, J., Menduiña García, R., Avilés Fernández, A., Bánffy, E., Bernabò-Brea, M., Billoin, D., Bonsall, C., Bonsall, L., Allen, T., Büster, L., Carver, S., Castells Navarro, L., Craig, O.E., Cook, G.T., Cunliffe, B., Denaire, A., Dinwiddy, K.E., Dodwell, N., Ernée, M., Evans, C., Kuchařík, M., Farré, J.F., Fowler, C., Gazenbeek, M., Garrido Pena, R., Haber-Uriarte, M., Haduch, E., Hey, G., Jowett, N., Knowles, T., Massy, K., Pfrengle,

- S., Lefranc, P., Lemercier, O., Lefebvre, A., Heras, C., Galera, V., Bastida, A., Lomba, J., Majó, T., McKinley, J.I., McSweeney, K., Gusztáv, M.B., Modi, A., Kulcsár, G., Kiss, V., Czene, A., Patay, R., Endródi, A., Köhler, K., Hajdu, T., Szeniczey, T., Dani, J., Bernert, Z., Hoole, M., Cheronet, O., Velemnský, P., Dobeš, M., Candilio, F., Brown, F., Flores, R., Herrero-Corral, A.M., Tusa, S., Carnieri, E., Lentini, L., Valenti, A., Zazini, A., Waddington, C., Delibes, G., Guerra-Doce, E., Neil, B., Brittain, M., Luke, M., Mortimer, R., Desideri, J., Besse, M., Brüken, G., Furmanek, M., Haluszko, A., Mackiewicz, M., Rapiński, A., Leach, S., Soriano, I., Lillios, K.T., Cardoso, J.L., Pearson, M.P., Włodarczak, P., Price, T.D., Prieto, P., Rey, P.J., Risch, R., Rojo Guerra, M.A., Schmitt, A., Serralongue, J., Silva, A.M., Smrčka, V., Vergnaud, L., Zilhão, J., Caramelli, D., Higham, T., Thomas, M.G., Kennett, D.J., Fokkens, H., Heyd, V., Sheridan, J.A., Sjögren, K.G., Stockhammer, P.W., Krause, J., Pinhasi, R., Haak, W., Barnes, I., Lalueza-Fox, C., Reich, D. (2018) The Beaker phenomenon and the genomic transformation of Northwest Europe. *Nature* 555:190–196
- Ortner D.J. 2003. Identification of Pathological Conditions in Human Skeletal Remains. Academic Press, San Diego.
- Pérez-Romero, A., Iriarte, E., Galindo-Pellicena, M. A., García-González, R., Rodríguez, L., Castilla, M., Francés-Negro, M., Santos, E., Valdiosera, C., Arsuaga, J. L., Alday, A., Carretero, J. M. (2017) An unusual Pre-Bell Beaker copper age cave burial context from El Portalón de Cueva Mayor site (Sierra de Atapuerca, Burgos). *Quaternary International* 433,142–155.
- Pin, C., Briot, D., Bassin, C., Poitrasson, F. (1994). Concomitant separation of strontium and samarium-neodymium for isotopic analysis in silicate samples, based on specific extraction chromatography. *Analytica Chimica Acta* 298 (2), 209–217.
- Price, T.D., Bentley, R.A., Gronenborn, D., Lüning, J., Wahl, J. (2001). Human migration in the linearbandkeramik of central europe. *Antiquity* 75, 593–603.
- Price, T.D., Burton, J.H., Bentley, R.A. (2002). The characterization of biologically available strontium isotope ratios for the study of prehistoric migration. *Archaeometry* 44 (1), 117–135.
- Salazar García, D. C. (2011). Aproximación a la dieta de la población calcolítica de La Vital a través del análisis de isótopos estables del carbono y del nitrógeno sobre restos óseos. In: Pérez G, Bernabeu J, Carrión Y, García- Puchol O, Molina LL, Gómez M (Eds.),

- Vida y muerte en la desembocadura del Serpis durante el III y el I milenio a.C. Museu de Prehistòria de València- Diputació de Valencia (T.V. 113)*, València, pp. 139–149.
- Salazar-García, D.C., (2012). Isótopos, dieta y movilidad en el País Valenciano. Aplicación a restos humanos del Paleolítico medio al Neolítico final. Universitat de València, Valencia (Tesis Doctoral).
- Salazar-García, D.C., (2014). Estudi de la dieta en la població de Cova dels Diablets mitjançant anàlisi d'isòtops estables del carboni i del nitrogen en col·lagen ossi. Resultats preliminars. In: Aguilera Arzo, G.A., Monroig, D., García-Borja, P. (Eds.), *La Cova dels Diablets (Alcalà de Xivert, Castelló). Prehistòria a la Serra d'Irta*. Diputació de la Castelló, Castellón, pp. 67–78.
- Salazar-García, D.C., García-Puchol, O., de Miguel-Ibañez, M.P., Talamo, S., (2016). Earliest evidence of neolithic collective burials from Eastern Iberia: radiocarbon dating at the archaeological site of Les Llometes (Alicante, Spain). *Radiocarbon* 58 (3), 679–692.
- Sarasketa-Gartzia, I., Villalba-Mouco, V., le Roux, P., Arrizabalaga, Á., Salazar-García, D. C. (2018). Late Neolithic-Chalcolithic socio-economical dynamics in Northern Iberia. A multi-isotope study on diet and provenance from Santimamiñe and Pico Ramos archaeological sites (Basque Country, Spain). *Quaternary International* 481, 14–27.
- Sarasketa-Gartzia, I., Villalba-Mouco, V., Le Roux, P., Arrizabalaga, Á., & Salazar-García, D. C. (2018). Anthropogenic resource exploitation and use of the territory at the onset of social complexity in the Neolithic-Chalcolithic Western Pyrenees: a multi-isotope approach. *Archaeological and Anthropological Sciences*. <https://doi.org/10.1007/s12520-018-0678-7>
- Schuhmacher, T. X., Banerjee, A. (2012). Procedencia e intercambio de marfil en el Calcolítico de la Península Ibérica. *Rubricatum: Revista Del Museu de Gavà*, (5), 289–298.
- Sjögren, K.G., Price, T.D., Kristiansen, K. (2016). Diet and mobility in the Corded Ware of Central Europe. *PloS one*, 11(5), e0155083.
- Szécsényi-Nagy, A., Roth, C., Brandt, G., Rihuete-Herrada, C., Tejedor-Rodríguez, C., Held, P., García-Martínez-de-Lagrán, I., Arcusa Magallón, H., Zesch, S., Knipper, C., Bánffy, E., Friederich, S., Meller, H., Bueno, P., Barroso, R., Balbín, R., Herrero-Corral, A.M., Flores, R., Alonso, C., Jiménez, J., Rindlisbacher, L., Oliart, C., Fregeiro, M.I., Soriano, I., Vicente, O., Micó, R., Lull, V., Soler, J., López, J.A., Roca de Togores, C., Hernández, M.S., Jover, F.J., Lomba, J., Avilés, A., Lillios, K.T., Silva, A.M., Magalhães, M., Oosterbeek, L.M.,

- Cunha, C., Waterman, A.J., Roig, J., Martínez, A., Ponce, J., Hunt, M., Mejías-García, J.C., Carlos Pecero, J.C., Cruz-Auñón, R., Tomé, T., Carmona, E., Cardoso, J.L., Araújo, A.C., Liesau von Lettow-Vorbeck, C., Blasco, C., Ríos, P., Pujante, A., Royo-Guillén, J.I., Esquembre, M.A., Dos Santos, V.M., Parreira, R., Morán, E., Méndez, E., Vega y Miguel, J., Mendiña, R., Martínez, V., López, O., Krause, J., Pichlerf, S.L., Garrido-Pena, R., Kunst, M., Risch, R., Rojo-Guerra, M.A., Haak, W., Alt, K.W. (2017) The maternal genetic make-up of the Iberian Peninsula between the Neolithic and the Early Bronze Age. *Scientific Reports*, 7(1), 15644.
- Ubelaker, D. (1978). Human skeletal remains. Excavation, analysis, interpretation. Chicago, IL: Aldine.
- Utrilla, P., Laborda, R. (2018). La Cueva de Chaves (Bastaras, Huesca), el gran lugar de habitat del prepirineo: 15000 años de ocupación. *Trabajos de Prehistoria*, 1–22.
- Utrilla, P., Mazo, C., Domingo, R. (2015). Fifty thousand years of prehistory at the cave of Abauntz (Arraitz, Navarre): a nexus point between the Ebro Valley, Aquitaine and the Cantabrian corridor. *Quaternary International*, 364, 294–305.
- Utrilla, P., Montes, L., Fernanda, B., Torres Pérez-Hidalgo, T. J., Ortiz Menéndez, J. E. (2010). La cueva de Gabasa revisada 15 años después: un cubil para las hienas y un cazadero para los Neandertales. *Zona Arqueológica*, (13), 376–389.
- Valenzuela-Lamas, S., Jimenez-Manchon, S., Evans, J., Lopez, D., Jornet, R., Albarella, U., (2016). Analysis of seasonal mobility of sheep in Iron Age Catalonia (north-eastern Spain) based on strontium and oxygen isotope analysis from tooth enamel: first results. *Journal of Archaeological Science: Reports* 6, 828–836.
- Villalba-Mouco, V., Martínez-labarga, C., Utrilla, P., Laborda, R., Ignacio, J., Salazar-garcía, D. C. (2018b). Reconstruction of human subsistence and husbandry strategies from the Iberian Early Neolithic: A stable isotope approach. *American Journal of Physical Anthropology* 167 (2), 257–271.
- Villalba-Mouco, V., Sarasketa-Gartzia, I., Utrilla, P., Oms, F. X., Mazo, C., Mendiola, S., Cebriá, A. Salazar-García, D. C. (2018a). Stable isotope ratio analysis of bone collagen as indicator of different dietary habits and environmental conditions in northeastern Iberia during the 4th and 3rd millennium cal B.C. *Archaeological and Anthropological Sciences*. <https://doi.org/10.1007/s12520-018-0657-z>
- Villalba-Mouco, V., Sauqué, V., Sarasketa-Gartzia, I., Pastor, M. V., le Roux, P. J., Vicente, D.,

Utrilla, P., Salazar-García, D. C. (2018c). Territorial mobility and subsistence strategies during the Ebro Basin Late Neolithic-Chalcolithic: A multi-isotope approach from San Juan cave (Loarre, Spain). *Quaternary International* 481, 28–41.

Waterman, A. J., Tykot, R. H., Silva, A. M. (2015). Stable Isotope Analysis of Diet-based Social Differentiation at Late Prehistoric Collective Burials in South-Western Portugal. *Archaeometry*, 58(1), 131–151.

FIGURAS Y TABLAS



Figura 1: a) Zona de Tierra Bucho en la que se localiza de la Cueva de los Cristales y otros yacimientos que aparecen citados en el texto, en una vista oblicua a partir de Google Earth (Montes *et al.*, 2016b) (nota: la escala es variable debido a la vista oblicua de la imagen). b) Fotografía de la Cueva de los Cristales y su entorno (Fotografía tomada por R. Domingo).

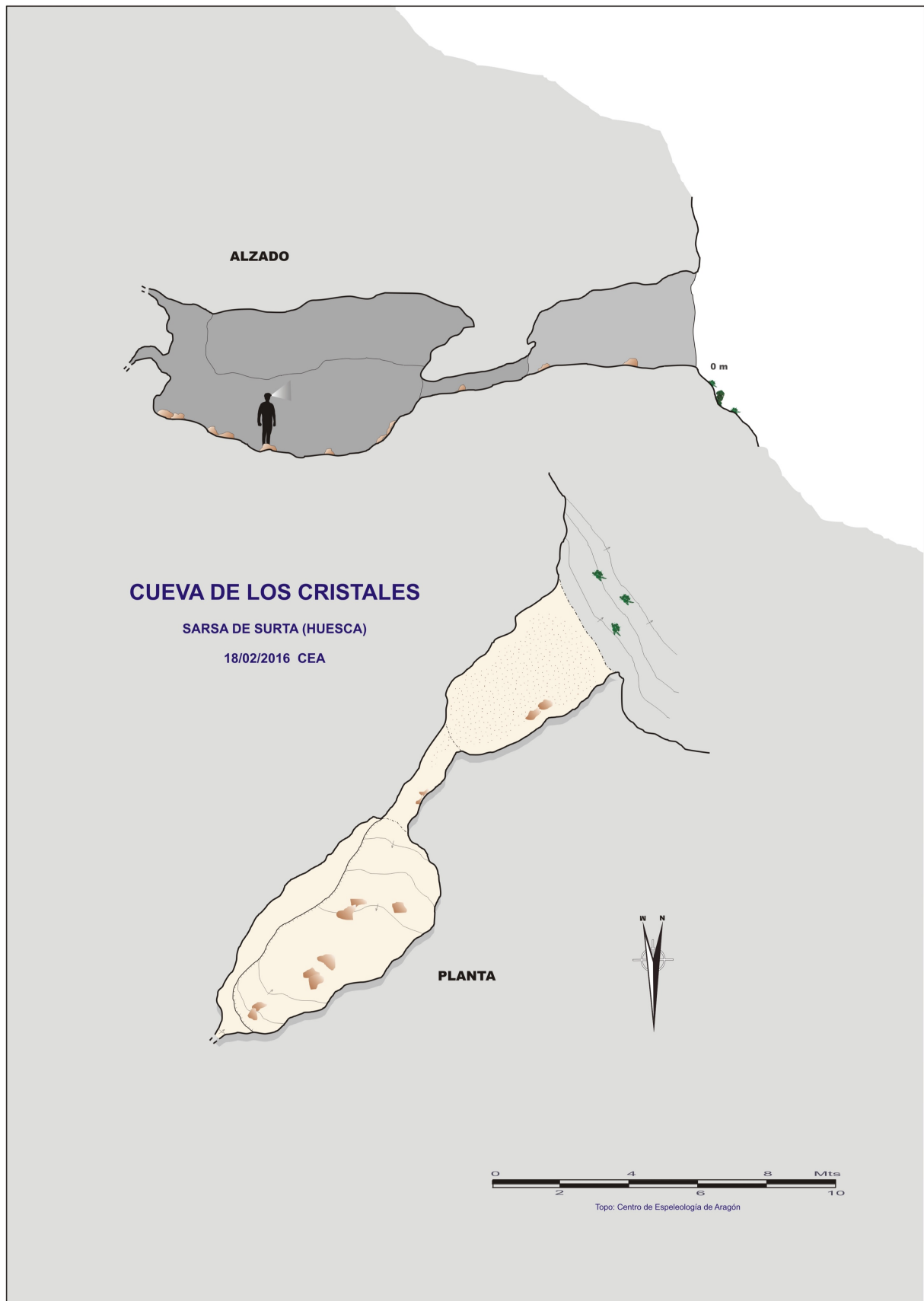
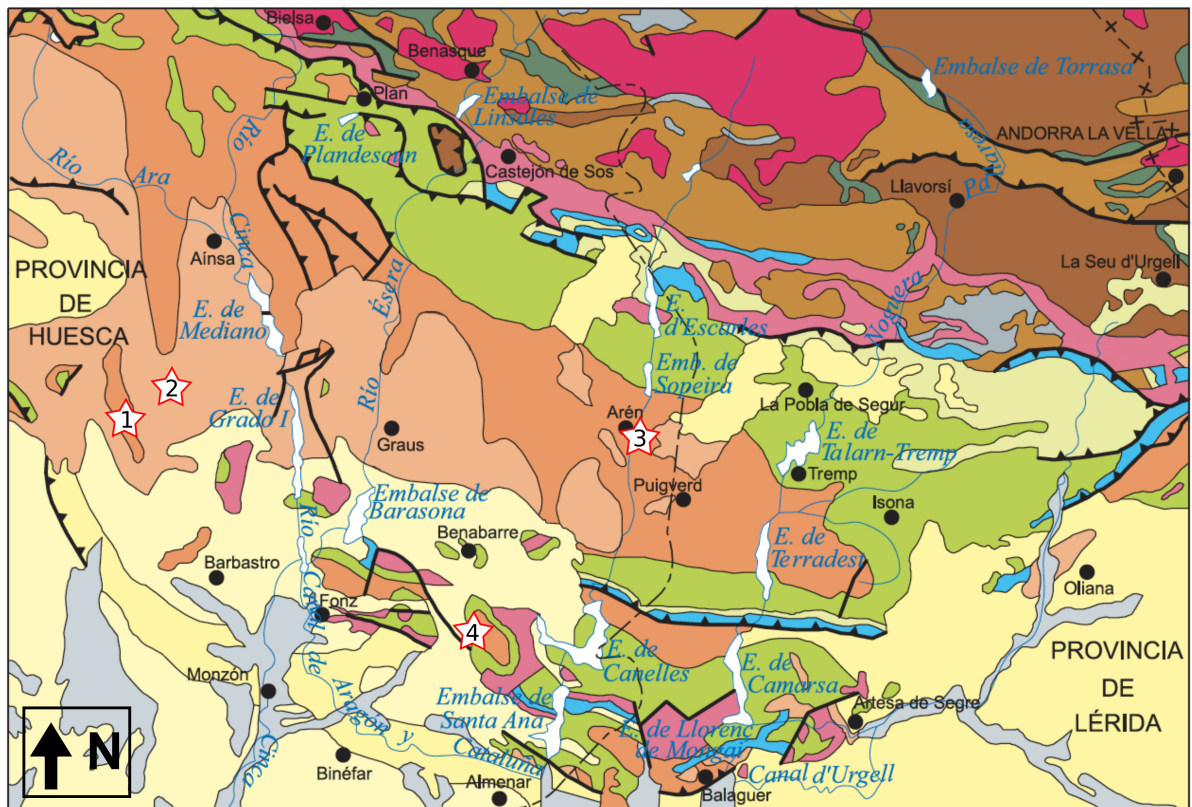


Figura 2: Topografía de la Cueva de los Cristales, mostrando el vestíbulo y la cámara interior, unidas por un reducido conducto.



Escala 1:1.000.000

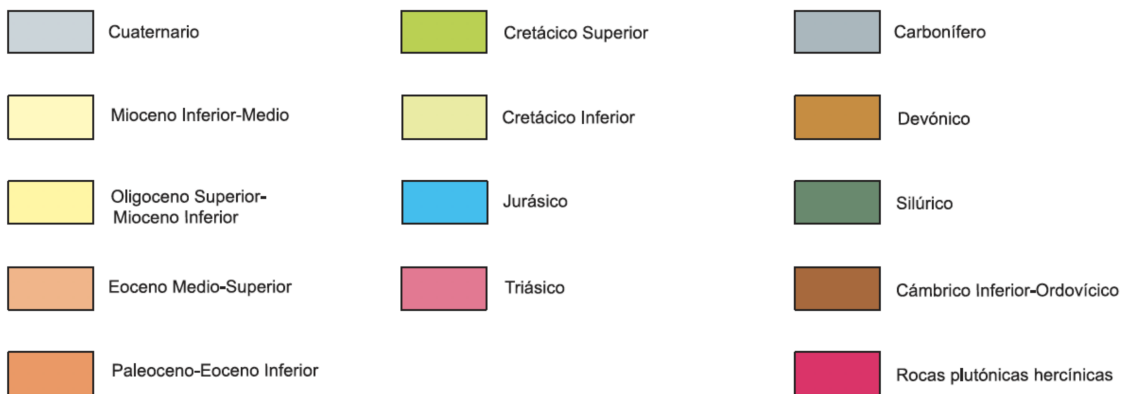


Figura 3: Lugares de mapeo de estroncio biodisponible señalados con estrellas en el mapa geológico simplificado y extraído de Instituto Geológico y Minero de España (IGME): 1) “Zona Cuevas” (Cueva de los Cristales y Cueva Dróica), 2) “Zona Dólmenes” (Dolmen de la Capilleta, Caseta de las Balanzas y Pueyoril) 3) Entorno de la localidad de Arén, y 4) Entorno de la localidad de Gabasa.

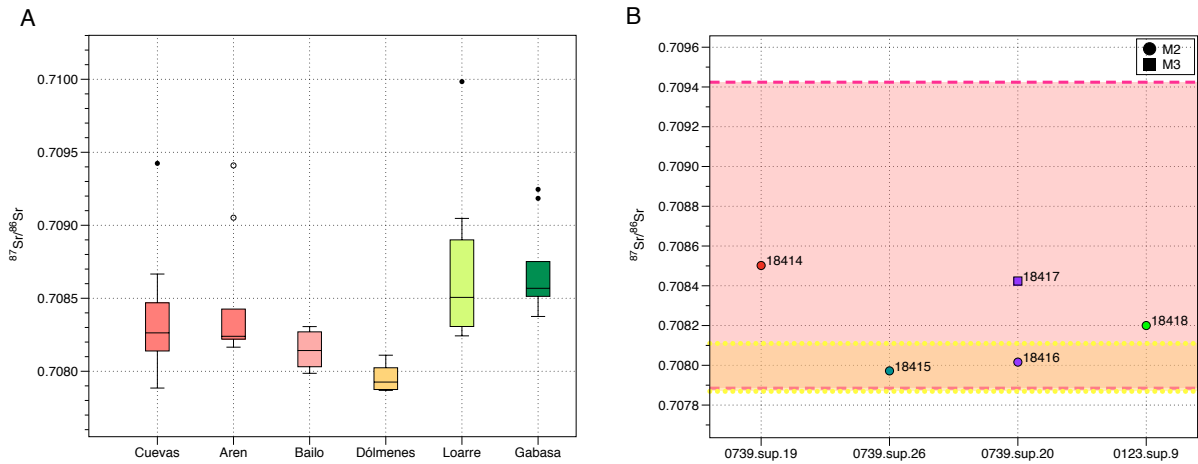


Figura 4: a) Valores biodisponibles calculados a partir de plantas y caracoles actuales. “Cuevas” y “Arén”: Paleoceno-Eoceno Inferior; “Bailo”: Oligoceno Superior-Mioceno Inferior; “Dólmenes”: Eoceno Medio-Superior; “Loarre”: Cretácico-Mioceno; y “Gabasa”: Paleoceno-Cretácico Superior. Los valores de la Cueva de San Juan de Loarre también incluyen esmalte de microvertebrados y aparecen publicados junto a los de Bailo en [Villalba-Mouco et al., 2018c](#). b) Valores de Sr en esmalte humano proyectados sobre el rango de los valores de Sr biodisponible de las dos zonas principales de estudio (Paleoceno-Eoceno Inferior: Zona Cuevas, color rosa delimitado por líneas discontinuas; Eoceno Medio-Superior: Zona Dólmenes, color naranja delimitado por puntos amarillos). Los círculos se corresponden con los valores de Sr medidos sobre el M2 y los cuadrados sobre el M3. Cada color representa un individuo.

Yacimiento	Muestra	Ref. Laboratorio	Fecha Laboratorio	Fecha Cal BC (2σ)	Publicación
Cueva Drólica (nivel ocupación a)	Carbón	GrN-30996	3790 ± 60	2457-2038	Montes y Martínez Bea, 2006
Cueva Drólica (nivel ocupación a)	Carbón	GrA-25757	3830 ± 45	2460-2146	Montes y Martínez Bea, 2006
Cueva Drólica (nivel ocupación a)	Carbón	GrA-33936	3975 ± 35	2579-2349	Montes y Martínez Bea, 2006
Cueva Drólica (nivel ocupación a)	Carbón	GrA-33935	4000 ± 35	2619-2462	Montes y Martínez Bea, 2006
Cueva Drólica (nivel ocupación a)	Carbón	GrA-38063	4105 ± 30	2864-2506	Montes y Martínez Bea, 2006
Cueva de los Cristales	Hueso humano	GrN-26967	3900 ± 100	2834-2041	Montes et al., 2016b.
Cueva de los Cristales	Hueso humano	GrA-38062	4121 ± 30	2867-2581	Montes et al., 2016b.
Cueva de los Cristales	Hueso humano	GrA-38061	4370 ± 30	3089-2907	Montes et al., 2016b
Dolmen de la Capilleta	Hueso humano	GrN-16051	4360 ± 35	3089-2901	Calvo, 1991a
Dolmen de Caseta de las Balanzas	Hueso humano	GrN-16052	3795 ± 35	2397-2061	Calvo, 1991b

Tabla 1: Fechas radiocarbónicas calibradas a 2 σ de los yacimientos localizados en la zona conocida como Tierra Bucho donde se encuentran los yacimientos de la Cueva de los Cristales, Cueva Drólica, Dolmen de la Capilleta y Dolmen de Caseta de las Balanzas. De Cueva Drólica solo aparecen las dataciones de los niveles de ocupación calcolíticos.

S-UCT (código de laboratorio)	Tipo de muestra/ Especie	Depósito geológico	Zona muestreada	$^{87}\text{Sr}/^{86}\text{Sr}$
18297	<i>Helix</i> sp.	Paleoceno-Eoceno Inferior	Cuevas (Drólica y Cristales)	0,708023
18298	<i>Helix</i> sp.	Paleoceno-Eoceno Inferior	Cuevas (Drólica y Cristales)	0,708139
18299	<i>Helix</i> sp.	Paleoceno-Eoceno Inferior	Cuevas (Drólica y Cristales)	0,708286
18300	<i>Helix</i> sp.	Paleoceno-Eoceno Inferior	Cuevas (Drólica y Cristales)	0,708155
18301	<i>Helix</i> sp.	Paleoceno-Eoceno Inferior	Cuevas (Drólica y Cristales)	0,707885
18133	Herbácea	Paleoceno-Eoceno Inferior	Cuevas (Drólica y Cristales)	0,708666
18134	<i>Buxus sempervirens</i>	Paleoceno-Eoceno Inferior	Cuevas (Drólica y Cristales)	0,708469
18135	<i>Quercus</i> sp.	Paleoceno-Eoceno Inferior	Cuevas (Drólica y Cristales)	0,709424
18136	<i>Buxus sempervirens</i>	Paleoceno-Eoceno Inferior	Cuevas (Drólica y Cristales)	0,708240
18137	<i>Abies</i> sp.	Paleoceno-Eoceno Inferior	Cuevas (Drólica y Cristales)	0,708465
18302	<i>Helix</i> sp.	Eoceno Medio- Superior	Dólmenes	0,707875
18303	<i>Helix</i> sp.	Eoceno Medio- Superior	Dólmenes	0,707932
18304	<i>Helix</i> sp.	Eoceno Medio- Superior	Dólmenes	0,707869
18305	<i>Helix</i> sp.	Eoceno Medio- Superior	Dólmenes	0,707891
18306	<i>Helix</i> sp.	Eoceno Medio- Superior	Dólmenes	0,707870

		Superior		
18138	<i>Buxus sempervirens</i>	Eoceno Medio-Superior	Dólmenes	0.708024
18139	<i>Pinus sp.</i>	Eoceno Medio-Superior	Dólmenes	0,708095
18140	<i>Juniperus sp.</i>	Eoceno Medio-Superior	Dólmenes	0,708018
18141	Herbácea	Eoceno Medio-Superior	Dólmenes	0,708110
18142	<i>Quercus sp.</i>	Eoceno Medio-Superior	Dólmenes	0,707920
18312	<i>Helix sp.</i>	Paleoceno-Eoceno Inferior	Arén	0,708230
18313	<i>Helix sp.</i>	Paleoceno-Eoceno Inferior	Arén	0,708165
18314	<i>Helix sp.</i>	Paleoceno-Eoceno Inferior	Arén	0,708392
18315	<i>Helix sp.</i>	Paleoceno-Eoceno Inferior	Arén	0,708219
18316	<i>Helix sp.</i>	Paleoceno-Eoceno Inferior	Arén	0,708220
18148	<i>Quercus sp.</i>	Paleoceno-Eoceno Inferior	Arén	0,709052
18149	<i>Buxus sempervirens</i>	Paleoceno-Eoceno Inferior	Arén	0,708426
18150	<i>Quercus sp.</i>	Paleoceno-Eoceno Inferior	Arén	0,708233
18151	<i>Buxus sempervirens</i>	Paleoceno-Eoceno Inferior	Arén	0,708246
18152	Herbácea	Paleoceno-Eoceno Inferior	Arén	0,709410
18287	<i>Helix sp.</i>	Paleoceno-	Gabasa	0,708476

		Cretácico Superior		
18288	<i>Helix</i> sp.	Paleoceno- Cretácico Superior	Gabasa	0,708513
18289	<i>Helix</i> sp.	Paleoceno- Cretácico Superior	Gabasa	0,708375
18290	<i>Helix</i> sp.	Paleoceno- Cretácico Superior	Gabasa	0,708530
18291	<i>Helix</i> sp.	Paleoceno- Cretácico Superior	Gabasa	0,708555
18123	<i>Quercus</i> sp.	Paleoceno- Cretácico Superior	Gabasa	0,709246
18124	<i>Buxus sempervirens</i>	Paleoceno- Cretácico Superior	Gabasa	0,709184
18125	<i>Juniperus</i> sp.	Paleoceno- Cretácico Superior	Gabasa	0,708657
18126	<i>Rosmarinus officinalis</i>	Paleoceno- Cretácico Superior	Gabasa	0,708582
18127	Herbácea	Paleoceno- Cretácico Superior	Gabasa	0,708751

Tabla 2: Muestras actuales analizadas, zona geológica y valores de $^{87}\text{Sr}/^{86}\text{Sr}$ para cada una de ellas.

S-UCT (código de laboratorio)	Sigla arqueológica	Edad	Diente muestreado	$^{87}\text{Sr}/^{86}\text{Sr}$	Concentración Sr (ppm)
18414	0739.sup.1P	Subadult	M2	0,708502	246,4
18415	0739.sup.26	Adult	M2	0,707972	191,5
18416	0739.sup.20	Adult	M2	0,708016	146,4
18417	0739.sup.20	Adult	M3	0,708424	87,06
18418	0123.sup.9	Adult	M2	0,708200	113,0

Tabla 3: Valores de $^{87}\text{Sr}/^{86}\text{Sr}$ y concentración de Sr de cada muestra de esmalte dental humano con su correspondiente sigla arqueológica y código de laboratorio.

10.5 Use and reuse of funerary spaces. Strontium isotopes and bayesian radiocarbon modelling to approach Late Neolithic/Chalcolithic funerary behaviour in Northern Iberia

Use and reuse of funerary spaces. Strontium isotopes and bayesian radiocarbon modelling to approach Late Neolithic/Chalcolithic funerary behaviour in Northern Iberia.

Vanessa Villalba-Mouco^{1}, Pilar Utrilla¹, Izaskun Sarasketa-Gartzia², Carlos Mazo¹, Domingo C. Salazar-García^{3,4}*

¹ *Grupo Primeros Pobladores del Valle del Ebro (PPVE), Instituto de Investigación en Ciencias Ambientales (IUCA), Universidad de Zaragoza, Pedro Cerbuna 12, 50009, Zaragoza. Spain.*

² *Departamento de Geografía, Prehistoria y Arqueología. Universidad del País Vasco-Euskal Herriko Unibertsitatea. C/Francisco Tomás y Valiente s/n. 01006, Vitoria-Gasteiz. Spain.*

³ *Grupo de Investigación en Prehistoria IT-622-13 (UPV-EHU)/IKERBASQUE-Basque Foundation for Science (Vitoria, Spain)*

³ *Department of Geological Sciences. University of Cape Town (Cape Town, South Africa).*

Abstract

Chalcolithic period is poorly understood in Northern Iberia due to the scarce presence of excavated settlements. In this area, the evidences to approach the Chalcolithic period mainly come from the study of the collective funerary structures. In this sense, the term Late Neolithic-Chalcolithic is commonly accepted to define a common period when the people were buried together, without evidence of disruptions in time nor culture along the 4th to 3rd millennium cal B.C.

To study this potential transition and the use of these collective funerary enclosures, here we apply Bayesian radiocarbon modelling together with the study of human enamel strontium isotopes to shed light on time use and provenance of the people. Human samples analysed come from Cueva de Abauntz, a Late Neolithic-Chalcolithic burial cave located in the North of Iberia. In total, 16 radiocarbon dates, together with 44 strontium isotope analyses in human

dental enamel, were performed. The results have allowed us to identify two burial phases inside the cavity and three different geological areas of individual provenance, showing the earlier individuals the highest proportion of local values. Our results could be in agreement with the increase of the usage of the sepulchral cave, being non-local people added through time. This study shows that the application of strontium isotope analysis together with radiocarbon dates can shed light on population changes and funerary uses during the Late Neolithic-Chalcolithic periods in Northern Iberia.

Keywords: Burial caves, Mobility, Provenance, Bayesian model, Incineration, Cueva de Abauntz.

1. INTRODUCTION

Iberian Late Neolithic and Chalcolithic periods are characterized by the presence of a high number of burials where people were usually buried together in shared spaces, caves ([Fernández-Crespo, 2016](#); [Villalba-Mouco et al., 2018](#)) or megalithic structures (e.g. [Andrés, 2005](#); [Alt et al., 2015](#); [Fernández-Crespo and de la Rúa, 2015](#)). Despite the amount of human remains are higher than for the rest of prehistoric periods, the information that we have about the transition between the Late Neolithic and the Chalcolithic periods is scarce and partially divided between the South and North of Iberia.

The beginning of the Iberian Chalcolithic is classically represented by the Millares Culture, which spreads along the South of Iberia ([Micó, 1995](#); [Almagro and Arribas, 1963](#)). This new culture represents a clear change, with the presence of the first fortified settlements ([Esquivel and Navas, 2007](#)) and the consolidation of copper metallurgy ([Nocete et al., 2011](#)). Contrary, the beginning of the Chalcolithic period in Northern Iberia is poorly understood due to the scarce presence of excavated settlements, all of them concentrated along the Iberian Central Plateau ([Delibes et al., 1995](#); [Blasco et al., 2007](#)). Most of the information in this area comes from burial structures, which are not always a clear reflection of the many cultural and economic aspects of society. Moreover, the Neolithic-Chalcolithic transition could be archaeologically questionable because of the continued occupation of some Late Neolithic settlements ([Bernabeu et al., 2003](#); [Blasco et al., 2007](#); [Rojo et al., 2008](#)). This continuity is also

perceptible in most of these collective burials, where the radiocarbon dates show a sustained use since 4th to 3rd millennium cal B.C. (Salazar-García et al., 2016; Utrilla et al., 2015, Villalba-Mouco et al., 2017; Fernández-Crespo, 2016) (**Figure 1**). Furthermore, stable isotope analysis (e.g. García-Borja et al., 2013; McClure et al., 2011, Salazar-García 2012 and 2014, Salazar-García et al., 2018, Villalba-Mouco et al., 2018; Waterman et al., 2016 and 2017) and DNA studies (Alt et al., 2016, Szécsényi-Nagy et al., 2017; Olalde et al., 2017) neither shed light on this transitional period, showing an homogeneity during the Late Neolithic and the Chalcolithic.

To study this potential transition and the use of these collective funerary enclosures, here we apply radiocarbon Bayesian modelling based on the archaeological information together with strontium isotope analysis to address on time of use of the burial caves and provenance of the people buried in shared spaces along the 4th to 3rd millennium cal B.C. Here we analyse the individuals of the Northern Iberian Late Neolithic-Chalcolithic burial cave Cueva de Abauntz (**Figure 1**). Contrary to what happens with carbon and nitrogen stable isotope analysis, strontium isotope analyses are scarce in Iberia (Alt et al., 2016; Díaz-del-Río et al., 2017; Sarasketa-Gartzia et al., 2018; Villalba-Mouco et al., 2018; Díaz-Zorita et al., 2014; Waterman et al., 2014), probably due to the higher cost of the analyses and the necessity of working in *clean laboratories*. The same problematic issue happens with radiocarbon dates, whose price is high for dating all the individuals recovered from these crowded funerary enclosures. In this context, we usually find a single or reduced set of radiocarbon dates or old date methods, without AMS and/or dates from bone aggregates or long-life samples, which present a high deviation and less precision (e.g. Apellániz, 1974, Baldeón et al. 1983, Fernandez Eraso, 1997, 2003).

1.1 $^{87}\text{Sr}/^{86}\text{Sr}$ isotopes from tooth enamel and their use in individual mobility studies

Strontium isotope ratios ($^{87}\text{Sr}/^{86}\text{Sr}$) of tooth enamel can provide insight on the use of the territory by tracking individual mobility (Bentley, 2013), understanding mobility as temporal or permanent territorial movements of individuals for an unknown reason. In this sense, $^{87}\text{Sr}/^{86}\text{Sr}$ have proved to be useful in many archaeological issues which involve human or animal displacements: livestock mobility patterns and transhumance activities (e.g.

Valenzuela-Lamas et al., 2016), seasonal mobility of wild species (e.g. Britton et al., 2009 and 2011; Copeland et al., 2016) and female exogamy in hominins and prehistoric cultures (e.g. Copeland et al., 2011; Haak et al., 2008; Knipper et al., 2017).

Strontium isotopes do not show isotopic fractionation when incorporated through the foodweb through the water, plants and animals, including human tissues. Human enamel, contrary to what happens in bones, is formed during childhood or early adulthood (depending on the tooth) and does not show remodelling during the individual's life (Bentley, 2006). On the other hand, $^{87}\text{Sr}/^{86}\text{Sr}$ ratio depends on geology, showing different values among different geologies, which vary according to the bedrock age and or the amount of ^{87}Rb . The heavier strontium isotope (^{87}Sr) is an unstable isotope that is formed from the radioactive decay of ^{87}Rb , while the lighter (^{86}Sr) is stable (Bentley, 2006). Different weather conditions like sea spray effect (Bentley, 2006), or the input of varied materials coming from the different environments like dust precipitation or alluvial deposition could influence and modify the estimated bedrock values (Sjögren et al., 2016). So that, bioavailable Sr values have to be measured in the surrounding areas of the study (Price et al., 2002).

This $^{87}\text{Sr}/^{86}\text{Sr}$ signature is fixed during enamel mineralization and reflects the bioavailable strontium values from the region where the individual lived when enamel mineralization took place (Ericson, 1985; Price et al., 2002). Second (M2) and third (M3) molars are preferentially selected for this kind of analysis in humans because they allow the comparison of childhood signature (aprox. period of M2 mineralization) with the signature from late adolescence/ early adulthood (aprox. period of M3 mineralization) (Hillson, 1996). Deciduous teeth, which mineralized during pregnancy, and permanent teeth whose enamel mineralizes during possible breastfeeding or weaning periods must be avoided due to different physiological processes could influence in the $^{87}\text{Sr}/^{86}\text{Sr}$ values.

1.2 The studied site: Cueva de Abauntz

The burial cave studied in this work is Cueva de Abauntz, located in Northeast of the Iberian Peninsula, in the village of Arraitz (Navarra) (X. 610735; Y. 4763270, UTM30N, WGS84) at 610 m.a.s.l. The cavity has undergone an intensive use during whole Prehistory (Utrilla et al.,

2015). The first evidence comes from the Middle Palaeolithic, followed by a very rich Upper Paleolithic sequence with Solutrean, Magdalenian and Azilian levels (Utrilla et al., 2009). The explanation for this Paleolithic affluence could be related to its strategic position, which connects Aquitaine (Southwest of France) with the Mediterranean (Northeast of Iberia) through the Ebro Valley natural corridor (Utrilla et al., 2015). Although the cave was used as a refuge by some groups of Neolithic shepherds, it does not return to its splendor until the so-called Late Neolithic-Chalcolithic period (Utrilla et al., 2015). During this period the cavity was used as a burial space and the human corpses were accumulated inside, without any archaeological evidence of simultaneous deposition (**Figure 1**). Previous radiocarbon record shows the use of the cavity as a burial enclosure around one millennia, from 4rd to 3rd millennium cal B.C., with a total of five radiocarbon dates. The Minimum Number of Individuals (MNI) was 108, calculated with isolated teeth number but the methodology used was poorly explained (Utrilla et al., 2014). Although most of the remains appeared commingled and disarticulated as a result of simple deposition over the surface of the cave, some different kind of burials were found: pit burials concentrated along the corridor and second chamber, and stone cist graves in the first chamber (Utrilla et al., 2007). During the burial period, a fire event was recorded in the archaeological assemblage and some of the human remains from the first chamber of the cave were burned. This behaviour was initially interpreted as a corpse treatment for hygienic reasons (Utrilla et al., 2015), although other later studies pointed out that the thermic treatment was carried out post soft-tissue lost, thesis becoming the Hygienic hypothesis less feasible (Fernández-Crespo, 2016). The fire event took place around 2800 cal BC, contemporary to similar events in other near-by funerary cavities (**Figure 1**). In these cavities the fire record was linked to the end of the funerary use (Fernández-Crespo, 2016), but in Cueva de Abauntz the funerary use continues after the fire event, also directly dated around 2800 cal BC (Utrilla et al., 2015). This situation leads us to test the hypothesis of the burial use of Cueva de Abauntz by different communities that did not coincide in time but in space. This issue makes us propose two hypothetical scenarios for Cueva de Abauntz: 1) the existence of funerary use in a long-term scale without significant time interruptions and where the event of fire did not have the same meaning than in other nearby burial caves; or 2) that the burial cave experimented a turnover in the sepulchral use after the fire event. In this sense, we carried out two different Bayesian models in order to test which one fits better and provide a more probable answer to this question and identify

the beginning and the end of these assumed phases. Here we apply strontium isotope analysis in human dental enamel and radiocarbon Bayesian modelling to test the different time in use and the provenance of individuals buried in Cueva de Abauntz.

2. MATERIAL AND METHODS

2.1 Samples for radiocarbon analyses and ^{14}C dataset

We selected human mandibles to combine radiocarbon dates and strontium isotopic analyses with the aim of getting information about the period and the provenance of the same individuals (**Table 1**). Burned remains were avoided in order to analyse the best possible preserved collagen. The newest 11 radiocarbon dates were processed and analysed by The Curt-Engelhorn-Centre for Archaeometry Mannheim, Germany (samples using lab codes MAMS), using ultrafiltrated collagen (fraction >30kD) and dated using the MICADAS-AMS of the Klaus-Tschira-Archäometrie-Zentrum. Two of this samples were published in a previous work ([Villalba-Mouco et al., 2018](#)) and the other nine are included in this study for first time.

There are another five radiocarbon dates which were already published in previous studies of the cave ([Utrilla et al., 2007](#)). In this case, the radiocarbon analysis was carried out in different laboratories: Groningen (lab codes GrA), Centro Superior de Investigaciones Científicas (lab codes CSIC) and Lyon (lab codes Ly). All the radiocarbon dates come from human remains except one from a charcoal recovered from the area where the fire was performed, possibly pointing out the time for this event. **Table 1** shows the total number of radiocarbon dates and their archaeological description.

2.2 ^{14}C calibration and Bayesian Chronological models

The radiocarbon dates were calibrated using Oxcal v4.2.24 and IntCal13 ([Bronk Ramsey, 2009](#); [Reimer et al., 2013](#)) with 2σ (95.4 % probability). The reservoir effect was not taken into account because of the absence of marine diet ([Lillie et al., 2009](#)), tested with stable isotope analyses carried out in a previous study over the same individuals ([Villalba-Mouco et al., 2018](#)). **Table 2** summarizes the carbon and nitrogen isotopic values.

The first model tested has been one phase model, grouping all the human radiocarbon dates as a single burial phase. The radiocarbon from charcoal was ruled out from this phase model because of the high deviation. This is the model previously used for the burial phases in closer caves and megalithic burials (Fernandez-Crespo, 2016; Fernández-Crespo and Schulting, 2017). The second model grouped samples in two phases according to the archaeological information. The stratigraphic order is not clear for all the samples because most of the human remains appeared scrambled and commingled, but we have used different archaeological information to define the order of depositions: type of burial, kind of gravegoods, and in some cases stratigraphic position. We defined an older phase called Pre-Fire phase which groups pit burials or remains associated to pit structures which normally appeared buried together with bone spatulas as a common gravegood. This kind of burial was more frequent in the Corridor and Chamber 2, and when they appear in Chamber 1 they are clearly identified under the cremated bones which means that they are older than the fire event. The later phase was called Post-Fire phase and takes the individual samples which appeared with a simple deposition over the surface of the cavity, sometimes recovered from superficial levels and mixed with roman or contemporaneous materials. We also have included cist burials in this Post-Fire phase because there is the stratigraphic evidence that they were built over some of the burned human remains. All the archaeological information was summarized in **Table 1** and **Figure 2**. The transition boundary between two phases was restricted to the charcoal radiocarbon date. For both models, we used Phase bayesian modelling implemented in Oxcal 4.2.4 (Bronk Ramsey, 2009). Constrain values were not used because the beginning and the end of the funerary use is unknown. All results higher than 60% of agreement were considerable accepted for the model (Bronk Ramsey, 2009). We also have implemented Kerner plot function in order to determinate the density and the distribution of events in each phase (Bronk Ramsey, 2017).

2.3 Sample preparation for strontium isotope analysis

2.3.1. Enamel samples

We use strontium isotopes from tooth enamel to approach the mobility patterns of Late Neolithic-Chalcolithic humans who were buried in Cueva de Abauntz. Forty-four tooth samples attached to mandibles from 32 humans were selected for strontium isotope analysis. Second (M2) and third (M3) molars were preferentially selected and both sampled for each individual when it was possible. When M2 are not available, premolars (P1 or P2) or canines (C) were chosen instead of first molars (M1) (**Table 2**). This sampling strategy increases the track of individual movements because ensures having two different life periods represented: childhood (M2, P, C) and late adolescence/ early adulthood (M3). Mandibles with only M3 were excluded because they only reflect the late adolescence/ early adulthood signal, which purportedly could mask previous movements by already reflecting the latest environment where the individual lives (most probable the local signal). We also excluded teeth whose enamel mineralized during a possible breastfeeding or weaning stage of childhood development (incisors and first molars) (Hillson, 1996). The same sampling strategy has been followed in previous studies (Sarasketa-Gartzia et al., 2017; Sarasketa-Gartzia et al., 2018).

Sample preparation and analysis were done in dedicated isotope facilities of the University of Cape Town (South Africa), as described below. Prior to analysis, a portion of enamel (ca. 20 mg) was cleaned by abrasion and possible dentine remains were removed using a Dremel 3500 drill bit, rinsed and ultrasonicated for 20 minutes in MilliQ water. Diamond drill bits were cleaned with ethanol and ultrasonicated in MilliQ water between samples to avoid cross-contamination (Budd et al., 2000). After this, the cleaned enamel sample was digested with 2mL bi-distilled distilled 65% HNO₃ in a closed Teflon beaker placed on a hotplate at 140 °C for an hour. Digested samples were then dried and redissolved in 1.5 mL of bi-distilled 2M HNO₃. These redissolved samples were centrifuged at 4000 rpm for 20 minutes, and the supernatant was collected for strontium separation chemistry. A separate fraction for each sample in this step was used to calculate the concentration with ⁸⁸Sr intensity (V) regression equation built with SRM987 standard from NIST (National Institute of Standards and Technology, Gaithersburg, MD, USA).

Strontium was isolated with 200µl of Eichrom Sr.Spec resin loaded in Bio-Spin Disposable Chromatography Bio-Rad Columns following the method of Pin et al. (1994). The separated strontium fraction for each sample was dried down, dissolved in 2 ml 0.2% bi-distilled HNO₃

and diluted to 200 ppb Sr concentrations for isotope analysis. $^{87}\text{Sr}/^{86}\text{Sr}$ ratios were measured using a NuPlasma HR multicollector inductively-coupled-plasma mass spectrometer (MC-ICP-MS). Sample analyses were referenced to bracketing analyses of SRM987, using a $^{87}\text{Sr}/^{86}\text{Sr}$ reference value of 0.710255 from NIST. All strontium isotope data are corrected for isobaric rubidium interference at 87 amu using the measured signal for ^{85}Rb and the natural $^{85}\text{Rb}/^{87}\text{Rb}$ ratio. Instrumental mass fractionation was corrected using the measured $^{86}\text{Sr}/^{88}\text{Sr}$ ratio and the exponential law, and a true $^{86}\text{Sr}/^{88}\text{Sr}$ value of 0.1194. Results for repeat analyses of an in-house carbonate standard processed and measured with the batches of samples in this study ($^{87}\text{Sr}/^{86}\text{Sr} = 0.708936$; 2 sigma 0.000041; n=33) are in agreement with long-term results for this in-house standard ($^{87}\text{Sr}/^{86}\text{Sr}$; 0.708915; 2 sigma 0.000047; n=125). For every two batches one blank was added to assess the cleanliness of the process; there was no peak and, thus, no contamination from external Sr in any of the batches.

2.3.2. Organic samples for bioavailable strontium values

Cueva de Abauntz is developed through Cretaceous limestones layers, but it is surrounded by different geological areas. The nearest surroundings are made up of Triassic layers and Permo-Triassic volcanic intrusions. Carboniferous and Devonian basins show a further away location (see map in **Figure 3**). $^{87}\text{Sr}/^{86}\text{Sr}$ bioavailable ranges of Cretaceous, Triassic and Permo-Triassic geological areas were calculated with modern snails and plants, following Bentley (2004) and Price (2002). The same strontium extraction and purification procedure previously described was used on modern snail shells, taking an amount of 40 mg of snail shell. Plant procedure needed a previous step of incineration of the green parts. The digestion in this case was done with 48% HF and bi-distilled 65% HNO_3 (4:1 respectively) as it is described in Copeland et al., (2016). No strontium concentrations were measured in modern samples because diagenetic effects were not expected (**Figure 3, Table 3**).

3. RESULTS

3.1 Radiocarbon analysis

All the samples processed and analysed in The Curt-Engelhorn-Centre for Archaeometry

Mannheim, Germany, had enough >30KDa good quality collagen preserved within the accepted C:N ratio range (2.9-3.6) (Van Klinken, 1999). Samples from CSIC and Groningen (GrA) laboratories were also done with AMS techniques, but the quality controls were not supplied by the laboratories. Ly-1963 charcoal sample from Lyon laboratory was dated without AMS techniques.

The first Bayesian model, which considers all human radiocarbon dates coming from a same burial phase, shows an index of agreement of 93.0 ($A_{\text{model}}=93.0\%$) (supplementary **Figure S1 and Table S1**). According to the boundaries estimated by the model, the burial use of Cueva de Abauntz began in the Late-Neolithic (3573-3157 cal. B.C., Boundary start) and ended during the late moments of the Chalcolithic (2481-2191 cal. B.C, Boundary end). Kerner density analysis shows the presence of two smooth peaks reflecting the concentration of radiocarbon dates along two time transects inside the burial period.

The two phases model (Pre-Fire and Post-Fire burial stages) showed a Model agreement index of 102% ($A_{\text{model}}=102.6\%$) (**Figure 4 and Table S2**). Individual agreement index was higher than 60% in all the samples and range between 111.7 to 74.8% (**Table S2**). In this case, boundaries estimated by the model are reflecting a burial use from 3810-3170 cal B.C. (Boundary Start, 95,4% of probability) to 2880-2570 (Boundary Fire, 95,4% of probability), which acts as a transition to the second phase which ends at 2562-2325 cal B.C. (Boundary End, 95,4% of probability). **Table S2** show the unmodelled and modelled radiocarbon dates according to two phase bayesian modelling. **Figure 4** shows the multiple plot for the two modelled phases and the summarized modelled radiocarbon dates of each phase using Kerner plot (Bronk Ramsey, 2017).

3.2 Sr and provenance study

The $^{87}\text{Sr}/^{86}\text{Sr}$ values from plants and snails were analysed to calculate the bioavailable $^{87}\text{Sr}/^{86}\text{Sr}$ signature of the immediate surroundings of Cueva de Abauntz as well as near-by geological areas, and are presented in **Table 3**. The location of sampling areas is shown in the geological map (**Figure 3**). $^{87}\text{Sr}/^{86}\text{Sr}$ from the surrounding area of Cueva de Abauntz (Cretaceous) was calculated with plants and snails (**Area 1 in Figure 3**), showing a range between 0.708581 -

0.709112 for plants, and 0.708268 - 0.708522 for snails. Cueva de Abauntz is located only a few meters away from the river Ultzama, which runs over different geological layers. In order to make sure that the river deposits are not modifying the expected bioavailable values for the Cretaceous geology, another area from the same geological period was sampled (this time only with snails), and ranged between of 0.707940-0.708340 (Area 2 in **Figure 3**). All these samples from Cretaceous areas 1 and 2 are overlapped and they were grouped as a “Cretaceous range” in the plot, although Sampling Area 2 presented a slight lower mean value. The second geological area analysed is composed by volcanic ophites, dated back to the Permo-Triassic period (Area 3 in **Figure 3**), and shows a bioavailable $^{87}\text{Sr}/^{86}\text{Sr}$ value range between 0.709195 - 0.710092 for plants. The third geological area analysed belongs to the Triassic (Area 4 in **Figure 3**) and its bioavailable strontium values range between 0.710920 - 0.71339 for plants. No snails were found in the last two areas. Forty-four enamel chunks from 32 humans were also analysed. The $^{87}\text{Sr}/^{86}\text{Sr}$ ratio and Sr concentration (ppm) results from human enamel samples are presented in **Table 2**. The plot with bioavailable $^{87}\text{Sr}/^{86}\text{Sr}$ values from all the areas and human enamel $^{87}\text{Sr}/^{86}\text{Sr}$ values is shown in **Figure 5**.

There are 24 enamel samples whose $^{87}\text{Sr}/^{86}\text{Sr}$ values are inside the $^{87}\text{Sr}/^{86}\text{Sr}$ bioavailable Cretaceous value range (Areas 1 and 2 in **Figure 3**). There are also 20 enamel samples whose $^{87}\text{Sr}/^{86}\text{Sr}$ values are outside the Cretaceous bioavailable $^{87}\text{Sr}/^{86}\text{Sr}$ range. Inside this group, there are 14 samples whose values are compatibles with Permo-Triassic volcanic deposits (Area 3 in **Figure 3**), and 3 samples compatible with Triassic deposits (Area 4 in **Figure 3**). Finally, there are another 3 samples whose values are outside the three bioavailable ranges positioned between Area 3 and Area 4 ranges.

Per individuals, 18 of the 32 individuals have a Cretaceous signature and potentially show no changes in mobility (this last only assessed when it was possible to analyse two different teeth from the same individual), seven of the 32 individuals have Permo-Triassic volcanic values without changes in mobility (four of them show both values M2 and M3 inside this bioavailable range and three with one single data), and two of the 32 individuals have Triassic values (measured in one tooth). Other 4 individuals of the 32 analysed show discrepancies in their strontium signature between their two teeth analysed: (i) individual S-UCT 19036 has Sr values compatible with the Permo-Triassic in M2 and with the Triassic in M3; (ii) individual S-

UCT 19033 has $^{87}\text{Sr}/^{86}\text{Sr}$ values compatible with Cretaceous values in M2 and Permo-Triassic values in M3; (iii) individual S-UCT 19039 has Sr values compatible with Permo-Triassic volcanic values in M2 and Cretaceous values in M3; (iv) individual S-UCT 19049 has Sr values compatible with Cretaceous values in M2 and without correspondence with any bioavailable range analysed in M3, showing a middle value between Permo-Triassic volcanic and Triassic ranges in this last one. Finally, there is one only individual whose values from both the second and third molars do not show correspondence with any of the bioavailables ranges analysed here, but are located in between Permo-Triassic volcanic and Triassic bioavailable value areas (**Figure 5, Table 2**).

4. DISCUSSION

During the Iberian Late Neolithic appears the so-called phenomenon of the Funerary Collectivism when caves and megalithic monuments are used as shared burial places ([Andrés, 1998](#)). In Northern Iberia there is a widespread use of megalithic monuments, some of them used from the latest moments of the Middle Neolithic to the Late Chalcolithic (around 3600-1600 cal BC for Northern Iberia) ([López de la Calle, 1993](#); [Pérez Arrondo, 1986](#); [Fernández-Crespo, 2012](#)), sometimes with time gaps in use for some of them ([Andrés, 2009](#)). Overlapping in time, around 3500 to 2800 cal BC, many caves and rock shelters also started to be used as collective burials in Northern Iberia ([Fernández-Crespo and Schulting, 2018](#)). Although both kind of structures were used at the same time, the number of individuals recovered tend to be higher in caves, which has been interpreted that only a special selection of individuals were buried in a megalithic structure ([Fernández-Crespo and de-la-Rúa, 2015](#)). In this regard, burial caves usually harbour from tens to hundreds of individuals (e.g. [Lorenzo, 2014](#), [Fernández-Crespo 2010](#); [Gimeno, 2009](#)). Due to this high amount of buried individuals and their usually simple deposition over the surface of the cavities, human remains tend to appear comingled and disarticulated, making it very difficult to discern different burial moments along the Late Neolithic and the Chalcolithic periods. The only way to ensure their chronological adscription is implementing direct radiocarbon dates to the minimum number of individuals, but this strategy sometimes requires high economical resources. There are only a few examples in Iberia where the total or almost total of individuals from Late Neolithic-Chalcolithic burial caves are dated ([Salazar-García et al. 2016](#); [García-Guixé, 2011](#)). This situation is somewhat better in Chalcolithic Megalithic monuments in Southern Iberia (e.g. [Aranda Jiménez et al.,](#)

2018; García Sanjuán et al., 2018), but still further away from what happens in other European territories for this time periods (e.g. Stockhammer et al., 2015). In this context, Cueva de Abauntz has 15 radiocarbon dates on human remains, which contrasts positively with the number of radiocarbon dates available from other near-by Late Neolithic-Chalcolithic burial caves where radiocarbon dates are not only scarce but also many times too old to have been performed by AMS techniques (Apellániz, 1974; Basabe and Benasar, 1983). This considerable radiocarbon dataset of Cueva de Abauntz, together with the archaeological information, have allowed to perform bayesian models for ^{14}C radiocarbon dates (Bronk Ramsey, 2009).

Cueva de Abauntz is located in an area surrounded by many sepulchral caves and megalithic monuments (**Figure 1**). In many of these burial caves, the use of fire has been recorded at the end of the use of the cavities as funerary enclosures. This event has been proposed as a sign of closure of the funerary activity, and in all the cavities it appears around 2800 cal B.C (Fernandez-Crespo, 2016). The presence of fire in Cueva de Abauntz has also been recorded at that same time, although the radiocarbon date for this moment comes from one charcoal sample and the *old wood* effect should not be ruled out (Bowman, 1990). The main difference between Cueva de Abauntz and the other burial caves with presence of fire is that in the first one, the radiocarbon dates point out to a further funerary use after the fire event until 2476-2286 cal BC (GrA-377323, unmodelled). This issue leads us to suggest the presence of a second burial phase after the fire in Cueva de Abauntz or, possibly, a different cultural meaning for the fire event in this case. We have tried to test these different scenarios with Bayesian modelling, testing a single funerary event or the presence of two different moments, divided by the fire moment. In this sense, the two-phase model shows a higher agreement ($A_{\text{model}}=102.6\%$) than the single-phase model, although the latter also fits statistically ($A_{\text{model}}=93.0\%$) (**Table S1 and Table S2**). Moreover, if we look at the kerner plot which summarized the events in one phase model, we can infer the presence of two smooth peaks which suggest the presence of two moments of more intensive use (**Figure S1**). These two reasons make it more plausible to propose the presence of two phases of burials, divided by the moment of the fire event (**Figure 4**). This, possibly has the same meaning than in the other surrounding caves, the closure of the burial space, although in Cueva de Abauntz we will have another burial phase time after the fire event.

The early burial phase, called “Pre-Fire phase” (3573-3157 cal B.C., Boundary Start [95,4% of probability]; to 2880-2570 cal B.C., Boundary Fire [95,4% of probability]), is represented by the oldest burials and would arrive up to the presence of fire in the first hall. In this phase, the samples follow a distribution from the depth to the entrance of the cave, being the most recent one in the first hall where the fire even occurred (**Figure 2, Figure 4**). Despite being a great disparity in bone appearance, we suggest that the fire happened with the absence of soft tissues because many bones show a cracked surface linked to burned dry bone and without evidence of warping (Ubelaker, 2008; Whyte, 2001). Moreover, we found many human bones that show a grey-blue appearance as a result of being subject to high temperatures, which is also more compatible with the absence of soft tissues (Walker and Miller, 2005; Ubelaker, 2008). We find interesting to highlight that some of the earliest burials were not simply deposited over the surface but appeared instead buried in pits, which is characteristic from the Middle Neolithic and first moments of the Late Neolithic in the *Sepulcros de Fosa* Culture that occupied the near-by region of Northeast Iberia (e.g Morrel et al., 2017, Gibaja et al., 2012).

The second burial phase, called “Post-Fire phase” (from 2880-2570 cal B.C., Boundary Fire [95,4% of probability] to 2562-2325 cal B.C., Boundary End [95,4% of probability]), is represented by the latest burial phase, which would take place after the fire event (**Figure 4**). This phase is composed by a bigger set of radiocarbon dates, and suggests a prolonged use after the fire event. In this regard, Cueva de Abauntz would have a second burial phase that does not appear in the archaeological record of the nearby cavities that show the suggested funerary site closure. Despite this funerary behaviour not being able to be extended to other territories, the possible presence of closures and openings of funerary spaces suggest that the defined Funerary Collectivism is not as homogeneous as has been previously conceived. More radiocarbon dates in sepulchral caves are necessary to confirm different funerary behaviours along the entire Iberian Peninsula.

Cueva de Abauntz was a burial place during the Late Neolithic-Chalcolithic period. As it includes a long time span for burial, as well as because of the inherent limitations of strontium isotope analysis interpretation, defining local or non-local individuals is sometimes difficult and interpretation should be taken with caution. This limitation comes first because we only

analyse at most two different time windows (M2 and M3) but mobility could happen sometime in between the mineralization of both molars. Second limitation arrives because there are different geological areas with the same Sr bioavailable values which could mask the mobility too. Thus, if we consider Cretaceous values as a local signal, we could estimate that 56% (18 out 32) of the population were locals (at least during the two moments of life represented by the two teeth analysed per individual); 19% (6 out 32) were non-locals showing Permo-Triassic values; and 6% (2 out 32) were non-locals showing Triassic values. Movement between different geological areas is also recorded from Permo-Triassic to Triassic areas (1 out 32), from Permo-Triassic to Cretaceous areas (1 out 32), and from Cretaceous to Permo-Triassic areas (1 out 32). Finally, there are also 2 individuals (6%) some of whose Sr values are outside of the bioavailable ranges analysed in this study, between Cretaceous and Permo-Triassic values (**Figure 5, Figure 6**). This makes us consider the potential use of these two territories in a way the individual got an averaged signature between them. However, that they do come from further away can't be ruled out.

When combining radiocarbon dates together with strontium isotopes analysis we can obtain more in-depth information regarding provenance through time, even if the number of available radiocarbon dates is less than the strontium data. In this sense, we find a local $^{87}\text{Sr}/^{86}\text{Sr}$ signal (considering local the Cretaceous values although provenance can be from further areas) in the individuals who present the oldest radiocarbon dates (**Figure 6**). This could suggest the early use of Cueva de Abauntz as a burial space by the communities of people living closer to the burial site. Looking at the later periods, we find individuals whose $^{87}\text{Sr}/^{86}\text{Sr}$ values are compatible with the bioavailable values for further away territories (Permo-Triassic and Triassic) (**Figure 3**). This higher mobility pattern observed in the more recent periods of use of the burial site have been already tested in other Late Neolithic-Chalcolithic burials caves with less radiocarbon dates available ([Villalba-Mouco et al., 2017](#)).

This increase in individuals with non-local $^{87}\text{Sr}/^{86}\text{Sr}$ values over time could be in agreement with the increase of the identity of Cueva de Abauntz as a burial place through time and also could explain the presence of the second burial phase after the fire event. It would also be compatible with a more prolonged burial use than what is observed in other nearby cavities ([Fernández-Crespo and Schulting, 2018](#)) (**Figure 1**). If Cueva de Abauntz started to be used also

by further away communities means that there should exist a displacement of dead individuals from further areas to Cueva de Abauntz. This issue could be supported by individuals who present “non local” $^{87}\text{Sr}/^{86}\text{Sr}$ values in both enamel samples, M2 and M3 (they would have arrived at the site dead) (**Figure 5 and Figure 6**). The same point has been suggested for individuals buried in the Kurtzebide Dolmen, only around 100 km away from Cueva de Abauntz. In that case, 100 per 100 of the individuals showed a non-local signal ([Sarasketa-Gartzia et al., 2018](#)). This type of megalithic burial structure is usually located in remote places, normally in highlands where the settlements are not frequent, which makes more plausible the hypothesis of corpse transport.

Despite the all the individuals can be migrants on life and this cannot be detected by Sr isotope analysis, In the case of Cueva de Abauntz, another more plausible option could be that individuals were migrants, and that they travelled during life to an area close to Cueva de Abauntz after their tooth mineralization (childhood for M2 and early adulthood for M3) ([Hillson, 1996](#)). In this sense, we could suggest a real displacement during life for the individuals that show different $^{87}\text{Sr}/^{86}\text{Sr}$ values from different geological areas in each dental piece (3 individuals). Whatever the reason, radiocarbon dates together with strontium isotopes suggest a change in the funerary use at Cueva de Abauntz that could not be detected through conventional archaeological approaches (**Figure 6**). More studies combining direct radiocarbon dating together with strontium isotopes analyses are required for better understanding the use of the funerary spaces during the Late Neolithic-Chalcolithic transition in the Iberian Peninsula.

5. CONCLUSIONS

This study assesses funerary use of Cueva de Abauntz, a collective burial located in northern Iberia in an area with a high presence of funerary caves and megalithic monuments used during the Late Neolithic-Chalcolithic period. Radiocarbon Bayesian modelling together with strontium isotope analysis reported differences in time use and provenance of individuals buried in Cueva de Abauntz sepulchral cave. The 17 radiocarbon dates have been modelled as two phases of burials, which are separated by the presence of a fire event recorded inside the cave. Contrary to what happens in other near-by burial caves, Cueva the Abauntz continues being used as a burial site intensively until 2300 cal. BC. Despite not analyzing both isotopes

and radiocarbon dates in all humans sampled, we found a local signal for the first humans buried in pit structures but a higher mobility and/or intensive use of Cueva de Abauntz by different communities in the second burial phase. Despite this funerary behaviour not being reported in other near-by territories, the possible presence of closures and openings of the funerary space sheds light about the defined Funerary Collectivism and the unclear period of the Late Neolithic-Chalcolithic period in Northern Iberia. More radiocarbon dates and strontium isotope analysis in sepulchral caves are necessary to test the different funerary behaviours along the Iberian Peninsula.

Acknowledgments

VVM has a predoctoral scholarship funded by the Gobierno de Aragón and the Fondo Social Europeo (BOA20150701025), and did a research stay at the University of Cape Town funded by the Fundación Ibercaja-CAI (2016) and DC's UCT research grants. DCSG acknowledges also funding for this research from the BBVA Foundation (I Ayudas a Investigadores, Innovadores y Creadores Culturales). VVM and PU are members of the Spanish project HAR2014-59042-P (Transiciones climáticas y adaptaciones sociales en la prehistoria de la Cuenca del Ebro), and of the regional government of Aragón PPVE research group (H-07: Primeros Pobladores del Valle del Ebro). ISG has a predoctoral scholarship funded by Basque Government and is a member of the Spanish project HAR2014-53536-P and IT-662-13. All authors would like to thank Centro de Espeleología de Aragón (CEA), specially Mario Gisbert for the topography of the cave and for the help with sampling modern materials. We would like to thank Feyrooza Rawoot, Kerryn Gray and Petrus Leroux for technical assistance, and Chrystel Tinguely for helping in obtaining the Sr concentration values. We would also have to thank Garcia Gazolaz and Jose Ignacio Lorenzo for providing the human samples.

BIBLIOGRAPHY

Almagro, M., Arribas, A., 1963. *El poblado y la necrópolis megalíticas de Los Millares: (Santa Fe de Mondújar, Almería)*. Consejo Superior de Investigaciones Científicas, Inst. Español de Prehistoria, 1963.

Alt, K.W., Zesch, S., Garrido-Pena, R., Knipper, C., Szécsényi-Nagy, A., Roth, C., Tejedor-Rodríguez, C., Held, P., García-Martínez-de-Lagrán, I., Navitainuck, D., Arcusa, H., Rojo-Guerra, M.A., 2016. A community in life and death: the Late Neolithic megalithic tomb at Alto de Reinoso (Burgos, Spain). *PloS One*, 11(1), e0146176.

Andrés, M.T., 1998. Colectivismo funerario neo-eneolítico. Aproximación metodológica sobre datos de la Cuenca Alta y Media del Ebro. Institución Fernando el Católico. Diputación de Zaragoza, Zaragoza.

Andrés, M.T., 2005. Concepto y análisis del cambio cultural: su percepción en la materia funeraria del Neolítico y Eneolítico. In: *Monografías Arqueológicas*, vol. 42. Departamento de Ciencias de la Antigüedad, Universidad de Zaragoza, Zaragoza.

Apellániz, J.M. 1974. El Grupo de Los Husos durante la prehistoria con cerámica del País Vasco. *Estudios de Arqueología Alavesa* 7: 1-409.

Aranda Jiménez, G., Lozano Medina, Á., Sánchez Romero, M., Díaz-Zorita Bonilla, M., Bocherens, H. (2018). Chronology of Megalithic Funerary Practices in Southeastern Iberia: The Necropolis of Panoria (Granada, Spain). *Radiocarbon*, 60(1), 1-19.

Baldeón A, García E, Ortiz L, Lobo P (1983) Excavaciones en el yacimiento de Fuente Hoz (Anúcita, Alava). *Estudios de Arqueología Alavesa*: 7–68.

Bentley, R.A., 2006. Strontium isotopes from the earth to the archaeological skeleton: a review. *J. Archaeol. Method Theory* 13 (3), 135e187.

Bentley, R. A. (2013). Mobility and the diversity of Early Neolithic lives: isotopic evidence from skeletons. *Journal of Anthropological Archaeology*, 32(3), 303-312.

Bentley, R.A., Price, T.D., Stephan, E., 2004. Determining the 'local' Sr-87/Sr-86 range for archaeological skeletons: a case study from Neolithic Europe. *Journal of Archaeological Science* 31 (4), 365–375.

Blasco, C., Delibes, G., Baena, J., Liesau, C., Ríos, P., 2007. El poblado calcolítico de 701 Camino de las Yeseras (San Fernando de Henares, Madrid): un escenario favorable para el estudio de la incidencia campaniforme en el interior peninsular. *Trabajos de Prehistoria* 703 64(1), 151–163.

Bernabeu, J., Orozco, T., Díez, A., Gómez, M., Molina, F. J., 2003. Mas d'Is (Penàguila, Alicante): aldeas y recintos monumentales del Neolítico Inicial en el valle del Serpis. *Trabajos de prehistoria* 60(2), 39–59.

Bowman, S. 1990. Radiocarbon Dating. Interpreting the past. London: British Museum.

Britton, K., Grimes, V., Dau, J., & Richards, M. P. (2009). Reconstructing faunal migrations using intra-tooth sampling and strontium and oxygen isotope analyses: a case study of modern caribou (*Rangifer tarandus granti*). *Journal of Archaeological Science*, 36(5), 1163-1172.

Britton, K., Grimes, V., Niven, L., Steele, T. E., McPherron, S., Soressi, M., ... & Richards, M. P. (2011). Strontium isotope evidence for migration in late Pleistocene *Rangifer*: Implications for Neanderthal hunting strategies at the Middle Palaeolithic site of Jonzac, France. *Journal of human evolution*, 61(2), 176-185.

Bronk Ramsey, C., 2009. Bayesian analysis of radiocarbon dates. *Radiocarbon* 51 (1), 337–360.

Bronk Ramsey, C., (2017). Methods for Summarizing Radiocarbon Datasets. *Radiocarbon* 59, 1809–1833.

Budd, P., Montgomery, J., Barriero, B., Thomas, R.G., 2000. Differential diagenesis of strontium in archaeological human dental tissues. *Appl. Geochem.* 15, 687e694.

Copeland, S.R., Cawthra, H.C., Fisher, E.C., Lee-Thorp, J.A., Richard, M.C., le Roux, P.J., Hodgkins, J., Marean, C.W., 2016. Strontium isotope investigation of ungulate movement patterns on the pleistocene paleo-agulhas plain of the greater Cape floristic region, South Africa. *Quat. Sci. Rev.* 141, 65–84.

Copeland, S.R., Sponheimer, M., de Ruiter, D.J., Lee-Thorp, J.A., Codron, D., le Roux, P.J., Grimes, V., Richards, M.P., 2011. Strontium isotope evidence for landscape use by early hominins. *Nature* 474 (7349), 76–78.

Delibes, G., Herrán, J.I., Santiago, J., de Val, J., 1995. Evidence for social complexity in the Copper Age of the Northern Meseta. In: K.T. Lillios (ed.): *The origins of complex societies in late prehistoric Iberia. International Monographs in Prehistory* 8, pp. 44–63.

Díaz-del-Río, P., Waterman, A. J., Thomas, J. T., Peate, D. W., Tykot, R. H., Martínez-Navarrete, M. I., Vicent, J. M., 2017. Diet and mobility patterns in the Late Prehistory of central Iberia (4000–1400 cal bc): the evidence of radiogenic ($^{87}\text{Sr}/^{86}\text{Sr}$) and stable ($\delta^{18}\text{O}$, $\delta^{13}\text{C}$) isotope ratios. *Archaeological and Anthropological Sciences*, 9(7), 1439-1452.

Díaz-Zorita, M., 2014. The copper age. In: *South-west Spain: a Bioarchaeological Approach to Prehistoric Social Organisation*. Durham University, Durham (Doctoral thesis).

Esquivel, J.A., Navas, E., 2007. Geometric architectural pattern and constructive energy 761 analysis at Los Millares Copper Age Settlement (Santa Fé de Mondújar, Almería, 762 Andalusia). *Journal of Archaeological science*, 34(6), 894–904.

Ericson, J.E., 1985. Strontium isotope characterization in the study of prehistoric human ecology. *Journal of Human Evolution* 14, 503–514.

Fernández-Crespo, T., 2010. *Caracterización antropológica y tratamiento funerario de las*

poblaciones del Neolítico a la Edad del Bronce en la comarca de La Rioja: estado de la cuestión. *Munibe*. Suplemento 32, 414–424.

Fernández-Crespo, T., 2016a. El papel del fuego en los enterramientos neolíticos finales/calcolíticos iniciales de los abrigos de la Sierra de Cantabria y sus estribaciones (valle medio-alto del Ebro). *Trabajos de Prehistoria* 73(1), 128–146

Fernández-Crespo, T., de-la-Rúa, C., 2015. Demographic evidence of selective burial in megalithic graves of northern Spain. *Journal of Archaeological Science* 53, 604–617.

Fernández Eraso, J. 1997. Peña Larga . Memorias de yacimientos alaveses 4. Diputación Foral de Álava. Vitoria-Gasteiz.

Fernández Eraso, J. 2003. Las Yurdinas II: Un depósito entre finales del IV y comienzos del III milenio BC. Memorias de yacimientos alaveses 8. Diputación Foral de Álava. Vitoria-Gasteiz.

Gibaja AF, Carvalho AF, Chambon P, editors. 2012. *Funerary Practices in the Iberian Peninsula from the Mesolithic to the Chalcolithic*. Oxford: BAR International Series.

Gimeno, B., 2009. Estudio antropológico de la cueva sepulcral de Loarre. *Saldvie Estudios de Prehistoria y Arqueología* 9, 369–392.

García-Guixé, E., 2011. Estudi paleoantropològic i paleopatològic del sepulcre col·lectiu de Forat de Conqueta (Santa Linya, Lleida). *Treballs d'arqueologia* 17, 37–98.

García Sanjuán, L., Cáceres Puro, L., Costa Caramé, M. E., Díaz-Guardamino-Urbe, M., Díaz-Zorita Bonilla, M., Fernández Flores, Á., Hurtado Pérez, V., López Aldana, P. M., Méndez Izquierdo, E., Pajuelo Pando, A., Rodríguez Vidal, J., Vargas Jiménez, J. M., Wheatley, D., Dunbar, E., Bronk Ramsey, C., Bayliss, A., Beavan, N., Hamilton, D. y Whittle, A., 2018. Assembling the dead, gathering the living: Radiocarbon dating and Bayesian modelling for Copper Age Valencina de la Concepción (Sevilla, Spain). *Journal of World Prehistory* (num).

Haak, W., Guido B., Hylke N. de Jong, Christian Meyer, Robert Ganslmeier, Volker Heyd, Chris Hawkesworth, Alistair WG Pike, Harald Meller, and Kurt W. Alt. "Ancient DNA, Strontium isotopes, and osteological analyses shed light on social and kinship organization of the Later Stone Age." *Proceedings of the National Academy of Sciences* 105, no. 47 (2008): 18226-18231.

Hillson, S., 1996. *Dental Anthropology*. Cambridge University Press, Cambridge.

Knipper, Corina, Alissa Mittnik, Ken Massy, Catharina Kociumaka, Isil Kucukkalipci, Michael Maus, Fabian Wittenborn et al. "Female exogamy and gene pool diversification at the transition from the Final Neolithic to the Early Bronze Age in central Europe." *Proceedings of the National Academy of Sciences* (2017): 201706355.

Lillie, M., Budd, C., Potekhina, I., Hedges, R. (2009). The radiocarbon reservoir effect: new evidence from the cemeteries of the middle and lower Dnieper basin, Ukraine. *Journal of Archaeological Science*, 36(2), 256-264.

Lorenzo, J.I., 2014. Estudio antropológico de los restos de Forcas II. In: Utrilla y, P., Mazo, C. (Eds.), *La Penea de las Forcas (Graus, Huesca). Un asentamiento estratégico en la con uencia del Esera y el Isabena*. Monografías Arqueológicas/ Prehistoria 46, Zaragoza, pp. 337–341.

McClure, S.B., García, O., de Toghores, C.R., Culleton, B.J., Kennett, D.J., 2011. Osteological and paleodietary investigation of burials from Cova de la Pastora, Alicante, Spain. *Journal of Archaeological Science* 38 (2), 420–428.

Micó, R., 1995. Los Millares and the Copper Age of the Iberian Southeast. *The Origins of Complex Societies in Late Prehistoric Iberia* :169.

Morell, B., Duboscq, S., Masclans, A., Remolins, G., Pou, R., Martí, M., Barceló, J.A., Oms, X., Santos, F.J., Mozota, M., Subirà, M.E., Gibaja, J.F., 2017. Chronology of the Neolithic Necropolis at Camí de Can Grau (NE-Iberian Peninsula). Funerary pattern changes and long-distance raw material exchanges. *Comptes Rendus Palevol* (in press).

Nocete, F., Sáez, R., Bayona, M. R., Peramo, A., Inacio, N., & Abril, D. (2011). Direct chronometry (^{14}C AMS) of the earliest copper metallurgy in the Guadalquivir Basin (Spain) during the Third millennium BC: first regional database. *Journal of Archaeological Science*, 38(12), 3278-3295.

Olalde, I., Brace, S., Allentoft, M.E., Armit, I., Kristiansen, K., Rohland, N., Mallick, S., Booth, T., Szécsényi-Nagy, A., Mittnik, A., Altena, E., Lipson, M., Lazaridis, I., Patterson, N.J., Broomandkoshbacht, N., Diekmann, Y., Faltyskova, Z., Fernandes, D.M., Ferry, M., Harney, E., de Knijff, P., Michel, M., Oppenheimer, J., Stewardson, K., Barclay, A., Alt, K.W., Avilés Fernández, A., Bánffy, E., Bernabò-Brea, M., Billoin, D., Blasco, C., Bonsall, C., Bonsall, L., Allen, T., Büster, L., Carver, S., Castells Navarro, L., Craig, O.E., Cook, G.T., Cunliffe, B., Denaire, A., Dinwiddy, K.E., Dodwell, N., Ernée, M., Evans, C., Kuchařík, M., Farré, J.F., Fokkens, H., Fowler, C., Gazenbeek, M., Garrido Pena, R., Haber-Uriarte, M., Haduch, E., Hey, G., Jowett, N., Knowles, T., Massy, K., Pfrengle, S., Lefranc, P., Lemerrier, O., Lefebvre, A., Joaquín, L. M., Majó, T., McKinley, J.I., McSweeney, K., Gusztáv, M. B., Modi, A., Kulcsár, G., Kiss, V., Czene, A., Patay, R., Endródi, A., Köhler, K., Hajdu, T., Cardoso, J. L., Liesau, C., Pearson, M. P., Włodarczak, P., Price, T. D., Prieto, P., Rey, P.J., Ríos, P., Risch, R., Rojo Guerra, M.A., Schmitt, A., Serrallongue, J., Silva, A.M., Smrčka, V., Vergnaud, L., Zilhão, J., Caramelli, D., Higham, T., Heyd, V., Sheridan, J.A., Sjögren, K.G., Thomas, M.G., Stockhammer, P. W., Pinhasi, R., Krause, J., Haak, W., Barnes, I., Lalueza-Fox, C., Reich, D. (2017) *The Beaker phenomenon and the genomic transformation of northwest Europe*. bioRxiv.

Price, T.D., Burton, J.H., Bentley, R.A., 2002. The characterization of biologically available strontium isotope ratios for the study of prehistoric migration. *Archaeometry* 44 (1), 117–135.

Reimer, P.J., Bard, E., Bayliss, A., Beck, J.W., Blackwell, P.G., Bronk Ramsey, C., Grootes, P.M., Guilderson, T.P., Hafliðason, H., Hajdas, I., Hatt_e, C., Heaton, T.J., Hoffmann, D.L., Hogg, A.G., Hughen, K.A., Kaiser, K.F., Kromer, B., Manning, S.W., Niu, M., Reimer, R.W., Richards, D.A., Scott, E.M., Southon, J.R., Staff, R.A., Turney, C.S.M., Van der Plicht, J., 2013. IntCal13 and Marine13 radiocarbon age calibration curves 0-50,000 Years cal BP. *Radiocarbon* 55 (4), 1869–1887.

Salazar-García, D.C., 2012. Aproximación a la dieta de la población calcolítica de La Vital a través del análisis de isótopos estables del carbono y del nitrógeno sobre restos óseos. In: Pérez, G., Bernabeu, J., Carrión, Y., García-Puchol, O., Molina, L.L., Gómez, M. (Eds.), La Vital (Gandia, Valencia). Vida y muerte en la desembocadura del Serpis durante el III y el I milenio a.C. Museu de Prehistòria de València-Diputació de Valencia (T.V. 113), València, pp. 139–143.

Salazar-García, D.C., 2014a. Estudi de la dieta en la població de Cova dels Diablets mitjançant anàlisi d'isòtops estables del carboni i del nitrogen en collàgen ossi. Resultats preliminars. In: Aguilera Arzo, G.A., Monroig, D., García-Borja, P. (Eds.), La Cova dels Diablets (Alcalà de Xivert, Castelló). Prehistòria a la Serra d'Irta. Diputació de la Castelló, Castellón, pp. 67–78.

Salazar-García, D.C., García-Puchol, O., de Miguel-Ibañez, M.P., Talamo, S., 2016. Earliest evidence of neolithic collective burials from Eastern Iberia: radiocarbon dating at the archaeological site of Les Llometes (Alicante, Spain). *Radiocarbon* 58 (3), 679–692.

Sarasketa-Gartzia, I., Villalba-Mouco, V., le Roux, P., Arrizabalaga, Á., Salazar-García, D. C., 2017. Late Neolithic-Chalcolithic socio-economical dynamics in Northern Iberia. A multi-isotope study on diet and provenance from Santimamiñe and Pico Ramos archaeological sites (Basque Country, Spain). *Quaternary International* (*in press*).

Sarasketa-Gartzia, I., Villalba-Mouco, V., Arrizabalaga, Á., Salazar-García, D. C., 2018. Anthropogenic resource exploitation and use of the territory at the onset of social complexity in the Western Pyrenees: a multi-isotope approach. *Archaeological and Anthropological Science* (*in press*).

Fernández-Crespo, T., Schulting, R.J., 2017. Living different lives: Early social differentiation identified through linking mortuary and isotopic variability in Late Neolithic/Early Chalcolithic north-central Spain. *PLoS one* 12(9), e0177881.

Rojo, M., Garrido, R., García-Martínez de Lagrán, I., Kunst, M., 2008. Los recintos del poblado

del Neolítico Antiguo de la Revilla del Campo (Ambrona, Soria). In: *IV Congreso del Neolítico Peninsular*. Museo Arqueológico de Alicante-MARQ, pp. 252–258.

Sjögren, K.G., Price, T.D., Kristiansen, K. (2016). Diet and mobility in the Corded Ware of Central Europe. *PLoS one*, 11(5), e0155083.

Stockhammer, P. W., Massy, K., Knipper, C., Friedrich, R., Kromer, B., Lindauer, S., Radosavljević, J., Krause, J. (2015). Rewriting the central European Early Bronze Age chronology: Evidence from large-scale radiocarbon dating. *PLoS One*, 10(10), e0139705.

Szécsényi-Nagy, A., Roth, C., Brandt, G., Rihuete-Herrada, C., Tejedor-Rodríguez, C., Held, P., García-Martínez-de-Lagrán, I., Arcusa Magallón, H., Zesch, S., Knipper, C., Bánffy, E., Friederich, S., Meller, H., Bueno, P., Barroso, R., Balbín R., Herrero- Corral, A.M., Flores, R., Alonso, C., Jiménez, J., Rindlisbacher, L., Oliart, C., Fregeiro, M.I., Soriano, I., Vicente, O., Micó, R., Lull, V., Soler, J., López J.A., Roca de Togores, C., Hernández, M.S., Jover, F.J., Lomba, J., Avilés, A., Lillios, K.T., Silva, A.M., Magalhães, M., Oosterbeek, L.M., Cunha, C., Waterman, A.J., Roig, J., Martínez, A., Ponce J., Hunt, M., Mejías-García, J.C., Carlos Pecero J.C., Cruz-Auñón, R., Tomé, T., Carmona, E., Cardoso, J.L., Araújo, A.C., Liesau, C., von Lettow-Vorbeck, Blasco, C., Ríos, P., Pujante, A., Royo-Guillén, J.I., Esquembre, M.A., Dos Santos, V.M., Parreira, R., Morán, E., Méndez, E., Vega, J., Menduiña, R., Martínez, V., López, O., Krause, J., Pichlerf, S.L., Garrido-Pena, R., Kunst, M., Risch, R., Rojo-Guerra, M.A., Haak, W., Atl, K.W., 2017. The maternal genetic make-up of the Iberian Peninsula between the Neolithic and the Early Bronze Age. bioRxiv

Ubelaker, D. H. (2009). The forensic evaluation of burned skeletal remains: a synthesis. *Forensic Science International*, 183(1-3), 1-5.

Utrilla, P., Mazo, C., Domingo, R., 2015. Fifty thousand years of prehistory at the cave of Abauntz (Arraitz, Navarre): a nexus point between the Ebro valley, aquitaine and the cantabrian corridor. *Quaternary International* 364, 294–305.

Utrilla, P., Mazo, C., Lorenzo, J.I., 2007. Enterramientos humanos en el Calcolítico de Abauntz. In: *La tierra te sea leve. Arqueología de la Muerte en Navarra*, pp. 66–72. Museo de Navarra.

Utrilla, P., Mazo, C., Sopena, M. C., Martínez-Bea, M., & Domingo, R. (2009). A palaeolithic map from 13,660 calBP: engraved stone blocks from the Late Magdalenian in Abauntz Cave (Navarra, Spain). *Journal of Human Evolution*, 57(2), 99–111.

Utrilla, P., Mazo, C., Lorenzo, J.I., 2014. Rituales funerarios en el calcolítico de Abauntz. Un ejemplo de lesión con supervivencia. *Salduie 13-14*, 297–314.

Valenzuela-Lamas, S., Jiménez-Manchón, S., Evans, J., López, D., Jornet, R., & Albarella, U. (2016). Analysis of seasonal mobility of sheep in Iron Age Catalonia (north-eastern Spain) based on strontium and oxygen isotope analysis from tooth enamel: first results. *Journal of Archaeological Science: Reports*, 6, 828-836.

Van Klinken, G.J., 1999. Bone collagen quality indicators for palaeodietary and radiocarbon measurements. *Journal of Archaeological Science* 26, 687–695.

Villalba-Mouco, V., Sarasketa-Gartzia, I., Utrilla, P, Oms, X., Mendiola, S., Mazo, C., Cebrià, A., Salazar-García, D.C. 2018. Stable isotope ratio analysis of bone collagen as indicator of different environment conditions and dietary habits in Northeastern Iberia during IV and III millennium cal B.C. *Archaeological and Anthropological Science (in press)*.

Villalba-Mouco, V., Sauqué, V., Sarasketa-Gartzia, I., Pastor, M.V., le Roux, P.J., Vicente, D., Utrilla, P., Salazar-García, D.C., 2017. Territorial mobility and subsistence strategies during the Ebro Basin Late Neolithic-Chalcolithic: A multi-isotope approach from San Juan cave (Loarre, Spain). *Quaternary International (in press)*.

Walker, P.L., Miller, K.P., 2005. Time, temperature, and oxygen availability: an experimental study of the effects of environmental conditions on the color and organic content of cremated bone, *Am. J. Phys. Anthropol. Suppl.* 40, 216–217.

Waterman, A. J., Tykot, R. H., & Silva, A. M. (2016). Stable Isotope Analysis of Diet-based Social Differentiation at Late Prehistoric Collective Burials in South-Western Portugal. *Archaeometry*, 58(1), 131-151.

Waterman, A. J., Peate, D. W., Silva, A. M., & Thomas, J. T. (2014). In search of homelands: using strontium isotopes to identify biological markers of mobility in late prehistoric Portugal. *Journal of Archaeological Science*, 42, 119-127.

Waterman, A.J., Beck, J.L., Thomas, J.T., Tykot, R.H. 2017. Stable Isotope Analysis of Human Remains from Los Millares (Almería, Spain, c. 2500-1800 BC): Regional Comparisons and Dietary Variability, Menga. *Journal of Andalusian Prehistory* 8, 15–27.

Whyte, T.R., (2001). Distinguishing remains of human cremations from burned animal bones, *J. Field Archaeol.* 28 (3/4) (2001) 437–448.

Pin C, Briot D, Bassin C, Poitrasson F (1994) Concomitant separation of strontium and samarium-neodymium for isotopic analysis in silicate samples, based on specific extraction chromatography. *Anal Chim Acta* 298: 209–217.

Van Klinken, G.J. (1999). Bone collagen quality indicators for palaeodietary and radiocarbon measurements. *Journal of Archaeological Science*, 26, 687–695.

Villalba-Mouco, V., Sauqué, V., Sarasketa-Gartzia, I., Pastor, M.V., le Roux, P.J., Vicente, D., Utrilla, P., Salazar-García, D.C., 2017. Territorial mobility and subsistence strategies during the Ebro Basin Late Neolithic-Chalcolithic: A multi-isotope approach from San Juan cave (Loarre, Spain). *Quaternary International* (in press).

Villalba-Mouco, V., Sarasketa-Gartzia, I., Utrilla, P., Oms, F.X., Mazo, C., Mendiola, S., Cebrià, A., Salazar-García, D.C., 2018. Stable isotope ratio analysis of bone collagen as indicator of different dietary habits and environment conditions in Northeastern Iberia during the 4th and 3rd millennium cal B.C. *Archaeological and Antropological Science* (in press).

FIGURES AND TABLES

FIGURES

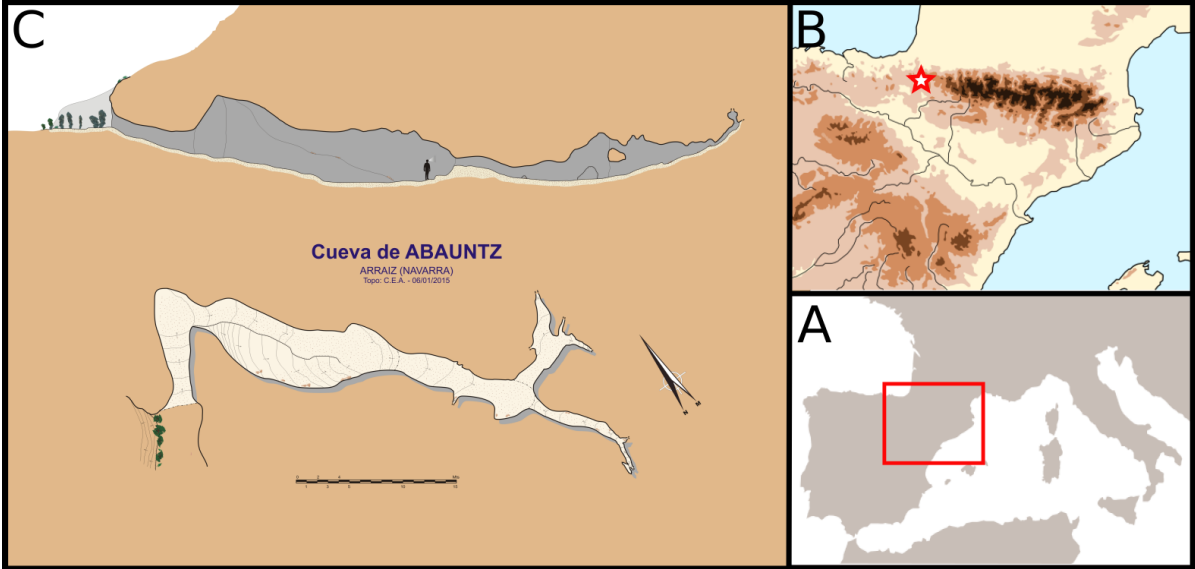


Figure 1: Location map. a Location of the Iberian Peninsula inside Western Europe. b Map of the northeast of the Iberian Peninsula, the star shows the location of Cueva de ABAUNTZ. c Topography of Cueva de ABAUNTZ with plan and profile views.

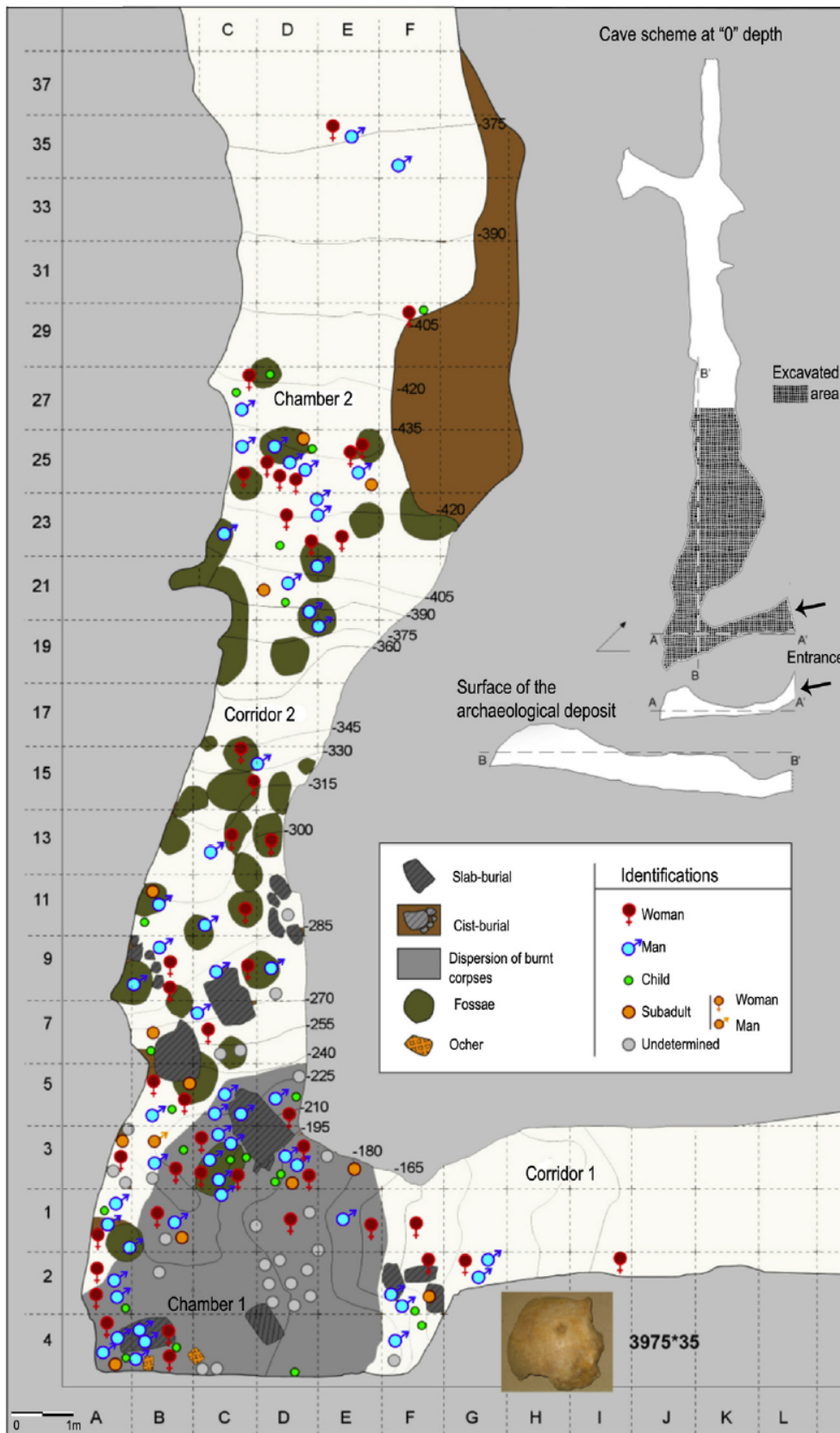


Figure 2: Burial distribution over the Cueva de Abauntz plan views (from Utrilla et al. 2015).

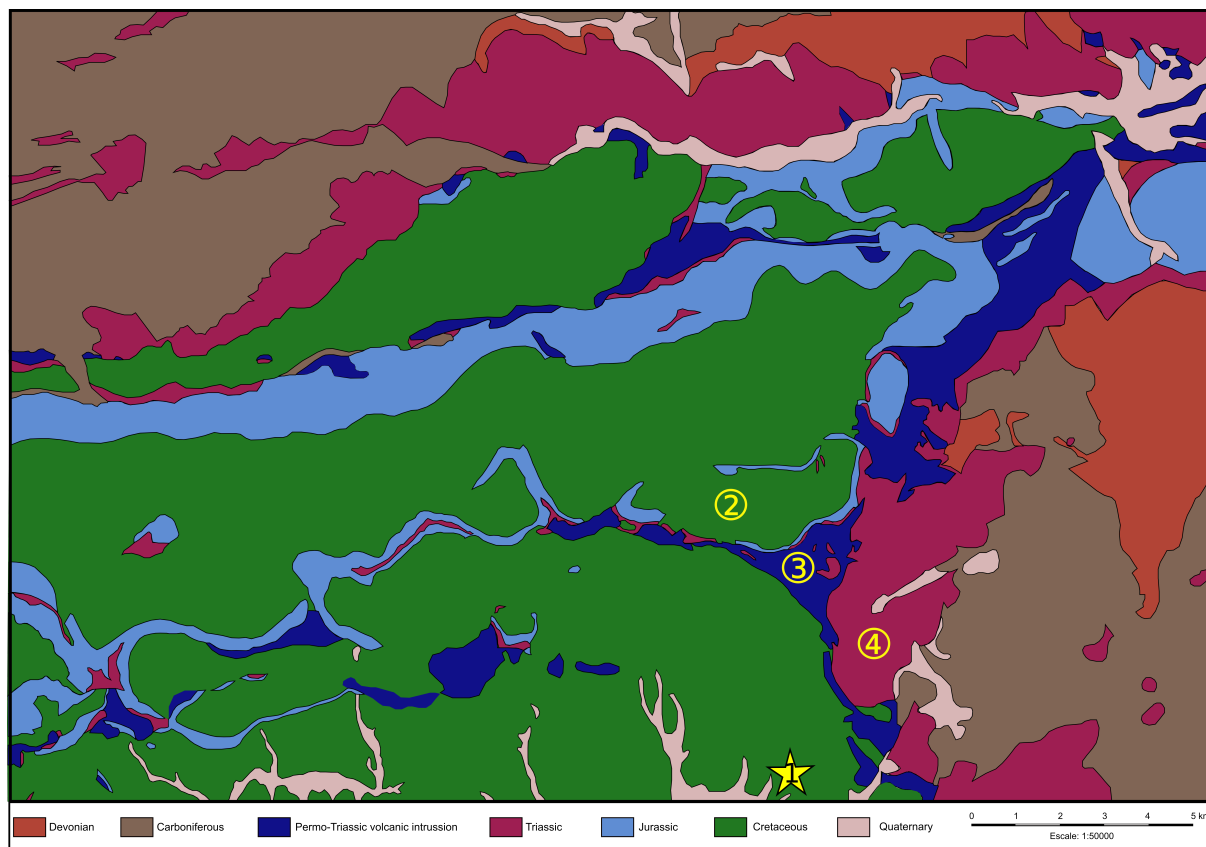


Figure 3: Simplified geological map of Cueva de Abauntz surroundings discussed in the text. Circles show the sampling areas for bioavailable $^{87}\text{Sr}/^{86}\text{Sr}$ range.

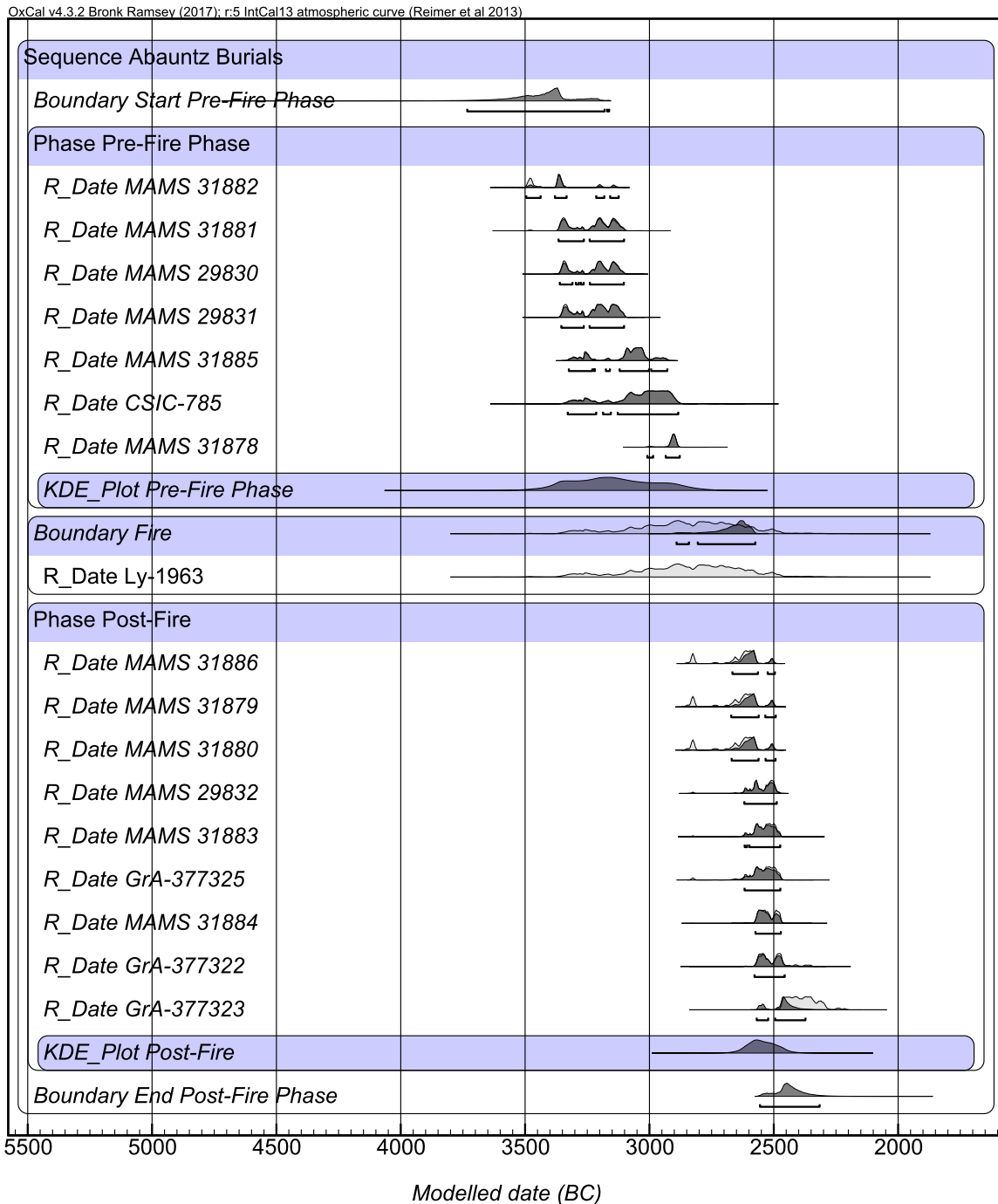


Figure 4: Radiocarbon 2 phases Bayesian modelling of Abauntz individuals Calibration and Bayesian model was performed with OxCal v4.2.3 using the IntCal13 calibration curve (Bronk Ramsey, 2009; Reimer et al., 2013).

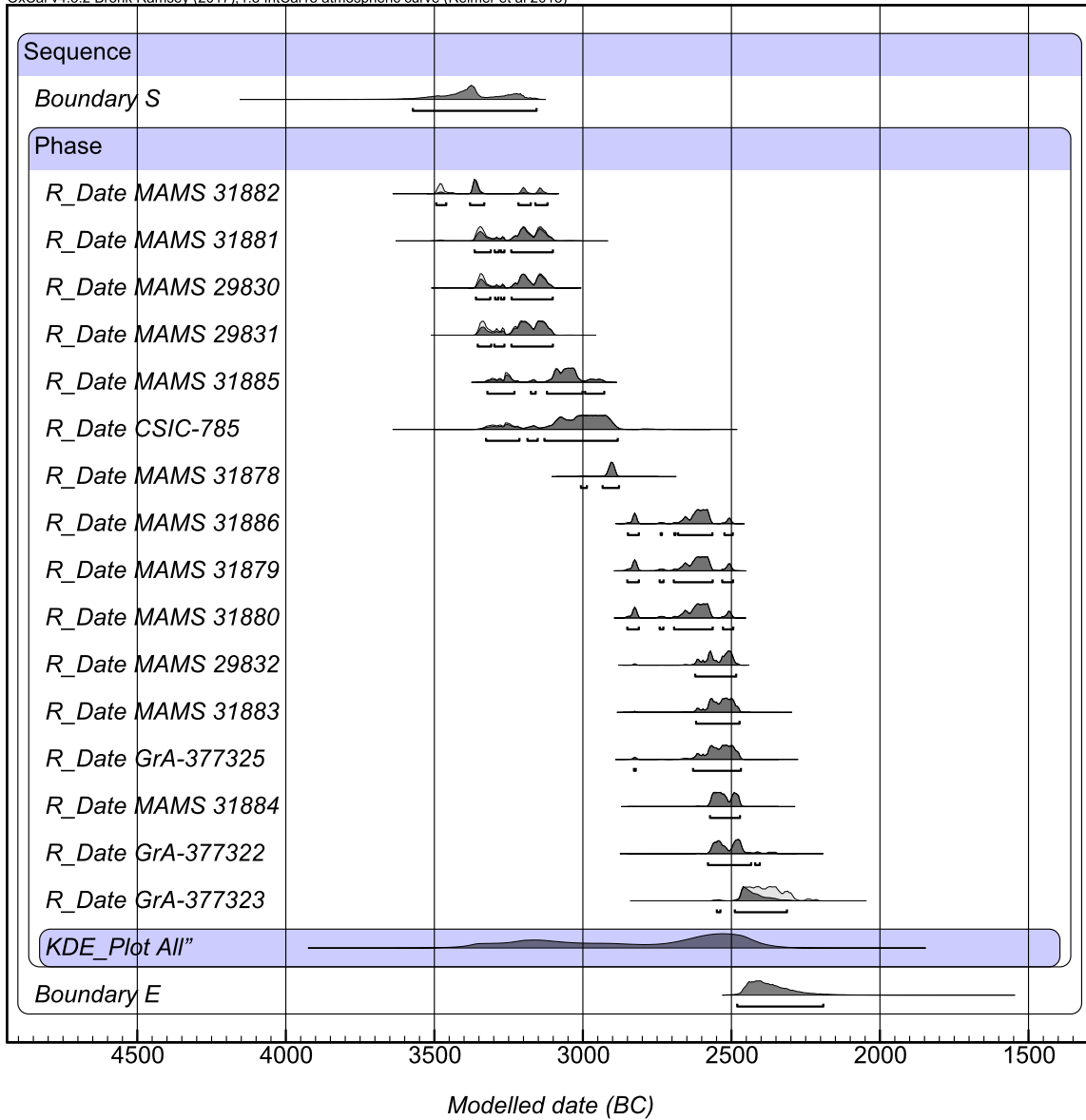


Figure S1: Radiocarbon 1 phase Bayesian modelling of Abautz individuals Calibration and Bayesian model was performed with OxCal v4.2.3 using the IntCal13 calibration curve (Bronk Ramsey, 2009; Reimer et al., 2013).

Archaeological ID	Lab Code	Date uncalibrated	Unmodelled (calibrated at 2sigma cal BC)	Archaeological description
Ab.25D.371.746	MAMS 31882	4600 ± 28	3500-3139	Pit burial-related from Chamber 2
Ab.25D.371.768	MAMS 31881	4544 ± 32	3366-3104	Pit burial-related from Chamber 2
Ab.21D.360.7	MAMS 29830	4534 ± 24	3362-3105	Pit burial-related from Chamber 2
Ab.21D.360.8	MAMS 29831	4523 ± 24	3356-3104	Pit burial-related from Chamber 2
Ab.1D.146.11	MAMS 31885	4443 ± 27	3327-3104	Chamber 1
Ab. 1C/3C.205	CSIC-785	4370 ± 70	3331-2885	Pit burial from Chamber 1 (Carlos b1)
Ab.1A.169.169	MAMS 31878	4296 ± 26	3009-2879	Pit burial from Chamber 1 (Alberto)
Ab. 4C.114.1	Ly-1963	4240 ± 140	3332-2476	Charcoal from Chamber 1
Ab.29F.rev.2	MAMS 31886	4077 ± 23	2850-2497	Surface, without ritual
Ab.27C.r.50	MAMS 31879	4076 ± 27	2851-2495	Surface, without ritual
Ab.rev(35).672	MAMS 31880	4076 ± 26	2851-2495	Surface without ritual
Ab.17C.283.31	MAMS 29832	4040 ± 23	2623-2483	Surface without ritual (bronze axe potentially associated)
Ab.23D/F.rev(19041)	MAMS 31883	4026 ± 28	2620-2473	Surface, without ritual
Ab.5D.196.13	GrA-377325	4025 ± 35	2831-2468	Cist burial (burned remains under cists)
Ab.rev(35).619	MAMS 31884	4000 ± 25	2573-2471	Surface without ritual
Ab. rev. p. 105 (caja 997)	GrA-377322	3975 ± 35	2579-2349	Surface without ritual, trepanated skull
Ab.25D.377.409	GrA-377323	3900 ± 35	2476-2286	Surface, without ritual (Kimby)

Table 1: radiocarbon dates from Cueva de Abauntz sepulchral levels. All dates have been calibrated with OxCal v4.2.3 and using the IntCal13 calibration curve (Bronk Ramsey 2009; Reimer et al. 2013) and their correspondence with the archaeological context and ID

S-UCT code	Species	Sampled bone	Archaeological ID	$\delta^{13}\text{C}$ ‰	$\delta^{15}\text{N}$ ‰	Age	Collagen yield (%)	C (%)	N (%)	C: N (Elemental)	Sampled tooth	$^{87}\text{Sr}/^{86}\text{Sr}$	Sr conc. (ppm)
19064	Human	mandible	Ab.4F.139.1	-20.2	8.9	Infant I	3.45	39.8	14.4	3.2	-	-	-
19063	Human	mandible	Ab.27D.342.155	-20.5	9.0	Infant I	5.71	44.1	15.6	3.3	-	-	-
19058	Human	mandible	Ab.2F.95.2	-20.5	9.0	Infant I	7.22	44.1	15.6	3.3	P1	0.708416	69.58
19056	Human	mandible	Ab.3D.142.2.68	-20.0	8.3	Infant II	2.76	43.7	15.3	3.3	-	-	-
19067	Human	mandible	Ab.5C.b1b2.159	-20.3	9.1	Infant II	3.72	43.0	15.6	3.2	P1	0.708933	101.4
19059	Human	mandible	Ab.1D.146.11	-19.3	9.8	Infant I	2.05	40.4	14.7	3.2	M2	0.711560	194.3
19060	Human	mandible	Ab.3D.142.2.67	-21.0	9.7	Infant II	4.81	44.4	14.5	3.2	M2	0.709057	106.1
19062	Human	mandible	Ab.27-33.100?	-20.0	8.5	Infant II	4.46	42.9	15.7	3.2	-	-	-
19057	Human	mandible	Ab.35E.401.6	-20.7	7.9	Juvenile	2.57	39.5	14.2	3.3	M2	0.708456	78.25
19061	Human	mandible	Ab.9C.230.860	-20.6	9.3	Juvenile	4.78	43.4	15.0	3.4	M2	0.708850	126.6
19065	Human	mandible	Ab.3C.161.19.134	-20.8	8.9	Juvenile	2.40	43.0	14.7	3.4	M2	0.709209	184.2
19066	Human	mandible	Ab.7A.146.295	-20.4	8.3	Juvenile	2.80	40.8	14.5	3.2	M2	0.708616	154.7
19033	Human	mandible	Ab.29F.rev.2	-20.3	8.8	17-25 y.	3.17	39.8	14.6	3.2	M2	0.708320	131.7
											M3	0.709559	107.0
19038	Human	mandible	Ab.25D.371.746	-20.5	9.5	17-25 y.	1.74	37.6	13.5	3.2	M2	0.708092	167.2
											M3	0.709043	130.6
19039	Human	mandible	Ab.23D.421.221	-19.8	9.0	17-25 y.	4.26	40.8	15.3	3.1	M2	0.709628	98.56
											M3	0.709106	130.3
19041	Human	mandible	Ab. 23D/F.rev..	-20.2	8.2	17-25 y.	5.68	42.8	15.7	3.2	P2	0.710026	122.7
19042	Human	mandible	Ab.2C.64.42	-20.1	9.1	17-25 y.	2.79	39.9	14.6	3.2	M2	0.708775	139.7
19045	Human	mandible	Ab.rev(35)439	-20.2	8.8	17-25 y.	2.83	40.8	14.7	3.2	M2	0.708882	90.43
19047	Human	mandible	Ab.4B.100.638	-20.5	9.1	17-25 y.	2.96	41.1	14.7	3.3	-	-	-
19049	Human	mandible	Ab.29F.b1.2	-20.1	8.8	17-25 y.	5.28	42.9	15.6	3.2	M2	0.709482	70.37
											M3	0.709132	88.92
19051	Human	mandible	Ab.25D.nivel I. X:375	-20.3	9.5	17-25 y.	4.40	43.5	15.8	3.2	M2	0.709164	140.1
											M3	0.709116	108.1
19055	Human	mandible	Ab.25D.nivel I.430-431	-20.1	8.4	17-25 y.	4.96	43.1	15.5	3.2	M2	0.708645	135.7
19028	Human	mandible	Ab.25D.371.768	-20.1	9.0	25-35 y.	2.37	38.1	13.7	3.2	-	-	112.5
19029	Human	mandible	Ab.21D.360.7	-19.3	11.3	25-35 y.	4.75	41.7	15.1	3.2	M2	0.709849	199.7
											M3	0.709255	162.5
19034	Human	mandible	Ab.rev(35).146	-19.6	9.2	25-35 y.	2.30	41.0	15.3	3.1	-	-	-
19035	Human	mandible	Ab.rev(35).672	-20.1	9.1	25-35 y.	2.89	39.7	14.7	3.1	M2	0.709754	105.3
											M3	0.709419	68.41
19036	Human	mandible	Ab.rev(35).619	-20.1	9.0	25-35 y.	5.55	42.2	15.7	3.1	M2	0.709182	62.24
											M3	0.710984	62.48
19037	Human	mandible	Ab.27-33.109	-20.2	8.2	25-30 y.	3.08	41.7	15.5	3.1	M2	0.709608	119.2
											M3	0.709882	90.66
19053	Human	mandible	Ab.19E.364.2	-19.9	8.8	25-35 y.	2.38	38.8	16.0	3.3	-	-	-
19030	Human	mandible	Ab.1A.169.169	-20.8	9.3	33-45	6.32	42.5	15.2	3.3	M2	0.709922	89.42
											M3	0.709825	78.92
19040	Human	mandible	Ab.27-33.108	-19.9	9.0	33-45	4.52	41.2	15.3	3.1	P2	0.708431	164.9
19044	Human	mandible	Ab.25C.nivel I.x: 375?? (17)	-20.2	8.6	33-45	2.80	41.0	14.8	3.2	-	-	-
19048	Human	mandible	Ab.21D.360.8	-20.4	9.7	33-45	4.09	41.2	14.8	3.3	M2	0.708513	125.6
											M3	0.708529	79.98
19046	Human	mandible	Ab.rev(35).126	-20.3	9.0	33-45	2.36	38.8	14.0	3.2	-	-	-
19031	Human	mandible	Ab.27C.r.50	-20.3	8.8	45+	5.06	41.2	14.8	3.3	-	-	59.60
19043	Human	mandible	Ab.25D.r.845	-20.4	9.5	senil	3.05	38.0	14.0	3.2	P2	0.709195	65.41
19054	Human	mandible	Ab.23D/E.rev.181	-19.9	9.4	senil	2.96	40.5	14.5	3.3	C	0.708310	138.2
19032	Human	mandible	Ab.23r.421.219	-20.3	9.2	adult	5.72	42.8	15.6	3.2	-	-	-
19050	Human	mandible	Ab.35E.430.138	-20.0	9.2	adult	2.61	41.2	14.8	3.2	-	-	-
19052	Human	mandible	Ab.25E.rev.51	-17.6	9.8	adult	3.69	40.0	17.3	3.3	P2	0.708526	187.6

Table 2: Cueva de Abauntz stable C and N and Sr isotope ratio, including S-UCT code, sampled bone, biological age group, %Collagen (> 30 kDa fraction), $\delta^{13}\text{C}$ and $\delta^{15}\text{N}$ average values, collagen control indicators (%C, %N, C:N elemental), sampled tooth, $^{87}\text{Sr}/^{86}\text{Sr}$ values and Sr concentration(ppm).

Name	Unmodelled (BC/AD) at 2sigma		Modelled (BC/AD) at 2sigma		Agreement (Model=93)
	From	to	From	to	
MAMS 31882	-3500	-3139	-3494	-3120	71.7
MAMS 31881	-3366	-3104	-3365	-3102	99.8
MAMS 29830	-3362	-3105	-3361	-3102	100.4
MAMS 29831	-3356	-3104	-3355	-3102	102
MAMS 31885	-3327	-2929	-3322	-2929	102
CSIC-785	-3331	-2885	-3327	-2883	102.2
MAMS 31878	-3009	-2879	-3007	-2879	99
MAMS 31886	-2850	-2497	-2849	-2496	99.2
MAMS 31879	-2851	-2495	-2851	-2495	99.5
MAMS 31880	-2851	-2495	-2851	-2495	99.4
MAMS 29832	-2623	-2483	-2623	-2485	99
MAMS 31883	-2620	-2473	-2620	-2473	99.6
GrA-377325	-2831	-2468	-2829	-2469	99.9
MAMS 31884	-2573	-2471	-2573	-2472	99.4
GrA-377322	-2579	-2349	-2580	-2405	103.7
GrA-377323	-2476	-2286	-2550	-2314	102.2

Table S1: 1-phase modelled radiocarbon dates. Calibration and Bayesian model was performed with OxCal v4.2.3 using the IntCal13 calibration curve ([Bronk Ramsey, 2009](#); [Reimer et al., 2013](#)).

Name	Unmodelled (BC/AD) at 2sigma		Modelled (BC/AD) at 2sigma		Agreement (Model=102.2)
	From	to	From	to	
MAMS 31882	-3500	-3139	-3496	-3124	87.9
MAMS 31881	-3366	-3104	-3366	-3103	99.7
MAMS 29830	-3362	-3105	-3361	-3104	99.7
MAMS 29831	-3356	-3104	-3355	-3103	100.5
MAMS 31885	-3327	-2929	-3325	-2929	100.7
CSIC-785	-3331	-2885	-3329	-2885	101.1
MAMS 31878	-3009	-2879	-3009	-2879	98.3
MAMS 31886	-2850	-2497	-2667	-2496	111.2
MAMS 31879	-2851	-2495	-2672	-2493	111.9
MAMS 31880	-2851	-2495	-2670	-2494	111.8
MAMS 29832	-2623	-2483	-2619	-2489	100.6
MAMS 31883	-2620	-2473	-2618	-2475	101.3
GrA-377325	-2831	-2468	-2618	-2474	104.1
MAMS 31884	-2573	-2471	-2574	-2472	100.2
GrA-377322	-2579	-2349	-2578	-2457	106.6
GrA-377323	-2476	-2286	-2569	-2373	76.1

Table S2: 2-phase modelled radiocarbon dates. Calibration and Bayesian model was performed with OxCal v4.2.3 using the IntCal13 calibration curve ([Bronk Ramsey, 2009](#); [Reimer et al., 2013](#)).

10.6 Survival of Late Pleistocene Hunter-gatherer ancestry in the Iberian Peninsula.

Please cite this article in press as: Villalba-Mouco et al., Survival of Late Pleistocene Hunter-Gatherer Ancestry in the Iberian Peninsula, *Current Biology* (2019), <https://doi.org/10.1016/j.cub.2019.02.006>

Current Biology
Report

CellPress

Survival of Late Pleistocene Hunter-Gatherer Ancestry in the Iberian Peninsula

Vanessa Villalba-Mouco,^{1,2} Marieke S. van de Loosdrecht,¹ Cosimo Posth,¹ Rafael Mora,³ Jorge Martínez-Moreno,³ Manuel Rojo-Guerra,⁴ Domingo C. Salazar-García,⁵ José I. Royo-Guillén,⁶ Michael Kunst,⁷ H el ene Rougier,⁸ Isabelle Crevecoeur,⁹ H ector Arcusa-Magall on,¹⁰ Cristina Tejedor-Rodr iguez,¹¹ I nigo Garc a-Mart nez de Lagr an,¹² Rafael Garrido-Pena,¹³ Kurt W. Alt,^{14,15} Choongwon Jeong,¹ Stephan Schiffels,¹ Pilar Utrilla,² Johannes Krause,¹ and Wolfgang Haak^{1,16,*}

¹Department of Archaeogenetics, Max Planck Institute for the Science of Human History, Kahlaische Stra e 10, 07745 Jena, Germany

²Departamento de Ciencias de la Antigüedad, Grupo Primeros Pobladores del Valle del Ebro (PPVE), Instituto de Investigación en Ciencias Ambientales (IUCA), Universidad de Zaragoza, Pedro Cerbuna, 50009 Zaragoza, Spain

³Centre d'Estudis del Patrimoni Arqueol gic de la Prehist ria (CEPAP), Facultat de Lletres, Universitat Aut noma Barcelona, 08190 Bellaterra, Spain

⁴Department of Prehistory, University of Valladolid, Plaza del Campus, 47011 Valladolid, Spain

⁵Grupo de Investigaci n en Prehistoria IT-622-13 (UPV-EHU)/IKERBASQUE-Basque Foundation for Science, Euskal Herriko Unibertsitatea, Francisco Tomas y Valiente s/n., 01006 Vitoria, Spain

⁶Direcci n General de Cultura y Patrimonio, Gobierno de Arag n, Avenida de Ranillas, 5 D., 50018 Zaragoza, Spain

⁷Instituto Arqueol gico Alem n, Calle Serrano 159, E-28002 Madrid, Spain

⁸Department of Anthropology, California State University, Northridge, Northridge, California 91330, USA

⁹Universit  de Bordeaux, CNRS, UMR 5199-PACEA, 33615 Pessac Cedex, France

¹⁰Arcadia-FUNGE, Fundaci n General de la Universidad de Valladolid, 47002 Valladolid, Spain

¹¹Juan de la Cierva-Formaci n Program, Institute of Heritage Sciences, Spanish National Research Council (Incipit, CSIC), Av. de Vigo, 15705 Santiago de Compostela, Spain

¹²Juan de la Cierva-Incorporaci n Program, Department of Prehistory, Valladolid University, Plaza del Campus, 47011 Valladolid, Spain

¹³Department of Prehistory, Universidad Aut noma de Madrid, Campus de Cantoblanco, 28049 Madrid, Spain

¹⁴Center of Natural and Cultural Human History, Danube Private University, Steiner Landstr. 124, A-3500 Krems, Austria

¹⁵Department of Biomedical Engineering, University of Basel, Gewerbestrasse 14-16, CH-4123 Allschwil, Switzerland

¹⁶Lead Contact

*Correspondence: haak@shh.mpg.de

<https://doi.org/10.1016/j.cub.2019.02.006>

Current Biology

Survival of Late Pleistocene Hunter-Gatherer Ancestry in the Iberian Peninsula

Highlights

- Iberian hunter-gatherers show dual Late Pleistocene genetic ancestry
- Dual hunter-gatherer ancestry is the result of admixture from different refugia
- This mixed Late Pleistocene ancestry can be traced in Iberian Neolithic farmers

Authors

Vanessa Villalba-Mouco, Marieke S. van de Loosdrecht, Cosimo Posth, ..., Pilar Utrilla, Johannes Krause, Wolfgang Haak

Correspondence

haak@shh.mpg.de

In Brief

Villalba-Mouco et al. generate genome-wide data from prehistoric Iberian hunter-gatherers and early farmers and show that two lineages of Late Pleistocene ancestry survived in Iberian foragers, likely as a result of admixture from different southern refugia. Newly arrived Neolithic farmers retain this genetic signature, suggesting local admixture.

Survival of Late Pleistocene Hunter-Gatherer Ancestry in the Iberian Peninsula

Vanessa Villalba-Mouco,^{1,2} Marieke S. van de Loosdrecht,¹ Cosimo Posth,¹ Rafael Mora,³ Jorge Martínez-Moreno,³ Manuel Rojo-Guerra,⁴ Domingo C. Salazar-García,⁵ José I. Royo-Guillén,⁶ Michael Kunst,⁷ H el ene Rougier,⁸ Isabelle Crevecoeur,⁹ H ector Arcusa-Magall on,¹⁰ Cristina Tejedor-Rodr iguez,¹¹ I nigo Garc a-Mart nez de Lagr an,¹² Rafael Garrido-Pena,¹³ Kurt W. Alt,^{14,15} Choongwon Jeong,¹ Stephan Schiffels,¹ Pilar Utrilla,² Johannes Krause,¹ and Wolfgang Haak^{1,16,*}

¹Department of Archaeogenetics, Max Planck Institute for the Science of Human History, Kahlaische Stra e 10, 07745 Jena, Germany

²Departamento de Ciencias de la Antigüedad, Grupo Primeros Pobladores del Valle del Ebro (PPVE), Instituto de Investigación en Ciencias Ambientales (IUCA), Universidad de Zaragoza, Pedro Cerbuna, 50009 Zaragoza, Spain

³Centre d'Estudis del Patrimoni Arqueol gic de la Prehist ria (CEPAP), Facultat de Lletres, Universitat Aut noma Barcelona, 08190 Bellaterra, Spain

⁴Department of Prehistory, University of Valladolid, Plaza del Campus, 47011 Valladolid, Spain

⁵Grupo de Investigaci n en Prehistoria IT-622-13 (UPV-EHU)/IKERBASQUE-Basque Foundation for Science, Euskal Herriko Unibertsitatea, Francisco Tomas y Valiente s/n., 01006 Vitoria, Spain

⁶Direcci n General de Cultura y Patrimonio, Gobierno de Arag n, Avenida de Ranillas, 5 D., 50018 Zaragoza, Spain

⁷Instituto Arqueol gico Alem n, Calle Serrano 159, E-28002 Madrid, Spain

⁸Department of Anthropology, California State University, Northridge, Northridge, California 91330, USA

⁹Universit  de Bordeaux, CNRS, UMR 5199-PACEA, 33615 Pessac Cedex, France

¹⁰Arcadia-FUNGE, Fundaci n General de la Universidad de Valladolid, 47002 Valladolid, Spain

¹¹Juan de la Cierva-Formaci n Program, Institute of Heritage Sciences, Spanish National Research Council (Incipit, CSIC), Av. de Vigo, 15705 Santiago de Compostela, Spain

¹²Juan de la Cierva-Incorporaci n Program, Department of Prehistory, Valladolid University, Plaza del Campus, 47011 Valladolid, Spain

¹³Department of Prehistory, Universidad Aut noma de Madrid, Campus de Cantoblanco, 28049 Madrid, Spain

¹⁴Center of Natural and Cultural Human History, Danube Private University, Steiner Landstr. 124, A-3500 Krems, Austria

¹⁵Department of Biomedical Engineering, University of Basel, Gewerbestrasse 14-16, CH-4123 Allschwil, Switzerland

¹⁶Lead Contact

*Correspondence: haak@shh.mpg.de

<https://doi.org/10.1016/j.cub.2019.02.006>

SUMMARY

The Iberian Peninsula in southwestern Europe represents an important test case for the study of human population movements during prehistoric periods. During the Last Glacial Maximum (LGM), the peninsula formed a periglacial refugium [1] for hunter-gatherers (HGs) and thus served as a potential source for the re-peopling of northern latitudes [2]. The post-LGM genetic signature was previously described as a cline from Western HG (WHG) to Eastern HG (EHG), further shaped by later Holocene expansions from the Near East and the North Pontic steppes [3–9]. Western and central Europe were dominated by ancestry associated with the ~14,000-year-old individual from Villabruna, Italy, which had largely replaced earlier genetic ancestry, represented by 19,000–15,000-year-old individuals associated with the Magdalenian culture [2]. However, little is known about the genetic diversity in southern European refugia, the presence of distinct genetic clusters, and correspondence with geography. Here, we report new genome-wide data from 11 HGs and Neolithic individuals that highlight the late survival of Paleolithic ancestry in Iberia, reported previously in Magdale-

nian-associated individuals. We show that all Iberian HGs, including the oldest, a ~19,000-year-old individual from El Mir n in Spain, carry dual ancestry from both Villabruna and the Magdalenian-related individuals. Thus, our results suggest an early connection between two potential refugia, resulting in a genetic ancestry that survived in later Iberian HGs. Our new genomic data from Iberian Early and Middle Neolithic individuals show that the dual Iberian HG genomic legacy pertains in the peninsula, suggesting that expanding farmers mixed with local HGs.

RESULTS AND DISCUSSION

We successfully generated autosomal genome-wide data and mitochondrial genomes of 10 new individuals from key sites in the Iberian Peninsula ranging from ~13,000–6,000 calibrated years before present (years cal BP): Late Upper Paleolithic (n = 2), Mesolithic (n = 1), Early Neolithic (EN; n = 4), and Middle Neolithic (n = 3) (Figure 1, Data S1A, and STAR Methods). We furthermore improved the sequencing depth of one Upper Paleolithic individual from Troisi me caverne of Goyet (Belgium) dated to ~15,000 years cal BP and associated with the Magdalenian culture [2]. For each individual, we generated multiple DNA libraries with unique index pairs [10, 11] for next-generation



Figure 1. Geo-chronological Location of Ancient Individuals from the Iberian Peninsula

(A) Map showing the geographical location of the new individuals and sites included in this study (black outlines) and relevant published data for HGs and EN/MN individuals from the Iberian Peninsula (no outlines).

(B) Radiocarbon dates of newly reported individuals in years cal BP (error bars indicate the 2-sigma range).

See also [Data S1](#).

sequencing from ancient DNA (aDNA) extracted from teeth and bones [12] ([Data S1B](#) and [STAR Methods](#)). These were subsequently enriched using targeted in-solution capture for ~1240K informative nuclear SNPs [13], and independently for the complete mitogenome [14], and sequenced on Illumina platforms. All libraries contained short DNA fragments (46–65 bp length on average) with post mortem deamination patterns characteristic for aDNA (4%–16% for partial uracil-DNA glycosylase [UDG] and 19%–31% for non-UDG treated libraries at the first base pair position; [Data S1C](#) and [S1D](#) and [STAR Methods](#)). We estimated contamination rates from nuclear DNA in males to be 1.0%–3.4% for final merged libraries using ANGSD method 2 [15] and for mitogenomes in both sexes to be 0.14%–2.20% using ContamMix [16] ([Data S1E](#) and [S1F](#) and [STAR Methods](#)). After quality filtering, we obtained an endogenous DNA content of 1.3%–29.5% on the targeted 1240K SNPs ([Data S1C](#) and [STAR Methods](#)). We called pseudo-haploid genotypes for each individual (merged libraries) by randomly choosing a single base per site and intersected our data with a set of global modern populations genotyped for ~1240K nuclear SNP positions [17], including published ancient individuals from [2, 5, 7–9, 13, 14, 18–25]. The final dataset from the newly reported individuals contained 19,269–814,072 covered SNPs ([Data S1G](#) and [STAR Methods](#)). For principal-component analysis (PCA), we intersected our new data and published ancient individuals with a panel of worldwide modern populations genotyped on the Affymetrix Human Origins (HO) array [26].

Genetic Structure in Iberian Hunter-Gatherers

To characterize the genetic differentiation between HG individuals, we calculated genetic distances, defined as $1 - f_3$, where f_3 denotes the f_3 -outgroup statistics [26], for pairwise compari-

sons among all published and newly generated HG and visualized the results using multidimensional scaling (MDS) ([STAR Methods](#), [Figure 2A](#) and [STAR Methods](#)). The hunter-gatherer (HG) individuals form distinguishable clusters on the MDS plot, supported by f_4 -statistics and clustering analysis ([Figure S1](#) and [STAR Methods](#)), which we label in line with Fu et al. [2] as *Villabruna*, *Vestonice*, *Satsurblia*, and *Mal'ta* clusters, respectively. Henceforth, we present genetic clusters in italics and individuals in normal print. We introduce the *GoyetQ2* cluster (based on the highest genomic coverage) representing the Magdalenian-associated individuals Goyet Q-2, Hohle Fels 49, Rigney 1, El Mirón, and Burkhardshtöhle. With the newly generated data, we notice that Iberian HGs form a cline between the *GoyetQ2* and *Villabruna* clusters ([Figures 2A](#) and [S2](#)). This cline also includes El Mirón (the oldest individual from Iberia), which had previously been considered representing its own *El Mirón* cluster together with all individuals of the *GoyetQ2* cluster (yellow symbols in [Figure 2A](#)) [2]. Here, Canes 1 and La Braña 1 (Mesolithic individuals from the Cantabrian region in northern Iberia) are falling closer to the *Villabruna* cluster, while Chan (northwestern Iberia) and our newly reported individuals from Moita do Sebastião (Portuguese Atlantic coast) and Balma Guilanyà (Pre-Pyrenean region, northeastern Iberia) have more affinity with El Mirón, which is in turn closer to the Magdalenian *GoyetQ2* cluster.

This observation is confirmed by f_4 -statistics of the form $f_4(\text{GoyetQ2}, \text{Villabruna}; \text{test}, \text{Mbuti})$, which measures whether a test population shares more genetic drift with Goyet Q-2 than with the Villabruna individual. Three Iberian HGs (Chan, Moita do Sebastião, and El Mirón), as well as Hohle Fels 49 and the 35,000-year-old Goyet Q116-1, show significantly positive f_4 -values, indicating that these individuals shared more ancestry with Goyet Q-2 than with Villabruna ([Figure 2B](#)). This

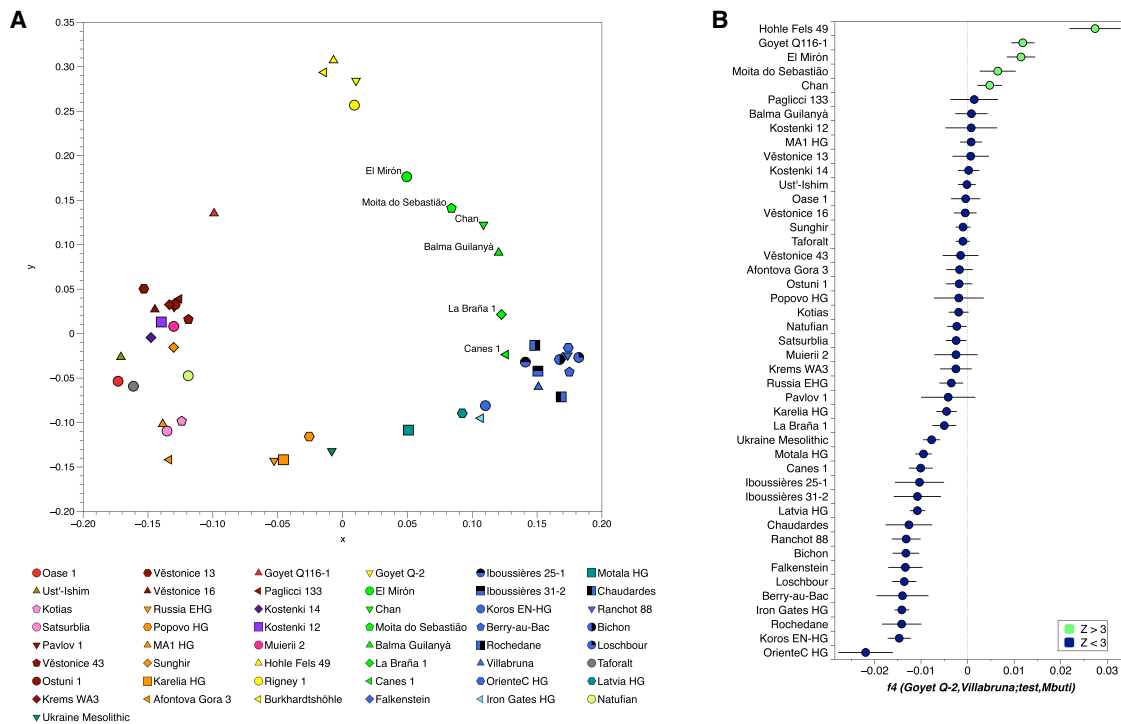


Figure 2. Genetic Distances between European HGs and Key f_4 -Statistics

(A) MDS plot of genetic distances between Eurasian HG individuals (>30,000 SNPs). The main genetic clusters defined previously [2] are: *Vestonice* (dark red), *Mal'ta* (orange: MA1 and Afontova Gora 3), *Satsurblia* (light pink: Kotias and Satsurblia), *Villabruna* (blue: Koros EN-HG, Berry-au-Bac 1, Rochedane, Villabruna, Chaudardes 1, Ranchot 88, La Braña 1, Loschbour), and *GoyetQ2* (yellow; newly defined). Iberian HGs are shown as green symbols.

(B) f_4 -statistics highlighting the excess affinity to Goyet Q-2 in Iberian and European HGs (>20,000 SNPs; error bars indicate ± 3 SE; $Z > 3$ [green]). See also Figures S1 and S2.

heterogeneity in Iberian HGs cannot be explained by genetic drift alone (against which this type of F-statistics is robust) but only by admixture between two sources related to Goyet Q-2 and Villabruna, respectively. We visualize this admixture cline using contrasting f_3 -outgroup statistics of the form $f_3(\text{GoyetQ2}; \text{test}, \text{Mbuti})$ and $f_3(\text{Villabruna}; \text{test}, \text{Mbuti})$ (Figure 3A). The individuals from the *Villabruna* cluster deviate from the symmetry line $x = y$ toward the y axis, expectedly, indicating excess genetic drift shared with Villabruna. In contrast, individuals of the *GoyetQ2* cluster deviate from the symmetry line $x = y$ toward the x axis, indicating excess genetic drift with Goyet Q-2. Iberian HGs fall between the two clusters, which is inconsistent with them forming a clade with either group, but can only be explained by admixture. Here, Iberian HG Canes 1 and La Braña 1 share more Villabruna-like ancestry while El Mirón, Moita do Sebastião, and Chan share more Goyet Q-2-like ancestry.

To further confirm the potential admixture of El Mirón, we used $f_4(\text{GoyetQ2 cluster}, \text{El Mirón}; \text{Villabruna}, \text{Mbuti})$ to test if Magdalenian-associated individuals were cladal with El Mirón. Here, we obtained significantly negative Z scores for Hohle Fels 49, Goyet Q-2, and Burkhardtshöhle. Among these, Goyet Q-2 has the highest data quality and most negative Z score and thus represents the best proxy for the non-*Villabruna*-like ancestry proportion in individuals such as El Mirón ($Z = -6.82$) (Data S1H). Based on this observation, we used the test $f_4(\text{Goyet Q-2}, \text{GoyetQ2 cluster}; \text{Villabruna}, \text{Mbuti})$, for which El Mirón is

significantly negative (Figure 3B and Data S1H), confirming shared ancestry with Villabruna.

To show that the affinity of El Mirón with the Villabruna individual cannot be explained by El Mirón representing a basal split from Villabruna and the other *GoyetQ2* individuals, we used the test $f_4(\text{GoyetQ2 cluster}, \text{Villabruna}; \text{El Mirón}, \text{Mbuti})$. Here, all individuals of the *GoyetQ2* cluster are significantly positive, indicating that this cluster does not represent a sister branch of Villabruna and that El Mirón is not an outgroup to both the *Villabruna* and *GoyetQ2* clusters (Figure 3C and Data S1H). The mixed ancestry of El Mirón could also explain its reduced affinity to Goyet Q116-1 when compared to the younger *GoyetQ2* cluster in the test $f_4(\text{GoyetQ2 cluster}, \text{Goyet Q-2}; \text{Goyet Q116-1}, \text{Mbuti})$ (Data S1H).

Having established two potential Paleolithic source populations surviving in Iberia from $\sim 19,000$ years cal BP onward, we used the admixture modeling programs *qpWave* and *qpAdm* (Figure 3D and STAR Methods) to explore the ancestry of all Iberian HGs. We used Villabruna and Goyet Q-2 as ultimate sources to model the dual ancestry in European HGs relative to outgroups that can distinguish these two sources from shared deeper ancestries (STAR Methods). Our two-source admixture model provides a good fit for the genetic profiles of most European HGs and is consistent with the cline between Villabruna- and Goyet Q-2-like ancestries described above (Figure 3D and STAR Methods). Here, Villabruna-like ancestry is the dominant component ($69.8\% \pm 4.3\% - 100\%$) in individuals of the *Villabruna* cluster,

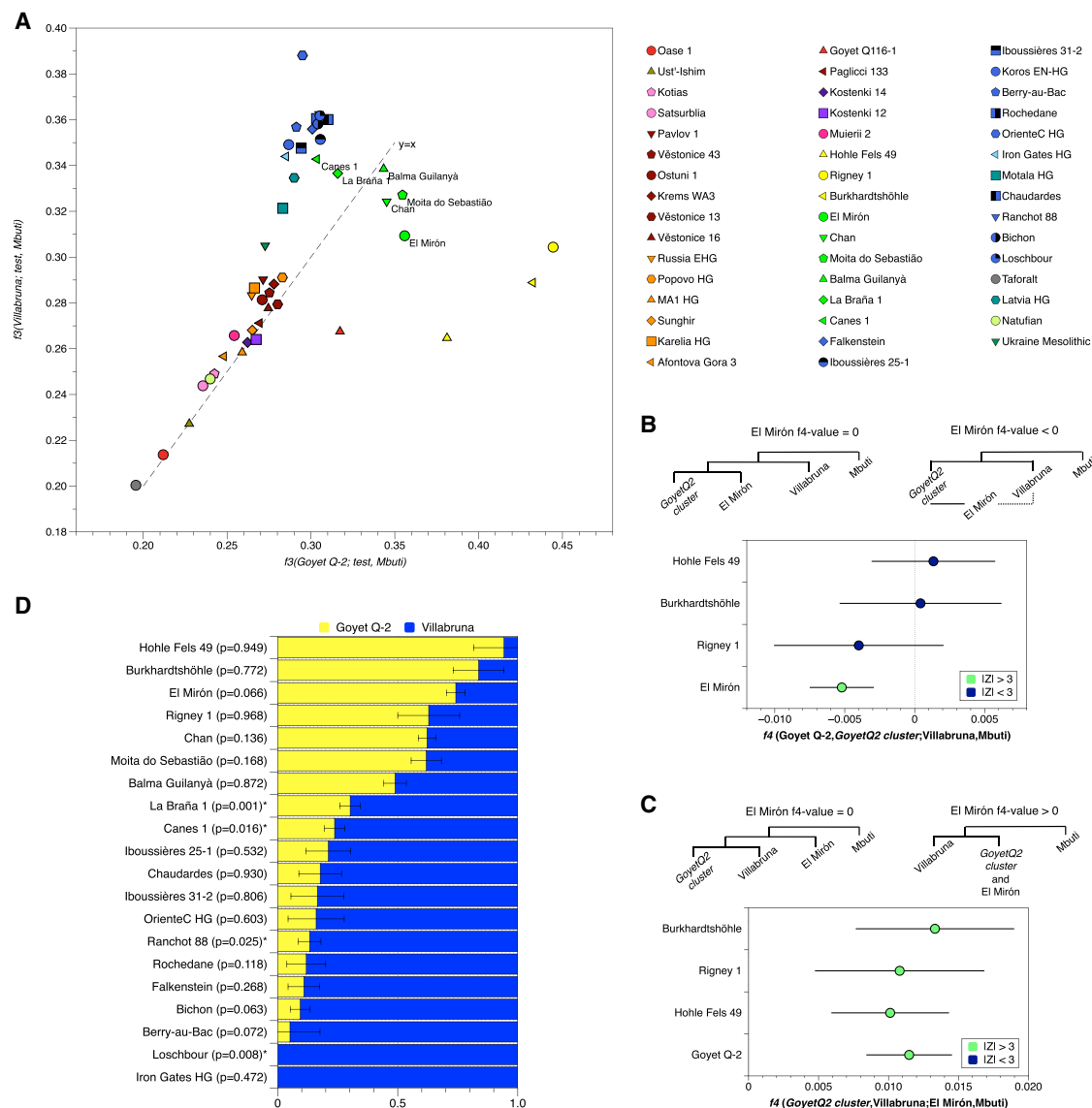


Figure 3. Key f_3 -Outgroup Tests, f_4 -Statistics, and $qpAdm$ Results

(A) Biplot of f_3 -outgroup tests illustrating the Villabrana-like and Goyet Q-2-like ancestries in European HGs. The $x = y$ axis marks full symmetry between Goyet Q-2- and Villabrana-like ancestries, and deviations mark excess ancestry shared with Goyet Q-2 (yellow) or Villabrana (blue).

(B) Results of f_4 -statistics highlighting the shared genetic drift between El Mirón and Villabrana individuals ($\geq 20,000$ SNPs; error bars indicated ± 3 SE).

(C) Results of f_4 -statistics showing that El Mirón is not a sister clade of Villabrana (error bars indicated ± 3 SE).

(D) Modeling European HGs as a two-way admixture of Villabrana- and Goyet Q-2-like ancestry (error bars indicated ± 1 SE).

See also Figure 3B and Data S1.

and Goyet Q-2-like ancestry the dominant component ($61.9\% \pm 6.3\% - 94.3\% \pm 5.7\%$) in GoyetQ2 cluster individuals (Figure 3D and Data S1). These results underline the power of our outgroups and choice of proxies to differentiate Goyet Q-2- from Villabrana-like ancestry within our test individuals (STAR Methods; see Figure S3A for a replication with more proximal sources El Mirón and Loschbour). Congruent with the pattern observed in MDS (Figure 2A), clustering analysis (Figure S1), PCA (Figure S2), F-statistic-based tests (Figure 2B), and the biplot of f_3 -outgroup tests (Figure 3B), the two-source admixture model assigns a higher proportion of Goyet Q-2-like ancestry to Iberian HGs (ranging from

23.7% to 75.3%) than to contemporaneous Western HG (WHG) outside of Iberia. In fact, Balma Guilanyà, La Braña 1, and Canes 1 show elevated Villabrana admixture proportions but still higher Goyet Q-2 proportions than non-Iberian HGs (Figure 3D and Data S1). We notice an additional contribution of Villabrana-like ancestry in the 12,000-year-old Balma Guilanyà individual from northeastern Iberia. Villabrana-like ancestry becomes even stronger during the Mesolithic in the Cantabrian region (La Braña 1 and Canes 1), suggesting extra HG flux into north/northeastern Iberia, which must have had a higher impact in this region. We were able to track a correlation between increasing Villabrana-like ancestry

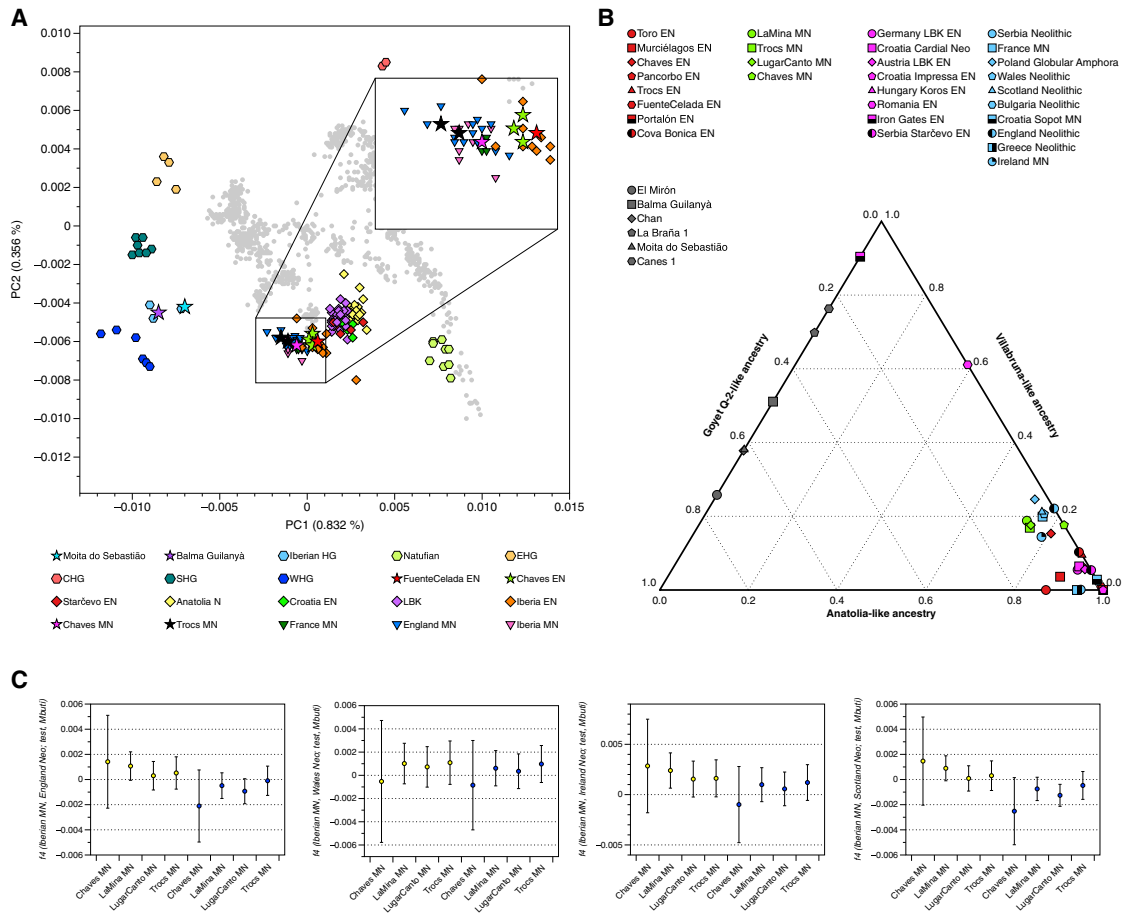


Figure 4. PCA Results and qpAdm Admixture Models

(A) Published ancient and newly reported individuals (stars) projected onto 777 present-day West Eurasians.

(B) Modeling EN and MN populations from Iberian and western Europe as admixture of three ancestral sources: Anatolian Neolithic, Goyet Q-2, and Villabruna (Data S1J).

(C) $f_4(\text{Iberian MN, Neolithic British Isles, test, Mbuti})$, where test is Goyet Q-2 (yellow) or Villabruna (blue), highlighting the excess of Goyet Q-2 ancestry in Iberian MN compared to Neolithic England and Scotland (error bars indicated ± 3 SE). The affinity to Villabruna is shown for comparison to avoid potential bias created by unspecified HG attraction.

See also Data S1.

and time in this region (Figure S3A), while Mesolithic HGs outside this region (Chan and Moita do Sebaštiao) retain more GoyetQ2 ancestry and do not fit this pattern (Figures S3A and S3C). Interestingly, we find no traces of African ancestry (Figure S3B and STAR Methods).

Dual Hunter-Gatherer Genetic Legacy in Iberian Neolithic Individuals

During the Neolithic transition $\sim 7,600$ years ago, human expansions reached the Iberian Peninsula relatively swiftly via expanding early farmers from western Anatolia [3–5]. The rapid expansion of EN individuals associated with farming practices across Europe resulted in a relatively low genetic variability in the reported Neolithic genomes, which makes it difficult to distinguish between the Mediterranean and Danubian routes of expansion of Neolithic lifeways [27, 28]. However, Olalde et al. [9] noted subtle regional differences between WHG individuals and used the proportion of HG ancestry from La Braña 1 in

Neolithic Iberians to trace the expansion from southwestern Europe along the Atlantic coast to Britain. This movement corresponds well with the megalithic burial practices of these regions observed in the archaeological record [29, 30]. Under the assumption that these proportions reflect one, or potentially more, local admixture events along the routes of expansion, it is thus possible to distinguish Neolithic groups by their varying autochthonous HG signatures [18].

Given the presence of two ancestral lineages in Iberian HGs, we thus explored this potential genetic legacy in our newly generated EN and Middle Neolithic (MN) individuals. We first used PCA to assess the genetic affinities qualitatively (Figure 4A). Here, the new Neolithic Iberian individuals spread along a cline from Neolithic Anatolia to WHG, on which the new individuals cluster with contemporaneous Iberian Neolithic individuals [5, 7, 8, 13, 24, 25]. As shown before, MN individuals are shifted toward WHG individuals [3], including the newly reported MN individuals from Cova de Els Trocs and Cueva de Chaves.

Using *qpAdm* models consistent with those above (Figures 3D and S3), we aimed to trace and quantify the proportion of Goyet Q-2- and Villabruna-like HG ancestry in EN and MN groups from Iberia and western/central Europe as a mixture of three ancestral sources: Anatolian Neolithic, Goyet Q-2, and Villabruna, respectively. We show that EN Iberians shared a higher proportion of Goyet Q-2-like ancestry than EN individuals from outside Iberia (Figure 4B and Data S1J). Goyet Q-2-like ancestry is higher in EN from southern Iberia (Andalusia), suggesting additional admixture with local Iberian HGs, who carried mixed Upper Paleolithic ancestry.

Goyet Q-2 ancestry is continuously detectable in all Iberian MN individuals, including broadly contemporaneous individuals from Scotland, Wales, Ireland, and France, but not in Neolithic England, for which the *qpAdm* model with three sources fails ($p = 6.91e-05$) in favor of two sources, despite being poorly supported ($p = 0.001$) (Data S1J). Goyet Q-2-like ancestry is, however, highest in all Iberian MN (except Chaves MN) when compared with other MN populations that share a similar overall amount of HG ancestry (Figures 4B and 4C). We note the presence of Goyet Q-2 ancestry in MN Trocs, where this ancestry was not observed during the EN, but importantly also in MN individuals from France and Globular Amphora from Poland.

Olalde and colleagues [9] reported an elevated signal of La Braña 1 ancestry in Neolithic individuals from Wales and England (using KO1 HG from Hungary and Anatolian Neolithic as the other two sources) and thus argued for an Iberian contribution to the Neolithic in Britain [9]. We replicated these findings by using similar sources (El Mirón instead of Goyet Q-2; Data S1J), showing that these results are sensitive to the source populations used. However, our models with Goyet Q-2 as ultimate source highlight not only the admixed nature of La Braña 1 and El Mirón, but also that Goyet Q-2-like ancestry in MN individuals outside Iberia hints at Iberia as one possible source, but not the exclusive source, of the Neolithic in Britain. Further sampling from regions in today's France, the Netherlands, Belgium, Luxembourg, and Germany is needed to answer this question.

Conclusions

Our results highlight the unique genetic structure observed in Iberian HG individuals, which results from admixture of individuals related to the *GoyetQ2* and *Villabruna* clusters. This suggests a survival of two lineages of Late Pleistocene ancestry in Holocene western Europe, in particular the Iberian Peninsula, whereas HG ancestry in most other regions was largely replaced by Villabruna-like ancestry. With an age estimate of $\sim 18,700$ years cal BP for the El Mirón individual, the oldest representative of this mixed ancestry, the timing of this admixture suggests an early connection (*terminus ante quem*) between putative ancestries from different LGM refugia. It is possible that Goyet Q-2 ancestry could have existed in Iberia in unadmixed form, where it was complemented by Villabruna ancestry as early as $\sim 18,700$ years ago. Alternatively, both Magdalenian-associated Goyet Q-2 and Villabruna ancestries originated in regions outside Iberia and arrived in Iberia independently, where both lineages admixed, or had already existed in admixed form outside Iberia. Interestingly, the dual Upper Paleolithic ancestry was also found in EN individuals

from the Iberian Peninsula, supporting the hypothesis of additional local admixture with resident HGs in Iberia during the time of the Mesolithic-Neolithic transition.

STAR★METHODS

Detailed methods are provided in the online version of this paper and include the following:

- KEY RESOURCES TABLE
- CONTACT FOR REAGENT AND RESOURCE SHARING
- EXPERIMENTAL MODEL AND SUBJECT DETAILS
 - Archaeological sites and sample description
 - Ancient DNA processing and quality control
- QUANTIFICATION AND STATISTICAL ANALYSIS
 - Read processing and assessment of ancient DNA authenticity
 - Contamination tests
 - Genotyping and merging with dataset
 - Kinship relatedness and individual assessment
 - Phenotypic traits analysis
 - Mitochondrial and Y chromosome haplogroups
 - Population genetic analysis
- DATA AND SOFTWARE AVAILABILITY

SUPPLEMENTAL INFORMATION

Supplemental Information can be found with this article online at <https://doi.org/10.1016/j.cub.2019.02.006>.

A video abstract is available at <https://doi.org/10.1016/j.cub.2019.02.006#mmc4>.

ACKNOWLEDGMENTS

We thank the members of the Archaeogenetics Department of the Max Planck Institute for the Science of Human History, especially Maïté Rivollat, Theseas Lamnidis, Cody Parker, Rodrigo Barquera, Stephen Clayton, Aditya Kumar, and all technicians. We thank Iñigo Olalde for valuable comments on the manuscript. We are indebted to the Museo de Huesca, Patrick Semal, the Royal Belgian Institute of Natural Sciences, and all archaeologists involved in the excavations. The genetic research was funded by the Max Planck Society and the European Research Council ERC-CoG 771234 PALEoRIDER (W.H.). V.V.-M. was funded by a predoctoral scholarship of the Gobierno de Aragón and the Fondo Social Europeo (BOA20150701025) and a 3-month research stay grant (CH 76/16) by Programa CAI-Ibercaja de Estancias de Investigación. V.V.-M. and P.U. are members of the Spanish project HAR2014-59042-P (Transiciones climáticas y adaptaciones sociales en la prehistoria de la Cuenca del Ebro), and of the regional government of Aragón PPVE research group (H-07: Primeros Pobladores del Valle del Ebro). The Goyet project was funded by the Wenner-Gren Foundation (7837 to H.R.), the College of Social and Behavioral Sciences of CSUN, and the CSUN Competition for Research, Scholarship, and Creative Activity Awards.

AUTHOR CONTRIBUTIONS

V.V.-M., J.K., and W.H. conceived the study; R.M., J.M.-M., M.R.-G., D.C.S.-G., J.I.R.-G., M.K., H.R., I.C., H.A.-M., C.T.-R., I.G.-M.d.L., R.G.-P., K.W.A., and P.U. assembled samples and provided archaeological context; V.V.-M., M.S.v.d.L., and C.P. performed aDNA lab work and sequencing; V.V.-M., C.P., M.S.v.d.L., S.S., C.J., and W.H. analyzed data; and V.V.-M., C.P., M.S.v.d.L., and W.H. wrote the manuscript with input from all co-authors.

DECLARATION OF INTERESTS

The authors declare no competing interests.

Received: October 16, 2018

Revised: January 4, 2019

Accepted: February 1, 2019

Published: March 14, 2019

REFERENCES

1. Stewart, J.R., and Stringer, C.B. (2012). Human evolution out of Africa: the role of refugia and climate change. *Science* **335**, 1317–1321.
2. Fu, Q., Posth, C., Hajdinjak, M., Petr, M., Mallick, S., Fernandes, D., Furtwängler, A., Haak, W., Meyer, M., Mittnik, A., et al. (2016). The genetic history of Ice Age Europe. *Nature* **534**, 200–205.
3. Haak, W., Lazaridis, I., Patterson, N., Rohland, N., Mallick, S., Llamas, B., Brandt, G., Nordenfelt, S., Harney, E., Stewardson, K., et al. (2015). Massive migration from the steppe was a source for Indo-European languages in Europe. *Nature* **522**, 207–211.
4. Günther, T., and Jakobsson, M. (2016). Genes mirror migrations and cultures in prehistoric Europe—a population genomic perspective. *Curr. Opin. Genet. Dev.* **41**, 115–123.
5. Valdiosera, C., Günther, T., Vera-Rodríguez, J.C., Ureña, I., Iriarte, E., Rodríguez-Varela, R., Simões, L.G., Martínez-Sánchez, R.M., Svensson, E.M., Malmström, H., et al. (2018). Four millennia of Iberian biomolecular prehistory illustrate the impact of prehistoric migrations at the far end of Eurasia. *Proc. Natl. Acad. Sci. USA* **115**, 3428–3433.
6. Allentoft, M.E., Sikora, M., Sjögren, K.-G., Rasmussen, S., Rasmussen, M., Stenderup, J., Damgaard, P.B., Schroeder, H., Ahlström, T., Vinner, L., et al. (2015). Population genomics of Bronze Age Eurasia. *Nature* **522**, 167–172.
7. Martiniano, R., Cassidy, L.M., Ó'Maoldúin, R., McLaughlin, R., Silva, N.M., Manco, L., Fidalgo, D., Pereira, T., Coelho, M.J., Serra, M., et al. (2017). The population genomics of archaeological transition in west Iberia: Investigation of ancient substructure using imputation and haplotype-based methods. *PLoS Genet.* **13**, e1006852.
8. Olalde, I., Schroeder, H., Sandoval-Velasco, M., Vinner, L., Lobón, I., Ramirez, O., Civit, S., García Borja, P., Salazar-García, D.C., Talamo, S., et al. (2015). A Common Genetic Origin for Early Farmers from Mediterranean Cardial and Central European LBK Cultures. *Mol. Biol. Evol.* **32**, 3132–3142.
9. Olalde, I., Brace, S., Allentoft, M.E., Armit, I., Kristiansen, K., Booth, T., Rohland, N., Mallick, S., Szécsényi-Nagy, A., Mittnik, A., et al. (2018). The Beaker phenomenon and the genomic transformation of northwest Europe. *Nature* **555**, 190–196.
10. Meyer, M., and Kircher, M. (2010). Illumina sequencing library preparation for highly multiplexed target capture and sequencing. *Cold Spring Harb. Protoc.* **2010**.
11. Kircher, M., Sawyer, S., and Meyer, M. (2012). Double indexing overcomes inaccuracies in multiplex sequencing on the Illumina platform. *Nucleic Acids Res.* **40**, e3.
12. Dabney, J., Knapp, M., Glocke, I., Gansauge, M.-T., Weihmann, A., Nickel, B., Valdiosera, C., García, N., Pääbo, S., Arsuaga, J.-L., and Meyer, M. (2013). Complete mitochondrial genome sequence of a Middle Pleistocene cave bear reconstructed from ultrashort DNA fragments. *Proc. Natl. Acad. Sci. USA* **110**, 15758–15763.
13. Mathieson, I., Lazaridis, I., Rohland, N., Mallick, S., Patterson, N., Roodenberg, S.A., Harney, E., Stewardson, K., Fernandes, D., Novak, M., et al. (2015). Genome-wide patterns of selection in 230 ancient Eurasians. *Nature* **528**, 499–503.
14. Mittnik, A., Wang, C.-C., Pfringler, S., Daubaras, M., Zariņa, G., Hallgren, F., Allmäe, R., Khartanovich, V., Moiseyev, V., Törv, M., et al. (2018). The genetic prehistory of the Baltic Sea region. *Nat. Commun.* **9**, 442.
15. Korneliussen, T.S., Albrechtsen, A., and Nielsen, R. (2014). ANGSD: Analysis of Next Generation Sequencing Data. *BMC Bioinformatics* **15**, 356.
16. Fu, Q., Mittnik, A., Johnson, P.L.F., Bos, K., Lari, M., Bollongino, R., Sun, C., Giemsch, L., Schmitz, R., Burger, J., et al. (2013). A revised timescale for human evolution based on ancient mitochondrial genomes. *Curr. Biol.* **23**, 553–559.
17. Mallick, S., Li, H., Lipson, M., Mathieson, I., Gymrek, M., Racimo, F., Zhao, M., Chennagiri, N., Nordenfelt, S., Tandon, A., et al. (2016). The Simons Genome Diversity Project: 300 genomes from 142 diverse populations. *Nature* **538**, 201–206.
18. Lipson, M., Szécsényi-Nagy, A., Mallick, S., Pósa, A., Stégmár, B., Keerl, V., Rohland, N., Stewardson, K., Ferry, M., Michel, M., et al. (2017). Parallel palaeogenomic transects reveal complex genetic history of early European farmers. *Nature* **551**, 368–372.
19. Mathieson, I., Alpaslan-Roodenberg, S., Posth, C., Szécsényi-Nagy, A., Rohland, N., Mallick, S., Olalde, I., Broomandkhoshbacht, N., Candilio, F., Cheronet, O., et al. (2018). The genomic history of southeastern Europe. *Nature* **555**, 197–203.
20. Cassidy, L.M., Martiniano, R., Murphy, E.M., Teasdale, M.D., Mallory, J., Hartwell, B., and Bradley, D.G. (2016). Neolithic and Bronze Age migration to Ireland and establishment of the insular Atlantic genome. *Proc. Natl. Acad. Sci. USA* **113**, 368–373.
21. Sikora, M., Seguin-Orlando, A., Sousa, V.C., Albrechtsen, A., Korneliussen, T., Ko, A., Rasmussen, S., Dupanloup, I., Nigst, P.R., Bosch, M.D., et al. (2017). Ancient genomes show social and reproductive behavior of early Upper Paleolithic foragers. *Science* **358**, 659–662.
22. van de Loosdrecht, M., Bouzouggar, A., Humphrey, L., Posth, C., Barton, N., Aximu-Petri, A., Nickel, B., Nagel, S., Talbi, E.H., El Hajraoui, M.A., et al. (2018). Pleistocene North African genomes link Near Eastern and sub-Saharan African human populations. *Science* **360**, 548–552.
23. Jones, E.R., Gonzalez-Fortes, G., Connell, S., Siska, V., Eriksson, A., Martiniano, R., McLaughlin, R.L., Gallego Llorente, M., Cassidy, L.M., Gamba, C., et al. (2015). Upper Palaeolithic genomes reveal deep roots of modern Eurasians. *Nat. Commun.* **6**, 8912.
24. Gonzalez-Fortes, G., Jones, E.R., Lightfoot, E., Bonsall, C., Lazar, C., Grandal-d'Anglade, A., Garraza, M.D., Drak, L., Siska, V., Simalcik, A., et al. (2017). Paleogenomic Evidence for Multi-generational Mixing between Neolithic Farmers and Mesolithic Hunter-Gatherers in the Lower Danube Basin. *Curr. Biol.* **27**, 1801–1810.
25. Fregel, R., Méndez, F.L., Bokbot, Y., Martín-Socas, D., Camalich-Massieu, M.D., Santana, J., Morales, J., Ávila-Arcos, M.C., Underhill, P.A., Shapiro, B., et al. (2018). Ancient genomes from North Africa evidence prehistoric migrations to the Maghreb from both the Levant and Europe. *Proc. Natl. Acad. Sci. USA* **115**, 6774–6779.
26. Patterson, N., Moorjani, P., Luo, Y., Mallick, S., Rohland, N., Zhan, Y., Genschoreck, T., Webster, T., and Reich, D. (2012). Ancient admixture in human history. *Genetics* **192**, 1065–1093.
27. Manning, K., Timpson, A., Colledge, S., Crema, E., Edinborough, K., Kerig, T., and Shennan, S. (2014). The chronology of culture: a comparative assessment of European Neolithic dating approaches. *Antiquity* **88**, 1065–1080.
28. Perrin, T., Manen, C., Valdeyron, N., and Guilaine, J. (2018). Beyond the sea... The Neolithic transition in the southwest of France. *Quat. Int.* **470**, 318–332.
29. Sherratt, A. (1995). Instruments of conversion? The role of megaliths in the mesolithic/neolithic transition in Northwest Europe. *Oxf. J. Archaeol.* **14**, 245–260.
30. Masset, C. (1993). *Les dolmens: Sociétés néolithiques, pratiques funéraires* (Paris: Ed. Errance).
31. Li, H., Handsaker, B., Wysoker, A., Fennell, T., Ruan, J., Homer, N., Marth, G., Abecasis, G., and Durbin, R.; 1000 Genome Project Data Processing Subgroup (2009). The Sequence Alignment/Map format and SAMtools. *Bioinformatics* **25**, 2078–2079.

32. Peltzer, A., Jäger, G., Herbig, A., Seitz, A., Kniep, C., Krause, J., and Nieselt, K. (2016). EAGER: efficient ancient genome reconstruction. *Genome Biol.* 17, 60.
33. Patterson, N., Price, A.L., and Reich, D. (2006). Population structure and eigenanalysis. *PLoS Genet.* 2, e190.
34. Weissensteiner, H., Pacher, D., Kloss-Brandstätter, A., Forer, L., Specht, G., Bandelt, H.-J., Kronenberg, F., Salas, A., and Schönherr, S. (2016). HaploGrep 2: mitochondrial haplogroup classification in the era of high-throughput sequencing. *Nucleic Acids Res.* 44 (W1), W58–63.
35. Poznik, G.D. (2016). Identifying Y-chromosome haplogroups in arbitrarily large samples of sequenced or genotyped men. *bioRxiv*. <https://doi.org/10.1101/088716>.
36. Kearse, M., Moir, R., Wilson, A., Stones-Havas, S., Cheung, M., Sturrock, S., Buxton, S., Cooper, A., Markowitz, S., Duran, C., et al. (2012). Geneious Basic: an integrated and extendable desktop software platform for the organization and analysis of sequence data. *Bioinformatics* 28, 1647–1649.
37. Monroy Kuhn, J.M., Jakobsson, M., and Günther, T. (2018). Estimating genetic kin relationships in prehistoric populations. *PLoS ONE* 13, e0195491.
38. Terradas, X., Pallarés, M., Mora, R., and Moreno, J.M. (1993). Estudi preliminar de les ocupacions humanes de la balma de Guilanyà (Navès, Solsonès). *Rev. d'Arqueologia Ponent*, 231–248.
39. Martínez-Moreno, J., Mora, R., and Casanova, J. (2006). Balma Guilanyà y la ocupación de la vertiente sur del Prepirineo del Noreste de la Península Ibérica durante el Tardiglaciario. In *La cuenca mediterránea durante el paleolítico superior: 38.000-10.000 años*, pp. 444–457.
40. Martínez-Moreno, J., Mora, R., and Casanova, J. (2007). El contexto cronométrico y tecno-tipológico durante el Tardiglaciario y Postglaciario de la vertiente sur de los Pirineos orientales. *Rev. d'Arqueologia Ponent*, 7–44.
41. Martínez-Moreno, J., and Mora, R. (2009). Balma Guilanyà (Prepirineo de Lleida) y el Aziliense en el noreste de la Península Ibérica. *Trabajos de Prehistoria* 66, 45–60.
42. García-Guixé, E., Martínez-Moreno, J., Mora, R., Núñez, M., and Richards, M.P. (2009). Stable isotope analysis of human and animal remains from the Late Upper Palaeolithic site of Balma Guilanyà, southeastern Pre-Pyrenees, Spain. *J. Archaeol. Sci.* 36, 1018–1026.
43. Ruiz, J., García-Sívoli, C., Martínez-Moreno, J., and Subirá, M.E. (2006). Los restos humanos del Tardiglaciario de Balma Guilanyà. In *La cuenca mediterránea durante el paleolítico superior: 38.000-10.000 años*, pp. 458–467.
44. Martzluff, M., Martínez-Moreno, J., Guilaine, J., Mora, R., and Casanova, J. (2012). Transformaciones culturales y cambios climáticos en los Pirineos catalanes entre el Tardiglaciario y Holoceno antiguo: Aziliense y Sauveterriense en Balma de la Margineda y Balma Guilanyà. *Cuaternario y Geomorfología* 26, 61–78.
45. Straus, L.G. (2015). Chronostratigraphy of the Pleistocene/Holocene boundary: the Azilian problem in the Franco-Cantabrian region. *Palaeohistoria* 27, 89–122.
46. Szécsényi-Nagy, A., Roth, C., Brandt, G., Rihuete-Herrada, C., Tejedor-Rodríguez, C., Held, P., García-Martínez-de-Lagrán, Í., Arcusa Magallón, H., Zesch, S., Knipper, C., et al. (2017). The maternal genetic make-up of the Iberian Peninsula between the Neolithic and the Early Bronze Age. *Sci. Rep.* 7, 15644.
47. Lubell, D., Jackes, M., Schwarcz, H., Knyf, M., and Meiklejohn, C. (1994). The Mesolithic-Neolithic transition in Portugal: isotopic and dental evidence of diet. *J. Archaeol. Sci.* 21, 201–216.
48. Jackes, M., and Alvim, P. (1999). Reconstructing Moita do Sebastião, the first step. In *Do Epipaleolítico ao Calcolítico na Península Ibérica*, Actas do IV Congresso de Arqueologia Peninsular, pp. 13–25.
49. Bicho, N.F. (1994). The End of the Paleolithic and the Mesolithic in Portugal. *Curr. Anthropol.* 35, 664–674.
50. Gronenborn, D. (2017). Migrations before the Neolithic? The Late Mesolithic blade-and-trapeze horizon in Central Europe and beyond. *Migration and Integration from Prehistory to the Middle Ages* (Halle, Germany: LandesMuseum für Vorgeschichte), pp. 113–122.
51. Perrin, T., Marchand, G., Allard, P., Binder, D., Collina, C., Garcia Puchol, O., and Valdeyron, N. (2009). Le second Mésoolithique d'Europe occidentale: origines et gradient chronologique. *Annales de la Fondation Fyssen* 24, 160–176.
52. Utrilla Miranda, P., and Laborda Lorente, R. (2018). La cueva de Chaves (Bastaras, Huesca): 15 000 años de ocupación prehistórica. *Trabajos de Prehistoria* 75, 248–269.
53. Castaños, P.M. (2004). Estudio arqueozoológico de los macromamíferos del Neolítico de la Cueva de Chaves (Huesca: Saldvie Estud. Prehist. y Arqueol.), pp. 125–172.
54. Baldellou Martínez, V. (2011). La Cueva de Chaves (Bastarás-Casbas, Huesca). *SAGVNTVM* 12, 141–144.
55. Utrilla, P., and Baldellou, V. (2001). Cantos pintados neolíticos de la Cueva de Chaves (Bastarás, Huesca: Saldvie Estud. Prehist. y Arqueol.), pp. 45–126.
56. Utrilla, P., and Baldellou, V. (2007). Les galets peints de la Grotte de Chaves. *Bull. la Société Préhistorique Ariège-Pyrénées* 62, 73–88.
57. Zilhão, J. (2001). Radiocarbon evidence for maritime pioneer colonization at the origins of farming in west Mediterranean Europe. *Proc. Natl. Acad. Sci. USA* 98, 14180–14185.
58. Isern, N., Zilhão, J., Fort, J., and Ammerman, A.J. (2017). Modeling the role of voyaging in the coastal spread of the Early Neolithic in the West Mediterranean. *Proc. Natl. Acad. Sci. USA* 114, 897–902.
59. Bernabeu, J., Balaguer, L.M., Esquembre-Bebíá, M.A., Pérez, J.R.O., and Soler, J.d.B. (2009). La cerámica impresa mediterránea en el origen del Neolítico de la península Ibérica. In *De Méditerranée et d'ailleurs...: mélanges offerts à Jean Guilaine*, pp. 83–96.
60. Martins, H., Oms, F.X., Pereira, L., Pike, A.W.G., Rowsell, K., and Zilhão, J. (2015). Radiocarbon dating the beginning of the Neolithic in Iberia: new results, new problems. *J. Mediterr. Archaeol.* 28, 105–131.
61. Villalba-Mouco, V., Utrilla, P., Laborda, R., Lorenzo, J.I., Martínez-Labarga, C., and Salazar-García, D.C. (2018). Reconstruction of human subsistence and husbandry strategies from the Iberian Early Neolithic: A stable isotope approach. *Am. J. Phys. Anthropol.* 167, 257–271.
62. Cuenca-Romero, M.d.C.A., Carmona Ballester, E., Pascual Blanco, S., Martínez, Díez, G., and Díez Pastor, C. (2011). El "campo de hoyos" calcolítico de Fuente Celada (Burgos): datos preliminares y perspectivas. *Complutum* 22, 47–69.
63. Rojo-Guerra, M., Peña-Chocarro, L., Royo-Guillén, J.I., Tejedor, C., García-Martínez de Lagrán, I., Arcusa, H., Garrido Pena, R., Moreno, M., Mazzucco, N., Gibaja, J.F., et al. (2013). Pastores trashumantes del Neolítico Antiguo en un entorno de alta montaña: secuencia crono-cultural de la Cova de Els Trocs (San Feliú de Veri, Huesca: BSAA Arqueol.), pp. 9–55.
64. Posth, C., Nägele, K., Colleran, H., Valentin, F., Bedford, S., Kami, K.W., Shing, R., Buckley, H., Kinaston, R., Walworth, M., et al. (2018). Language continuity despite population replacement in Remote Oceania. *Nat. Ecol. Evol.* 2, 731–740.
65. Rohland, N., Harney, E., Mallick, S., Nordenfelt, S., and Reich, D. (2015). Partial uracil-DNA-glycosylase treatment for screening of ancient DNA. *Philos. Trans. R. Soc. B Biol. Sci.* 370.
66. Maricic, T., Whitten, M., and Pääbo, S. (2010). Multiplexed DNA sequence capture of mitochondrial genomes using PCR products. *PLoS ONE* 5, e14004.
67. Fu, Q., Hajdinjak, M., Moldovan, O.T., Constantin, S., Mallick, S., Skoglund, P., Patterson, N., Rohland, N., Lazaridis, I., Nickel, B., et al. (2015). An early modern human from Romania with a recent Neanderthal ancestor. *Nature* 524, 216–219.
68. Schubert, M., Lindgreen, S., and Orlando, L. (2016). AdapterRemoval v2: rapid adapter trimming, identification, and read merging. *BMC Res. Notes* 9, 88.

69. Li, H., and Durbin, R. (2009). Fast and accurate short read alignment with Burrows-Wheeler transform. *Bioinformatics* 25, 1754–1760.
70. Gamba, C., Fernández, E., Tirado, M., Deguilloux, M.F., Pemonge, M.H., Utrilla, P., Edo, M., Molist, M., Rasteiro, R., Chikhi, L., and Arroyo-Pardo, E. (2012). Ancient DNA from an Early Neolithic Iberian population supports a pioneer colonization by first farmers. *Mol. Ecol.* 21, 45–56.
71. Gamba, C., Jones, E.R., Teasdale, M.D., McLaughlin, R.L., Gonzalez-Fortes, G., Mattiangeli, V., Domboróczki, L., Kóvári, I., Pap, I., Anders, A., et al. (2014). Genome flux and stasis in a five millennium transect of European prehistory. *Nat. Commun.* 5, 5257.
72. Hofmanová, Z., Kreutzer, S., Hellenthal, G., Sell, C., Diekmann, Y., Díez-Del-Molino, D., van Dorp, L., López, S., Kousathanas, A., Link, V., et al. (2016). Early farmers from across Europe directly descended from Neolithic Aegeans. *Proc. Natl. Acad. Sci. USA* 113, 6886–6891.
73. Lazaridis, I., Patterson, N., Mittnik, A., Renaud, G., Mallick, S., Kirsanow, K., Sudmant, P.H., Schraiber, J.G., Castellano, S., Lipson, M., et al. (2014). Ancient human genomes suggest three ancestral populations for present-day Europeans. *Nature* 513, 409–413.
74. Lazaridis, I., Nadel, D., Rollefson, G., Merrett, D.C., Rohland, N., Mallick, S., Fernandes, D., Novak, M., Gamarra, B., Sirak, K., et al. (2016). Genomic insights into the origin of farming in the ancient Near East. *Nature* 536, 419–424.

STAR★METHODS

KEY RESOURCES TABLE

REAGENT or RESOURCE	SOURCE	IDENTIFIER
Biological samples		
Ancient individual	This study/ Troisième caverne of Goyet archaeological site	Goyet Q-2
Ancient individual	This study/ Balma Guilanyà archaeological site	BAL001/ E1206 Shown to be identical with BAL005
Ancient individual	This study/ Balma Guilanyà archaeological site	BAL005/ BG E 3214 Shown to be identical with BAL001
Ancient individual	This study/ Balma Guilanyà archaeological site	BAL003/ E9605
Ancient individual	This study/ Moita do Sebastião archaeological site	CMS001/ 22
Ancient individual	This study/ Cueva de Chaves archaeological site	CHA001/ 84C
Ancient individual	This study/ Cueva de Chaves archaeological site	CHA002/ CH.NIG.11559
Ancient individual	This study/ Cueva de Chaves archaeological site	CHA003/ CH.NIG.11558
Ancient individual	This study/ Cueva de Chaves archaeological site	CHA004/ Ch.Banda13
Ancient individual	This study/ Fuente Celada archaeological site	FUC003/ H62 UE 622
Ancient individual	This study/ Cova de Els Trocs archaeological site	ELT002/ UE 69 C: 589 S:7 No Inv: 14227
Ancient individual	This study/ Cova de Els Trocs archaeological site	ELT006/ UE:1 C: 650 S:1 No Inv: 22404
Chemicals, Peptides, and Recombinant Proteins		
0.5 M EDTA pH 8.0	Life Technologies	AM9261
1x Tris-EDTA pH 8.0	AppliChem	A8569,0500
Proteinase K	Sigma-Aldrich	P2308-100MG
Guanidine hydrochloride	Sigma-Aldrich	G3272-500 g
3M Sodium Acetate pH 5,2	Sigma-Aldrich	S7899-500ML
Tween 20	Sigma-Aldrich	P9416-50ML
Water Chromasolv Plus	Sigma-Aldrich	34877-2.5L
Ethanol	Merck	1009832511
Isopropanol	Merck	1070222511
Buffer Tango	Life Technologies	BY5
T4 DNA Polymerase	New England Biosciences	M0203 L
T4 Polynucleotide Kinase	New England Biosciences	M0201 L
User Enzyme	New England Biosciences	M5505 L
Uracil Glycosylase inhibitor (UGI)	New England Biosciences	M0281 S
Bst 2.0 DNA Polymerase	New England Biosciences	M0537 S
BSA 20mg/mL	New England Biosciences	B9000 S
ATP	New England Biosciences	P0756 S
dNTPs 25 mM	Thermo Scientific	R1121
D1000 ScreenTapes	Agilent Technologies	5067-5582
D1000 Reagents	Agilent Technologies	5067-5583
Pfu Turbo Cx Hotstart DNA Polymerase	Agilent Technologies	600412

(Continued on next page)

Continued

REAGENT or RESOURCE	SOURCE	IDENTIFIER
Herculase II Fusion DNA Polymerase	Agilent Technologies	600679
1x TE-Puffer pH 8,0 low EDTA	AppliChem	A8569,0500
Sodiumhydroxide Pellets	Fisher Scientific	10306200
Sera-Mag Speed CM	GE Healthcare Lifescience	65152105050250
Dynabeads MyOne Streptavidin T1	Life Technologies	65601
GeneRuler Ultra Low Range DNA Ladder	Life Technologies	SM1211
10x GeneAmp PCR Gold Buffer and MgCl ₂	Life Technologies	4379874
Human Cot-1 DNA	Life Technologies	15279011
1M Tris-HCl pH 8.0	Life Technologies	15568025
20x SCC Buffer	Life Technologies	AM9770
UltraPure™ Salmon Sperm DNA Solution	Life Technologies	15632011
PEG 8000 Powder, Molecular Biology Grade	Promega	V3011
20% SDS Solution	Serva	39575.01
3M Sodium Acetate buffer solution pH 5,2	Sigma-Aldrich	S7899-500ML
5 M Sodium chloride solution	Sigma-Aldrich	S5150-1L
Denhardt's solution	Sigma-Aldrich	D9905-5MI
Critical Commercial Assays		
High Pure Viral Nucleic Acid Large Volume Kit	Roche	5114403001
Quick Ligation Kit	New England Biosciences	M2200 L
MinElute PCR Purification Kit	QIAGEN	28006
DyNAmo Flash SYBR Green qPCR Kit	Life Technologies	F-415L
Oligo aCGH/Chip-on-Chip Hybridization Kit	Agilent Technologies	5188-5220
HighSeq 4000 SBS Kit	Illumina	FC-410-1001/2
NextSeq 500/550 High Output Kit v2	Illumina	FC-404-2002
Deposited Data		
Raw and analyzed data (European nucleotide archive)	This paper	ENA: PRJEB30985
Software and Algorithms		
Samtools	[31]	http://samtools.sourceforge.net/
EAGER	[32]	https://eager.readthedocs.io/en/latest/
ADMIXTOOLS	[25]	https://github.com/DReichLab/AdmixTools
smartpca	[33]	https://www.hsph.harvard.edu/alkes-price/software/
ANGSD	[15]	http://www.popgen.dk/angsd/index.php/Main_Page Contamination
Haplogrep 2	[34]	http://haplogrep.uibk.ac.at/
ContamMix	[16]	https://github.com/StanfordBioinformatics/DEFUNCT-env-modules/tree/master/contamMix
Yhaplo	[35]	https://github.com/23andMe/yhaplo
Geneious R8.1.974	[36]	https://www.geneious.com
READ	[37]	https://bitbucket.org/tguenther/read

CONTACT FOR REAGENT AND RESOURCE SHARING

Further information and requests for resources and reagents should be directed to and will be fulfilled by the Lead Contact, Wolfgang Haak (haak@shh.mpg.de).

EXPERIMENTAL MODEL AND SUBJECT DETAILS

The Iberian Peninsula in southwestern Europe is understood as a periglacial refugium for Pleistocene hunter-gatherers (HG) during the Last Glacial Maximum (LGM). The post-LGM genetic signature in western and central Europe was dominated by ancestry similar to the Villabruna individual, commonly described as WHG ancestry or ‘Villabruna’ cluster [2]. This Villabruna cluster had largely

replaced the earlier *El Mirón* genetic cluster, comprised of 19,000–15,000-year-old individuals from central and western Europe associated with the Magdalenian culture [2].

By generating new genome-wide data from Belgian HG, Iberian HG and Neolithic individuals we aimed to further refine the HG genetic structure in the Iberian Peninsula during the Upper Paleolithic and Mesolithic, and to characterize the HG ancestry sources that contributed genetically to Neolithic groups. We hypothesize that (i) admixture events of different Upper Paleolithic HG ancestries resulted in genetic structure among various Iberian HG groups, which can be observed as asymmetric genetic affinities to the *Villabruna* and *El Mirón* cluster or another potential source, respectively, (ii) this structure during the Early Holocene is stronger in the Iberian Peninsula than in Central Europe (iii) the genetic structure was inherited by Neolithic individuals through mixture with local HG ancestry, especially in regions that initially were more affected by expanding farmers. All teeth and bone samples analyzed were obtained with relevant institutional permissions from the Gobierno de Aragón, Universitat Autònoma de Barcelona, Universidad de Valladolid, the German Archeological Institute Madrid.

Archaeological sites and sample description

Troisième caverne of Goyet (Upper Paleolithic)

The Troisième caverne of Goyet (Belgium) is a cave with an extensive Paleolithic record, from the Middle to the Upper Paleolithic periods (Aurignacian, Gravettian, and Magdalenian). The site was previously described and eight individuals were analyzed by Fu et al. [2]. For this study we have generated deeper sequencing data from individual Goyet Q-2 who is attributed to the Magdalenian period.

Goyet Q-2, juvenile individual (12,650 ± 50 BP [GrA-46168], 15,232–14,778 years cal BP [2-sigma value]) [2].

Balma Guilanyà (Late Upper Paleolithic)

Balma Guilanyà is a rock shelter located in Northeastern Iberia, at 1,150 m.a.s.l. (meters above sea level) in the Serra de Busa Pre-Pyrenean range (Navés, Lleida). After an initial test pit where Late Upper Paleolithic remains were recovered [38], the site was excavated between 2001 to 2008 [39, 40]. Two main chrono-cultural phases were defined. The oldest dates back to the Late Upper Paleolithic (15,000–11,000 years cal BP) and the youngest corresponds to the Early Mesolithic (11,000 – 9,500 years cal BP). The two chrono-cultural units are separated by a big fallen boulder which sealed the Late Upper Paleolithic levels [41]. A set of human skeletal remains were found under this big stone block without any evidence of funerary structures. Direct radiocarbon dates from two human remains (one human tooth and one human bone fragment) recovered from the same context dated to 13,380–12,660 years cal BP (Ua-34297) and 12,830–10,990 years cal BP (Ua- 34298) [42]. These dates fall inside the Bølling/Allerød interstadial and Younger Dryas stadial, which correspond to the Late Glacial. The Minimum Number of Individuals (MNI) was estimated to be three based on dental morphology: two adults and one immature individual [43]. The stable carbon and nitrogen isotope analyses performed on human bone collagen suggested a diet based on terrestrial herbivores, without any evidence of marine or freshwater resources [42]. The material cultural artifacts recovered from the same level as the human remains have been attributed to the Azilian techno-complex [41]. Balma Guilanyà shows clear technical parallels with the near Azilian site Balma Marguineda [44]. However, in general the Azilian is considered to be more common in Vasco-Cantabrian northern Iberia and on the other side of the Pyrenees [45]. Here, we report the genome-wide data from two individuals from this site:

BAL0051, adult individual

BAL003, adult individual

Moita do Sebastião (Mesolithic)

This site was previously described in Szécsényi-Nagy et al. [46]. Moita do Sebastião is a Late Mesolithic shell midden site located in the Muge region (Salvaterra de Magos, Portugal) on the Atlantic coastline of Portugal. The Muge and Sado regions were very fertile estuaries and marshes during the Mesolithic, which were exploited by hunter-gatherers to obtain marine resources [47]. Although Mesolithic groups are not considered fully sedentary, Moita do Sebastião presents some cultural characteristics that suggest permanence at the site: the presence of post holes associated with hut building, and a big burial space [48]. These features have been interpreted as a systematic occupation of the estuarine areas, which is also reflected in the shell midden conformation. The Moita do Sebastião site was excavated by different archaeologists since the last century. The total minimum number of individuals (MNI) is unknown, but it could reach up to 100 individuals when summarizing the different campaigns [48]. The lithic assemblage of the Mesolithic phase is characterized by microburin technique and geometrics [49]. The Mesolithic geometric phenomenon is spread widely along eastern and western Europe and North Africa, but its origin is still debated [50]. Based on a chronological gradient an African origin was suggested, from where it spread into Europe through the South of Italy (Sicily) and from where it followed a Mediterranean expansion to Iberia [51]. In this study, we genetically analyze one Mesolithic individual from this site:

CMS001, adult individual, (7,240 ± 70 BP [To-131], 8,185–7,941 years cal BP [2-sigma value]) [46].

Cueva de Chaves (Early Neolithic)

Cueva de Chaves is located in Northeastern Iberia, at 663 m.a.s.l. in the Pre-Pyrenean mountain range of Sierra de Guara (Bastarás, Huesca). The site was excavated under the direction of Pilar Utrilla and Vicente Baldellou in between 1984 and 2007. Cueva de

Chaves was occupied during the Paleolithic, Neolithic, and sporadically during the Bronze Age and Late Roman periods. Neolithic deposits were divided in two archaeological levels and dated to the Early Neolithic period (Ia: 5,600–5,300 years cal BCE; Ib 5,300–5,000 years cal BCE) [52]. Both levels show a full Neolithic package consisting of domestic fauna [53], Cardial pottery [54] and schematic rock art painted on pebbles [55, 56]. The earliest Neolithic sites in the Iberian Peninsula are located in coastal areas [57, 58]. A long-standing hypothesis in archaeology to explain this is that the first arrival of the Neolithic in the Iberian Peninsula resulted from a Cardial expansion by a maritime route. In this context, Cueva de Chaves represents an interesting case study, because radiocarbon dates for the occupation of this cave overlap in time with other Cardial Early Neolithic sites in coastal Iberia [59, 60]. The pottery style, together with the radiocarbon dates, suggest an early expansion of the first farmers from coastal to the inland areas following the Ebro Basin [52]. An MNI of four individuals, directly radiocarbon dated, were recovered from this Early Neolithic context (although one radiocarbon date points back to the early Middle Neolithic). One of individuals was in a complete anatomical articulation. A human isotopic dietary study shows a high animal protein intake consumed by all individuals [61]. This was related to the existence of a specialized animal husbandry management community in which agriculture was not intensively developed. We included four Neolithic individuals for genetic analyses in this study:

CHA001, adult (6,230 ± 45 BP [GrA-26912], 7,257–7,006 years cal BP [2-sigma value]) [54].

CHA002, adult (6,227 ± 28 BP [MAMS 29127], 7,250–7,018 years cal BP [2-sigma value]) [61].

CHA003, infant (6,180 ± 54 BP [D-AMS 015821], 7,245–6,947 years cal BP [2-sigma value]) [61].

CHA004, adult (5,645 ± 31 BP [MAMS 28128], 6,494–6,321 years cal BP [2-sigma value]) [61].

Fuente Celada (Early Neolithic)

This site was described in Szécsényi-Nagy et al. [46]. Fuente Celada is an open-air settlement located in the northern Iberian Central Plateau (Quintanaduenas, Burgos). All the archaeological materials are from a rescue excavation carried out in 2008 by Alameda Cuenca-Romero et al. [62]. The site presents many negative structures, most of them from the Chalcolithic period, suggesting a habitat settlement. Some of these negative structures contain Chalcolithic human remains. One of these burials gave an older date corresponding to the Early Neolithic. This burial contained an individual in a flexed position, with three bone rings close to the cervical vertebrae, which was interpreted as a necklace [62]. Here we include this Early Neolithic individual in our genetic analyses:

FUC003, adult (6,120 ± 30 BP [UGA-7565], 7,157–6,910 years cal BP [2-sigma value]) [62].

Cova de Els Trocs (Middle Neolithic)

This site was also described in Szécsényi-Nagy et al. [46]. Cova de Els Trocs is a cave located in Northeastern Iberia, at 1,564 m.a.s.l. in San Feliú de Verí (Bisaurri, Huesca) in the South of the Axial Pyrenees [63]. The excavation of the site is ongoing and led by Manuel Rojo Guerra and José Ignacio Royo Guillén. Within the large stratigraphic sequence three different occupation phases are discerned that are supported by more than twenty radiocarbon dates [63]. The first phase corresponds to the Early Neolithic (ca. 5,300–4,800 years cal BCE.) for which genomic data has been published in Haak et al. [3] for seven individuals. The second phase dates back to the Middle Neolithic (ca. 4,500–4,300 years cal BCE.) when the cave was possibly used by animals and no human remains have been retrieved. During the third phase (ca. 4,000–3,700; 3,350–2,900 years cal BCE) the cave was again used as a burial place despite not being the only purpose. From the third phase, we have included two individuals in the present genomic study:

ELT002, adult (5,008 ± 23 BP [MAMS-16160], 5,882–5,658 years cal BP [2-sigma value]) [63].

ELT006, adult (5,035 ± 23 BP [MAMS-16165], 5,895–5,716 years cal BP [2-sigma value]) [63].

Ancient DNA processing and quality control

Sampling of ancient human remains

For the ancient individuals analyzed in this study, we sampled various bones (a humerus, phalanges, metacarpals, mandibles and a cranial fragment) and teeth (molars) in the clean room of the Max Planck Institute for the Science of Human History (MPI-SHH) in Jena, Germany, and at the Institute of Anthropology, Johannes Gutenberg University, Mainz (Data S1B). Prior to sampling, samples were irradiated with UV-light for 30 min at all sides. Different sampling methods were used for different bone types, including sandblasting, grinding with mortar and pestle, and cutting and drilling in the denser regions (Data S1B). Teeth surfaces were cleaned with a low concentration bleach solution (3%). For the teeth sampled at the MPI-SHH, the crown was separated from the root by cutting with a hand saw along the cementum/enamel junction followed by drilling inside the pulp chamber [64]. For the teeth sampled in Mainz the complete tooth was ground using a mixer mill [46].

DNA extraction

DNA extraction was done following a modified version of the Dabney protocol [12], with an initial amount of 50–100 mg of bone or tooth powder. Samples were digested with extraction buffer (EDTA, UV H₂O and Proteinase K) during 16–24h in a rotator at 37°C. The suspension was centrifuged and the supernatant transferred into binding buffer (GuHCl, UV H₂O and Isopropanol) and then into silica columns (High Pure Viral Nucleic Acid Kit; Roche). The columns were first washed with wash buffer (High Pure Viral Nucleic Acid Kit; Roche) and then eluted in 100 μL TET (TE-buffer with 0.05% Tween). We included one or two extraction blanks in each extraction series to check for cross-contamination between samples and background contamination from the lab.

Library preparation

A total of 27 double-stranded (ds) libraries were created from 25 μ L DNA template extract at the MPI-SHH, following a protocol by Meyer & Kircher [10] with unique index pairs [11]. We used a partial Uracil DNA Glycosylase treatment (UDG-half) that repairs damaged nucleotides by removing deaminated cytosines except for the final nucleotides at the 5' and 3' read ends to retain a damage pattern characteristic for ancient DNA [65]. The libraries generated from Goyet Q-2 were ds-non-UDG and ss-UDG-half treated. We repaired the terminal ends of the DNA fragments using T4 DNA Polymerase (NBE) and joined the Illumina adaptors using the Quick Ligation Kit (NBE). We also added one or two library blanks per batch. One aliquot of each library was used to quantify the DNA copy number with IS7/IS8 primers [10] outside the clean room using DyNAmo SYBP Green qPCR Kit (Thermo Fisher Scientific) on the LightCycler 480 (Roche). Libraries were double indexed with unique index combinations [11] before doing PCR amplifications outside the cleanroom with PfuTurbo DNA Polymerase (Agilent). After amplification, the indexed products were purified with MinElute columns (QIAGEN) and eluted in 50 μ L TET buffer and quantified with IS5/IS6 primers using the DyNAmo SYBP Green qPCR Kit (Thermo Fisher Scientific) on the LightCycler 480 (Roche) [10]. We used Herculase II Fusion DNA Polymerase (Agilent) with the same IS5/IS6 primers for the further amplification of the indexed products up to a copy number of 10×10^{13} molecules/ μ L. After another purification round, we quantified the indexed libraries on a TapeStation (TapeStation Nucleic Acid System, Agilent 4200) and made a 10nM equimolar pool. [Data S1B](#) shows an overview of the extracts and libraries generated for each ancient individual.

Shotgun screening and in-solution enrichment of nuclear DNA (1240k capture) and mtDNA (mitocapture)

The pooled double indexed libraries were sequenced on an Illumina HiSeq2500 for a depth of ~ 5 million read cycles, using either a single (1x75bp reads) or double end (2x50bp reads) configuration. Reads were analyzed with EAGER 1.92.32 [32] to check the quality and quantity of endogenous human DNA in each library. We selected samples for targeted in-solution capture enrichment that showed a damage pattern characteristic for ancient DNA and with $> 0.2\%$ endogenous DNA. We further amplified these libraries with the IS5/IS6 primer set to a concentration of 200–400 ng/ μ L. After that, the libraries were hybridized in-solution to different oligonucleotide probe sets synthesized by Agilent Technologies to enrich for the complete mitogenome (mtDNA capture [66]) and for 1,196,358 informative nuclear SNP markers (1240K capture [67]).

QUANTIFICATION AND STATISTICAL ANALYSIS

Read processing and assessment of ancient DNA authenticity

We demultiplexed the sequenced libraries according to expected read indexes, allowing for one mismatch. We clipped adapters with AdapterRemoval v2.2.0 [68]. For paired end reads, we restricted to merged fragments with an overlap of at least 30 bp. Single end reads shorter than 30 bp were discarded. We mapped fragments to the Human Reference Genome Hs37d5 using the Burrows-Wheeler Aligner (BWA, v0.7.12-r1039) *aln* and *samse* commands (-l 16500, -n0.01, -q30) [69] and removed duplicate reads using DeDup v0.12.1. We excluded reads with a mapping quality phred score < 30 . A summary of quality statistics is given for 1240K SNP captured libraries in [Data S1C](#) and for mtDNA captured libraries in [Data S1D](#).

Contamination tests

Prior to genotype calling we assessed the level of contamination in the mitochondrial and nuclear genome using several methods.

DNA damage

We determined and plotted the deamination rate pattern in our UDG-half libraries using MapDamage v.2.0.6 from EAGER 1.92.32 [32]. Although damage rates at the terminal read ends vary (5.3%–14.8%) in libraries for individuals from different sites, all libraries show deamination patterns expected for ancient DNA ([Data S1C](#)). Then we trimmed the reads for 2 bp at both terminal ends of the UDG-half libraries to reduce the bias of deamination from our genotype calls. Non-UDG libraries generated from Goyet Q-2 were trimmed for 10 bp.

Contamination based on the match rate to the mtDNA dataset (ContamMix)

We used ContamMix 1.0.10 to estimate the mitochondrial contamination levels in our mito-captured libraries taking a worldwide mitochondrial dataset to compare as a potential contamination source [16] ([Data S1F](#)). We find contamination rates below 2.2% for all libraries ([Data S1F](#)). We visualized the mitochondrial read alignment with Geneious R8.1.974 [36] and manually checked for heterozygous calls to confirm the ContamMix estimates. We found a substantial mitogenome heterozygosity level for BAL003_MT in the manual check, contrasting its respective ContamMix estimate of 2.2%, and therefore excluded this library from further genome analyses.

Sex determination and X-contamination

We determined genetic sex by calculating the X-ratio (targeted X-Chromosome SNPs/ targeted autosomal SNPs) and Y-ratio (targeted Y-Chromosome SNPs/ targeted autosomal SNPs) ([Data S1F](#)). For uncontaminated libraries, we expect an X ratio ~ 1 and Y ratio ~ 0 for females and X and Y ratio of 0.5 in males [2]. Potential individuals that fall in an intermediate position could indicate the presence of DNA contamination.

Method 2 of the ANGSD package was used on merged and unmerged libraries from male individuals to test the heterozygosity of polymorphic sites on the X chromosome [15]. For low coverage libraries from the same individual with < 200 SNPs on the X chromosome we merged them into a single BAM file using samtools v0.1.19 [31] to facilitate contamination estimation of the merged libraries ([Data S1F](#)). Finally, merged libraries with less than 3.3% contamination were selected for population genetic analysis.

Genotyping and merging with dataset

After trimming of potentially damaged terminal ends bamfiles were genotyped with pileupCaller (<https://github.com/stschiff/sequenceTools/tree/master/src-pileupCaller>), which call one SNP per position considering the human genome as pseudo-haploid genome. Genotyped data were merged with Human Origins panel (~600K SNPs) [26] and 1240K panel [17]. For Goyet Q-2 the genotyping was applied to clipped and unclipped bamfiles, calling only transversions in the latter to avoid residual ancient DNA damage and merging these extra SNPs in the final genotype. The number of SNPs covered per individual is shown in [Data S1G](#).

Kinship relatedness and individual assessment

We first calculated the pairwise mismatch rate between bam files to rule out a potential duplication of individuals. We found the same low mismatch rate comparing different bamfiles combination from libraries of BAL001 and BAL005, respectively, suggesting that both samples come from the same individual. We consequently merged them as BAL051.

We then used Relationship Estimation from Ancient DNA (READ) to estimate the degree of genetic kinship relatedness among the final set of individuals [37]. This method can determine first and second-degree relatedness among individuals and can also be used to test for potential cross-contamination among libraries from the same batch of sampling processing. We calculated the proportion of non-matching alleles and normalized the results separating Neolithic from HG individuals taking into account the potential genetic diversity within each group to calculate the proportions of non-matching alleles (P_0). After the normalization of both groups, P_0 of HG ranged between 0.964–1.029 and between 0.974–1.074 for Neolithic individuals, which in both cases is higher than 0.90625, the top value for second-degree related individuals. In sum, there are no first- or second-degree relatives among our newly reported ancient Iberian individuals.

Phenotypic traits analysis

We extracted a list of 36 SNPs of functional importance or related to known phenotypic traits [22] (e.g., lactase persistence, pigmentation, eye colors) ([Figure S4](#)) and calculated the genotype likelihood based on the number of reads (using a quality filter q30) for each specific position to determinate the presence of the ancestral or derived alleles [22].

We interrogated different SNPs positions on the gene *OCA2* related to light eye color. We obtain the ancestral allele (rs12913832, 3 reads) in individuals CHA001 and ELT002, and heterozygous allele calls for ELT006, suggesting dark color eyes for all of them. The SNP coverage was not sufficient to reliable type the remaining individuals. Another allele from the same gene (rs1800404) related to eye pigmentation could support darker pigmentation in ELT006 than in ELT002. We also checked different SNPs positions in the gene *SLC45A2*. We obtain the ancestral alleles (rs1426654, 2 reads) in BAL0051 and (rs16891982, 4 reads) in CHA001 which suggest a darker skin color than ELT002 and ELT006, who are heterozygous or homozygous for the derived allele. The coverage in the other individuals is very low to allow comparisons. The allele rs3827760 of the *EDAR* gene, related to straight and thick hair, is ancestral in all individuals, albeit with variable coverage (CHA001, 4 reads; CHA003, 3 reads; ELT002, 14 reads and; ELT006, 8 reads). Also, as reported before for pre-farming and Neolithic individuals [13], none of our newly typed individuals show evidence for Lactase persistence. Individuals from the Neolithic times (ELT002, ELT006 and FUC003) show different combinations of derived and ancestral alleles of the gene *rs174546*, which is related to the capacity of regulation of the production of long-chain polyunsaturated fatty acids (FADS1/FADS2). Results are shown in [Figure S4](#).

Mitochondrial and Y chromosome haplogroups

Using an in-house mtDNA capture assay, we could recover complete mitochondrial genomes from individuals CHA002, CHA003, CHA004, ELT002, ELT006, and FUC003. The coverage of the mtDNA genome for the rest or the samples ranges from 88.86%–99.99% ([Data S1D](#)). We used samtools v1.3.1 to extract reads from mitocapture data [31] and mapped them to the rCRS and called the consensus sequences using Geneious R8.1.974 [36]. We downloaded these consensus sequences in *fasta* format and they were used to determinate mitochondrial haplotypes using Haplogrep 2 [34] ([Data S1F](#)).

Iberian HG individuals from Balma Guilanyà and Moita do Sebastião belong to haplogroup U, together with the two MN individuals CHA004 and ELT006 ([Data S1F](#)). Individual BAL003 could be assigned to U2'3'4'7'8'9', also found in the Paglicci 108 (~27,000 years cal BP, Italy), Rigney 1 (~15,500 years cal BP, France) [2], and Grotta d'Oriente C HG (~14,000 years cal BP, Italy) [19]. Individual BAL0051 belongs to U5b2a, also found in Neolithic Scotland [9]. Moita do Sebastião (CMS001) carries haplogroup U5b1, which was reported from MN, Bell Beaker and Middle Bronze Age individuals from Portugal and Spain [7, 9], and in the Ranchot 88 HG (~10,000 years cal BP, France) [2].

Early Neolithic individuals from Cueva de Chaves do not carry U haplogroups. Individual CHA001 could be assigned to haplogroup HV0+195, but was previously reported as K based on PCR-based results [70]. This haplogroup has been reported from MN Ireland [20], as well as MN Scotland and Bell Beaker individuals from England [9]. Individual CHA002 was assigned to K1a2a, which is common in Early Neolithic Iberia, e.g., Cova Bonica [8], Cova de Els Trocs [3] and Cueva del Toro [30], but also in Chalcolithic and Bell Beaker individuals from Iberia and Italy [9, 13]. CHA003 was assigned to K1a3a, so far reported from Neolithic Anatolia [13], Neolithic and Chalcolithic Scotland, and Bell Beaker individuals from Sicily [9]. Middle Neolithic individual CHA004 carried haplogroup U4a2f, found in HG from the Iron Gates, Romania, and Lithuania [14, 19]. The MN individual ELT002 carries haplogroup J1c1b, present in the Körös Early Neolithic [18], Neolithic from Scotland [9], Iberian Late Neolithic-Chalcolithic [7], and Bronze Age from Italy and Germany [6]. ELT006 was assigned to haplogroup U3a1, which has been reported from MN France and Germany [9, 19], and Chalcolithic Iberia [13]. Early Neolithic Fuente Celada carries haplogroup X2b+226, found in MN Hungary [71] and Middle Bronze Age Iberia [7]. X2b was

found in Iberian Late Neolithic [5], Chalcolithic [18] and Bell-Beaker individuals [9], Neolithic England [9] and Greece [72], and EN/LN Morocco [25].

For Y haplogroup determination, we first called the Y chromosome SNPs of the 1240K SNP panel from all male individuals using pileupCaller with MajorityCalling mode, (<https://github.com/stschiff/sequenceTools>), and mapping quality ≥ 30 and base quality ≥ 30 (Data S1E). Y chromosome haplogroups were called from the list of Y-SNPs included in the 1240K capture assay using the script *yhaplo* [35].

BAL0051 could be assigned to haplogroup I1, while BAL003 carries the C1a1a haplogroup. To the limits of our typing resolution, EN/MN individuals CHA001, CHA003, ELT002 and ELT006 share haplogroup I2a1b, which was also reported for Loschbour [73] and Motala HG [13], and other LN and Chalcolithic individuals from Iberia [7, 9], as well as Neolithic Scotland, France, England [9], and Lithuania [14]. Both C1 and I1/ I2 are considered typical European HG lineages prior to the arrival of farming. Interestingly, CHA002 was assigned to haplogroup R1b-M343, which together with an EN individual from Cova de Els Trocs (R1b1a) confirms the presence of R1b in Western Europe prior to the expansion of steppe pastoralists that established a related male lineage in Bronze Age Europe [3, 6, 9, 13, 19]. The geographical vicinity and contemporaneity of these two sites led us to run genomic kinship analysis in order to rule out any first or second degree of relatedness. Early Neolithic individual FUC003 carries the Y haplogroup G2a2a1, commonly found in other EN males from Neolithic Anatolia [13], Starçevo, LBK Hungary [18], *Impressa* from Croatia and Serbia Neolithic [19] and Czech Neolithic [9], but also in MN Croatia [19] and Chalcolithic Iberia [9].

Population genetic analysis

Labeling population groups

For the Paleolithic individuals, we adopted the labels from Fu et al. [2] and used the improved genotype calls from Mathieson et al. [19]. We included the HG with more than 15,000 SNPs covered in the PCA (Figure S1). If the HG individuals from the same site or chrono-cultural context clustered in the PCA analysis, we grouped them using the same label for the following population genetic analysis [14, 19, 21]. Neolithic individuals from Iberia were grouped by sites and by chrono-cultural context. For Neolithic individuals from outside of Iberia, we kept the label names from the respective initial publications [9, 13, 19, 20, 24, 74].

Principal Component Analysis

PCA analysis was run with the Human Origins dataset using *smartpca* v10210 (EIGENSOFT) with the option *SHRINKMODE* [33] using 777 modern populations to calculate eigenvectors on which aDNA samples were projected [74]. PC1 was multiplied by -1 ($-PC1$) in order to mirror geography.

F-statistics

D-statistics and F-statistics were calculated with *qpDstat* from ADMIXTOOLS (<https://github.com/DReichLab>). We used the 1240K panel to increase the number of SNPs covered by the ancient individuals and get more resolution in the statistic tests. Standard errors were calculated with the default block jackknife. We report and plot three standard errors in all F-statistics.

qpAdm and qpWave

We used *qpWave* and *qpAdm* from the ADMIXTOOLS package (<https://github.com/DReichLab>) to estimate admixture proportions. We used this framework to model and quantify the ancestry proportions of HG individuals in- and outside of Iberia (we only use HG or groups of HG with more than 30,000 SNPs). First, we tested whether Goyet Q-2 and Villabruna formed a clade with respect to the following set outgroups: Mota, Ust'-Ishim, Mal'ta 1 (MA1), Koros EN-HG, Goyet Q116-1, Mbuti, Papuan, Onge, Han, Karitiana and Natufian extending the set used by Olalde et al. [9]. The resulting *qpWave* model showed an extremely poor fit (p value = $3.07705115e-91$), which means that our set of outgroups can be used to differentiate between Goyet Q-2 and Villabruna-related ancestry. We then modeled the ancestry in the HG groups as a mixture of Goyet Q-2 and Villabruna (Figure 3D and Data S1I). Alternatively, we also used El Mirón and Loschbour as potential source populations and the same ten outgroups, after checking that El Mirón and Loschbour are not equally related to the outgroups (p value = $5.41365181e-68$) (Figure S3A and Data S1I).

We also used *qpWave* and *qpAdm* to explore the HG admixture in the Neolithic populations. In this case, the sources (left populations) were Anatolia Neolithic, Goyet Q-2 and Villabruna. We chose the same set of outgroups, and first checked that Anatolia Neolithic, Goyet Q-2 and Villabruna were not equally related to the outgroups (p value = $8.63552043e-92$) (Figure 4B and Data S1J). We repeated the model with Anatolia Neolithic, El Mirón and Villabruna as sources using the same set of outgroups. However, the resulting *qpWave* model also resulted in a poor fit (p value = $9.5033482e-59$) (Data S1J).

The results of all *qpWave* and *qpAdm* models are reported in Data S1I and S1J. The criteria to report these values were as follows: If the resulting p values were higher than 0.05 we report the three-sources model. If the p values were lower than 0.05 we show the best p value obtained from the three- or two-sources model (i.e., the nested model). In case of negative values for some of the sources, we report the two-sources model (nested model) and the respective p value of these models. We applied the same criteria to two-sources models.

Multi-Dimensional Scaling analysis (MDS)

We computed Multi-Dimensional Scaling (MDS) analysis using the R package *cmdscale* to measure the genetic dissimilarity among hunter-gatherers (HG), and then used the inverted [$1-f_3(HG1; HG2, Mbuti)$] pairwise values among all the combinations [2].

DATA AND SOFTWARE AVAILABILITY

Data is available at ENA under study accession number PRJEB30985.

Current Biology, Volume 29

Supplemental Information

Survival of Late Pleistocene Hunter-Gatherer

Ancestry in the Iberian Peninsula

Vanessa Villalba-Mouco, Marieke S. van de Loosdrecht, Cosimo Posth, Rafael Mora, Jorge Martínez-Moreno, Manuel Rojo-Guerra, Domingo C. Salazar-García, José I. Royo-Guillén, Michael Kunst, Hélène Rougier, Isabelle Crevecoeur, Héctor Arcusa-Magallón, Cristina Tejedor-Rodríguez, Iñigo García-Martínez de Lagrán, Rafael Garrido-Pena, Kurt W. Alt, Choongwon Jeong, Stephan Schiffels, Pilar Utrilla, Johannes Krause, and Wolfgang Haak

Supplemental Figures

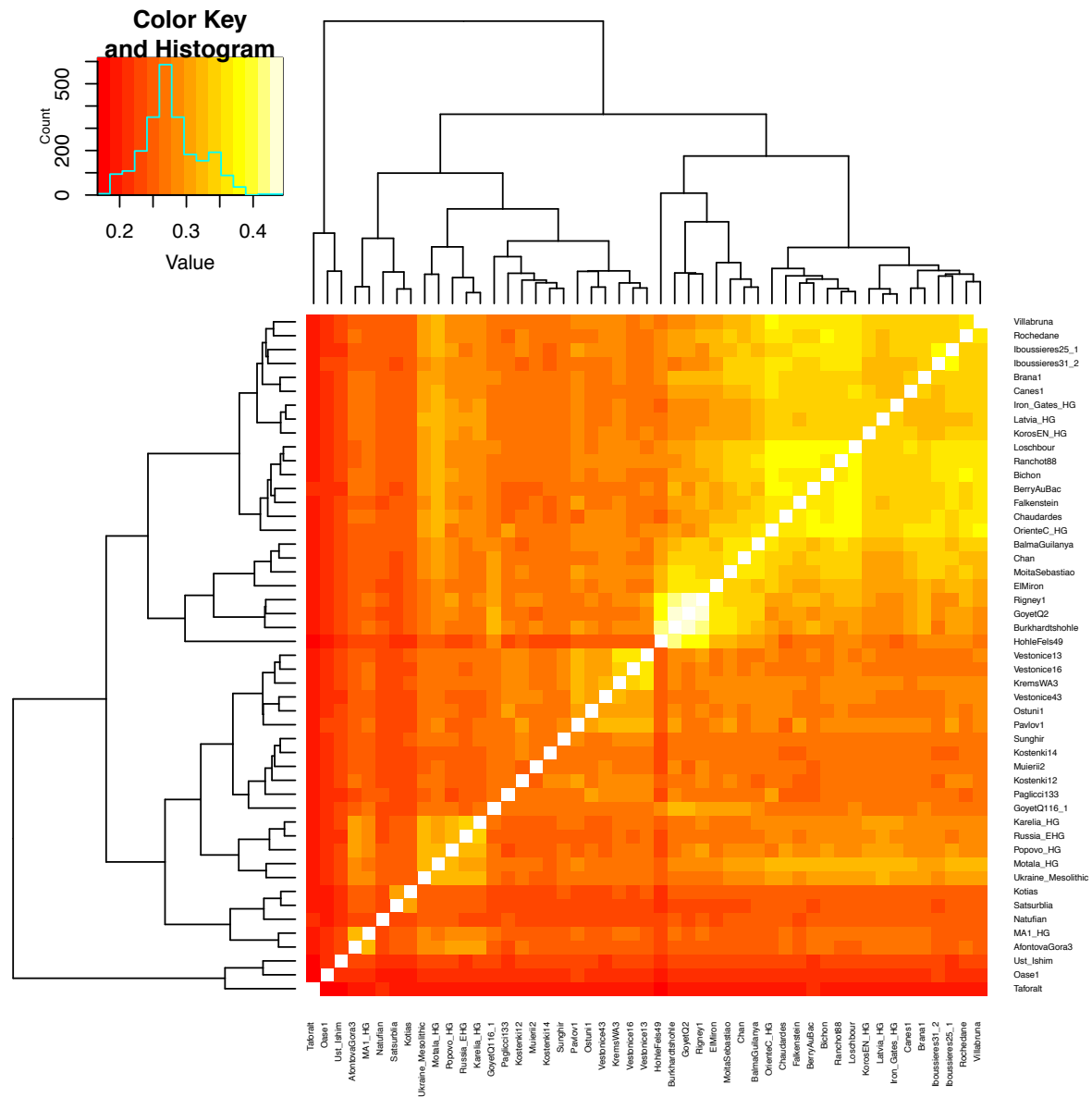


Figure S1. Heat plot showing the genetic distances between Eurasian HG, Related to Figure 2A. Genetic distances were calculated using $f3$ -outgroup statistics of the form $f3(X;Y, Mbuti)$, with X and Y being Eurasian hunter-gatherers in all possible pairwise comparisons. The analysis has been restricted to samples with more than 30,000 SNPs, following Fu et al. [S1]. The clustering pattern is similar to the MDS plot (STAR methods, Figure 2A): the newly reported Moita do Sebastião [~8ky cal BP], Balma Guilanyà [~12ky cal BP], and Chan [~9ky cal BP] cluster with El Mirón and Goyet Q-2, whereas La Braña 1 and Canes 1 cluster with Villabruna.

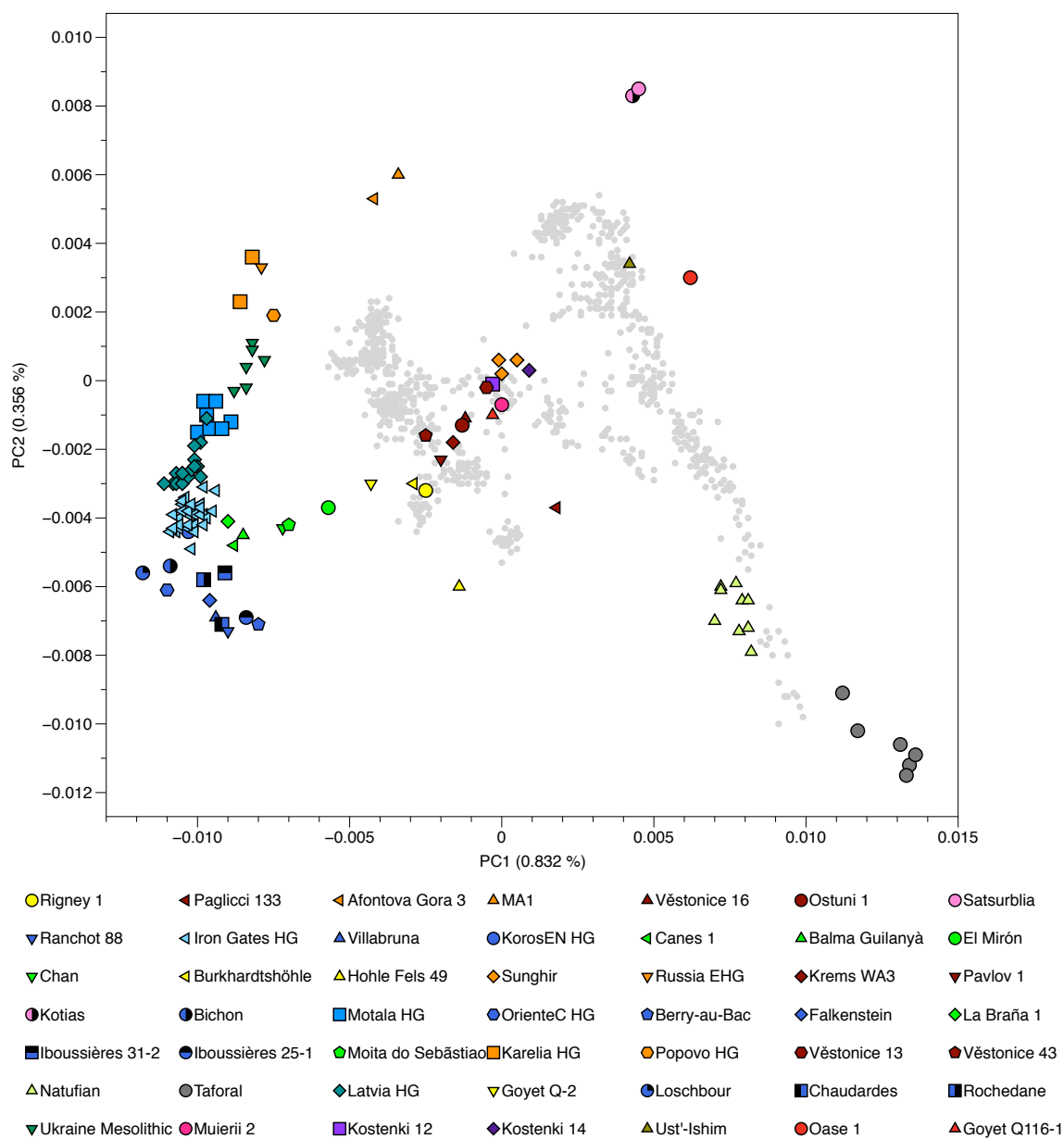


Figure S2. Principal Component Analysis of Hunter-gatherer individuals, Related to Figure 2A. PCA analysis calculated with 777 present day West Eurasians [S2] with option shrinkmode:YES on which HG individuals were projected.

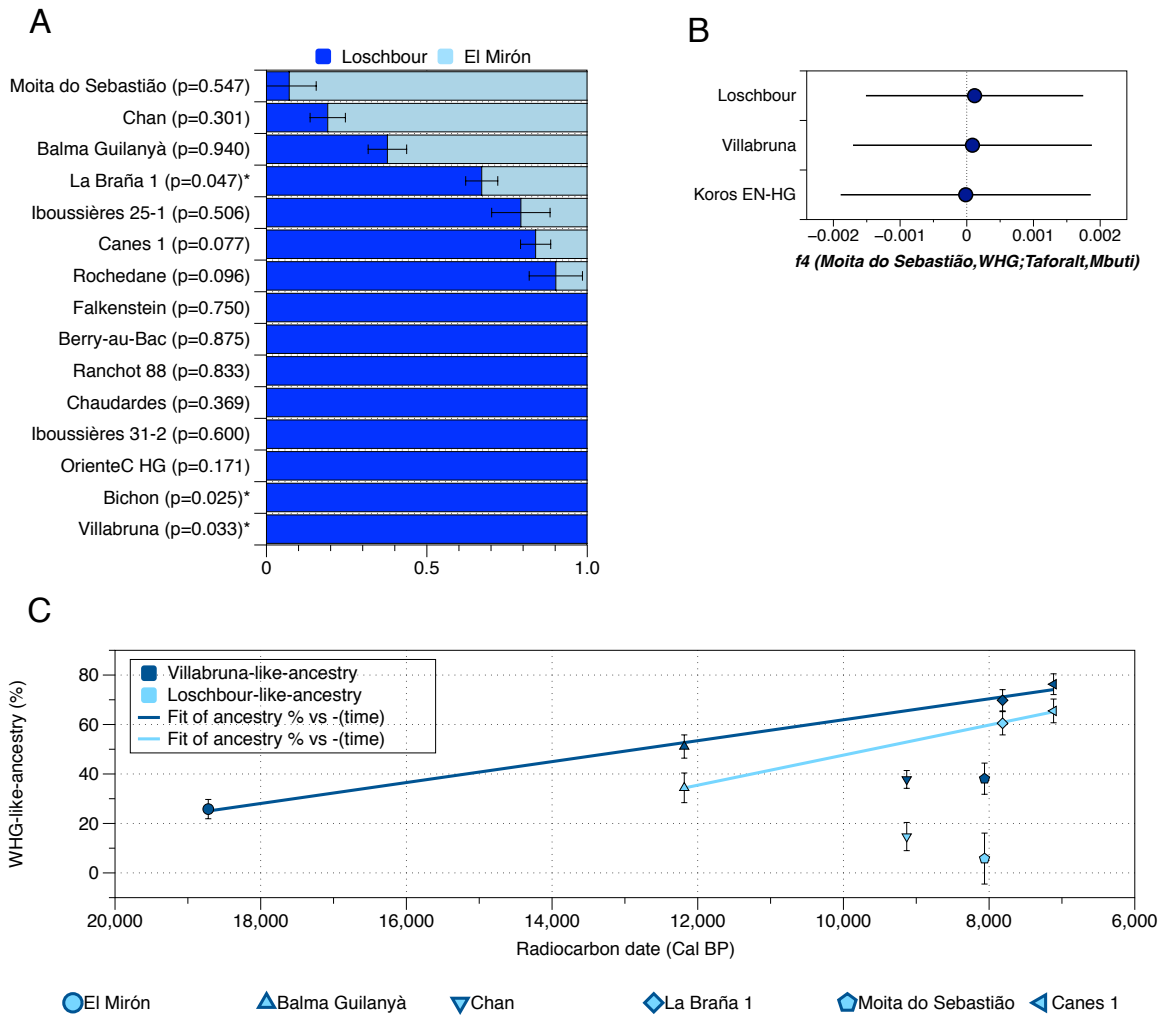


Figure S3. Hunter-gatherer ancestry and geographical correlation, Related to Figure 3D
A) Modelling European HG as admixture of Villabruna-like and El Mirón-like ancestry using *Loschbour* and *El Mirón* as proximal sources, respectively (error bars indicate ± 1 standard error). **B)** f_4 -statistics showing **no** affinity between Geometric Mesolithic Moita do Sebastião from Portugal and Iberomaurusian HG from Taforalt, Morocco, North Africa. Taforalt individuals are a good proxy to test the African-Iberian connections due to the genetic continuity attested in North Africa from the Late Pleistocene to the Holocene (Early Neolithic) despite their chronologically older age [S3]; errors bars indicate ± 3 standard errors **C)** Correlation between Villabruna-like ancestry (dark blue; Figure 3D) and Loschbour-like ancestry (light blue; Figure S3A) and time (error bars indicate the radiocarbon 2-sigma range). Both models result in a fit of $R = 0.99$ for individuals from north and northeast of Iberia Peninsula (to the exclusion of Chan and Moita do Sebastião), where we observe an increase of WHG-like ancestry similar to other parts of Europe.

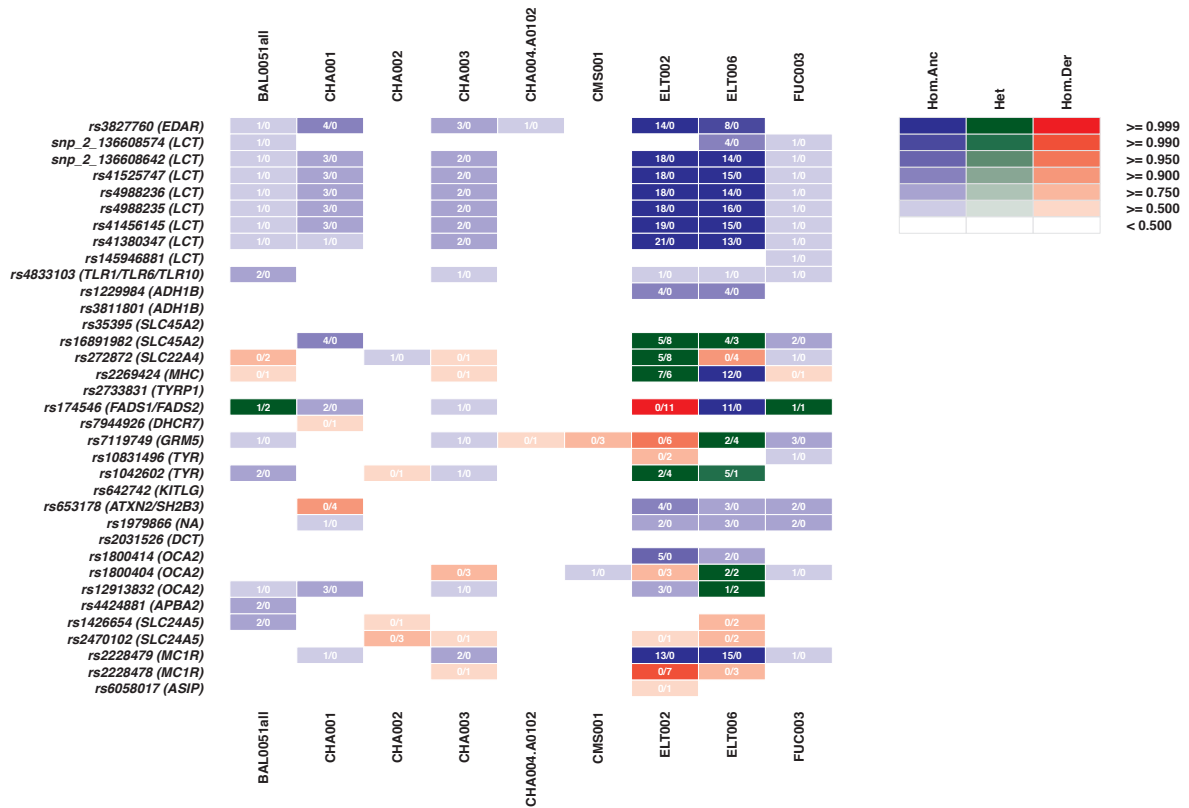


Figure S4. Summary of genotypes of phenotypic and functional SNPs, related to STAR methods. Colours indicate the homozygous ancestral/derived or heterozygous state of the SNPs reported in the left-hand column. Numbers in cells indicate the number of reads matching the ancestral/derived allele.

Supplemental References

- S1. Fu, Q., Posth, C., Hajdinjak, M., Petr, M., Mallick, S., Fernandes, D., Furtwängler, A., Haak, W., Meyer, M., Mitnik, A., *et al.* (2016). The genetic history of Ice Age Europe. *Nature* 534, 200-205.
- S2. Lazaridis, I., Nadel, D., Rollefson, G., Merrett, D.C., Rohland, N., Mallick, S., Fernandes, D., Novak, M., Gamarra, B., Sirak, K., *et al.* (2016). Genomic insights into the origin of farming in the ancient Near East. *Nature* 536, 419-424.
- S3. Fregel, R., Méndez, F.L., Bokbot, Y., Martín-Socas, D., Camalich-Massieu, M.D., Santana, J., Morales, J., Ávila-Arcos, M.C., Underhill, P.A., Shapiro, B., *et al.* (2018). Ancient genomes from North Africa evidence prehistoric migrations to the Maghreb from both the Levant and Europe. *Proc. Natl. Acad. Sci.*
<https://doi.org/10.1073/pnas.1800851115>
- S4. Posth, C., Renaud, G., Mitnik, A., Drucker, D.G., Rougier, H., Cupillard, C., Valentin, F., Thevenet, C., Furtwängler, A., Wißing, C., *et al.* (2016). *Current Biology* 26, 827-833.

Archaeological Site	Individual ID	Archaeological ID	Radiocarbon ID	Lab. Radiocarbon	Cal BCE (2 σ)	Cal BP (2 σ)	Chrono-Cultural context
Troisième caverne of Goyet cave	Goyet Q-2	Goyet Q-2	GrA-46168	12650 ± 50	13,283–12,829	15,232–14,778	Upper Paleolithic/ Magdalenian
Balma Guilanyà	BAL001	E1206	Ua-34297; Ua-34298	11095±195; 10195±25	11,384–10,733; 10,681–9,263	13,380–12,660; 12,830–10,990	Late Upper Paleolithic/Azilian
	BAL005	BG-E-3214					
	BAL003	E9605					
Moita do Sebastião	CMS001	22	To-131	7240±70	6,235 – 5,994	8,185 – 7,941	Mesolithic / Geometric
	CHA001	84C	GrA-26912	6230 ± 45	5,308 – 5,057	7,257 – 7,006	Early Neolithic/ Cardial
Cueva de Chaves	CHA002	CH.NIG.11559	MAMS 29127	6227 ± 28	5,299 – 5,070	7,250 – 7,018	
	CHA003	CH.NIG.11558	D-AMS 015821	6180 ± 54	5,296 – 4,998	7,245 – 6,947	
	CHA004	Ch.Banda13	MAMS 28128	5645 ± 31	4544-4373	6,494 – 6,321	
Cova de Els Trocs	ELT002	UE 69 C: 589 S:7 N° Inv	MAMS-16160	5008 ± 23	3,933 – 3,709	5,882 – 5,658	Middle Neolithic
	ELT006	UE:1 C: 650 S:1 N° Inv	MAMS-16165	5035 ± 23	3,945 – 3,769	5,895 – 5,716	Early Neolithic/ EpiCardial
Fuente Celada	FUC003	H62 UE 622	UGA-7565	6120 ± 30	5,208 – 4,961	7,157 – 6,910	
* BAL001 and BAL005 are the same individual. It appears as BAL051 along the manuscript							

Data S1A Chrono-cultural information, Related to Figure 1 and STAR methods.

Individual ID	Sample ID	Type of sample	Sampling process	Extraction ID	Library ID	Type of library	Library treatment
GoyetQ2	GoyetQ2	Humerus	Described in Fu et al. (1)	GX176	GA231snp GA247snp MA166snp	ssLibrary dsLibrary dsLibrary	UDG-half no-UDG no-UDG
BAL001	BAL001.A	Phalanx	Sandblustered and grinded	BAL001.A01	BAL001.A0102	dsLibrary	UDG-half
				BAL001.A02	BAL001.A0201 BAL001.A0202	dsLibrary dsLibrary	UDG-half UDG-half
BAL005	BAL005.A	Cranial fragment	Sandblustered and grinded	BAL005.A01	BAL005.A0102	dsLibrary	UDG-half
				BAL005.A02	BAL005.A0201 BAL005.A0202	dsLibrary dsLibrary	UDG-half UDG-half
BAL003	BAL003.A	Molar	Crown cut, drilled pulp	BAL003.A01	BAL003.A0101	dsLibrary	UDG-half
CHA001	CHA001.A	Metacarpal	Sandblustered and grinded	CHA001.A01	CHA001.A0102	dsLibrary	UDG-half
	CHA001.B	Metacarpal	Sandblustered and grinded	CHA001.B01	CHA001.B0102	dsLibrary	UDG-half
	CHA001.D	Phalanx	Sandblustered, cut and drilled inside	CHA001.D01	CHA001.D0102	dsLibrary	UDG-half
	CHA001.E	Phalanx	Sandblustered and grinded	CHA001.E01	CHA001.E0102	dsLibrary	UDG-half
CHA002	CHA002.A	Mandible	Surface removed, drilled inside the chin	CHA002.A01	CHA002.A0102	dsLibrary	UDG-half
	CHA002.B	Second molar	Crown cut, drilled pulp	CHA002.B01	CHA002.B0102	dsLibrary	UDG-half
CHA003	CHA003.A	Mandible	Sandblustered and grinded	CHA003.A01	CHA003.A0102 CHA003.A0103	dsLibrary dsLibrary	UDG-half UDG-half
CHA004	CHA004.A	Second molar	Crown cut, drilled pulp	CHA004.A01	CHA004.A0102	dsLibrary	UDG-half
CMS001	CMS001.A	Second molar	Sandblustered and smashed	CMS001.A02	CMS001.A0201	dsLibrary	UDG-half
					CMS001.A0202	dsLibrary	UDG-half
FUC003	FUC003.B	Unspecified tooth	Sandblustered and smashed	FUC003.B01	FUC003.B0101	dsLibrary	UDG-half
					FUC003.B0102	dsLibrary	UDG-half
ELT002	ELT002.A	First molar	Sandblustered and smashed	ELT002.A0101	ELT002.A0101	dsLibrary	UDG-half
	ELT002.B	Unspecified tooth	Sandblustered and smashed	ELT002.B0101	ELT002.B0101	dsLibrary	UDG-half
ELT006	ELT006.A	First molar	Sandblustered and smashed	ELT006.A0101	ELT006.A0101	dsLibrary	UDG-half
	ELT006.B	Second molar	Sandblustered and smashed	ELT006.B0101	ELT006.B0101	dsLibrary	UDG-half

Data S1B Sampling method and library treatment, Related to STAR methods.

Library	Raw Reads	Dedup Mapped Reads	End. DNA Capture (%)	Cluster factor	Mean coverage	Genome coverage X (%)	mt/nuclear ratio	DMG 1" Base 3'	DMG 2" Base 3'	DMG 1" Base 5'	DMG 2" Base 5'	Average length (bp)
GA231mg (IscAge resequenced)	22902190	1295761	2.096	3.103	3.103	0.0933	3.04	847.53	0.305	0.1777	0.3397	0.2124
GA231mg (NS500559)	8904514	1295761	1.978	2.886	2.886	0.0565	2.02	682.17	0.2798	0.1654	0.3389	0.2108
GA231mg (R479)	15180074	1148386	15.959	3.109	3.109	0.4133	15.34	683.42	0.3016	0.1905	0.3385	0.2109
GA231mg (R506)	9754168	818840	14.867	2.959	2.959	0.1312	13.18	585.66	0.3048	0.1392	0.3388	0.2085
GA231mg (IscAge resequenced)	24503905	1395356	12.851	6.384	6.384	0.0333	12.81	171.63	0.1605	0.1065	0.2399	0.1344
GA231mg (IscAge resequenced)	24503905	1395356	12.851	6.384	6.384	0.0333	12.81	171.63	0.1605	0.1065	0.2399	0.1344
MA166mp (D16402-12_CP)	29198138	1523286	3.441	3.839	3.839	0.0534	3.88	1248.17	0.3865	0.0133	0.1523	0.1005
MA166mp (R479)	13108192	964895	18.242	3.929	3.929	0.3767	18.4	695.51	0.0387	0.0133	0.1523	0.1005
MA166mp (R506)	10103660	798862	17.542	2.929	2.929	0.3226	16.85	644.02	0.0397	0.0145	0.1469	0.1024
BAU01.A0102	11478048	76997	6.236	11.327	11.327	0.0259	1.83	90.03	0.091	0.0192	0.0719	0.0134
BAU01.A0201.TF1.1	7577828	6.029	6.029	3.524	3.524	0.0414	3.51	15.83	0.0637	0.0089	0.0773	0.0112
BAU01.A0202.TF1.1	18340748	77859	1.731	3.608	3.608	0.0211	1.79	78.67	0.067	0.0152	0.0804	0.015
BAU03.A0101.TF2.1	6175070	138116	12.996	6.61	6.61	0.0221	1.76	296.82	0.11	0.022	0.0779	0.0221
BAU05.A0102	8870844	298220	14.967	6.384	6.384	0.0995	7.46	77.01	0.0564	0.0137	0.0699	0.0116
BAU05.A0201.TF1.1	6568822	348488	7.997	1.856	1.856	0.1207	10.4	48.86	0.034	0.0079	0.0675	0.009
BAU05.A0202.TF1.1	23786164	438489	4.529	2.438	2.438	0.1283	10.46	21.53	0.028	0.0107	0.0732	0.006
BAU05.A0203.TF1.1	1866868	136686	1.866	1.866	1.866	0.028	1.866	136.68	0.028	0.0107	0.0732	0.006
CH4001.B0102	8132020	13146	1.327	8.762	8.762	0.0054	0.42	188.84	0.1667	0.0242	0.1569	0.0239
CH4001.B0102	11237015	1090183	25.542	3.944	3.944	0.3856	26.43	67.73	0.0486	0.0142	0.0622	0.0198
CH4001.E0102	8158526	171147	11.068	7.713	7.713	0.0545	4.04	85.63	0.0795	0.0202	0.0884	0.0173
CH4002.A0102	9252666	520215	29.459	8.08	8.08	0.1324	8.98	196.13	0.0433	0.0127	0.0478	0.01
CH4002.B0102	9620935	208216	10.254	7.172	7.172	0.0546	4.04	38888.12	0.0228	0.0233	0.0993	0.0188
CH4003.A0102	8781464	563877	24.915	5.834	5.834	0.1723	12.63	219.48	0.0664	0.0164	0.0727	0.0127
CH4003.A0103.TF1.1	23774728	1299514	12.526	2.599	2.599	0.3408	24.41	110.98	0.0669	0.0118	0.0788	0.0124
CH4004.A0102	6999476	386221	5.869	3.959	3.959	0.0688	5.78	980.46	0.1431	0.0247	0.1406	0.0206
CH5001.A0201.TF1.1	23745124	310386	4.286	3.113	3.113	0.0882	7.74	209.44	0.142	0.021	0.1493	0.0214
CH5001.A0201.TF2.1	32925904	220124	2.189	2.128	2.128	0.085	5.79	203.49	0.138	0.0223	0.1496	0.022
CH5001.A0201.TF1.1	32925904	220124	2.189	2.128	2.128	0.085	5.79	203.49	0.138	0.0223	0.1496	0.022
EU1002.B0101.TF1.1	4466389	4466389	24.773	1.444	1.444	1.6561	55.16	181.11	0.0446	0.0105	0.0786	0.0119
EU1002.B0101.TF1.1	26593448	5266731	24.589	1.432	1.432	1.9274	57.52	95.08	0.0628	0.0101	0.0786	0.0119
EU1006.A0101.TF1.1	26530294	2624033	14.709	1.575	1.575	0.9234	41.54	270.23	0.0559	0.0093	0.0678	0.0101
EU1006.A0101.TF1.1	26758094	3444773	16.203	1.517	1.517	1.2348	48.8	303.49	0.0457	0.0081	0.0611	0.0089
FUJ003.B0101.TF2.1	23325884	1193529	12.567	2.307	2.307	0.261	19.76	1628.44	0.139	0.0168	0.1564	0.018
FUJ003.B0102.TF1.1	23946696	1395835	15.326	2.801	2.801	0.3341	24.66	1468.37	0.1481	0.017	0.1614	0.0181

Data S1C Ancient DNA information for 1240K captured libraries UDG-half treated. DNA Capture (%) represents the percentage of overlapped reads with the targeted 1240K capture SNPs, Related to STAR methods.

Sample Name	# of Raw Reads prior Clip & Merge (C&M)	Mapped Reads after RMDup	Endogenous DNA (%)	Cluster Factor	Mean Coverage	Coverage >= 1X in %	DMG 1st Base 3'	DMG 2nd Base 3'	DMG 1st Base 5'	DMG 2nd Base 5'	average fragment length
BAL001.A0102.MT1.1	67434	839	7.94	2.737	2.7854	88.26	0.0503	0.0058	0.0552	0.0114	55.01
BAL001.A0201.MT1.1	104276	1416	7.397	2.674	4.7619	94.76	0.0662	0.0037	0.0899	0.0069	55.72
BAL001.A0202.MT1.1	60914	750	6.104	1.992	2.3807	86.42	0.0667	0	0.0577	0	52.59
BAL003.A0101.MT1.1	435912	2955	48.467	42.304	9.1505	98.84	0.0436	0	0.0408	0.0019	51.31
BAL005.A0102.MT1.1	661324	7021	32.474	18.544	23.2249	99.91	0.0502	0.002	0.0578	0.0013	54.81
BAL005.A0201.MT1.1	870766	15412	28.372	9.594	51.0267	99.99	0.0462	0.0023	0.0662	0.0025	54.86
BAL005.A0202.MT1.1	658976	10044	17.989	5.747	32.0355	99.94	0.061	0.0029	0.0695	0.0045	52.85
CHA001.D0102.MT1.1	125302	8531	31.579	2.789	30.0051	99.91	0.0304	0.0044	0.0541	0.0027	58.28
CHA001.E0102.MT1.1	61596	1273	9.854	2.599	4.3401	95.29	0.0286	0	0.0596	0.0036	56.49
CHA002.A0102.MT1.1	238410	7411	52.846	10.862	23.6925	99.93	0.0329	0.0045	0.0479	0.0013	52.97
CHA002.B0102.MT1.1	2843734	267368	71.142	4.402	938.7933	100	0.0764	0.0026	0.0791	0.0022	58.18
CHA003.A0102.MT1.1	1009458	24425	55.598	14.087	75.1807	100	0.0578	0.003	0.0706	0.0031	51
CHA003.A0103.MT1.1	1439204	53992	52.49	7.462	165.6296	100	0.0807	0.0028	0.0839	0.003	50.83
CHA004.A0102.MT1.1	631222	54016	47.861	3.188	173.8365	100	0.0812	0.0022	0.0877	0.002	53.32
CMS001.A0201.MT1.1	112962	6200	15.04	1.365	16.6778	99.76	0.1575	9.00E-04	0.1443	0.0041	44.57
CMS001.A0202.MT1.1	136728	7213	15.036	1.314	18.7112	99.69	0.1525	0.0039	0.156	0.0036	42.98
ELT002.A0101.MT1.1	2321834	189446	73.134	5.961	739.9797	100	0.0551	0.0026	0.0617	0.0026	64.72
ELT002.B0101.MT1.1	1470198	132509	69.986	5.034	517.7293	100	0.0498	0.0025	0.0567	0.003	64.74
ELT006.A0101.MT1.1	249386	43076	55.778	1.909	162.8928	100	0.0353	0.002	0.048	0.0024	62.66
ELT006.B0101.MT1.1	1451670	75740	64.744	7.973	296.9315	100	0.0334	0.0026	0.0443	0.0024	64.96
FUC003.B0101.MT1.1	1742478	160789	63.178	3.559	460.519	100	0.1679	0.0027	0.1682	0.0026	47.46
FUC003.B0102.MT1.1	1864686	188257	65.444	3.148	535.0713	100	0.1779	0.0025	0.1737	0.0029	47.09

Data S1D Ancient DNA information for mtDNA captured in UDG-half treated libraries. DNA Capture (%) represents the percentage of overlapped reads with the targeted mitochondrial capture SNPs, Related to STAR methods.

Individual (merged libraries)	X Cov.	Y Cov.	Auto Cov.	X ratio	Y ratio	Sex det.	X Cont.	S.E.	X SNP	Y haplogroup
GoyetQ2	0.351468	0.380196	0.844449	0.41620986	0.45022968	XY	0.019212	6.48E-03	1516	Reported in Fu et al (1)
BAL003	0.00850481	0.0139578	0.0206987	0.41088619	0.6743322	XY	No possible	No possible	21	C1a1a
BAL0051	0.16716	0.207285	0.410781	0.40693216	0.50461195	XY	0.033733	1.47E-02	468	I1
CHA001	0.171056	0.221273	0.436666	0.3917319	0.50673283	XY	-0.00138	6.51E-04	511	I2a1b
CHA002	0.0729965	0.0872666	0.178294	0.40941647	0.48945337	XY	0.009718	1.03E-02	250	R1b
CHA003	0.201175	0.24772	0.493914	0.40730775	0.5015448	XY	0.010887	8.06E-03	619	I2a1b
CHA004	0.0482696	0.00097949	0.0660543	0.73075636	0.01482859	XX	-	-	96	
CMS001	0.157832	0.00348944	0.187378	0.84231874	0.01862246	XX	-	-	337	
ELT002	1.26234	2.15657	3.5167	0.35895584	0.61323684	XY	0.002448	1.51E-03	5277	I2a1a1
ELT006	0.321906	0.512489	0.90203	0.3568684	0.56815073	XY	0.003059	2.08E-03	3398	I2a1a1
FUC003	0.247032	0.277472	0.573374	0.43083921	0.48392847	XY	0.005881	5.26E-03	740	G2a2a1

Data S1E Sex determination and nuclear contamination estimation on X Chromosome in male samples, Related to STAR methods.

Merged Library code	mt Contamination (ContamMix)	Haplogroup	Quality (Haplogrep)	Sample Polymorphisms
BAL0051_MT	1.60%	U5b2a	86.53%	551T, 51C, 59C, 79G, 150T, 263G, 3201G, 750G, 1438G, 1721T, 2706G, 3107A, 3107C, 3394C, 4732G, 4769G, 5471A, 7028T, 7766G, 8860G, 9477A, 11467G, 11719A, 12308G, 12372A, 13637G, 13637G, 14182C, 14766T, 15326G, 16114A, 16192T, 16270T
BAL003_MT	2.20%	U2'3'4'7'8'9	79.52%	73G, 150T, 152C, 263G, 3211G, 750G, 964A, 964A, 1391C, 1438G, 1811R, 2294R, 2706G, 3107A, 4769G, 4843T, 5268R, 5319G, 6152C, 7028T, 7920N, 8860G, 9110C, 10020Y, 10981M, 11453T, 11467G, 11719A, 12245C, 12308G, 12372A, 15326G, 15466A, 15466A, 16362C, 16390R, 16519C, 16535K
CHA001_MT	1.20%	HV0 + 195	97.02%	72C, 195C, 263G, 3091CC, 315.1C, 750G, 1438G, 2706G, 3107A, 4769G, 7028T, 8860G, 14305A, 15326G, 16298C
CHA002_MT	0.16%	K1a2a	99.32%	73G, 263G, 3211G, 497T, 519.1AA, 750G, 1189C, 1438G, 1811G, 2706G, 3107A, 3480G, 4769G, 5773A, 7028T, 8860G, 9055A, 9698C, 10398G, 10550G, 11025C, 11299C, 11467G, 11719A, 12308G, 12372A, 14167T, 14766T, 14798C, 15326G, 16224C, 16311C, 16519C
CHA003_MT	0.35%	K1a3a	98.06%	73G, 263G, 309Y, 310C, 497T, 750G, 1189C, 1438G, 1811G, 2706G, 3107A, 3480G, 4769G, 7028T, 7599C, 8860G, 9055A, 9698C, 10398G, 10550G, 11299C, 11467G, 11719A, 12308G, 12372A, 13117G, 14167T, 14766T, 14798C, 15326G, 16224C, 16311C, 16519C
CHA004_MT	0.17%	U4a2f	98.86%	73G, 195C, 263G, 310C, 498A, 521.1AA, 750G, 1189C, 1438G, 1811G, 1978G, 2706G, 3107A, 4644C, 4769G, 5999C, 6047G, 7028T, 8818T, 8860G, 11332T, 11467G, 11719A, 12308G, 12372A, 12397G, 14620T, 14766T, 15326G, 15693C, 16356C, 16519C
CMS001_MT	0.46%	U5b1 + 16189	95.97%	73G, 150T, 263G, 750G, 1438G, 2706G, 3107A, 3197C, 4769G, 5656G, 7028T, 7768G, 8860G, 9477A, 11467G, 11719A, 11734G, 12308G, 12372A, 13146T, 13617C, 14182C, 14766T, 15326G, 16164G, 16189C, 16192T, 16270T
ELT002_MT	0.29%	J1c1b	98.72%	73G, 185A, 263G, 295T, 315.1C, 462T, 482C, 489C, 750G, 1438G, 2706G, 3010A, 3107A, 3394C, 4216C, 4769G, 7028T, 7184G, 8860G, 10398G, 11251G, 11719A, 12612G, 13708A, 14766T, 14798C, 15326G, 15452A, 16009T, 16126C
ELT006_MT	0.22%	U3a1	100%	73G, 150T, 263G, 3211G, 750G, 1438G, 1811G, 2294G, 2706G, 3010A, 3107A, 4703C, 4769G, 6518T, 7028T, 8860G, 9266A, 10506G, 11467G, 11719A, 12308G, 12372A, 13934T, 14139G, 14766T, 15326G, 15454C, 16343G, 16390A, 16519C
FUC003_MT	0.14%	X2b + 226	100%	73G, 153G, 195C, 225A, 226C, 263G, 321.1GG, 750G, 1438G, 1719A, 2706G, 3107A, 4769G, 6221C, 6371T, 7028T, 8393T, 8860G, 11719A, 12705T, 13708A, 13966G, 14470C, 14766T, 15326G, 15927A, 16189C, 16223T, 16278T, 16519C
GoyetQ2	0.05%	Reported in Posth et al. 2016 [54]	Reported in Posth et al. 2016 [54]	Reported in Posth et al. 2016 [54]

Data S1F Mitochondrial contamination and haplogroup determination, Related to STAR methods.

Sample ID	Final autosomal SNPs sites covered in 1240K panel	Final autosomal SNPs sites covered in HO panel
GoyetQ2	379768	203321
BAL003	19269	10602
BAL0051	330931	183543
CHA001	336249	184527
CHA002	141287	77284
CHA003	373101	207744
CHA004	64502	34725
CMS001	174710	96653
ELT002	814072	447287
ELT006	701320	390247
FUC003	431296	237647

Data S1G Number of SNPs called and % SNPs covered in 1240K and HO panel, Related to STAR methods.

X	Y	test	out	f4	st.err	Z	BABA	ABBA	SNPs	Explanation
Burkhardtshohle	Iberia_ElMiron	Italy_Villabruna	Mbuti.DG	-0.005736	0.001661	-3.453	1100	1253	26646	El Mirón and other members from
Hohle Fels 49	Iberia_ElMiron	Italy_Villabruna	Mbuti.DG	-0.005497	0.001185	-4.64	1872	2143	49364	Goyet Q-2 cluster do not conform a
Goyet Q-2	Iberia_ElMiron	Italy_Villabruna	Mbuti.DG	-0.005209	0.000764	-6.819	10253	11520	243116	clade respect to Villabruna. We
Rigney 1	Iberia_ElMiron	Italy_Villabruna	Mbuti.DG	-0.003141	0.001779	-1.765	995	1068	23072	selectect GoyetQ-2
GoyetQ2_review2	Iberia_ElMiron	Italy_Villabruna	Mbuti.DG	-0.005209	0.000764	-6.819	10253	11520	243116	This test confirm that El Miron
GoyetQ2_review2	Germany_HohleFels49_published	Italy_Villabruna	Mbuti.DG	0.001339	0.001472	0.91	817	786	23120	Individual shared genetic drift with
GoyetQ2_review2	France_Rigney1_published	Italy_Villabruna	Mbuti.DG	-0.003997	0.002019	-1.98	459	512	13172	Villabruna individual only explained
GoyetQ2_review2	Germany_Burkhardtshohle_published	Italy_Villabruna	Mbuti.DG	0.000417	0.001927	0.217	586	580	15051	by admixture. The rest of
GoyetQ2_review2	Italy_Villabruna	Iberia_ElMiron	Mbuti.DG	0.011475	0.00102	11.253	14310	11520	243116	This test confirm that El Miron
Germany_HohleFels49_published	Italy_Villabruna	Iberia_ElMiron	Mbuti.DG	0.010119	0.001402	7.22	2642	2143	49364	Individual did not split earlier from
France_Rigney1_published	Italy_Villabruna	Iberia_ElMiron	Mbuti.DG	0.010797	0.002018	5.349	1317	1068	23072	Villabruna branch. El Mirón and all
Germany_Burkhardtshohle_published	Italy_Villabruna	Iberia_ElMiron	Mbuti.DG	0.013318	0.001887	7.058	1608	1253	26646	the individuals inside El Goyet Q-2
Germany_HohleFels49_published	GoyetQ2_review2	Belgium_GoyetQ116_1_1	Mbuti.DG	-0.004111	0.001577	-2.607	635	717	19979	El Mirón is the individuals inside the
France_Rigney1_published	GoyetQ2_review2	Belgium_GoyetQ116_1_1	Mbuti.DG	-0.002586	0.002045	-1.264	449	481	12346	Goyet Q-2 cluster with less affinity to
Germany_Burkhardtshohle_published	GoyetQ2_review2	Belgium_GoyetQ116_1_1	Mbuti.DG	0.000137	0.001973	0.069	552	550	14223	Goyet Q-116 despite being the
Iberia_ElMiron	GoyetQ2_review2	Belgium_GoyetQ116_1_1	Mbuti.DG	-0.00331	0.000822	-4.025	9593	10325	221337	oldest. This could be explained by

Data S1H F4-statistics, Related to Figure 3B and Figure 3C.

Sources	Right populations	p-value
Goyet Q-2, Villabruna	Mota, Ust'-Ishim, Mal'ta 1 (MA1), Koros EN-HG, Goyet Q-116-1, Mbuti, Papuan, Onge, Han, Karitiana and Natufian	3.08E-91
El Mirón, Loschbour	Mota, Ust'-Ishim, Mal'ta 1 (MA1), Koros EN-HG, Goyet Q-116-1, Mbuti, Papuan, Onge, Han, Karitiana and Natufian	5.41E-68

Test population	Source 1	Source 2	p-value	Mixture proportions		SE	
				Source 1	Source 2	Source 1	Source 2
Berry-Au-Bac	Goyet Q-2	Villabruna	0.07206638	0.051	0.949	0.125	0.125
Berry-Au-Bac	El Mirón	Loschbour	0.875394	0	1	0	0
Bichon	Goyet Q-2	Villabruna	0.06332111	0.094	0.906	0.041	0.041
Bichon	El Mirón	Loschbour	0.0254175	0	1	0	0
Iron Gates HG	Goyet Q-2	Villabruna	0.472363	0	1	0	0
Iron Gates HG	El Mirón	Loschbour	2.38E-04	0	1	0	0
Loschbour	Goyet Q-2	Villabruna	0.00803701	0	1	0	0
Villabruna	El Mirón	Loschbour	0.0328396	0	1	0	0
Rochedane	Goyet Q-2	Villabruna	0.11752874	0.119	0.881	0.081	0.081
Rochedane	El Mirón	Loschbour	0.09624124	0.098	0.902	0.083	0.083
Ranchot88	Goyet Q-2	Villabruna	0.02503332	0.133	0.867	0.047	0.047
Ranchot88	El Mirón	Loschbour	0.833264	0	1	0	0
OrienteC HG	Goyet Q-2	Villabruna	0.60273047	0.16	0.84	0.117	0.117
OrienteC HG	El Mirón	Loschbour	0.170645	0	1	0	0
Falkenstein	Goyet Q-2	Villabruna	0.26846816	0.109	0.891	0.066	0.066
Falkenstein	El Mirón	Loschbour	0.750326	0	1	0	0
Ibous sieres31-2	Goyet Q-2	Villabruna	0.805701229	0.165	0.835	0.11	0.11
Ibous sieres31-2	El Mirón	Loschbour	0.599562	0	1	0	0
Chaudardes	Goyet Q-2	Villabruna	0.92959425	0.177	0.823	0.089	0.089
Chaudardes	El Mirón	Loschbour	0.369156	0	1	0	0
Ibous sieres25-1	Goyet Q-2	Villabruna	0.53154669	0.211	0.789	0.093	0.093
Ibous sieres25-1	El Mirón	Loschbour	0.5055104	0.207	0.793	0.091	0.091
Canes 1	Goyet Q-2	Villabruna	0.01610227	0.237	0.763	0.042	0.042
Canes 1	El Mirón	Loschbour	0.07701889	0.161	0.839	0.047	0.047
La Braña 1	Goyet Q-2	Villabruna	0.00044605	0.302	0.698	0.043	0.043
La Braña 1	El Mirón	Loschbour	0.04694271	0.329	0.671	0.05	0.05
Balma Guilanyà	Goyet Q-2	Villabruna	0.87148639	0.489	0.511	0.047	0.047
Balma Guilanyà	El Mirón	Loschbour	0.93985913	0.623	0.377	0.06	0.06
Chan	Goyet Q-2	Villabruna	0.13624607	0.622	0.378	0.036	0.036
Chan	El Mirón	Loschbour	0.30098571	0.809	0.191	0.055	0.055
Moita do Sebastião	Goyet Q-2	Villabruna	0.16815929	0.619	0.381	0.063	0.063
Moita do Sebastião	El Mirón	Loschbour	0.54734104	0.929	0.071	0.084	0.084
Rigney1	Goyet Q-2	Villabruna	0.96827428	0.629	0.371	0.129	0.129
El Mirón	Goyet Q-2	Villabruna	0.06640881	0.742	0.258	0.039	0.039
Burkhardtshohle	Goyet Q-2	Villabruna	0.77200323	0.837	0.163	0.106	0.106
HohleFels49	Goyet Q-2	Villabruna	0.94924453	0.943	0.057	0.126	0.126

Data S11 qpAdm models for HG individuals, Related to Figure 3D and Figure S3A.

Sources	Right populations	p-value
Anatolia Neolithic, Goyet Q-2, Villabruna	Mota, Ust'-Ishim, Mal'ta 1 (MA1), Koros EN-HG, Goyet Q-116-1, Mbuti, Papuan, Onge, Han, Karitiana and Natufian	8.64E-92
Anatolia Neolithic, El Mirón, Villabruna	Mota, Ust'-Ishim, Mal'ta 1 (MA1), Koros EN-HG, Goyet Q-116-1, Mbuti, Papuan, Onge, Han, Karitiana and Natufian	9.50E-59

Test population	Mixture proportions				SE				
	Source 1	Source 2	Source 3	p-value	Source 1	Source 2	Source 3		
Toro_EN	Anatolia Neolithic	Goyet Q-2	Villabruna	0.051487643	0.871	0.129	0	0.051	0
Toro_EN	Anatolia Neolithic	El Mirón	Villabruna	0.141986493	0.863	0.137	0	0.042	0
LaMina_MN	Anatolia Neolithic	Goyet Q-2	Villabruna	0.018891576	0.734	0.078	0.188	0.025	0.024
LaMina_MN	Anatolia Neolithic	El Mirón	Villabruna	0.325412124	0.755	0.128	0.117	0.021	0.029
Murcielagos_EN.SG	Anatolia Neolithic	Goyet Q-2	Villabruna	0.584717669	0.885	0.079	0.036	0.041	0.037
Murcielagos_EN.SG	Anatolia Neolithic	El Mirón	Villabruna	0.442409108	0.874	0.073	0.053	0.035	0.046
Trocs_MN	Anatolia Neolithic	Goyet Q-2	Villabruna	0.478508828	0.751	0.081	0.169	0.031	0.028
Trocs_MN	Anatolia Neolithic	El Mirón	Villabruna	0.17737303	0.744	0.107	0.149	0.026	0.032
Chaves_EN	Anatolia Neolithic	Goyet Q-2	Villabruna	0.19555451	0.805	0.041	0.153	0.037	0.034
Chaves_EN	Anatolia Neolithic	El Mirón	Villabruna	0.566675838	0.802	0.107	0.092	0.028	0.036
LugarCanto_MN.SG	Anatolia Neolithic	Goyet Q-2	Villabruna	0.126203213	0.749	0.075	0.176	0.026	0.025
LugarCanto_MN.SG	Anatolia Neolithic	El Mirón	Villabruna	0.274703223	0.78	0.066	0.154	0.022	0.028
Serbia_Neolithic	Anatolia Neolithic	Goyet Q-2	Villabruna	0.548126443	0.949	0.05	0.001	0.024	0.022
Serbia_Neolithic	Anatolia Neolithic	El Mirón	Villabruna	0.07077072	0.972	0.01	0.019	0.02	0.026
Germany_LBK_EN	Anatolia Neolithic	Goyet Q-2	Villabruna	0.063587653	0.915	0.03	0.055	0.013	0.012
Germany_LBK_EN	Anatolia Neolithic	El Mirón	Villabruna	0.213773934	0.932	0.033	0.035	0.011	0.014
France_MN	Anatolia Neolithic	Goyet Q-2	Villabruna	0.631094334	0.764	0.037	0.199	0.027	0.024
France_MN	Anatolia Neolithic	El Mirón	Villabruna	0.505772137	0.781	0.023	0.196	0.022	0.028
Croatia_Cardial_Neolithic	Anatolia Neolithic	Goyet Q-2	Villabruna	0.888968065	0.914	0.022	0.064	0.025	0.022
Croatia_Cardial_Neolithic	Anatolia Neolithic	El Mirón	Villabruna	0.394062031	0.957	0.013	0.03	0.021	0.026
Poland_Globular_Amphora	Anatolia Neolithic	Goyet Q-2	Villabruna	0.420786048	0.723	0.031	0.246	0.026	0.025
Poland_Globular_Amphora	Anatolia Neolithic	El Mirón	Villabruna	0.443163688	0.74	0.033	0.227	0.021	0.027
Pancorbo_EN	Anatolia Neolithic	Goyet Q-2	Villabruna	0.273413255	0.926	0.013	0.06	0.039	0.034
Pancorbo_EN	Anatolia Neolithic	El Mirón	Villabruna	0.870706608	0.908	0.023	0.069	0.031	0.037
Austria_LBK_EN	Anatolia Neolithic	Goyet Q-2	Villabruna	0.423910178	0.93	0.013	0.056	0.017	0.015
Austria_LBK_EN	Anatolia Neolithic	El Mirón	Villabruna	0.482689058	0.951	0	0.049	0.011	0
Croatia_Impressa_EN	Anatolia Neolithic	Goyet Q-2	Villabruna	0.491612	1	0	0	0	0
Croatia_Impressa_EN	Anatolia Neolithic	El Mirón	Koros EN-HG	0.302783026	0.975	0.009	0.016	0.028	0.036
Wales_Neolithic	Anatolia Neolithic	Goyet Q-2	Villabruna	0.286242574	0.764	0.03	0.206	0.036	0.035
Wales_Neolithic	Anatolia Neolithic	El Mirón	Villabruna	0.105910786	0.791	0.02	0.189	0.031	0.038
Scotland_Neolithic	Anatolia Neolithic	Goyet Q-2	Villabruna	0.017269685	0.756	0.032	0.212	0.014	0.012
Scotland_Neolithic	Anatolia Neolithic	El Mirón	Villabruna	0.011835181	0.769	0.033	0.197	0.012	0.016
Bulgaria_Neolithic	Anatolia Neolithic	Goyet Q-2	Villabruna	0.685479279	0.976	0	0.024	0.014	0
Bulgaria_Neolithic	Anatolia Neolithic	El Mirón	Villabruna	0.644836955	0.975	0	0.025	0.013	0
Chaves_MN	Anatolia Neolithic	Goyet Q-2	Villabruna	0.001363106	0.824	0	0.176	0.071	0
Chaves_MN	Anatolia Neolithic	El Mirón	Villabruna	0.003197065	0.775	0	0.225	0.062	0
Croatia_Sopot_MN	Anatolia Neolithic	Goyet Q-2	Villabruna	0.555679085	0.972	0	0.028	0.016	0
Croatia_Sopot_MN	Anatolia Neolithic	El Mirón	Villabruna	0.550179548	0.974	0	0.026	0.014	0
England_Neolithic	Anatolia Neolithic	Goyet Q-2	Villabruna	0.000618117	0.779	0	0.221	0.013	0
England_Neolithic	Anatolia Neolithic	El Mirón	Villabruna	0.00120836	0.778	0.026	0.196	0.016	0.021
Hungary_Koros_EN	Anatolia Neolithic	Goyet Q-2	Villabruna	0.492461	1	0	0	0	0
Hungary_Koros_EN	Anatolia Neolithic	El Mirón	Villabruna	0.460287	1	0	0	0	0
Romania_EN.SG	Anatolia Neolithic	Goyet Q-2	Villabruna	0.000302956	0.389	0	0.611	0.035	0
Romania_EN.SG	Anatolia Neolithic	El Mirón	Villabruna	0.000163555	0.402	0	0.598	0.032	0
Romania_Iron_Gates_EN	Anatolia Neolithic	Goyet Q-2	Villabruna	0.035186381	0	0.096	0.904	0	0.046
Romania_Iron_Gates_EN	Anatolia Neolithic	El Mirón	Villabruna	0.002060765	0.1	0	0.9	0.036	0
Serbia_Starevo_EN	Anatolia Neolithic	Goyet Q-2	Villabruna	0.015504589	0.946	0	0.054	0.024	0
Serbia_Starevo_EN	Anatolia Neolithic	El Mirón	Villabruna	0.014042054	0.938	0	0.062	0.022	0
Trocs_EN	Anatolia Neolithic	Goyet Q-2	Villabruna	0.022358817	0.905	0	0.095	0.016	0
Trocs_EN	Anatolia Neolithic	El Mirón	Villabruna	0.028028175	0.891	0.046	0.063	0.021	0.027
FuenteCelada_EN	Anatolia Neolithic	Goyet Q-2	Villabruna	0.099130192	0.991	0	0.009	0.031	0
FuenteCelada_EN	Anatolia Neolithic	El Mirón	Villabruna	0.598857042	0.976	0.024	0	0.042	0
Greece_Neolithic	Anatolia Neolithic	Goyet Q-2	Villabruna	0.758761153	0.941	0.059	0	0.033	0
Greece_Neolithic	Anatolia Neolithic	El Mirón	Villabruna	0.399083959	0.978	0.022	0	0.032	0
Hungary_Starevo_EN	Anatolia Neolithic	Goyet Q-2	Villabruna	0.03719349	0.996	0	0.004	0.017	0
Hungary_Starevo_EN	Anatolia Neolithic	El Mirón	Villabruna	0.681185	1	0	0	0	0
Portalon_EN.SG	Anatolia Neolithic	Goyet Q-2	Villabruna	0.215857	1	0	0	0	0
Portalon_EN.SG	Anatolia Neolithic	El Mirón	Villabruna	0.117447	1	0	0	0	0
Bonica_EN.SG	Anatolia Neolithic	Goyet Q-2	Villabruna	0.668976669	0.894	0.003	0.103	0.042	0.041
Bonica_EN.SG	Anatolia Neolithic	El Mirón	Villabruna	0.214951558	0.871	0.082	0.047	0.035	0.049
Ireland_MN	Anatolia Neolithic	Goyet Q-2	Villabruna	0.253449818	0.789	0.067	0.144	0.036	0.036
Ireland_MN	Anatolia Neolithic	El Mirón	Villabruna	0.150462048	0.804	0.062	0.134	0.032	0.043

Data S1J qpAdm models for Neolithic individuals, Related to Figure 4B.

11 DISCUSSION

This chapter includes an extended discussion of the main results from different publications from the ‘Results’ chapter. Discussion has been divided in two main subchapters. The first one includes all the discussion related to the isotope publications and second one includes the discussion of DNA publication.

11.1 Discussion of carbon and nitrogen isotopic results

11.1.1 Fish consumption abandonment during the Neolithic

The arrival of the first Neolithic societies into Iberia associated with the first farming practices produced not only a shift in the genomic make up, but also in the resource management and the diet. Undoubtedly, the main evidence comes from the archaeological record itself, but isotopic analysis help estimate the direct impact on the individuals quantitatively.

Iberian HG isotopic analysis show some contribution of marine or estuarine resources in HG diet, with a higher proportion in the Atlantic façade compared to the Mediterranean one (Arias, 2007; García-Guixe et al. 2006; Lubell et al. 1994; Salazar-García et al., 2014). Despite none of these cases show a fully marine diet, the subsequent Neolithic individuals show a clear shift to a fully terrestrial diet commonly recorded in Iberia and elsewhere in Europe (Salazar-García et al., 2018) with the exception of Balkans and Baltic regions (Bonsall et al., 2004; Borić et al. 2004; Lidén et al. 2004).

As it has been observed in previous studies and the results of this thesis confirm, also the Late Neolithic and Chalcolithic individuals show a complete abandon of marine or brackish resources. In our studied sites a complete C₃ diet is even clear due to the inland location of all the sites (Villalba-Mouco et al., 2018; Villalba-Mouco et al., 2018). Of the sites here studied, only the Early Neolithic site Cueva de Chaves could include an input of other kind of riverine or dairy resources (Villalba-Mouco et al., 2018).

11.1.1.1 The Early Neolithic individuals from Cueva de Chaves

In our isotopic study of the Early Neolithic individuals from Cueva de Chaves there is one individual (S-UCT 21024/ 84C) who does not cluster with the others, whose body was recovered from a special burial. This individual shows higher $\delta^{13}\text{C}$ and $\delta^{15}\text{N}$ values (by 1.5‰ and 0.7‰ higher than the other humans, respectively; 6.6‰ and 1.7‰ higher than herbivores, respectively). For this individual, a small input of another type of protein resource could be suggested, perhaps marine or estuarine protein consumption in low quantities but enough as to be recorded in the isotopic collagen composition (**Figure 41**).

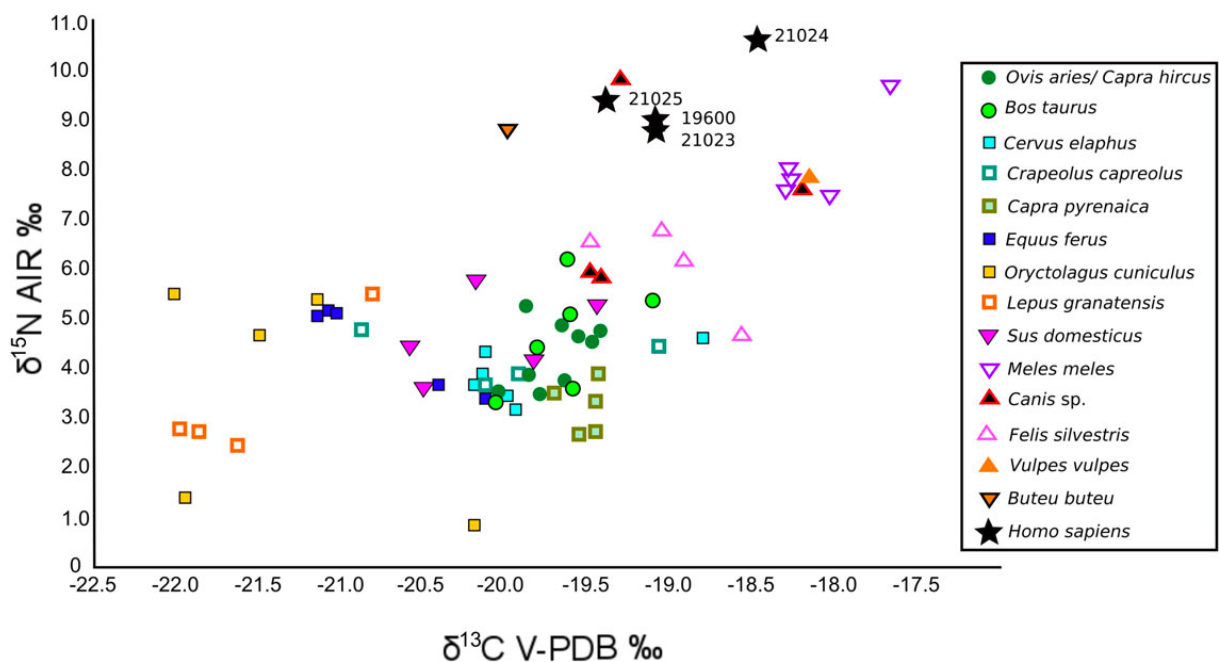


Figure 41: Scatter plot of human and fauna bone collagen $\delta^{13}\text{C}$ and $\delta^{15}\text{N}$ values from Cueva de Chaves.

Cueva de Chaves is located close to the Solencio ravine, which presents a torrential water flux, something likely not compatible with the extensive presence of freshwater fish. Moreover, the higher $\delta^{15}\text{N}$ and $\delta^{13}\text{C}$ values at the same time is more common for marine than freshwater resource consumption (Lillie et al., 2011) (**Figure 41**). If this was the case and the individual had eaten marine or estuarine fish, as they are not available locally, this would be another point to support the existence of coastal-inland routes for this time period. This has been proposed previously by schematic rock art studies (Utrilla and Baldellou, 2001; Pérez, 2016) as well as by the huge set of Cardial pottery and marine shells used for Cardial decoration recovered at the site (Utrilla and Laborda, 2018). When plotting together all the adult Early Neolithic humans from Iberia (3 sites, 9 adult humans including Cueva de Chaves), individual S-UCT

21024 from Cueva de Chaves shows the highest $\delta^{13}\text{C}$ and $\delta^{15}\text{N}$ values only followed by one individual from Cueva de Nerja where a small C_4 input has been suggested (Salazar-García et al., 2017). In contrast to Cueva de Nerja, no faunal remains have shown typical values from C_4 ecosystems at Cueva de Chaves, so the hypothesis of marine protein intake is more plausible for this individual, as well as due to the presence of a higher $\delta^{15}\text{N}$ increase at Cueva de Chaves than at Cueva de Nerja in comparison to their respective faunal baselines (Figure 42). This could imply that the Cueva de Chaves first farmers had some connections with contemporaneous coastal sites. Strontium isotope analysis in dental enamel could help to know more about the mobility of this Cardial individual with a special burial treatment during his life as long as the migration happened after the enamel mineralization and if the geology of the two areas (where the enamel mineralization took place and Cueva de Chaves) were different (Bentley, 2013; Price et al. 2001) (Figure 42).

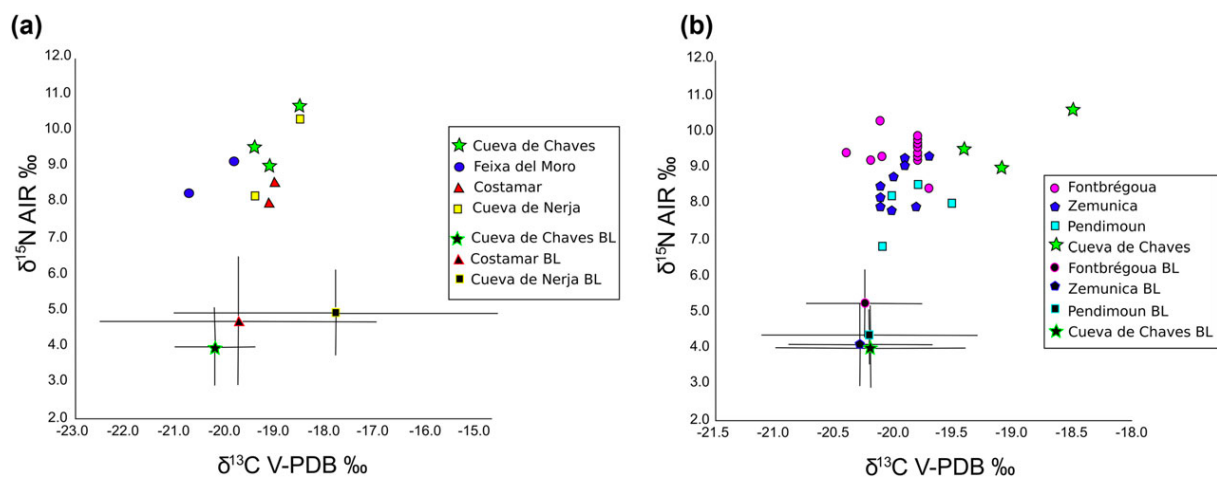


Figure 42: **A)** Plot of bone collagen $\delta^{13}\text{C}$ and $\delta^{15}\text{N}$ values of different Early Neolithic adult humans from Iberia [Costamar (Salazar-García, 2009); Cueva de Nerja (Salazar-García et al., 2017); Feixa del Moro (Remolins et al., 2016) and Cueva de Chaves (Villalba-Mouco et al., 2018)]; **B)** Plot of bone collagen $\delta^{13}\text{C}$ and $\delta^{15}\text{N}$ values of different Early Neolithic from the Western Mediterranean region [Fontbrégoua (France) (Le Bras-Goude et al. 2010), Pendimoun (Le Bras-Goude et al., 2006), Zemunica (Croatia) (Guiry et al., 2017) and Cueva de Chaves (Villalba-Mouco et al., 2018)]. The X and Y axes are plotted at different scales in order to make all the samples more visible. The $\delta^{13}\text{C}$ and $\delta^{15}\text{N}$ baselines were calculated with contemporaneous herbivore data of each site when was available excluding domestic pigs. Subadult individuals were excluded; BL: Baseline.

Note: The strontium isotope analysis of individuals from Cueva de Chaves is on preparation. We already have data for S-UCT 19600 and S-UCT 21025. When I performed the sampling on

the Museo of Huesca, the mandible of the individual S-UCT 21024/ 84C was missing. Now that the mandible of this individual has been located, we can continue studying the provenance of the individual S-UCT 21024/ 84C.

11.1.2 Husbandry practices during Early Neolithic

Despite the homogeneous diet of the producer societies, it is interesting to understand the husbandry management strategies of the first farming societies from an isotopic point of view. Moreover, exploring the fauna data (and plant remains when available) could help us to improve the human diet interpretation. To do that, it is mandatory to study entire settlements to assess all the possible domestic and wild species that contributed to the human diet. The Iberian Peninsula presents few Early Neolithic sites where fauna and humans can be analyzed together from an isotopic perspective. Most of the Early Neolithic human remains were recovered from only sepulchral contexts (e.g Oms et al., 2017; Oms et al., 2015; Zilhão, 1992) where fauna remains do not need to be representative of the individual diet, and not all the individuals have to come from the same settlement. Cueva de Chaves was mostly a habitat settlement, although it also had some areas dedicated to funerary practices. Besides the funerary area (Utrilla et al., 2008), evidence of different daily activities typical of a Neolithic community have been discovered inside the cave, shedding light on the broad Neolithic lifestyle: evidence of hunting (Castaños, 2004; Domingo, 2009), butchery and harvest activities (Domingo, 2014; López-García & López-Sáez, 2000; López García, 1992; Mazzucco et al., 2015), schematic art representations in pebbles, (Utrilla and Baldellou, 2002; Utrilla and Baldellou, 2007), fireplaces and storage structures (Alcolea et al. 2017). Many of these tasks can be recorded separately, and evidence of most of them together usually happen only in open-air settlements such as La Draga (Bosch et al., 2011) and Guixeres de Vilobí (Oms et al., 2014). In this sense, the isotopic study on the site of Cueva de Chaves is an example for understanding the dietary and economical changes that took place during Early Neolithic in Iberia (Villalba-Mouco et al., 2018).

11.1.2.1 *Wild and domestic herbivores in Cueva de Chaves*

In this study, no significant differences were found between wild and domestic herbivores from Cueva de Chaves. Finding the same values among wild and domestic herbivores could point towards a possible common plant resource consumption. On the other hand, domestic herbivore data also present less dispersion than wild ones. Specifically, domestic ovicaprids show the

smallest dispersion in both $\delta^{13}\text{C}$ and $\delta^{15}\text{N}$ values and suggest a common environment and feeding that could be associated with stabling practices to protect the livestock from the wild carnivores as described for other Iberian Early Neolithic sites (Oms et al., 2014; Saña et al., 2015). This common feeding/environment would imply the absence of sheep flocks or transhumance activities amongst the Early Neolithic community living in the cave. However, since bulk bone collagen reflects an average of the last years of life, it is difficult to find differences in isotopic values resulting from the seasonal movements between environments; sequential $\delta^{13}\text{C}$ and $\delta^{18}\text{O}$ isotopic analysis of teeth would be necessary to prove the absence of these types of husbandry practices (Tornero et al., 2016, 2018) (**Figure 41**).

Some isotopic analysis between wild and domestic herbivores have been carried out in order to test differences in husbandry management practices in other contemporary Iberian sites such as La Draga or Cova de Frare (Navarrete et al., 2017). At the first site, the domestic fauna showed higher $\delta^{13}\text{C}$ and $\delta^{15}\text{N}$ values. These slight isotopic differences could suggest different feeding strategies, such as using agricultural crops as one of the potential fodders for domestic species. The reason for these higher $\delta^{13}\text{C}$ and $\delta^{15}\text{N}$ values could be the use of natural fertilizers. Although the presence of crops in La Draga is clear (Antolín, 2016; Antolín and Buxó, 2011), Navarrete et al. (2017) proposed that the increase in $\delta^{15}\text{N}$ values is quite low to propose an intensive manuring effect (Amy Bogaard et al., 2013). However, the other Early Neolithic site, Cova de Frare, presents no isotopic differences between wild and domestic herbivores (Navarrete et al., 2017), likewise as observed at Cueva de Chaves (**Figure 41**).

11.1.2.2 Pig livestock in Cueva de Chaves

Suids are omnivores with a flexible ecological niche because of their opportunistic feeding (Macdonald and Barrett, 1993; Schley and Roper, 2003). Humans have taken advantage of this to feed domestic pigs (*Sus domesticus*) with whatever suited them. As a result, the diet of pigs has proved to reflect many aspects of human community structure in both prehistoric (Madgwick et al. 2012) and historic periods (Halley and Rosvold, 2014). In this sense, two main management models for pig husbandry have been proposed. The first one is based on a free-range management where pigs feed on their own and most of the diet comes from plants (Madgwick et al. 2012), resulting in an herbivorous isotopic signal. The other one is the household management one, where pigs feed on leftovers and human debris and therefore commonly show a mixed isotopic signature resulting from combining the different types of

foods consumed by humans in each case (Balasse et al., 2016; Madgwick et al., 2012; Müldner and Richards, 2005; Privat et al., 2002; Richards et al., 2006). Some authors consider that both suid husbandry management models can occur simultaneously in what is called a "household model" with mixed diets only depending on the size of livestock (Navarrete et al., 2017). Other authors argue that pig management practices change according to the chrono-cultural period, showing more household feeding of pigs in historic rather than prehistoric times (Madgwick et al. 2012) (Figure 41).

Domestic suids from Cueva de Chaves showed an herbivore diet. The same $\delta^{15}\text{N}$ range as herbivores shows, points out they are in a same trophic level, ruling out a significant input of animal protein in their diet (Bocherens and Drucker, 2003). The $\delta^{15}\text{N}$ values are also the same for ruminant and non-ruminant herbivores, suggesting that isotopic digestive fractionation could cause an incorrect herbivore profile in pigs (Halley and Rosvold, 2014; Hedges, 2003). This herbivore trophic attribution would be compatible with a free-range pig husbandry management similar to what is proposed for the Early Neolithic Iberian sites of Cova del Frare and Serra de Mas Bonet (Navarrete et al., 2017). However, and contrary to what is observed at these sites, Cueva de Chaves has a large-sized pig livestock, more similar to the one from La Draga where an herbivore pig diet has also been suggested (Navarrete et al., 2017) (Figure 41).

This result led us to propose a controlled and limited dispersion range for suid husbandry, or their keeping in an enclosure where they would be fed only plant foods (Hadjikoumis, 2012; Halstead and Isaakidou, 2011). In this sense, anthracological evidence shows the importance of acorns in Cueva de Chaves during the older Early Neolithic level (Alcolea et al., 2017; Zapata et al., 2008) when the presence of a woodland environment is suggested (Marta Alcolea et al., 2017). The consumption of acorns could have decreased over time (Hamilton et al., 2009), parallel to the woodland clearing at the recent Early Neolithic level (Marta Alcolea et al., 2017). It is also necessary to consider that, as ethnography shows (Halstead and Isaakidou, 2011), a fattening diet based on animal products could take place at the end of the pig's life and would therefore not be shown in the collagen bulk signature. However, it seems that the overall introduction of leftover feeding of pigs happened over time, linked to the complexity of the settlements (Madgwick et al. 2012) (Figure 41).

11.1.3 Diet continuity or a methodological bias?

The biggest data set for carbon and nitrogen analysis performed in human collagen in Iberia comes from the Late Neolithic to Chalcolithic transect (including some Bronze Age). A higher precision in time scale is not possible due to most of these sites published are collective burials and not all their individuals have a direct radiocarbon date. During that time transect the human isotope values portray a quite homogeneous overall diet among humans (**Figure 43**). This homogeneous pattern of diet based on C₃ terrestrial resources seems to be general along the entire Iberian Peninsula during the Late Neolithic and Chalcolithic (e.g. Alt et al., 2016; Diaz-Zorita-Bonilla, 2014; Fernández-Crespo et al., 2018; Fernández-Crespo and Schulting, 2017; Fontanals-Coll et al., 2015; García-Borja et al., 2013; López-Costas et al., 2015; McClure et al., 2011; Salazar-García, 2011; Sarasketa-Gartzia et al., 2018a; Sarasketa-Gartzia et al., 2018b; Villalba-Mouco et al., 2018a; Villalba-Mouco et al., 2018b; Waterman et al., 2015). The reason of this homogeneity could be the consolidated economy based on agriculture and livestock, together with a higher mobility among the different communities and the increase of trade networks, not only in prestigious objects (Schuhmacher and Banerjee, 2012) but also in food products.

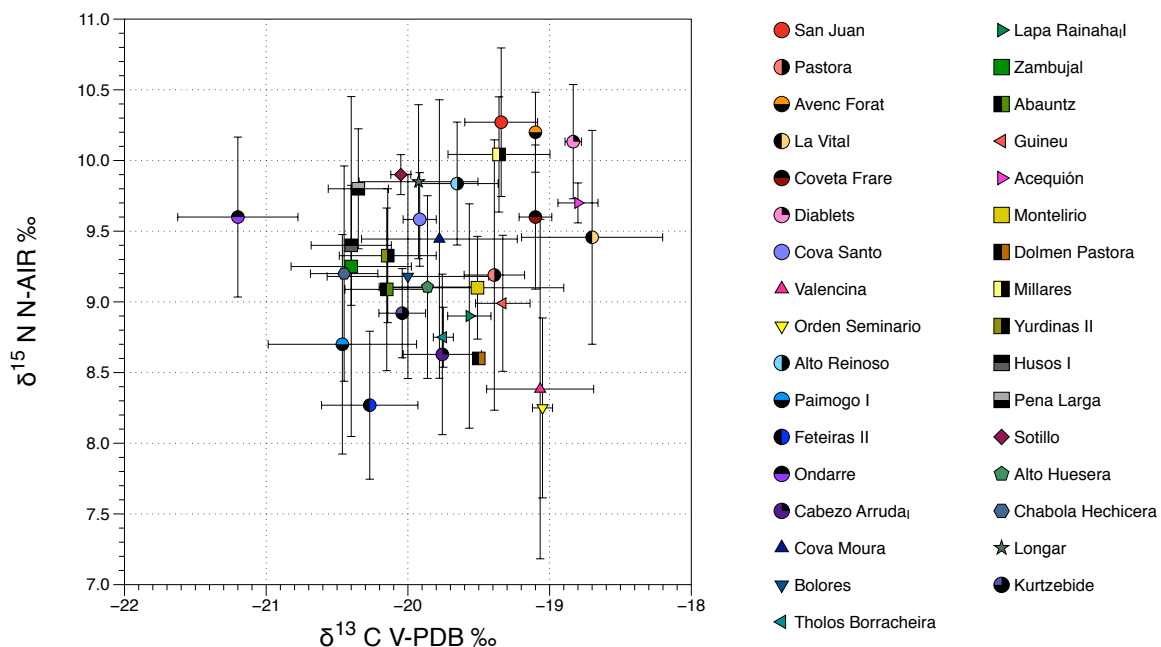


Figure 43: Plot of bone collagen $\delta^{13}\text{C}$ and $\delta^{15}\text{N}$ values of different Late Neolithic-Chalcolithic and Bronze sites from Iberian Peninsula (data and references available Annex 1).

However, another interesting point to address would be the limit of the resolution using carbon and nitrogen stable isotope from the bulk collagen. Recent studies highlight this limitation power of dietary studies using stable isotope compositions. Webb et al. (2017) have shown in a controlled feeding experiment on pigs (considered physiologically comparable to humans) that the $\delta^{13}\text{C}$ value of bulk of collagen could mask some diet information and also could provide a wrong interpretation about resource consumption. Moreover, bulk isotopic values are influenced by aminoacid routing (Webb et al., 2017). High protein diet directly routes non-essential aminoacids because it is more efficient the assimilation than the synthetization energetically speaking. But, when the diet is poor in protein content, the novo synthesis happens more frequently. In this case, the carbon can also come from carbohydrates and lipids (Jim et al., 2006). This could mean that if one individual has a low protein diet consisted on few marine resources and higher amount of plants, the novo synthesis of non-essential aminoacids could mask the marine $\delta^{13}\text{C}$ values (Webb et al., 2017). Future approaches to explore human diet would need to combine the isotopic analysis on specific aminoacids (LC-IRMS) (Krummen et al., 2004) with bulk collagen analysis in order to get more resolution and discern if there is a homogeneous diet among the individuals during the Neolithic and the Chalcolithic and Bronze Age or if on the other hand we have a problem in the method resolution that is creating this homogeneity (Figure 43).

11.1.4 Environmental influence on isotopic values

Despite the homogeneity among individuals during the Late Neolithic to Bronze Age transect we still can differentiate some patterns. Firstly, the individuals tend to cluster together by sites (Figure 43). This could be reflecting more specific shared diets in each site. When we look at groups of sites, we observed that sites located in the same eco-geographical region also shared more affinity to others located outside the region (Figure 44, Figure 45). This still can be reflecting differences in diet, potentially driven by ecosystem resource availability. However, when looking at faunal isotopic results, we can still differentiate these eco-geographical regions (Figure 46, Figure 47). This only could mean that the human values are also influenced by environmental factors. This is something already known, but we still find many examples in the literature where researchers do not include fauna remains or the number of analysis performed in fauna is not enough to estimate an accurate baseline for each eco-geographical region; we acknowledge that sometimes these faunal remains simply are not available in the archaeological record, but in this case this should be clearly stated and discussed regarding

interpretation of human results when comparing to faunal remains from other sites and/or other time periods. Moreover, many reviewers ask for a comparison of all the contemporaneous sites in Iberia for a certain time period; based on these differences direct comparison is neither always possible nor useful even if all samples to be compared have a C₃ full diet from an isotopic perspective.

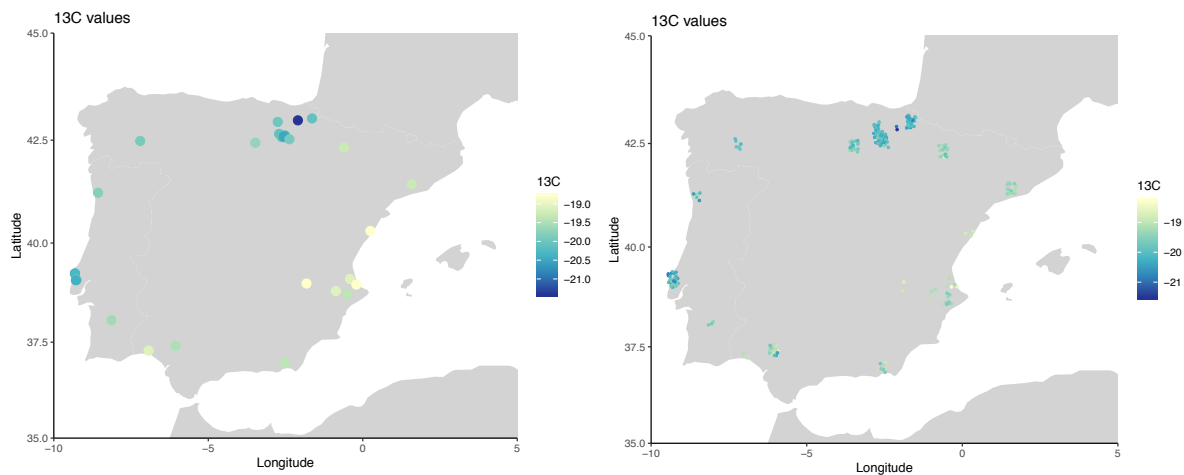


Figure 44: **A)** Average of $\delta^{13}\text{C}$ values from the published data with individuals grouped by sites. **B)** $\delta^{13}\text{C}$ values from the published individuals plotted individually with jitter option in R. The data set includes studies with age group and good collagen quality control values. Subadult individuals have been excluded (Annex 1).

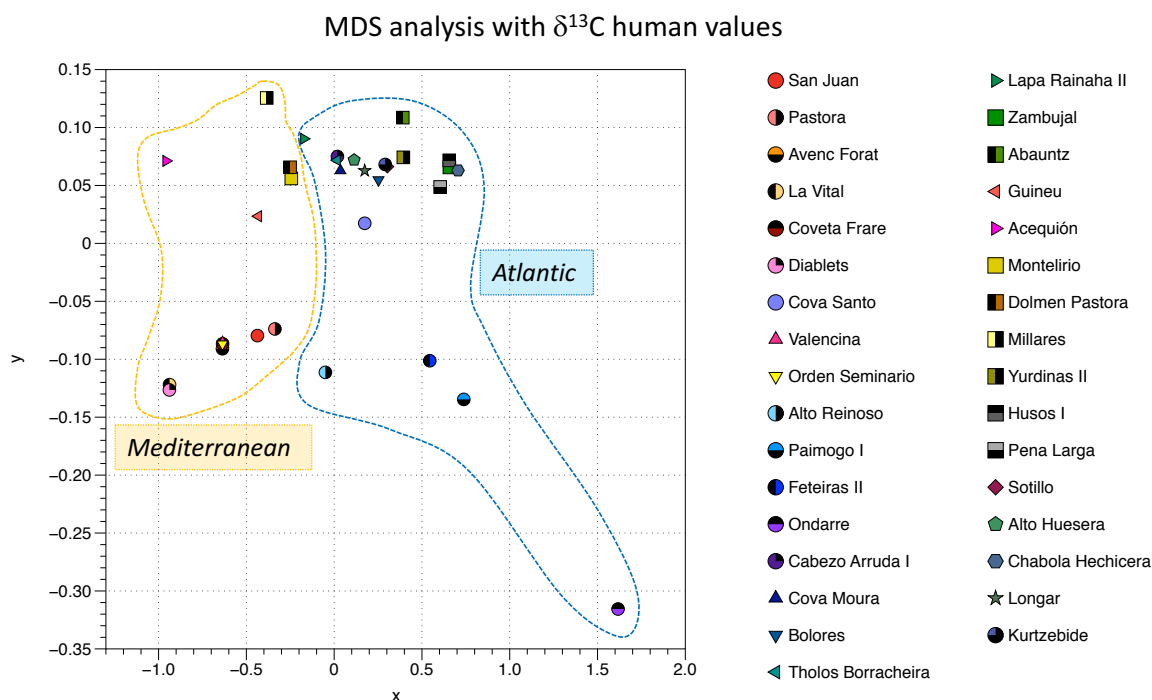


Figure 45: Multi Dimensional Scale analysis built with the absolute value of pairwise differences among the site $\delta^{13}\text{C}$ average value. Mann-Whitney non-parametric test between groups show statistical significance (p . value = $8.211\text{e-}30$; Annex 2 and 5).

The highest differences are found comparing the $\delta^{13}\text{C}$ values, although for some regions we can also infer some differences for the $\delta^{15}\text{N}$ (**Figure 48**). The results suggest that the observed human difference between sites should not be attributed entirely to diet, but most possibly to the existence of enough environmental differences to be recorded in the collagen $\delta^{13}\text{C}$ values along the food web. Plants are very sensitive to different environmental factors (altitude, temperature, luminosity or water availability) and their physiological adaptation to its factors can generate a variation in their isotopic values as happens with C_3 and C_4 adaptations (Ambrose, 1991; O’Leary, 1981). This spectrum of values has been used to assess several aspects about past environmental conditions when studying the $\delta^{13}\text{C}$ and $\delta^{15}\text{N}$ isotopic values of a species with a fixed diet over time (e.g. González-Guarda et al., 2017; Stevens et al., 2008). Moreover, this gradual $\delta^{13}\text{C}$ and $\delta^{15}\text{N}$ variation among different environments is very helpful to discriminate altitudinal movements in herbivores with a high precision method based on serial dentine analysis (Tornero et al., 2016). These differences demand caution when interpreting human diets from different sites that are not contemporary and/or not in a same area, as it is possible that the environmental influence is responsible for changes otherwise attributed to different subsistence patterns and social structures (Fernández-Crespo and Schulting, 2017), as has been demonstrated in neighbouring territories (Goude and Fontugne, 2016; Herrscher and Le Bras-Goude, 2010).

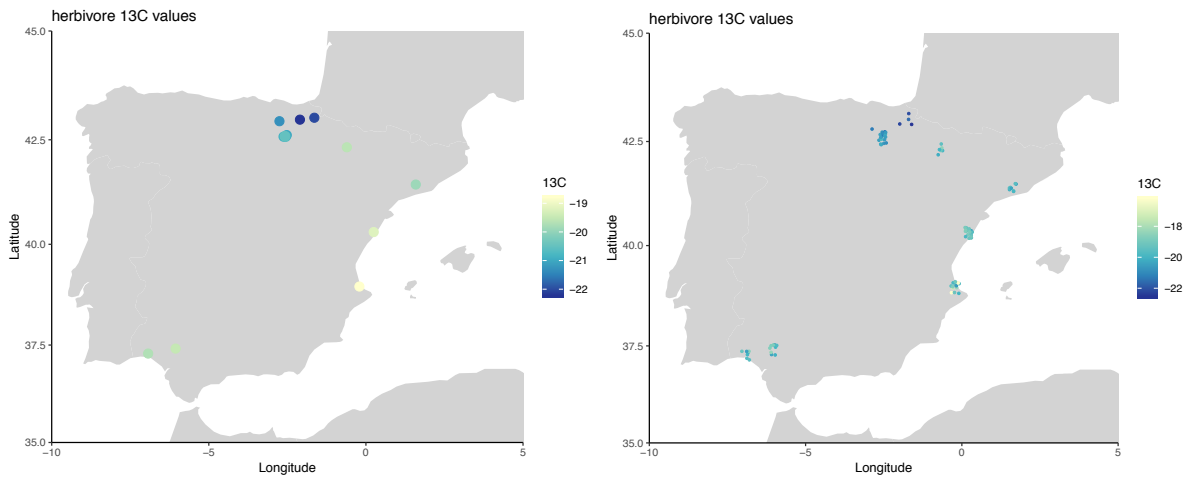


Figure 46: A) Average of $\delta^{13}\text{C}$ values from the published data with herbivores grouped by sites. B) $\delta^{13}\text{C}$ values from the published herbivores plotted individually with jitter option. The data set includes wild and domestic herbivores. Suids and other omnivores have been excluded (Annex 1).

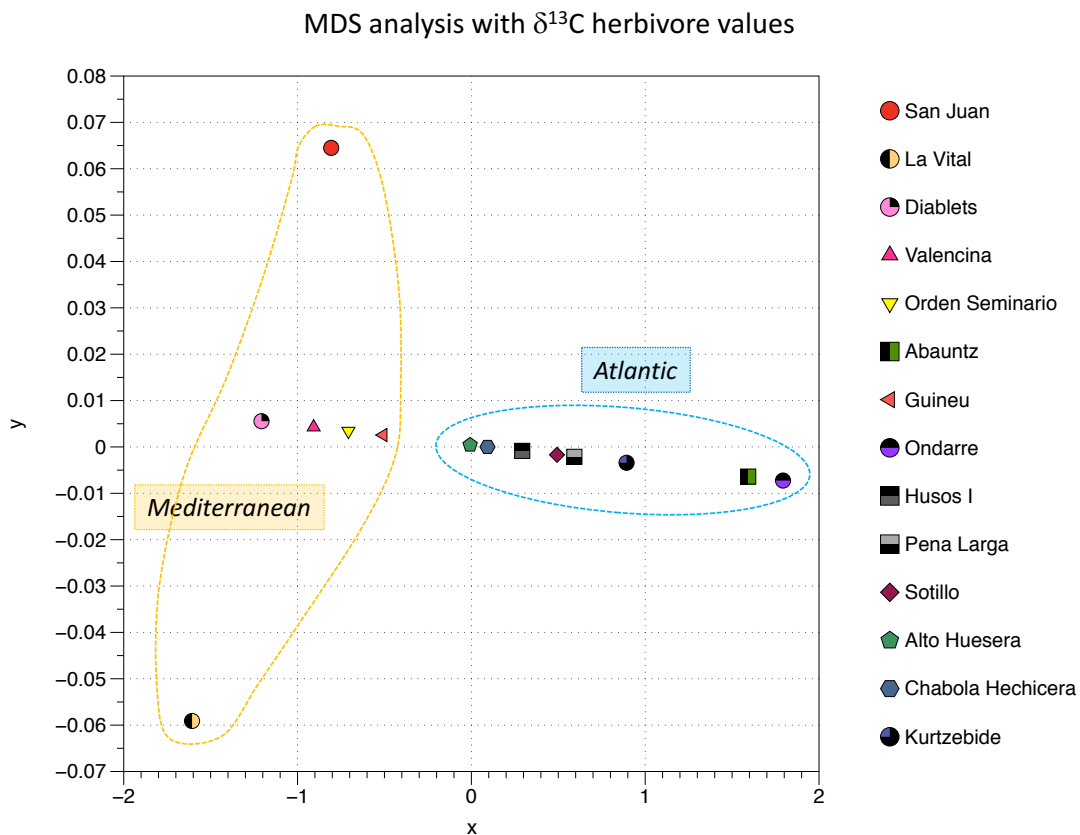


Figure 47: Multi Dimensional Scale analysis built with the absolute value of pairwise differences among the herbivore $\delta^{13}\text{C}$ average value per site. Mann-Whitney non-parametric test between groups show statistical significance (p. value = 2.561e-11; Annex 4 and 6).

This environmental influence could also affect the diet estimation using Bayesian modelling approaches (Fernandes et al., 2014; Moore and Semmens, 2008; Phillips and Gregg, 2003). Most of this model applied for humans was developed for ecological studies where the environmental conditions are shared by the entire ecosystem. But, human diet is more complex and is influenced by many factors like personal preferences, cooking and food products trading. Moreover, the significant influence of the environmental factors on bone collagen open again the discussion to consider stable isotope analysis performed on bulk collagen as a precise method to estimate quantitatively the human diet. Otherwise, we need to explore further if humans with a full C_3 diet could be also used as an environmental approach like animals. We will have to explore in detail if the two variables (diet and environment) show some correlation. If not, we always have to fix one of them to study the other appropriately. That means study the environmental conditions when the diet is fixed, as it happens in fauna studies (e.g. Stevens et al., 2008) or fix the environmental conditions (only select compatible eco-geographical regions) to study human diet. Future research can be addressed to study weather conditions which can influence most on isotopic values and the delimitation of these eco-geographical regions in detail.

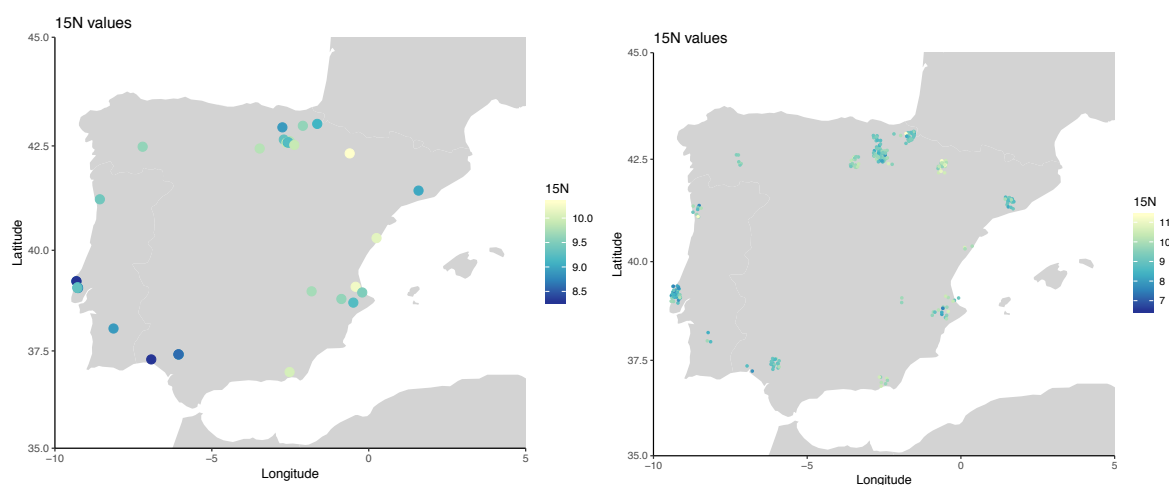


Figure 48: **A)** Average of $\delta^{15}\text{N}$ values from the published data with individuals grouped by sites. **B)** $\delta^{15}\text{N}$ values from the published individuals plotted individually with jitter option in R. The data set includes studies with age group and quality controls reported. Subadult individuals have been excluded (Annex 1).

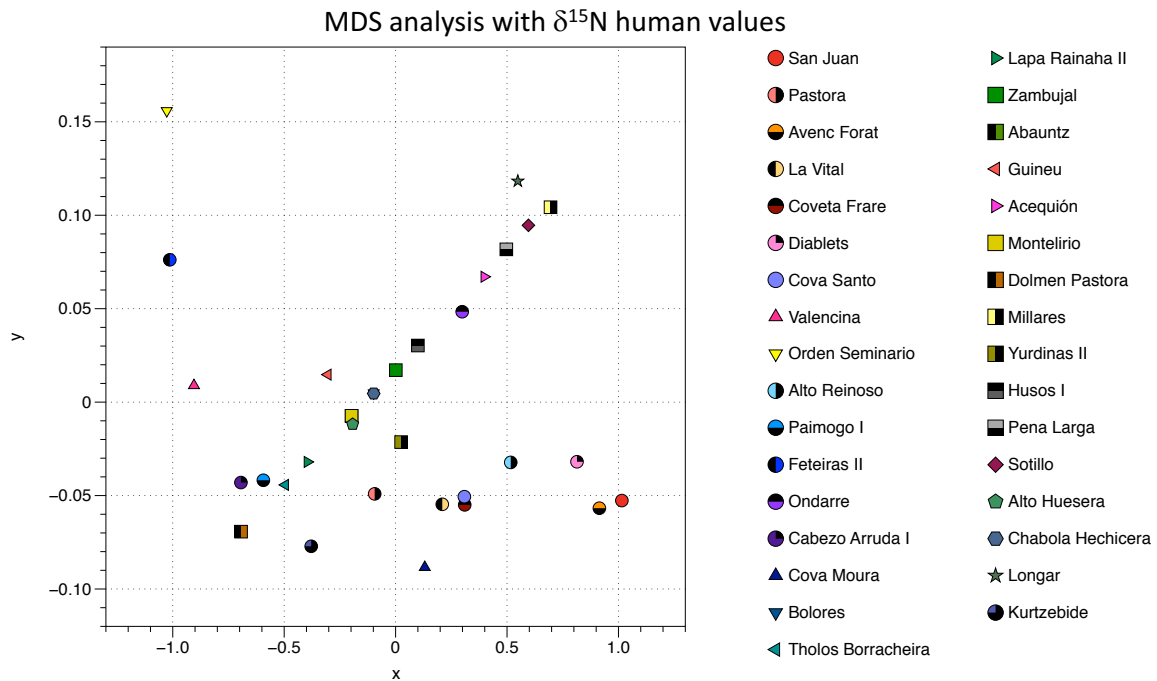


Figure 49: Multi Dimensional Scale Analysis built with the absolute value of pairwise differences among the site $\delta^{15}\text{N}$ average value. $\delta^{15}\text{N}$ does not show a clear eco-geographical clustering (Annex 3 and 5).

11.2 Discussion of strontium results

11.2.1 Method accuracy to estimate the bioavailable Sr range.

During the develop of this thesis we noticed that the range of bioavailable $^{87}\text{Sr}/^{86}\text{Sr}$ values for plants was larger than for snails systematically (Villalba-Mouco et al. 2018). We assumed that the range in this group is likely caused by the different kinds of plants sampled, herbaceous, bushes and trees, which take water from different depths within the ground. Contrary, we interpreted that the small range for $^{87}\text{Sr}/^{86}\text{Sr}$ values from snails reflects the extremely limited movement over the landscape. But, there is also an issue of $^{87}\text{Sr}/^{86}\text{Sr}$ median values calculated with snails and plants from the same specific sampled area using the same number of samples in each group (n=5) (Figure 50).

We are not able to distinguish which is the best marker (plants or snails) for the calculation of bioavailable range of $^{87}\text{Sr}/^{86}\text{Sr}$ values with the methodology of sampling used along this thesis. Future studies should approach this question focusing specifically in the method improvement, including also archaeological faunal remains.

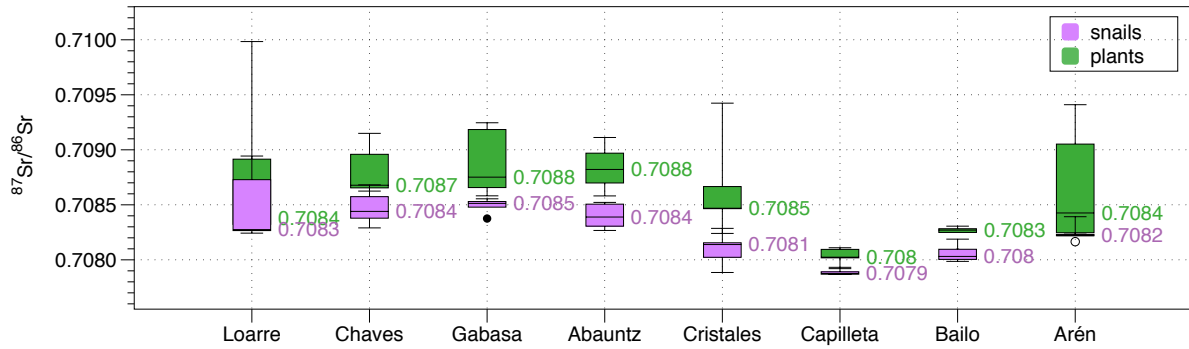


Figure 50: Pair-comparison of $^{87}\text{Sr}/^{86}\text{Sr}$ values in the areas where both, plant and snail were sampled. Median is the reported value, boxes are represented by 1st and 3rd quartile. Whiskers show the maximum and the minimum values.

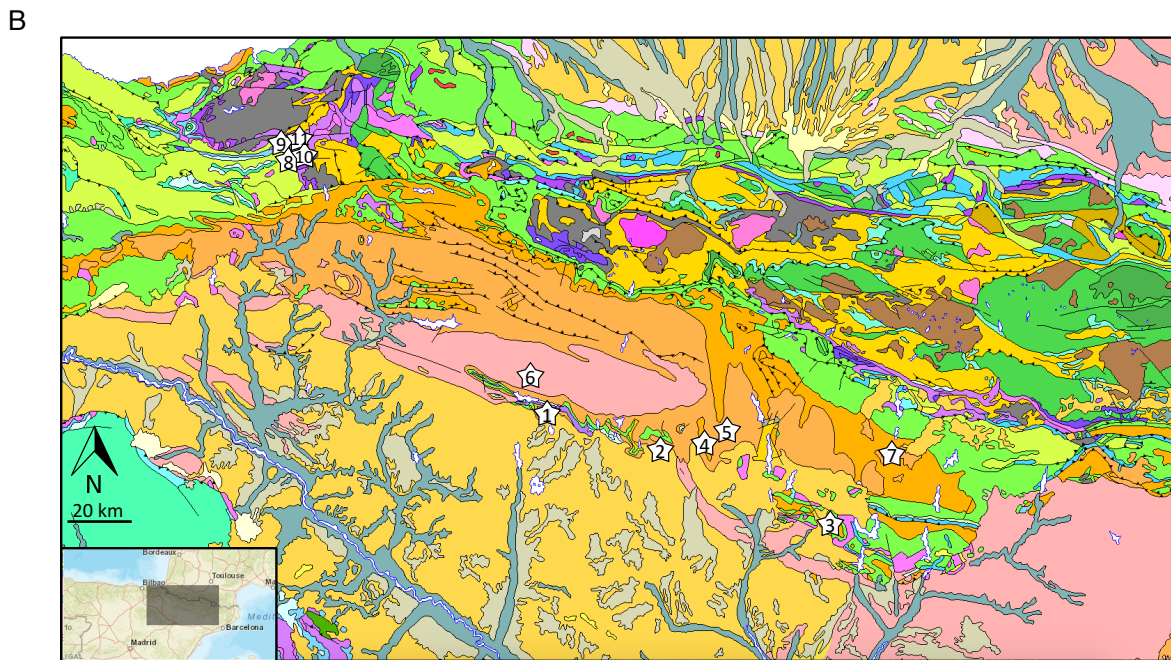
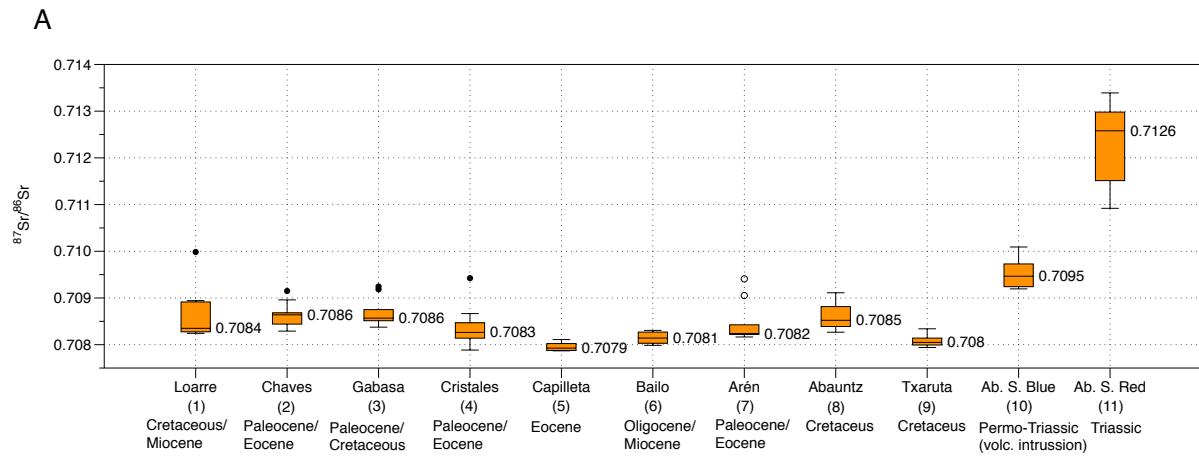


Figure 51: A) $^{87}\text{Sr}/^{86}\text{Sr}$ values in the sampled areas (plants and snails when both were analyzed from the same area). Median is the reported value, boxes are represented by 1st and 3rd quartile. Whiskers show the maximum and the minimum values. **B)** Geological map with

the location of the sampled areas (to see more resolution on a specific area, consult the geological description in the articles, “Results” chapter).

11.2.2 Archaeological discussion of strontium results

The study of individual provenance in this thesis has had two main limitations. First one comes from the kind of sites. All the studied sites are sepulchral caves from the Late Neolithic-Chalcolithic period. Non-local individuals found in a sepulchral cave could have different meanings. They could be actual migrants that travelled at some point during their life to settle at a community living close to place (the cave) where they were eventually buried. Or, alternatively, could mean that the site was used as a shared funerary space by communities living in a wider area encompassing different major geological regions other than the one from the immediate burial surrounding. In order to better assess these two possibilities, distances should be considered. If a non-local individual shows values compatible with those from nearby geological areas, we can't rule out the possibility that the individual is no real migrant but instead was transported to the cave from its “local” community once dead. However, if the non-local values correspond to geological domains situated further away, it is less plausible that the corpse was brought into the cave from far away distances, and we are possibly talking in this case of a real migrant. This example was found in Cueva de San Juan (Loarre). Three individuals showed higher $^{87}\text{Sr}/^{86}\text{Sr}$ values than the bioavailable Sr range from San Juan cave surroundings (Cretaceous-Miocene) and nearby Ebro Basin deposits. Because of proximity, it is likely that these individuals arrived from other regions with abundant Lower Triassic formations: the Iberian System in the south of San Juan cave or the Navarre Pyrenees in the north. In this three cases the Lower Triassic deposits with considerable surface area are more than 100 km away from San Juan cave, and it is therefore likely that these three individuals (M30, M42 and C7) are actual migrants coming from afar. As a result, and further supported by the fact that all this far away regions are full of cavities potentially available for burying the dead, the corpse transportation hypothesis is in these three individuals less plausible.

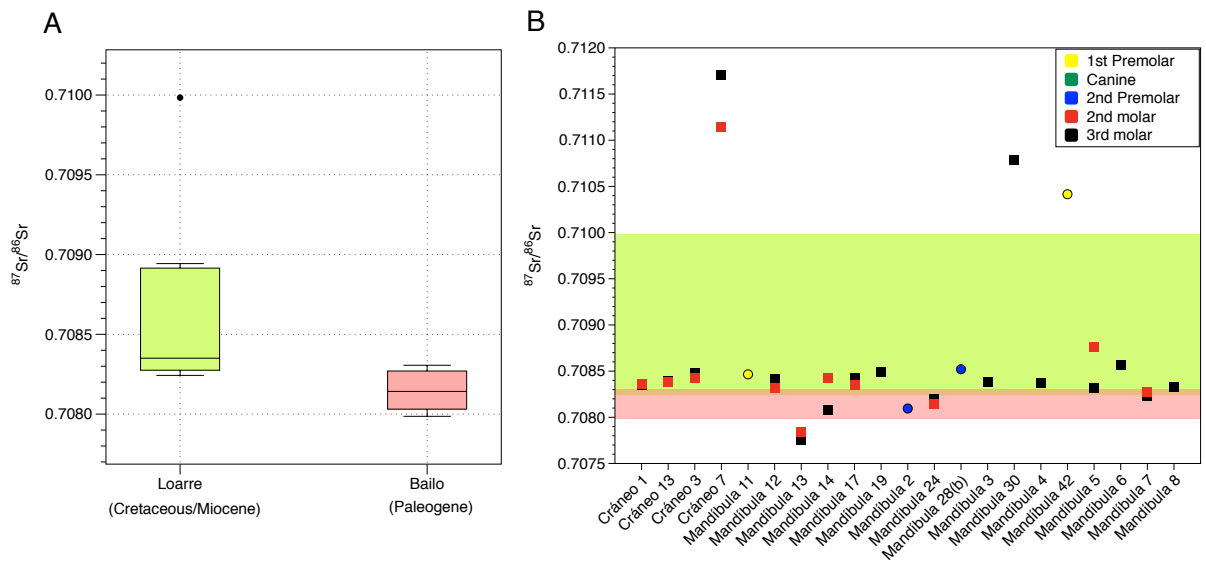


Figure 52: A) Box plot of $^{87}\text{Sr}/^{86}\text{Sr}$ range for bioavailable areas. B) Human enamel values reported over the bioavailable range.

The second limitation comes from the surrounding landscape of the Ebro Basin and concretely our studied area, is highly dominated by Tertiary and Quaternary deposits (**Figure 51**). We have detected many overlapping Sr bioavailable values among the different Paleogene and Miocene deposits and this was the main problem to assess the provenance of the individuals from Cueva de los Cristales (Sarsa de Surta) (**Figure 51**). But contrary, finding individuals with high $^{87}\text{Sr}/^{86}\text{Sr}$ values can make us confirm with certain assurance the non-local conditions of the individuals, like it happens in Cueva de San Juan (**Figure 52**, **Figure 53**).

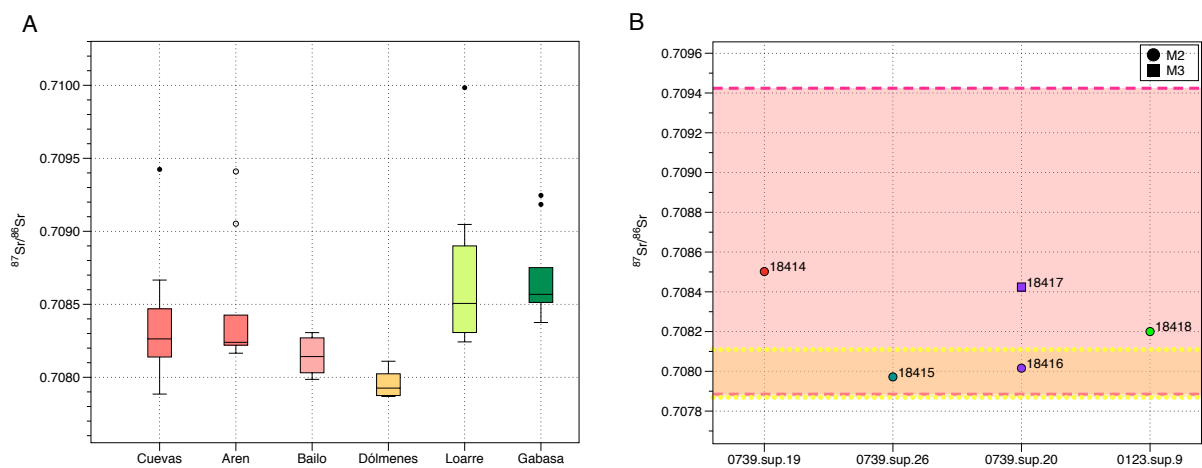


Figure 53: A) Box plot of $^{87}\text{Sr}/^{86}\text{Sr}$ range for bioavailable areas. B) Human enamel values reported over the bioavailable range.

Otherwise, Cueva de Abauntz sepulchral cave located in Arraitz (Navarra) shows a quite different geological landscape, with Cretaceous, Triassic, Permo-Triassic and Jurassic surrounding deposits. In this case, considering some individuals local or not is complicated and confused so finally we established to call “local” all the individuals who presented values compatible with Cretaceous deposits, where the cave is settled. On the other hand, the presence of different kind of geological deposits made possible to differentiate individuals with different provenances which can be compatible with the use of the burial enclosure by different communities. Thanks to combine the Sr values with direct radiocarbon dating and the Bayesian modelling of the dates based on the archaeological information, we were able to distinguish two burial phases split by the moment when a fire event is recorded in Cueva the Abauntz. When combining radiocarbon dates together with strontium isotopes analysis we can obtain more in-depth information regarding provenance through time. In this sense, we find a local $^{87}\text{Sr}/^{86}\text{Sr}$ signal (Cretaceous values) in the individuals who present the oldest radiocarbon dates. This could suggest the early use of Cueva de Abauntz as a burial space by the communities of people living closer to the burial site. Looking at the later periods, we find individuals whose $^{87}\text{Sr}/^{86}\text{Sr}$ values are compatible with the bioavailable values for further away territories (Permo-Triassic and Triassic). This feature is in agreement with the results of Cueva de San Juan where the individual mobility seems to have happened at the end of the cave's use as burial site, during the end of the Late Neolithic-Chalcolithic period, as shown by the radiocarbon dates of the non-local individuals (**Figure 54**).

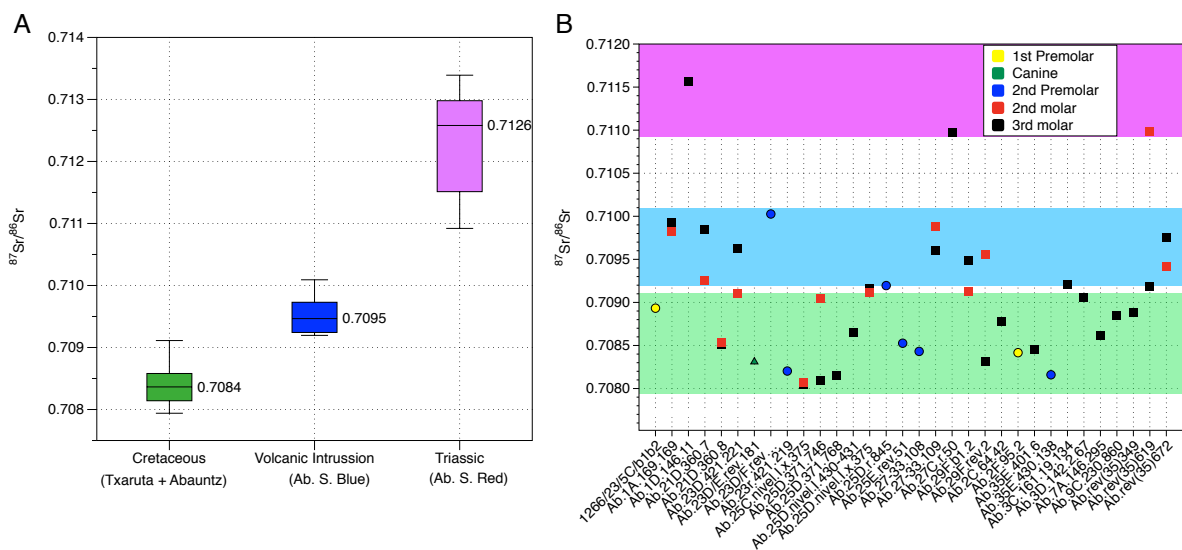
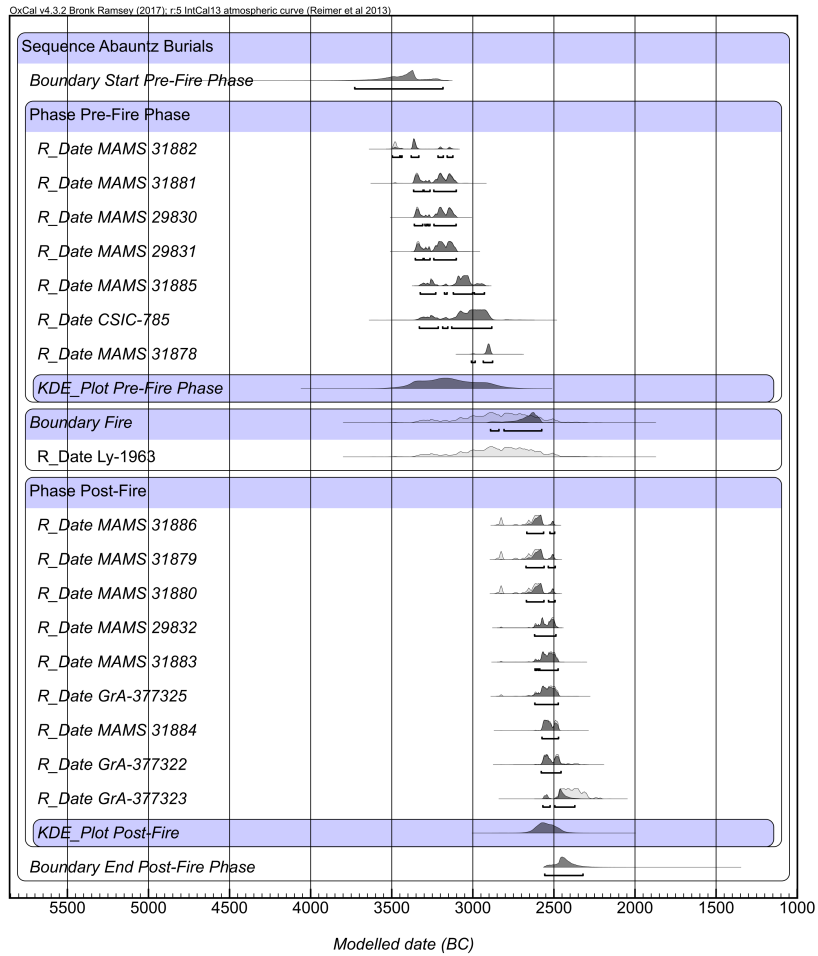


Figure 54: A) Box plot of $^{87}\text{Sr}/^{86}\text{Sr}$ range for bioavailable areas. B) Human enamel values reported over the bioavailable range.

Another interesting point of Cueva de Abauntz is the moment when the fire event is recorded and the presence of a second burial phase. Cueva de Abauntz is located in an area surrounded by many sepulchral caves. In many of these burial caves, the use of fire has been recorded at the end of the use of the cavities as funerary enclosures. This event has been proposed as a sign of closure of the funerary activity, and in all the cavities it appears around 2800 cal B.C (Fernández-Crespo, 2016). The presence of fire in Cueva de Abauntz has also been recorded at that same time, although the radiocarbon date for this moment comes from one charcoal sample and the *old wood* effect should not be ruled out (Bowman, 1990). The main difference between Cueva de Abauntz and the other burial caves with presence of fire is that in the first one, the radiocarbon dates point out to a further funerary use after the fire event until 2476-2286 cal BC (GrA-377323, unmodelled). This issue leads us to suggest the presence of a second burial phase after the fire in Cueva de Abauntz or, possibly, a different cultural meaning for the fire event in this case (**Figure 55**).

It is still too tentative to connect the fire events in the sepulchral cavities with the arrival of Steppe ancestry to the Iberian Peninsula but, both phenomenon dated to the 2,800 cal BC and that could be a possible cultural explanation for the closure of some funerary spaces, and the presence of more diverse provenance individuals in Cueva de Abauntz (Olalde et al., 2018). Up to this moment, it is supposed that the arrival of steppe ancestry came into Iberia from Central Europe crossing the Pyrenees (Olalde et al., 2018, 2019). Maybe Navarra was an easier way to go into Iberia. On the other hand, it is also possible to think in a safety explanations. Some researchers have suggested the association of fire with hygienic reasons (Utrilla et al. 2015). The fact that the spread of the steppe ancestry has been linked to the spread of plague in Europe (Andrades Valtueña et al., 2017) could suggest those sites as potential candidate to find *Yersinia Pestis* or another infectious pathogen.

A



B

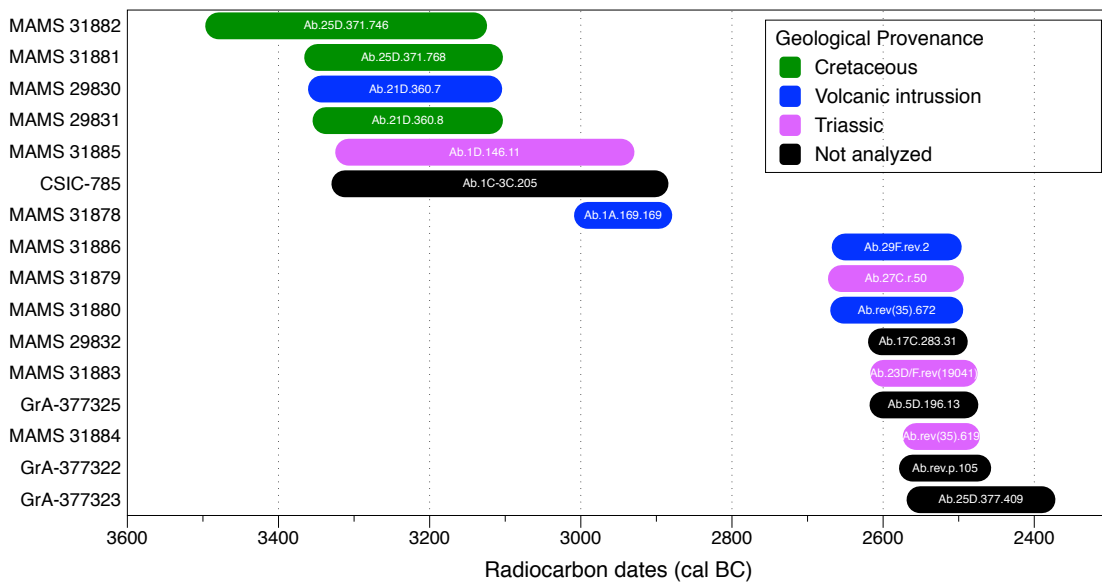


Figure 55: A) Radiocarbon 2 phases Bayesian modelling of Abauntz individuals. **B)** Provenance of the analyses individuals with direct radiocarbon date. Calibration and Bayesian model was performed with OxCal v4.2.3 using the IntCal13 calibration curve (Bronk Ramsey, 2009; Reimer et al., 2013).

11.3 Archaeological discussion of aDNA results

11.3.1 El Mirón admixture

As it is described in the ‘Genetic structure of Iberian HG’ sub-header in the publication Villalba-Mouco et al., 2019 (chapter 9.6 of the ‘Results’), the genetic ancestry of El Mirón individual is a mixture of that was previously defined as two different genetic clusters (Fu et al., 2016).

El Mirón individual is the oldest genomic data available for the Iberian Paleolithic up to date. This individual, directly dated to 18,720 cal BP, is associated with the Magdalenian technocomplex, for which it is also the oldest representative in Europe (Fu et al., 2016). This early date might suggest that Goyet-Q-2-like ancestry was present, at least in Iberia, during the preceding Solutréan period. The Solutrean technocomplex spread throughout Iberia and France during the Last Glacial Maximum (23 to 19 Ka cal BP). Inside Iberia, the transition from Upper Solutréan to the Lower Magdalenian differs in the Cantabrian when compared to the Mediterranean side of Iberia. In the Cantabrian region this shift has been termed the “de-solutreanized” transition, and occurred at the end of the Upper Solutrean (Straus, 1975). This transition ended earlier than in the Mediterranean area (Aura et al., 2012), and was followed by a stability of the lithic assemblage as in the lower Magdalenian (Utrilla, 2004). On the other hand, the Mediterranean transition from Upper Solutrean to Archaic Magdalenian was different due to the Upper Solutrean still retaining some Gravettian traits, and thus is known as the Solutreo-Gravettian. This regional difference is later homogenized during the Lower Magdalenian despite a later appearance in the Mediterranean region (Aura et al., 2012).

The genetic data from the Cantabrian region suggests that at the end of Last Glacial Maximum individuals associated with the Lower Magdalenian admixed with individuals associated with the Epigravettian assemblages from different southern *refugia*, probably the Italian or Balkan peninsulas. The longer and more archaic Solutréan traditions in the Mediterranean region, and their cultural links with the Gravettian technocomplex during the first stages, may suggest the possibility of finding relatively unmixed Goyet-Q-2-like ancestry in Mediterranean Iberia, in an older time period. Future aDNA analysis in HG from the Mediterranean side of Iberia could help us to test this hypothesis.

The fact that this admixture only appeared in the oldest and most southern Magdalenian individual from Iberia, but not in northern latitudes, suggests that the admixture event happened during the Last Glacial Maximum, when the displacements along southern latitudes were much easier than the northern ones. Moreover, the small amount of Villabruna-like ancestry in El Mirón individual would imply a limited contact. Future aDNA studies performed on HGs from different Last Glacial Maximum biogeographical *refugia* must focus on the analysis of bidirectional, or unidirectional geneflow, looking for Goyet-Q-2-like ancestry in Epigravettian individuals.

11.3.2 Aurignacian lineage survival in Magdalenian-associated individuals

The observation that Goyet Q-2-like ancestry must be older than the actual date of the current genetic type specimen, was already suggested by the genetic link with the Aurignacian-period individual Goyet Q-116-1, who shares more genetic ancestry with Magdalenian-associated individuals than Gravettian-associated individuals from Central Europe (Fu et al., 2016). From a genetic point of view, Gravettian individuals (also known as the ‘Vêstonice cluster’), show some geneflow from Eastern Europe (e.g. in the ~34,000-year-old Sunghir individuals or the ~37,000-years-old Kostenki-14 individual) (Sikora et al., 2017). This link with Eastern Europe is not present/detectable in all the Magdalenian individuals, even in the oldest individual from El Mirón (Fu et al., 2016). Up to this moment, the lack of Gravettian individuals from Western Europe does not allow us to presume genetic homogeneity along the widespread Gravettian techno-complex, despite the similarities in the lithic and artistic assemblages (Roebroeks, 1999). However, the survival of Aurignacian-like ancestry in Magdalenian individuals, such as in the *Goyet Q-2* individuals, could have been possible if a Gravettian population from western Europe that carried a different genetic makeup than that of Central Europe, had also directly drifted from Aurignacians.

11.3.3 Second arrival of Villabruna like-ancestry related to the Azilian technocomplex

The so-called Azilian industry is the dominant techno-complex in Vasco-Cantabria (Straus and González Morales 2003) and the Pre-Pyrenean region of the Iberian Peninsula during the Pleistocene-Holocene transition (Barandiarán and Cava, 1994; Martínez-Moreno and Mora, 2009), and in central/southern France (Clottes, 1979, 1983) around 14,000 cal BP. This wider

geographic region formed a natural corridor which connected Iberia and France, and where the Azilian techno-complex was shared, but was absent in the rest of the Iberian Peninsula (**Figure 56**). Traditionally, the transition to the Azilian techno-complex has been viewed as a direct result of the climatic amelioration which took place during the Bølling/Allerød warming phase (14,700 -12,700 cal BP) (Heiri et al., 2014) when hunter-gatherers broadened their subsistence spectrum, specializing in small prey hunting and combining terrestrial and aquatic resources, a trend, which then continued during the Holocene (Straus, 2015). It is also in this period that the naturalistic art paintings, which were very common in the region, disappeared, and were replaced by geometric motifs mostly found in mobile art (Sieveking, 1987). The material assemblage also presents changes with respect to the preceding Magdalenian culture. Classically, the Azilian technocomplex was defined by the presence of flat, asymmetrical harpoons, painted cobbles, thumb end-scrapers and curve backed ‘Azilian’ points. This set has been re-defined, incorporating new elements and criteria such as a generalized simplification of the knapping method combined with a microlithization/miniaturization effect, in particular of backed points and end scrapers (Alonso, 2008; Martzluff et al., 2012; Quintana and Velasco, 1994). However, in many of these Azilian sites the chronostratigraphic continuity between the Magdalenian and Azilian levels makes it difficult to establish a clear rupture between both phases (**Figure 56**).

Up to this point in time, the genomic data available for Iberian hunter-gatherers support a gradual replacement of the genomic structure present in Iberia during the Magdalenian period (represented by the El Mirón individual) in the northern areas where the Azilian spread during a later period, as shown by individuals such as Balma Guilanyà. Villabruna-like ancestry became stronger during the Mesolithic in the same area where the Azilian was spread before (La Braña 1 and Canes 1) suggesting additional hunter-gatherer flux into north/northeastern Iberia, which must have had a higher impact in this region. In contrast, Mesolithic hunter-gatherers outside of this region retain more ancestry shared with the *Goyet Q-2* cluster or have a significantly higher amount of El Mirón-like-ancestry (Chan from Galicia or Moita do Sebastião in Portugal) when modelled with El Mirón as a local source (**Figure 56**).

In this sense, the Iberian Peninsula can be considered to be a special case because Villabruna-like ancestry only had a high impact in the Cantabrian corridor, which started during the Azilian, and continued increasing during the Mesolithic. At the same time, the Mesolithic individuals outside of this region still retained the genetic signature of El Mirón. In France,

however, where the Magdalenian assemblage was also common, we observe a complete replacement of Goyet Q-2-like ancestry since the Azilian which continues with the following Epipaleolithic and Mesolithic groups.

An alternative Epipaleolithic assemblage which could also have carried Villabruna-like ancestry into Iberia was the Sauveterrian, which was common across Northern Italy and France, and had influenced the Mediterranean side of Iberia ([Roman-Monroig, 2012](#); [Soto et al., 2015](#)). This assemblage reflects the first microlithization and geometrization. That could have suggested the onset of the Geometric Mesolithic tradition unless the microlithization and geometrization process is completely interrupted by the Notch and Denticulate Mesolithic, chronologically in between both traditions, Sauveterrian and Geometric Mesolithic, in the same area (eg. [\(Lourdes Montes et al., 2016\)](#)). However, the proportion of Villabruna-like ancestry in the Mediterranean area is not as high as in the Cantabrian corridor. This suggests that, if Sauveterrian technocomplex was imported from Italy or France, they did not have a large impact on the local hunter-gatherers, or that the tradition was not directly imported by incoming people in the case of Iberia. The latter hypothesis can be tested in the Geometric Mesolithic groups because genomic data is available from both the Mediterranean (Cingle del Mas Nou and Cueva de la Cocina (merged data) plus La Carigüela), ([\(Olalde et al., 2019\)](#)) and the Atlantic region (Moita do Sebastião, this thesis). Here, the high Magdalenian component in the Geometric Mesolithic from both areas rejects the hypothesis that incoming gene-flow was associated with Geometric Mesolithic technological assemblage.

Note: In this thesis we have aimed to analyse DNA also from individuals from the Notch and Denticulate Mesolithic site of El Collado ([\(Gibaja et al., 2015\)](#)), but these did not yield sufficient DNA for downstream analyses. Obtaining data from individuals associated to this lithic assemblage would be important to confirm the continuity in the Mediterranean area from the Epipaleolithic to the Late Mesolithic.

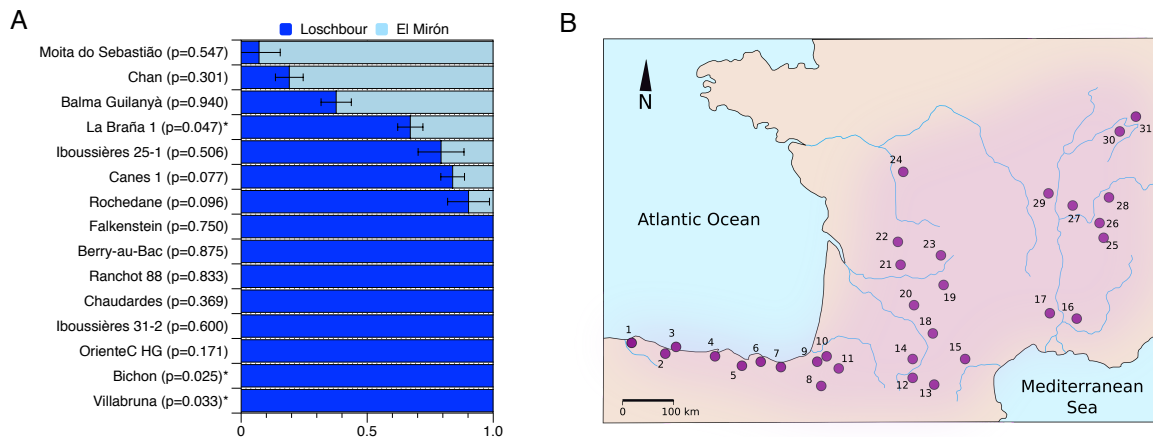


Figure 56: A) Modelling European HG as mixture of Villabruna-like and El Mirón-like ancestry using Loschbour and El Mirón as proximal sources, respectively (error bars indicate ± 1 standard error; p-values > 0.05 indicate a statistically supported model). **B)** Map showing the distribution of the main sites related to the Azilian Culture, adapted from Strauss (2015): 1. La Paloma, Cueva Oscura de Ania; 2. Los Azules; 3. La Riera; 4. El Pendo, Cueva Morin; 5. Arenaza; 6. Santimamiñe; 7. Urtiaga, Ekain, Erralla; 8. Zatoya, Abauntz; 9. Isturitz; 10. Duruthy, Dufaure; 11. Poeymau; 12. Mas d'Azil; 13. La Vache, Rhodes II; 14. La Tourasse; 15. Gazel 16. Chinchon, La Salpetriere; 17. Saut du Loup; 18. Tete du Chien; 19. Pegourie, Graves Pielago, Rascano, El Otero; 20. Borie del Rey; 21. Faurelie; 22. Pont d' Ambon; 23. Chez Jugie; 24. Bois Ragot; 25. Jean Pierre I; 26. Thoys; 27. Abri Gay; 28. Les Douattes, Blame-de-Thuy; 29. Varennes-Ies-Mâcon; 30. Rochedane; 31. Mannlefelsen.

11.3.4 Differences between Villabruna components in the Magdalenian, Azilian and Mesolithic individuals

In the ‘Genetic structure of Iberian HG’ sub-header of the publication Villalba-Mouco et al., 2019 (chapter 9.6 of the ‘Results’) we characterized the different affinities of Iberian HGs to individuals including in *Goyet Q-2* and *Villabruna* clusters. Next aDNA studies could be addressed to define better the *Villabruna* component detected in the 19,000 year-old El Mirón individual is different from the Villabruna-like component that spread from 14,000 years in Europe. This can be shown by comparing the Villabruna-like ancestry in the oldest El Mirón individual and the latest more recent Iberian HGs with the following test: $f_4(\text{Iberian HG}, \text{GoyetQ2}; \text{WHG}, \text{Mbuti})$, with Loschbour, Koros EN-HG, OrienteC and Villabruna as WHG.

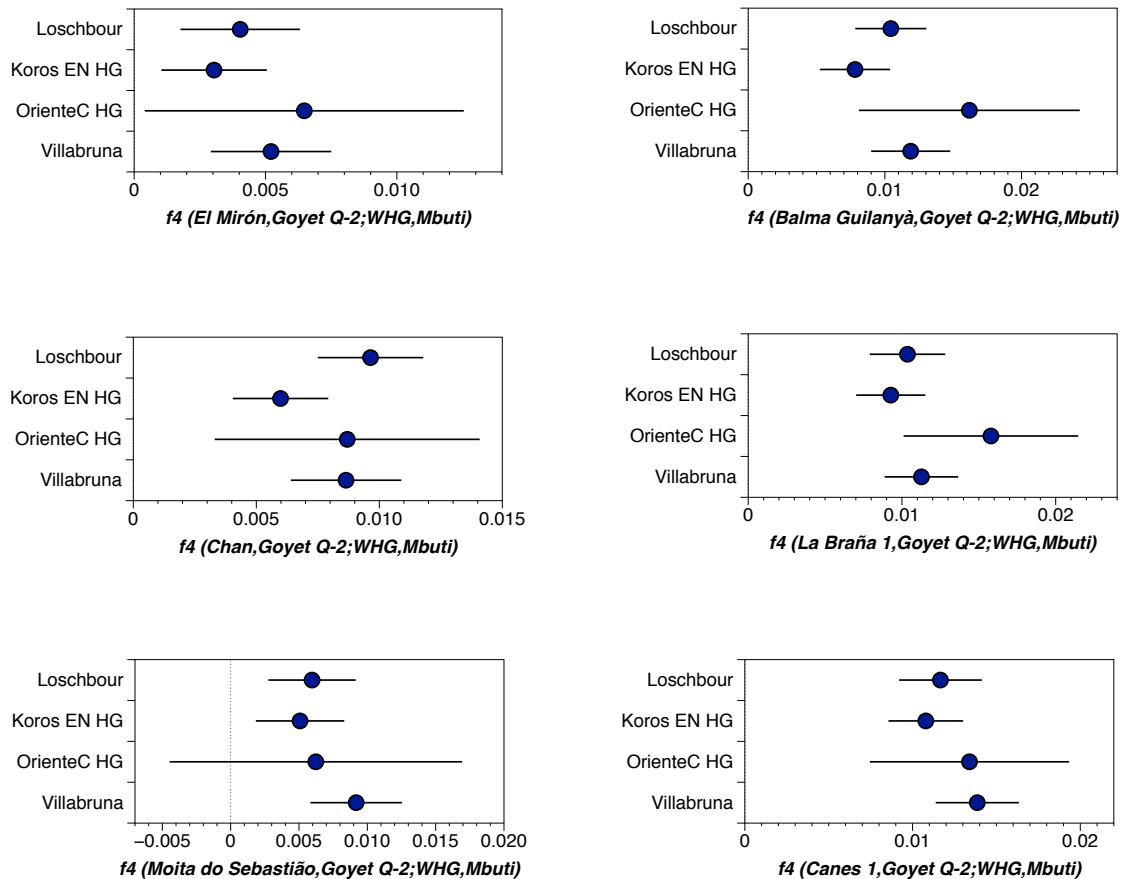


Figure 57: F_4 -statistics showing the affinities of Iberian HG to different WHGs, highlighting the presence of different WHG components (error bars indicate ± 3 standard error).

With this test we observe that the Villabruna-like ancestry is not the same in all Iberian hunter-gatherers. In the case of Balma Guilanyà and La Braña 1, they show more attraction to OrienteC than the others, despite this difference is not significant due to the bad coverage of the last individual translated into large error bars. Another interesting point would be the lower genetic affinity of Chan to Koros EN-HG comparing with the other tested HGs. This fact could be related to the issue of a higher Eastern HG component present in Koros EN-HG (Mathieson et al., 2018) that would be absent in Chan individual, probably due to their most-western geographical location. More analysis would be needed to find differential Villabruna-like ancestry in the Iberian HGs along different time periods and/or geographical regions. (Figure 57).

11.3.5 The Last Iberian HGs Canes 1 and La Braña 1 and their Eastern HG ancestry

The Mesolithic genetic signature was previously described as a cline from Western HG (WHG) to Eastern HG (EHG) (Mathieson et al., 2018). Based on this finding and the special HG genetic structure in Iberia, we wanted to explore further if we can also see an increase of EHG affinity in the Iberian HGs, that could correlate with a geographical and/or chronological distribution. Performing the test $f_4(\text{Iberian HG}, \text{Goyet Q-2}; \text{AG3}, \text{Mbuti})$ we observed that the latest hunter-gatherers (La Braña 1 and Los Canes 1, red symbols in **Figure 58**) carried a higher amount of eastern hunter-gatherer component that could be interpreted as a signal of the latest entrance of new hunter-gatherers into the Peninsula. If we consider the radiocarbon dates of the latest hunter-gatherers, it appears as if this exogenous pulse could have been driven by an early presence of farmers in the nearby territories, such as the *Impressa* associated-individuals in southeastern France (Perrin et al., 2018).

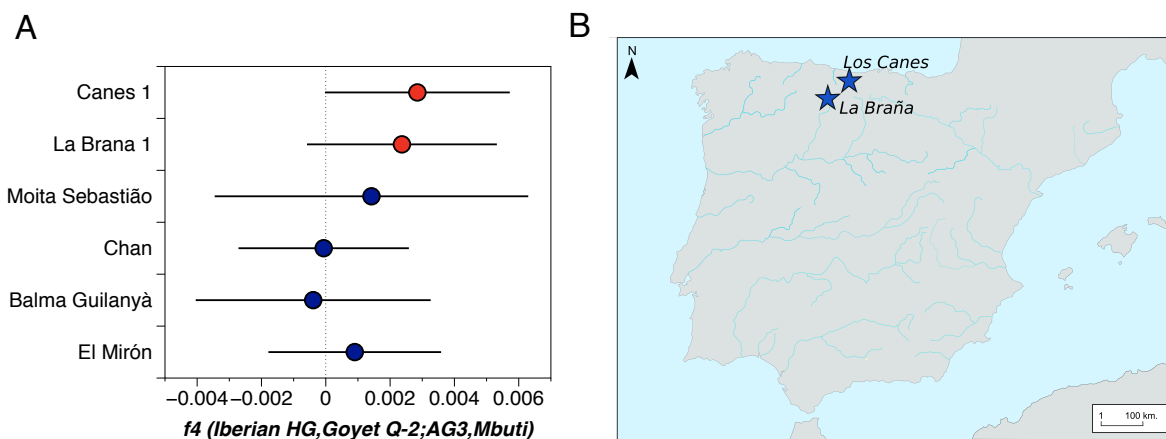


Figure 58: **A)** f_4 -statistics that highlight the extra EHG ancestry (more positive values although they are not significant) observed in the late Iberian HGs La Braña 1 and Canes 1 (red symbols, error bars indicate ± 3 standard error). **B)** Geographical location of La Braña and Los Canes.

However, to show strong evidence for this connection, we would need to increase the number of data points from Late Mesolithic individuals from south-eastern France. From an archaeological point of view, the individuals from Los Canes 1 that are associated to the geometric Mesolithic techno-complex were not as common in the Cantabrian region as in the Mediterranean, including late Castelnovian individuals from France (Perrin et al. 2009). Previous studies explained the difference between Los Canes and other Mesolithic hunter-gatherers from the same regions as a possible movement from the Iberian Central Plateau to the

Cantabrian region for Los Canes (Arias, 2007). However, the subtle signal of EHG ancestry makes it more plausible that the latest hunter-gatherer groups came from outside of Iberia, e.g. from France where the presence of geometric microliths are strongly confirmed in the latest hunter-gatherers (Perrin et al. 2009), or even further east (Figure 58).

11.3.6 No African connections during Mesolithic times

The Iberian Peninsula, in the southwestern-most part of Europe, has been suggested as the connecting bridge between Europe and the African continent. The oldest evidence for such potential connections dates back to the Early Upper Paleolithic and is attributed to the African Aurignacian or Lower Capsian (Obermaier, 1925). This potential connection has been suggested to have also persisted in later periods, such as during the Epipaleolithic microlithic bladelet technocomplex (Epipaleolítico Laminar in Iberia), the Epipaleolithic microlithic bladelet Iberomaurusian technocomplex (Barton et al., 2013), as well as during the Geometric Mesolithic (Perrin et al. 2009).

The main characteristic technological change during the Late Mesolithic is the shift to the Blade and Trapeze industry, which is commonly grouped as Mesolithic Geometric (Trapezes and Triangles phases) in Iberia. Although the distribution of this phenomenon is widespread along eastern, western and north Africa, its origin is still debated (Gronenborn, 2017). Based on a chronological gradient, an African origin was suggested, from where it spread into Europe through the south of Italy (Sicily), and from where it followed a Mediterranean expansion into Iberia (Perrin et al. 2009). Other authors posit Crimea as the place of origin for the Blade and Trapeze industries (Biagi 2016). Inside Iberia this cultural phenomenon is distributed along both the Mediterranean (Puchol et al., 2009) and Atlantic (Bicho et al., 2017) coastlines. This contrasts with the situation in northern Iberia where Mesolithic Geometric flint tools are found in significantly lower numbers (Arias and Fano 2009), with the exception of the Ebro Valley, a natural corridor between the Mediterranean region and Cantabria (Utrilla et al. 2009). Interestingly, this is the geographic region where, and the time period and when, the Villabruna/Loschbour-related ancestry increased, as shown in individuals from La Braña 1 and Canes 1, in contrast to the individual Moita do Sebastião from Portugal where the Geometric Mesolithic was predominant (Bicho et al., 2013). Importantly, our genomic results from Moita do Sebastião, attributed to the Geometric Mesolithic, show a strong affinity with El Mirón, but lack any genetic evidence in support of the hypothesis of an African origin for the Mesolithic

Geometric (**Figure 59**). Here, f_4 -statistics of the form $f_4(\text{Moita do Sebastião, WHG; Taforalt, Mbuti})$ in **Figure 59** indicate no extra genetic affinity of Moita do Sebastião to Pleistocene Iberomaurusian HG from Taforalt (North Africa) ([van de Loosdrecht et al., 2018](#)). Taforalt individuals are considered a good proxy to test the African-Iberian connections due to the genetic continuity shown in North Africa from the Late Pleistocene to the Holocene (Early Neolithic), despite their chronologically older age ([Fregel et al., 2018](#)). The observation that the genomic structure at the Atlantic coast has not significantly changed since the Magdalenian currently supports the idea of cultural diffusion or analogous technological changes rather than direct gene flow. However, more data, especially from the Mediterranean Mesolithic Geometric individuals, is needed to address this question in more detail.

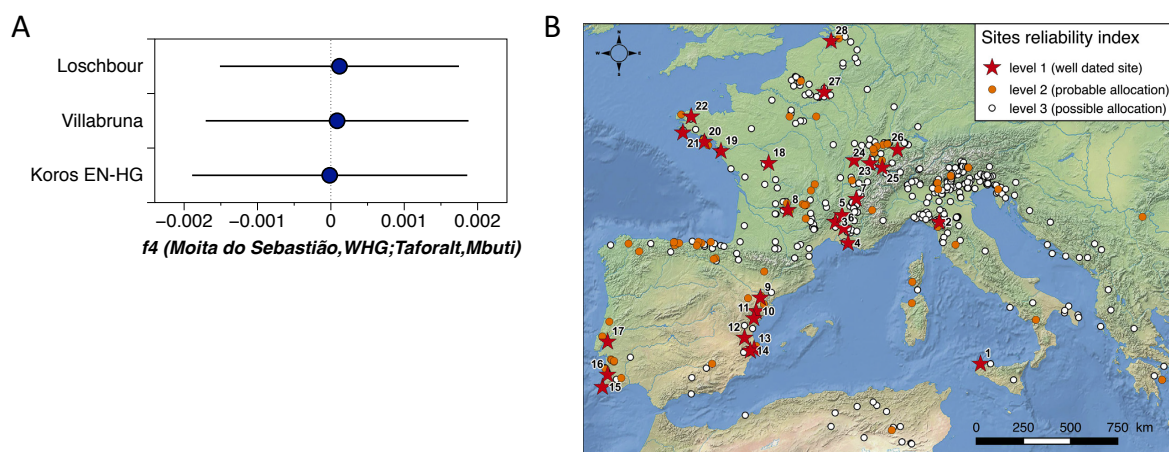


Figure 59: A) f_4 -statistics indicating no affinity between Geometric Mesolithic Moita do Sebastião from Portugal and Iberomaurusian HG from Taforalt, Morocco, North Africa (error bars indicate ± 3 standard error). **B)** Geographic dispersion of Geometric Mesolithic sites, from Marchand and Perrin (2010).

11.3.7 The genetic legacy of hunter-gatherers in Iberian farmers

Previous studies have shown that it is possible to distinguish Neolithic groups by their different admixture proportions from temporally close autochthonous hunter-gatherers, assuming that these proportions reflect one, or potentially more, local admixture events along the expansion route ([Lipson et al., 2017](#)). In the ‘Dual HG genetic legacy’ sub-header of the publication [Villalba-Mouco et al., 2019](#) (chapter 9.6 of the ‘Results’ chapter), we showed that we were able to distinguish two hunter-gatherer lineages in the Iberian Early and Middle Neolithic

individuals. The Villalbruna-like ancestry is present in all Early Neolithic individuals across western Europe, but the additional presence of Goyet-Q-2-like ancestry appears to be specific for some Iberian Early Neolithic individuals. The individuals with highest amounts of Goyet-Q-2-like ancestry were located in southern Iberia (Andalucía; Cueva del Toro and Cueva de los Murciélagos sites), and were associated with the Almagra cultural complex. Conversely, Early Neolithic individuals from northern Peninsula showed more Villalbruna-like ancestry, and little to no Goyet-Q-2-like ancestry. This distribution reflects the genetic structure of the previous, local hunter-gatherers with less Villalbruna-like ancestry in southern areas, or the arrival of early farmers with more influence Villalbruna-like ancestry in northern Iberia, or potentially a mix of both. The location of the earliest evidence of *Impressa*-like pottery in the southern regions, such as modern-day Alicante (Bernabeu et al., 2009) allows me to conclude that the idea that the Early Neolithic also reflects the genetic structure of preceding hunter-gatherers appears more plausible (**Figure 60**).

During the Middle Neolithic the HG signal started to become more homogenized, however the Iberian sites continued having higher Goyet-2 like ancestry. Olalde et al. (2018) noted the subtle differences between WHG individuals and used the proportion of ancestry from the Iberian hunter-gatherer individual La Braña 1 found in Neolithic Iberian groups to trace the movement of Neolithic groups from southwestern Europe, to Britain along the Atlantic coast. In fact, Olalde and colleagues (Olalde et al., 2018) reported an elevated signal of La Braña 1 ancestry in Neolithic individuals from Wales and England (using KO1 HG from Hungary and Anatolian Neolithic as the other two sources) and thus argued for an Iberian contribution to the Neolithic populations in Britain.

In the ‘Dual HG genetic legacy’ sub-header of the publication Villalba-Mouco et al., 2019 (chapter 9.6 of the ‘results’ chapter), we used this rationale and replicated these findings by using similar sources (El Mirón instead of Goyet Q-2), showing that these results are sensitive to the source populations used (Supplementary Data S1J of Villalba-Mouco et al., 2019). In fact, our models with Goyet Q-2 as an ultimate source highlight not only the admixed nature of La Braña 1 and El Mirón. Moreover, the Goyet Q-2-like ancestry in Middle Neolithic individuals outside of Iberia hint at Iberia as one possible but not the exclusive source of the Neolithic in Britain (Villalba-Mouco et al., 2019). Further sampling from regions in modern-day France, the Netherlands, Belgium, Luxembourg, and Germany is needed to answer this question.

11.3.8 LBK and Cardial-related routes of the Neolithic expansion

The relatively rapid expansion of Early Neolithic individuals associated with farming practices from western Anatolia across Europe resulted in a relatively low genetic variability in the reported European Neolithic genomes, who are closely related to a Western Anatolian source population (Mathieson et al., 2015). This lack of genetic differentiation makes it difficult to distinguish between the Mediterranean and Danubian expansion route, as suggested by the archaeological record (Manning et al., 2014; Perrin et al., 2018). Moreover, a direct comparison is also not possible because the tests in the way $f_4(\text{Cardial}, \text{LBK}; \text{test}, \text{Mbuti})$ are biased by the amount of HG ancestry. The Iberian Early Neolithic individuals show, in general, more hunter-gatherer ancestry than other Early Neolithic Starçevo or LBK groups (Mathieson et al., 2018; Olalde et al., 2018; Vanessa Villalba-Mouco et al., 2019).

Archaeological research suggests that the maritime route associated with *Impressa* and Cardial ware was faster, and this was the first to reach Iberia (Martins et al., 2015). For Iberia itself, it is still not clear whether the Danubian-route reached the Peninsula slightly later in the northern parts, where it could be attributed to incised-impressed groups (also called Epicardial), or whether those groups only represent a derived form/phase of the Cardial horizon from when it expanded from coastal to inland areas (Isern et al., 2017; Zilhão, 2001).

From a genetic point of view, there is not enough genetic differentiation among early farmers in Iberia to the limits of our current resolution. However, it is worth noting that early farmer individuals associated with earlier phases of Early Neolithic show a higher proportion of HG admixture (Toro EN, Murciélagos EN, Chaves EN, Trocs EN and Bonica EN vs. Portalon EN, Fuentecelada EN and Pancorbo EN) (**Figure 60**). However, this observation might not be directly related to any cultural complex, and is potentially only the signal in the first arriving/pioneering farmers that were able to interact more with local hunter-gatherers. The first group composed by the more ancient Early Neolithic individuals show more Goyet Q-2-like ancestry than the other and individuals. Individuals from the La Almagra context (Toro EN and Murciélagos EN) show a more elevated proportion Goyet Q-2-like ancestry than the rest of the Early Neolithic individuals which can suggest a higher admixture with local hunter-gatherers. However, the early Cardial individual from Cova Bonica, Vallirana (Barcelona), does not show Goyet Q-2-like ancestry. The Late Mesolithic gap in the Catalonia region could explain the lower amount of Goyet Q-2-like ancestry in Cardial ware individuals from the same region (Morales and Oms, 2012). On the other hand, individuals from the Ebro-Valley, where late

Mesolithic was attested and where Cueva de Chaves (Cardial-associated individuals), show higher amount of hunter-gatherer ancestry, including Goyet Q-2-like ancestry. (**Figure 61**).

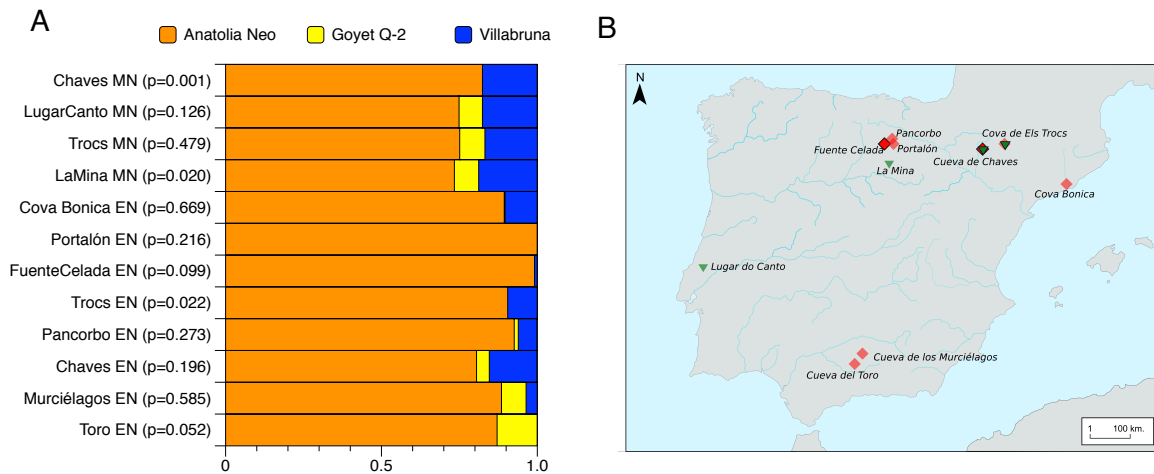


Figure 60: A) Modelling Iberian Early and Middle Neolithic as mixture of Villabruna-like Goyet Q-2-like and Anatolia Neolithic-like ancestries (p-values > 0.05 indicate a statistically supported model). **B)** Geographic dispersion of Early and Middle Neolithic sites in Iberia.

On a larger scale, these subtle differences in the amount of hunter-gatherer ancestry also render a direct comparison between Cardial and LBK individuals difficult. All LBK related individuals analysed so far indicate a lower proportion of hunter-gatherer ancestry and due to this, all of the individuals with higher amounts of hunter-gatherer ancestry will automatically show more genetic affinity to Iberian Early Neolithic, directly related to the Mediterranean/Cardial route. One possibility to test whether the Iberian individuals share more ancestry with either of the cultural groups is to explore the Middle Neolithic populations for which the amount of hunter-gatherer ancestry is higher than it is in the Early Neolithic populations, which increases the power of resolution. In this way, we observe that England Neolithic share more genetic ancestry with LBK-like Neolithic groups than Middle Neolithic populations from Portugal. However, this attraction is not significant if we perform the same test with an Iberian Cardial site instead of LBK individuals. The meaning of these differences could be explained if Portuguese Neolithic only received Cardial contribution (Mediterranean route) and Britain Neolithic a mix of both (LBK and Cardial, ergo Central European and Mediterranean routes). On the other hand, this result can also be explained if the Iberian Cardial Neolithic (represented here by Chaves EN and Bonica EN) already carried a mix of Central Europe and Mediterranean mix of ancestries. The analysis of new Cardial individuals from southern regions of Iberian and new

Middle Neolithic Iberian populations would be needed to confirm if this result can be directly related to different Neolithic expansion routes (**Figure 61**).

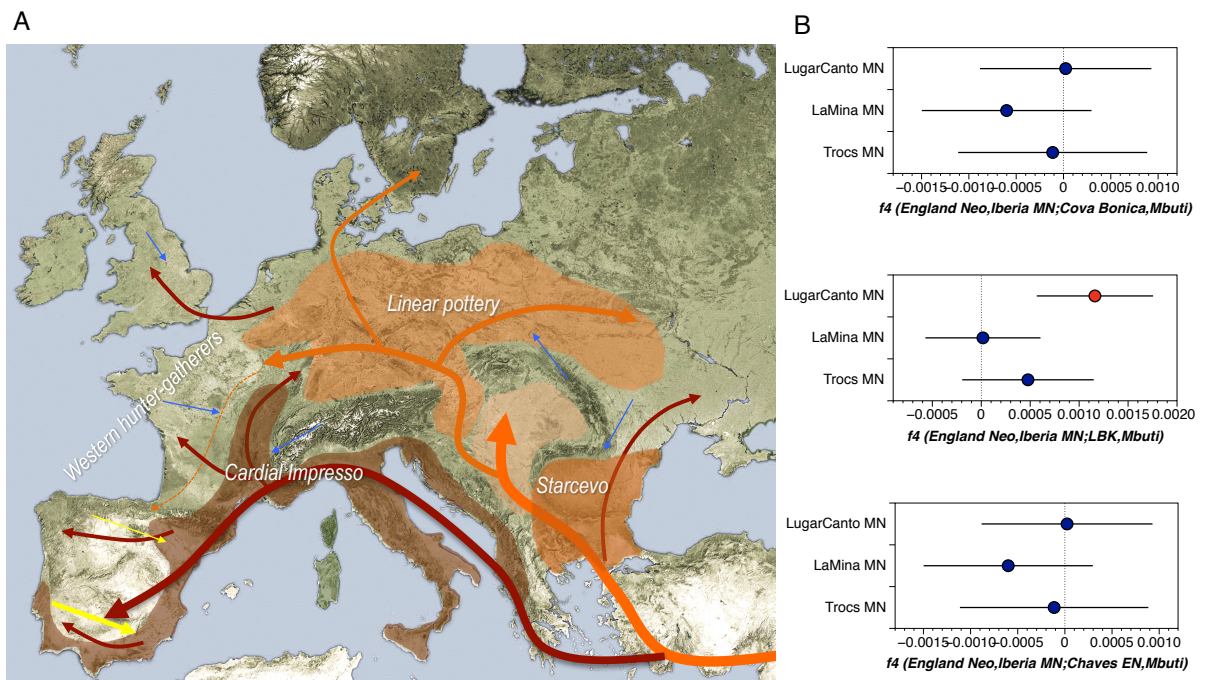


Figure 61: A) European map with the Early Neolithic expansion from Western Anatolia, modified from Haak et al. 2015. **B)** f4-statistics indicating a significant attraction of LBK for England Neolithic compared to Portuguese Middle Neolithic (error bars indicate ± 3 standard error).

Despite this work only includes genomic data from ten new individuals from Iberia ranging from ~12,000 to ~5000 years old, we have been able to describe a previously unknown genetic structure in the Iberian HGs. We have shown that some of the Iberian HG still retain a higher Magdalenian-like ancestry, that was supposed to be replaced by Villabruna-like ancestry after 14,000 years ago in Western Europe. As a result, the two ancestral lineages survived in the Iberian Peninsula in admixed form conforming a new genetic cline.

The survival of these two genetic lineages has been attested in the Early and Middle Neolithic populations in the same region. That has make possible to strongly suggest the admixture among HG and Early Farmers locally. A more detailed study encompassing a wider area and more Early and Middle Neolithic individuals will be needed to study geographical pattern where the admixture happened more frequently as well as the potential origins of different Neolithic groups characterized by stylistic wares.

12 CONCLUSIONS AND FUTURE PERSPECTIVES

The objective of this thesis was to contribute with the understanding of the Mesolithic-Neolithic transition and its evolution in Iberia using a direct biomolecular approach on human remains. The data obtained during four years of research has been useful to infer the demographic change between the Iberian HG and the first farmers as well as infer information about the interaction among these two different population groups. To reach these objectives we have used the most advanced methods applied to paleogenomic research nowadays, like NGS and the capture protocol of 1240K SNPs along the generated human genomes. Thanks to these methods we have been able to recovered genome-wide data from eleven individuals who range from ~ 13000 cal BP to 5000 cal BP.

Moreover, we have inferred indirect biological changes related to this population shift, like the subsistence strategies, the beginning husbandry management and the mobility patterns among the Neolithic groups. To reach these objectives we have produced more than 200 carbon ($\delta^{13}\text{C}$) and nitrogen ($\delta^{15}\text{N}$) isotopic collagen values (measured in duplicated), increasing considerably the dataset available for the Iberian Peninsula at this period, and even more the isotopic collagen data available on Early Neolithic fauna remains. This analysis has allowed us to suggest a higher importance on husbandry than agriculture, although the domestic species did not show a special feeding compared to the wild ones. Besides, the big data set available now for humans from the Late Neolithic and the Chalcolithic period allows to test the presence of two different eco-geographical regions with significant statistics robustness in isotopic values.

Apart from that, we have generated the first big published data set of Sr values of human enamel values (more than 80 samples). This is because of the absence of any dedicated laboratory where perform this type of analysis in Iberia make this analysis underestimated compared with other countries. Thus, we were also able to create a preliminary Sr bioavailable map of the Prepyrenean landscape with more than 100 samples which for sure will be useful for many future researchs. The use of Sr with the radiocarbon dates has allowed us to study in detail the collective burial phenomenon that appear in the latest moments of the Middle Neolithic and spans up to the beginning of the Bronze Age.

To sum up, these are the specific important points of the conclusions and the future perspectives to be addressed to each of them:

1. $\delta^{13}\text{C}$ and $\delta^{15}\text{N}$ collagen isotopic values are good estimators of study the husbandry practices when the entire settlement is available.

The isotopic study of Cueva de Chaves represents one of the few Early Neolithic isotope analysis studies carried out on the Iberian Peninsula where humans and a large set of fauna coming from the same chrono-cultural context have been analysed together. While the number of domestic animal remains reflects the importance of animal husbandry at inland early farming communities, animal dietary strategies show a basic husbandry management. Domestic and wild species showed similar values, suggesting the use of common resources or areas for grazing. Even the domestic pig showed an herbivorous diet, ruling out a human leftover feeding. The human isotopic dietary study shows a high animal protein intake by all individuals. This high meat consumption would be related to the existence of a specialized animal husbandry management community in which agriculture was not intensively developed.

Future work can be addressed to answer some specific questions where the bulk collagen analysis does not have enough resolution. For example, it would be important to address a serial isotopic analysis in the pig dentine (carbon and nitrogen analysis) in pigs in order to prove that there is not a fattening moment in the last stages of their life where they potentially can show a shift to the more omnivorous diet. Additionally, the isotopic analysis of herbivore enamel (e.g. oxygen, strontium and carbon) would be useful to complete rule out the transhumance activities in domestic species.

2. $\delta^{13}\text{C}$ and $\delta^{15}\text{N}$ collagen isotopic values slightly different in individual 84C from Cueva de Chaves

The big animal dataset analyzed for Early Neolithic of Cueva de Chaves allowed us to confirm a high animal protein intake by all individuals. This high meat consumption would be related to the existence of a specialized animal husbandry management community in which agriculture was not intensively developed. Specially, the values

from the individual $\delta^{13}\text{C}$ might reflect a slight isotopic signature of marine/estuarine or dairy protein intake at some point of the individual's life.

The analysis of carbon and nitrogen on specific aminoacids could help us to distinguish among this type of resources. Moreover, the enamel Sr values of this specific individual might be useful to determinate his provenance.

3. There is an “homogeneous” overall human diet based on C_3 terrestrial resources among the entire Iberian Peninsula during the Late Neolithic and Chalcolithic.

The isotopic dietary approach for the individuals analysed from the Late Neolithic-Chalcolithic period shows a diet based on C_3 terrestrial resources, common for the whole Iberian Peninsula during this period. We have proposed the consolidated economy based on agriculture and livestock as the reason of this homogeneity. But, we need to take into consideration that the limit of the resolution using carbon and nitrogen stable isotope from the bulk collagen could be masking potential differences on human diet inside Iberia.

In this sense, it would be important to always combine the human isotopic analysis with a big set of faunal remains recovered from the same context (not all the published sites have including the herbivore baseline), and also combine with other methods like proteomics and metagenomics which have more resolution and determine the species and product consumed even the latter only shows the short-term food consumption (latest food remains trapped in dental calculus).

4. There are two main eco-geographical regions in the Iberian Peninsula which show significant different $\delta^{13}\text{C}$ values.

The environmental influenced on isotope values has been tested in the human dataset available for the Iberian Late Neolithic-Chalcolithic. Human and fauna $\delta^{13}\text{C}$ values show significant differences between two areas which correlate with geography of the Peninsula, the Mediterranean-influence and the Atlantic-influence areas. The fact that we find the same isotopic behavior in humans and fauna only means that the human $\delta^{13}\text{C}$ values are also influenced by environmental factors. This re-opens again the

discussion about the use of, at least $\delta^{13}\text{C}$ isotopic bulk collagen value, as a good estimator of diet.

Future work should be addressed to find which are the specific environmental factors in these two areas which have more influence in the $\delta^{13}\text{C}$ (light hours, rainfall, temperature...). As there not as specific information for all these factors in the paleoenvironmental record, it would probably useful to measure contemporaneous values (e.g. wild fauna) from both regions. Moreover, it would be interesting to test if the variable “time” has as strong influence as the variable “eco-geographical region”. That means if the different samples from same time period are still showing significant differences between these two eco-geographical regions. As a future work, we are planning to test for differences using also the dataset available from other chronologies.

- 5. The Ebro basin is not the optimal area to track human displacements in life using strontium isotopes because its geology shows an overlap in the Sr values but contrary, good to determine non-locals with sureness.**

The studied landscape of the Ebro Basin is highly dominated by different Paleogene and Miocene deposits. We have detected many overlapping Sr bioavailable values among the different Paleogene and Miocene deposits and even in the Cretaceous ones. That fact can be masking more non-local people who could come from different areas along the Ebro basin. But on the other hand, if the Sr values exceed the Cretaceous values, we can assume the non-local rank confidentially.

In this point, we don't think that including more sampling Paleogene, Miocene or Cretaceous areas or increasing the sample size on every area (we already have 70 samples for the middle Ebro Basin) is going to improve the resolution.

- 6. More ‘non-local’ individuals were found at the end of the funerary use of sepulchral caves, which proves that combining Sr and the direct radiocarbon date is a powerful method that should be always used together.**

The further location of landscapes with higher Sr values makes it easier to detect “non-local” individuals with certain assurance. The clear non-local individuals from San Juan

de Loarre directly dated from the latest moments of the funerary use of the cave. This also happens in Abauntz, where we found a local signal for the first humans buried in pit structures and then a higher mobility in the second burial phase.

We think that this is an interesting methodology to study the collective burials from a different perspective, and many other burial cavities (and also megalithic burials) could be studied.

7. There is a unique genetic structure in the Iberian HG

This genetic structure results from admixture of individuals related to the GoyetQ-2 and Villabruna clusters. This suggests a survival of two lineages of Late Pleistocene ancestry in Holocene western Europe, in particular the Iberian Peninsula, whereas HG ancestry in most other regions was largely replaced by Villabruna-like ancestry. That could be possible due to geographical location of the Iberian Peninsula and the role as a biogeographical *refugium* for Pleistocene HG.

8. The oldest representant of the Magdalenian-ancestry, the individual from El Mirón, is already an admixture of Goyet Q-2 and Villabruna-like ancestries.

The 18700 years-old El Mirón individual is the oldest representative of this mixed ancestry. The timing of this admixture suggests an early connection (*terminus ante quem*) between putative ancestries from different LGM refugia. It is possible that Goyet Q-2 ancestry could have existed in Iberia in unadmixed form, where it was complemented by Villabruna ancestry as early as 18,700 years ago. Alternatively, both Magdalenian-associated Goyet Q-2 and Villabruna ancestries originated in regions outside Iberia and arrived in Iberia independently, where both lineages admixed, or had already existed in admixed form outside Iberia.

9. The additional contribution of Villabruna-like ancestry correlates well with the Azilian technocomplex in the Cantabrian region. During the Mesolithic times, the same region received new HGs with more EHG ancestry.

We notice an additional contribution of Villabruna-like ancestry in the 12,000-year-old Balma Guilanyà individual from northeastern Iberia. The Villabruna-like ancestry becomes even stronger during the Mesolithic in the Cantabrian region (La Braña 1 and Canes 1), suggesting extra HG flux into north/northeastern Iberia, which must have had a higher impact in this region. This extra HG flux which already carries EHG ancestry could be created by the pressure of *Impressa*-Neolithic groups from the French territory.

10. There is no correlation of Mesolithic Geometric techno-complex and a change in the genomic makeup in the Iberian Peninsula.

Our individual associated to the Mesolithic Geometric techno-complex from Moita do Sebastião shows a similar genetic ancestry to El Mirón and no African ancestry was found in her genome. The fact that the genomic structure at the Atlantic coast has not significantly changed since the Magdalenian currently supports the idea of cultural diffusion or analogous technological changes rather than a direct gene-flow for the spread of Mesolithic Geometric techno-complex.

11. There was a local admixture between HG and Early farmer with a higher impact in Southern Mediterranean areas, in individuals related to the Almagra complex.

The different genetic structure resulted from admixture of the two hunter-gatherer lineages (Goyet Q-2 and Villabruna) was also found in Iberian Early Neolithic individuals. The individuals with higher amount of Goyet Q-2-like ancestry were located in Southern Iberia (Andalucía; Cueva del Toro and Cueva de los Murciélagos sites), and they were associated to the Almagra cultural complex. During the Middle Neolithic times this signal start to be more homogenized but the Iberian sites continue having the higher Goyet-2-like ancestry.

The genomic analysis is the most powerful tool to approach the evolutionary history of the populations and no direct source populations are always needed to infer changes in the genetic ancestries. However, it would be interesting to continue exploring this time transect in Iberia including the analysis of more individuals. For example, it would be really interesting to analyse older individuals than El Mirón, from different regions of Iberia, to test if the unadmixed

Magdalenian ancestry there was also present in the Iberia Peninsula. Another interesting point would be to study the Mesolithic and Neolithic connections with the neighbouring French territory and include more middle Neolithic samples that are underrepresented in many studies and they can be the way to test for the different expansion routes of the Neolithic due to this high and equivalent proportion of HG ancestry in different territories.

13 BIBLIOGRAPHY

- Åberg, G., Fosse, G., & Stray, H. (1998). Man, nutrition and mobility: A comparison of teeth and bone from the Medieval era and the present from Pb and Sr isotopes. *Science of The Total Environment*, 224(1), 109–119. [https://doi.org/https://doi.org/10.1016/S0048-9697\(98\)00347-7](https://doi.org/https://doi.org/10.1016/S0048-9697(98)00347-7)
- Adler, C. J., Haak, W., Donlon, D., & Cooper, A. (2011). Survival and recovery of DNA from ancient teeth and bones. *Journal of Archaeological Science*, 38(5), 956–964. <https://doi.org/https://doi.org/10.1016/j.jas.2010.11.010>
- Alcolea, M. (2017). *Paisaje vegetal y gestión de los recursos leñosos durante la transición Epipaleolítico-Neolítico en el valle del Ebro. Aportaciones desde la antracología* (University, doctoral thesis).
- Alcolea, M., Utrilla, P., Piqué, R., Laborda, R., & Mazo, C. (2017). Fuel and acorns: Early Neolithic plant use from Cueva de Chaves (NE Spain). *Quaternary International*, 457, 228–239. <https://doi.org/https://doi.org/10.1016/j.quaint.2016.10.019>
- Alexander Bentley, R. (2006). Strontium Isotopes from the Earth to the Archaeological Skeleton: A Review. *Journal of Archaeological Method and Theory*, 13(3), 135–187. <https://doi.org/10.1007/s10816-006-9009-x>
- Allentoft, M. E., Sikora, M., Sjögren, K.-G., Rasmussen, S., Rasmussen, M., Stenderup, J., ... Willerslev, E. (2015). Population genomics of Bronze Age Eurasia. *Nature*, 522, 167–172. Retrieved from <http://dx.doi.org/10.1038/nature14507>
- Alonso, D. Á. (2008). La cronología del tránsito Magdalenense/Aziliense en la región cantábrica/The chronology of the Magdalenian/Azilian transition in the Cantabrian region. *Complutum*, 19(1), 67–78.
- Alt, K. W., Zesch, S., Garrido-Pena, R., Knipper, C., Szécsényi-Nagy, A., Roth, C., ... Rojo-Guerra, M. A. (2016). A Community in Life and Death: The Late Neolithic Megalithic Tomb at Alto de Reinoso (Burgos, Spain). *PLOS ONE*, 11(1), e0146176. Retrieved from <https://doi.org/10.1371/journal.pone.0146176>
- Álvarez-Fernández, E. (2011). Humans and marine resource interaction reappraised: Archaeofauna remains during the late Pleistocene and Holocene in Cantabrian Spain. *Journal of Anthropological Archaeology*, 30(3), 327–343. <https://doi.org/https://doi.org/10.1016/j.jaa.2011.05.005>
- Ambrose, S. H. (1990). Preparation and characterization of bone and tooth collagen for isotopic analysis. *Journal of Archaeological Science*, 17(4), 431–451. [https://doi.org/https://doi.org/10.1016/0305-4403\(90\)90007-R](https://doi.org/https://doi.org/10.1016/0305-4403(90)90007-R)
- Ambrose, S. H. (1991). Effects of diet, climate and physiology on nitrogen isotope abundances in terrestrial foodwebs. *Journal of Archaeological Science*, 18(3), 293–317. [https://doi.org/https://doi.org/10.1016/0305-4403\(91\)90067-Y](https://doi.org/https://doi.org/10.1016/0305-4403(91)90067-Y)
- Ambrose, S. H. (1993). Isotopic analysis of paleodiet: methodological and interpretive considerations. *Investigations of Ancient Human Tissue: Chemical Analysis in Anthropology*, Gordon and Breach Science publishers, New York, pp. 59–130.
- Ambrose, S. H., & Norr, L. (1993). Experimental Evidence for the Relationship of the Carbon Isotope Ratios of Whole Diet and Dietary Protein to Those of Bone Collagen and Carbonate BT - Prehistoric Human Bone: Archaeology at the Molecular Level. In J. B. Lambert & G. Grupe (Eds.) (pp. 1–37). Berlin, Heidelberg: Springer Berlin Heidelberg. https://doi.org/10.1007/978-3-662-02894-0_1
- Ammerman, A. J. (1973). A population model for the diffusion of early farming in Europe. In: Renfrew, C. (Ed.), *The Explanation of Culture Change: Models in Prehistory.*, Duckworth, London, pp. 343–357.
- Ammerman, A. J., & Cavalli-Sforza, L. L. (1971). Measuring the rate of spread of early

- farming in Europe. *Man* 6, 674–688.
- Ammerman, A. J., & Cavalli-Sforza, L. L. (2014). *The Neolithic transition and the genetics of populations in Europe* (Vol. 836). Princeton University Press.
- Andrades Valtueña, A., Mittnik, A., Key, F. M., Haak, W., Allm e, R., Belinskij, A., ... Krause, J. (2017). The Stone Age Plague and Its Persistence in Eurasia. *Current Biology*, 27(23), 3683–3691.e8. <https://doi.org/https://doi.org/10.1016/j.cub.2017.10.025>
- Andr s Rup rez, M. (1998). Colectivismo funerario neoneol tico. Aproximaci n metodol gica sobre datos de la cuenca alta y media del Ebro. *Zaragoza: Instituci n Fernando El Cat lico*.
- Andrews, R. M., Kubacka, I., Chinnery, P. F., Lightowlers, R. N., Turnbull, D. M., & Howell, N. (1999). Reanalysis and revision of the Cambridge reference sequence for human mitochondrial DNA. *Nature Genetics*, 23(2), 147. <https://doi.org/10.1038/13779>
- Antol n, F. (2016). *Local, intensive and diverse?: Early farmers and plant economy in the North-East of the Iberian Peninsula (5500-2300 cal BC)* (Vol. 2). Barkhuis publishing (Groningen).
- Antol n, F., & Bux , R. (2000). L'exploraci  de les plantes al jaciment de la Draga: contribuci  a la hist ria de l'agricultura i de l'alimentaci  vegetal del neol tic a Catalunya. *El Poblat Lacustre Del Neol tic Antic de La Draga: Excavacions de 200 - 2005*, Monografias del CASC, Girona MAC-CASC, pp 147–174.
- Arias, P. (2005). Determinaciones de is topos estables en restos humanos de la regi n Cant brica: aportaci n al estudio de la dieta de las poblaciones del Mesol tico y el Neol tico. *Munibe Antropologia-Arkeologia*, (57), 359–374.
- Arias, P. (2007). Neighbours but diverse: social change in north-west Iberia during the transition from the Mesolithic to the Neolithic (5500-4000 cal BC). In Whittle A. and Cummings, V. (Eds.) *Going over: the Mesolithic-Neolithic transitions in north-western Europe, Proceedings-British Academy* (Vol. 144, p. 53-71). Oxford University Press Inc.
- Arias P., & Fano, A. (2009).   Mesol tico geom trico o Mesol tico con geom tricos?: el caso de la regi n cant brica. In *El mesol tico geom trico en la Pen nsula Ib rica* (pp. 69–92). Departamento de Ciencias de la Antigüedad.
- Arranz-Otaegui, A., Gonzalez Carretero, L., Ramsey, M. N., Fuller, D. Q., & Richter, T. (2018). Archaeobotanical evidence reveals the origins of bread 14,400 years ago in northeastern Jordan. *Proceedings of the National Academy of Sciences*, 115(31), 7925 LP-7930. <https://doi.org/10.1073/pnas.1801071115>
- Aura, J. E., Tiffagom, M., Jord  Pardo, J. F., Duarte, E., Fern ndez de la Vega, J., Santamaria, D., ... Perez Ripoll, M. (2012). The Solutrean–Magdalenian transition: A view from Iberia. *Quaternary International*, 272–273, 75–87. <https://doi.org/https://doi.org/10.1016/j.quaint.2012.05.020>
- Bada, J. L., Peterson, R. O., Schimmelmann, A., & Hedges, R. E. M. (1990). Moose teeth as monitors of environmental isotopic parameters. *Oecologia*, 82(1), 102–106. <https://doi.org/10.1007/BF00318540>
- Balasse, M., Evin, A., Tornero, C., Radu, V., Fiorillo, D., Popovici, D., ... B l şescu, A. (2016). Wild, domestic and feral? Investigating the status of suids in the Romanian Gumelni a (5th mil. cal BC) with biogeochemistry and geometric morphometrics. *Journal of Anthropological Archaeology*, 42, 27–36. <https://doi.org/https://doi.org/10.1016/j.jaa.2016.02.002>
- Balasse, M., Tornero, C., Br hard, S., Ughetto-Monfrin, J., Voinea, V., & B l şescu, A. (2014). Cattle and Sheep Herding at Cheia, Romania, at the Turn of the Fifth Millennium cal BC. In *Proceedings of the British Academy* (Vol. 198, pp. 115–142).
- Baldellou, V. (2011). La Cueva de Chaves (Bastar s-Casbas, Huesca). *SAGVNTVM Extra*, 12, 141–144.
- Bar-Yosef, O. (1983). The Natufian in the southern Levant. In P. E. L. Young, C. T., Smith &

- P. and Mortensen (Eds.), *The Hilly Flanks and Beyond. "Essays on the Prehistory of Southwestern Asia presented to R. J. Braidwood* (pp. 11–42). Chicago: Oriental Institute, University of Chicago Press.
- Barandiarán, I., & Cava, A. (1994). Zatoya, sitio magdalenense de caza en medio pirenaico. *Homenaje Al Dr. J. Gonzalez Echegaray, Museo y Centro de Investigación Altamira*, 71–85.
- Barandiarán, I., & Cava Almuzara, A. (2000). A propósito de unas fechas del Bajo Aragón: reflexiones sobre el Mesolítico y el Neolítico en la Cuenca del Ebro. *Spal*, 9, 293–326.
- Barton, R. N. E., Bouzouggar, A., Hogue, J. T., Lee, S., Collcutt, S. N., & Ditchfield, P. (2013). Origins of the Iberomaurusian in NW Africa: New AMS radiocarbon dating of the Middle and Later Stone Age deposits at Taforalt Cave, Morocco. *Journal of Human Evolution*, 65(3), 266–281. <https://doi.org/10.1016/j.jhevol.2013.06.003>
- Benson, L., Cordell, L., Vincent, K., Taylor, H., Stein, J., Farmer, G. L., & Futa, K. (2003). Ancient maize from Chacoan great houses: Where was it grown? *Proceedings of the National Academy of Sciences*, 100(22), 13111 LP–13115. <https://doi.org/10.1073/pnas.2135068100>
- Bentley, R. A. (2004). Characterising human mobility by strontium isotope analysis of the skeletons. In C.F.W Higham and R. Thosarat (Eds), *Khok Phanom Di: Summary and Conclusions* (pp 159–166), Oxford: Oxbow Books.
- Bentley, R. A. (2013). Mobility and the diversity of Early Neolithic lives: Isotopic evidence from skeletons. *Journal of Anthropological Archaeology*, 32(3), 303–312. <https://doi.org/10.1016/j.jaa.2012.01.009>
- Bernabeu, J., Balaguer, L. M., Esquembre-Bebiá, M. A., Pérez, J. R. O., & Soler, J. de D. B. (2009). La cerámica impresa mediterránea en el origen del Neolítico de la península Ibérica. In *De Méditerranée et d'ailleurs...: mélanges offerts à Jean Guilaine* (pp. 83–96).
- Bernabeu, J., Pérez, O. G., Balaguer, L. M., & Borja, P. G. (2011). La cerámica neolítica durante el VI milenio CAL AC en el Mediterráneo central peninsular. *Saguntum: Papeles Del Laboratorio de Arqueología de Valencia*, (12), 153–178.
- Biagi, P. (2016). The Last Hunter-Gatherers of the Northern Coast of the Black Sea and their Role in the Mesolithic of Europe. In R. Kraus and H. Floss (Eds), *Southeast Europe Before neolithisation*, (pp 113–131), Tübingen: Universität Tübingen.
- Biagi, P., & Spataro, M. (2005). New observations on the radiocarbon chronology of the Starčevo-Criş and Körös cultures. In L. Nikolova, J. Higgings (Eds), *Prehistoric Archaeology & Anthropological Theory and Education. Reports of Prehistoric Research Projects*, 6–7 (pp. 35–52) Salt Lake City: International Institute of Anthropology, Argosy University.
- Bicho, N., Cascalheira, J., Gonçalves, C., Umbelino, C., Rivero, D. G., & André, L. (2017). Resilience, replacement and acculturation in the Mesolithic/Neolithic transition: The case of Muge, central Portugal. *Quaternary International*, 446, 31–42. <https://doi.org/10.1016/j.quaint.2016.09.049>
- Bicho, N., Cascalheira, J., Marreiros, J., Gonçalves, C., Pereira, T., & Dias, R. (2013). Chronology of the Mesolithic occupation of the Muge valley, central Portugal: The case of Cabeço da Amoreira. *Quaternary International*, 308–309, 130–139. <https://doi.org/10.1016/j.quaint.2012.10.049>
- Binder, D., & Sénépart, I. (2010). La séquence de l'Impresso-Cardial de l'abri Pendimoun et l'évolution des assemblages céramiques en Provence. In C. Manen, F. Covertini, D. Binder and I. Sénépart (Eds), *Premières Sociétés Paysannes de Méditerranée Occidentale. Structures Des Productions Céramiques. Mémoire*, 51, (pp. 149–167), Mémoire LI de la Société Préhistorique française.
- Blasco, C., Delibes, G., Baena, J., Liesau, C., & Ríos, P. (2007). El poblado calcolítico de

- Camino de las Yeseras (San Fernando de Henares, Madrid): un escenario favorable para el estudio de la incidencia campaniforme en el interior peninsular. *Trabajos de Prehistoria*, 64(1), 151–163.
- Blasco, C., & Ríos, P. (2010). La función del metal entre los grupos campaniformes. Oro versus cobre. El ejemplo de la Región de Madrid. *Trabajos de Prehistoria*, 67(2), 359–372.
- Bocherens, H., & Drucker, D. (2003). Trophic level isotopic enrichment of carbon and nitrogen in bone collagen: case studies from recent and ancient terrestrial ecosystems. *International Journal of Osteoarchaeology*, 13(1-2), 46–53. <https://doi.org/10.1002/oa.662>
- Bogaard, A., Fraser, R., Heaton, T. H. E., Wallace, M., Vaiglova, P., Charles, M., ... Stephan, E. (2013). Crop manuring and intensive land management by Europe's first farmers. *Proceedings of the National Academy of Sciences*, 110(31), 12589 LP-12594. <https://doi.org/10.1073/pnas.1305918110>
- Bogaard, A., Heaton, T. H. E., Poulton, P., & Merbach, I. (2007). The impact of manuring on nitrogen isotope ratios in cereals: archaeological implications for reconstruction of diet and crop management practices. *Journal of Archaeological Science*, 34(3), 335–343. <https://doi.org/https://doi.org/10.1016/j.jas.2006.04.009>
- Bogaard, A., Henton, E., Evans, J. A., Twiss, K. C., Charles, M. P., Vaiglova, P., & Russell, N. (2014). Locating Land Use at Neolithic Çatalhöyük, Turkey: The Implications of 87Sr/86Sr Signatures in Plants and Sheep Tooth Sequences. *Archaeometry*, 56(5), 860–877. <https://doi.org/10.1111/arc.12049>
- Bonsall, C., Cook, G. T., Hedges, R. E. M., Higham, T. F. G., Pickard, C., & Radovanović, I. (2004). Radiocarbon and Stable Isotope Evidence of Dietary Change from the Mesolithic to the Middle Ages in the Iron Gates: New Results from Lepenski Vir. *Radiocarbon*, 46(1), 293–300. <https://doi.org/DOI: 10.1017/S0033822200039606>
- Borić, D., Grupe, G., Peters, J., & Mikić, Ž. (2004). Is the Mesolithic–Neolithic Subsistence Dichotomy Real? New Stable Isotope Evidence from the Danube Gorges. *European Journal of Archaeology*, 7(3), 221–248. <https://doi.org/DOI: 10.1177/1461957104056500>
- Borić, D., & Price, T. D. (2013). Strontium isotopes document greater human mobility at the start of the Balkan Neolithic. *Proceedings of the National Academy of Sciences*, 110(9), 3298 LP-3303. <https://doi.org/10.1073/pnas.1211474110>
- Bos, K. I., Schuenemann, V. J., Golding, G. B., Burbano, H. A., Waglechner, N., Coombes, B. K., ... Krause, J. (2011). A draft genome of *Yersinia pestis* from victims of the Black Death. *Nature*, 478, 506–510. Retrieved from <https://doi.org/10.1038/nature10549>
- Bosch, À. B., de Catalunya, M. d'Arqueologia, & Catalunya. (2011). *El poblat lacustre neolític de La Draga: excavacions 2000-2005*. Generalitat de Catalunya.
- Bowman, S. (1990). *Radiocarbon dating* (Vol. 1). Univ of California Press.
- Boyd, B. (2006). On 'sedentism' in the Later Epipalaeolithic (Natufian) Levant. *World Archaeology*, 38(2), 164–178. <https://doi.org/10.1080/00438240600688398>
- Brandt, G., Haak, W., Adler, C. J., Roth, C., Szécsényi-Nagy, A., Karimnia, S., ... Alt, K. W. (2013). Ancient DNA Reveals Key Stages in the Formation of Central European Mitochondrial Genetic Diversity. *Science*, 342(6155), 257 LP-261. <https://doi.org/10.1126/science.1241844>
- Brandt, G., Szécsényi-Nagy, A., Roth, C., Alt, K. W., & Haak, W. (2015). Human paleogenetics of Europe – The known knowns and the known unknowns. *Journal of Human Evolution*, 79, 73–92. <https://doi.org/https://doi.org/10.1016/j.jhevol.2014.06.017>
- Brea, L. B. (1949). Le culture preistoriche della Francia meridionale e della Catalogna e la successione stratigrafica delle Arene Candide. *Rivista Di Studi Liguri*, (15), 21–45.
- Briggs, A. W., Good, J. M., Green, R. E., Krause, J., Maricic, T., Stenzel, U., ... Pääbo, S.

- (2009). Targeted Retrieval and Analysis of Five Neandertal mtDNA Genomes. *Science*, 325(5938), 318 LP-321. <https://doi.org/10.1126/science.1174462>
- Briggs, A. W., Krause, J., Kircher, M., Meyer, M., Pääbo, S., & Stenzel, U. (2009). Removal of deaminated cytosines and detection of in vivo methylation in ancient DNA. *Nucleic Acids Research*, 38(6), e87–e87. <https://doi.org/10.1093/nar/gkp1163>
- Briggs, A. W., Stenzel, U., Johnson, P. L. F., Green, R. E., Kelso, J., Prüfer, K., ... Pääbo, S. (2007). Patterns of damage in genomic DNA sequences from a Neandertal. *Proceedings of the National Academy of Sciences*, 104(37), 14616 LP-14621. <https://doi.org/10.1073/pnas.0704665104>
- Briscoe, H. V. A., & Robinson, P. L. (1925). XCIX.—A redetermination of the atomic weight of boron. *Journal of the Chemical Society, Transactions*, 127, 696–720.
- Britton, K., Grimes, V., Dau, J., & Richards, M. P. (2009). Reconstructing faunal migrations using intra-tooth sampling and strontium and oxygen isotope analyses: a case study of modern caribou (*Rangifer tarandus granti*). *Journal of Archaeological Science*, 36(5), 1163–1172. <https://doi.org/https://doi.org/10.1016/j.jas.2009.01.003>
- Britton, K., Grimes, V., Niven, L., Steele, T. E., McPherron, S., Soressi, M., ... Richards, M. P. (2011). Strontium isotope evidence for migration in late Pleistocene Rangifer: Implications for Neanderthal hunting strategies at the Middle Palaeolithic site of Jonzac, France. *Journal of Human Evolution*, 61(2), 176–185. <https://doi.org/https://doi.org/10.1016/j.jhevol.2011.03.004>
- Bronk Ramsey, C. (2009). Bayesian Analysis of Radiocarbon Dates. *Radiocarbon*, 51(1), 337–360. <https://doi.org/DOI:10.1017/S0033822200033865>
- Brookins, D. G., Moore, D. I., & Gosz, J. R. (1983). Using Strontium Isotope Ratios to Estimate Inputs to Ecosystems. *BioScience*, 33(1), 23–30. <https://doi.org/10.2307/1309240>
- Brothwell, D. R. (1987). Desenterrando huesos. *La Excavación, Tratamiento y Estudio de Restos Del Esqueleto Humano*.
- Brown, T. A., Nelson, D. E., Vogel, J. S., & Southon, J. R. (1988). Improved Collagen Extraction by Modified Longin Method. *Radiocarbon*, 30(2), 171–177. <https://doi.org/DOI:10.1017/S0033822200044118>
- Budd, P., Montgomery, J., Barreiro, B., & Thomas, R. G. (2000). Differential diagenesis of strontium in archaeological human dental tissues. *Applied Geochemistry*, 15(5), 687–694. [https://doi.org/https://doi.org/10.1016/S0883-2927\(99\)00069-4](https://doi.org/https://doi.org/10.1016/S0883-2927(99)00069-4)
- Burbano, H. A., Hodges, E., Green, R. E., Briggs, A. W., Krause, J., Meyer, M., ... Pääbo, S. (2010). Targeted Investigation of the Neandertal Genome by Array-Based Sequence Capture. *Science*, 328(5979), 723 LP-725. <https://doi.org/10.1126/science.1188046>
- Burger, J., Kirchner, M., Bramanti, B., Haak, W., & Thomas, M. G. (2007). Absence of the lactase-persistence-associated allele in early Neolithic Europeans. *Proceedings of the National Academy of Sciences*, 104(10), 3736 LP-3741. <https://doi.org/10.1073/pnas.0607187104>
- Burton, J. H., Price, T. D., & Middleton, W. D. (1999). Correlation of Bone Ba/Ca and Sr/Ca due to Biological Purification of Calcium. *Journal of Archaeological Science*, 26(6), 609–616. <https://doi.org/https://doi.org/10.1006/jasc.1998.0378>
- Buxó, R., & Piqué, R. (2008). *Arqueobotánica: los usos de las plantas en la península Ibérica*. Grupo Planeta (GBS).
- Cai, L., & Qiu, S. (1984). Carbon-13 evidence for ancient diets in China. *Kaogu*, 10, 949.
- Cann, R. L., Stoneking, M., & Wilson, A. C. (1987). Mitochondrial DNA and human evolution. *Nature*, 325(6099), 31–36. <https://doi.org/10.1038/325031a0>
- Capo, R. C., Stewart, B. W., & Chadwick, O. A. (1998). Strontium isotopes as tracers of ecosystem processes: theory and methods. *Geoderma*, 82(1), 197–225. [https://doi.org/https://doi.org/10.1016/S0016-7061\(97\)00102-X](https://doi.org/https://doi.org/10.1016/S0016-7061(97)00102-X)

- Carvalho, A. F. (2011). Produção cerâmica no início do Neolítico de Portugal. *SAGVNTVM Extra*, 12, 237–250.
- Castaños, P. M. (2004). Estudio arqueozoológico de los macromamíferos del Neolítico de la Cueva de Chaves (Huesca). *Saldvie: Estudios de Prehistoria y Arqueología*, (4), 125–172.
- Cava Almuzara, A. (1994). El Mesolítico en la Cuenca del Ebro. Un estado de la cuestión. *Zephyrus*, 47, 65–91.
- Childe, V. G. (1964). *What happened in history*. Penguin books.
- Childe, V. G. (2013). *The dawn of European civilization*. Routledge.
- Clottes, J. (1979). Midi-Pyrénées. *Gallia Préhistoire*, 22(2), 629–671.
- Clottes, J. (1983). Midi-Pyrénées. *Gallia Préhistoire*, 26(2), 465–510.
- Consortium, T. I. H. G. M., McPherson, J. D., Marra, M., Hillier, L., Waterston, R. H., Chinwalla, A., ... Lehrach, H. (2001). A physical map of the human genome. *Nature*, 409, 934. Retrieved from <https://doi.org/10.1038/35057157>
- Cooper, A., Austin, J., Sanchez, J. J., Beaumont, M., Endicott, P., Barnett, R., & Brotherton, P. (2007). Novel high-resolution characterization of ancient DNA reveals C & U-type base modification events as the sole cause of post mortem miscoding lesions. *Nucleic Acids Research*, 35(17), 5717–5728. <https://doi.org/10.1093/nar/gkm588>
- Copeland, S. R., Cawthra, H. C., Fisher, E. C., Lee-Thorp, J. A., Cowling, R. M., le Roux, P. J., ... Marean, C. W. (2016). Strontium isotope investigation of ungulate movement patterns on the Pleistocene Paleo-Agulhas Plain of the Greater Cape Floristic Region, South Africa. *Quaternary Science Reviews*, 141, 65–84. <https://doi.org/10.1016/j.quascirev.2016.04.002>
- Copeland, S. R., Sponheimer, M., de Ruiter, D. J., Lee-Thorp, J. A., Codron, D., le Roux, P. J., ... Richards, M. P. (2011). Strontium isotope evidence for landscape use by early hominins. *Nature*, 474, 76. Retrieved from <https://doi.org/10.1038/nature10149>
- Copeland, S. R., Sponheimer, M., le Roux, P. J., Grimes, V., Lee-Thorp, J. A., de Ruiter, D. J., & Richards, M. P. (2008). Strontium isotope ratios ($^{87}\text{Sr}/^{86}\text{Sr}$) of tooth enamel: a comparison of solution and laser ablation multicollector inductively coupled plasma mass spectrometry methods. *Rapid Communications in Mass Spectrometry*, 22(20), 3187–3194. <https://doi.org/10.1002/rcm.3717>
- Coplen, T. B. (1996). New guidelines for reporting stable hydrogen, carbon, and oxygen isotope-ratio data. *Geochimica et Cosmochimica Acta*, 60(17), 3359–3360.
- Coplen, T. B., & Clayton, R. N. (1973). Hydrogen isotopic composition of NBS and IAEA stable isotope water reference samples. *Geochimica et Cosmochimica Acta*, 37(10), 2347–2349. [https://doi.org/10.1016/0016-7037\(73\)90108-7](https://doi.org/10.1016/0016-7037(73)90108-7)
- Coplen, T. B., Kendall, C., & Hopple, J. (1983). Comparison of stable isotope reference samples. *Nature*, 302(5905), 236–238. <https://doi.org/10.1038/302236a0>
- Cox, G., & Sealy, J. (1997). Investigating Identity and Life Histories: Isotopic Analysis and Historical Documentation of Slave Skeletons Found on the Cape Town Foreshore, South Africa. *International Journal of Historical Archaeology*, 1(3), 207–224. <https://doi.org/10.1023/A:1027349115474>
- Cunningham, C., Scheuer, L., & Black, S. (2016). *Developmental juvenile osteology*. Academic Press.
- Dabney, J., Knapp, M., Glocke, I., Gansauge, M.-T., Weihmann, A., Nickel, B., ... Meyer, M. (2013). Complete mitochondrial genome sequence of a Middle Pleistocene cave bear reconstructed from ultrashort DNA fragments. *Proceedings of the National Academy of Sciences*, 110(39), 15758 LP-15763. Retrieved from <http://www.pnas.org/content/110/39/15758.abstract>
- Dabney, J., Meyer, M., & Pääbo, S. (2013). Ancient DNA damage. *Cold Spring Harbor Perspectives in Biology*, 5(7), a012567.

- Davis, S., & Simões, T. (2016). The velocity of Ovis in prehistoric times: the sheep bones from Early Neolithic Lameiras, Sintra, Portugal. *O Neolítico Em Portugal Antes Do Horizonte 2020: Perspectivas Em Debate*, 2, 51–66.
- Delibes, G., Herrán, J. I., Santiago, J. de, & Val, J. del. (1995). Evidence for social complexity in the Copper Age of the Northern Meseta. In K.T. Lillios (Ed), *The Origins of Complex Societies in Late Prehistoric Iberia*, (pp. 44–63), International Monographs in Prehistory, 8..
- Delibes, G., & Manzano, J. F. (2000). La trayectoria cultural de la Prehistoria Reciente (6400-2500 BP) en la Submeseta Norte: principales hitos de un proceso. In *3º Congresso de Arqueologia Peninsular: UTAD, Vila Real, Portugal, setembro de 1999* (pp. 95–122). ADECAP.
- Delwiche, C. C., & Steyn, P. L. (1970). Nitrogen isotope fractionation in soils and microbial reactions. *Environmental Science & Technology*, 4(11), 929–935.
<https://doi.org/10.1021/es60046a004>
- DeNiro, M. J. (1985). Postmortem preservation and alteration of in vivo bone collagen isotope ratios in relation to palaeodietary reconstruction. *Nature*, 317(6040), 806–809.
<https://doi.org/10.1038/317806a0>
- DeNiro, M. J., & Epstein, S. (1978). Influence of diet on the distribution of carbon isotopes in animals. *Geochimica et Cosmochimica Acta*, 42(5), 495–506.
[https://doi.org/https://doi.org/10.1016/0016-7037\(78\)90199-0](https://doi.org/https://doi.org/10.1016/0016-7037(78)90199-0)
- Diaz-Zorita-Bonilla, M. (2013). The Copper Age in south-west Spain: a bioarchaeological approach to prehistoric social organisation. Durham University, Doctoral thesis.
- Dobzhansky, T. (1937). Genetic Nature of Species Differences. *The American Naturalist*, 71(735), 404–420. <https://doi.org/10.1086/280726>
- Domingo, R. (2009). Caracterización funcional de los microlitos geométricos: el caso del Valle del Ebro. In *El mesolítico geométrico en la Península Ibérica* (pp. 375–389). Departamento de Ciencias de la Antigüedad.
- Domingo, R. (2012). Beyond Chaves: Functional analysis of neolithic blades from the Ebro Valley. In *International conference on use-wear analysis* (pp. 672–681).
- Drucker, D., Bocherens, H., Bridault, A., & Billiou, D. (2003). Carbon and nitrogen isotopic composition of red deer (*Cervus elaphus*) collagen as a tool for tracking palaeoenvironmental change during the Late-Glacial and Early Holocene in the northern Jura (France). *Palaeogeography, Palaeoclimatology, Palaeoecology*, 195(3), 375–388.
[https://doi.org/https://doi.org/10.1016/S0031-0182\(03\)00366-3](https://doi.org/https://doi.org/10.1016/S0031-0182(03)00366-3)
- Ehleringer, J. R., Cerling, T. E., & Helliker, B. R. (1997). C4 photosynthesis, atmospheric CO2, and climate. *Oecologia*, 112(3), 285–299. <https://doi.org/10.1007/s004420050311>
- Enlow, D. H. (1963). Principles of bone remodeling. Springfield, IL: Charles C. Thomas Publishing.
- Ericson, J. E. (1985). Strontium isotope characterization in the study of prehistoric human ecology. *Journal of Human Evolution*, 14(5), 503–514.
[https://doi.org/https://doi.org/10.1016/S0047-2484\(85\)80029-4](https://doi.org/https://doi.org/10.1016/S0047-2484(85)80029-4)
- Eske, W., & Alan, C. (2005). Review Paper. Ancient DNA. *Proceedings of the Royal Society B: Biological Sciences*, 272(1558), 3–16. <https://doi.org/10.1098/rspb.2004.2813>
- Esquivel, J. A., & Navas, E. (2007). Geometric architectural pattern and constructive energy analysis at Los Millares Copper Age Settlement (Santa Fé de Mondújar, Almería, Andalusia). *Journal of Archaeological Science*, 34(6), 894–904.
<https://doi.org/https://doi.org/10.1016/j.jas.2006.09.003>
- Ezzo, J. A. (1994). Putting the “Chemistry” Back into Archaeological Bone Chemistry Analysis: Modeling Potential Paleodietary Indicators. *Journal of Anthropological Archaeology*, 13(1), 1–34. <https://doi.org/https://doi.org/10.1006/jaar.1994.1002>
- Fernandes, R., Millard, A. R., Brabec, M., Nadeau, M.-J., & Grootes, P. (2014). Food

- Reconstruction Using Isotopic Transferred Signals (FRUITS): A Bayesian Model for Diet Reconstruction. *PLOS ONE*, 9(2), e87436. Retrieved from <https://doi.org/10.1371/journal.pone.0087436>
- Fernández-Crespo, T. (2016). El papel del fuego en los enterramientos neolíticos finales/calcolíticos iniciales de los abrigos de la Sierra de Cantabria y sus estribaciones (valle medio-alto del Ebro). *Trabajos de Prehistoria*, 73(1), 128–146.
- Fernández-Crespo, T., Ordoño, J., Barandiarán, I., Andrés, M. T., & Schulting, R. J. (2018). The Bell Beaker multiple burial pit of La Atalayuela (La Rioja, Spain): stable isotope insights into diet, identity and mortuary practices in Chalcolithic Iberia. *Archaeological and Anthropological Sciences*. <https://doi.org/10.1007/s12520-018-0610-1>
- Fernández-Crespo, T., & Schulting, R. J. (2017). Living different lives: Early social differentiation identified through linking mortuary and isotopic variability in Late Neolithic/ Early Chalcolithic north-central Spain. *PLOS ONE*, 12(9), e0177881. Retrieved from <https://doi.org/10.1371/journal.pone.0177881>
- Fernández Eraso, J., Ollero Ojeda, A., Ormaetxea Arenaza, O., Castaños, P., Iriarte Chiapusso, M. J., & Merino Nazabal, I. (1997). Excavaciones en el abrigo de Peña Larga(Cripán-Alava). *Memorias de Yacimientos Alaveses*.
- Fincham, A. G., Moradian-Oldak, J., & Simmer, J. P. (1999). The Structural Biology of the Developing Dental Enamel Matrix. *Journal of Structural Biology*, 126(3), 270–299. <https://doi.org/https://doi.org/10.1006/jsbi.1999.4130>
- Flannery, K. V. (1973). The origins of agriculture. *Annual Review of Anthropology*, 2(1), 271–310.
- Fontanals-Coll, M., Díaz-Zorita Bonilla, M., & Subirà, M. E. (2015). A Palaeodietary Study of Stable Isotope Analysis from a High-status Burial in the Copper Age: The Montelirio Megalithic Structure at Valencina de la Concepción–Castilleja de Guzmán, Spain. *International Journal of Osteoarchaeology*, 26(3), 447–459. <https://doi.org/10.1002/oa.2435>
- Fregel, R., Méndez, F. L., Bokbot, Y., Martín-Socas, D., Camalich-Massieu, M. D., Santana, J., ... Bustamante, C. D. (2018). Ancient genomes from North Africa evidence prehistoric migrations to the Maghreb from both the Levant and Europe. *Proceedings of the National Academy of Sciences*. Retrieved from <http://www.pnas.org/content/early/2018/06/11/1800851115.abstract>
- Fu, Q., Hajdinjak, M., Moldovan, O. T., Constantin, S., Mallick, S., Skoglund, P., ... Pääbo, S. (2015). An early modern human from Romania with a recent Neanderthal ancestor. *Nature*, 524, 216–219. Retrieved from <http://dx.doi.org/10.1038/nature14558>
- Fu, Q., Meyer, M., Gao, X., Stenzel, U., Burbano, H. A., Kelso, J., & Pääbo, S. (2013). DNA analysis of an early modern human from Tianyuan Cave, China. *Proceedings of the National Academy of Sciences*, 110(6), 2223 LP-2227. <https://doi.org/10.1073/pnas.1221359110>
- Fu, Q., Mittnik, A., Johnson, P. L. F., Bos, K., Lari, M., Bollongino, R., ... Krause, J. (2013). A Revised Timescale for Human Evolution Based on Ancient Mitochondrial Genomes. *Current Biology*, 23(7), 553–559. <https://doi.org/https://doi.org/10.1016/j.cub.2013.02.044>
- Fu, Q., Posth, C., Hajdinjak, M., Petr, M., Mallick, S., Fernandes, D., ... Reich, D. (2016). The genetic history of Ice Age Europe. *Nature*, 534, 200–205. Retrieved from <http://dx.doi.org/10.1038/nature17993>
- Fuller, B. T., Fuller, J. L., Harris, D. A., & Hedges, R. E. M. (2006). Detection of breastfeeding and weaning in modern human infants with carbon and nitrogen stable isotope ratios. *American Journal of Physical Anthropology*, 129(2), 279–293. <https://doi.org/10.1002/ajpa.20249>
- Gamba, C., Fernández, E., Tirado, M., Deguilloux, M. F., Pemonge, M. H., Utrilla, P., ...

- Arroyo-Pardo, E. (2011). Ancient DNA from an Early Neolithic Iberian population supports a pioneer colonization by first farmers. *Molecular Ecology*, *21*(1), 45–56. <https://doi.org/10.1111/j.1365-294X.2011.05361.x>
- Gamba, C., Jones, E. R., Teasdale, M. D., McLaughlin, R. L., Gonzalez-Fortes, G., Mattiangeli, V., ... Pinhasi, R. (2014). Genome flux and stasis in a five millennium transect of European prehistory. *Nature Communications*, *5*, 5257. Retrieved from <http://dx.doi.org/10.1038/ncomms6257>
- García-Puchol, O., Diez Castillo, A. A., & Pardo-Gordó, S. (2017). Timing the Western Mediterranean Last Hunter-Gatherers and First Farmers BT - Times of Neolithic Transition along the Western Mediterranean. In O. García-Puchol & D. C. Salazar-García (Eds.) (pp. 69–99). Cham: Springer International Publishing. https://doi.org/10.1007/978-3-319-52939-4_4
- García-Puchol, O., McClure, S. B., Juan-Cabanilles, J., Diez-Castillo, A. A., Bernabeu-Aubán, J., Martí-Oliver, B., ... Kennett, D. J. (2018). Cocina cave revisited: Bayesian radiocarbon chronology for the last hunter-gatherers and first farmers in Eastern Iberia. *Quaternary International*, *472*, 259–271. <https://doi.org/https://doi.org/10.1016/j.quaint.2016.10.037>
- García Borja, P. (2017). Las cerámicas neolíticas de la Cova de la Sarsa (Bocairent, Valencia). Tipología, estilo e identidad. Serie de Trabajos Varios del SIP.
- García Borja, P. J., Tortosa, A., Emili, J., Jordá Pardo, J. F., & Salazar García, D. C. (2014). La cerámica neolítica de la Cueva de Nerja (Málaga, España): salas del Vestíbulo y la Mina. *Archivo de Prehistoria Levantina*, *30*, 81–131.
- García Borja, P., Pérez Fernández, Á., Biosca Cirujeda, V., Ribera Gómez, A., & Salazar García, D. C. (2013). Los restos humanos de la Coveta del Frare (La Font de la Figuera, València).
- García, M. D.-A., Lladró, A. C., & Liesau, C. (1992). El poblado calcolítico de la Loma de Chiclana (Vallecas, Madrid): excavaciones de urgencia realizadas en 1987. *Arqueología, Paleontología y Etnografía*, (3), 31–116.
- Garn, S. M. (1970). *The earlier gain and the later loss of cortical bone, in nutritional perspective*. Springfield, IL: Charles C. Thomas.
- Gavilán, B; Escacena, J. L. (2009). Acerca del Primer Neolítico de Andalucía Occidental. Los Tramos Medio y Bajo de la Cuenca del Guadalquivir. *Mainake XXXI*, 311–351.
- Gibaja, J. F., Subirà, M. E., Terradas, X., Santos, F. J., Agulló, L., Gómez-Martínez, I., ... Fernández-López de Pablo, J. (2015). The Emergence of Mesolithic Cemeteries in SW Europe: Insights from the El Collado (Oliva, Valencia, Spain) Radiocarbon Record. *PLOS ONE*, *10*(1), e0115505. Retrieved from <https://doi.org/10.1371/journal.pone.0115505>
- Ginolhac, A., Jónsson, H., Orlando, L., Schubert, M., & Johnson, P. L. F. (2013). mapDamage2.0: fast approximate Bayesian estimates of ancient DNA damage parameters. *Bioinformatics*, *29*(13), 1682–1684. <https://doi.org/10.1093/bioinformatics/btt193>
- Gnirke, A., Melnikov, A., Maguire, J., Rogov, P., LeProust, E. M., Brockman, W., ... Nusbaum, C. (2009). Solution hybrid selection with ultra-long oligonucleotides for massively parallel targeted sequencing. *Nature Biotechnology*, *27*, 182–189. Retrieved from <https://doi.org/10.1038/nbt.1523>
- González-Fortes, G., Jones, E. R., Lightfoot, E., Bonsall, C., Lazar, C., Grandal-d'Anglade, A., ... Hofreiter, M. (2017). Paleogenomic Evidence for Multi-generational Mixing between Neolithic Farmers and Mesolithic Hunter-Gatherers in the Lower Danube Basin. *Current Biology*, *27*(12), 1801–1810.e10. <https://doi.org/https://doi.org/10.1016/j.cub.2017.05.023>
- González-Guarda, E., Domingo, L., Tornero, C., Pino, M., Hernández Fernández, M., Sevilla,

- P., ... Agustí, J. (2017). Late Pleistocene ecological, environmental and climatic reconstruction based on megafauna stable isotopes from northwestern Chilean Patagonia. *Quaternary Science Reviews*, 170, 188–202.
<https://doi.org/https://doi.org/10.1016/j.quascirev.2017.06.035>
- González-Sampériz, P., Utrilla, P., Mazo, C., Valero-Garcés, B., Sopena, M. C., Morellón, M., ... Martínez-Bea, M. (2009). Patterns of human occupation during the early Holocene in the Central Ebro Basin (NE Spain) in response to the 8.2 ka climatic event. *Quaternary Research*, 71(2), 121–132. <https://doi.org/DOI: 10.1016/j.yqres.2008.10.006>
- Goude, G., & Fontugne, M. (2016). Carbon and nitrogen isotopic variability in bone collagen during the Neolithic period: Influence of environmental factors and diet. *Journal of Archaeological Science*, 70, 117–131.
<https://doi.org/https://doi.org/10.1016/j.jas.2016.04.019>
- Graustein, W. C., & Armstrong, R. L. (1983). The Use of Strontium-87/Strontium-86 Ratios to Measure Atmospheric Transport into Forested Watersheds. *Science*, 219(4582), 289 LP-292. <https://doi.org/10.1126/science.219.4582.289>
- Green, R. E., Krause, J., Briggs, A. W., Maricic, T., Stenzel, U., Kircher, M., ... Pääbo, S. (2010). A Draft Sequence of the Neandertal Genome. *Science*, 328(5979), 710 LP-722. <https://doi.org/10.1126/science.1188021>
- Gronenborn, D. (2017). Migrations before the Neolithic? The Late Mesolithic blade-and-trapeze horizon in Central Europe and beyond. In *Migration and Integration from Prehistory to the Middle Ages, LandesMuseum für Vorgeschichte, Halle, Germany* (pp. 113–122).
- Grupe, G. (2001). Archaeological Microbiology. In A. M. Brothwell, D. R., Pollard (Ed.), *Handbook of Archaeological Sciences* (John Wille, pp. 351–358). New York.
- Guerra, M. Á. R., Chocarro, L. P., Guillén, J. I. R., Rodríguez, C. T., de Lagrán, I. G.-M., Magallón, H. A., ... Bao, J. F. G. (2013). Pastores trashumantes del Neolítico Antiguo en un entorno de alta montaña: secuencia crono-cultural de la Cova de Els Trocs (San Feliu de Veri, Huesca). *BSAA Arqueología*, (79), 9–55.
- Guilaine, Jean; Manen, C. (2007). Du Mésolithique au Néolithique en Méditerranée de l'Ouest : aspects culturels. In J. . Guilaine, J.; Manen C.; Vigne (Ed.), *Pont de Roque-Haute (Portiragnes, Hérault). Nouveaux regards sur la néolithisation de la France méditerranéenne* (Pont de Ro, pp. 303–322). Toulouse, Archives d'Ecologie préhistorique.
- Guilaine, J. (2018). A personal view of the neolithisation of the Western Mediterranean. *Quaternary International*, 470, 211–225.
<https://doi.org/https://doi.org/10.1016/j.quaint.2017.06.019>
- Guilaine, J., & Manen, C. (1995). Contacts sud-nord au Néolithique ancien: témoignages de la grotte de Gazel en Languedoc. In *22ème colloque interrégional sur le Néolithique* (pp. 301–311).
- Guiry, E., Karavanić, I., Klindžić, R. Š., Talamo, S., Radović, S., & Richards, M. P. (2017). Stable Isotope Palaeodietary and Radiocarbon Evidence from the Early Neolithic Site of Zemunica, Dalmatia, Croatia. *European Journal of Archaeology*, 20(2), 235–256.
<https://doi.org/DOI: 10.1017/ea.2016.24>
- Guixé, E. G. (2011). Estudi paleoantropològic i paleopatològic del sepulcre col· lectiu de Forat de Conqueta (Santa Linya, Lleida). *Treballs d'arqueologia*, 17, 37–98.
- Guixé, E. G., Richards, M. P., & Subirà, M. E. (2006). Palaeodiets of humans and fauna at the Spanish Mesolithic site of El Collado. *Current Anthropology*, 47(3), 549.
- Guy Straus, L., & González Morales, M. (2003). El Mirón Cave and the 14C Chronology of Cantabrian Spain. *Radiocarbon*, 45(01), 41–58.
<https://doi.org/10.1017/S0033822200032380>
- Haak, W., Brandt, G., de Jong, H. N., Meyer, C., Ganslmeier, R., Heyd, V., ... Alt, K. W.

- (2008). Ancient DNA, Strontium isotopes, and osteological analyses shed light on social and kinship organization of the Later Stone Age. *Proceedings of the National Academy of Sciences*, 105(47), 18226–18231. Retrieved from <http://www.pnas.org/content/early/2008/11/17/0807592105.abstract>
- Haak, W., Forster, P., Bramanti, B., Matsumura, S., Brandt, G., Tänzer, M., ... Burger, J. (2005). Ancient DNA from the First European Farmers in 7500-Year-Old Neolithic Sites. *Science*, 310(5750), 1016 LP-1018. <https://doi.org/10.1126/science.1118725>
- Haak, W., Lazaridis, I., Patterson, N., Rohland, N., Mallick, S., Llamas, B., ... Reich, D. (2015). Massive migration from the steppe was a source for Indo-European languages in Europe. *Nature*, 522, 207–211. Retrieved from <http://dx.doi.org/10.1038/nature14317>
- Hadjikoumis, A. (2012). Traditional pig herding practices in southwest Iberia: Questions of scale and zooarchaeological implications. *Journal of Anthropological Archaeology*, 31(3), 353–364. <https://doi.org/https://doi.org/10.1016/j.jaa.2012.02.002>
- Hagelberg, E., Sykes, B., & Hedges, R. (1989). Ancient bone DNA amplified. *Nature*, 342(6249), 485.
- Halley, D. J., & Rosvold, J. (2014). Stable isotope analysis and variation in medieval domestic pig husbandry practices in northwest Europe: absence of evidence for a purely herbivorous diet. *Journal of Archaeological Science*, 49, 1–5. <https://doi.org/https://doi.org/10.1016/j.jas.2014.04.006>
- Halstead, P., & Isaakidou, V. (2011). A pig fed by hand is worth two in the bush: ethnoarchaeology of pig husbandry in Greece and its archaeological implications. *Ethnozooarchaeology: The Present and Past of Human-Animal Relations*. Oxbow.
- Hamilton, J., Hedges, R. E. M., & Robinson, M. (2009). Rooting for pigfruit: pig feeding in Neolithic and Iron Age Britain compared. *Antiquity*, 83(322), 998–1011. <https://doi.org/DOI:10.1017/S0003598X00099300>
- Handley, L. L., Austin, A. T., Stewart, G. R., Robinson, D., Scrimgeour, C. M., Raven, J. A., ... Schmidt, S. (1999). The $\delta^{15}\text{N}$ natural abundance ($\delta^{15}\text{N}$) of ecosystem samples reflects measures of water availability. *Functional Plant Biology*, 26(2), 185–199. Retrieved from <https://doi.org/10.1071/PP98146>
- Handley, L. L., & Raven, J. A. (1992). The use of natural abundance of nitrogen isotopes in plant physiology and ecology. *Plant, Cell & Environment*, 15(9), 965–985. <https://doi.org/10.1111/j.1365-3040.1992.tb01650.x>
- Hansen, A. J., Willerslev, E., Wiuf, C., Mourier, T., & Arctander, P. (2001). Statistical Evidence for Mismatching Lesions in Ancient DNA Templates. *Molecular Biology and Evolution*, 18(2), 262–265. <https://doi.org/10.1093/oxfordjournals.molbev.a003800>
- Heaton, T. H. E. (1987). $^{15}\text{N}/^{14}\text{N}$ ratios of nitrate and ammonium in rain at Pretoria, South Africa. *Atmospheric Environment (1967)*, 21(4), 843–852. [https://doi.org/https://doi.org/10.1016/0004-6981\(87\)90080-1](https://doi.org/https://doi.org/10.1016/0004-6981(87)90080-1)
- Hebsgaard, M. B., Phillips, M. J., & Willerslev, E. (2005). Geologically ancient DNA: fact or artefact? *Trends in Microbiology*, 13(5), 212–220. <https://doi.org/https://doi.org/10.1016/j.tim.2005.03.010>
- Hedges, R. E. M. (2002). Bone diagenesis: an overview of processes. *Archaeometry*, 44(3), 319–328.
- Hedges, R. E. M. (2003). On bone collagen—apatite-carbonate isotopic relationships. *International Journal of Osteoarchaeology*, 13(1-2), 66–79. <https://doi.org/10.1002/oa.660>
- Hedges, R. E. M., Clement, J. G., Thomas, C. D. L., & O'Connell, T. C. (2007). Collagen turnover in the adult femoral mid-shaft: Modeled from anthropogenic radiocarbon tracer measurements. *American Journal of Physical Anthropology*, 133(2), 808–816. <https://doi.org/10.1002/ajpa.20598>
- Hedges, R. E. M., & Reynard, L. M. (2007). Nitrogen isotopes and the trophic level of

- humans in archaeology. *Journal of Archaeological Science*, 34(8), 1240–1251.
<https://doi.org/https://doi.org/10.1016/j.jas.2006.10.015>
- Heiri, O., Brooks, S. J., Renssen, H., Bedford, A., Hazekamp, M., Ilyashuk, B., ... Lotter, A. F. (2014). Validation of climate model-inferred regional temperature change for late-glacial Europe. *Nature Communications*, 5, 4914. Retrieved from
<https://doi.org/10.1038/ncomms5914>
- Herrscher, E., Goude, G., & Metz, L. (2017). Longitudinal Study of Stable Isotope Compositions of Maternal Milk and Implications for the Palaeo-Diet of Infants. *BMSAP*, 29(3–4), 131–139. Retrieved from <https://doi.org/10.1007/s13219-017-0190-4>
- Herrscher, E., & Le Bras-Goude, G. (2010). Southern French Neolithic populations: Isotopic evidence for regional specificities in environment and diet. *American Journal of Physical Anthropology*, 141(2), 259–272. <https://doi.org/10.1002/ajpa.21141>
- Higgins, D., Kaidonis, J., Townsend, G., Hughes, T., & Austin, J. J. (2013). Targeted sampling of cementum for recovery of nuclear DNA from human teeth and the impact of common decontamination measures. *Investigative Genetics*, 4(1), 18.
<https://doi.org/10.1186/2041-2223-4-18>
- Higuchi, R., Bowman, B., Freiberger, M., Ryder, O. A., & Wilson, A. C. (1984). DNA sequences from the quagga, an extinct member of the horse family. *Nature*, 312(5991), 282–284. <https://doi.org/10.1038/312282a0>
- Hill, P. A. (1998). Bone remodelling. *British Journal of Orthodontics*, 25(2), 101–107.
- Hodell, D. A., Quinn, R. L., Brenner, M., & Kamenov, G. (2004). Spatial variation of strontium isotopes ($^{87}\text{Sr}/^{86}\text{Sr}$) in the Maya region: a tool for tracking ancient human migration. *Journal of Archaeological Science*, 31(5), 585–601.
<https://doi.org/https://doi.org/10.1016/j.jas.2003.10.009>
- Hoefs, J. (n.d.). *Stable Isotope Geochemistry*, 3rd ed., Springer-Verlag, New York.
- Hofmanová, Z., Kreutzer, S., Hellenthal, G., Sell, C., Diekmann, Y., Díez-del-Molino, D., ... Burger, J. (2016). Early farmers from across Europe directly descended from Neolithic Aegeans. *Proceedings of the National Academy of Sciences*, 113(25), 6886 LP-6891. Retrieved from <http://www.pnas.org/content/113/25/6886.abstract>
- Hofreiter, M., Jaenicke, V., Serre, D., Haeseler, A. von, & Pääbo, S. (2001). DNA sequences from multiple amplifications reveal artifacts induced by cytosine deamination in ancient DNA. *Nucleic Acids Research*, 29(23), 4793–4799.
<https://doi.org/10.1093/nar/29.23.4793>
- Hofreiter, M., Serre, D., Poinar, H. N., Kuch, M., & Pääbo, S. (2001). Ancient DNA. *Nature Reviews Genetics*, 2(5), 353–359. <https://doi.org/10.1038/35072071>
- Hoppe, K. A., Koch, P. L., Carlson, R. W., & Webb, S. D. (1999). Tracking mammoths and mastodons: Reconstruction of migratory behavior using strontium isotope ratios. *Geology*, 27(5), 439–442. [https://doi.org/10.1130/0091-7613\(1999\)027<0439:TMAMRO>2.3.CO;2](https://doi.org/10.1130/0091-7613(1999)027<0439:TMAMRO>2.3.CO;2)
- Höss, M., Jaruga, P., Zastawny, T. H., Dizdaroglu, M., & Paabo, S. (1996). DNA Damage and DNA Sequence Retrieval from Ancient Tissues. *Nucleic Acids Research*, 24(7), 1304–1307. <https://doi.org/10.1093/nar/24.7.1304>
- Hut, G. (1987). Consultants' group meeting on stable isotope reference samples for geochemical and hydrological investigations. In *Consultants' group meeting on stable isotope reference samples for geochemical and hydrological investigations*. International Atomic Energy Agency (IAEA). Retrieved from
http://inis.iaea.org/search/search.aspx?orig_q=RN:18075746
- Ingman, M., Kaessmann, H., Pääbo, S., & Gyllensten, U. (2000). Mitochondrial genome variation and the origin of modern humans. *Nature*, 408, 708–713. Retrieved from
<https://doi.org/10.1038/35047064>
- Isern, N., Zilhão, J., Fort, J., & Ammerman, A. J. (2017). Modeling the role of voyaging in

- the coastal spread of the Early Neolithic in the West Mediterranean. *Proceedings of the National Academy of Sciences*, 114(5), 897 LP-902. Retrieved from <http://www.pnas.org/content/114/5/897.abstract>
- Jackes, M., & Alvim, P. (1999). Reconstructing Moita do Sebastião, the first step. In *Do Epipaleolítico ao Calcolítico na Península Ibérica*, Actas do IV Congresso de Arqueologia Peninsular, pp 13–25.
- Jim, S., Jones, V., Ambrose, S. H., & Evershed, R. P. (2006). Quantifying dietary macronutrient sources of carbon for bone collagen biosynthesis using natural abundance stable carbon isotope analysis. *British Journal of Nutrition*, 95(6), 1055–1062. <https://doi.org/DOI: 10.1079/BJN20051685>
- Juan-Cabanilles, J., & Oliver, B. M. (2017). Poblamiento y procesos culturales en la Península Ibérica del VII al V milenio AC. *SAGVNTVM Extra*, 5, 45–87.
- Kearse, M., Moir, R., Wilson, A., Stones-Havas, S., Cheung, M., Sturrock, S., ... Drummond, A. (2012). Geneious Basic: An integrated and extendable desktop software platform for the organization and analysis of sequence data. *Bioinformatics*, 28(12), 1647–1649. <https://doi.org/10.1093/bioinformatics/bts199>
- Keeling, C. D. (1961). A mechanism for cyclic enrichment of carbon-12 by terrestrial plants. *Geochimica et Cosmochimica Acta*, 24(3), 299–313. [https://doi.org/https://doi.org/10.1016/0016-7037\(61\)90024-2](https://doi.org/https://doi.org/10.1016/0016-7037(61)90024-2)
- Key, F. M., Posth, C., Krause, J., Herbig, A., & Bos, K. I. (2017). Mining Metagenomic Data Sets for Ancient DNA: Recommended Protocols for Authentication. *Trends in Genetics*, 33(8), 508–520. <https://doi.org/https://doi.org/10.1016/j.tig.2017.05.005>
- Kircher, M., Sawyer, S., & Meyer, M. (2012). Double indexing overcomes inaccuracies in multiplex sequencing on the Illumina platform. *Nucleic Acids Research*, 40(1), e3. <https://doi.org/10.1093/nar/gkr771>
- Knipper, C., Mittnik, A., Massy, K., Kociumaka, C., Kucukkalipci, I., Maus, M., ... Stockhammer, P. W. (2017). Female exogamy and gene pool diversification at the transition from the Final Neolithic to the Early Bronze Age in central Europe. *Proceedings of the National Academy of Sciences*, 114(38), 10083 LP-10088. <https://doi.org/10.1073/pnas.1706355114>
- Korneliussen, T. S., Albrechtsen, A., & Nielsen, R. (2014). ANGSD: Analysis of Next Generation Sequencing Data. *BMC Bioinformatics*, 15(1), 356. <https://doi.org/10.1186/s12859-014-0356-4>
- Krause, J., & Pääbo, S. (2016). Genetic Time Travel. *Genetics*, 203(1), 9 LP-12. <https://doi.org/10.1534/genetics.116.187856>
- Krings, M., Geisert, H., Schmitz, R. W., Krainitzki, H., & Pääbo, S. (1999). DNA sequence of the mitochondrial hypervariable region II from the Neandertal type specimen. *Proceedings of the National Academy of Sciences*, 96(10), 5581 LP-5585. <https://doi.org/10.1073/pnas.96.10.5581>
- Krokan, H. E., & Bjørås, M. (2013). Base Excision Repair. *Cold Spring Harbor Perspectives in Biology*, 5(4):a012583. Retrieved from <http://cshperspectives.cshlp.org/content/5/4/a012583.abstract>
- Krummen, M., Hilker, A. W., Juchelka, D., Duhr, A., Schlüter, H.-J., & Pesch, R. (2004). A new concept for isotope ratio monitoring liquid chromatography/mass spectrometry. *Rapid Communications in Mass Spectrometry*, 18(19), 2260–2266. <https://doi.org/10.1002/rcm.1620>
- Laborda, R. (2018). *El Neolítico antiguo en el Valle Medio del Ebro. Cerámica decorada y dataciones radiocarbónicas entre 5600-4800 cal BC*. University of Zaragoza, Doctoral Thesis.
- Larson, G., Albarella, U., Dobney, K., Rowley-Conwy, P., Schibler, J., Tresset, A., ... Cooper, A. (2007). Ancient DNA, pig domestication, and the spread of the Neolithic into

- Europe. *Proceedings of the National Academy of Sciences*, 104(39), 15276 LP-15281. <https://doi.org/10.1073/pnas.0703411104>
- Lazaridis, I., Nadel, D., Rollefson, G., Merrett, D. C., Rohland, N., Mallick, S., ... Reich, D. (2016). Genomic insights into the origin of farming in the ancient Near East. *Nature*, 536, 419–424. Retrieved from <http://dx.doi.org/10.1038/nature19310>
- Le Bras-Goude, G., Binder, D., Formicola, V., Duday, H., Couture-Veschambre, C., Hublin, J.-J., & Richards, M. (2006). Stratégies de subsistance et analyse culturelle de populations néolithiques de Ligurie: approche par l'étude isotopique ($\delta^{13}\text{C}$ et $\delta^{15}\text{N}$) des restes osseux. *Bulletins et Mémoires de La Société d'Anthropologie de Paris*, (18 (1-2)), 43–53.
- Le Bras-Goude, G., Binder, D., Zémour, A., & Richards, M. P. (2010). New radiocarbon dates and isotope analysis of Neolithic human and animal bone from the Fontbrégoua Cave (Salernes, Var, France). *Journal of Anthropological Sciences= Rivista Di Antropologia: JASS*, 88, 167–178.
- Lee-Thorp, J. A. (2008). On isotopes and old bones*. *Archaeometry*, 50(6), 925–950. <https://doi.org/10.1111/j.1475-4754.2008.00441.x>
- Lemmen, C., Gronenborn, D., & Wirtz, K. W. (2011). A simulation of the Neolithic transition in Western Eurasia. *Journal of Archaeological Science*, 38(12), 3459–3470. <https://doi.org/https://doi.org/10.1016/j.jas.2011.08.008>
- Li, H., & Durbin, R. (2009). Fast and accurate short read alignment with Burrows–Wheeler transform. *Bioinformatics*, 25(14), 1754–1760. <https://doi.org/10.1093/bioinformatics/btp324>
- Li, H., Handsaker, B., Wysoker, A., Fennell, T., Ruan, J., Homer, N., ... Subgroup, 1000 Genome Project Data Processing. (2009). The Sequence Alignment/Map format and SAMtools. *Bioinformatics*, 25(16), 2078–2079. <https://doi.org/10.1093/bioinformatics/btp352>
- Lidén, K., Eriksson, G., Nordqvist, B., Götherström, A., & Bendixen, E. (2004). “The wet and the wild followed by the dry and the tame” – or did they occur at the same time? Diet in Mesolithic – Neolithic southern Sweden. *Antiquity*, 78(299), 23–33. <https://doi.org/DOI:10.1017/S0003598X00092899>
- Liden, K., Takahashi, C., & Nelson, D. E. (1995). The Effects of Lipids in Stable Carbon Isotope Analysis and the Effects of NaOH Treatment on the Composition of Extracted Bone Collagen. *Journal of Archaeological Science*, 22(2), 321–326. <https://doi.org/https://doi.org/10.1006/jasc.1995.0034>
- Lillie, M., Budd, C., & Potekhina, I. (2011). Stable isotope analysis of prehistoric populations from the cemeteries of the Middle and Lower Dnieper Basin, Ukraine. *Journal of Archaeological Science*, 38(1), 57–68. <https://doi.org/https://doi.org/10.1016/j.jas.2010.08.010>
- Lillie, M. C., & Richards, M. (2000). Stable Isotope Analysis and Dental Evidence of Diet at the Mesolithic–Neolithic Transition in Ukraine. *Journal of Archaeological Science*, 27(10), 965–972. <https://doi.org/https://doi.org/10.1006/jasc.1999.0544>
- Lindahl, T. (1993). Instability and decay of the primary structure of DNA. *Nature*, 362(6422), 709–715.
- Lipson, M., Szécsényi-Nagy, A., Mallick, S., Pósa, A., Stégmár, B., Keerl, V., ... Reich, D. (2017). Parallel palaeogenomic transects reveal complex genetic history of early European farmers. *Nature*, 551, 368–372. Retrieved from <http://dx.doi.org/10.1038/nature24476>
- Llorente, M. G., Jones, E. R., Eriksson, A., Siska, V., Arthur, K. W., Arthur, J. W., ... Manica, A. (2015). Ancient Ethiopian genome reveals extensive Eurasian admixture in Eastern Africa. *Science*, 350(6262), 820 LP-822. <https://doi.org/10.1126/science.aad2879>

- Longin, R. (1971). New Method of Collagen Extraction for Radiocarbon Dating. *Nature*, 230(5291), 241–242. <https://doi.org/10.1038/230241a0>
- López-Costas, O., Müldner, G., & Martínez Cortizas, A. (2015). Diet and lifestyle in Bronze Age Northwest Spain: the collective burial of Cova do Santo. *Journal of Archaeological Science*, 55, 209–218. <https://doi.org/https://doi.org/10.1016/j.jas.2015.01.009>
- López-García, P., & López-Sáez, J. A. (2000). Le paysage et la phase Épipaléolithique-Mésolithique dans les Pré-Pyrénées Aragonaises et le Bassin Moyen de l'Èbre à partir de l'analyse palynologique. In *Les derniers chasseurs-cueilleurs d'Europe occidentale (13000–5500 av. J.-C.): Actes du colloque international de Besançon, 23–25 October 1998* (pp. 59–69).
- López, P. (1992). Análisis polínicos de cuatro yacimientos arqueológicos situados en el Bajo Aragón. In *Aragón-litoral Mediterráneo: intercambios culturales durante la prehistoria: en homenaje a Juan Maluquer de Motes* (pp. 235–242). Institución Fernando el Católico.
- Lubell, D., Jackes, M., Schwarcz, H., Knyf, M., & Meiklejohn, C. (1994). The Mesolithic-Neolithic transition in Portugal: isotopic and dental evidence of diet. *Journal of Archaeological Science*, 21, 201–216.
- Sampietro, M.L., Caramelli, D., Lari, M., Pou, R., Martí, M., ... Lalueza-Fox, C. (2007). Palaeogenetic evidence supports a dual model of Neolithic spreading into Europe. *Proceedings of the Royal Society B: Biological Sciences*, 274(1622), 2161–2167. <https://doi.org/10.1098/rspb.2007.0465>
- Macdonald, D. W., & Barrett, P. (1993). *Mammals of Britain & Europe*. HarperCollins.
- Madgwick, R., Mulville, J., & Stevens, R. E. (2012). Diversity in foddering strategy and herd management in late Bronze Age Britain: An isotopic investigation of pigs and other fauna from two midden sites. *Environmental Archaeology*, 17(2), 126–140. <https://doi.org/10.1179/1461410312Z.00000000011>
- Makarewicz, C. A., & Sealy, J. (2015). Dietary reconstruction, mobility, and the analysis of ancient skeletal tissues: Expanding the prospects of stable isotope research in archaeology. *Journal of Archaeological Science*, 56, 146–158. <https://doi.org/https://doi.org/10.1016/j.jas.2015.02.035>
- Mallick, S., Li, H., Lipson, M., Mathieson, I., Gymrek, M., Racimo, F., ... Reich, D. (2016). The Simons Genome Diversity Project: 300 genomes from 142 diverse populations. *Nature*, 538, 201–206. Retrieved from <http://dx.doi.org/10.1038/nature18964>
- Manen, C. (2007). La production céramique de Pont de Roque-Haute : synthèse et comparaisons. In J. D. Guilaine, J., Manen, C., Vigne (Ed.), *Pont de Roque-Haute (Portiragnes, Hérault). Nouveaux regards sur la néolithisation de la France méditerranéenne* (Archives d, pp. 151–166). Toulouse.
- Manning, K., Timpson, A., Colledge, S., Crema, E., Edinborough, K., Kerig, T., & Shennan, S. (2014). The chronology of culture: a comparative assessment of European Neolithic dating approaches. *Antiquity*, 88(342), 1065–1080. <https://doi.org/DOI:10.1017/S0003598X00115327>
- Mannino, M. A., Catalano, G., Talamo, S., Mannino, G., Di Salvo, R., Schimmenti, V., ... Sineo, L. (2012). Origin and Diet of the Prehistoric Hunter-Gatherers on the Mediterranean Island of Favignana (Ègadi Islands, Sicily). *PLoS ONE*, 7(11), 1–12. Retrieved from <http://10.0.5.91/journal.pone.0049802>
- Mannino, M. A., Salvo, R. Di, Schimmenti, V., Patti, C. Di, Incarbona, A., Sineo, L., & Richards, M. P. (2011). Upper Palaeolithic hunter-gatherer subsistence in Mediterranean coastal environments: an isotopic study of the diets of the earliest directly-dated humans from Sicily. *Journal of Archaeological Science*, 38(11), 3094–3100. <https://doi.org/https://doi.org/10.1016/j.jas.2011.07.009>
- Maricic, T., Whitten, M., & Pääbo, S. (2010). Multiplexed DNA Sequence Capture of Mitochondrial Genomes Using PCR Products. *PLOS ONE*, 5(11), e14004. Retrieved

- from <https://doi.org/10.1371/journal.pone.0014004>
- Marino, B. D., & McElroy, M. B. (1991). Isotopic composition of atmospheric CO₂ inferred from carbon in C₄ plant cellulose. *Nature*, *349*(6305), 127–131. <https://doi.org/10.1038/349127a0>
- Mariotti, A. (1983). Atmospheric nitrogen is a reliable standard for natural ¹⁵N abundance measurements. *Nature*, *303*(5919), 685–687. <https://doi.org/10.1038/303685a0>
- Martín-Socas, D., Camalich Massieu, M. D., Herrero, J. L. C., & Rodríguez-Santos, F. J. (2018). The beginning of the Neolithic in Andalusia. *Quaternary International*, *470*, 451–471. <https://doi.org/https://doi.org/10.1016/j.quaint.2017.06.057>
- Martin, R. B., Burr, D. B., Sharkey, N. A., & Fyhrie, D. P. (1998). *Skeletal tissue mechanics* (Vol. 190). Springer.
- Martínez-Moreno, J., & Mora, R. (2009). Balma Guilanyà (Prepirineo de Lleida) y el Aziliense en el noreste de la Península Ibérica. *Trabajos de Prehistoria*, *66*(2), 45–60.
- Martínez, P. A., & Catalán, M. P. (1997). *El Neolítico y Calcolítico de la Cueva de Nerja en el contexto andaluz*. Patronato de la Cueva de Nerja.
- Martiniano, R., Cassidy, L. M., Ó'Maoldúin, R., McLaughlin, R., Silva, N. M., Manco, L., ... Bradley, D. G. (2017). The population genomics of archaeological transition in west Iberia: Investigation of ancient substructure using imputation and haplotype-based methods. *PLoS Genetics*, *13*(7), e1006852. Retrieved from <https://doi.org/10.1371/journal.pgen.1006852>
- Martins, H., Oms, F. X., Pereira, L., Pike, A. W. G., Rowsell, K., & Zilhão, J. (2015). Radiocarbon dating the beginning of the Neolithic in Iberia: new results, new problems. *Journal of Mediterranean Archaeology*, *28*(1), 105–131.
- Martzluff, M., Moreno, J. M., Guilaine, J., Mora, R., & Casanova, J. (2012). Transformaciones culturales y cambios climáticos en los Pirineos catalanes entre el Tardiglacial y Holoceno antiguo: Aziliense y Sauveterriense en Balma de la Margineda y Balma Guilanyà. *Cuaternario y Geomorfología*, *26*(3–4), 61–78.
- Masset, C. (1993). Les dolmens: Sociétés néolithiques, pratiques funéraires. *Editions Errance, Paris*.
- Mathieson, I., Alpaslan-Roodenberg, S., Posth, C., Szécsényi-Nagy, A., Rohland, N., Mallick, S., ... Reich, D. (2018). The genomic history of southeastern Europe. *Nature*, *555*, 197–203. Retrieved from <http://dx.doi.org/10.1038/nature25778>
- Mathieson, I., Lazaridis, I., Rohland, N., Mallick, S., Patterson, N., Roodenberg, S. A., ... Reich, D. (2015). Genome-wide patterns of selection in 230 ancient Eurasians. *Nature*, *528*, 499–503. Retrieved from <http://dx.doi.org/10.1038/nature16152>
- Mazzarello, P. (1999). A unifying concept: the history of cell theory. *Nature Cell Biology*, *1*(1), E13–E15. <https://doi.org/10.1038/8964>
- Mazzucco, N., Clemente-Conte, I., Gassiot, E., & Gibaja, J. F. (2015). Insights into the economic organization of the first agro-pastoral communities of the NE of the Iberian Peninsula: A traceological analysis of the Cueva de Chaves flaked stone assemblage. *Journal of Archaeological Science: Reports*, *2*, 353–366. <https://doi.org/https://doi.org/10.1016/j.jasrep.2015.02.010>
- Mazzucco, N., & Gibaja, J. F. (2018). A palaeoeconomic perspective on the Early Neolithic lithic assemblages of the N–NE of the Iberian Peninsula. *Quaternary International*, *472*, 236–245. <https://doi.org/https://doi.org/10.1016/j.quaint.2016.05.012>
- McArthur, J. M., Howarth, R. J., & Bailey, T. R. (2001). Strontium Isotope Stratigraphy: LOWESS Version 3: Best Fit to the Marine Sr-Isotope Curve for 0–509 Ma and Accompanying Look-up Table for Deriving Numerical Age. *The Journal of Geology*, *109*(2), 155–170. <https://doi.org/10.1086/319243>
- McClure, S. B., García, O., Roca de Togores, C., Culleton, B. J., & Kennett, D. J. (2011). Osteological and paleodietary investigation of burials from Cova de la Pastora, Alicante,

- Spain. *Journal of Archaeological Science*, 38(2), 420–428.
<https://doi.org/https://doi.org/10.1016/j.jas.2010.09.023>
- Menozzi, P., Piazza, A., & Cavalli-Sforza, L. (1978). Synthetic maps of human gene frequencies in Europeans. *Science*, 201(4358), 786 LP-792.
<https://doi.org/10.1126/science.356262>
- Meyer, M., Arsuaga, J.-L., de Filippo, C., Nagel, S., Aximu-Petri, A., Nickel, B., ... Pääbo, S. (2016). Nuclear DNA sequences from the Middle Pleistocene Sima de los Huesos hominins. *Nature*, 531, 504–507. Retrieved from <https://doi.org/10.1038/nature17405>
- Meyer, M., & Kircher, M. (2010). Illumina Sequencing Library Preparation for Highly Multiplexed Target Capture and Sequencing. *Cold Spring Harbor Protocols*, 2010(6), pdb.prot5448. <https://doi.org/10.1101/pdb.prot5448>
- Meyer, M., Kircher, M., Gansauge, M.-T., Li, H., Racimo, F., Mallick, S., ... Pääbo, S. (2012). A High-Coverage Genome Sequence from an Archaic Denisovan Individual. *Science*, 338(6104), 222 LP-226. <https://doi.org/10.1126/science.1224344>
- Minagawa, M., & Wada, E. (1984). Stepwise enrichment of $\delta^{15}\text{N}$ along food chains: Further evidence and the relation between $\delta^{15}\text{N}$ and animal age. *Geochimica et Cosmochimica Acta*, 48(5), 1135–1140. [https://doi.org/https://doi.org/10.1016/0016-7037\(84\)90204-7](https://doi.org/https://doi.org/10.1016/0016-7037(84)90204-7)
- Monroy Kuhn, J. M., Jakobsson, M., & Günther, T. (2018). Estimating genetic kin relationships in prehistoric populations. *PLOS ONE*, 13(4), e0195491. Retrieved from <https://doi.org/10.1371/journal.pone.0195491>
- Montes, L., & Domingo, R. (2014). La ocupación de las Sierras Exteriores durante el Calcolítico. *La Peña de Las Forcas (Graus, Huesca). Un Asentamiento Estratégico En La Confluencia Del Ésera y El Isábena. Monografías Arqueológicas/Prehistoria*, 46, 409–426.
- Montes, L., Domingo, R., González-Sampériz, P., Sebastián, M., Aranbarri, J., Castaños, P., ... Laborda, R. (2016). Landscape, resources and people during the Mesolithic and Neolithic times in NE Iberia: The Arba de Biel Basin. *Quaternary International*, 403, 133–150. <https://doi.org/https://doi.org/10.1016/j.quaint.2015.05.041>
- Montgomery, J., & Evans, J. (2006). *Immigrants on the Isle of Lewis: combined traditional funerary and modern isotope evidence to investigate social differentiation, migration and dietary changes in the Outer Hebrides*. Oxbow Books.
- Moore, J. W., & Semmens, B. X. (2008). Incorporating uncertainty and prior information into stable isotope mixing models. *Ecology Letters*, 11(5), 470–480.
<https://doi.org/10.1111/j.1461-0248.2008.01163.x>
- Morales, J. I., & Oms, F. X. (2012). Las últimas evidencias mesolíticas del NE peninsular y el vacío pre-neolítico. *Rubricatum: Revista Del Museu de Gavà*, (5), 35–42.
- Müldner, G., & Richards, M. P. (2005). Fast or feast: reconstructing diet in later medieval England by stable isotope analysis. *Journal of Archaeological Science*, 32(1), 39–48.
<https://doi.org/https://doi.org/10.1016/j.jas.2004.05.007>
- Müller, W., Fricke, H., Halliday, A. N., McCulloch, M. T., & Wartho, J.-A. (2003). Origin and Migration of the Alpine Iceman. *Science*, 302(5646), 862 LP-866.
<https://doi.org/10.1126/science.1089837>
- Mullis, K. B., & Faloona, F. A. B. T.-M. in E. (1987). Specific synthesis of DNA in vitro via a polymerase-catalyzed chain reaction. In *Recombinant DNA Part F* (Vol. 155, pp. 335–350). Academic Press. [https://doi.org/https://doi.org/10.1016/0076-6879\(87\)55023-6](https://doi.org/https://doi.org/10.1016/0076-6879(87)55023-6)
- Munoz, A. M. (1965). *Cultura neolítica catalana de los "Sepulcros de Fosa"*. Publicaciones eventuales.
- Nair, A. K., Gautieri, A., Chang, S.-W., & Buehler, M. J. (2013). Molecular mechanics of mineralized collagen fibrils in bone. *Nature Communications*, 4, 1724. Retrieved from <https://doi.org/10.1038/ncomms2720>
- Navarrete, V., Colonese, A. C., Tornero, C., Antolín, F., Von Tersch, M., Eulàlia Subirà, M.,

- ... Saña, M. (2017). Feeding Management Strategies among the Early Neolithic Pigs in the NE of the Iberian Peninsula. *International Journal of Osteoarchaeology*, 27(5), 839–852. <https://doi.org/10.1002/oa.2598>
- Nielsen-Marsh, C. M., & Hedges, R. E. M. (2000). Patterns of Diagenesis in Bone I: The Effects of Site Environments. *Journal of Archaeological Science*, 27(12), 1139–1150. <https://doi.org/https://doi.org/10.1006/jasc.1999.0537>
- O’Connell, T. C., Kneale, C. J., Tasevska, N., & Kuhnle, G. G. C. (2012). The diet-body offset in human nitrogen isotopic values: A controlled dietary study. *American Journal of Physical Anthropology*, 149(3), 426–434. <https://doi.org/10.1002/ajpa.22140>
- O’Leary, M. H. (1981). Carbon isotope fractionation in plants. *Phytochemistry*, 20(4), 553–567. [https://doi.org/https://doi.org/10.1016/0031-9422\(81\)85134-5](https://doi.org/https://doi.org/10.1016/0031-9422(81)85134-5)
- O’Leary, M. H. (1988). Carbon isotopes in photosynthesis. *Bioscience*, 38(5), 328–336.
- Obermaier, H. (1925). El Hombre Fósil. *Comisión de Investigaciones Paleontológicas y Prehistóricas, J. A. E.*
- Olalde, I., Allentoft, M. E., Sánchez-Quinto, F., Santpere, G., Chiang, C. W. K., DeGiorgio, M., ... Lalueza-Fox, C. (2014). Derived immune and ancestral pigmentation alleles in a 7,000-year-old Mesolithic European. *Nature*, 507, 225–228. Retrieved from <http://dx.doi.org/10.1038/nature12960>
- Olalde, I., Brace, S., Allentoft, M. E., Armit, I., Kristiansen, K., Booth, T., ... Reich, D. (2018). The Beaker phenomenon and the genomic transformation of northwest Europe. *Nature*, 555, 190–196. Retrieved from <http://dx.doi.org/10.1038/nature25738>
- Olalde, I., Mallick, S., Patterson, N., Rohland, N., Villalba-Mouco, V., Silva, M., ... Reich, D. (2019). The genomic history of the Iberian Peninsula over the past 8000 years. *Science*, 363(6432), 1230 LP-1234. <https://doi.org/10.1126/science.aav4040>
- Olalde, I., Schroeder, H., Sandoval-Velasco, M., Vinner, L., Lobón, I., Ramirez, O., ... Lalueza-Fox, C. (2015). A Common Genetic Origin for Early Farmers from Mediterranean Cardial and Central European LBK Cultures. *Molecular Biology and Evolution*, 32(12), 3132–3142. Retrieved from <http://dx.doi.org/10.1093/molbev/msv181>
- Oms, F. X. (2017). *La neolitització del nord-est de la península Ibèrica* (2017th ed.). Barcelona: Societat Catalana d’Arqueologia.
- Oms, F. X., Cebrià, A., Morales, J. I., & Pedro, M. (2015). Una inhumació cardial a la cova Foradada (Calafell, Baix Penedès)? *Jornades d’Arqueologia Del Penedès*, 59–64.
- Oms, F. X., Daura, J., Sanz, M., Mendiola, S., Pedro, M., & Martínez, P. (2017). First Evidence of Collective Human Inhumation from the Cardial Neolithic (Cova Bonica, Barcelona, NE Iberian Peninsula). *Journal of Field Archaeology*, 42(1), 43–53. <https://doi.org/10.1080/00934690.2016.1260407>
- Oms, F. X., Esteve, X., Mestres, J., Martín, P., & Martins, H. (2014). La neolitización del nordeste de la Península Ibérica: datos radiocarbónicos y culturales de los asentamientos al aire libre del Penedès. *Trabajos de Prehistoria*, 71(1), 42–55.
- Oms, F. X., García, J. M. L., Llach, X. M., Martín, P., Mendiola, S., Morales, J. I., ... Gómez, M. Y. (2013). Hàbitat en cova i espai pels ramats ca. 6200-6000 BP: dades preliminars de la Cova Colomera (Prepirineu de Lleida) durant el neolític antic. *Saguntum: Papeles Del Laboratorio de Arqueología de Valencia*, (45), 25–38.
- Orlando, L., Ginolhac, A., Zhang, G., Froese, D., Albrechtsen, A., Stiller, M., ... Willerslev, E. (2013). Recalibrating Equus evolution using the genome sequence of an early Middle Pleistocene horse. *Nature*, 499, 74–78. Retrieved from <https://doi.org/10.1038/nature12323>
- Otero, N., Vitòria, L., Soler, A., & Canals, A. (2005). Fertiliser characterisation: Major, trace and rare earth elements. *Applied Geochemistry*, 20(8), 1473–1488. <https://doi.org/https://doi.org/10.1016/j.apgeochem.2005.04.002>
- Pääbo, S. (1985). Molecular cloning of Ancient Egyptian mummy DNA. *Nature*, 314(6012),

- 644–645. <https://doi.org/10.1038/314644a0>
- Pääbo, S. (1989). Ancient DNA: extraction, characterization, molecular cloning, and enzymatic amplification. *Proceedings of the National Academy of Sciences*, 86(6), 1939 LP-1943. <https://doi.org/10.1073/pnas.86.6.1939>
- Patterson, N., Moorjani, P., Luo, Y., Mallick, S., Rohland, N., Zhan, Y., ... Reich, D. (2012). Ancient Admixture in Human History. *Genetics*, 192(3), 1065–1093. <https://doi.org/10.1534/genetics.112.145037>
- Patterson, N., Price, A. L., & Reich, D. (2006). Population Structure and Eigenanalysis. *PLOS Genetics*, 2(12), e190. Retrieved from <https://doi.org/10.1371/journal.pgen.0020190>
- Peltenburg, E., Colledge, S., Croft, P., Jackson, A., McCartney, C., & Murray, M. A. (2000). Agro-pastoralist colonization of Cyprus in the 10th millennium BP: initial assessments. *Antiquity*, 74(286), 844–853. <https://doi.org/DOI:10.1017/S0003598X0006049X>
- Peltzer, A., Jäger, G., Herbig, A., Seitz, A., Kniep, C., Krause, J., & Nieselt, K. (2016). EAGER: efficient ancient genome reconstruction. *Genome Biology*, 17(1), 60. <https://doi.org/10.1186/s13059-016-0918-z>
- Pérez-Romero, A., Iriarte, E., Galindo-Pellicena, M. Á., García-González, R., Rodríguez, L., Castilla, M., ... Carretero, J.-M. (2017). An unusual Pre-bell beaker copper age cave burial context from El Portalón de Cueva Mayor site (Sierra de Atapuerca, Burgos). *Quaternary International*, 433, 142–155. <https://doi.org/https://doi.org/10.1016/j.quaint.2015.06.063>
- Pérez, M. S. H. (2016). Arte Macroesquemático vs. Arte Esquemático. Reflexiones en torno a una relación intuitiva. In *Del neolític a l'edat de bronze en el Mediterrani occidental: Estudis en homenatge a Bernat Martí Oliver* (pp. 481–490). Museu de Prehistòria de València.
- Perrin, T., Marchand, G., Allard, P., Binder, D. (2009). Le second Mésoolithique d'Europe occidentale : origines et gradient chronologique. In *Fondation Fyssen, Annales 24* (pp. 162–172).
- Perrin, T., & Binder, D. (2011). Le Mésoolithique à trapèzes et la néolithisation de l'Europe sud-occidentale. In *La transition néolithique en Méditerranée. Actes du colloque Transitions en Méditerranée, ou comment des chasseurs devinrent agriculteurs, Muséum de Toulouse* (pp. 271–281). Errance et Archives d'Ecologie Préhistorique.
- Perrin, T., & Defranould, E. (2016). The Montclus rock shelter (Gard) and the continuity hypothesis between 1st and 2nd Mesolithic in Southern France. *Quaternary International*, 423, 230–241. <https://doi.org/https://doi.org/10.1016/j.quaint.2015.09.046>
- Perrin, T., Manen, C., Valdeyron, N., & Guilaine, J. (2018). Beyond the sea... The Neolithic transition in the southwest of France. *Quaternary International*, 470, 318–332. <https://doi.org/https://doi.org/10.1016/j.quaint.2017.05.027>
- Phillips, D. L., & Gregg, J. W. (2003). Source partitioning using stable isotopes: coping with too many sources. *Oecologia*, 136(2), 261–269. <https://doi.org/10.1007/s00442-003-1218-3>
- Pin, C., Briot, D., Bassin, C., & Poitrasson, F. (1994). Concomitant separation of strontium and samarium-neodymium for isotopic analysis in silicate samples, based on specific extraction chromatography. *Analytica Chimica Acta*, 298(2), 209–217. [https://doi.org/https://doi.org/10.1016/0003-2670\(94\)00274-6](https://doi.org/https://doi.org/10.1016/0003-2670(94)00274-6)
- Pinhasi, R., Fernandes, D., Sirak, K., Novak, M., Connell, S., Alpaslan-Roodenberg, S., ... Hofreiter, M. (2015). Optimal Ancient DNA Yields from the Inner Ear Part of the Human Petrous Bone. *PLOS ONE*, 10(6), e0129102. Retrieved from <https://doi.org/10.1371/journal.pone.0129102>
- Posth, C., Nägele, K., Colleran, H., Valentin, F., Bedford, S., Kami, K. W., ... Powell, A. (2018). Language continuity despite population replacement in Remote Oceania. *Nature Ecology & Evolution*, 2(4), 731–740. <https://doi.org/10.1038/s41559-018-0498-2>

- Posth, C., Renaud, G., Mittnik, A., Drucker, D. G., Rougier, H., Cupillard, C., ... Krause, J. (2016). Pleistocene Mitochondrial Genomes Suggest a Single Major Dispersal of Non-Africans and a Late Glacial Population Turnover in Europe. *Current Biology*, 26(6), 827–833. <https://doi.org/https://doi.org/10.1016/j.cub.2016.01.037>
- Poszwa, A., Dambrine, E., Ferry, B., Pollier, B., & Loubet, M. (2002). Do deep tree roots provide nutrients to the tropical rainforest? *Biogeochemistry*, 60(1), 97–118. <https://doi.org/10.1023/A:1016548113624>
- Poznik, G. D. (2016). Identifying Y-chromosome haplogroups in arbitrarily large samples of sequenced or genotyped men. *BioRxiv*. Retrieved from <http://biorxiv.org/content/early/2016/11/19/088716.abstract>
- Price, T. D., Bentley, R. A., Lüning, J., Gronenborn, D., & Wahl, J. (2001). Prehistoric human migration in the Linearbandkeramik of Central Europe. *Antiquity*, 75(289), 593–603. <https://doi.org/DOI: 10.1017/S0003598X00088827>
- Price, T. D., Blitz, J., Burton, J., & Ezzo, J. A. (1992). Diagenesis in prehistoric bone: Problems and solutions. *Journal of Archaeological Science*, 19(5), 513–529. [https://doi.org/https://doi.org/10.1016/0305-4403\(92\)90026-Y](https://doi.org/https://doi.org/10.1016/0305-4403(92)90026-Y)
- Price, T. D., Burton, J. H., & Bentley, R. A. (2002). The Characterization of Biologically Available Strontium Isotope Ratios for the Study of Prehistoric Migration. *Archaeometry*, 44(1), 117–135. <https://doi.org/10.1111/1475-4754.00047>
- Privat, K. L., O'connell, T. C., & Richards, M. P. (2002). Stable Isotope Analysis of Human and Faunal Remains from the Anglo-Saxon Cemetery at Berinsfield, Oxfordshire: Dietary and Social Implications. *Journal of Archaeological Science*, 29(7), 779–790. <https://doi.org/https://doi.org/10.1006/jasc.2001.0785>
- Prüfer, K., Racimo, F., Patterson, N., Jay, F., Sankararaman, S., Sawyer, S., ... Pääbo, S. (2013). The complete genome sequence of a Neanderthal from the Altai Mountains. *Nature*, 505, 43. Retrieved from <https://doi.org/10.1038/nature12886>
- Puchol, O. G., Balaguer, L. M., Tortosa, J. E. A., & Aubán, J. B. (2009). From the Mesolithic to the Neolithic on the Mediterranean Coast of the Iberian Peninsula. *Journal of Anthropological Research*, 65(2), 237–251. <https://doi.org/10.3998/jar.0521004.0065.205>
- Quintana, F. J., & Velasco, J. A. F.-T. (1994). Los arpones azilienses de la cueva de los Azules (Cangas de Onís, Asturias). In *Homenaje al Dr. Joaquín González Echegaray* (pp. 87–96). Dirección General de Bellas Artes y Archivos.
- Rau, G. (1978). Carbon-13 Depletion in a Subalpine Lake: Carbon Flow Implications. *Science*, 201(4359), 901 LP-902. <https://doi.org/10.1126/science.201.4359.901>
- Reich, D., Thangaraj, K., Patterson, N., Price, A. L., & Singh, L. (2009). Reconstructing Indian population history. *Nature*, 461, 489. Retrieved from <https://doi.org/10.1038/nature08365>
- Reimer, P. J., Bard, E., Bayliss, A., Beck, J. W., Blackwell, P. G., Ramsey, C. B., ... van der Plicht, J. (2013). IntCal13 and Marine13 Radiocarbon Age Calibration Curves 0–50,000 Years cal BP. *Radiocarbon*, 55(4), 1869–1887. https://doi.org/DOI: 10.2458/azu_js_rc.55.16947
- Remolins, G., Gibaja, J. F., Allié, F., Fontanals, M., Martin, P., Masclans, A., ... Llovera, X. (2016). The Neolithic Necropolis of La Feixa del Moro (Juberri, Andorra): New data on the first farming communities in the Pyrenees. *Comptes Rendus Palevol*, 15(5), 537–554. <https://doi.org/https://doi.org/10.1016/j.crpv.2015.11.005>
- Richards, M. P., Fuller, B. T., & Molleson, T. I. (2006). Stable isotope palaeodietary study of humans and fauna from the multi-period (Iron Age, Viking and Late Medieval) site of Newark Bay, Orkney. *Journal of Archaeological Science*, 33(1), 122–131. <https://doi.org/https://doi.org/10.1016/j.jas.2005.07.003>
- Richards, M. P., & Hedges, R. E. M. (2003). Variations in bone collagen $\delta^{13}\text{C}$ and $\delta^{15}\text{N}$

- values of fauna from Northwest Europe over the last 40 000 years. *Palaeogeography, Palaeoclimatology, Palaeoecology*, 193(2), 261–267.
[https://doi.org/https://doi.org/10.1016/S0031-0182\(03\)00229-3](https://doi.org/10.1016/S0031-0182(03)00229-3)
- Richards, M. P., Pettitt, P. B., Trinkaus, E., Smith, F. H., Paunović, M., & Karavanić, I. (2000). Neanderthal diet at Vindija and Neanderthal predation: The evidence from stable isotopes. *Proceedings of the National Academy of Sciences*, 97(13), 7663 LP-7666.
<https://doi.org/10.1073/pnas.120178997>
- Rizzi, E., Lari, M., Gigli, E., De Bellis, G., & Caramelli, D. (2012). Ancient DNA studies: new perspectives on old samples. *Genetics Selection Evolution*, 44(1), 21.
<https://doi.org/10.1186/1297-9686-44-21>
- Roebroeks, W. (1999). *Hunters of the Golden Age: The Mid Upper Palaeolithic of Eurasia, 30,000-20,000 BP* (Vol. 31). University of Leiden.
- Rohland, N., Harney, E., Mallick, S., Nordenfelt, S., & Reich, D. (2015). Partial uracil–DNA–glycosylase treatment for screening of ancient DNA. *Philosophical Transactions of the Royal Society B: Biological Sciences*, 370(1660). Retrieved from
<http://rstb.royalsocietypublishing.org/content/370/1660/20130624.abstract>
- Rohland, N., & Hofreiter, M. (2007). Ancient DNA extraction from bones and teeth. *Nature Protocols*, 2, 1756. Retrieved from <https://doi.org/10.1038/nprot.2007.247>
- Rojo-Guerra, M. A., García-Martínez de Lagrán, Í., & Royo-Guillén, J. I. (2018). The beginning of the Neolithic in the mid-Ebro valley and in Iberia’s Inland (Northern and Southern submeseta), Spain. *Quaternary International*, 470, 398–438.
<https://doi.org/https://doi.org/10.1016/j.quaint.2017.12.037>
- Rojo-Guerra, M. A., Garrido-Pena, R., Tejedor Rodríguez, C., García Martínez de Lagrán, Í., & Alt, K. W. (2015). El tiempo y los ritos de los antepasados: La Mina y El Alto del Reinoso, novedades sobre el megalitismo en la Cuenca del Duero. *Arpi. Arqueología y Prehistoria Del Interior Peninsular*, 3, 133–147.
- Rojo-Guerra, M. A., Kunst, M., Garrido-Pena, R., & de Lagrán, E. I. G. (2006). La Neolitización de la Meseta Norte a la luz del C-14: análisis de 47 dataciones absolutas inéditas de dos yacimientos domésticos del Valle de Ambrona, Soria, España. *Archivo de Prehistoria Levantina*, 26, 39–100.
- Roman-Monroig, D. (2012). Nouveautés sur la séquence du Pléistocène final et l’Holocène initial dans le versant méditerranéen de la péninsule Ibérique à travers l’industrie lithique. *L’Anthropologie*, 116(5), 665–679.
<https://doi.org/https://doi.org/10.1016/j.anthro.2012.09.002>
- Royo, J. I. (1987). El poblado y necrópolis neolíticos del Barranco de la Mina Vallfera, Mequinzenza (Zaragoza). Campaña de 1985. *Arqueología Aragonesa 1985*, 27–29.
- Salazar-García, D. C. (2009). Estudio de la dieta en la población neolítica de Costamar. Resultados preliminares de análisis de isótopos estables de Carbono y Nitrógeno. *Monografies de Prehistòria i Arqueologia Castellonenques*, 8, 411–418.
- Salazar-García, D. C., Aura, J. E., Olària, C. R., Talamo, S., Morales, J. V., & Richards, M. P. (2014). Isotope evidence for the use of marine resources in the Eastern Iberian Mesolithic. *Journal of Archaeological Science*, 42, 231–240.
<https://doi.org/https://doi.org/10.1016/j.jas.2013.11.006>
- Salazar-García, D. C., Fontanals-Coll, M., Goude, G., & Subirà, M. E. (2018). “To ‘seafood’ or not to ‘seafood’?” An isotopic perspective on dietary preferences at the Mesolithic–Neolithic transition in the Western Mediterranean. *Quaternary International*, 470, 497–510. <https://doi.org/https://doi.org/10.1016/j.quaint.2017.12.039>
- Salazar-García, D. C., García-Puchol, O., de Miguel-Ibáñez, M. P., & Talamo, S. (2016). Earliest Evidence of Neolithic Collective Burials from Eastern Iberia: Radiocarbon Dating at the Archaeological Site of Les Llometes (Alicante, Spain). *Radiocarbon*, 58(3), 679–692. <https://doi.org/DOI:10.1017/RDC.2016.34>

- Salazar-García, D. C., Pérez-Ripoll, M., García-Borja, P., Jordá Pardo, J. F., & Aura Tortosa, J. E. (2017). A Terrestrial Diet Close to the Coast: A Case Study from the Neolithic Levels of Nerja Cave (Málaga, Spain) BT - Times of Neolithic Transition along the Western Mediterranean. In O. García-Puchol & D. C. Salazar-García (Eds.) (pp. 281–307). Cham: Springer International Publishing. https://doi.org/10.1007/978-3-319-52939-4_11
- Salazar García, D. C. (2011). Aproximación a la dieta de la población calcolítica de La Vital a través del análisis de isótopos estables del carbono y del nitrógeno sobre restos óseos. In B. J. Pérez G & G. M. Carrión Y, García- Puchol O, Molina LL (Eds.), *Vida y muerte en la desembocadura del Serpis durante el III y el I milenio a.C. Museu de Prehistòria de València- Diputación de Valencia (T.V. 113)* (pp. 139–149).
- Saña, M., Antolín, F., Bergadà, M., Castells, L., Craig, O., Edo, M., ... Spiteri, C. (2015). Prácticas agropecuarias durante el neolítico antiguo y el neolítico medio en la cueva de Can Sadurní: una aproximación interdisciplinar.
- Sanger, F., Nicklen, S., & Coulson, A. R. (1977). DNA sequencing with chain-terminating inhibitors. *Proceedings of the National Academy of Sciences*, 74(12), 5463 LP-5467. <https://doi.org/10.1073/pnas.74.12.5463>
- Sanjuán, L. G. (2013). El asentamiento de la Edad del Cobre en Valencina de la Concepción: Estado actual de la investigación, debates y perspectivas. In *El asentamiento prehistórico de Valencina de la Concepción (Sevilla): investigación y tutela en el 150 aniversario del Descubrimiento de La Pastora* (pp. 21–60).
- Sanjuán, L. G., Triviño, M. L., Schuhmacher, T. X., Wheatley, D., & Banerjee, A. (2013). Ivory Craftsmanship, Trade and Social Significance in the Southern Iberian Copper Age: The Evidence from the PP4-Montelirio Sector of Valencina de la Concepción (Seville, Spain). *European Journal of Archaeology*, 16(4), 610–635. <https://doi.org/10.1179/1461957113Y.0000000037>
- Sarasketa-Gartzia, I., Villalba-Mouco, V., le Roux, P., Arrizabalaga, Á., & Salazar-García, D. C. (2016). Late Neolithic-Chalcolithic socio-economical dynamics in Northern Iberia. A multi-isotope study on diet and provenance from Santimamiñe and Pico Ramos archaeological sites (Basque Country, Spain). *Quaternary International*, 481, 14–27 <https://doi.org/10.1016/j.quaint.2017.05.049>
- Sarasketa-Gartzia, I., Villalba-Mouco, V., Le Roux, P., Arrizabalaga, Á., & Salazar-García, D. C. (2018). Anthropoc resource exploitation and use of the territory at the onset of social complexity in the Neolithic-Chalcolithic Western Pyrenees: a multi-isotope approach. *Archaeological and Anthropological Sciences*. <https://doi.org/10.1007/s12520-018-0678-7>
- Sawyer, S., Krause, J., Guschanski, K., Savolainen, V., & Pääbo, S. (2012). Temporal Patterns of Nucleotide Misincorporations and DNA Fragmentation in Ancient DNA. *PLOS ONE*, 7(3), e34131. Retrieved from <https://doi.org/10.1371/journal.pone.0034131>
- Schell, D. M. (1983). Carbon-13 and Carbon-14 Abundances in Alaskan Aquatic Organisms: Delayed Production from Peat in Arctic Food Webs. *Science*, 219(4588), 1068 LP-1071. <https://doi.org/10.1126/science.219.4588.1068>
- Schley, L., & Roper, T. J. (2003). Diet of wild boar *Sus scrofa* in Western Europe, with particular reference to consumption of agricultural crops. *Mammal Review*, 33(1), 43–56. <https://doi.org/10.1046/j.1365-2907.2003.00010.x>
- Schoeninger, M. J. (1985). Trophic level effects on $^{15}\text{N}/^{14}\text{N}$ and $^{13}\text{C}/^{12}\text{C}$ ratios in bone collagen and strontium levels in bone mineral. *Journal of Human Evolution*, 14(5), 515–525. [https://doi.org/https://doi.org/10.1016/S0047-2484\(85\)80030-0](https://doi.org/https://doi.org/10.1016/S0047-2484(85)80030-0)
- Schoeninger, M. J. (1988). Reconstructing prehistoric human diet. *Homo*, 39(2), 78–99.
- Schoeninger, M. J. (1990). Anthropology: Carbon isotope ratios. In S. P. Parker (Ed.), *McGraw- Hill Yearbook of Science and Technology* (McGraw-Hil, pp. 16–18). New

York.

- Schoeninger, M. J., & DeNiro, M. J. (1984). Nitrogen and carbon isotopic composition of bone collagen from marine and terrestrial animals. *Geochimica et Cosmochimica Acta*, 48(4), 625–639. [https://doi.org/https://doi.org/10.1016/0016-7037\(84\)90091-7](https://doi.org/https://doi.org/10.1016/0016-7037(84)90091-7)
- Schoeninger, M. J., & Moore, K. (1992). Bone stable isotope studies in archaeology. *Journal of World Prehistory*, 6(2), 247–296. <https://doi.org/10.1007/BF00975551>
- Schubert, M., Lindgreen, S., & Orlando, L. (2016). AdapterRemoval v2: rapid adapter trimming, identification, and read merging. *BMC Research Notes*, 9(1), 88. <https://doi.org/10.1186/s13104-016-1900-2>
- Schuhmacher, T. X., & Banerjee, A. (2012). Procedencia e intercambio de marfil en el Calcolítico de la Península Ibérica. *Rubricatum: Revista Del Museu de Gavà*, (5), 289–298.
- Schulting, R. (2015). Stable Isotopes and Neolithic Subsistence. In D. Fowler, C., Harding, J., Hofmann (Ed.), *The Oxford Handbook of Neolithic Europe* (pp. 361–883). Oxford University Press.
- Schulting, R. J. (1998). Slighting the sea: stable isotope evidence for the transition to farming in northwestern Europe. *Documenta Praehistorica*, 25, 203–218.
- Seibt, U., Rajabi, A., Griffiths, H., & Berry, J. A. (2008). Carbon isotopes and water use efficiency: sense and sensitivity. *Oecologia*, 155(3), 441. <https://doi.org/10.1007/s00442-007-0932-7>
- Sharp, Z. (2017). Principles of stable isotope geochemistry, Prentice Hall, New York.
- Shearer, G., Kohl, D. H., & Chien, S.-H. (1978). The Nitrogen-15 Abundance in a Wide Variety of Soils. *Soil Science Society of America Journal*, 42, 899–902. <https://doi.org/10.2136/sssaj1978.03615995004200060013x>
- Shennan, S. (2018). *The First Farmers of Europe: An Evolutionary Perspective*. Cambridge University Press.
- Sherratt, A. (1995). Instruments of conversion? The role of megaliths in the Mesolithic/Neolithic transition in northwest Europe. *Oxford Journal of Archaeology*, 14(3), 245–260.
- Sievekings, A. (1987). L'Art azilien, origine-survivance. By Claude Couraud. 28× 22 cm. Pp. 184, 50 figs., 22 tables+ 40 pls. Paris: CNRS (XX e supplément à Gallia Préhistoire), 1985. ISBN 2-222-03488-4. Fr. 280. *The Antiquaries Journal*, 67(2), 394–395.
- Sikora, M., Seguin-Orlando, A., Sousa, V. C., Albrechtsen, A., Korneliusen, T., Ko, A., ... Willerslev, E. (2017). Ancient genomes show social and reproductive behavior of early Upper Paleolithic foragers. *Science*. Retrieved from <http://science.sciencemag.org/content/early/2017/10/04/science.aao1807.abstract>
- Sillen, A. (1986). Biogenic and diagenetic Sr/Ca in Plio-Pleistocene fossils of the Omo Shungura Formation. *Paleobiology*, 12(3), 311–323. <https://doi.org/DOI:10.1017/S0094837300013816>
- Silva, A. (2003). Portuguese populations of Late Neolithic and Chalcolithic periods exhumed from collective burials. *Anthropologie (1962-)*, 41(1/2), 55–64. Retrieved from <http://www.jstor.org/stable/26292629>
- Skoglund, P., Northoff, B. H., Shunkov, M. V., Derevianko, A. P., Pääbo, S., Krause, J., & Jakobsson, M. (2014). Separating endogenous ancient DNA from modern day contamination in a Siberian Neandertal. *Proceedings of the National Academy of Sciences*, 111(6), 2229 LP-2234. <https://doi.org/10.1073/pnas.1318934111>
- Skoglund, P., Thompson, J. C., Prendergast, M. E., Mitnik, A., Sirak, K., Hajdinjak, M., ... Reich, D. (2017). Reconstructing Prehistoric African Population Structure. *Cell*, 171(1), 59–71.e21. <https://doi.org/https://doi.org/10.1016/j.cell.2017.08.049>
- Smith, B. N., & Epstein, S. (1971). Two Categories of $\delta^{13}\text{C}/\delta^{12}\text{C}$ Ratios for Higher Plants.

- Plant Physiology*, 47(3), 380 LP-384. <https://doi.org/10.1104/pp.47.3.380>
- Soto, A., Alday, A., Montes, L., Utrilla, P., Perales, U., & Domingo, R. (2015). Epipalaeolithic assemblages in the Western Ebro Basin (Spain): The difficult identification of cultural entities. *Quaternary International*, 364, 144–152. <https://doi.org/https://doi.org/10.1016/j.quaint.2014.05.041>
- Spyrou, M. A., Tikhbatova, R. I., Wang, C.-C., Valtueña, A. A., Lankapalli, A. K., Kondrashin, V. V., ... Krause, J. (2018). Analysis of 3800-year-old *Yersinia pestis* genomes suggests Bronze Age origin for bubonic plague. *Nature Communications*, 9(1), 2234. <https://doi.org/10.1038/s41467-018-04550-9>
- Stevens, R. E., Jacobi, R., Street, M., Germonpré, M., Conard, N. J., Münzel, S. C., & Hedges, R. E. M. (2008). Nitrogen isotope analyses of reindeer (*Rangifer tarandus*), 45,000 BP to 9,000 BP: Palaeoenvironmental reconstructions. *Palaeogeography, Palaeoclimatology, Palaeoecology*, 262(1), 32–45. <https://doi.org/https://doi.org/10.1016/j.palaeo.2008.01.019>
- Stewart, J. R., & Stringer, C. B. (2012). Human Evolution Out of Africa: The Role of Refugia and Climate Change. *Science*, 335(6074), 1317 LP-1321. Retrieved from <http://science.sciencemag.org/content/335/6074/1317.abstract>
- Straus, L. G. (1975). Solutrense o magdalenense inferior cantábrico?: significado de la diferencia. *Boletín Del Instituto de Estudios Asturianos*, 29(86), 782–800.
- Straus, L. G. (2015). Chronostratigraphy of the Pleistocene/Holocene boundary: the Azilian problem in the Franco-Cantabrian region. *Palaeohistoria*, 27, 89–122.
- Szécsényi-Nagy, A., Roth, C., Brandt, G., Rihuete-Herrada, C., Tejedor-Rodríguez, C., Held, P., ... Alt, K. W. (2017). The maternal genetic make-up of the Iberian Peninsula between the Neolithic and the Early Bronze Age. *Scientific Reports*, 7(1), 15644. <https://doi.org/10.1038/s41598-017-15480-9>
- Szpak, P. (2014). Complexities of nitrogen isotope biogeochemistry in plant-soil systems: implications for the study of ancient agricultural and animal management practices. *Frontiers in Plant Science*. Retrieved from <https://www.frontiersin.org/article/10.3389/fpls.2014.00288>
- Tauber, H. (1981). ^{13}C evidence for dietary habits of prehistoric man in Denmark. *Nature*, 292(5821), 332–333. <https://doi.org/10.1038/292332a0>
- Tauber, H. (1986). *Analysis of stable isotopes in prehistoric populations*. Berliner Gesellschaft für Anthropologie, Ethnologie und Urgeschichte.
- Thomson, J. J., Aston, F. W., Soddy, F., Merton, T. R., & Lindemann, F. A. (1921). Discussion on Isotopes. *Proceedings of the Royal Society of London. Series A, Containing Papers of a Mathematical and Physical Character*, 99(697), 87–104. Retrieved from <http://www.jstor.org/stable/93977>
- Tieszen, L. L. (1991). Natural variations in the carbon isotope values of plants: Implications for archaeology, ecology, and paleoecology. *Journal of Archaeological Science*, 18(3), 227–248. [https://doi.org/https://doi.org/10.1016/0305-4403\(91\)90063-U](https://doi.org/https://doi.org/10.1016/0305-4403(91)90063-U)
- Tieszen, L. L., & Fagre, T. (1993). Effect of Diet Quality and Composition on the Isotopic Composition of Respiratory CO_2 , Bone Collagen, Bioapatite, and Soft Tissues BT - Prehistoric Human Bone: Archaeology at the Molecular Level. In J. B. Lambert & G. Grupe (Eds.) (pp. 121–155). Berlin, Heidelberg: Springer Berlin Heidelberg. https://doi.org/10.1007/978-3-662-02894-0_5
- Tilley, C. (1994). Interpreting material culture. *Interpreting Objects and Collections*, 67–75.
- Tornero, C., Aguilera, M., Ferrio, J. P., Arcusa, H., Moreno-García, M., García-Reig, S., & Rojo-Guerra, M. (2018). Vertical sheep mobility along the altitudinal gradient through stable isotope analyses in tooth molar bioapatite, meteoric water and pastures: A reference from the Ebro valley to the Central Pyrenees. *Quaternary International*, 484, 94–106. <https://doi.org/https://doi.org/10.1016/j.quaint.2016.11.042>

- Tornero, C., Balasse, M., Bălăşescu, A., Chataigner, C., Gasparyan, B., & Montoya, C. (2016). The altitudinal mobility of wild sheep at the Epigravettian site of Kalavan 1 (Lesser Caucasus, Armenia): Evidence from a sequential isotopic analysis in tooth enamel. *Journal of Human Evolution*, *97*, 27–36.
<https://doi.org/https://doi.org/10.1016/j.jhevol.2016.05.001>
- Tuross, N., Behrensmeyer, A. K., & Eanes, E. D. (1989). Strontium increases and crystallinity changes in taphonomic and archaeological bone. *Journal of Archaeological Science*, *16*(6), 661–672. [https://doi.org/https://doi.org/10.1016/0305-4403\(89\)90030-7](https://doi.org/https://doi.org/10.1016/0305-4403(89)90030-7)
- Utrilla, P., & Baldellou, V. (2001). Cantos pintados neolíticos de la Cueva de Chaves (Bastarás, Huesca). *Saldvie: Estudios de Prehistoria y Arqueología*, (2), 45–126.
- Utrilla, P., Montes, L., Mazo, C., Bea, M., & Domingo, R. (2009). El Mesolítico geométrico en Aragón. In *El mesolítico geométrico en la Península Ibérica* (pp. 131–190). Departamento de Ciencias de la Antigüedad.
- Utrilla, P., Laborda, R. (2018). La Cueva de Chaves (Bastaras, Huesca), el gran lugar de habitat del prepirineo: 15000 años de ocupación. *Trabajos de Prehistoria*, 1–22.
- Utrilla, P. (2004). Evolución histórica de las sociedades cantábricas durante el Tardiglacial: el Magdaleniense inicial, inferior y medio (16500/13000 BP). *Las Sociedades Del Paleolítico En. a Región Cantábrica. Kobie, Anejos*, 8.
- Utrilla, P., & Baldellou, V. (2007). Les galets peints de la Grotte de Chaves. *Bulletin de La Société Préhistorique Ariège-Pyrénées*, *62*, 73–88.
- Utrilla, P., Lorenzo, J. I., Baldellou, V., Sopena, M. C., & Ayuso, P. (2008). Enterramiento masculino en fosa, cubierto de cantos rodados, en el Neolítico antiguo de la Cueva de Chaves. In *IV Congreso del Neolítico Peninsular (Alicante 2006)* (Vol. 2, pp. 131–140).
- Utrilla, P., Mazo, C., & Domingo, R. (2015). Fifty thousand years of prehistory at the cave of Abautz (Arraitz, Navarre): a nexus point between the Ebro Valley, Aquitaine and the Cantabrian corridor. *Quaternary International*, *364*, 294–305.
- Vågene, Å. J., Herbig, A., Campana, M. G., Robles García, N. M., Warinner, C., Sabin, S., ... Krause, J. (2018). Salmonella enterica genomes from victims of a major sixteenth-century epidemic in Mexico. *Nature Ecology & Evolution*, *2*(3), 520–528.
<https://doi.org/10.1038/s41559-017-0446-6>
- Valdiosera, C., Günther, T., Vera-Rodríguez, J. C., Ureña, I., Iriarte, E., Rodríguez-Varela, R., ... Jakobsson, M. (2018). Four millennia of Iberian biomolecular prehistory illustrate the impact of prehistoric migrations at the far end of Eurasia. *Proceedings of the National Academy of Sciences*. Retrieved from
<http://www.pnas.org/content/early/2018/03/06/1717762115.abstract>
- Valentin, J. (2002). Basic anatomical and physiological data for use in radiological protection: reference values: ICRP Publication 89. *Annals of the ICRP*, *32*(3), 1–277.
[https://doi.org/https://doi.org/10.1016/S0146-6453\(03\)00002-2](https://doi.org/https://doi.org/10.1016/S0146-6453(03)00002-2)
- Valenzuela-Lamas, S., Jiménez-Manchón, S., Evans, J., López, D., Jornet, R., & Albarella, U. (2016). Analysis of seasonal mobility of sheep in Iron Age Catalonia (north-eastern Spain) based on strontium and oxygen isotope analysis from tooth enamel: First results. *Journal of Archaeological Science: Reports*, *6*, 828–836.
<https://doi.org/https://doi.org/10.1016/j.jasrep.2015.08.042>
- Valera, A. C., Silva, A. M., & Romero, J. E. M. (2014). The temporality of Perdigões enclosures: absolute chronology of the structures and social practices. *SPAL-Revista de Prehistoria y Arqueología*, (23), 11–26.
- Valla, F. R. (1981). Les établissements natoufiens dans le nord d’Israël in *Préhistoire du Levant*. In A. Cauvin, J. & P. Sanlaville (Eds.), *Préhistoire du Levant, CNRS, Paris* (pp. 409–420). CNRS, Paris.
- van de Loosdrecht, M., Bouzouggar, A., Humphrey, L., Posth, C., Barton, N., Aximu-Petri, A., ... Krause, J. (2018). Pleistocene North African genomes link Near Eastern and sub-

- Saharan African human populations. *Science*, 360(6388), 548 LP-552. Retrieved from <http://science.sciencemag.org/content/360/6388/548.abstract>
- van der Merwe, N. J. (1982). Carbon Isotopes, Photosynthesis, and Archaeology: Different pathways of photosynthesis cause characteristic changes in carbon isotope ratios that make possible the study of prehistoric human diets. *American Scientist*, 70(6), 596–606. Retrieved from <http://www.jstor.org/stable/27851731>
- van Klinken, G. J. (1999). Bone Collagen Quality Indicators for Palaeodietary and Radiocarbon Measurements. *Journal of Archaeological Science*, 26(6), 687–695. <https://doi.org/https://doi.org/10.1006/jasc.1998.0385>
- Van Klinken, G. J., Richards, M. P., & Hedges, B. E. M. (2002). An Overview of Causes for Stable Isotopic Variations in Past European Human Populations: Environmental, Ecophysiological, and Cultural Effects BT - Biogeochemical Approaches to Paleodietary Analysis. In S. H. Ambrose & M. A. Katzenberg (Eds.) (pp. 39–63). Boston, MA: Springer US. https://doi.org/10.1007/0-306-47194-9_3
- van Willigen, S. (2018). Between Cardial and Linearbandkeramik: From no-man's-land to communication sphere. *Quaternary International*, 470, 333–352. <https://doi.org/https://doi.org/10.1016/j.quaint.2017.08.031>
- Van Willigen, S. (2004). Aspects culturels de la néolithisation en Méditerranée occidentale : le Cardial et l'Épicardial. *Bulletin de La Société Préhistorique Française*, 463–495. Retrieved from https://www.persee.fr/doc/bspf_0249-7638_2004_num_101_3_13028
- Venter, J. C., Adams, M. D., Myers, E. W., Li, P. W., Mural, R. J., Sutton, G. G., ... Zhu, X. (2001). The Sequence of the Human Genome. *Science*, 291(5507), 1304 LP-1351. <https://doi.org/10.1126/science.1058040>
- Villalba-Mouco, V., Martínez-Labarga, C., Utrilla, P., Laborda, R., Ignacio, J., & Salazar-garcía, D. C. (2018). Reconstruction of human subsistence and husbandry strategies from the Iberian Early Neolithic : A stable isotope approach, *American Journal of Physical Anthropology*, 167, 257–271. <https://doi.org/10.1002/ajpa.23622>
- Villalba-Mouco, V., Sarasketa-Gartzia, I., Utrilla, P., Oms, F. X., Mazo, C., Mendiola, S., ... Salazar-García, D. C. (2018). Stable isotope ratio analysis of bone collagen as indicator of different dietary habits and environmental conditions in northeastern Iberia during the 4th and 3rd millennium cal B.C. *Archaeological and Anthropological Sciences*. <https://doi.org/10.1007/s12520-018-0657-z>
- Villalba-Mouco, V., Sauqué, V., Sarasketa-Gartzia, I., Pastor, M. V., le Roux, P. J., Vicente, D., ... Salazar-García, D. C. (2018). Territorial mobility and subsistence strategies during the Ebro Basin Late Neolithic-Chalcolithic: A multi-isotope approach from San Juan cave (Loarre, Spain). *Quaternary International*, 481, 28–41. <https://doi.org/10.1016/j.quaint.2017.05.051>
- Villalba-Mouco, V., van de Loosdrecht, M. S., Posth, C., Mora, R., Martínez-Moreno, J., Rojo-Guerra, M., ... Haak, W. (2019). Survival of Late Pleistocene Hunter-Gatherer Ancestry in the Iberian Peninsula. *Current Biology*, 29(7), 1169–1177.e7. <https://doi.org/https://doi.org/10.1016/j.cub.2019.02.006>
- Vogel, J. C., Talma, A. S., Hall-Martint, A. J., & Viljoen, P. J. (1990). Carbon and nitrogen isotopes in elephants. *Am. J. Psychiat*, 142, 163–170.
- Wada, E. (1980). Nitrogen isotope fractionation and its significance in biogeochemical processes occurring in marine environments. *Isotope Marine Chemistry*, 375–398.
- Waterman, A. (2012). *Marked in life and death: identifying biological markers of social differentiation in lateprehistoric Portugal* (PhD thesis). Iowa: University of Iowa.
- Waterman, A. J., Tykot, R. H., & Silva, A. M. (2015). Stable Isotope Analysis of Diet-based Social Differentiation at Late Prehistoric Collective Burials in South-Western Portugal. *Archaeometry*, 58(1), 131–151. <https://doi.org/10.1111/arcm.12159>
- Watson, J. D., & Crick, F. H. C. (1953). Molecular structure of nucleic acids. *Nature*,

171(4356), 737–738.

- Webb, E. C., Lewis, J., Shain, A., Kastrisianaki-Guyton, E., Honch, N. V., Stewart, A., ... Evershed, R. P. (2017). The influence of varying proportions of terrestrial and marine dietary protein on the stable carbon-isotope compositions of pig tissues from a controlled feeding experiment. *STAR: Science & Technology of Archaeological Research*, 3(1), 28–44. <https://doi.org/10.1080/20548923.2016.1275477>
- Weissensteiner, H., Pacher, D., Kloss-Brandstätter, A., Forer, L., Specht, G., Bandelt, H.-J., ... Schönherr, S. (2016). HaploGrep 2: mitochondrial haplogroup classification in the era of high-throughput sequencing. *Nucleic Acids Research*, 44(W1), W58–W63. Retrieved from <http://dx.doi.org/10.1093/nar/gkw233>
- White, T. D., & Folkens, P. A. (2005). *The human bone manual*. Elsevier.
- Whittle, A. W. R. (1996). *Europe in the Neolithic: the creation of new worlds*. Cambridge University Press.
- Willcox, G., Buxo, R., & Herveux, L. (2009). Late Pleistocene and early Holocene climate and the beginnings of cultivation in northern Syria. *The Holocene*, 19(1), 151–158. <https://doi.org/10.1177/0959683608098961>
- Willerslev, E., Cappellini, E., Boomsma, W., Nielsen, R., Hebsgaard, M. B., Brand, T. B., ... Collins, M. J. (2007). Ancient Biomolecules from Deep Ice Cores Reveal a Forested Southern Greenland. *Science*, 317(5834), 111 LP-114. <https://doi.org/10.1126/science.1141758>
- Willerslev, E., Hansen, A. J., Binladen, J., Brand, T. B., Gilbert, M. T. P., Shapiro, B., ... Cooper, A. (2003). Diverse Plant and Animal Genetic Records from Holocene and Pleistocene Sediments. *Science*, 300(5620), 791 LP-795. <https://doi.org/10.1126/science.1084114>
- Wilson, A. C., Cann, R. L., Carr, S. M., George, M., Gyllensten, U. L. F. B., Helm-Bychowski, K. M., ... Stoneking, M. (2008). Mitochondrial DNA and two perspectives on evolutionary genetics. *Biological Journal of the Linnean Society*, 26(4), 375–400. <https://doi.org/10.1111/j.1095-8312.1985.tb02048.x>
- Wilson, J. W. (1947). Virchow's Contribution to the Cell Theory. *Journal of the History of Medicine and Allied Sciences*, 2(2), 163–178. Retrieved from <http://www.jstor.org/stable/24619588>
- Wright, H. E., Thorpe, J. L., Mackay, A., Battarbee, R., Birks, J., & Oldfield, F. (2003). Climatic change and the origin of agriculture in the Near East. *Global Change in the Holocene*, 49–62.
- Zapata, L., & Baldellou, V. (2008). Bellotas de cronología neolítica para consumo humano en la cueva de Chaves (Bastarás, Huesca). In *IV Congreso del Neolítico Peninsular: 27-30 de noviembre de 2006* (pp. 402–410). Museo Arqueológico de Alicante-MARQ.
- Zapata, L., Peña-Chocarro, L., Pérez-Jordá, G., & Stika, H.-P. (2004). Early Neolithic Agriculture in the Iberian Peninsula. *Journal of World Prehistory*, 18(4), 283–325. <https://doi.org/10.1007/s10963-004-5621-4>
- Zeder, M. A. (2008). Domestication and early agriculture in the Mediterranean Basin: Origins, diffusion, and impact. *Proceedings of the National Academy of Sciences*, 105(33), 11597 LP-11604. <https://doi.org/10.1073/pnas.0801317105>
- Zilhao, J. (1993). The spread of agro-pastoral economies across Mediterranean Europe: a view from the far west. *Journal of Mediterranean Archaeology*, 6(1), 5–63.
- Zilhão, J. (1992). *Gruta do Caldeirão o neolítico antigo*. Trabalhos de Arqueologia 6. Lisboa: Instituto Português do Património Cultural.
- Zilhão, J. (2001). Radiocarbon evidence for maritime pioneer colonization at the origins of farming in west Mediterranean Europe. *Proceedings of the National Academy of Sciences*, 98(24), 14180 LP-14185. Retrieved from <http://www.pnas.org/content/98/24/14180.abstract>

Zilhão, J., & Real, F. (1984). *A gruta da Feteira (Lourinhã): escavações de salvamento de uma necrópole neolítica.*

14 ANNEX

SITE	INDIVIDUAL (human)	$\delta^{13}\text{C}$	$\delta^{15}\text{N}$	LONGITUDE	LATITUDE	Mean $\delta^{13}\text{C}$	Mean $\delta^{15}\text{N}$	Reference
San Juan cave	18475	-19.3	10.4	42.324047	-0.607341	-19.3	10.3	Villalba-Mouco et al., 2018
San Juan cave	18484	-19.3	10.1	42.324047	-0.607341			Villalba-Mouco et al., 2018
San Juan cave	18485	-19.1	10.4	42.324047	-0.607341			Villalba-Mouco et al., 2018
San Juan cave	18495	-19.4	10.4	42.324047	-0.607341			Villalba-Mouco et al., 2018
San Juan cave	18502	-19.2	9.9	42.324047	-0.607341			Villalba-Mouco et al., 2018
San Juan cave	18473	-19.7	9.7	42.324047	-0.607341			Villalba-Mouco et al., 2018
San Juan cave	18478	-19.2	10.6	42.324047	-0.607341			Villalba-Mouco et al., 2018
San Juan cave	18479	-19.5	9.9	42.324047	-0.607341			Villalba-Mouco et al., 2018
San Juan cave	18483	-19.3	11	42.324047	-0.607341			Villalba-Mouco et al., 2018
San Juan cave	18487	-19.1	10	42.324047	-0.607341			Villalba-Mouco et al., 2018
San Juan cave	18494	-19.6	10.4	42.324047	-0.607341			Villalba-Mouco et al., 2018
San Juan cave	18496	-19.3	9.8	42.324047	-0.607341			Villalba-Mouco et al., 2018
San Juan cave	18501	-19.6	10.5	42.324047	-0.607341			Villalba-Mouco et al., 2018
San Juan cave	18503	-19.4	9.2	42.324047	-0.607341			Villalba-Mouco et al., 2018
San Juan cave	18504	-19.2	10.2	42.324047	-0.607341			Villalba-Mouco et al., 2018
San Juan cave	18505	-18.7	11.2	42.324047	-0.607341			Villalba-Mouco et al., 2018
San Juan cave	18476	-19	10.9	42.324047	-0.607341			Villalba-Mouco et al., 2018
San Juan cave	18482	-19.2	11	42.324047	-0.607341			Villalba-Mouco et al., 2018
San Juan cave	18491	-19.7	9.6	42.324047	-0.607341			Villalba-Mouco et al., 2018
San Juan cave	18486	-19.4	10.6	42.324047	-0.607341			Villalba-Mouco et al., 2018
San Juan cave	18489	-19.2	10.9	42.324047	-0.607341			Villalba-Mouco et al., 2018
San Juan cave	18490	-19.9	9.4	42.324047	-0.607341			Villalba-Mouco et al., 2018
San Juan cave	18481	-19.4	10.2	42.324047	-0.607341			Villalba-Mouco et al., 2018
San Juan cave	18498	-19.5	10.2	42.324047	-0.607341			Villalba-Mouco et al., 2018
La Pastora	LP-m-14	-19.5	9	38.711107	-0.491188	-19.4	9.2	McClure et al., 2011

La Pastora	LP-m-39	-19	10	38.711107	-0.491188				McClure et al., 2011
La Pastora	LP-m-23	-19.1	9.7	38.711107	-0.491188				McClure et al., 2011
La Pastora	LP-3	-19.6	8.1	38.711107	-0.491188				McClure et al., 2011
La Pastora	LP-9	-19.5	9.5	38.711107	-0.491188				McClure et al., 2011
La Pastora	LP-m-31	-19.3	9.7	38.711107	-0.491188				McClure et al., 2011
La Pastora	LP-m-17	-19.3	10.6	38.711107	-0.491188				McClure et al., 2011
La Pastora	LP-m-21	-19.6	9.5	38.711107	-0.491188				McClure et al., 2011
La Pastora	LP-5 BA	-19.4	8.3	38.711107	-0.491188				McClure et al., 2011
La Pastora	LP-m-6	-19.6	7.5	38.711107	-0.491188				McClure et al., 2011
Avenc Forat	AVF6	-19.1	10	39.103956	-0.417931	-19.1	10.2		McClure et al., 2011
Avenc Forat	AVF7	-19.1	10.4	39.103956	-0.417931				McClure et al., 2011
La Vital	7400	-18.28	9.03	38.963065	-0.207311	-18.7	9.5		Salazar-García, 2011
La Vital	7401	-18.57	9.01	38.963065	-0.207311				Salazar-García, 2011
La Vital	7402	-19.25	10.33	38.963065	-0.207311				Salazar-García, 2011
Coveta del Frare	27187	-19	9.8	38.801692	-0.871795	-19.1	9.6		García-Borja et al., 2013
Coveta del Frare	26902	-19	9.6	38.801692	-0.871795				García-Borja et al., 2013
Coveta del Frare	26190	-19.2	8.9	38.801692	-0.871795				García-Borja et al., 2013
Coveta del Frare	26903	-19.2	10.1	38.801692	-0.871795				García-Borja et al., 2013
Diablets	26784	-18.8	9.9	40.297869	0.247774	-18.8	10.1		Salazar-García, 2014
Diablets	26785	-18.8	10.6	40.297869	0.247774				Salazar-García, 2014
Diablets	26792	-18.9	9.9	40.297869	0.247774				Salazar-García, 2014
Cova do Santo	101	-19.8	9.7	42.481107	-7.204619	-19.9	9.6		López-Costas et al., 2015
Cova do Santo	102	-20.1	9.5	42.481107	-7.204619				López-Costas et al., 2015
Cova do Santo	105	-19.9	9.4	42.481107	-7.204619				López-Costas et al., 2015
Cova do Santo	106	-19.9	9.3	42.481107	-7.204619				López-Costas et al., 2015
Cova do Santo	107	-19.8	10.2	42.481107	-7.204619				López-Costas et al., 2015
Cova do Santo	109	-20	9.4	42.481107	-7.204619				López-Costas et al., 2015

Valencina-Castilleja	ALC1	-19	9	37.411124	-6.057099	-19.1	8.4	Diaz-Zorita-Bonilla, 2014
Valencina-Castilleja	ALC4	-18.8	8.7	37.411124	-6.057099			Diaz-Zorita-Bonilla, 2014
Valencina-Castilleja	C1	-19.8	6.5	37.411124	-6.057099			Diaz-Zorita-Bonilla, 2014
Valencina-Castilleja	ALG13	-18.8	8.7	37.411124	-6.057099			Diaz-Zorita-Bonilla, 2014
Valencina-Castilleja	CC1	-18.9	7.5	37.411124	-6.057099			Diaz-Zorita-Bonilla, 2014
Valencina-Castilleja	10.049-1	-19.1	9.9	37.411124	-6.057099			Diaz-Zorita-Bonilla, 2014
La Orden-Seminario		-19.1	8.7	37.285024	-6.930417	-19.05	8.25	Diaz-Zorita-Bonilla, 2014
La Orden-Seminario		-19	7.8	37.285024	-6.930417			Diaz-Zorita-Bonilla, 2014
Alto del Reinoso	1	-19.7	9.7	42.438587	-3.475999	-19.7	9.8	Alt et al., 2016
Alto del Reinoso	2	-19.5	9.4	42.438587	-3.475999			Alt et al., 2016
Alto del Reinoso	3	-19.4	10.2	42.438587	-3.475999			Alt et al., 2016
Alto del Reinoso	4	-19.3	9.7	42.438587	-3.475999			Alt et al., 2016
Alto del Reinoso	6	-19.5	9.8	42.438587	-3.475999			Alt et al., 2016
Alto del Reinoso	8	-19.4	9.7	42.438587	-3.475999			Alt et al., 2016
Alto del Reinoso	9	-19.4	9.8	42.438587	-3.475999			Alt et al., 2016
Alto del Reinoso	10	-19.6	9.6	42.438587	-3.475999			Alt et al., 2016
Alto del Reinoso	1173-74	-19.5	10.3	42.438587	-3.475999			Alt et al., 2016
Alto del Reinoso	1171-72	-19.6	10.2	42.438587	-3.475999			Alt et al., 2016
Alto del Reinoso	1149-50	-19.4	9.7	42.438587	-3.475999			Alt et al., 2016
Alto del Reinoso	1158-60	-19.4	10.3	42.438587	-3.475999			Alt et al., 2016
Alto del Reinoso	2867-70	-19.6	10.1	42.438587	-3.475999			Alt et al., 2016
Alto del Reinoso	1295-98	-19.7	9.5	42.438587	-3.475999			Alt et al., 2016
Alto del Reinoso	1014-15	-20.2	9.1	42.438587	-3.475999			Alt et al., 2016
Alto del Reinoso	115-16	-19.9	9.9	42.438587	-3.475999			Alt et al., 2016
Alto del Reinoso	2499-501	-20	11	42.438587	-3.475999			Alt et al., 2016
Alto del Reinoso	381	-20.2	9.4	42.438587	-3.475999			Alt et al., 2016
Alto del Reinoso	1000-02	-20.1	9.5	42.438587	-3.475999			Alt et al., 2016

Paimogo I	PM12268	-21.3	8.1	39.240117	-9.316867	-20.46	8.7	Waterman et al., 2015
Paimogo I	PM12263	-21	10.3	39.240117	-9.316867			Waterman et al., 2015
Paimogo I	PM12261	-20.4	9.3	39.240117	-9.316867			Waterman et al., 2015
Paimogo I	PM12338	-20.8	8.5	39.240117	-9.316867			Waterman et al., 2015
Paimogo I	PM12951	-19.8	8.8	39.240117	-9.316867			Waterman et al., 2015
Paimogo I	PM12282	-20.1	8.5	39.240117	-9.316867			Waterman et al., 2015
Paimogo I	PM12821	-20	8	39.240117	-9.316867			Waterman et al., 2015
Paimogo I	PM12600	-20.3	8.1	39.240117	-9.316867			Waterman et al., 2015
Feteira II	Fet1222	-20.2	8.4	39.240337	-9.313904	-20.26	8.27	Waterman et al., 2015
Feteira II	fet1219	-19.9	8.6	39.240337	-9.313904			Waterman et al., 2015
Feteira II	Fet1547	-20.6	7.5	39.240337	-9.313904			Waterman et al., 2015
Feteira II	Fet342	-20.4	8.6	39.240337	-9.313904			Waterman et al., 2015
Feteira II	Fet944	-20.1	8.2	39.240337	-9.313904			Waterman et al., 2015
Feteira II	Fet1092	-19.7	9.1	39.240337	-9.313904			Waterman et al., 2015
Feteira II	Fet92	-20.7	7.8	39.240337	-9.313904			Waterman et al., 2015
Feteira II	Fet1245	-20.5	7.6	39.240337	-9.313904			Waterman et al., 2015
Feteira II	Fet968	-20.1	8.3	39.240337	-9.313904			Waterman et al., 2015
Feteira II	Fet799	-20.3	8.2	39.240337	-9.313904			Waterman et al., 2015
Feteira II	Fet1229	-20.9	7.6	39.240337	-9.313904			Waterman et al., 2015
Feteira II	Fet313	-20.1	8.6	39.240337	-9.313904			Waterman et al., 2015
Feteira II	Fet1006	-20	9	39.240337	-9.313904			Waterman et al., 2015
Ondarre	OND2	-20.9	10	42.970799	-2.099776	-21.2	9.6	Fernandez-Crespo et al., 2017
Ondarre	OND4	-21.5	9.2	42.970799	-2.099776			Fernandez-Crespo et al., 2017
Cabeco da Arruda I	CAI 13	-19.5	8.5	39.085405	-9.273086	-19.75	8.63	Waterman et al., 2015
Cabeco da Arruda I	CAI 11	-19.8	8.6	39.085405	-9.273086			Waterman et al., 2015
Cabeco da Arruda I	CAI 17	-19.5	8.4	39.085405	-9.273086			Waterman et al., 2015
Cabeco da Arruda I	CAI 1	-19.6	8.8	39.085405	-9.273086			Waterman et al., 2015

Cabeco da Arruda I	CAI 25	-19.8	9.7	39.085405	-9.273086			Waterman et al., 2015
Cabeco da Arruda I	CAI 3	-20.3	8.6	39.085405	-9.273086			Waterman et al., 2015
Cabeco da Arruda I	CAI 7	-19.8	7.8	39.085405	-9.273086			Waterman et al., 2015
Cova Moura	CM12	-20.1	7.6	41.233848	-8.568657	-19.78	9.4	Waterman et al., 2015
Cova Moura	CM2	-19.3	9.7	41.233848	-8.568657			Waterman et al., 2015
Cova Moura	CM84	-19.5	9.5	41.233848	-8.568657			Waterman et al., 2015
Cova Moura	CM159	-19.5	9.9	41.233848	-8.568657			Waterman et al., 2015
Cova Moura	CM9	-19.5	9.3	41.233848	-8.568657			Waterman et al., 2015
Cova Moura	CM95	-20	9.1	41.233848	-8.568657			Waterman et al., 2015
Cova Moura	CM30	-19	10	41.233848	-8.568657			Waterman et al., 2015
Cova Moura	CM22	-20.6	11.2	41.233848	-8.568657			Waterman et al., 2015
Cova Moura	CM81	-20.5	8.7	41.233848	-8.568657			Waterman et al., 2015
Bolores	11.4.B93/B14	-19.6	9	39.092772	-9.276829	-20	9.18	Waterman et al., 2015
Bolores	B1.11N.4.B663	-19.5	9.5	39.092772	-9.276829			Waterman et al., 2015
Bolores	B1.9,10.0.BL5	-20.8	9.8	39.092772	-9.276829			Waterman et al., 2015
Bolores	B1.2.1.B14	-19.7	9.6	39.092772	-9.276829			Waterman et al., 2015
Bolores	B1.CR1.x.B89	-20.4	8	39.092772	-9.276829			Waterman et al., 2015
Tholos Borracheira	Bor 1007	-19.7	8.9	39.07221	-9.261147	-19.75	8.75	Waterman et al., 2015
Tholos Borracheira	Bor 57	-19.8	8.6	39.07221	-9.261147			Waterman et al., 2015
Lapa da Rainaha II	LR 261	-19.6	8.6	38.064633	-8.132973	-19.57	8.9	Waterman et al., 2015
Lapa da Rainaha II	LR 95	-19.4	8.3	38.064633	-8.132973			Waterman et al., 2015
Lapa da Rainaha II	LR 47	-19.7	9.8	38.064633	-8.132973			Waterman et al., 2015
Zambujal	Z831	-20.7	8.4	39.074489	-9.28553	-20.4	9.25	Waterman et al., 2015
Zambujal	Z776	-20.1	10.1	39.074489	-9.28553			Waterman et al., 2015
Abauntz	19033	-20.3	8.8	43.015368	-1.641456	-20.1	9.1	Villalba-Mouco et al., 2018
Abauntz	19038	-20.5	9.5	43.015368	-1.641456			Villalba-Mouco et al., 2018
Abauntz	19039	-19.8	9.0	43.015368	-1.641456			Villalba-Mouco et al., 2018

Abauntz	19041	-20.2	8.2	43.015368	-1.641456			Villalba-Mouco et al., 2018
Abauntz	19042	-20.1	9.1	43.015368	-1.641456			Villalba-Mouco et al., 2018
Abauntz	19045	-20.2	8.8	43.015368	-1.641456			Villalba-Mouco et al., 2018
Abauntz	19047	-20.5	9.1	43.015368	-1.641456			Villalba-Mouco et al., 2018
Abauntz	19049	-20.1	8.8	43.015368	-1.641456			Villalba-Mouco et al., 2018
Abauntz	19051	-20.3	9.5	43.015368	-1.641456			Villalba-Mouco et al., 2018
Abauntz	19055	-20.1	8.4	43.015368	-1.641456			Villalba-Mouco et al., 2018
Abauntz	19028	-20.1	9.0	43.015368	-1.641456			Villalba-Mouco et al., 2018
Abauntz	19029	-19.3	11.3	43.015368	-1.641456			Villalba-Mouco et al., 2018
Abauntz	19034	-19.6	9.2	43.015368	-1.641456			Villalba-Mouco et al., 2018
Abauntz	19035	-20.1	9.1	43.015368	-1.641456			Villalba-Mouco et al., 2018
Abauntz	19036	-20.1	9.0	43.015368	-1.641456			Villalba-Mouco et al., 2018
Abauntz	19037	-20.2	8.2	43.015368	-1.641456			Villalba-Mouco et al., 2018
Abauntz	19053	-19.9	8.8	43.015368	-1.641456			Villalba-Mouco et al., 2018
Abauntz	19032	-20.3	9.2	43.015368	-1.641456			Villalba-Mouco et al., 2018
Abauntz	19050	-20.0	9.2	43.015368	-1.641456			Villalba-Mouco et al., 2018
Abauntz	19030	-20.8	9.3	43.015368	-1.641456			Villalba-Mouco et al., 2018
Abauntz	19040	-19.9	9.0	43.015368	-1.641456			Villalba-Mouco et al., 2018
Abauntz	19044	-20.2	8.6	43.015368	-1.641456			Villalba-Mouco et al., 2018
Abauntz	19048	-20.4	9.7	43.015368	-1.641456			Villalba-Mouco et al., 2018
Abauntz	19046	-20.3	9.0	43.015368	-1.641456			Villalba-Mouco et al., 2018
Abauntz	19031	-20.3	8.8	43.015368	-1.641456			Villalba-Mouco et al., 2018
Abauntz	19043	-20.4	9.5	43.015368	-1.641456			Villalba-Mouco et al., 2018
Abauntz	19054	-19.9	9.4	43.015368	-1.641456			Villalba-Mouco et al., 2018
Guineu	18973	-19.8	9.5	41.441531	1.586308	-19.3	9.0	Villalba-Mouco et al., 2018
Guineu	18976	-19.3	9.0	41.441531	1.586308			Villalba-Mouco et al., 2018
Guineu	18978	-19.2	9.2	41.441531	1.586308			Villalba-Mouco et al., 2018

Guineu	18982	-19.4	9.2	41.441531	1.586308			Villalba-Mouco et al., 2018
Guineu	18983	-19.4	8.4	41.441531	1.586308			Villalba-Mouco et al., 2018
Guineu	18984	-18.8	9.0	41.441531	1.586308			Villalba-Mouco et al., 2018
Guineu	18985	-19.3	8.7	41.441531	1.586308			Villalba-Mouco et al., 2018
Guineu	18987	-19.5	9.1	41.441531	1.586308			Villalba-Mouco et al., 2018
Guineu	18992	-19.4	8.5	41.441531	1.586308			Villalba-Mouco et al., 2018
Guineu	18994	-19.1	9.3	41.441531	1.586308			Villalba-Mouco et al., 2018
Guineu	18997	-19.3	8.2	41.441531	1.586308			Villalba-Mouco et al., 2018
Guineu	18998	-19.3	8.8	41.441531	1.586308			Villalba-Mouco et al., 2018
Guineu	19001	-19.3	8.7	41.441531	1.586308			Villalba-Mouco et al., 2018
Guineu	19002	-19.4	9.9	41.441531	1.586308			Villalba-Mouco et al., 2018
Guineu	19004	-19.4	8.7	41.441531	1.586308			Villalba-Mouco et al., 2018
Guineu	19007	-19.3	8.6	41.441531	1.586308			Villalba-Mouco et al., 2018
Guineu	19008	-19.5	9.9	41.441531	1.586308			Villalba-Mouco et al., 2018
Guineu	19009	-19.2	9.0	41.441531	1.586308			Villalba-Mouco et al., 2018
Acequión	1	-18.9	9.6	38.990736	-1.821029	-18.8	9.7	Salazar-García et al., 2013
Acequión	2	-18.7	9.8	38.990736	-1.821029			Salazar-García et al., 2013
Montelirio	Mo2	-18.3	8.7	37.409837	-6.05932	-19.5	9.1	Fontanals-Coll et al., 2015
Montelirio	Mo3	-19.1	9	37.409837	-6.05932			Fontanals-Coll et al., 2015
Montelirio	Mo4	-19.1	8.9	37.409837	-6.05932			Fontanals-Coll et al., 2015
Montelirio	Mo5	-19.9	-19.1	37.409837	-6.05932			Fontanals-Coll et al., 2015
Montelirio	Mo6	-19.4	10	37.409837	-6.05932			Fontanals-Coll et al., 2015
Montelirio	Mo10	-20.3	8.9	37.409837	-6.05932			Fontanals-Coll et al., 2015
Montelirio	Mo11	-19.5	9.5	37.409837	-6.05932			Fontanals-Coll et al., 2015
Montelirio	Mo13	-20	8.9	37.409837	-6.05932			Fontanals-Coll et al., 2015
Montelirio	Mo14	-19.3	8.9	37.409837	-6.05932			Fontanals-Coll et al., 2015
Montelirio	Mo15	-19.3	9	37.409837	-6.05932			Fontanals-Coll et al., 2015

Montelirio	Mo16	-20.4	9.2	37.409837	-6.05932				Fontanals-Coll et al., 2015
Dolmen La Pastora		-19.5	8.6	37.413145	-6.064496	-19.5	8.6		Fontanals-Coll et al., 2015
Millares	Ind. 55.0	-19.6	9.5	36.964635	-2.522633	-19.4	10		Waterman et al., 2018
Millares	Ind. 55.1	-18.9	10.5	36.964635	-2.522633				Waterman et al., 2018
Millares	Ind. 57.1	-19.8	9.7	36.964635	-2.522633				Waterman et al., 2018
Millares	Ind. 57.4	-19.2	10.4	36.964635	-2.522633				Waterman et al., 2018
Millares	Ind. 74.3	-19.6	10.1	36.964635	-2.522633				Waterman et al., 2018
Millares	Ind. 74.0	-19.5	10.4	36.964635	-2.522633				Waterman et al., 2018
Millares	Ind. 63	-18.9	9.7	36.964635	-2.522633				Waterman et al., 2018
Las Yurdinas II	LYI34	-20.1	8.8	42.649263	-2.706487	-20.1	9.3		Fernandez-Crespo and Schulting, 2017
Las Yurdinas II	LYI29	-20.2	8.5	42.649263	-2.706487				Fernandez-Crespo and Schulting, 2017
Las Yurdinas II	LYI26	-19.9	9.6	42.649263	-2.706487				Fernandez-Crespo and Schulting, 2017
Las Yurdinas II	LYI25	-20	9.7	42.649263	-2.706487				Fernandez-Crespo and Schulting, 2017
Las Yurdinas II	LYI27	-19.9	9.5	42.649263	-2.706487				Fernandez-Crespo and Schulting, 2017
Las Yurdinas II	LYI30	-20.1	9.7	42.649263	-2.706487				Fernandez-Crespo and Schulting, 2017
Las Yurdinas II	LYI40	-20.2	8.3	42.649263	-2.706487				Fernandez-Crespo and Schulting, 2017
Las Yurdinas II	LYI41	-20.3	9.3	42.649263	-2.706487				Fernandez-Crespo and Schulting, 2017
Las Yurdinas II	LYI56	-20.1	9.4	42.649263	-2.706487				Fernandez-Crespo and Schulting, 2017
Las Yurdinas II	LYI43	-20.7	9.1	42.649263	-2.706487				Fernandez-Crespo and Schulting, 2017
Las Yurdinas II	LYI38	-20.4	9.3	42.649263	-2.706487				Fernandez-Crespo and Schulting, 2017
Las Yurdinas II	LYI42	-20.8	9	42.649263	-2.706487				Fernandez-Crespo and Schulting, 2017
Las Yurdinas II	LYI44	-20.4	9.3	42.649263	-2.706487				Fernandez-Crespo and Schulting, 2017
Las Yurdinas II	LYI65	-19.4	10.4	42.649263	-2.706487				Fernandez-Crespo and Schulting, 2017
Las Yurdinas II	LYI19	-19.8	9.4	42.649263	-2.706487				Fernandez-Crespo and Schulting, 2017
Las Yurdinas II	LYI31	-20.5	9.6	42.649263	-2.706487				Fernandez-Crespo and Schulting, 2017
Las Yurdinas II	LYI33	-20.4	9.5	42.649263	-2.706487				Fernandez-Crespo and Schulting, 2017
Las Yurdinas II	LYI46	-20	9.1	42.649263	-2.706487				Fernandez-Crespo and Schulting, 2017

Las Yurdinas II	LYII49	-20.6	8.9	42.649263	-2.706487			Fernandez-Crespo and Schulting, 2017
Las Yurdinas II	LYII45	-19.9	8.6	42.649263	-2.706487			Fernandez-Crespo and Schulting, 2017
Las Yurdinas II	LYII53	-20	9.9	42.649263	-2.706487			Fernandez-Crespo and Schulting, 2017
Las Yurdinas II	LYII24	-19.7	9.9	42.649263	-2.706487			Fernandez-Crespo and Schulting, 2017
Las Yurdinas II	LYII32	-19.6	9.8	42.649263	-2.706487			Fernandez-Crespo and Schulting, 2017
Las Yurdinas II	LYII50	-19.9	9.6	42.649263	-2.706487			Fernandez-Crespo and Schulting, 2017
Las Yurdinas II	LYII51	-20.5	9.1	42.649263	-2.706487			Fernandez-Crespo and Schulting, 2017
Las Yurdinas II	LYII48	-20.3	9.2	42.649263	-2.706487			Fernandez-Crespo and Schulting, 2017
Los Husos I	LHI60	-20.6	9.7	42.570975	-2.548521	-20.4	9.4	Fernandez-Crespo and Schulting, 2017
Los Husos I	LHI57	-20.2	9.1	42.570975	-2.548521			Fernandez-Crespo and Schulting, 2017
Peña Larga	CPL5	-20.5	10.1	42.610342	-2.519232	-20.4	9.8	Fernandez-Crespo and Schulting, 2017
Peña Larga	CPL14'	-20.2	9.5	42.610342	-2.519232			Fernandez-Crespo and Schulting, 2017
El Sotillo	ES103	-20	10	42.573691	-2.621899	-20.1	9.9	Fernandez-Crespo and Schulting, 2017
El Sotillo	ES104	-20.1	9.8	42.573691	-2.621899			Fernandez-Crespo and Schulting, 2017
Alto de la Huesera	LHUE51	-19.8	8.8	42.580629	-2.582655	-19.9	9.1	Fernandez-Crespo and Schulting, 2017
Alto de la Huesera	LHUE32	-20.1	9.7	42.580629	-2.582655			Fernandez-Crespo and Schulting, 2017
Alto de la Huesera	LHUE2i	-19.3	8.3	42.580629	-2.582655			Fernandez-Crespo and Schulting, 2017
Alto de la Huesera	LHUE16c	-20	8.8	42.580629	-2.582655			Fernandez-Crespo and Schulting, 2017
Alto de la Huesera	LHUE49	-20.5	8.7	42.580629	-2.582655			Fernandez-Crespo and Schulting, 2017
Alto de la Huesera	LHUE36	-20	9.8	42.580629	-2.582655			Fernandez-Crespo and Schulting, 2017
Alto de la Huesera	LHUE52	-19.6	9.1	42.580629	-2.582655			Fernandez-Crespo and Schulting, 2017
Alto de la Huesera	LHUE50	-19.9	8.9	42.580629	-2.582655			Fernandez-Crespo and Schulting, 2017
Alto de la Huesera	LHUE37	-19.2	9.7	42.580629	-2.582655			Fernandez-Crespo and Schulting, 2017
Alto de la Huesera	LHUE45	-19.8	9.7	42.580629	-2.582655			Fernandez-Crespo and Schulting, 2017
Alto de la Huesera	LHUE33	-20	10.1	42.580629	-2.582655			Fernandez-Crespo and Schulting, 2017
Alto de la Huesera	LHUE19c	-19.6	9.5	42.580629	-2.582655			Fernandez-Crespo and Schulting, 2017
Alto de la Huesera	LHUE53	-19.5	9.8	42.580629	-2.582655			Fernandez-Crespo and Schulting, 2017

Alto de la Huesera	LHUE7c	-20.2	7.8	42.580629	-2.582655			Fernandez-Crespo and Schulting, 2017
Alto de la Huesera	LHUE18c	-19.7	9.1	42.580629	-2.582655			Fernandez-Crespo and Schulting, 2017
Alto de la Huesera	LHUE12c	-19.9	9.1	42.580629	-2.582655			Fernandez-Crespo and Schulting, 2017
Alto de la Huesera	LHUE14c	-19.6	8.9	42.580629	-2.582655			Fernandez-Crespo and Schulting, 2017
Alto de la Huesera	LHUE38	-20.3	9.4	42.580629	-2.582655			Fernandez-Crespo and Schulting, 2017
Alto de la Huesera	LHUE44	-20.2	8.4	42.580629	-2.582655			Fernandez-Crespo and Schulting, 2017
Alto de la Huesera	LHUE42	-19.6	9.7	42.580629	-2.582655			Fernandez-Crespo and Schulting, 2017
Alto de la Huesera	LHUE3c'	-20.3	7.9	42.580629	-2.582655			Fernandez-Crespo and Schulting, 2017
Chabola de la Hechicera	CH96	-20.3	9.8	42.586092	-2.564612	-20.5	9.2	Fernandez-Crespo and Schulting, 2017
Chabola de la Hechicera	CH93	-20.8	9.6	42.586092	-2.564612			Fernandez-Crespo and Schulting, 2017
Chabola de la Hechicera	CH94	-20.3	9.3	42.586092	-2.564612			Fernandez-Crespo and Schulting, 2017
Chabola de la Hechicera	CH95	-20.4	8.1	42.586092	-2.564612			Fernandez-Crespo and Schulting, 2017
Longar	LON37	-19.5	10.6	42.521961	-2.372541	-19.9	9.9	Fernandez-Crespo and Schulting, 2017
Longar	LON19	-20.5	9.4	42.521961	-2.372541			Fernandez-Crespo and Schulting, 2017
Longar	LON7	-19.8	9.5	42.521961	-2.372541			Fernandez-Crespo and Schulting, 2017
Longar	LON5	-19.9	9.9	42.521961	-2.372541			Fernandez-Crespo and Schulting, 2017
Kurtzebide	TBI.15A	-19.9	8.4	42.934554	-2.751712	-20.0	8.9	Sarasketa-Gartzia et al. 2018
Kurtzebide	TBI.42B	-19.8	9	42.934554	-2.751712			Sarasketa-Gartzia et al. 2018
Kurtzebide	TBI.51	-20.3	9.3	42.934554	-2.751712			Sarasketa-Gartzia et al. 2018
Kurtzebide	TBI.58	-20.1	9.1	42.934554	-2.751712			Sarasketa-Gartzia et al. 2018
Kurtzebide	TBI.64	-20.1	8.7	42.934554	-2.751712			Sarasketa-Gartzia et al. 2018
Kurtzebide	TBI.11	-20	9	42.934554	-2.751712			Sarasketa-Gartzia et al. 2018
Kurtzebide	TBI.18	-20	9	42.934554	-2.751712			Sarasketa-Gartzia et al. 2018
Kurtzebide	TBI.49	-20.3	8.6	42.934554	-2.751712			Sarasketa-Gartzia et al. 2018
Kurtzebide	TBI.16	-19.9	9.4	42.934554	-2.751712			Sarasketa-Gartzia et al. 2018
Kurtzebide	TBI.14	-20	8.7	42.934554	-2.751712			Sarasketa-Gartzia et al. 2018

Annex 1: Adult human bone collagen $\delta^{13}\text{C}$ and $\delta^{15}\text{N}$ values of different Late Neolithic-Chalcolithic and Bronze sites from Iberian Peninsula.

San Juan	Patron	Avenida Font La Vial	Coveta Fraz Diabets	Cova Sano Valencina	Orden Semi Alto Reinosa Pannoga I	Fetrasa II	Ordaz	Cabezo Arc Coveta Mour Boieres	Thos Ber Lapa Raina Zumbal	Albantz	Guinea	Acaculote	Monestrio	Dobitza Pe Millares	Yamata II Haos I	Pena Larja Scutilla	Alto Huesca Chabata Ht Longar	Kuruzide																		
0	1.110	0.800	0.700	0.167	2.950	0.463	1.600	2.031	0.700	1.700	0.836	1.100	1.500	1.400	1.300	0.600	1.310	1.200	1.000	1.200	0.900	0.900	0.700	0.600	0.500	0.400	1.195	1.100	0.450	1.380						
1.100	0	1.000	0.900	0.167	1.917	0.463	1.600	2.031	0.700	1.700	0.836	1.100	1.500	1.400	1.300	0.600	1.310	1.200	1.000	1.200	0.900	0.900	0.700	0.600	0.500	0.400	1.195	1.100	0.450	1.380						
1.000	1.000	0	0.800	0.167	1.917	0.463	1.600	2.031	0.700	1.700	0.836	1.100	1.500	1.400	1.300	0.600	1.310	1.200	1.000	1.200	0.900	0.900	0.700	0.600	0.500	0.400	1.195	1.100	0.450	1.380						
0.800	0.800	0.800	0	0.633	0.083	0.117	1.250	0.337	0.800	1.231	0.100	0.900	0.756	0.300	0.400	0.510	0.200	0.400	0.500	0.300	0.400	0.300	0.400	0.300	0.200	0.300	0.400	0.300	0.400	0.300	0.400	0.300	0.400			
0.700	0.400	0.600	0.100	0	0.533	0.017	1.217	1.350	0.237	0.900	1.331	0.000	1.000	1.000	0.400	0.800	0.700	0.300	0.500	0.300	0.400	0.300	0.400	0.300	0.200	0.300	0.400	0.300	0.400	0.300	0.400	0.300	0.400			
0.167	0.383	0.067	0.633	0.533	0	0.517	1.217	1.350	0.237	0.900	1.331	0.000	1.000	1.000	0.400	0.800	0.700	0.300	0.500	0.300	0.400	0.300	0.400	0.300	0.200	0.300	0.400	0.300	0.400	0.300	0.400	0.300	0.400			
0.717	0.383	0.067	0.633	0.533	0	0.517	1.217	1.350	0.237	0.900	1.331	0.000	1.000	1.000	0.400	0.800	0.700	0.300	0.500	0.300	0.400	0.300	0.400	0.300	0.200	0.300	0.400	0.300	0.400	0.300	0.400	0.300	0.400			
0.717	0.383	0.067	0.633	0.533	0	0.517	1.217	1.350	0.237	0.900	1.331	0.000	1.000	1.000	0.400	0.800	0.700	0.300	0.500	0.300	0.400	0.300	0.400	0.300	0.200	0.300	0.400	0.300	0.400	0.300	0.400	0.300	0.400			
2.650	0.850	1.950	1.250	1.550	1.850	1.350	0.450	1.537	0.400	0.031	1.300	0.300	1.000	1.000	0.400	0.800	0.700	0.300	0.500	0.300	0.400	0.300	0.400	0.300	0.200	0.300	0.400	0.300	0.400	0.300	0.400	0.300	0.400			
0.463	0.637	0.363	0.337	0.237	1.437	1.537	0	1.100	1.531	0.200	1.200	0.356	0.900	0.900	0.400	0.800	0.700	0.300	0.500	0.300	0.400	0.300	0.400	0.300	0.200	0.300	0.400	0.300	0.400	0.300	0.400	0.300	0.400			
1.600	0.500	1.500	0.800	0.900	1.400	0.900	0.400	1.100	0	0.431	0.900	0.100	0.744	0.900	0.100	0.200	0.600	0.400	0.800	0.600	0.400	0.300	0.400	0.300	0.200	0.300	0.400	0.300	0.400	0.300	0.400	0.300	0.400			
2.031	0.931	1.931	1.231	1.331	1.831	1.331	0.031	1.300	0.431	1.300	0.300	1.144	0.900	0.300	1.000	0.600	0.400	0.800	0.600	0.400	0.300	0.400	0.300	0.200	0.300	0.400	0.300	0.400	0.300	0.400	0.300	0.400	0.300	0.400		
1.400	0.300	1.300	0.600	0.700	1.200	0.800	0.600	0.900	0.200	0.600	0.700	0.300	0.900	0.300	1.000	0.600	0.400	0.800	0.600	0.400	0.300	0.400	0.300	0.200	0.300	0.400	0.300	0.400	0.300	0.400	0.300	0.400	0.300	0.400		
1.700	0.600	1.600	0.900	1.000	1.500	1.000	0.300	1.200	0.100	0.300	1.000	0	0.854	0.900	0.300	0.700	0.300	0.500	0.300	0.400	0.300	0.400	0.300	0.200	0.300	0.400	0.300	0.400	0.300	0.400	0.300	0.400	0.300	0.400		
0.854	0.244	0.756	0.056	0.156	1.044	1.144	0.156	0.844	0	0.200	0.600	0.300	0.900	0.300	1.000	0.600	0.400	0.800	0.600	0.400	0.300	0.400	0.300	0.200	0.300	0.400	0.300	0.400	0.300	0.400	0.300	0.400	0.300	0.400		
1.100	0.000	1.000	0.300	0.400	0.900	0.800	0.900	0.600	0.400	0.600	0.200	0	0.400	0.300	1.000	0.100	0.500	0.300	0.400	0.300	0.400	0.300	0.200	0.300	0.400	0.300	0.400	0.300	0.400	0.300	0.400	0.300	0.400	0.300	0.400	
1.500	0.400	1.400	0.700	0.800	1.300	0.800	0.400	0.500	0.100	0.500	0.800	0.200	0.600	0.400	0	0.400	0.300	0.400	0.300	0.400	0.300	0.200	0.300	0.400	0.300	0.400	0.300	0.400	0.300	0.400	0.300	0.400	0.300	0.400	0.300	0.400
1.400	0.300	1.300	0.600	0.700	1.200	0.800	0.600	0.900	0.200	0.600	0.700	0.300	0.900	0.300	1.000	0.600	0.400	0.800	0.600	0.400	0.300	0.400	0.300	0.200	0.300	0.400	0.300	0.400	0.300	0.400	0.300	0.400	0.300	0.400	0.300	0.400
1.200	0.100	1.100	0.400	0.500	1.000	0.800	0.700	0.400	0.800	0.500	0.500	0	0.110	0.600	0.800	0.200	0.200	0.200	0.200	0.200	0.200	0.200	0.200	0.200	0.200	0.200	0.200	0.200	0.200	0.200	0.200	0.200	0.200	0.200	0.200	0.200
1.310	0.210	1.210	0.510	0.610	1.110	0.610	0.590	0.690	0.810	0.290	0.610	0.390	0.410	0.210	0.190	0.090	0.310	0.110	0	0.700	0.100	0.400	1.000	0.327	0.400	0.800	0.900	0.105	0.200	0.300	0.400	0.500	0.600	0.700	0.800	
0.600	0.500	0.500	0.200	0.100	0.400	0.100	1.000	1.400	1.000	0.400	0.800	0.800	0.500	0.300	0.300	0.300	0.300	0.300	0.300	0.300	0.300	0.300	0.300	0.300	0.300	0.300	0.300	0.300	0.300	0.300	0.300	0.300	0.300	0.300	0.300	
1.200	0.100	1.100	0.400	0.500	1.000	0.800	0.700	0.400	0.800	0.500	0.500	0	0.100	0.600	0.800	0.200	0.200	0.200	0.200	0.200	0.200	0.200	0.200	0.200	0.200	0.200	0.200	0.200	0.200	0.200	0.200	0.200	0.200	0.200	0.200	0.200
0.300	0.800	0.200	0.400	0.100	0.400	0.400	0.400	0.400	0.400	0.400	0.400	0.400	0.400	0.400	0.400	0.400	0.400	0.400	0.400	0.400	0.400	0.400	0.400	0.400	0.400	0.400	0.400	0.400	0.400	0.400	0.400	0.400	0.400	0.400	0.400	0.400
0.973	0.127	0.873	0.173	0.273	1.027	1.027	0.473	0.627	0.627	0.627	0.627	0.627	0.627	0.627	0.627	0.627	0.627	0.627	0.627	0.627	0.627	0.627	0.627	0.627	0.627	0.627	0.627	0.627	0.627	0.627	0.627	0.627	0.627	0.627	0.627	
0.900	0.200	0.800	0.100	0.200	1.000	1.100	0.400	0.700	1.100	0.200	0.800	0.000	0.200	0.600	0.100	0	0.400	0.300	0.300	0.300	0.300	0.300	0.300	0.300	0.300	0.300	0.300	0.300	0.300	0.300	0.300	0.300	0.300	0.300	0.300	
0.500	0.600	0.400	0.300	0.200	1.400	1.500	0.000	1.100	0.500	0.200	1.200	0.400	0.600	1.000	0.700	0.800	0.100	0.100	0.100	0.100	0.100	0.100	0.100	0.100	0.100	0.100	0.100	0.100	0.100	0.100	0.100	0.100	0.100	0.100	0.100	
0.400	0.700	0.300	0.400	0.300	1.300	1.600	0.100	1.200	1.600	0.300	1.300	0.600	0.800	1.000	0.700	0.800	0.100	0.100	0.100	0.100	0.100	0.100	0.100	0.100	0.100	0.100	0.100	0.100	0.100	0.100	0.100	0.100	0.100	0.100	0.100	
0.400	0.700	0.300	0.400	0.300	1.300	1.600	0.100	1.200	1.600	0.300	1.300	0.600	0.800	1.000	0.700	0.800	0.100	0.100	0.100	0.100	0.100	0.100	0.100	0.100	0.100	0.100	0.100	0.100	0.100	0.100	0.100	0.100	0.100	0.100	0.100	
0.450	0.650	0.350	0.450	0.350	1.450	1.550	0.050	1.150	1.550	0.250	1.250	0.450	0.650	1.050	0.750	0.850	0.150	0.150	0.150	0.150	0.150	0.150	0.150	0.150	0.150	0.150	0.150	0.150	0.150	0.150	0.150	0.150	0.150	0.150		
1.380	0.280	1.280	0.580	0.680	1.180	0.680	0.220	0.620	0.820	0.320	0.620	0	0.320	0.180	0.480	0.880	0.280	0.180	0.180	0.180	0.180	0.180	0.180	0.180	0.180	0.180	0.180	0.180	0.180	0.180	0.180	0.180	0.180	0.180		

Annex 3: Distant matrix built with the absolute value of pairwise differences among the site $\delta^{15}\text{N}$ average value calculated with adult individuals.

	San_Juan	La_Vital	Diablots	Valencina	Orden_Semi	Abauntz	Guineu	Ondarre	Husos_I	Pena_Larga	Sotillo	Alto_Hueser	Chabola_Hec	Kurtzebide
San_Juan	0	0.810	0.400	0.100	0.100	2.400	0.300	2.600	1.100	1.400	1.300	0.800	0.900	1.700
La_Vital	0.810	0	0.400	0.700	0.900	3.200	1.100	3.400	1.900	2.200	2.100	1.600	1.700	2.500
Diablots	0.400	0.400	0	0.300	0.500	2.800	0.700	3.000	1.500	1.800	1.700	1.200	1.300	2.100
Valencina	0.100	0.700	0.300	0	0.200	2.500	0.400	2.700	1.200	1.500	1.400	0.900	1.000	1.800
Orden_Semi	0.100	0.900	0.500	0.200	0	2.300	0.200	2.500	1.000	1.300	1.200	0.700	0.800	1.600
Abauntz	2.400	3.200	2.800	2.500	2.300	0	2.100	0.200	1.300	1.000	1.100	1.600	1.500	0.700
Guineu	0.300	1.100	0.700	0.400	0.200	2.100	0	2.300	0.800	1.100	1.000	0.500	0.600	1.400
Ondarre	2.600	3.400	3.000	2.700	2.500	0.200	2.300	0	1.500	1.200	1.300	1.800	1.700	0.900
Husos_I	1.100	1.900	1.500	1.200	1.000	1.300	0.800	1.500	0	0.300	0.200	0.300	0.200	0.600
Pena_Larga	1.400	2.200	1.800	1.500	1.300	1.000	1.100	1.200	0.300	0	0.100	0.600	0.500	0.300
Sotillo	1.300	2.100	1.700	1.400	1.200	1.100	1.000	1.300	0.200	0.100	0	0.500	0.400	0.400
Alto_Hueser	0.800	1.600	1.200	0.900	0.700	1.600	0.500	1.800	0.300	0.600	0.500	0	0.100	0.900
Chabola_Hec	0.900	1.700	1.300	1.000	0.800	1.500	0.600	1.700	0.200	0.500	0.400	0.100	0	0.800
Kurtzebide	1.700	2.500	2.100	1.800	1.600	0.700	1.400	0.900	0.600	0.300	0.400	0.900	0.800	0

Annex 4: Distant matrix built with the absolute value of pairwise differences among the site $\delta^{13}\text{C}$ average value calculated with herbivores.

Pop	X ($\delta^{13}\text{C}$)	Y ($\delta^{13}\text{C}$)	X ($\delta^{15}\text{N}$)	Y ($\delta^{15}\text{N}$)
San_Juan	-0.43707833	-0.07961231	1.01524366	-0.052676495
Pastora	-0.33743841	-0.07385136	-0.093930455	-0.049092023
Avenc_Forat	-0.63634613	-0.09094911	0.914417523	-0.056758397
La_Vital	-0.93750498	-0.12190678	0.209384494	-0.054680823
Coveta_Frare	-0.63538185	-0.08668095	0.310103498	-0.054977619
Diablets	-0.93842181	-0.12649979	0.813946878	-0.031910915
Cova_Santo	0.17418694	0.01733826	0.308539776	-0.050599523
Valencina	-0.63550833	-0.08547799	-0.904751877	0.008910701
Orden_Seminario	-0.63606721	-0.08691767	-1.026776568	0.155890139
Alto_Reinoso	-0.04976225	-0.11131976	0.516632198	-0.032256949
Paimogo_I	0.73826187	-0.13465878	-0.593458048	-0.041815812
Feteiras_II	0.54462198	-0.10127486	-1.013302451	0.07615129
Ondarre	1.61690255	-0.315573	0.298766124	0.048376283
Cabezo_Arruda_I	0.01859046	0.0749607	-0.694090927	-0.04304006
Cova_Moura	0.035712	0.06284387	0.130922664	-0.088394561
Bolores	0.25263483	0.05477078	-0.098244697	0.004840223
Tholos_Borracheira	0.01660005	0.07184887	-0.49514968	-0.044284012
Lapa_Rainaha_II	-0.17277522	0.09028807	-0.395923435	-0.032002953
Zambujal	0.65626199	0.0655655	0.000981549	0.017121282
Abauntz	0.39094226	0.10855045	-0.197470943	-0.007440835
Guineu	-0.43210308	0.02344472	-0.303857504	0.014716412
Acequi3n	-0.95733338	0.07116614	0.397665421	0.067082975
Montelirio	-0.24402883	0.05602176	-0.197503874	-0.007316108
Dolmen_Pastora	-0.25103325	0.06567516	-0.693478287	-0.069315344
Millares	-0.38403024	0.12549292	0.695250068	0.104282517
Yurdinas_II	0.39402592	0.07425394	0.024618263	-0.021368138
Husos_I	0.65527647	0.0716991	0.100074839	0.030286261
Pena_Larga	0.60363471	0.04869615	0.496826926	0.081748432
Sotillo	0.30313059	0.06626227	0.596014947	0.094613975
Alto_Huesera	0.11382389	0.07198139	-0.192772096	-0.011821399
Chabola_Hechicera	0.70546286	0.06296704	-0.098291505	0.004601692
Longar	0.17404669	0.06276148	0.54836201	0.118269952
Kurtzebide	0.29069727	0.0681338	-0.37874849	-0.077140171

Annex 5: MDS coordinates for $\delta^{13}\text{C}$ and $\delta^{15}\text{N}$ human values

Pop	X ($\delta^{13}\text{C}$)	Y ($\delta^{13}\text{C}$)
San_Juan	-0.806334107	0.06453626
La_Vital	-1.606856912	-0.05906031
Diablets	-1.207314585	0.00555155
Valencina	-0.907297437	0.004271765
Orden_Seminario	-0.707286004	0.003418575
Abauntz	1.592845469	-0.006393108
Guineu	-0.507274572	0.002565385
Ondarre	1.792856902	-0.007246298
Husos_I	0.292771158	-0.000847374
Pena_Larga	0.592788307	-0.002127159
Sotillo	0.492782591	-0.001700564
Alto_Huesera	-0.007245991	0.00043241
Chabola_Hechicera	0.092759726	5.81548E-06
Kurtzebide	0.892805456	-0.003406944

Annex 6: MDS coordinates for $\delta^{13}\text{C}$ faunal values